Illinois U Library

The American Mineralogist

Journal of the Mineralogical Society of America

Vol. 38 NOVEMBER-DECEMBER, 1953 Nos. 11 and 12

STUDIES IN PETROLOGY AND MINERALOGY

Dedicated to

CLARENCE S. ROSS
and
WALDEMAR T. SCHALLER

By Their Present and Former Colleagues
of the U. S. Geological Survey
on the occasion
of their formal retirement

Edited by the Staff
Geochemistry and Petrology Branch
U. S. Geological Survey

EDITOR: WALTER F. HUNT
ASSISTANT EDITOR: LEWIS S. RAMSDELL
BOARD OF ASSOCIATE EDITORS:
ESPER S. LARSEN, JR.
MICHAEL FLEISCHER
ELBURT F. OSBORN
AUSTIN F. ROGERS (1950–1953)
GEORGE TUNELL (1951–1954)
ADOLF PABST (1952–1955)

Published bi-monthly by the Society

Mineralogical Society of America*

ASSOCIATED WITH THE GEOLOGICAL SOCIETY OF AMERICA

President: **J. D. H. Donnay**, The Johns Hopkins University, Baltimore, Maryland.
Acting Vice President: **Sterling B. Hendricks**, Plant Industry Station, Beltsville, Maryland.
Secretary: **C. S. Hurlbut, Jr.**, Harvard University, Cambridge, Massachusetts.
Treasurer: **Earl Ingerson**, U. S. Geological Survey, Washington 25, D. C.
Editor: **Walter F. Hunt**, University of Michigan, Ann Arbor, Michigan.
Councillors: **E. F. Osborn**, School of Mineral Industries, Pennsylvania State College, Pennsylvania.
George T. Faust, U. S. Geological Survey, Washington 25, D. C.
Victor T. Allen, Institute of Geophysical Technology, St. Louis, Missouri.
C. Osborne Hutton, Stanford University, Palo Alto, California.
Michael Fleischer, U. S. Geological Survey, Washington 25, D. C.

The enlarged issues of this journal for 1953 are made possible by a grant from the Penrose Fund of the Geological Society of America.

The American Mineralogist—Journal of the Mineralogical Society of America

A journal containing articles on mineralogy, crystallography, petrography, and allied sciences, is issued every two months. Contributions are invited from everyone.

Office of Publication, Mineralogical Laboratory, Ann Arbor, Mich.

The general conduct of the journal is in the hands of the editor, **Walter F. Hunt**, Ann Arbor, Michigan, to whom all manuscripts should be submitted. To assist the editor the council of the Mineralogical Society has appointed **Lewis S. Ramsdell**, Ann Arbor, Michigan, assistant editor, and the following board of associate editors:

Michael Fleischer, U. S. Geological Survey, Washington, D. C.
Esper S. Larsen, Jr., U. S. Geological Survey, Washington, D. C.
Elburt F. Osborn, Pennsylvania State College, State College, Pa.
Adolf Pabst, University of California, Berkeley 4, California.
Austin F. Rogers, 2412 Durant Ave., Berkeley, California.
George Tunell, University of California at Los Angeles, California.

Contributors of leading articles are given without charge 100 reprints (without covers) of their article. If additional reprints are desired these can be purchased at the following rates:

Pages	*1–4*	*5–8*	*9–12*	*13–16*	*17–20*	*21–24*	*25–28*	*29–32*	*Covers*
Copies									
25	$3.50	$5.00	$ 8.00	$ 9.50	$11.00	$13.00	$15.00	$16.00	$4.90
50	3.80	5.55	8.80	10.40	12.10	14.20	16.40	17.50	5.50
75	4.10	6.10	9.60	11.30	13.20	15.40	17.80	19.00	6.10
100	4.40	6.65	10.40	12.20	14.30	16.60	19.20	20.50	6.70
Addl. C's	1.20	2.20	3.20	3.60	4.40	4.80	5.60	6.00	2.40

Cover Composition $1.55.

Sent to all members and fellows of the Mineralogical Society of America. Subscription price, $4.00 per year (single copies of normal issues, $1.00 plus postage).

Entered as second class matter at the post office at Menasha, Wis., under Act of March 3, 1879. Acceptance for mailing at the special rate of postage provided for in section 1103, Act of Oct. 3, 1917, paragraph 4 section 429 P. L. & R. authorized March 13, 1922.

Notice of change of address, orders, and remittances should be sent to Dr. Earl Ingerson, U. S. Geological Survey, Washington 25, D. C.

Printed by the George Banta Publishing Company, Menasha, Wisconsin
Printed in the United States of America

STUDIES IN PETROLOGY AND MINERALOGY

Dedicated to

CLARENCE S. ROSS

and

WALDEMAR T. SCHALLER

By Their Present and Former Colleagues
of the U. S. Geological Survey
on the occasion
of their formal retirement

1953

Publication of this volume has been greatly aided by grants from the Geological Society of America and the National Science Foundation and by contributions from the following:

Leason H. Adams
Victor T. Allen
Z. S. Altschuler
Charles A. Anderson
David A. Andrews
Joseph M. Axelrod
Roy A. Bailey
Thomas F. Bates
Sarah Berthold
Leona Boardman
Theodore Botinelly
Norman L. Bowen
Wilmot H. Bradley
N. M. Bramlette
Josiah Bridge
A. F. Buddington
Paul B. Bunton
Eugene Callaghan
Martha S. Carr
Maxwell K. Carron
Evelyn Cisney
Fred M. Chace
Felix Chayes
C. L. Christ
Esther W. Claffy
Joan R. Clark
Preston E. Cloud, Jr.
Frank Cuttitta
Maurice Deul
Gabrielle Donnay
Joseph D. H. Donnay
Albert E. J. Engel
Richard C. Erd
Howard T. Evans, Jr.
Joseph J. Fahey
George T. Faust
Henry G. Ferguson
D. Jerome Fisher
Frances J. Flanagan
Michael Fleischer
Mary H. Fletcher
William F. Foshag
Margaret D. Foster
Jacob Freedman
Carl Fries, Jr.
Clifford Frondel
Judith Frondel
H. R. Gault
Robert M. Garrels
Joseph L. Gillson
James Gilluly
Jewell J. Glass
Samuel S. Goldich
Joseph W. Greig
Allen B. Griggs
Frank S. Grimaldi
Robert A. Hatch
Herbert E. Hawkes, Jr.
Armin W. Helz
Edward P. Henderson
Sterling B. Hendricks
Frank L. Hess
Donnel F. Hewett
Fred A. Hildebrand
Marjorie Hooker
Charles B. Hunt
Walter F. Hunt
C. S. Hurlbut, Jr.
C. Osborne Hutton
Earl Ingerson
Herbert Insley
Richard H. Jahns
Serah C. Johnson
William D. Johnston, Jr.
Joe H. Kerr
Paul F. Kerr
Charles A. Kinser
Adolph Knopf
Edward H. Kraus
Harry S. Ladd
Esper S. Larsen, Jr.
Esper S. Larsen, III
Dwight M. Lemmon
Marie Louise Lindberg
Kenneth E. Lohman
G. D. Louderback
Gordon A. Macdonald
John P. Marble
Brian H. Mason
Irving May
Vincent E. McKelvey
John L. Mergner
Herbert E. Merwin
Roswell Miller, III
Charles Milton
Hugh D. Miser
Watson H. Monroe
G. W. Morey
Mary E. Mrose
K. J. Murata
Joseph Murdoch
Alfred T. Myers
Charles R. Naeser
Thomas B. Nolan
Elburt F. Osborn
Adolph Pabst
Charles Palache
Charles F. Park, Jr.
William T. Pecora
Joe Webb Peoples
Stuart H. Perry
George Phair
Frederick H. Pough
John C. Rabbitt
Joseph L. Ramisch
Lewis S. Ramsdell
Frank S. Reed
John C. Reed
John B. Reeside, Jr.
Laura Reichen
Donald Richter
Daphne Riska
G. D. Robinson
William W. Rubey
E. H. Sarles
A. Nelson Sayre
John F. Schairer
Alexander M. Sherwood
Quentin D. Singewald
Chester B. Slawson
Robert L. Smith
Ward C. Smith
Taisia Stadnichenko
Thomas W. Stern
Rollin E. Stevens
Lorin R. Stieff
Marcellus H. Stow
George Switzer
Thomas P. Thayer
Martin S. Tischler
Carl Tolman
George Tunell
Orville F. Tuttle
Angelina Vlisidis
Magnus Vonsen
Charlotte M. Warshaw
Israel Warshaw
Russell D. Wayland
Alice D. Weeks
Edgar T. Wherry
James Steele Williams
Alexander N. Winchell
C. Wroe Wolfe
Wendell P. Woodring
Theodore Woodward
William E. Wrather
Frederick E. Wright
Hatten S. Yoder, Jr.
Emanuel G. Zies
Samuel Zerfoss
Peter Zubovic

Contents

CLARENCE S. ROSS . . . . *George T. Faust* 879

WALDEMAR T. SCHALLER . . . . *Joseph J. Fahey* 881

RHODONITE, JOHANNSENITE, AND FERROAN JOHANNSENITE AT VANADIUM, NEW MEXICO . . . . *Victor T. Allen and Joseph J. Fahey* 883

CHEMICAL PETROLOGY AND MINERALOGY OF HORNBLENDE IN NORTHWEST ADIRONDACK GRANITIC ROCKS . . . . *A. F. Buddington and B. F. Leonard* 891

LINDGRENITE AND CUPROTUNGSTITE FROM THE SEVEN DEVILS DISTRICT, IDAHO . . . . *Ralph S. Cannon, Jr. and Frank S. Grimaldi* 903

STUDIES OF BORATE MINERALS (II): X-RAY CRYSTALLOGRAPHY OF INYOITE AND MEYERHOFFERITE; X-RAY AND MORPHOLOGICAL CRYSTALLOGRAPHY OF $2CaO \cdot 3B_2O_3 \cdot 9H_2O$ . . . . *C. L. Christ* 912

COMPOSITION, TENEBRESCENCE AND LUMINESCENCE OF SPODUMENE MINERALS . . . . *Esther W. Claffy* 919

THE CRYSTALLOGRAPHY OF BASTNAESITE, PARISITE, ROENTGENITE, AND SYNCHISITE . . . . *Gabrielle Donnay and J. D. H. Donnay* 932

FAUSTITE, A NEW MINERAL, THE ZINC ANALOGUE OF TURQUOIS . . . . *Richard C. Erd, Margaret D. Foster, and Paul D. Proctor* 964

STEVENSITE, REDEFINED AS A MEMBER OF THE MONTMORILLONITE GROUP . . . . *George T. Faust and K. J. Murata* 973

THE BAVENITE PROBLEM . . . . *Michael Fleischer and George Switzer* 988

GEOCHEMICAL STUDIES OF CLAY MINERALS (II): RELATION BETWEEN IONIC SUBSTITUTION AND SWELLING IN MONTMORILLONITE . . . . *Margaret D. Foster* 994

HYDROXYL SUBSTITUTION IN THORITE AND ZIRCON . . . . *Clifford Frondel* 1007

STUDIES OF URANIUM MINERALS (XII): THE STATUS OF BILLIETITE AND BECQUERELITE . . . . *Judith W. Frondel and Frank Cuttitta* 1019

THE MAYODAN METEORITE, ROCKINGHAM COUNTY, NORTH CAROLINA . . . . *Edward P. Henderson and Stuart H. Perry* 1025

TWO URANIUM-BEARING PEGMATITE BODIES IN SAN BERNARDINO COUNTY, CALIFORNIA . . . . *D. F. Hewett and Jewell J. Glass* 1040

MINIMIZING THE EFFECTS OF PREFERRED ORIENTATION IN x-RAY POWDER DIFFRACTION PATTERNS . . . . *Fred A. Hildebrand* 1051

GIANT AMYGDULES IN ANDESITE FROM THE SOUTHERN QUITMAN MOUNTAINS, TEXAS . . . . *Earl Ingerson* 1057

AMYGDULAR CAMPTONITE DIKES FROM MOUNT JO, MOUNT MARCY QUADRANGLE, ESSEX COUNTY, NEW YORK . . . . *Howard W. Jaffe* 1065

THE GENESIS OF PEGMATITES (II): QUANTITATIVE ANALYSIS OF LITHIUM-BEARING PEGMATITE, MORA COUNTY, NEW MEXICO . . . . *Richard H. Jahns* 1078

CLINTONITE AS A CONTACT-METASOMATIC PRODUCT OF BOULDER BATHYLITH, MONTANA . . . . *Adolph Knopf* 1113

ZONED ZIRCON FROM OKLAHOMA . . . . *Esper S. Larsen, Jr., C. L. Waring, and Joseph Berman* 1118

MORAESITE, A NEW HYDROUS BERYLLIUM PHOSPHATE FROM MINAS GERAIS, BRAZIL . . . . *M. L. Lindberg, W. T. Pecora, and A. L. de M. Barbosa* 1126

THE WEBSTER-ADDIE ULTRAMAFIC RING, JACKSON COUNTY, NORTH CAROLINA, AND SECONDARY ALTERATION OF ITS CHROMITE . . . . *Roswell Miller, III* 1134

THE IDENTITY OF TINZENITE WITH MANGANOAN AXINITE . . . . *C. Milton, F. A. Hildebrand, and A. M. Sherwood* 1148

STUDIES OF URANIUM MINERALS (XIII): SYNTHETIC URANOSPINITES............... *Mary E. Mrose* 1159
BURBANKITE AND CALKINSITE, TWO NEW CARBONATE MINERALS FROM MONTANA.. .... *W. T. Pecora and Joe H. Kerr* 1169
PREPARATION OF ROCK THIN SECTIONS.........*Frank S. Reed and John L. Mergner* 1184
THE LEONA RHYOLITE, ALAMEDA COUNTY, CALIFORNIA............*G. D. Robinson* 1204
HIDALGOITE, A NEW MINERAL.................*Robert L. Smith, Frank S. Simons, and Angelina C. Vlisidis* 1218
RE-EXAMINATION OF MOSESITE................*George Switzer, K. J. Murata, J. J. Fahey, and W. F. Foshag* 1225
MONTROSEITE, A NEW VANADIUM OXIDE FROM THE COLORADO PLATEAUS...............*Alice D. Weeks, Evelyn A. Cisney, and Alexander M. Sherwood* 1235
THE CRYSTAL STRUCTURE OF MONTROSEITE, A VANADIUM MEMBER OF THE DIASPORE GROUP...........................*Howard T. Evans, Jr., and Stanley Block* 1242
SOME THERMODYNAMIC RELATIONS AMONG THE VANADIUM OXIDES AND THEIR RELATION TO THE OXIDATION STATES OF THE URANIUM ORES OF THE COLORADO PLATEAUS..*Robert M. Garrels* 1251
NOTES AND NEWS: OCCURRENCE OF BASSANITE IN TWO DESERT BASINS IN SOUTHEASTERN CALIFORNIA....................*Robert D. Allen and Henry Kramer* 1266
A SIMPLE HIGH-TEMPERATURE MICROSCOPE HEATING STAGE.....................................*Donald H. Richter and Joseph F. Abell* 1269
BIBLIOGRAPHY OF CLARENCE SAMUEL ROSS (THROUGH 1953).......................................COMPILED BY MARJORIE HOOKER 1272
BIBLIOGRAPHY OF WALDEMAR THEODORE SCHALLER (THROUGH 1953).......................................COMPILED BY MARJORIE HOOKER 1276

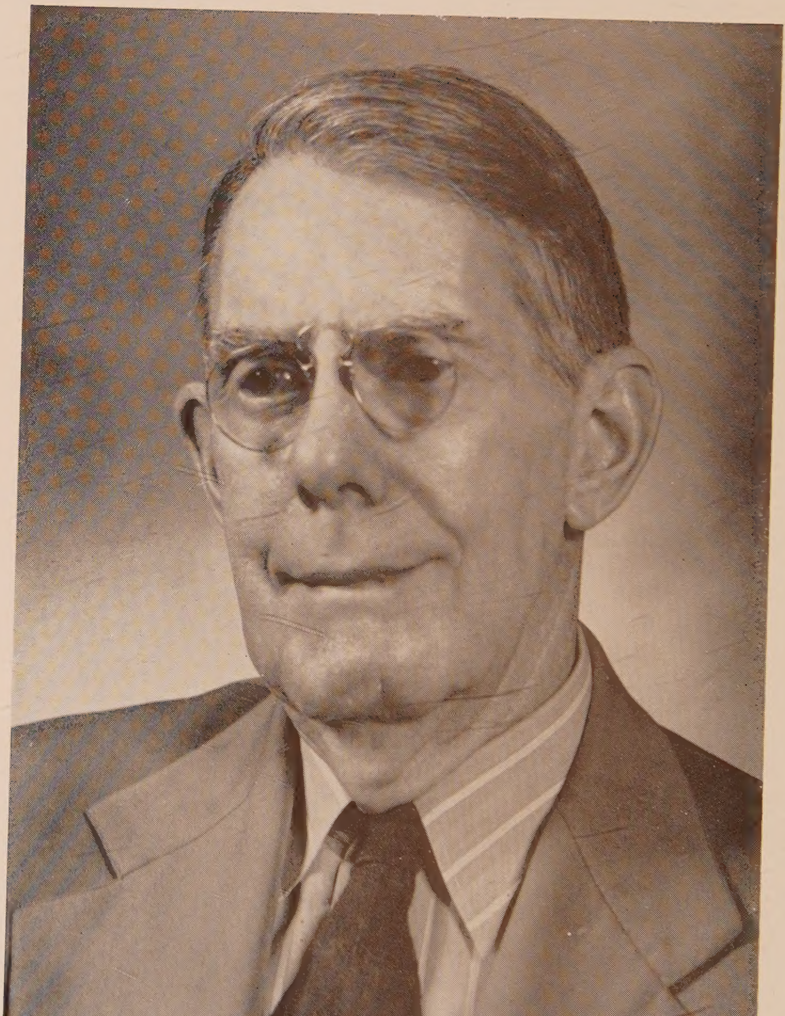

Clarence S. Ross

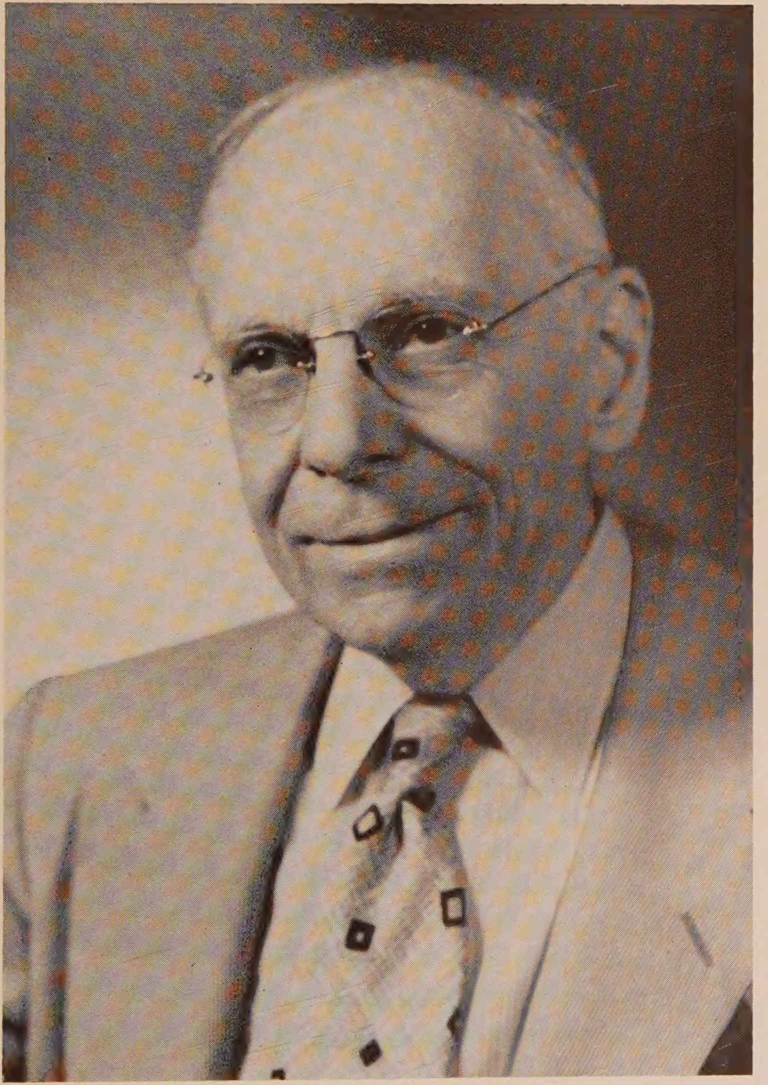

Waldemar T. Schaller

Digitized by the Internet Archive
in 2024

https://archive.org/details/american-mineralogist_november-december-1953_38_11-12

THE AMERICAN MINERALOGIST
JOURNAL OF THE MINERALOGICAL SOCIETY OF AMERICA

Vol. 38 NOVEMBER-DECEMBER 1953 Nos. 11 and 12

CLARENCE S. ROSS*

GEORGE T. FAUST, *U. S. Geological Survey, Washington, D. C.*

Clarence S. Ross is one of the eminent triumvirate of Ross, Schaller, and Larsen, of the U. S. Geological Survey, that has contributed so much to the basic data of mineralogy and petrology during the past 35 years.

Ross entered the University of Illinois to study engineering and had the good fortune to take a course in Engineering Geology under Professor William S. Bayley. Before the course was over the student was lost to engineering but gained by geology. Dr. Bayley exerted a profound influence on Ross, not only in inspiring him to study geology, but also in acting as a second father to him. At Illinois, Ross received thorough training in the basic cognate disciplines; and, as a consequence, he has always stressed the value of a broad background for work in the geological sciences. His doctoral dissertation was on the Snowbank granite of the Lake Superior region.

Dr. Ross joined the Survey in 1917 and for two years was engaged in oil studies in Oklahoma and Texas. The gateway to his life interests opened when he joined Cross and Larsen in the studies of volcanic rocks of the San Juan region of Colorado. Since that day, his association with Larsen and Schaller has been exceedingly close.

His major fields of study have been the physical chemistry of the formation of certain types of ore deposits, the clay minerals, and volcanology. The contribution that Dr. Ross has made to the mineralogy of the clay minerals is truly significant. When he started work on these minerals, the literature on the subject was in a state of utter confusion. An attitude of hopelessness concerning the study of such fine-grained minerals prevailed in many laboratories. It was Ross who unequivocally demonstrated that what was considered to be kaolinite consisted of three different minerals, which he named kaolinite, dickite, and nacrite. He extended his studies to the kaolin-group minerals—halloysite and allophane—and he published many papers on the clay minerals. His work on the montmorillonite group culminated in the Professional Paper published in 1945 with Dr. Sterling B. Hendricks. In addition to the descriptive work on the clays, Ross has been greatly interested in relating the clay minerals to the paragenesis and origin of rocks and ore deposits. As a result of his work in clearly defining the clay minerals and in establishing their paragenesis, a new field was opened for advances in the study of ore deposits, the alteration of rocks, and the development of soils.

---

* Publication authorized by the Director, U. S. Geological Survey.

Some of Dr. Ross' friends have wondered why, in the past ten years, he has transferred his major efforts from clays to volcanoes. Ross explains that no great jump is involved. He first became interested in clay materials by way of bentonites and their origin as volcanic materials. Thus, in going back to the study of volcanic rocks, he is only completing a circle.

Dr. Ross was for about 20 years head of the Section of Petrology of the U. S. Geological Survey. It has been one of his proudest boasts that he has never proposed a new rock name.

To those of us who have had the privilege of working closely with Clarence Ross, it is not a simple thing to set down in words our indebtedness to him. Ever willing to help us interpret what we see under the microscope, to repair or make a piece of unusual laboratory equipment, to give good counsel when sought, he inspires us by his example and arouses a healthy enthusiasm for research. Clarence Ross has lived up to the standards set by his illustrious predecessors. In dedicating this volume to Ross and Schaller, we pay tribute to two eminent scholars whose modesty makes it doubly a pleasure thus to acclaim them.

WALDEMAR T. SCHALLER*

JOSEPH J. FAHEY, *U. S. Geological Survey, Washington, D. C.*

In a small improvised chemical laboratory located behind the family residence in San Francisco, Theodore P. Schaller, using Remsen's textbook, began to teach his son Waldemar the elementary principles of chemistry. Little did he realize then that he was planting a seed that would grow and blossom forth, yielding in great abundance fruit that has vastly enriched the science of mineralogy throughout the last fifty years.

After graduation from high school, young Waldemar attended the University of California, where, under the stimulating influence of Professors Andrew C. Lawson, head of the Department of Geology, Arthur S. Eakle, who taught him mineralogy and goniometry, and Walter C. Blasdale, who gave to him a well-rounded course in analytical chemistry, he completed his undergraduate work and received his Bachelor of Science degree in 1903.

An appointment as Assistant Chemist on the U. S. Geological Survey three months after his graduation brought Schaller to Washington, D. C. Here, in the Division of Physical and Chemical Research with Geologist George F. Becker as Chief, he was associated with such giants in the field of geochemistry as Frank Wigglesworth Clarke, William F. Hillebrand, George Steiger, Eugene T. Allen, and Eugene C. Sullivan, who were to contribute so largely to their chosen field. In this environment he stored up a wealth of knowledge and experience that served him as a background for his future research.

On the twentieth day of August nineteen hundred and eight Schaller married Mary Ellen Boyland of Virginia. Though no children blessed this union, it has been a most happy one. Three nieces were raised from early childhood and received the same tender care that would have been lavished on their own children.

Schaller resigned from the Survey, March 1, 1912, and he and Mrs. Schaller went to Europe. There they visited mineralogical museums and collections, and he conferred with the leading European mineralogists. In June of that year he received his Doctor of Philosophy degree, summa cum laude, under Paul Groth at the University of Munich. This was followed by studies under Victor Goldschmidt at Heidelberg. October found Dr. Schaller reinstated on the Survey after his very rewarding six months abroad. Except for this short period and another six months during 1920 when he was employed in private industry, he has had continuous service on the Survey since 1903.

The greatness of Waldemar Schaller as a scientist is reflected in his bibliography of nearly 200 titles. He has described more than 40 new mineral species, and his classic study of the paragenesis of the saline minerals in the Permian deposits of New Mexico has pointed the way for the British mineralogists in their recent investigation of the English evaporites of the same age. However, any outline, brief though it be, of his scientific achievements, would be inadequately drawn if only the published record were considered. He has played the role of consultant and adviser to scores of his colleagues, and teacher to many of his younger associates. Repeatedly, time was cheerfully taken from study of a research problem to painstakingly answer, in his own thorough fashion, the very elementary question of a neophyte in the field of mineralogy or crystallography.

---

* Publication authorized by the Director, U. S. Geological Survey.

A severe critic of those who do not hew to the line of scientific rectitude, Waldemar Schaller exerts a strong stimulating influence, not only on his associates in the Geochemistry and Petrology Branch, but also on the geologists throughout the Survey. It is indeed a great privilege for his associates to honor this eminent scientist and his colleague of many years, Clarence S. Ross, by dedicating to them this issue of the *American Mineralogist.*

RHODONITE, JOHANNSENITE, AND FERROAN JOHANNSENITE AT VANADIUM, NEW MEXICO*

VICTOR T. ALLEN, *Institute of Technology,
Saint Louis University, St. Louis, Mo.*

AND

JOSEPH J. FAHEY, *U. S. Geological Survey, Washington, D. C.*

ABSTRACT

The occurrences and relations of rhodonite, johannsenite, and ferroan johannsenite at the Star, Hobo, and Princess mines, near Vanadium, Grant County, N. Mex., are described, and the optical properties and chemical compositions of these minerals are recorded. In the deep levels of these mines rhodonite replaces johannsenite and ferroan johannsenite and was probably formed by the introduction of manganese in the ore solutions that later deposited magnetite, sphalerite, and other sulfides.

INTRODUCTION

This paper describes the occurrences of rhodonite, johannsenite, and ferroan johannsenite at the Star, Hobo, and Princess mines near Vanadium, N. Mex., and is essentially a report of progress on our study of the pyroxenes associated with the pyrometasomatic zinc deposits of N. Mex. and Mexico. These mines are located in Grant County, about 12 miles east of Silver City, N. Mex., and are included in the Central Mining District, parts of which have been mapped and described by Lindgren, Graton, and Gordon (1910), by Paige (1916), by Spencer and Paige (1935), and by Lasky (1936).

Johannsenite was named by Schaller in 1938, so it appears appropriate to record here the extension of known occurrences of this manganese pyroxene and its association with rhodonite. Furthermore, the term ferroan johannsenite used here to designate the composition of another manganese pyroxene in this district indicates the usefulness of the adjectival modifiers to mineral names as proposed by Schaller in 1930.

The Central Mining District (Fig. 1) contains several stocks of granodiorite and allied rocks that are associated with ore deposits. The Hanover stock is known from the excellent paper of Schmitt (1939) on the Pewabic mine, one by Schaller (1938) on johannsenite from the Hanover Mine (1938), and earlier papers by Paige (1916), Spencer and Paige (1935), and others. A stock containing the important disseminated copper deposit that is mined by the Kennecott Copper Corporation in a

---

* Publication authorized by the Director, U. S. Geological Survey.

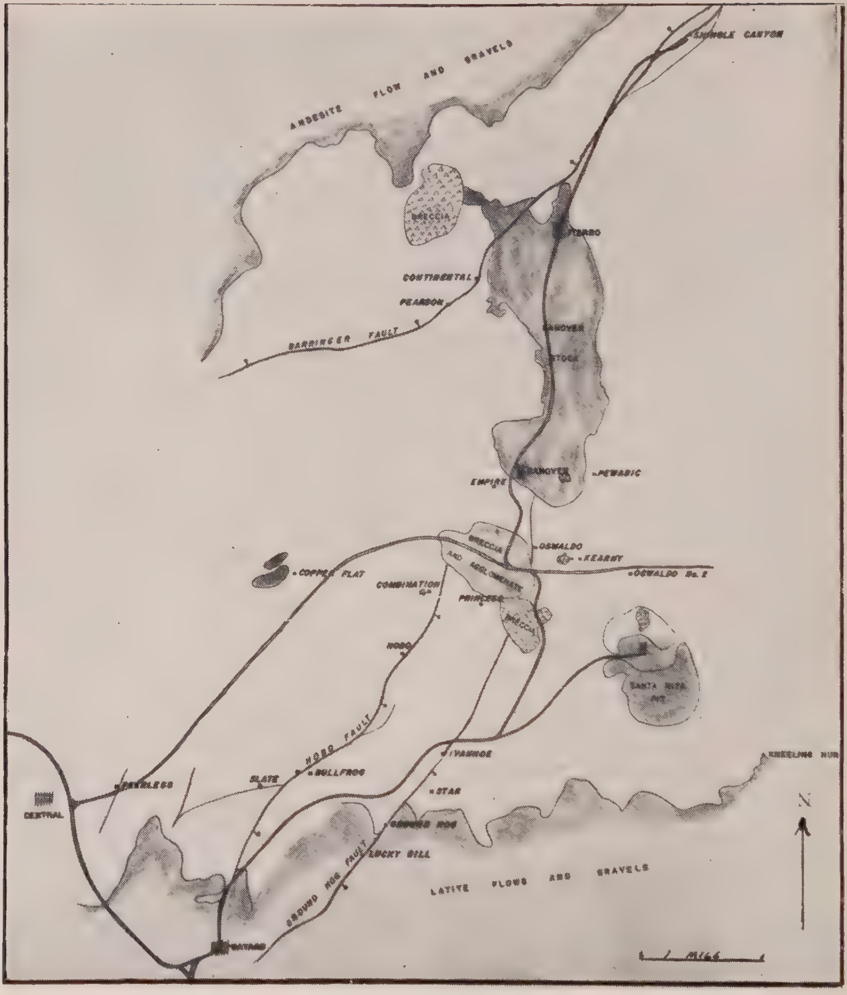

FIG. 1. Map showing location of mines of Central mining district, New Mexico.

large open pit occurs near the village of Santa Rita (Spencer and Paige, 1935; Kerr *et al.*, 1950). Two small stocks form the locus of the Copper Flat mine, which first attracted interest as a copper prospect (Lindgren, Graton, and Gordon, 1910) and during the Second World War was operated as a zinc mine by the Peru Mining Company. Mineralization related to the intrusive body at the Ground Hog mine was not discovered until later (Spencer and Paige, 1935; Lasky, 1936), but it is to this intrusion that the deposits of the Star, Hobo, and Princess mines are related.

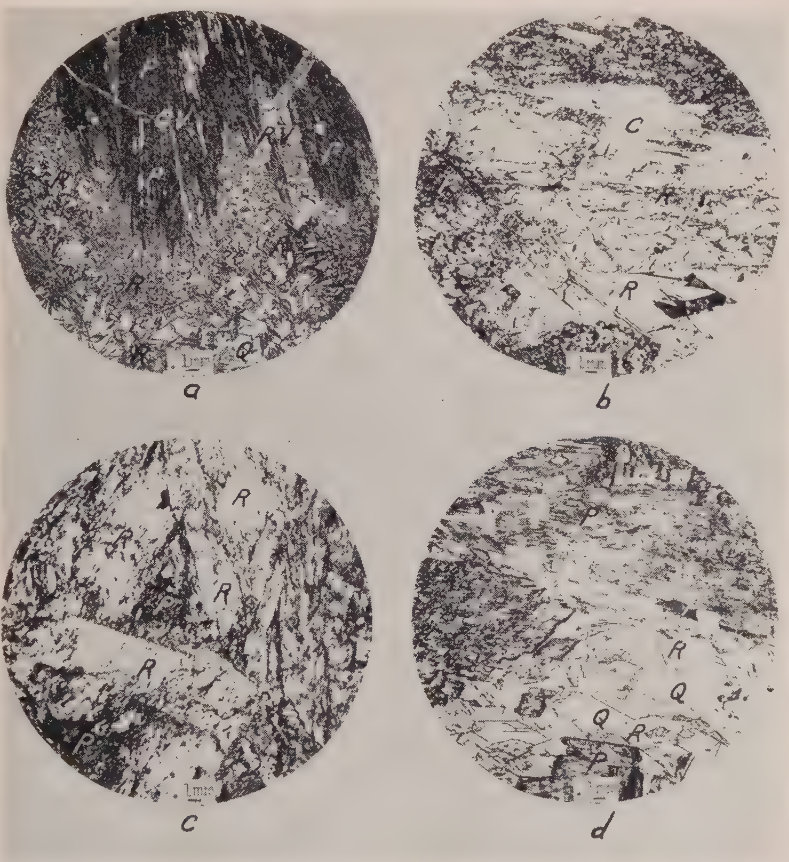

FIG. 2. Photomicrographs of rhodonite. a. Rhodonite (R) replaces pyroxene (P). Q is quartz (white). QV is a tiny quartz vein. RV is rhodonite cutting pyroxene (P). 1950-foot level, Star mine, Vanadium, N. Mex. b. Rhodonite (R) replaces pyroxene (P). C is calcite, 1950-foot level, Star mine, Vanadium, New Mex. c. Rhodonite crystals (R) developed in pyroxene (P). 1950-foot level, Star mine, Vanadium, N. Mex. d. Rhodonite crystals (R) in quartz (Q) formed from pyroxene (P). Hobo mine, Vanadium, N. Mex.

Occurrences and Properties of Rhodonite

In the development of the deep levels of the mines near Vanadium, N. Mex., a pink or flesh-colored silicate was observed that had not been recorded previously at the Ground Hog, Star, Hobo, and Princess mines (Northrop, 1944). Optical, spectrographic, chemical, and x-ray data indicate that this mineral is rhodonite with $\alpha = 1.717$; $\beta = 1.721$; $\gamma = 1.729$; $\gamma - \alpha = 0.012$; $2V = 76°$; positive; $Z' \wedge C = 32°$. These values are slightly low for pure rhodonite but agree with those of rhodonite containing some Mg, Fe, and Ca in addition to the Mn and SiO_2 required by its formula

(Larsen and Berman, 1934). Harry Rose of the U. S. Geological Survey estimated from the spectrograms examined by him that specimens from the Star and Hobo mines contain approximately 4 or 5 per cent Ca, 2 per cent Fe, and 1 or 2 per cent Mg, in addition to abundant manganese.

The textural relations in thin sections indicate that rhodonite has replaced the pyroxenes. In figure 2a, showing material from the 1950-foot level of the Star mine, needles of rhodonite occur in quartz at the end of the pyroxene, and a vein of rhodonite cuts the early pyroxene. Small quartz veins cut across the pyroxene and the rhodonite. The change of a

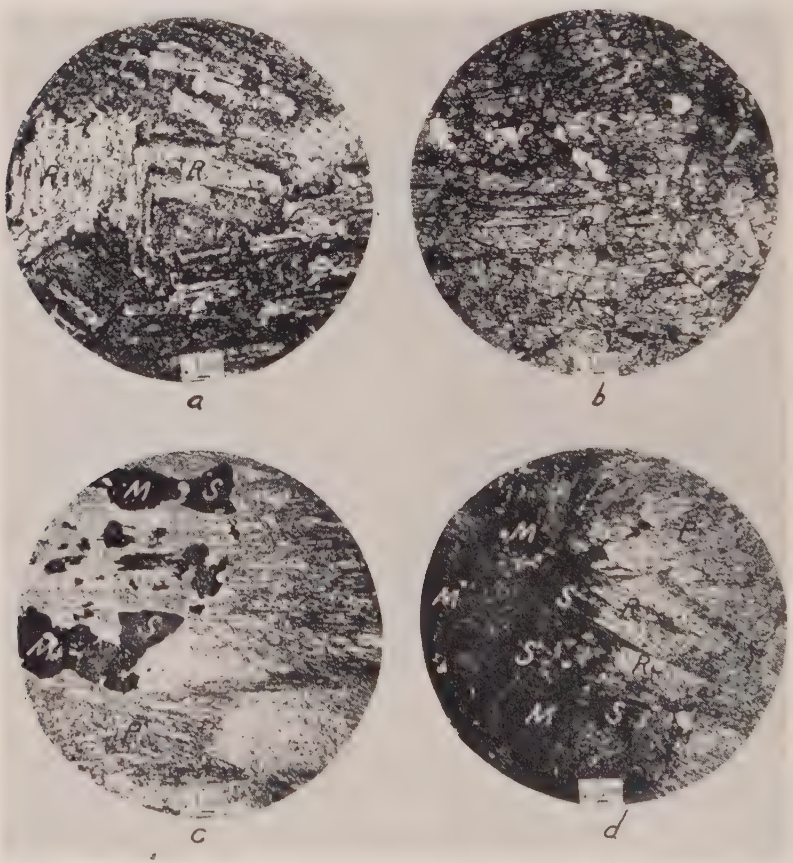

FIG. 3. Photomicrographs of rhodonite, pyroxene, magnetite, and sphalerite. a. Rhodonite (R) replaces pyroxene (P). Hobo mine, Vanadium, N. Mex. b. Rhodonite (R) replaces pyroxene (P). Princess mine, Vanadium, N. Mex. c. Magnetite (M) and sphalerite (S) are later than pyroxene (P). 1950-foot level, Star mine, Vanadium, N. Mex. d. Magnetite (M) and sphalerite (S) cut and fill space in pyroxene (P) and rhodonite (R). 1950-foot level, Star mine, Vanadium, N. Mex.

pyroxene containing Ca, Mg, Fe, Mn, and SiO_2 to rhodonite with a composition of $MnSiO_3$ would liberate Ca, Mg, Fe, and probably some silica. Schaller (1938) has suggested that the hydrous calcium silicate xonotlite, at Pueblo, Mexico, was formed under these conditions. No xonotlite has been observed at Vanadium, N. Mex., but the calcite, which occurs at the Star mine between rhodonite and pyroxene (see Fig. 2b), may represent calcium liberated from pyroxene. At the same locality large crystals of rhodonite occupy space formerly taken by pyroxene (see Fig. 2c). At the Hobo mine terminated crystals of rhodonite have grown at the expense of pyroxene (see Fig. 2d). Rhodonite replaces columnar pyroxene in a sample from the Hobo mine (Fig. 3a) and in another from the Princess mine (Fig. 3b). These relations were photographed in plane polarized light, but replacement features stand out even more clearly under crossed nicols because the birefringence of rhodonite is low as compared with that of the associated pyroxenes.

OCCURRENCE AND PROPERTIES OF FERROAN JOHANNSENITE

Some of the pyroxene that occurs at the Star mine in contact with rhodonite was separated by hand picking and by using heavy solutions. The partial analysis of it (No. 3, Table 1) by Fahey shows 10.9 per cent MnO and 9.7 FeO. Two specimens of salite described by Schmitt from the Pewabic mine, Hanover, N. Mex., contain 2.17 and 2.66 per cent MnO and 14.84 and 18.56 per cent FeO, respectively (Nos. 1 and 2, Table 1). The possibility that the high manganese content of the pyroxene from the Star mine is due to intergrown rhodonite is remote, because no rhodonite could be detected in the sample by optical tests or in the x-ray pattern of it studied by Fred A. Hildebrand, of the Geological Survey.

Two specimens of the pyroxene from the Star mine were selected and prepared for complete analyses, because they were free from any visible rhodonite in thin section. Sample 4, Table 1, contains 14.13 per cent MnO and 11.30 per cent FeO, and no rhodonite could be detected in its x-ray pattern. No. 5, Table 1, contains 15.53 per cent MnO and 10.68 per cent FeO, but the x-ray pattern of some reddish grains isolated from the sample suggests to Hildebrand that a very small amount of rhodonite may be present. The estimate of the number of pyroxene grains of the type that gives the broad, weak lines suggestive of rhodonite indicates that the amount of rhodonite in the total sample is so small that it can be neglected.

The indices of refraction of the pyroxene at the Star mine increase directly with increased amounts of MnO (Table 1, Nos. 3, 4, 5). This suggests that the manganese is an essential part of the pyroxene, and the composition of the mineral can be best expressed by the name ferroan johannsenite.

Typical occurrences of needles and prismatic columns of ferroan johannsenite are shown in Figure 2a, b, c associated with rhodonite and in Figure 3c, d associated with the ore minerals.

OCCURRENCE AND PROPERTIES OF JOHANNSENITE

The pyroxene in contact with the rhodonite at the Hobo mine (Fig. 2d) contains 25.90 per cent MnO and 2.58 per cent FeO (No. 6, Table 1) and has the optical properties of johannsenite (No. 8, Table 1). The

TABLE 1. ANALYSES AND OPTICAL PROPERTIES OF SOME PYROXENES

	1	2	3	4	5	6	7	8
SiO_2	52.20	48.52		48.98	48.94		48.15	48.62
Fe_2O_3	0.74	1.86	0.97	1.07	0.93	0.20	1.58	
FeO	14.84	18.56	9.70	11.30	10.68	2.58	4.28	
Al_2O_3	0.26	1.67		0.84	0.48		0.31	
TiO_2	0.01	0.08		0.14	0.10			
MnO	2.17	2.66	10.90	14.13	15.53	25.90	21.37	28.69
CaO	22.19	21.71		20.64	21.10		20.88	22.69
MgO	7.50	4.11		2.19	2.36		0.48	
Na_2O	nd*	nd		0.10	nd		nd	
K_2O	nd	nd		0.05	nd		nd	
H_2O	0.38	0.99		0.44	nd		1.20	
CO_2							1.39	
ZnS							0.17	
Total	100.29	100.16		99.88	100.12		99.81	100.00
α	1.687	1.690	1.695	1.703	1.708	1.708	1.713	1.710
β	1.692	1.693	1.702	1.711	1.718	1.718	1.721	1.719
γ	1.721	1.715	1.723	1.732	1.736	1.737	1.740	1.738
$\gamma-\alpha$	0.034	0.025	0.028	0.029	0.028	0.029	0.027	0.028
Sign	+	+	+	+	+	+	+	+
$Z\wedge c$	54°	38°	46°±	46°±	47°±	40°±	48°±	
2V	60°±	60°±	60°±	70°±	70°±	70°±	70°±	

* nd = not determined.

1, 2. Salite, Pewabic mine, Hanover, N. Mex. Chemical and optical data after Schmitt (1939).

3, 4, 5. Ferroan johannsenite, Star mine, Vanadium, N. Mex., J. J. Fahey, aanlyst.

6. Johannsenite, Hobo mine, Vanadium, N. Mex., J. J. Fahey, analyst.

7. Johannsenite, Empire Zinc Company mine, Hanover, N. Mex., Schaller (1938, 579).

8. Theoretical composition and optical properties of pure johannsenite, $CaMnSi_2O_6$. Schaller (1938, p. 581).

MnO content of the johannsenite at the Hobo mine is higher than that of the johannsenite from the Empire Zinc Company mine, Hanover, N. Mex., analyzed by Schaller, but it does not exceed the theoretical amount (compare Nos. 6, 7, 8, Table 1). The *x*-ray pattern contains weak, broad lines, suggesting that a very small amount of rhodonite may be present in the hand-picked sample.

Origin and Sequence of Minerals

The observation that ferroan johannsenite with 10.9 per cent MnO is replaced by rhodonite as easily as is johannsenite with 25.9 per cent MnO strongly supports the petrographic evidence that most of the MnO for the formation of rhodonite was introduced by the ore solutions rather than being supplied by the alteration in place of the pyroxenes with small amounts of manganese. The source of the ore solutions was the intrusive magma of the Ground Hog district, which invaded the limestones of Paleozoic age and formed replacement deposits with a typical pyrometasomatic mineral assemblage.

The sequence of minerals observed at the Star, Hobo, and Princess mines is as follows: Quartz was the earliest mineral to form, but quartz veins cut other minerals indicating that the veins continued to form throughout the period of ore mineralization. The pyroxenes ferroan johannsenite and johannsenite crystallized early and were changed locally to rhodonite, with the formation of some calcite. Magnetite, sphalerite, galena, and pyrite are later than the silicates (Fig. 3c, d). This order agrees with the paragenetic sequence of mineralization observed by Harrison Schmitt (1939, p. 802) at the Pewabic mine, Hanover, N. Mex.

Acknowledgments

Field collecting by Allen during the summer of 1952 was financed by a project grant from the Penrose Bequest of the Geological Society of America. Dr. Harrison Schmitt, consulting mining geologist of Silver City, N. Mex., made available his detailed knowledge of the district, offered suggestions on mineral localities, and extended many courtesies during the field work. Mr. Don Purvis, Superintendent, and Mr. Bert Morrison, Geologist, of the American Smelting & Refining Company, Mr. J. T. Lewis, Superintendent, and Mr. F. S. Cook, Geologist, of the U. S. Smelting & Refining Company, cooperated in the collecting of specimens from the mines near Vanadium. The *x*-ray patterns of the pyroxenes and rhodonite were made by Fred A. Hildebrand and the spectrograms were made by Harry Rose in the laboratories of the U. S. Geological Survey.

References

KERR, PAUL F., KULP, J. L., PATTERSON, C. M., AND WRIGHT, R. J. (1950), Hydrothermal alteration at Santa Rita, New Mexico: *Bull. Geol. Soc. Am.*, **61,** 275–348.

LARSEN, ESPER S., AND BERMAN, HARRY (1934), The microscopic determination of nonopaque minerals, *U. S. Geol. Survey Bull.*, **848,** 131, 134.

LASKY, SAMUEL G. (1936), Geology and ore deposits of the Bayard area, Central Mining District, New Mexico, *U. S. Geol. Survey Bull.*, **870,** 1–144.

LINDGREN, W., GRATON, L. C., AND GORDON, C. H. (1910), The ore deposits of New Mexico, *U. S. Geol. Survey Prof. Paper* **68,** 317–318.

NORTHROP, S. A. (1944), Minerals of New Mexico, New Mexico Univ. Press, p. 268.

PAIGE, SIDNEY (1916), Silver City Folio, New Mexico, *U. S. Geol. Survey, Geol. Atlas* **199.**

SCHALLER, WALDEMAR T. (1930), Adjectival ending of chemical elements used as modifiers to minerals names, *Am. Mineral.*, **15,** 566–575.

——— (1938), Johannsenite, a new manganese pyroxene, *Am. Mineral.*, **23,** 575–583.

SCHMITT, HARRISON (1939), The Pewabic Mine, *Bull. Geol. Soc. Am.*, **50,** 777–818.

SPENCER, A. C. AND PAIGE, SIDNEY (1935), Geology of the Santa Rita Mining Area, New Mexico, *U. S. Geol. Survey Bull.* **859,** 1–78.

CHEMICAL PETROLOGY AND MINERALOGY OF HORNBLENDES IN NORTHWEST ADIRONDACK GRANITIC ROCKS*

A. F. Buddington, *Princeton University, Princeton, New Jersey*

and

B. F. Leonard, *U. S. Geological Survey, Denver, Colorado*

Contents

Abstract 891
Introduction 891
Petrologic Notes 892
  Hornblende from granitic rocks of Diana-Stark complex 892
  Hornblende from younger granitic rocks 893
Optical and Chemical Data 897
  Optical properties of some Adirondack hornblendes 897
    Indices of refraction 897
    Birefringence 898
    Optic axial angle 898
    Dispersion 899
    Extinction angle 899
    Pleochroism and absorption 900
  General relations of the Adirondack hornblendes 900
References 901

Abstract

Chemical analyses and optical properties of seven hornblendes from granitic rocks of the northwest Adirondack Mountains, New York, are presented. The chemical analyses have been recalculated in terms of a theoretical amphibole formula. All the hornblendes belong to the femaghastingsite and ferrohastingsite varieties and carry chlorine as well as fluorine in significant amounts. The variations in composition of the hornblendes correlate with the degree of differentiation of the rock of which they are a part, or with the degree of modification of incorporated foreign material. The methods used in determining the optical properties are fully described and critically discussed. A satisfactory, detailed correlation of chemical and optical properties has not yet been achieved, even for the limited part of the hastingsite group investigated here.

Introduction

Granitic rocks with hornblende as a varietal mineral form very large masses and are a major element in the pre-Cambrian bedrock of the northwest Adirondack Mountains of New York (Buddington, 1939 and 1948). This paper is a contribution on the chemical composition and optical properties of the hornblendes, together with a brief discussion of their petrologic environment. Buddington initiated the study of the

---

* Publication authorized by the Director, U. S. Geological Survey.

hornblendes and prepared the section on chemical petrology. Leonard contributed the optical data.

The chemical analyses were made at the Rock Analysis Laboratory of the University of Minnesota. The cost of the analyses was borne by a grant of funds from the Eugene Higgins Trust allocated to Princeton University.

The hornblendes were concentrated for analysis by use of the Frantz magnetic separator and heavy liquids. This work was done by H. L. James and R. J. Smith. The hornblende concentrates submitted for chemical analysis were better than 99.5 per cent pure. Most of them were about 99.9 per cent pure. The contaminants were chiefly minute grains of quartz and potash feldspar that had not broken free from the hornblende, even after crushing to -100, $+200$ mesh.

There is no reason to doubt that the hornblendes in the fraction studied optically were identical with those in the concentrate submitted for chemical analysis.

The writers have followed Billings' subdivision (1928) of the hastingsite group, according to the molecular proportions of FeO and MgO; *ferrohastingsite*, $FeO/MgO > 2$; *femaghastingsite*, $FeO/MgO < 2$ but $> \frac{1}{2}$; and *magnesiohastingsite*, $FeO/MgO < \frac{1}{2}$.

PETROLOGIC NOTES

The granitic rocks of the northwest Adirondacks are of two different ages. The older granitic rocks, part of the Diana-Stark complex, have been intensely deformed, recrystallized, and intruded by a younger series of granitic rocks. These younger granites in large part have a sheetlike, phacolithic, and domical relationship to all older rocks.

Chemical analyses of rocks from which the hornblendes 1, 3, 4, and 6 (Table 1) and pyroxene no. 8 (Table 1) were concentrated are to appear in a forthcoming publication of the U. S. Geological Survey entitled "Geology and mineral deposits of the St. Lawrence County magnetite district, New York," by Buddington and Leonard.

Hornblende from Granitic Rocks of Diana-Stark Complex

The older granitic rocks are facies of the Diana-Stark complex. This complex has been described and interpreted (Buddington, 1939, pp. 73–109; Buddington, 1948, pp. 24–29) as a very great sheet of igneous rock that has been intensely deformed and recrystallized. The sheet has a stratiform character resulting from differentiation primarily by fractional crystallization. Pyroxene syenite gneiss with lenses of shonkinite and feldspathic ultramafic (ferroaugite, ilmenite, and magnetite) gneiss occurs in the lower part. This grades upward through pyroxene quartz syenite gneiss and hornblendic quartz-bearing syenite gneiss into hornblende granite gneiss, which forms the upper facies. The pyroxenic facies of this sheet are green in color, whereas the hornblendic facies are pink.

Hornblende 5 occurs as porphyroblasts in a pink granoblastic quartz-bearing syenite gneiss, which grades into a pyroxene quartz-bearing syenite gneiss stratigraphically below and a hornblende granite gneiss stratigraphically above. Hornblendes 6 and 7 are from wholly recrystallized granite gneiss characteristic of the upper facies of the Diana-Stark sheet. The variation of the mafic minerals from ferroaugite (nos. 8 and 9, Table 1) in the lower part of the sheet through femaghastingsite (no. 5) to ferrohastingsite (nos. 6 and 7) in the upper part of the sheet is consistent with what might be expected as a product of fractional crystallization and gravity sorting of successive crystal fractions. The ratio of mol per cent (FeO plus MnO)/MgO increases systematically from that in the ferroaugite (nos. 8 and 9 = 0.86 and 0.85, respectively) through femaghastingsite (no. 5 = 1.18) to ferrohastingsite (nos. 6 and 7 = 3.20 and 4.09, respectively). This increase in ratio of FeO to MgO is correlated with a higher percentage of quartz and a higher ratio of normative orthoclase to albite in the ferrohastingsite-bearing gneisses.

Hornblende from Younger Granitic Rocks

The predominant member of the younger granitic rocks is a hornblende-microperthite granite commonly with 20 to 30 per cent quartz. Hornblende 2 is from this type of rock. The hornblende granite is in part strongly deformed and recrystallized to a gneiss. Hornblende 3 is from this gneissic facies. The microperthite of the hornblende granite has been recrystallized in the gneissic facies to a granoblastic aggregate of oligoclase and potash feldspar. A little sphene has also developed in the gneiss as a reaction product. The hornblende of the normal hornblende-microperthite granite is a green variety, whereas the recrystallized hornblende of the gneissic facies is commonly pleochroic from green to bluish green. Both types were found in one sample of partly recrystallized rocks. The indices of refraction of three specimens from the normal granite indicate the hornblende to be just in the border zone between femaghastingsite and ferrohastingsite.

There is also a facies of the hornblende granite in which the quartz content is commonly greater than 27 per cent and the ratio K_2O/Na_2O is slightly higher than in the normal granite. The hornblende (no. 4) of this type of rock is a ferrohastingsite with a relatively high ratio of ferrous iron to magnesia. (The particular rock from which the analyzed hornblende was taken has a lower percentage of quartz than is normal for this facies of the granites.) All the chemical and mineralogical character-

TABLE 1. CHEMICAL ANALYSES OF SEVEN HORNBLENDES AND TWO PYROXENES FROM GRANITIC ROCKS OF THE NORTHWEST ADIRONDACKS

	Hornblende from microcline granite gneiss	Hornblendes from younger hornblende granite and hornblende granite gneiss			Hornblendes from Diana-Stark complex			Pyroxenes from Diana complex	
	1 (B-555)	2 (W-14)	3 (956)	4 (B-189)	5 (D-8)	6 (B-669)	7 (5100)	8	9
SiO_2	39.78	39.32	37.90	38.44	41.25	38.73	38.74	51.53	52.28
Al_2O_3	11.39	10.82	11.89	11.03	10.40	11.49	11.42	1.50	2.71
Fe_2O_3	5.93	5.52	7.75	5.80	3.85	5.22	4.34	2.72	2.58
FeO	14.21	20.43	20.71	24.67	16.28	22.89	23.28	13.13	12.61
MgO	9.62	6.16	4.16	1.97	8.02	4.10	3.25	8.92	8.70
CaO	9.68	9.17	9.54	9.56	10.26	9.45	10.16	20.17	16.69
Na_2O	1.57	1.99	1.57	1.81	1.58	1.68	1.98	0.67	0.78
K_2O	1.60	1.47	1.75	1.72	1.46	1.61	1.97	0.00	0.28
H_2O+	2.59	1.75	1.82	1.09	1.69	1.67	0.83	0.36	0.38
H_2O-	0.25	0.33	0.10	0.19	0.10	0.04	0.09	0.06	0.56
TiO_2	1.47	1.76	0.83	2.37	2.90	1.70	2.83	0.19	1.32
F	1.29	1.50	0.72	0.96	1.17	0.61	0.95	—	—
Cl	0.58	0.37	0.26	0.60	0.60	0.53	0.77	—	—
MnO	0.68	0.50	0.85	0.48	0.76	0.58	0.44	0.82	0.72
Total	100.64	101.09	99.85	100.69	100.32	100.30	101.05	100.07	99.61
Less O for F and Cl	0.67	0.71	0.36	0.54	0.62	0.38	0.57		
Total (corrected)	99.97	100.38	99.49	100.15	99.70	99.92	100.48		
Modal wt. per cent hornblende	2.9	2.5	5.0	8.6	7.1	10.7	11.0	58.0*	4.0*
Modal wt. per cent quartz	21.6	25.0	27.5	24.0	9.2	18.7	14.4	0.6	11.0
Normative ratio orthoclase/albite	2.97	1.18	1.33	1.26	0.86	0.99	0.96		
Ratio $\frac{FeO+MnO}{MgO}$ (mol. props.)	0.86	1.89	2.91	7.14	1.18	3.20	4.09	0.86	0.85
Ratio MgO/FeO (mol. props.)	1.22	0.54	0.36	0.14	0.89	0.32	0.25		

* Pyroxene.

TABLE 2. OPTICAL PROPERTIES OF SEVEN HORNBLENDES FROM GRANITIC ROCKS OF THE NORTHWEST ADIRONDACKS

	1 (B-555)	2 (W-14)	3 (956)	4 (B-189)	5 (D-8)	6 (B-669)	7 (5100)
α	1.666	1.674	1.682	1.6940	1.680	1.688	1.692
β	1.689	1.693	1.701	1.7170	1.692	1.709	1.712
γ	1.693	1.700	1.705	1.7235	1.696	1.714	1.716
$\gamma-\alpha$	0.027	0.026	0.023	0.0295	0.016	0.026	0.024
Optic sign	(−)	(−)	(−)	(−)	(−)	(−)	(−)
$2V_{\text{meas.}}$	51±1°	62±3°	49±3°	52±2°	58±4°	51±5°	52±3°
$2V_{\text{calc.}}$	46°	62½°	49½°	55°	60½°	52°	48°
Dispersion 1st axis	$r>v$ strong	$r<v$ distinct	$r>v$ strong	$r<v$ strong	$r<v$ strong	$r<v$ strong	$r<v$ strong
Dispersion 2nd axis	$r<v$ strong	same?	$r>v$ weak	$r<v$ distinct	$r>v$? very weak	$r>v$ distinct	$r<v$ weak
$Z\wedge c$	21±5°	14±3°	16½°	12–13°	15±5°	12±2°	9½±3°
X	Pale greenish yellow	Greenish yellow	Straw yellow	Pale olive	Greenish yellow	Pale greenish yellow	Yellowish green
Y	Olive	Olive	Green	Dark grayish olive	Olive	Dark olive	Very dark olive
Z	Greenish blue	Green	Bluish green	Dark green with bluish tint	Green	Dark green	Very dark green
Absorption	$Y>Z>X$	$Y\geqq Z>X$	$Y=Z>X$	$Y\geqq Z\gg X$	$Y\geqq Z>X$	$Y\geqq Z\gg X$	$Y\geqq Z\gg X$
Orientation	$Y=b$	$Y=b$	$Y=b$	$Y=b$	$Y=b$	$Y=b$	$Y=b$
G.	3.211	—	—	3.445	3.258	—	3.432
		Birefringences determined by means of Berek compensator					
$\gamma-\beta$	0.004	—	—	0.0063*	0.004	0.005	—
$\beta-\alpha$	—	—	—	0.0230*	0.0125	0.020	—
$\gamma-\alpha$	ca. 0.025+	—	—	0.0295*	—	—	0.024

* Determined by H. H. Hess.

TABLE 3. STRUCTURAL FORMULAE* OF SEVEN HORNBLENDES FROM GRANITIC ROCKS OF THE NORTHWEST ADIRONDACKS

		1 (B-555)		2 (W-14)		3 (956)		4 (B-189)		5 (D-8)		6 (B-669)		7 (5100)	
(W)	K	0.31		0.30		0.36		0.35		0.28		0.32		0.40	
	Na	0.46		0.60		0.50		0.56		0.48		0.51		0.61	
	Ca	1.56	2.33	1.53	2.43	1.62	2.48	1.65	2.56	1.68	2.44	1.60	2.43	1.74	2.75
(X)	Mg	2.17		1.43		0.98		0.47		1.84		0.97		0.78	
	Fe′′	1.77		2.65		2.74		3.31		2.07		3.03		3.12	
	Mn	0.09	4.03	0.07	4.15	0.11	3.83	0.07	3.85	0.09	4.00	0.08	4.08	0.06	3.96
(Y)	Al	0.01		0.09		0.23		0.29		0.17		0.28		0.33	
	Fe′′′	0.67		0.64		0.92		0.70		0.44		0.63		0.52	
	Ti	0.17	0.85	0.21	0.94	0.10	1.25	0.29	1.28	0.33	0.94	0.21	1.12	0.34	1.19
(Z)	Si	5.98		6.11		6.00		6.20		6.30		6.13		6.18	
	Al	2.02	8.00	1.89	8.00	2.00	8.00	1.80	8.00	1.70	8.00	1.87	8.00	1.82	8.00
	OH	2.60		1.81		1.92		1.17		1.72		1.77		0.88	
	F	0.61		0.74		0.36		0.48		0.56		0.30		0.48	
	Cl	0.16	3.37	0.09	2.64	0.07	2.35	0.15	1.80	0.15	2.43	0.13	2.20	0.21	1.57

* The structural type is taken as $W_{2-3}(XY)_5(Z_4O_{11})_2(OH, F, Cl)_2$.

1 (B-555) Femaghastingsite, from hornblende microcline-rich granite gneiss, quarry at crossing of Dead Creek and New York Route 3, Tupper Lake quadrangle. Analyst, Eileen K. Oslund.

2 (W-14) Femaghastingsite, from hornblende granite, 1.2 miles NNE of Bush's Corners, Lowville quadrangle. Analyst, Lee C. Peck. (From rock whose analysis is given in Geol. Soc. Amer. Mem. 7, Table 37, no. 133, p. 138.)

3 (956) Ferrohastingsite, from granoblastic hornblende granite gneiss, a mile S of Palmerville, Blanchard Hill, Russell quadrangle. Analyst, Lee C. Peck.

4 (B-189) Ferrohastingsite, from hornblende granite, 0.5 mile N of Cranberry Lake State Park, Cranberry Lake quadrangle. Analyst, Lee C. Peck.

5 (D-8) Femaghastingsite, from red granoblastic quartz-bearing syenite gneiss (Diana complex), 3.1 miles SSE of Harrisville bridge, 3.6 miles from Harrisville by road, Lake Bonaparte quadrangle. Analyst, Eileen K. Oslund.

6 (B-669) Ferrohastingsite, from red granoblastic phacoidal hornblende granite gneiss (Stark complex), 2 miles SE of Degrasse, Russell quadrangle. Analyst, Lee C. Peck.

7 (5100) Ferrohastingsite, from green granoblastic phacoidal hornblende granite gneiss (Stark complex), top of Downey Mountain, Santa Clara quadrangle. Analyst, Lee C. Peck.

8 Ferroaugite, from feldspathic ultramafic gneiss layer in pyroxene syenite gneiss, 1.25 miles W of Kalurah, Oswegatchie quadrangle. Analyst, Lee C. Peck. Atomic ratio, $Ca_{44.5}Mg_{27.25}Fe_{28.25}$. (Originally published in Hess, 1949, p. 652.)

9 Ferroaugite, from pyroxene quartz syenite gneiss, 1.25 miles SW of Harrisville, Lake Bonaparte quadrangle. Analyst, Lee C. Peck. Atomic ratio, $Ca_{40.5}Mg_{30}Fe_{29.5}$.

istics of this granite, as well as the field evidence, are consistent with the hypothesis that the more quartzose facies represents a slightly younger differentiate of the same magma that yielded the normal granite.

Microcline-rich granite gneiss occurs as sheetlike masses intimately associated with metasedimentary rocks and amphibolite. The microcline granite gneiss is interpreted as in large part the product of modification, granitization, and migmatitization of metasediments and amphibolite by potash-rich solutions. The hornblendic facies of the microcline granite gneisses are always associated with included layers, schlieren, and disintegrated relics of amphibolite. The hornblende ranges from femaghastingsite to ferrohastingsite. The variation in composition probably depends in part upon the degree of modification by granitizing solutions of the hornblende derived by incorporation from amphibolite.

Optical and Chemical Data

*Optical Properties of Some Adirondack Hornblendes**

Indices of Refraction

The indices of refraction were determined in sodium light by the immersion method, using freshly standardized liquids varying by intervals of 0.002 in the range from 1.660 to 1.700, and by slightly less than 0.005 in the range from 1.700 to 1.725. The temperature at which the measurements were made was closely controlled.

The indices α and γ were determined on cleavage flakes parallel to the $\{010\}$ parting. The index β was determined on rare grains perpendicular to an optic axis, or on very rare grains perpendicular to Bx_a.

Five separate determinations of α, β, and γ were made for most hornblendes, though the number of determinations ranged from 4 to 11. For hornblende 4, α was determined with exceptional precision; total and partial birefringences were measured by H. H. Hess, using a technique developed for the study of pyroxenes (Hess, 1949); and the values for β and γ were calculated from α and the partial birefringences.

The reported values for indices of refraction are thought to be the best approximations possible at this time. Two factors seriously affect the accuracy of the determinations:

1. Pure hornblende concentrates from a single hand specimen are slightly variable in composition. Because of weak absorption parallel to X, α can usually be determined with greater accuracy than β or γ; and on a given grain the value of α can be determined in sodium light with an

---

* To keep within the page limits imposed for this issue of the journal, it was necessary to delete a section on crystal form and cleavage of the hornblendes and to condense the sections on measurement of indices of refraction, 2V, and extinction angle.

error of 0.001 or less. However, the range in α for several grains in the same mount may be as much as 0.003. A similar range was observed for the values of β and γ. (But see factor 2, just below.)

2. Absorption parallel to Y and Z is so strong that the determinative error in β and γ may be slightly greater than 0.001.

Birefringence

The values for total birefringence reported just below the indices of refraction in Table 2 were determined, as usual, by difference. Because of the range in α and γ, reflecting variable composition, it was feared that these values for total birefringence might be slightly in error. To check this possibility, separate birefringence determinations were made by means of a Berek compensator for all hornblendes except nos. 2 and 3. The results are given at the bottom of Table 2. For hornblendes, except no. 4, described in the preceding section, the measurements were made on ordinary thin sections. The thickness of a quartz grain adjacent to, or only one grain removed from, a suitable hornblende was determined by means of the Berek compensator. The total or partial birefringence of the hornblende was then determined. The measurements for hornblendes 5 and 6 were made on the microscope stage, using X-Z sections of quartz and suitably oriented sections of hornblende. The measurements for hornblendes 1 and 7 were made on a universal stage according to the technique described by Emmons (1943, pp. 172–182).

The agreement between birefringences determined by immersion and by measurement of retardation in ordinary thin sections is generally good. (See table 2.) At least the direct determination of birefringence serves as a check against serious errors in the relative values of the indices of refraction of a given hornblende. For example, γ minus α for hornblende 5 seemed very low relative to the total birefringence of the other hornblendes. However, direct measurements of the partial birefringences of this hornblende confirmed the results of the immersion work.

Optic Axial Angle

The optic axial angle was measured in thin section on the universal stage, using a number of grains normal or nearly normal to Bx_a. This angle is reported in Table 2 as $2V_{meas}$. Under the best of conditions, the precision of measurement on these hornblendes ranges from $\frac{1}{2}$° to 2°. The range of values reported for $2V_{meas.}$ in Table 2 is due in part to slight variation in composition of the hornblende, from grain to grain, and in part to unavoidable errors in measurement. Strong absorption parallel to Y and Z makes proper orientation of sections subnormal to Bx_a exceedingly difficult on the universal stage, and the resulting determination of 2V is therefore suspect. In addition, total reflection from the surface of the grain may occasionally be confused with one extinction position.

Dispersion

The dispersion of the optic axes is inclined. It is always distinct or strong for one optic axis; it is less pronounced for the other, even when apparent dispersion is reported as strong for both axes (e.g., hornblende 1, Table 2). Dispersion was determined qualitatively by examining many optic axis figures for each hornblende. It was not possible to assign the relative intensity of dispersion to optic axes A or B, nor was it possible to measure 2V in red light and in blue light. A correct statement of the true optic axial dispersion for hornblende 1, and perhaps for hornblendes 5 and 6, would of course depend on such measurements.

Extinction Angle

The extinction angle $Z \wedge c$ was measured on the microscope stage, using hornblende sections parallel to the optic plane. The values reported in Table 2 are averages of repeated determinations made on a number of suitably oriented grains. Thin sections, rather than immersed fragments, were used. Because of strong absorption parallel to Z, it is difficult to get the correct extinction position of Z, as well as to see the trace of the cleavage whose zone axis is *c*. Moreover, the cleavage trace observed on sections parallel to the optic plane is moderately to highly irregular. Consequently, the extinction angle measured on a single grain may vary by as much as 9°. A range of 3° to 4° is common. Probably relatively little of this variation is due to compositional variation in the hornblende.

Owing to the difficulty of determining extinction positions and orienting cleavage planes on the universal stage, U-stage measurements of $Z \wedge c$ for hornblende 1 showed a greater range ($\pm 7°$) than microscope-stage measurements made on the same grains cut parallel to the optic plane. U-stage measurements of $Z \wedge c$ in re-oriented random sections of hornblende 1 were even less reliable, showing a range of $\pm 10°$. Measuring $Z \wedge c$ by observing the extinction position of X, and then rotating 90° on the outer vertical axis, may have increased the accuracy of some determinations by $\frac{1}{2}°$ or 1°.

At present, there seems to be no reliable method for accurately determining $Z \wedge c$ on the hastingsites described in this paper. Leonard prefers to measure $Z \wedge c$ on X-Z sections on the microscope stage, if necessary checking the orientation of the same grains on the universal stage and checking to see that *c* is truly the zone axis for the observed cleavage traces.

Pleochroism and Absorption

The colors reported for X, Y, and Z are those observed in thin sections having an average thickness of 0.020 to 0.025 mm. (These thicknesses were determined by measurements of retardation in suitably oriented quartz grains.) In thin sections 0.030 mm. thick, X is pale but Y and Z for most hornblendes are very dark or almost black, the body color of hornblendes seen in hand specimen. Crushed hornblendes immersed in oil transmit almost no light parallel to Y and Z unless the fragments are smaller than about 200 mesh. For most hornblendes, Y and Z remain very dark, though appreciably colored, for fragments as small as −400, +600 mesh.

The determination of the color of Y is sometimes difficult if the hornblende has strong dispersion. A section a few degrees subnormal to an optic axis will include more emergent red light or more emergent blue, depending on the orientation of the grain. A relatively small tilt will thus produce a substantial change in the observed color of Y, which is actually Y′. The difficulty is obviated, of course, if the sections are truly normal to the optic axis or acute bisectrix.

The absorption indicatrix of the hornblendes coincides with the optical indicatrix. This relation is quite different from that obtaining among certain common clinopyroxenes, especially among members rich in Fe′′′ (Hess, 1949).

General Relations of the Adirondack Hornblendes

All the Adirondack hornblendes in granitic rocks for which data are available show a noteworthy amount of chlorine. There are but few analyses of hornblendes in the literature that give the per cent of chlorine. If this is to be taken to indicate that chlorine is minor in amount, then the Adirondack hornblendes are exceptionally rich in this element. It is possible, however, that chlorine occurs in significant amounts in some hornblendes in which it has not been determined. A ferrohastingsite from the rapakivi granites of Finland, described by Sahama (1947), has 0.51 per cent Cl and 1.06 per cent F. A pargasite from the Tiree marble of the Hebrides, described by Hallimond (1947), has 0.46 per cent Cl and 0.16 per cent F. Hallimond (1947, pp. 237–238) notes that the amphibole approaches hastingsite in composition. A ferrohastingsite described by Krutov (1936) and named by him dashkessanite, has 7.24 per cent Cl. A femaghastingsite from garnetiferous amphibolite of the central Adirondacks, New York, described by Buddington (1952, p. 42, no. 9), has 0.63 per cent Cl and only 0.08 per cent F. A comparison of hornblendes from Adirondack amphibolites (Buddington, 1952, pp. 42 and 53) also shows that the total alkalis are higher in hornblendes having significant amounts of F or Cl than in those having only a slight amount of the halogens.

Both in the granitic rocks of the Diana-Stark complex and in the younger granitic rocks, the ferrohastingsite hornblendes carry a very slightly higher percentage of total alkalis than the femaghastingsites. Also, in each of the two rock series there is a systematic decrease in the per cent of total OH, F, and Cl as the ratio MgO/FeO decreases.

Hornblendes of similar chemical composition occur both in primary igneous rock and in the gneissic equivalents.

A pargasitic variety of hornblende is found in a thin layer of thoroughly recrystallized amphibolite enclosed in the granite from which hornblende 2 was concentrated. Pargasite from the amphibolite contains 0.91 per cent F and 0.03 per cent Cl (Buddington, 1952, p. 42, no. 1). This contrasts with 1.50 per cent F and 0.37 per cent Cl found in the femaghastingsite (no. 2) of the granite. The femaghastingsite (no. 2) of the granite has a much higher ratio of

$$\frac{\mathrm{FeO} + \mathrm{MnO}}{\mathrm{MgO}} = 1.89$$

than the pargasite of the amphibolite, which has

$$\frac{\mathrm{FeO} + \mathrm{MnO}}{\mathrm{MgO}} = 0.78,$$

as one would expect.

The main purpose of this investigation has been to define the chemical composition and optical properties of hornblendes from granitic rocks of the northwest Adirondacks, and to discuss their petrologic significance. A secondary goal was to correlate these data and the previously published data on similar amphiboles, in order to increase our understanding of the hastingsite group. So far, a reasonably precise correlation has not been achieved, owing mainly to the extreme complexity of the hastingsite group and to the lack of reliable and essentially complete chemical and optical data on its members. The lines of attack recently employed by Foslie (1945) and Sundius (1946) have been especially fruitful, but the need for additional data is great.

References

Billings, Marland (1928), The chemistry, optics, and genesis of the hastingsite group of amphiboles: *Am. Mineral.*, **13,** 287–296.

Buddington, A. F. (1939), Adirondack igneous rocks and their metamorphism: *Geol. Soc. Amer., Mem.* **7,** 354 pp.

——— (1948), Origin of granitic rocks of the northwest Adirondacks, in Gilluly, James, chm., Origin of granite: *Geol. Soc. Amer., Mem.* **28,** 21–43.

——— (1952), Chemical petrology of some metamorphosed Adirondack gabbroic, syenitic and quartz syenitic rocks: Bowen volume, *Am. Jour. Sci.*, 37–84.

Emmons, R. C. (1943), The universal stage: *Geol. Soc. Amer., Mem.* **8,** 205 pp.

Foslie, Steinar (1945), Hastingsites, and amphiboles from the epidote-amphibolite facies: *Norsk geol. tidsskr.*, **25,** 74–98.

Hallimond, A. F. (1947), Pyroxenes, amphibole, and mica from the Tiree marble (with chemical analyses by C. O. Harvey): *Mineralog. Mag.*, **28,** 230–243.

Hess, H. H., (1949), Chemical composition and optical properties of common clinopyroxenes, Part I: *Am. Mineral.*, **34,** 621–666.

Krutov, G. A. (1936), Dashkessanite—a new chlorine amphibole of the hastingsite group: *Acad. Sci. U.R.S.S. Bull., ser. geol.*, 341–373. (Cited in *Mineralog. Abs.*, 1937, **6,** 438.)

Sahama, T. G. (1947), Rapakivi amphibole from Uuksunjoki, Salmi area: *Comm. geol. Finlande Bull.* **140,** 159–162.

Sundius, Nils (1946), The classification of the hornblendes and the solid solution relations in the amphibole group: *Sveriges geol. Undersökning, ser. C, no.* **480,** 36 pp.

LINDGRENITE AND CUPROTUNGSTITE FROM THE SEVEN DEVILS DISTRICT, IDAHO*

RALPH S. CANNON, JR., AND FRANK S. GRIMALDI
U. S. Geological Survey, Washington, D. C.

CONTENTS

Abstract 903
Introduction 903
Occurrence 904
Properties 905
Chemical composition of lindgrenite 906
Cuprotungstite 906
Oxidation of molybdenite 908
Acknowledgments 910
References 910

ABSTRACT

Lindgrenite was recognized by Waldemar Schaller just before World War II in specimens of contact-metamorphic copper ores from the Seven Devils Mountains in western Idaho. Hitherto this basic copper molybdate had been described only from the copper deposit at Chuquicamata in Chile. The Idaho lindgrenite, like that at the type locality, is a supergene mineral formed as a product of weathering of molybdenite, but in Idaho the molybdenite has weathered in a geochemical environment that differs in several respects from the Chilean occurrence. Chemical analyses of the lindgrenite and of associated cuprotungstite from the Seven Devils district reported here are in accord with the original analysis of lindgrenite and with analyses of cuprotungstite from Cave Creek, Arizona.

INTRODUCTION

The copper molybdate lindgrenite was described in 1935 as a new mineral species in specimens from the great porphyry copper deposit at Chuquicamata, Chile, by Palache (1935). Since then it has been recognized as one of the more abundant molybdenum minerals in the oxidized zone of the Chuquicamata ore body (Bandy, 1938; López, 1939; Jarrell, 1939, 1944). Surprisingly, it has not been reported from any other localities, even though one might expect to find it in analogous environments in other molybdenum-bearing copper deposits, as in the porphyry copper deposits of the southwestern United States.[1]

A new occurrence from a notably different geologic environment was found in 1941 when Waldemar Schaller tentatively identified as lindgrenite a green mineral on a specimen of contact-metamorphic copper ore collected by Cannon in western Idaho. Studies of the chemical, x-ray crystallographic, and optical properties of the Idaho mineral established its identity with lindgrenite from Chile.

---

* Publication authorized by the Director, U. S. Geological Survey. This contribution is an outgrowth of a field investigation that was made in cooperation with the Idaho Bureau of Mines and Geology.

[1] Since this manuscript was written, lindgrenite has been recognized in one of these porphyry copper deposits: at Inspiration, Ariz., by N. P. Peterson, of the U. S. Geological Survey.

Occurrence

The lindgrenite described in this paper occurs on specimens of tactite collected on the dump of the upper tunnel of the Helena mine (SE $\frac{1}{4}$ sec. 25, T. 21 N., R. 3 W., Boise Meridian), about 4 miles northeast of Cuprum, in the Seven Devils mining district, Adams County, Idaho. This tunnel explores a contact between diorite and marble where an irregular zone of tactite contains shoots of copper ore with subordinate amounts of molybdenum and tungsten minerals typical of the contact-metamorphic deposits of the district. The material on the surface of the dump in the fall of 1941 was mostly low-grade oxidized copper ore that had been discarded in the course of current mining operations by H. G. and A. R. Kleinschmidt; and the material containing lindgrenite had probably been mined from a winze they sank below the tunnel floor in following a shoot of copper ore.

The matrix of the lindgrenite is hard granular tactite composed largely of quartz with subordinate amounts of silicates (fibrous hastingsite, epidote, and garnet) and suffused with a variety of oxidation products. Prior to oxidation the rock contained abundant grains of bornite, radiating clusters of plates of molybdenite, a few grains of molybdenian scheelite, and probably carbonate minerals.

Oxidation has converted the bornite almost completely to hard, resinous, dark-brown limonitic material; and its copper content has been dispersed in crusts and veinlets of chrysocolla, brochantite, lindgrenite, and other secondary copper minerals. Some of the molybdenite, especially where the rock is heavily stained with limonite, is still present as bright silvery plates that appear to show no effects of solution or alteration. Elsewhere molybdenite has been altered to pseudomorphs of powellite ($CaMoO_4$) that preserve not only the external form of the molybdenite plates but also their internal foliated structure as well, or it has been completely removed, leaving lamellar crystal cavities. The foliated powellite pseudomorphs are soft and claylike, with an earthy to waxy appearance, and range in color from gray to creamy white. A second variety of powellite, in pale-green, waxy, botryoidal masses, partly fills a cavity lined with quartz crystals and is likewise judged to be of supergene origin. The molybdenian scheelite is least affected of the ore minerals, but on most of the grains an outer shell has been partly attacked and altered to cuprotungstite, which is similar in appearance to the lindgrenite.

The lindgrenite occurs as veinlets, crusts, and possibly minor replacements of pseudomorphous powellite. A few veinlets, no thicker than 0.2 mm., fill cracks in the tactite. Some of the lindgrenite composing the veinlets is in the form of poorly developed tabular crystals lying parallel to the vein walls. Some cavities formerly occupied by molybdenite, and perhaps some formerly occupied by other minerals that have been removed by weathering, are now lined with drusy crusts of lindgrenite 0.2 to 0.5 mm. thick. These crusts are composed of better-formed tabular crystals arranged in radiating clusters approximately normal to the cavity walls. Thin films of a green copper mineral that may be lindgrenite are also interlayered with some of the foliated powellite pseudomorphs after molybdenite. The resulting mixture is so impure and so fine grained that identification of the mineral as lindgrenite is not certain. However, this green staining of pseudomorphic powellite was observed only in close proximity to veinlets and crusts of recognizable lindgrenite.

PROPERTIES

The physical and optical properties of the Idaho lindgrenite are virtually identical with those of the Chilean material. The Idaho mineral is transparent, and its color ranges from yellowish green in thin plates or aggregates to deep bottle green in thicker crystals or masses. Examined in immersion oils the powdered grains are yellowish green, nonpleochroic or possibly very faintly pleochroic, and have indices of refraction greater than 1.800 and strong birefringence. Inclined extinction measured on an unbroken crystal was $X \wedge c = 56°$ in the obtuse angle β, which compares with that reported by Palache (1935). The *x*-ray powder diffraction pattern of this mineral was found by W. E. Richmond to be identical with the pattern of the type lindgrenite from Chile.

Crystals of the Idaho lindgrenite are greatly inferior to the better crystals from Chile, but in the drusy cavities an occasional crystal is sufficiently well developed to permit comparison with the type material. These better crystals do not exceed 0.2 mm. in maximum dimension. Several of them were carefully examined with the binocular microscope, but goniometric measurements were not attempted. Referred to the orientation of Barnes (1949), the crystals are monoclinic and have a tabular habit parallel to the clinopinacoid *b* (010), some faces of which are striated parallel to the edge of the prominent prism *t* (130). The negative orthodome *A* ($\bar{1}01$) and a clinodome, presumably *r* (021), are also strongly developed, and the negative orthodome is bounded by a pair of faces representing a negative pyramid form, either M ($\bar{1}21$) or n ($\bar{1}11$). Only one form was observed that is not listed for the type material from Chile—namely, a small sharp face observed on one crystal, evidently a negative orthodome, possibly $\bar{1}02$.

CHEMICAL COMPOSITION OF LINDGRENITE

The chemical formula of lindgrenite is $3CuO \cdot 2MoO_3 \cdot H_2O$, derived from an analysis by F. A. Gonyer (Palache, 1935) of 1.5 grams of the mineral from Chile. The Idaho material is not abundant enough for complete chemical analysis, but a minute amount was separated from the largest specimen (#520) for microanalysis. A partial analysis of an ammoniacal extract of 3.5 milligrams yielded the results shown in Table 1. The molecular ratios of the major constitutents are in close agreement with those obtained from Gonyer's analysis.

TABLE 1. PARTIAL ANALYSIS OF LINDGRENITE FROM IDAHO BY F. S. GRIMALDI

	1 Gram	2 Ratio	3 Ratio
CuO	0.0015	3.0	3.0
MoO_3	0.00188	2.078	2.080
WO_3	0.000	—	—

1. Partial analysis of lindgrenite from Helena mine, Adams County, Idaho.
2. Molecular ratios from 1, calculated on basis of CuO=3.0.
3. Molecular ratios similarly calculated from Gonyer's analysis of lindgrenite from Chile.

CUPROTUNGSTITE

Microanalyses made by this same method on three samples of cuprotungstite provide a check on the analytical procedure. In each analysis a small fraction of a gram of sample was first extracted with ammonia; then copper, molybdenum, and tungsten in the ammoniacal extract were determined. The microanalysis of cuprotungstite from Cave Creek, Ariz., was made on a portion of the same sample analyzed by Schaller (1932). The close similarity of ratios found strengthens confidence in the meth-

TABLE 2. PARTIAL ANALYSES OF CUPROTUNGSTITE BY F. S. GRIMALDI

	1. Arizona			2. Idaho			3. Idaho		
	Gram	Ratios		Gram	Ratios		Gram	Ratios	
CuO	0.00776	0.976 or 2.00		0.0255	0.321 or 2.00		0.0456	0.573 or 2.00	
WO_3	0.01120	0.483	1.01	0.0438	0.189	1.22	0.0700	0.302	1.09
MoO_3	0.00012	0.008		0.0009	0.006		0.0015	0.010	

1. Cuprotungstite from Cave Creek, Maricopa County, Ariz.; portion of sample originally analyzed by Schaller (1932).
2. and 3. Cuprotungstite from South Peacock mine, Seven Devils mining district, Adams County, Idaho (specimen #486).

ods used. In addition, the analytical results on cuprotungstite from Idaho are internally consistent and also similar to results on the cuprotungstite from Arizona (Table 2).

The microsamples of Idaho cuprotungstite were taken from a specimen collected on the dump of the South Peacock mine, another of the contact-metamorphic copper mines of the Seven Devils district. This cuprotungstite occurs as crusts and apophyses that corrode and replace the outer portions of large crystals of molybdenian scheelite embedded in garnet tactite. Cannon prepared a larger sample of this material for more complete analysis (sample 486Z), using the Frantz isodynamic separator followed by hand-picking. Impurities in the sample were thus reduced to about 5 per cent and were determined by ultraviolet fluorescence to be predominantly molybdenian scheelite. Grimaldi made the analysis (Table 3) on 0.150 gram of this purified material.

TABLE 3. ANALYSIS OF CUPROTUNGSTITE FROM IDAHO BY F. S. GRIMALDI

	Per cent	Ratios		
CuO	34.40	0.4325	or 2.00	
WO_3	54.27	0.2340	1.08	1.12
MoO_3	1.23	0.0085	0.04	
SiO_2	None			
H_2O-	1.27			
H_2O+	4.95	0.2748	1.27	
Insoluble scheelite	3.93			
	100.05			
Sp. gr. 5.40		Formula $2CuO \cdot WO_3 \cdot H_2O$		

Grimaldi's analysis was made on the purest sample of cuprotungstite that has been analyzed to date. For this reason it is worthwhile to compare the molecular ratios implied by the new analysis with those from previous analyses as reviewed by Schaller (1932) when he established the formula $2CuO \cdot WO_3 \cdot H_2O$. Four alternative interpretations of ratios of the Idaho cuprotungstite (I) are shown in Table 4 in comparison with similar interpretations for (II) the average of four analyses (recalculated to 100) of Arizona material by Schaller (1932) and for (III) an analysis of cuprotungstite from Chile by Domeyko as listed in Dana's *System of Mineralogy* (6th ed., p. 988, 1892). Much of the molybdenum found by Grimaldi in the Idaho sample probably came from ammoniacal solution of finer-grained molybdenian scheelite impurity, in which the WO_3/MoO_3 ratio would be about 1.83. Therefore, in our opinion, the alternative I.C. ($CuO/WO_3/H_2O = 2.00/1.01/1.27$) probably represents the best evaluation of the Idaho data. Similarly Schaller (1932) implied preference for alternatives II.B.(2.00/1.01/1.38) and III.C.(2.00/1.08/1.33) for the data on cuprotungstite from Arizona and Chile, respectively. This comparison clearly supports Schaller's determination of the CuO/WO_3 ratio as 2/1 and appears to raise a question whether the ratio H_2O/WO_3 may not be somewhat greater than 1/1.

TABLE 4. RATIOS OF CUPROTUNGSTITE

	I. Idaho Grimaldi, analyst		II. Arizona Schaller, analyst		III. Chile Domeyko, analyst	
	Per cent	Ratios	Per cent	Ratios	Per cent	Ratios
CaO	—	—	3.51	0.0625	2.00	0.0357
MgO	—	—	0.56	0.0139	—	—
CuO	34.40	0.4325	32.67	0.4107	30.63	0.3851
WO_3	54.27	0.2340	57.20	0.2467	56.48	0.2435
MoO_3	1.23	0.0085	—	—	—	—
$H_2O(+)$	4.95	0.2748	6.07	0.3366	4.62	0.2564
A.	2.00/1.08/1.27		2.00/1.20/1.64		2.00/1.26/1.33	
B.	2.00/1.12/1.27		2.00/1.01/1.38		2.00/1.16/1.22	
C.	2.00/1.01/1.27		2.00/0.83/1.64		2.00/1.08/1.33	
D.	2.00/1.12/1.29		—		—	

A. Molecular ratios $CuO/WO_3/H_2O$, as analyzed.

B. Molecular ratios $CuO(+CaO+MgO)/WO_3(+MoO_3)/H_2O$.

C. Molecular ratios $CuO/WO_3/H_2O$, if all CaO, MgO, and MoO_3 are assumed components of (molybdenian) scheelite and the corresponding quantity of WO_3 is deducted.

D. Molecular ratios $CuO/WO_3/H_2O$, if all MoO_3 is assumed a component of lindgrenite and the corresponding quantities of CuO and H_2O are deducted.

OXIDATION OF MOLYBDENITE

Information on the oxidation of molybdenite and on the related formation of lindgrenite and other supergene molybdenum minerals at Chuquicamata has been provided in papers by Bandy (1938), López (1939), and Jarrell (1939, 1944) published subsequent to Palache's original description of lindgrenite. Much of this information has been summarized succinctly by Jarrell (1944):

> "Molybdenite is normally quite resistant to oxidation; hence where it formed part of the hypogene mineralization at Chuquicamata, residual molybdenite probably exists above the general top of the sulphides. When it finally capitulates to the oxidizing solutions, the molybdenum and sulphur go into solution, and a brown limonite remains pseudo-

morphic after molybdenite crystals. The molybdenum combines with copper in solution and deposits lindgrenite a few centimeters away; or it may be absorbed by coming into contact with the existing amorphous, extremely porous chenevixite, since assays of the latter mineral show it to contain up to 5 per cent Mo. Near the surface or under exceptional conditions elsewhere, yellow molybdic ochre may form. A very few specimens of wulfenite also have been found."

These limonitic pseudomorphs after molybdenite, mentioned above, deserve more study. Ferric oxide hydrate is not an expectable residue from dissolving molybdenum sulfide. According to López, the pseudomorphs are red (light gray in polished sections) and contain molybdenum as well as iron. He believes them to be a new molybdenum ochre: Bandy, however, believes them to be an iron-molybdenum sulfide.

Molybdenite in the forested Seven Devils Mountains has weathered under climatic conditions notably different from the high desert environment at Chuquicamata. Rainfall is far more abundant, and the water table is much nearer the surface and probably far more constant in the Seven Devils district. Although ratios of molybdenum to copper in the ores are similar, the mineralogy and chemistry of ores and country rock being weathered at the two localities are quite dissimilar in most respects, and it is probable that important differences exist in the chemical composition of ground waters. The marble and tactite country rocks of the contact-metamorphic deposits in the Seven Devils are characterized by abundance of calcium carbonate, and the ores themselves by scarcity of sulfur. Sulfide minerals associated with molybdenite in these Seven Devils ores generally do not exceed a few per cent and tend to be poor in sulfur. Bornite and chalcocite are the most common sulfides, chalcopyrite is scarce, and pyrite practically absent. The ore deposit at Chuquicamata, by contrast, is rich in sulfur, and the molybdenite there is associated with comparatively abundant sulfides, among which sulfur-rich pyrite predominates. Ground waters circulating through the Idaho contact-metamorphic deposits are presumed to be much richer in calcium bicarbonate and poorer in sulfate than ground waters at Chuquicamata. Their effectiveness in oxidizing metallic sulfides and transporting metals certainly has been limited for, unlike Chuquicamata, there is no zone of thorough oxidation nor any appreciable supergene enrichment.

In the Seven Devils district molybdenite does not seem notably more resistant than other sulfides to oxidation as it does at Chuquicamata, nor is it replaced by limonitic pseudomorphs like those at Chuquicamata or those described by Blanchard (1935) at other localities. Instead, much of the molybdenite has been replaced by powellite. The alteration process evidently retains most of the molybdenum within the host crystal while oxygen and calcium are substituted for sulfur. This alteration of molybdenite to powellite, together with other local evidence, suggests that very little migration of molybdenum normally accompanied oxidation of molybdenite in the Seven Devils district. Only under exceptional conditions, clearly where molybdenite was unusually abundant and perhaps where in addition ground waters were abnormally poor in calcium, was there any perceptible migration of molybdenum. Such anomalous conditions must have existed very locally at one time within the specimens that now contain lindgrenite. In parts of them molybdenite was dissolved completely away; molybdenum was taken into solution and precipitated together with copper, as lindgrenite, either in the crystal cavities or within a few centimeters of them; and some of the molybdenum combined with calcium to form a deposit of transported powellite, also only a few centimeters away. There is tenuous evidence that within this same localized area copper-bearing solutions may have attacked powellite pseudomorphs to form minor replacements by lindgrenite. No molybdic ochre nor other supergene molybdenum minerals have been identified in these specimens or elsewhere in the district.

ACKNOWLEDGMENTS

This note on the occurrence of lindgrenite in Idaho is an outgrowth of a study of the geology and ore deposits of the Seven Devils district by the U. S. Geological Survey in cooperation with the Idaho Bureau of Mines and Geology. We take pleasure in reporting this first discovery of lindgrenite in the United States as one more of Waldemar Schaller's contributions to the mineralogy of the molybdates and tungstates. It was he who first sensed the identity of the material and guided our efforts to identify and describe it. We are indebted also to Harvard University and to A. E. Weissenborn of the Geological Survey for material from Chuquicamata that was used for comparative study.

The finding of lindgrenite in one of the contact-metamorphic deposits of the Seven Devils district has interesting historical connotations. Waldemar Lindgren, in whose honor the mineral was named, once briefly reconnoitered the Seven Devils region for the U. S. Geological Survey, and with his description of these very deposits he first clearly defined the contact-metamorphic class of ore deposits in the United States. And the other molybdate with which this lindgrenite is associated was first discovered in a specimen from one of these same deposits and described as a new mineral species by one of Lindgren's colleagues, the chemist Melville, who named it powellite in honor of Major J. W. Powell, then Director of the U. S. Geological Survey.

REFERENCES

BANDY, M. C. (1938), Mineralogy of three sulphate deposits of northern Chile: *Am. Mineral.*, **23**, 669–760.

Barnes, W. H. (1949), The unit cell and space group of lindgrenite: *Am. Mineral.*, **34,** 163–172.

——— (1949), Corrections to recent papers on proberite and lindgrenite: *Am. Mineral.*, **34,** 611–612.

Blanchard, Roland (1935), "Limonite" of molybdenite derivation: *Econ. Geol.*, **30,** 313–319.

Jarrell, O. W. (1939), Marshite and other minerals from Chuquicamata, Chile: *Am. Mineral.*, **24,** 629–635.

——— (1944), Oxidation at Chuquicamata, Chile: *Econ. Geol.*, **39,** 251–286.

López, V. M. (1939), The primary mineralization at Chuquicamata, Chile, S. A.: *Econ. Geol.*, **34,** 674–711.

Palache, Charles (1935), Lindgrenite, a new mineral: *Am. Mineral.*, **20,** 484–491.

Schaller, W. T. (1932), Chemical composition of cuprotungstite: *Am. Mineral.*, **17,** 234–237.

STUDIES OF BORATE MINERALS (II): *X*-RAY CRYSTALLOGRAPHY OF INYOITE AND MEYERHOFFERITE; *X*-RAY AND MORPHOLOGICAL CRYSTALLOGRAPHY OF $2CaO \cdot 3B_2O_3 \cdot 9H_2O$*

C. L. Christ, *U. S. Geological Survey, Washington 25, D. C.*

Abstract

Inyoite is monoclinic, $P2_1/a$, $a_0=10.63$, $b_0=12.06$, $c_0=8.40_5$Å, $\beta=114°02'$. $2CaO \cdot 3B_2O_3 \cdot 9H_2O$ is triclinic $P\bar{1}$, $a_0=7.04_6$, $b_0=9.45_2$, $c_0=7.41_2$ Å, $\alpha=101°21'$, $\beta=101°19'$, $\gamma=99°49'$. The findings of Switzer in Palache (1938) for meyerhofferite are confirmed. Powder patterns, partially indexed, are given for inyoite, meyerhofferite, and $2CaO \cdot 3B_2O_3 \cdot 9H_2O$.

Introduction and Acknowledgments

A systematic study of borate minerals has been continued in the present investigation with the determination of the *x*-ray crystallography of inyoite, $2CaO \cdot 3B_2O_3 \cdot 13H_2O$, the *x*-ray crystallography and morphology of the synthetic mineral $2CaO \cdot 3B_2O_3 \cdot 9H_2O$, and the redetermination of the *x*-ray crystallography of meyerhofferite, $2CaO \cdot 3B_2O_3 \cdot 7H_2O$. Results obtained on meyerhofferite were in excellent agreement with those previously reported by Switzer in Palache (1938). Powder patterns of the three compounds have been measured and partially indexed.

The work was undertaken primarily as a preliminary to the determination of the structures.

The writer is indebted to various colleagues in the U. S. Geological Survey: Waldemar T. Schaller furnished the crystals studied; Mrs. Joan R. Clark made many of the calculations and film measurements; Howard T. Evans, Jr., made the goniometric measurements on and the drawing of $2CaO \cdot 3B_2O_3 \cdot 9H_2O$ and also rendered much helpful advice; Fred A. Hildebrand prepared the powder patterns reported.

Experimental Work

All of the crystals used were synthetic. Schaller (personal communication) has furnished the following description of the methods of preparation:

> Inyoite (2:3:13). Grown on ulexite fragments placed in water and held at room temperature for about two months.
>
> Artificial (2:3:9). Grown on ulexite fragments placed in water and held at 50° C. for approximately one month.
>
> Meyerhofferite (2:3:7). Grown on ulexite fragments placed in water and held at 70-80° C. for approximately six months.

The inyoite crystals were colorless, transparent, tabular {001}, with {110} and {001} dominant, i.e., having essentially the habit described by Schaller (1916) for the crystals found at the original Inyo County, Calif., occurrence. The crystals of the $2CaO \cdot 3B_2O_3 \cdot 9H_2O$ were likewise colorless and transparent and are described by the drawing given in Figure 1. The crystal is flattened on $\{\bar{1}01\}$. In order of decreasing importance the forms observed are: g $\{\bar{1}01\}$, a $\{100\}$, b $\{010\}$, e $\{0\bar{1}1\}$, M $\{1\bar{1}0\}$, t $\{\bar{1}\bar{1}1\}$, s $\{1\bar{2}1\}$, and l $\{1\bar{2}0\}$. The last three are not shown on the drawing. The morphological study shows no evidence for assigning less than holohedral symmetry to the crystal. The meyerhofferite crystals were colorless, transparent, prismatic elongated [001] with $\{100\}$ dominant and $\{110\}$ somewhat less dominant, i.e., having the habit given in figure 43 of Schaller's original description (1916).

---

* Publication authorized by the Director, U. S. Geological Survey.

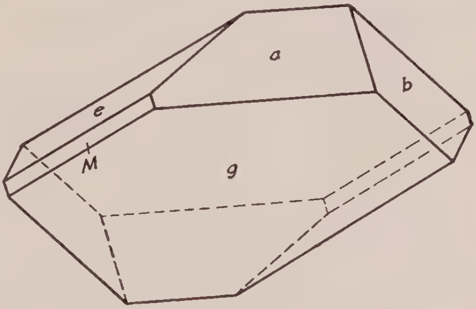

FIG. 1. Crystal of $2CaO \cdot 3B_2O_3 \cdot 9H_2O$ of typical habit (Evans, 1953 personal communication).

Forms:				
	b	010	e	$0\bar{1}1$
	a	100	g	$\bar{1}01$
	M	$1\bar{1}0$		

The determination of the lattice type and the measurements of the lattice constants were made using a quartz calibrated precession camera with Mo/Zr ($\lambda_\alpha = 0.71069$ Å; $\lambda_{\alpha_1} = 0.70926$ Å) radiation. The precession films were corrected for vertical and horizontal shrinkage. The powder patterns were prepared in a 114.57 mm. diameter camera with Cu/Ni radiation. Shrinkage corrections were applied. The values of the axial

TABLE 1. CRYSTALLOGRAPHIC ELEMENTS OF INYOITE—$2CaO \cdot 3B_2O_3 \cdot 13H_2O$

Symmetry: Monoclinic; space group $P2_1/a$ (C_{2h}^5)

Axial elements:
$a_0 = 10.63$ Å $\beta = 114°02'$
$b_0 = 12.06$
$c_0 = 8.40_5$
$a:b:c: = 0.8814:1:0.6969$
$V = 984.1$ Å^3 $Z = 2$ Density (calc.) $= 1.873$

TABLE 2. CRYSTALLOGRAPHIC ELEMENTS OF $2CaO \cdot 3B_2O_3 \cdot 9H2O$

Symmetry: Triclinic; space group $P\bar{1}$ (C_i^1)

Axial elements:

$a_0=7.04_6$ Å $\qquad \alpha=101°21'$
$b_0=9.45_2$ $\qquad \beta=101°19'$
$c_0=6.41_2$ $\qquad \gamma=99°49'$
$a:b:c=0.7455:1:0.6784$

Polar elements:

$a^*=0.1483$ $\qquad \lambda=76°13'$
$b^*=0.1106$ $\qquad \mu=76°14'$
$c^*=0.1638$ $\qquad \nu=77°26'$
$p_0:q_0:r_0=0.9055:0.6751:1$

Projection elements:

$x_0'=0.2001$ $\qquad p_0'=0.9508$
$y_0'=0.2502$ $\qquad q_0'=0.7089$
$\nu=77°26'$

Cartesian matrices:

$v_1=-0.2133$ $\qquad v_2=0.9570$

Direct:

$$M=\left\Vert \begin{array}{ccc} 6.909 & -2.016 & 0 \\ 0 & 9.045 & 0 \\ -1.383 & -1.860 & 6.412 \end{array} \right\Vert \text{ (in Å)}$$

Reciprocal:

$$M^{-1}=\left\Vert \begin{array}{ccc} 0.1447 & 0 & 0.0312 \\ 0.0323 & 0.1106 & 0.0390 \\ 0 & 0 & 0.1560 \end{array} \right\Vert \text{ (in Å}^{-1}\text{)}$$

$V=400.7$ Å^3 $\qquad Z=1$ $\qquad$ density (calc.)$=2.002$

lengths for inyoite and meyerhofferite are believed to be correct to 1.5 parts per 1000. The intervector angles are accurate to approximately 05′.

RESULTS

The results obtained from the *x*-ray single crystal study of inyoite are given in Table 1. The ratio of the axial elements and the value of the β-angle obtained in the *x*-ray work for inyoite are in excellent agreement with those obtained from morphological studies by Poitevin and Ellsworth (1921):

Present work	$a:b:c=0.8814:1:0.6969$	$\beta=114°02'$
Poitevin and Ellsworth	$a:b:c=0.8833:1:0.6950$	$\beta=114°01'$

The value of the *x*-ray density is 1.873. Schaller (1916) obtained 1.875 by the suspension method on Inyo material.

The crystallographic elements obtained from the *x*-ray work on $2CaO \cdot 3B_2O_3 \cdot 9H_2O$ are collected in Table 2. The formulas given by Evans (1948) were used in the calculations. The specific gravity of this compound was determined on the Berman balance to be 2.00. This value agrees well with the *x*-ray value of 2.002.

TABLE 3. COMPARISON OF X-RAY RESULTS FOR INYOITE, $2CaO \cdot 3B_2O_3 \cdot 9H_2O$, MEYERHOFFERITE, AND COLEMANITE

Mineral	Inyoite	Artificial	Meyerhofferite*	Colemanite**
Composition	$2CaO \cdot 3B_2O_3 \cdot 13H_2O$	$2CaO \cdot 3B_2O_3 \cdot 9H_2O$	$2CaO \cdot 3B_2O_3 \cdot 7H_2O$	$2CaO \cdot 3B_2O_3 \cdot 5H_2O$
System	Monoclinic	Triclinic	Triclinic	Monoclinic
Space Group	$P2_1/a$ (C_{2h}^5)	$P\bar{1}$ (C_i^1)	$P\bar{1}$ (C_i^1)	$P2_1/a$ (C_{2h}^5)
Z	2	1	1	2
a	10.63 Å	7.04_6 Å	6.61 Å	8.743 Å
b	12.06	9.45_2	8.35	11.264
c	8.40_5	6.41_2	6.49	6.102
α	(90°00′)	101°21′	90°00′	(90°00′)
β	114°02′	101°19′	101°31′	110°07′
γ	(90°00′)	99°49′	86°55′	(90°00′)
Volume	984.1 Å^3	400.7 Å^3	350.5 Å^3	564.2 Å^3
density (calc.)	1.873	2.002	2.118	2.419
a:b:c: (*x*-rays)	0.8814:1:0.6969	0.7455:1:0.6784	0.792:1:0.777	0.7762:1:0.5418
Vol./0-atom	20.5 Å^3	20.0 Å^3	19.5 Å^3	17.6 Å^3

* Switzer in Palache (1938) (original kX units converted to Å).
** Christ (1953).

The present study completes the determination of the crystallographic elements of the known members of the series: $2CaO \cdot 3B_2O_3 \cdot xH_2O$, where $x = 13, 9, 7$, and 5. The pertinent data on the four members of the series are collected in Table 3. One of the most interesting results of this comparison is that there is a progressive decrease in the volume occupied per oxygen atom with decreasing water content. In the case of colemanite the 17.6 Å^3 per oxygen atom is about the value expected if the structure is determined by the nearly close-packing of oxygen atoms (Christ, 1953). It is apparent that in the higher hydrates the percentage of oxygen atoms in nearly close-packing decreases. It is planned to study the thermal analysis for this series as an aid, and in addition, to the structural analysis.

The partially indexed powder patterns for inyoite, $2CaO \cdot 3B_2O_3 \cdot 9H_2O$, and meyerhofferite are given in Tables 4 to 6.

TABLE 4. X-RAY POWDER DATA: INYOITE—$2CaO \cdot 3B_2O_3 \cdot 13H_2O$
Monoclinic $P2_1/a$; $a_0=10.63$, $b_0=12.06$, $c_0=8.40^5$ Å, $\beta=114°02'$

Measured*		Calculated	
Cu/Ni	λ=1.5418 Å		
I	d_{hkl}	d_{hkl}	hkl
71	7.59	7.563	110
6	5.98	6.030	020
18	4.72	4.745	$21\bar{1}$
		4.743	021
		4.695	111
13	3.85	3.841	002
9	3.71	3.714	130
		3.690	$21\bar{2}$
4	3.45	3.449	$12\bar{2}$
6	3.37	3.369	211
6	3.13	3.126	310
100	3.03	3.033	221
		3.015	040
13	2.775	2.779	$20\bar{3}$
		2.777	032
9	2.643	2.643	231
18	2.494	2.503	013, $33\bar{2}$
		2.494	212
		2.483	132
3	2.410	2.406	321
25	2.286	2.287	241
		2.286	$23\bar{3}$
		2.281	$13\bar{3}$
4	2.185	2.190	410
		2.185	251, $42\bar{2}$
		2.181	142
		2.180	151
13	2.098	2.102	$20\bar{4}$
		2.092	$15\bar{2}$
		2.090	420
9	2.049	2.055	$43\bar{1}$
		2.049	$25\bar{2}$
		2.044	$2\bar{3}3$, 052
6	1.972		
13	1.916		
18	1.880		
3	1.752		
4	1.605		
6	1.528		
6	1.441		
Plus additional weak lines.			

* Shrinkage correction negligible.

TABLE 5. X-RAY POWDER DATA: $2CaO \cdot 3B_2O_3 \cdot 9H_2O$
Triclinic $P\bar{1}$; $a_0 = 7.04_6$, $b_0 = 9.45_2$, $c_0 = 6.41_2$ Å
$\alpha = 101°21'$, $\beta = 101°19'$, $\gamma = 99°49'$

Measured*		Calculated	
Cu/Ni	λ=1.5418 Å		
I	d_{hkl}	d_{hkl}	hkl
100	9.14	9.05	010
100	6.75	6.743	100
4	6.08	6.079	$\bar{1}10$
71	5.76	5.731	$0\bar{1}1$
50	5.20	5.181	$\bar{1}01$
6	4.88	4.916	110
50	4.56	4.564	$\bar{1}\bar{1}1$
71	4.19	4.207 4.195	$\bar{1}20$ $1\bar{1}1$
13	4.07	4.070	101
25	3.59	3.587	$1\bar{2}1$
18	3.36	3.364	111
13	3.14		
35	3.08		
50	3.02		
18	2.966		
18	2.864		
50	2.807		
25	2.700		
9	2.594		
71	2.573		
13	2.463		
4	2.405		
6	2.369		
13	2.333		
13	2.268		
4	2.228		
18	2.157		
9	2.133		
35	2.104		
13	2.048		
9	2.005		
9	1.940		
9	1.911		
9	1.878		
Plus additional weak lines.			

* Shrinkage correction negligible.

TABLE 6. X-RAY POWDER DATA: MEYERHOFFERITE—$2CaO\cdot 3B_2O_3\cdot 7H_2O$
Triclinic $P\bar{1}$; $a_0=6.61$, $b_0=8.35$, $c_0=6.49$ Å*
$\alpha=91°00'$, $\beta=101°31'$, $\gamma=86°55'$

Measured**		Calculated	
Cu/Ni	λ=1.5418 Å		
I	d_{hkl}	d_{hkl}	hkl
100	8.39	8.33	010
100	6.51	6.49 6.47	001 100
50	5.03	5.038	011
8	4.17	4.167 4.141	020 101
18	3.65	3.670	$1\bar{1}1$
12	3.50		
35	3.30		
100	3.17		
18	3.09		
18	2.974		
nil	2 900		
18	2.641		
50	2.540		
50	2.520		
4	2.463		
25	2.149		
18	2.093		
18	2.072		
18	2.019		
18	1.988		
18	1.956		
18	1.928		
18	1.894		
Plus additional weak lines.			

* Original units in kX. Given here in Å. Error ±0.02 Å.

** Shrinkage correction negligible.

REFERENCES

CHRIST, C. L. (1953), Studies of borate minerals: I x-ray crystallography of colemanite: *Am. Mineral.*, **38**, 411–415.

EVANS, H. T., JR. (1948), Relations among the crystallographic elements: *Am. Mineral.*, **33**, 60–63.

PALACHE, C. (1938), Crystallography of meyerhofferite: *Am. Mineral.*, **23**, 644–648.

POITEVIN, E., AND ELLSWORTH, H. V. (1921), Inyoite from New Brunswick: *Geol. Survey Canada, Bull.*, **32**.

SCHALLER, W. T. (1916), Inyoite and meyerhofferite, two new calcium borates: *U. S. Geol. Survey Bull.*, **610**, 35–55.

COMPOSITION, TENEBRESCENCE AND LUMINESCENCE OF SPODUMENE MINERALS

Esther W. Claffy, *Naval Research Laboratory, Washington, D. C.*

Abstract

Transparent spodumenes are shown to be of two types: chromian spodumene (green, the typical North Carolina "hiddenite") and non-chromian spodumene (colorless, yellow, pink and lilac "kunzite," green—whether natural or artificially induced). The pink color of non-chromian spodumene is correlated with the presence of Mn, and more specifically with a low Fe/Mn ratio. Only non-chromian spodumene is luminescent and tenebrescent. Absorption spectra of non-chromian spodumenes of various colors before and after x-ray irradiation, and after bleaching, show the preferential growth or decay of the 6400 Å band over the 5400 Å band. Both bands are probably due to Mn. The absorption spectrum of chromian spodumene is unchanged by irradiation or bleaching; its 6400 Å band is probably due to Cr, not Mn; its 11,000 Å band may be due to V.

Introduction

The striking luminescence and color changes of kunzite, the pink spodumene, have long been the subject of considerable research by mineralogists and physicists alike. Baskerville (1903), when naming kunzite, already noted its phosphorescence after x-ray irradiation, and Baskerville and Kunz (1904) reported on other sources of exciting radiation for kunzite. It is the general, although vague, impression that these properties are related to the presence of manganese. Furthermore, it is frequently assumed (Pringsheim, 1949; Bayley, 1928) that hiddenite, the green gem spodumene, is nature's equivalent of the green modification produced by high energy irradiation of kunzite.

It is proposed to demonstrate, by a critical review of the literature as well as on the basis of further investigations, that some of these beliefs are erroneous.

The mineral spodumene has the formula $LiAl(SiO_3)_2$, and is a member of the pyroxene family. Ford (1932) notes two gem varieties—green hiddenite and lilac kunzite. The name "triphane" is retained merely as a synonym. Jahns and Wright (1951), in a comprehensive report on lithium-pegmatites, classify the transparent spodumenes as triphane (colorless to yellow), kunzite (pink, lilac), and hiddenite (green).

The establishment of varietal names for transparent (gem) spodumenes on the basis of color is unfortunate. It will be demonstrated that, on the basis of chemical composition and luminescence and tenebresence behavior, gem spodumenes are of two types—a chromian spodumene (green, typically from North Carolina) and a non-chromian spodumene (colorless, yellow, pink, lilac or green—whether natural or artificially induced). Use of the varietal names will be avoided hereafter in this paper, except in referring to the literature.

LUMINESCENCE OF THE SPODUMENES

There is, apparently, some variation in the luminescence behavior of spodumenes, possibly even among similarly colored specimens from the same localities. This, coupled with occasionally loose application of the terms luminescence, fluorescence, and phosphorescence, has caused some confusion in the reported properties.*

According to Ford (1932), kunzite phosphoresces a strong orange-pink when excited by any source. Jahns and Wright (1951) report that gem spodumene is thermoluminescent and possibly triboluminescent, and that it is strongly phosphorescent when exposed to *x*-ray, ultraviolet, radium, or high tension electric currents. The Ultra-Violet Products Inc. handbook (1948) notes that some Pala kunzites fluoresce yellow and often phosphoresce for long periods, and that spodumene from Portland, Conn., sometimes has a persistent, deep red phosphorescence. Pochettino (1909, 1911) first records cathodoluminescence in various spodumenes when examined through a specially mounted polarizing microscope, and Nichols and Howes (1914) examine the cathodophosphorescence bands. None of our specimens shows strong phosphorescence under ultraviolet or electron excitation.

We have examined a total of 26 specimens of spodumene, including 5 common spodumenes (Andover, Me.; Portland, Conn.; Keystone, S. Dak.; Harding Mine, Taos Co., New Mex., Argentina), 7 colorless (Maharitra, Madagascar; Minas Geraes, Brazil; Pala, Calif.), 3 lilac (Pala), 3 pink (Pala), 1 yellow (Pala), 1 very light green (Pala), 4 light green and 2 dark green (Stony Pt., Alexander Co., N. C.).† The North Carolina green spodumenes show no luminescence whatsoever under ultraviolet light or spark discharge. Under 2537 Å ultraviolet excitation, fluorescence of the other spodumenes is very weak or missing. Under 3650 Å ultraviolet, all the other spodumenes fluoresce salmon pink—moderate to bright. Under electron excitation of a spark discharge from a Tesla coil, in partial vacuum, most show bright yellow-orange fluorescence but only a short weak phosphorescence; two colorless spodumenes (Brazil; Madagascar) fluoresce pink, and one or two of the common variety are non-luminescent.

---

* It should be remembered, of course, particularly when comparing recent data with data obtained in the early days of experimentation, that inherent mechanical differences in the equipment used by various workers, with corresponding significant differences in the intensity and wavelength-distribution of the radiation, may account for many of the apparent discrepancies in luminescence behavior. Pough and Rogers (1947), for example, report on the improved phosphorescence and tenebrescence response to the then newly developed, high intensity, Machlett-type *x*-ray tube.

† The North Carolina "hiddenities" were made available through the cooperation of Dr. William Foshag of the U. S. National Museum.

Another interesting property, which was intensively studied by Przibram and his colleagues (1922, 1923, 1924, 1932), is the radiophotoluminescence of kunzite. If kunzite is first irradiated with x-rays or radium γ-rays and is then excited by ultraviolet or other source, it fluoresces and phosphoresces strongly. The effect is sometimes noticeable even years later. All non-chromian spodumenes, regardless of color, behave similarly. It should be noted that Przibram (1921, 1932) specifically states that North Carolina hiddenite does not show radiophotoluminescence, even after long exposure to radium.

TENEBRESCENCE OF SPODUMENES

The property of tenebrescence is the reversible darkening and bleaching shown by certain crystalline solids. The darkening (or change in color) is induced by x-ray, cathode ray, or other high energy source and the bleaching by heat or irradiation with light of the same wavelength as the absorption band produced during darkening. Jahns and Wright (1951), for instance, note that many gem spodumenes, especially the green, lavender, and bluish varieties, fade on prolonged exposure to sunlight.

The tenebrescence of kunzite has been studied by Zekert (1927), Bělăr (1923), Lind and Bardwell (1923), Stuhlman and Daniel (1928), and Bayley (1928) among others. X-ray or γ-ray irradiation converts pink spodumene to the green; colorless spodumene when x-rayed passes through the pink stage (an intermediate colorless stage has sometimes been noted, presumably due to the combined effect of equal amounts of pink and green); and finally darkens to green. Exposure to daylight, ultraviolet, or moderate heat ($<250°$ C.) bleaches the colors, from green →pink→colorless. Firing at 500° C. converts the green directly to the colorless. The cycle can be started at any stage and can be repeated indefinitely. In Figure 1, the cyclic color changes in non-chromian gem spodumene are summarized.

It is reported by Pringsheim (1949) that the green modification emits the same phosphorescence color as the pink, but it is of longer duration. The heat-bleaching is accompanied by thermoluminescence (Pochettino, 1909, 1911; Przibram and Kara-Michailova, 1923). The colorless (bleached) modification no longer phosphoresces (Przibram, 1921).

We have found that chromian gem spodumene (green) from North Carolina cannot be bleached by such heat treatment nor by exposure to light. Nor can North Carolina specimens of pale green color be darkened

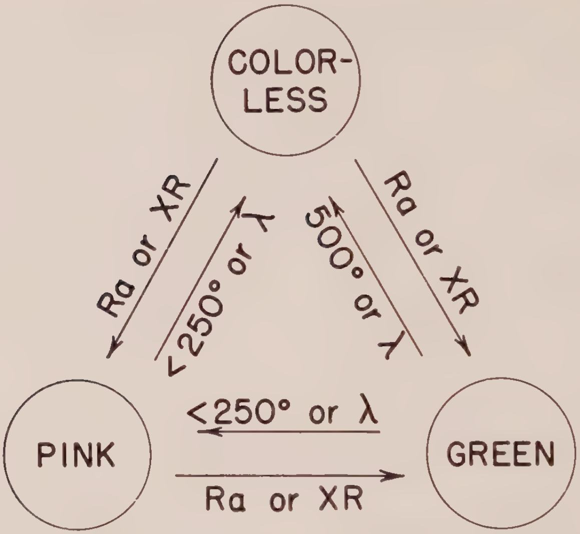

FIG. 1. Tenebrescence of non-chromian gem spodumene. λ=optical bleaching.

by x-rays or γ-rays. Whereas 4½ hours' heating at 250° C. produced no visible bleaching of color in a dark green chromian specimen, nor did one additional hour of firing at 500° C., a lilac non-chromian spodumene became completely colorless after one hour at 500° C. The so-called Pala "hiddenite," which fluoresced pale pink, was a deep blue-green after 3 hours' exposure to x-rays, and fluoresced and phosphoresced brightly. Two crystals of North Carolina chromian spodumene (one dark green, one light green) retained their original color after 3 hours' x-raying, and were still nonluminescent. Even 96 hours' exposure to a 500 mg. radium source did not darken a specimen of North Carolina chromian spodumene nor induce luminescence. Bayley (1928) also observed that hiddenite from North Carolina showed no marked change after x-ray irradiation.

The role of Mn in the tenebrescence of kunzite was explained by Stuhlman and Daniel (1928) in terms of a chemical oxidation-reduction process and chemiluminescence. In the light of modern knowledge of solids this explanation seems unlikely. Several workers (Meyer and Przibram, 1922; Zekert, 1927; Pough and Rogers, 1947) have reported the appearance of an intermediate, unstable brown coloration in kunzite after x-ray or γ-ray irradiation. According to Pough and Rogers (1947), immediately after irradiation the mineral was brown and showed strong phosphorescence—spontaneous afterglow—and not until this phosphorescence had ended did the usual green color appear. The fact that Mn^{+2} imparts a brown color to silicate glass and is responsible for its green or orange fluorescence (Weyl, 1951) is perhaps suggestive of a temporary photochemical reduction of Mn in spodumene by high energy radiation.

COMPOSITION AND STRUCTURE OF SPODUMENE

The presence of Mn as a minor constituent in spodumene has long been known, Davis (1904), the first to publish a chemical analysis of kunzite, reporting 0.11% MnO. Wild and Klemm (1925) made the earliest spectrographic analysis and found that all spodumenes, regardless of color, contained Mn, Ga, and Fe—with least Fe in pink kunzite. They were unable, by their technique, to correlate the concentration of Mn with the color of the spodumenes. Apparently equal amounts of Mn, and Ga, were present in all. Fe was believed responsible for the color of the yellow variety. Wild and Klemm did establish, however, that Cr was present in all hiddenites tested and that the deeper the green color, the more Cr was present. They suggested that V, together with Cr, may be responsible for the yellowish green color of some hiddenites.

More recently Gabriel, Slavin, and Carl (1942) analyzed spectrographically a number of transparent spodumenes, one lilac kunzite from Pala and ten colorless or nearly colorless spodumenes, from various localities. There was no attempt to study color as related to composition. We deduce one interesting relationship from their data, nevertheless. Of all eleven samples, the lilac kunzite, as opposed to the ten colorless spodumenes, contained the lowest concentration of Fe (0.020% Fe_2O_3) combined with high Mn (0.073% MnO). Recalculated in terms of Fe/Mn ratio, the lilac kunzite = 0.25; the colorless spodumenes range from 0.74 (0.44% Fe_2O_3/0.54% MnO) to 24.1 (0.64% Fe_2O_3/0.024% MnO).

The spectrochemical analyses of the minor and trace elements in our spodumenes, as recorded in Table 1, include all specimens for which absorption spectra were measured, as indicated below. The samples were carefully inspected under the binocular microscope for freedom from inclusions and were cleansed of superficial impurities by soaking in hydrochloric acid and rinsing with distilled water. A Baird 3-meter grating spectrograph was used for the analysis. Unfortunately, the press of other spectrographic work did not allow time for precise quantitative determinations.

Of particular interest are the elements Fe, Mn, Cr, V, and Sc. Mn is present in relatively high concentrations in all the spodumenes. These may be arranged in the following sequence of decreasing Mn concentration: #2 pink = #6 lilac = #8 lilac = #10 yellow > #1 colorless = #5 v. lt. green = #7 colorless = #9 colorless > #4 lt. green (N.C.) > #3 dk. green (N.C.). The group of highest Mn content includes the pink and lilac specimens, a yellow, and a colorless. The Fe content of the pink and lilac

TABLE 1. MINOR AND TRACE ELEMENTS IN SPODUMENES†

Element	Colorless #1	Pink 2	Dr. green 3	Lt. green 4	V. lt. green 5	Colorless 6	Colorless 7	Lilac 8	Colorless 9	Yellow 10
Na	.0X–.X%	.0X–.X%	.0X–.X%	.0X–.X%	.0X–.X%	.0X–.X%	.0X–.X%	.0X–.X%	.0X–.X%	.0X–.X%
K	—	—	—	—	—	—	—	—	—	—
Rb	—	—	—	—	—	—	—	—	—	—
Cs	—	—	—	—	—	—	—	—	—	—
Mg	<.0001	.000X	.0X	.0X	.000X	.000X	.000X	.000X	.000X	.000X
Sr	—	—	—	—	—	—	—	—	—	—
Ti	.000X	.000X	.0X	.0X	.00X	.0X	.0X–.X	.00X	.00X	.0X
Ga	.X	.X	.X	.X	.X	.X	.X	.X	.X	.X
Fe	.0X	.00X	.X–X.0	X.0	.0X	.X–X.0	.0X	.0X	.0X	.X–X.0
Mn	.X	.X	.0X–.X	.0X–.X	.X	.X	.X	.X	.X	.X
Cr	<.0001	<.0001	X.0	.X–X.0	<.0001	—	—	—	<.0001	<.0001
V	—	—	.X	.0X–.X	—	.000X	—	—	—	.000X
Co	.0X	.0X	.00X	.00X	.0X	.0X	.00X	.0X	.0X	.0X
Ni	<.0001	<.0001	.0X	.00X	.000X	.00X	.000X	.00X	.00X	.00X
Cu	—	<.0001	<.0001	<.0001	<.0001	<.0001	<.0001	<.0001	<.0001	<.0001
Sn	.X	.X	.X	.X	.X	.0X–.X	.X	.X	.X	.X
Ge	—	.000X	—	—	<.0001	.000X	.000X	.000X	.000X	.000X
Sc‡	—	—	<.05	—	—	—	—	—	<.05	—

1 —Colorless, Minas Geraes, Brazil.
2 —Pink, Katrina Mine, Pala, Calif.
3 —Dk. green hiddenite, Stony Pt., Alexander Co., N. C.
4*—Lt. green hiddenite, Stony Pt., Alexander Co., N. C.
5 —V. lt. green, Vanderburg Mine, Pala, Calif.
6*—Colorless, Pala, Calif.
7*—Colorless, Maharitra, Madagascar.
8*—Lilac, Pala, Calif.
9*—Colorless, Maharitra, Madagascar.
10*—Yellow, San Pedro Mine, Pala, Calif.

†—Absorption spectra recorded.
‡—Sc analysis by Martin Cavanagh.
*—Spectrochemical analysis by Samuel H. Cress.

specimens is among the lowest; the yellow and the colorless have considerably more Fe. Wherein the yellow differs from the colorless in this group is not clear from the available data.

The group of intermediate Mn content includes only colorless or very light green spodumenes. The Fe content of the group members is invariably high. The North Carolina green spodumenes contain the least Mn of all, and constitute a separate group; they also contain more Fe than any other spodumene, the yellow excepted. Cr is exceedingly low or absent in all the specimens except those from North Carolina, where the dark green shows more Cr than the light green. As to be expected, V and Ti accompany Fe and Cr. The concentration of V seems to be in direct proportion to the Cr concentration. Whether the presence of V influences the color of the chromian spodumenes is as yet unknown.

Our spectrochemical analyses, therefore, corroborate Wild and Klemm's identification of Cr as the chromophore in hiddenite. Moreover, the data substantiate the supposition that Mn is the probable coloring agent in pink kunzite.

Recently, Heinrich and Levinson (1953) published a detailed report on rose muscovites. The color was found to depend on the absence of Fe^{+2} and the predominance of Mn^{+3} over Fe^{+3}. In lepidolites, also, the color variations were related to fluctuations in the Fe/Mn ratio. The Fe/Mn ratio may play a similar role in the kunzites, as suggested by our chemical data. The valency condition of Mn in spodumene has not been established. Whereas chemical evidence suggests Mn^{+3}, the absorption spectra may be indicative of Mn^{+2}. It is conceivable that Mn exists in both states.

The fact that chromian spodumene, although colored green by Cr, still contains considerable Mn and yet does not luminesce may possibly be due to the "poisoning" or "killing" effect of Cr. As little as 0.001% Cr in a Mn-activated Zn_2SiO_4 (Marden and Meister, 1939), for example, causes detectable reduction in photoluminescence.

The presence of Sc in spodumenes has never before, as far as we have been able to determine, been reported in the literature. Sc is one of the rarer trace elements, although widely distributed in extremely low concentrations. It is more commonly found in granite pegmatite minerals, such as tourmaline, beryl, mica, pyroxene, and hornblende, where it replaces Mg and Fe^{+2}, ions of similar size.

Its occurrence in spodumene, however, does not seem unreasonable: (1) spodumene is a Li-pyroxene and a typical pegmatite mineral; and (2) Sc^{+3} (ionic radius 0.83) could replace Li^{+} (ionic radius 0.78). The presence of Sc in a spodumene from Madagascar, where the Sc mineral thortveitite occurs, is even less surprising.

Structure—Spodumene as it occurs in nature—the α or low temperature form—has a chain structure of Al_2O_3 and SiO_2 tetrahedra. The Li ions act as cross-linkages, and have six-fold coordination, forming LiO_6 groups.

The *x*-ray powder patterns (recorded with a large, 114.5 mm. camera) of spodumenes of varying color and composition are identical. There are no indications of lattice distortion or impurity phases. Whatever minor elements are present must be readily accommodated by the normal crystal lattice.

ABSORPTION SPECTRA

It is generally agreed that there are two predominant absorption bands in transparent spodumenes, a red band with a peak at about 5900 Å and a blue band at about 4320 Å. The variations reported in the extent or peak position of the bands are partly due to differences in technique (some early measurements were made with hand spectroscopes or by the use of filter combinations), partly to different crystallographic orientation of the minerals as examined (kunzite is pleochroic, hiddenite highly so), and partly to inherent differences—trace elements—in the mineral specimens.

We have recorded the absorption spectra of several different colored spodumenes, both before and after *x*-raying. For this purpose, polished plates approximately 5×8 mm. and 2 mm. thick were prepared from optically flawless portions of the crystals. Measurements were made with a Beckman, Model DU, spectrophotometer, over the range 2200 to 12,000 Å. Either a hydrogen or tungsten lamp, in combination with a blue-sensitive or red-sensitive phototube, was used as needed. The samples were firmly mounted so that the same portion of the plate was measured each time. To avoid inadvertent bleaching, the plates were kept in the dark when not in actual use. After *x*-ray irradiation, the plates were stored in the dark at least over-night before measurement, to allow for the decay of the *x*-ray induced phosphorescence, which otherwise could have caused anomalously high readings. The *x*-ray exposures consisted of approximately 29 hours' irradiation from a tungsten-target tube, with beryllium window, operated at 50 Kv and 15 milliamps., the samples being shielded from visible light during the entire period.

Bayley's (1928) seem to be the only published transmission spectra for any of the spodumenes. He examined one specimen of Pala kunzite and one North Carolina hiddenite, before and after *x*-raying, using a photographic technique. Our absorption data correspond well with Bayley's transmission data. However, where Bayley reports that no trace of absorption bands in the ultra-violet or violet could be found for kunzite,

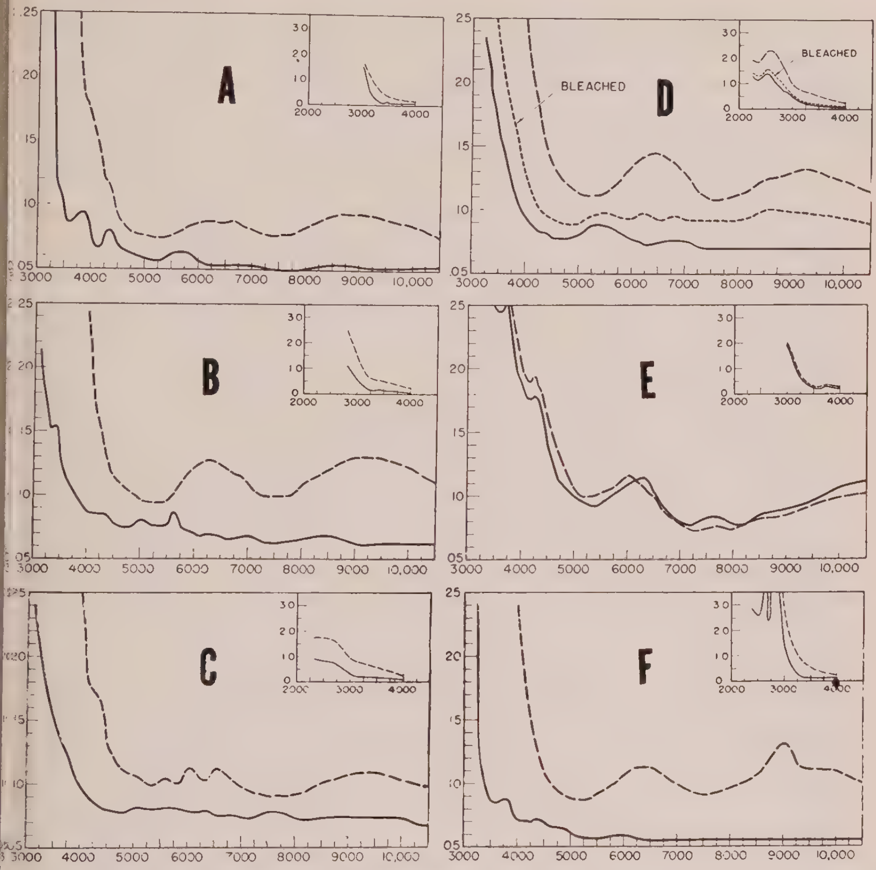

Fig. 2. Absorption spectra of spodumenes, as optical density (ordinate) vs. waveleng in A (abscissa). Inserts show ultraviolet absorption; solid lines = before *x*-ray, broken lines = after *x*-ray. A—colorless, Pala; B—colorless, Madagascar; C—colorless Sc-bearing, Madagascar; D—lilac, Pala; E—green, N.C.; F—yellow, Pala.

our spectra definitely show significant ultraviolet absorption at 2500 Å, and at 2600 Å and 2800 Å in yellow spodumene, as well as other bands in the violet for other specimens.

In Figure 2 are reproduced the absorption spectra of the various spodumenes, plotting optical density as a function of wavelength. Absorption bands which appear in most of the spectra and seem characteristic of the natural spodumenes are the 4300 Å and 5400 Å bands. The former may be related to the presence of Mn, as Turner and Weyl (1935) and Weyl (1951) report an absorption band at 4250 Å for Mn^{+2} in silicate glasses. The 5400 Å band may also be a Mn band. Absorption spectra of Mn^{+2}-activated silicates and pure $MnCl_2$ (Klick and Schulman, 1952) show several characteristic bands including one at about 5200 Å. Mn^{+3} in silicate glasses, according to Weyl (1951), has a strong absorption band whose maximum lies between 4700 Å and 5200 Å. Grum-Grzimailo (1945) shows spectra of ruby, tourmaline, and lepidolite with Mn^{+3} bands at about 5200 Å. The 5400 Å band is missing in the spectra of the green chromian and the yellow spodumenes. The 6400 Å band appears in all *x*-rayed spodumenes. Traces of an incipient 6400 Å band are seen in two natural colorless samples; it is fully developed in green chromian spodumene. A 9300 Å infrared band also characteristically develops after *x*-ray irradiation. Although apparently missing from *x*-rayed chromian spodumene, it may be masked by the tail of the broad shallow band peaking at approximately 11,000 Å.

By comparing the absorption spectra of a specimen before and after *x*-ray irradiation, the tenebrescence effects can be noted. The behavior of lilac spodumene (Fig. 2D) is typical. After exposure to *x*-rays, the 2500 Å ultraviolet band has increased in density almost two-fold. The very small 4300 Å band, the 5400 Å band, and the small 6800 Å band are masked by the growth of a strong absorption band with a maximum at 6400 Å. The latter is responsible for the green coloration produced by irradiation. In the infrared, a new band with a peak at about 9300 Å, has developed.

The effect of bleaching on the green, irradiated non-chromian spodumene is likewise recorded (Fig. 2D). In this instance, optical bleaching, by exposure to a 100-watt electric light bulb for five hours, was deliberately stopped far short of complete discoloration so that the interim decay—or growth—of the bands could be examined. The 2500 Å band has shrunk and has almost returned to its original density; the 5400 Å band has reappeared; and the 6400 Å band has been replaced by two small bands peaking at 6100 Å and 6800 Å, which were insignificant in the original lilac spodumene; and the 9300 Å infrared band has shrunk and now has apparently shifted to a peak at 8600 Å.

Of the two major bands involved in the color changes of non-chromian spodumene, it is seen that the 5400 Å band in pink spodumene is the more stable. It grows or bleaches more slowly and never becomes as dense as the 6400 Å band in the green. Earlier researchers (Lind and Bardwell, 1923; Stuhlman and Daniel, 1928) had studied these color changes in kunzite qualitatively. Bělăr (1923), who first attempted a quantitative spectrophotometric study and made measurements of the effects of increasing radium dosages at several selected wavelength positions, drew similar conclusions.

The absorption spectra of chromian green spodumene (Fig. 2E) before and after *x*-ray exposure are strikingly unlike those of the other spodumenes in that there is essentially no change in the spectra. New bands do not appear on *x*-raying, nor do the original bands disappear on attempted bleaching. There is only a slight increase in the overall density of some absorption bands with an apparently slight shift in some peak positions. The 6400 Å band is believed to be related to the presence of Cr, on the basis of Grum-Grzimailo's (1945) research on Cr in other minerals. Weyl and Thümen (1933) and Weyl (1951) studied Cr absorption in silicate glasses and also reported a 6500 Å band for Cr^{+3}. The 6400 Å band in chromian spodumene may be due in part, however, to the presence of V, for Weyl, Pincus, and Badger (1939) found absorption maxima at 4250 Å and 6250 Å in silicate glasses bearing V^{+3}. If so, then the 4250 Å band in chromian spodumene may also be related to V, as well as Mn.

The absorption spectra of green chromian spodumene (Fig. 2E) and green, irradiated non-chromian spodumene (Fig. 2D) should be compared. In the region 4000–7000 Å, the two spectra do seem similar, but the shape of the 6400 Å bands is different, as is their half-width—about 750 Å for chromian spodumene, about 1000 Å for the non-chromian. We believe that these two green bands are due to different types of absorbing centers and are to be correlated with the presence of Cr in the former and Mn in the latter, and that their similar location is coincidental. If these were both Mn bands, then there should also be some similarity in behavior between the two materials.

In the infrared region, the spectra are entirely different: green, irradiated non-chromian spodumene shows a band at 9300 Å; green chromian spodumene lacks this but has a band with a peak at 11,000 Å, which may be due to the presence of V. Fritz-Schmidt, Gehlhoff, and Thomas (1930) reported that V^{+5} in silicate glasses is characterized by fairly strong absorption near 11,500 Å. Farther out in the infrared, between 1.5–4.5 μ, the differences are even more extreme, as Bayley's (1928) spectra show.

Because of the presence of a 6300 Å band in both materials, and the presumed identity of a 10,000 Å band in hiddenite with a 9100 Å band in the green irradiated kunzite, Bayley concluded that natural hiddenite and green irradiated kunzite are alike. He further postulated that the presence of monazite sands near the North Carolina hiddenite deposit could account for the radiations that produced the green color in natural hiddenite.

Concluding Remarks

It is particularly fitting perhaps, that a report on spodumene should appear in a publication dedicated to Waldemar T. Schaller. Much of what is known today about pegmatite minerals in general, and Pala spodumenes in particular, is based on the outstanding early researches of Dr. Schaller.

REFERENCES

BASKERVILLE, C. (1903), Kunzite, a new gem: *Science,* **18,** 303–304.

BASKERVILLE, C., AND KUNZ, G. F. (1904), Kunzite and its unique properties: *Am. Jour. Sci.,* **18,** 25–28.

BAYLEY, P. L. (1928), The coloration of kunzite and hiddenite by *x*-rays: *Jour. Opt. Soc. Amer.,* **17,** 350–355.

BĚLĂR, M. (1923), Spektrophotometrische Untersuchung der Verfärbungserscheinungen durch Becquerelstrahlen: *Sitz. Akad. Wiss. Wien.,* **12,** 45–54.

DAVIS, R. O. E. (1904), Analysis of kunzite: *Am. Jour. Sci.,* **18,** 29.

FORD, W. E., (1932), Dana's Textbook of mineralogy: John Wiley & Sons, N. Y., 4th Ed.

FRITZ-SCHMIDT, M., GEHLHOFF, G. R., AND THOMAS, M. (1930), Die physikalischen Eigenschaften der Gläser in Abhängigkeit von der Zusammensetzung, IV. Die Durchlässigkeit der Gläser im ultravioletten, sichtbaren und ultraroten Gebiet: *Zeitschr. tech. Physik.,* **11,** 289–326.

GABRIEL, A., SLAVIN, M., AND CARL, J. F. (1942), Minor constituents in spodumene: *Econ. Geol.,* **37,** 116–125.

GRUM-GRZIMAILO, S. (1945), The influence of the structure of crystals on their colour produced by Cr, Mn, Fe, Ni, Co and Cu: *Acta Physicochimica U.R.S.S.,* **22,** 933–946.

HEINRICH, E. W., AND LEVINSON, A. A. (1953), Studies in the mica group; mineralogy of the rose muscovites: *Am. Mineral.,* **38,** 25–49.

JAHNS, R. H., AND WRIGHT, L. A. (1951), Gem and lithium-bearing pegmatites of the Pala District, San Diego County, California: *Div. of Mines, State of Calif. Dept. of Natural Resources, Special Rept.* **7-A.**

KLICK, C. C., AND SCHULMAN, J. H. (1952), On the luminescence of divalent manganese: *Jour. Opt. Soc. Amer.,* **42,** 910–916.

LIND, S. C., AND BARDWELL, T. (1923), Coloring and thermophosphorescence produced in transparent minerals and gems by radium radiation: *Jour. Franklin Inst.,* **196,** 357–390.

MARDEN, J. W., AND MEISTER, G. (1939), Effects of impurities on fluorescent compounds: *Trans. Illum. Eng. Soc.,* **34,** 503–513.

MEYER, S., AND PRZIBRAM, K. (1922), Bemerkungen über Verfärbung und Lumineszenz unter Einwerkung von Becquerelstrahlen: *Sitzb. Akad. Wiss. Wien,* **131,** 429–435.

NICHOLS, E. L., AND HOWES, H. L. (1914), Luminescence of kunzite: *Phys. Rev.,* **4,** 18–27.

POCHETTINO, A. (1909), Sui fenomeni di luminescenza nei minerali: *Il Nuovo Cimento,* **V-18,** 245–300.

——— (1911), Sui fenomeni di luminescenza catodica nei minerali: *Il Nuovo Cimento,* **VI-1,** 21–64.

POUGH, F. H., AND ROGERS, T. H. (1947), Experiments in *x*-ray irradiation of gem stones: *Am. Mineral.,* **32,** 31–43.

PRINGSHEIM, P. (1949), Fluorescence and phosphorescence: Interscience Publ., N. Y.

PRZIBRAM, K. (1921), Über Phosphoreszenz durch Becquerelstrahlen verfärbter Mineralien: *Sitzb. Akad. Wiss. Wien,* **130,** 265–270.

——— (1923), Verfärbung und Lumineszenz durch Becquerelstrahlen: *Zeitschr. f. Physik,* **20,** 196–208.

——— (1924), Zur Verfärbung und Lumineszenz durch Becquerelstrahlen: *Physikal. Zeitschr.,* **25,** 640–642.

——— (1932), Radiolumineszenz und Radiophotolumineszenz, III: *Sitzb. Akad. Wiss. Wien,* **141,** 283–289.

PRZIBRAM, W., AND KARA-MICHAILOVA, E. (1922, 1923), Über Radiolumineszenz und Radio-Photolumineszenz: *Sitab. Akad. Wiss. Wien,* **131,** 511–530; **132,** 285–298.

STUHLMAN, O., JR., AND DANIEL, A. F. (1928), The x-ray phosphorescent and thermophosphorescent radiations of kunzite: *Jour. Opt. Soc. America*, **17**, 289–293.

TURNER, W. E. S., AND WEYL, W. (1935), Constitution and color of glasses containing iron and manganese oxides: *Jour. Soc. Glass Tech., Trans.*, **19**, 208–216.

ULTRA-VIOLET PRODUCTS, INC. (1948), Rocks and minerals that fluoresce with Mineralight.

WEYL, W. (1951), Coloured glasses: Soc. Glass Tech., Publ., Sheffield, Eng.

WEYL, W., PINCUS, A. G., AND BADGER, A. E. (1939), Vanadium as a glass colorant: *Jour. Am. Ceram. Soc.*, **22**, 374–377.

WEYL, W., AND THÜMEN, E. (1933), Konstitution und Farbe der Chromgläser: *Sprechsaal*, **66**, 197–199.

WILD, G. O., AND KLEMM, R. (1925), Mitteilungen über spektroskopische Untersuchungen an Mineralien; V—Spodumen: *Centralbl. f. Mineral. A, nr.* **11**, 324–326.

ZEKERT, B. (1927), Zur Verfärbung des Steinsalzes und des Kunzits durch Becquerelstrahlen: *Sitzb. Akad. Wiss. Wien*, **136**, 337–365.

THE CRYSTALLOGRAPHY OF BASTNAESITE, PARISITE, ROENTGENITE, AND SYNCHISITE*

GABRIELLE DONNAY, *U. S. Geological Survey, Washington, D. C.*

AND

J. D. H. DONNAY, *The Johns Hopkins University, Baltimore, Md.*

CONTENTS

Abstract 932
Introduction 933
Unit-cell dimensions and symmetry 935
Syntaxic intergrowths 939
Chemical compositions of roentgenite and synchisite 942
Crystal structure 945
Crystal morphology 950
  Bastnaesite 950
  Parisite 952
  Roentgenite 952
  Synchisite 957
  Morphology of the intergrowths 957
Crystal optics 958
  Ionic refractivities 958
  Form birefringence 959
References 962

ABSTRACT

An x-ray study of parisite and related minerals from many localities establishes the existence of four species: bastnaesite, $CeFCO_3$; parisite, $2CeFCO_3 \cdot CaCO_3$; roentgenite, $3CeFCO_3 \cdot 2CaCO_3$; and synchisite, $CeFCO_3 \cdot CaCO_3$. Bastnaesite has space group $C\bar{6}2c$, $a = 7.16$, $c = 9.79$ Å, $Z = 6$. Parisite has space group R3, $a = 7.18$ for the ordered form, $a = 7.12$ for the disordered form, $c = 84.1$ Å, $Z = 18$. Roentgenite has space group R3, $a = 7.13$, $c = 69.4$ Å, $Z = 9$. Synchisite is orthorhombic or monoclinic with $\beta = 90°$, pseudo-hexagonal axes $a = 7.11$, $c = 54.7$ Å, $Z = 18$. All structures show a pronounced pseudo-H-centering of the lattice, which leads to a pseudo-axis $a' = a/2 \cos 30°$. When the structures are referred to the a' cell, several pseudo-periods along c are observed: one, $c''' = c/2$, in the case of bastnaesite; three, $c' = c/3$, $c'' = c/6$, and $c''' = c/18$, for parisite; two, $c' = c/3$, and $c''' = c/15$, for roentgenite; three, $c' = c/3$, $c'' = c/6$, and $c''' = c/12$, for synchisite. Oftedal's structural scheme is confirmed in its essentials. A linear relationship exists between c''' and the chemical composition.

Single crystals occur rarely. Most specimens are "polycrystals," syntaxic intergrowths of two species. Every pair has been observed, except bastnaesite-synchisite. Differential solubility in nitric acid reveals that the two species are in contact along an irregular surface or along repeated planes parallel to (0001). The complex morphology of these minerals, repeatedly discussed in the literature, is fully explained when the faces on the polycrystals are referred to the appropriate species. Indices of refraction are predicted in two ways:

---

* Publication authorized by the Director, U. S. Geological Survey.

(1) from ionic refractivities; (2) from form-birefrigence formulas, by letting slabs of the crystal structure be the components of Wiener's "mixed body." The indices thus predicted agree with those measured on specimens identified by *x*-rays.

INTRODUCTION

The main reason for undertaking this study was the promise it held of yielding additional information on syntaxic intergrowth, a phenomenon often mentioned in the literature since Ungemach coined the term *syntaxy* in 1935, and recently encountered in the andorite series (Donnay and Donnay, 1952). We are indebted to H. T. Evans, of the U. S. Geological Survey, for suggesting the problem to us. This work was completed as part of a program undertaken by the Geological Survey on behalf of the Division of Research of the Atomic Energy Commission.

The baffling morphology of parisite and related minerals, long a problem to crystallographers, had never been completely solved (Cesàro, 1907; Palache and Warren, 1911; Ungemach, 1935; Parker *et al*, 1939).

The question of the chemical composition of synchisite also required clarification. The formula for the mineral had been written[1] $CeFCO_3 \cdot CaCO_3$. It remained somewhat doubtful because, as was pointed out by H. Jaffe of the U. S. Geological Survey, the indices of refraction reported in the literature for synchisite ($CeFCO_3 \cdot CaCO_3$) and parisite ($2CeFCO_3 \cdot CaCO_3$) were almost identical. This similarity could not be reconciled with the difference in chemical composition. Moreover, Oftedal's calculations (1931b), by means of which he claimed to have confirmed the synchisite formula, were based on a specific gravity of 3.9 (determined by Flink, 1901, p. 35), whereas specific gravities as high as 4.15 were measured by us on crystals, small fragments of which were identified as synchisite by *x*-rays.

C. Frondel kindly placed at our disposal the material of the Harvard Museum, including some of the specimens measured and described by Palache and Warren (1911). G. Switzer made available to us all the relevant specimens of the U. S. National Museum. About 35 crystals were studied. They come from the following localities: Narsarsuk, Greenland; Quincy, Mass.; Muzo, Colombia; Pyrites, Mont.; Mountain Pass, Calif.; Bear Paw Mountains, Mont. More than 120 *x*-ray patterns were interpreted. They are rotation, precession, and Weissenberg photographs, taken with MoKα ($\lambda = 0.7107$ Å) or CuKα ($\lambda = 1.5418$ Å) radiation.

One of the results obtained was the discovery of a new mineral, roentgenite, $3CeFCO_3 \cdot 2CaCO_3$, the description of which has already been published (Gabrielle Donnay, 1953b).

---

[1] In this and all other formulas appearing in this paper, Ce actually stands for the rare earths of the cerium group.

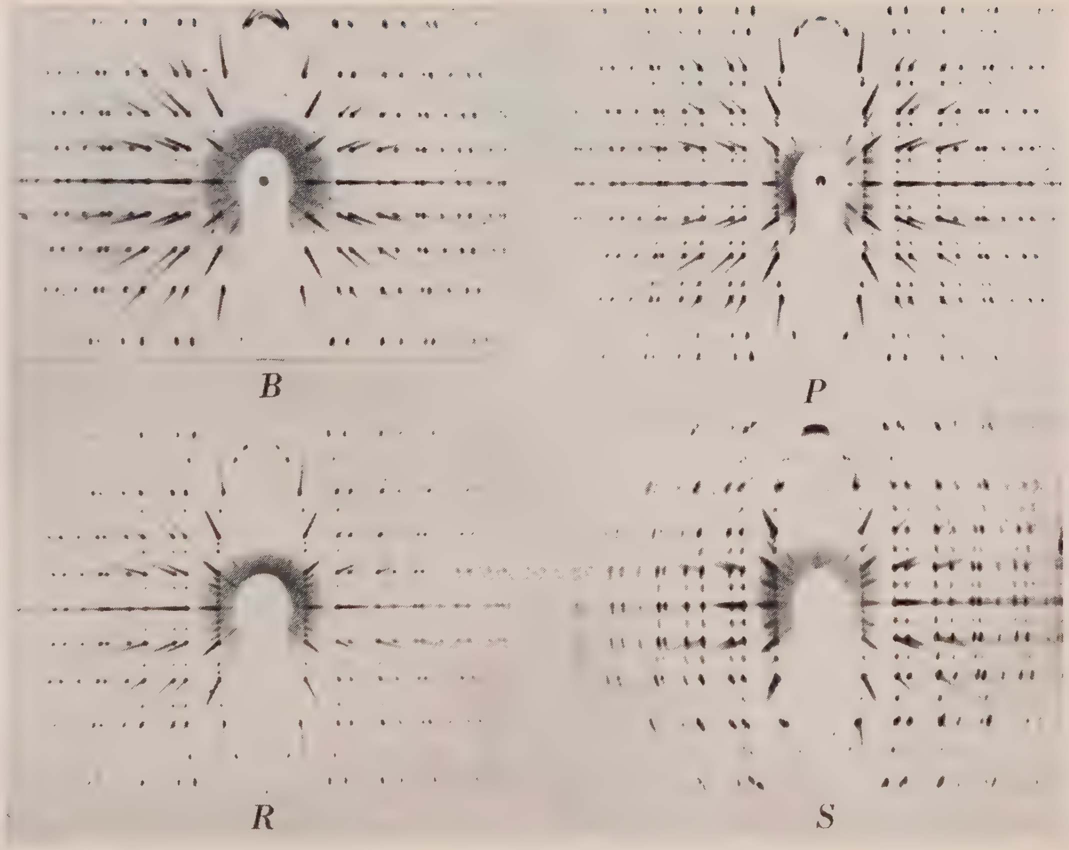

FIG. 1. Rotation photographs about the *c* axes of bastnaesite (B), parisite (P), roentgenite (R), synchisite (S). Note faint row lines which give true *a* axis. (MoKα radiation; 20-hour exposures.)

UNIT-CELL DIMENSIONS AND SYMMETRY

Some of the specimens examined give *x*-ray diffraction patterns that reveal only one crystalline species in a specimen. The data obtained from these single crystals will be presented first.

Rotation photographs about the *c* axes of the four species (Fig. 1) show the following *similarities*. (1) Intense row lines (reciprocal-lattice rows parallel to c^*) lead to a pseudo-axis a' of length 4.1 Å: very faint row lines give the true *a*, at 30° to a' and of length $4.1 \times 2 \cos 30^\circ = 7.1$ Å. The *a* lengths,[2] accurately determined from precession films, differ very little from species to species (Table 1). (2) The strongest layer lines (reciprocal-lattice nets perpendicular to *c*) correspond to a pseudo-period c''' decreasing from 4.9 to 4.6 Å from bastnaesite to synchisite. (3) An-

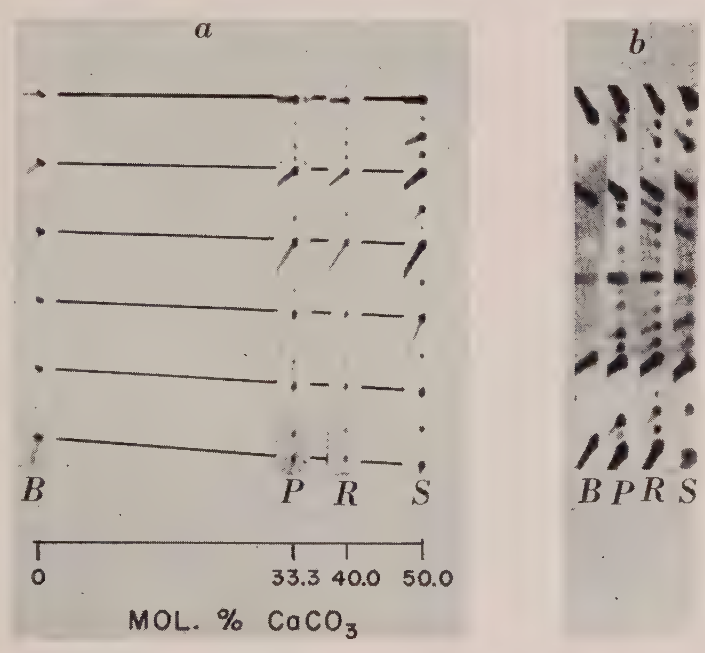

FIG. 2. Reflections $11\bar{2}l$ showing pseudo-period c'. (MoKα radiation; about 24-hour exposures.) (a) Reciprocal lattice rows from precession films mounted against composition to show linear variation of c'''^*. (b) Row lines of *c* axis rotation photographs.

---

[2] Oftedal recognized the true *a* of bastnaesite (1931a), but erroneously ascribed the faint row lines shown by parisite rotation patterns to a parallel intergrowth with a hypothetical substance, which he also postulated in synchisite (1931b, p. 444). Strunz (1949, p. 130) correctly transformed Oftedal's cells to the alternate setting, presumably to bring out the relationship with bastnaesite.

TABLE 1. CRYSTAL DATA

(All lengths expressed in Å units and known to ±0.3%)

	Bastnaesite $CeFCO_3$	Parisite $2CeFCO_3 \cdot CaCO_3$	Roentgenite $3CeFCO_3 \cdot 2CaCO_3$	Synchisite $CeFCO_3 \cdot CaCO_3$
a'	4.13_5	4.14_3[a] 4.11_3[b]	4.11_7	4.10_3
$a=a'\sqrt{3}$	7.16_2	7.17_6[a] 7.12_4[b]	7.13_1	7.10_7
c'''	4.89_4	4.67_3	4.62_7	4.56_0
c''	—	14.0_2 $c''=3c'''$	—	9.12_0 $c''=2c'''$
c'	—	28.0_4 $c'=6c'''$	23.1_4 $c'=5c'''$	18.2_4 $c'=4c'''$
c	9.78_7 $c=2c'''$	84.1_1 $c=18x'''$	69.4_1 $c=15c'''$	54.7_2 $c=12c'''$
c/a	1.36_7	11.7_2[a] 11.8_1[b]	9.73_3	7.69_9
Diffraction aspect (pseudo-cell $a'c'$)	C***	C***	C***	C***
Diffraction aspect (cell ac)	C**c	R**	R**	—
Laue class (cell ac)	$\frac{6}{m}\frac{2}{m}\frac{2}{m}$	$\bar{3}$	$\bar{3}$	—
Space group (cell ac)	$C\bar{6}2c$	R3	R3	Orthorhombic or monoclinic
Vol. of unit cell, V	217.4×2	208.4×18[a] 205.4×18[b]	203.8×15	199.5×12
Molecular weight, MW	219.14	538.37	857.60	319.23
Formula units/cell, Z	6	18	9	18
Spec. grav., G(calc.)	5.02	4.29[a] 4.35[b]	4.19	3.99
Spec. grav., G(obs.)[c]	4.78±0.1 4.99[d] 4.9–5.2[e]	4.05, 4.26, 4.39, 4.41, all±0.1	—	4.05, 4.15, all±0.1 3.902[f]

[a] Ordered.
[b] Disordered.
[c] Data probably obtained on polycrystals.
[d] Glass and Smalley (1945).
[e] Palache *et al.* (1951, p. 289).
[f] Flink (1901).

other well-marked pseudo-period, c'', is found in two of the species: in parisite, $c''=3c'''$, and in synchisite, $c''=2c'''$. (4) Every species save bastnaesite possesses yet another pseudo-period, c', which is not so easily recognized as c'' and is best seen on the first strong row line, consisting of reflections $11\bar{2}l$ (Fig. 2). Between the zero and first c''' layer line no such reflection appears on the bastnaesite pattern ($c'''=c'$); five reflections of medium-strong intensity appear on the parisite pattern

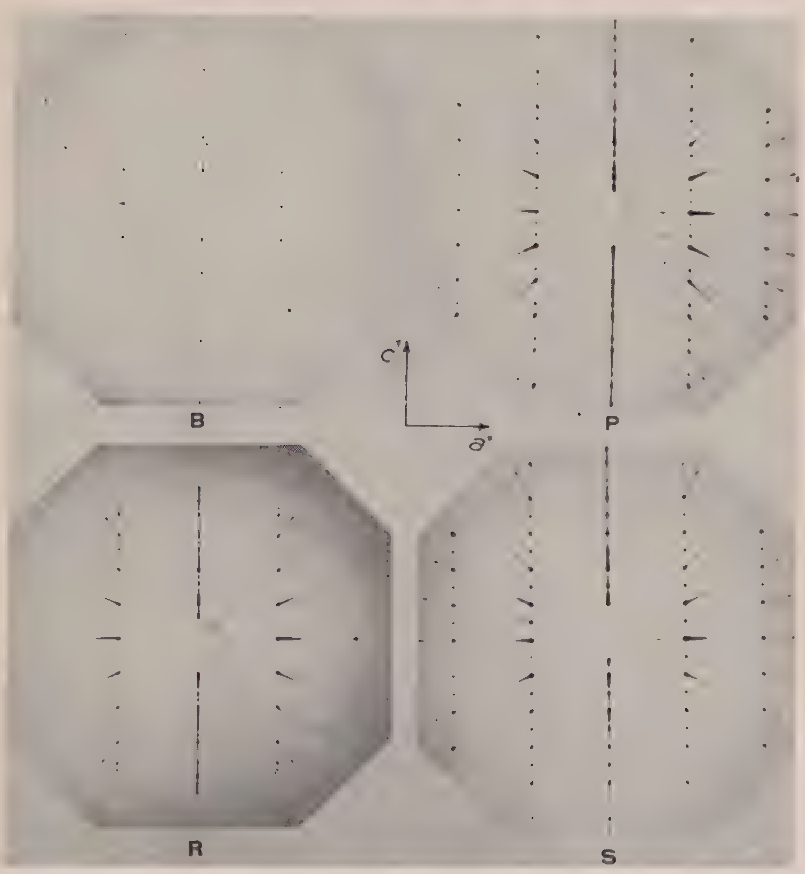

FIG. 3. Precession films of reciprocal lattice planes (010)*. Faint reflections, which lead to the true c period, appear on the row lines parallel to c^* for which $h \neq 3n$: (MoKα radiation; 24-hour exposures.)

($c' = 6c'''$); four on the roentgenite pattern ($c' = 5c'''$), and three on the synchisite pattern ($c' = 4c'''$). The true c values can be obtained from reflections that appear only on the faint row lines. They were measured on precession films exposed for about 24 hours (Fig. 3). For bastnaesite, $c = 2c'$. For the other three species $c = 3c'$. In terms of c''', $c = 18c'''$ for parisite, $c = 15c'''$ for roentgenite, and $c = 12c'''$ for synchisite.

The chemical compositions of only bastnaesite, $CeFCO_3$, and parisite, $2CeFCO_3 \cdot CaCO_3$, were well established when this study was begun (Palache, Berman and Frondel, 1951, p. 289, 282). With these formulas and the observed specific gravities (Table 1), the number of formula units in the true cell is found to be 6 for bastnaesite and 18 for parisite.

The diffraction aspect of every pseudo-cell $a'c'$ is C***; that of the true cell ac is C**c for bastnaesite and R** for parisite and roentgenite. The Laue class is $6/m\ 2/m\ 2/m$ for bastnaesite and $\bar{3}$ for parisite and roentgenite. The symmetry of synchisite is lower than hexagonal, either orthorhombic C-centered or monoclinic with an angle of 120°; even 40-hour exposures of upper levels on the precession camera did not bring out the faint reflections sufficiently to enable a decision to be reached. Morphological observations in the literature (Palache and Warren, 1911, Fig. 3), however, can be interpreted as due to orthorhombic symmetry. Bastnaesite is very strongly piezoelectric (Wooster, in Oftedal, 1931a, p. 465), so that the absence of a center of symmetry in its space group is established. The structural resemblance of the other three minerals to bastnaesite rules out centrosymmetric space groups for all of them. The symmetry of the true cell, $C\bar{6}2c$ (D_{3h}^4) for bastnaesite, $R3$ (C_3^4) for parisite and roentgenite, is obtained from structural considerations (see below, under crystal structure).

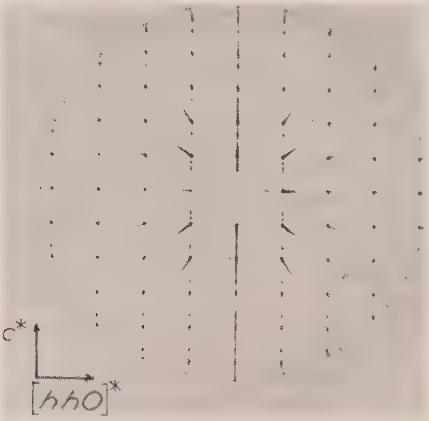

FIG. 4. Precession photograph of disordered parisite crystal from Quincy, Mass. (U. S. Nat. Mus. R2610). Note streaks, in addition to sharp reflections, parallel to c^*. (MoKα radiation; 16½-hour exposure.)

Two parisite crystals give diffraction patterns on which diffuse reflections, drawn out parallel to c^*, are superposed on the usual sharp reflections of every reciprocal-lattice row parallel to c^* (Fig. 4). Jagodzinski (1949) has shown that such a pattern is produced by disorder in the sequence of chemically different ordered layers. In this case the layers are perpendicular to c^*. Thus the two crystals examined belong to a disordered form. It is probable that they crystallized at elevated temperature. The *c* length is the same for the disordered form as for the ordered one, but the *a* lengths show a difference which, although small, is beyond experimental error (Table 1). It is probably accidental that disorder was observed in parisite only; roentgenite can be expected to show it too.

Syntaxic Intergrowths

The term *syntaxy* was coined by Ungemach (1935a, p. 184 and 187) by analogy with the term *epitaxy* previously introduced by Royer. Whereas epitaxy referred to an oriented overgrowth of one substance crystallizing on another, syntaxy was meant to designate the oriented intergrowth of two *chemically identical substances* alternating with each other, but having crystallized simultaneously, whose corresponding cell edges are in the ratio of small integers. Ungemach coined the term to describe the intergrowths of coquimbite and paracoquimbite (1935a, p. 165–190). As the surfaces of junction between constituents are planes (0001), he considered this kind of intergrowth a special case of epitaxy; in fact he writes (1935a, p. 184) that if the two minerals constituting the edifice were of different chemical compositions, he would consider the assemblage an example of repeated epitaxy.

In a subsequent paper Ungemach (1935b) looks for other examples of syntaxy. He stresses the fact that the phenomenon was already known in carborundum. He then describes parisite-synchisite intergrowths in great detail (1935b, pp. 6–18) and attempts to prove that they are syntaxic intergrowths, in his sense of the word. In effect he feels that the very occurrence of the intergrowths is in itself proof that the chemical compositions of the constituents must be identical. He, who as early as 1925 had suggested that synchisite as originally described should be split into two species (one of them parisite), now reverses his previous conclusion. A very searching morphological analysis leads him to distinguish three "polymorphs": "parisite α" (=synchisite), "parisite γ" (=parisite), and "parisite β," which we have been able to identify as being roentgenite.

Ungemach's definition of syntaxic intergrowth seems to be unduly restrictive, as this kind of intergrowth is found to occur also with *constituent substances that are chemically different.* We therefore propose to abandon the condition of identity of chemical compositions. Henceforth we shall use the term *syntaxy* in this extended meaning.

A large proportion of the "crystals" examined give *x*-ray patterns (Fig. 5) that reveal the co-existence of *two* crystalline species in syntaxic intergrowth. Indeed, the specimens discussed above, which give the diffraction pattern of a single species, may do so because only their very tip

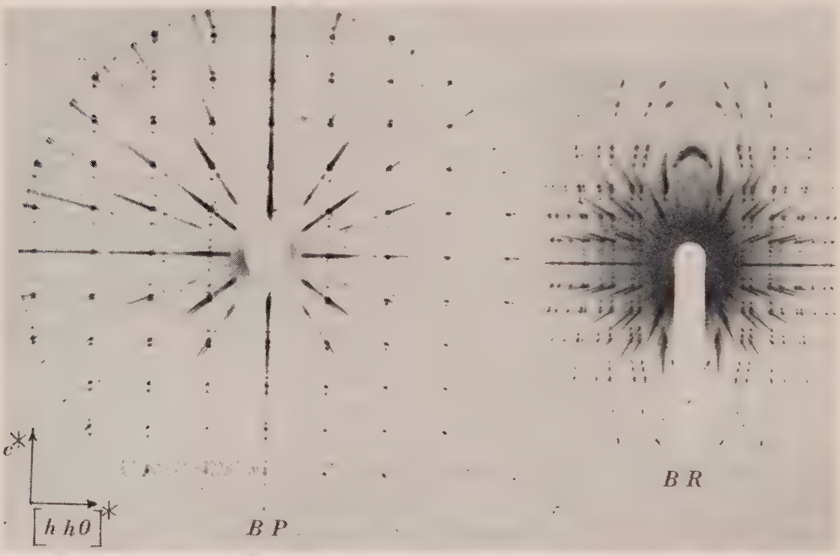

FIG. 5. Diffraction patterns of polycrystals. Left: Precession photograph of bastnaesite-parisite. Right: c-axis rotation photograph of bastnaesite-roentgenite. (MoKα radiation; 20-hour exposures.)

is bathed in the *x*-ray beam. There is morphological evidence that many of these specimens are also intergrowths. With the exception of the bastnaesite-synchisite combination, which has never been observed, all possible pairs have been found. It appears therefore that, in the group of minerals under investigation, syntaxic intergrowth can occur when the pseudo-periods c''' differ by as much as 5.5%, but it no longer occurs when the difference reaches 7.0%. The mutual orientation of the two species consists in a perfect parallelism of their coordinate axes. The a axes of the two species may have the same sense or opposite senses. In the latter case the two species are related to each other, like the two individuals of a twin, by a 60°-rotation about the 3-fold axis c. A parisite-roentgenite polycrystal (Harvard Museum No. 84233, labeled "synchisite" from Narsarsuk) showed this phenomenon. The *x*-ray reflections are sharp spots, indicating that each individual crystalline domain is at least 0.1 micron across. Streaks parallel to c^*, like those observed for pure parisite, were produced by one specimen from Montana (U. S. National Museum No. R84440), which was identified as an intergrowth of parisite and roentgenite. Whether the disorder occurs in the parisite, in the roentgenite, or in both was not determined.

Morphologically many of these intergrowths are not readily distinguishable from single crystals and have in fact often been referred to as "crystals" in the literature. As they are not homogeneous solids, this usage is unfortunate. To such an edifice, composed of two or more structurally distinct species in syntaxic intergrowth and simulating a single crystal, it has been found convenient to apply the term "polycrystal" (Gabrielle Donnay, 1953a).

The confusion that characterizes many morphological descriptions and which is emphasized by the etymology of the name synchisite—from the Greek word for "confounding"—is due to the prevalence of polycrystals. Most of the specimens lent to us, even carefully measured "crystals" described in the literature, were found on x-ray examination to be mislabeled. The morphology of these intergrowths is fully described by Ungemach (1935b); it will be explained in the section on morphology.

Occasionally an intergrowth is recognizable as such. In one case (Harvard Museum No. 84233 Narsarsuk) a parisite rhombohedron was attached to a bastnaesite prism. The surface of contact, henceforth referred to as interface, was planar but not a parting plane. The crystals were separated by a method described below. The other case is a group of a dozen intergrowths from a hand specimen of the U. S. National Museum (cordylite, R2613, Narsarsuk). Each intergrowth consists of a pyramid topped by a thin plate. The appearance, on a vastly smaller scale, recalls that of a tiny erosion pillar capped by a miniature mesa. The pyramid is a polycrystal of parisite and roentgenite, the plate is bastnaesite. Attempts to isolate the plate were unsuccessful because again the interface was not a plane of parting.

There exists a simple method of studying the physical nature of the intergrowth, based on the known differential solubility of the constituents. Bastnaesite is insoluble in concentrated cold acid, parisite dissolves slowly in it, roentgenite dissolves readily, and synchisite very quickly, even in dilute acid. The bastnaesite plate comes off easily when the intergrowth is dipped in concentrated nitric acid for a few minutes. Many of the polycrystals were observed under a binocular microscope while submerged in acid and afterwards again studied by x-rays. The dissolving of one of the forms could thus be verified. Two different types of syntaxic intergrowth appear, often on one and the same polycrystal. The one type (Fig. 6a) may be described as two-dimensional, because the interface is planar, parallel to (0001). The constituent layers vary from very thin to thick. This type of intergrowth is to be expected because the interface is the plane controlled only by the a axes, which are nearly identical for any two species. The second type (Fig. 6b) is three-dimensional; that is, the interface is irregular. By dissolving out the more soluble constituent, the acid leaves a deep crevice or a "drill hole" randomly oriented with respect to crystallographic directions.

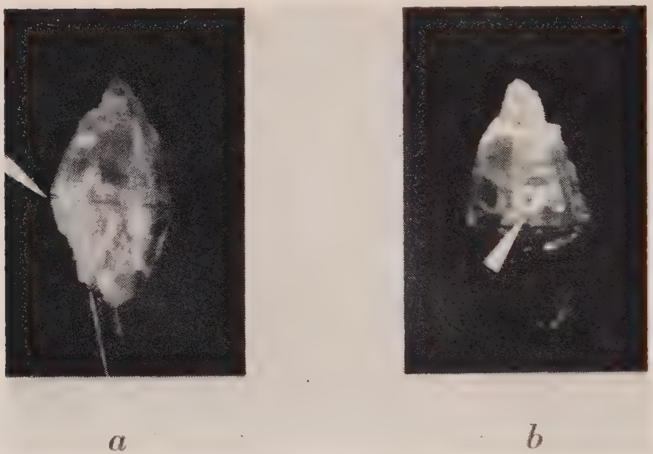

FIG. 6. Roentgenite-synchisite from Narsarsuk, Greenland. The polycrystal was dipped into dilute nitric acid for 10 minutes and synchisite dissolved out. (a) Two-dimensional intergrowth; interface is planar. (b) Three dimensional intergrowth; interface is irregular.

The frequent occurrence of polycrystals is an expression of the inability of the system $CeFCO_3$-$CaCO_3$ to form solid solutions. One crystal precipitates until the conditions in the solution have changed sufficiently for the next compound to separate out. The latter crystallizes on the original crystal. The two species alternate, so that periodic changes in the conditions of the system must be postulated. The two species do not necessarily have neighboring compositions on the phase diagram. These observations require conditions to change not only periodically but also discontinuously. Variations in the pH of the solution may well be the controlling factor during crystal growth, and dissolution of a large part of the polycrystal may account for the mushroom-like specimens. They would, at one time, have had the appearance of a single crystal yet have consisted of three species, a situation which would be expected to occur frequently but which has not been observed.

Another intergrowth of bastnaesite, namely with fluocerite (tysonite), CeF_3, has been described by Oftedal (1931c). Bastnaesite, in this case, is an alteration product of fluocerite.

THE CHEMICAL COMPOSITIONS OF ROENTGENITE AND SYNCHISITE

Because of the predominant occurrence of polycrystals, it would have been necessary to examine innumerable small crystals by x-rays in order to obtain enough pure material for chemical or spectroscopic analysis. Practical considerations, among them a lack of specimens, rendered such a procedure impossible. Crystallographic deductions, however, led to the chemical formulas.

All reflections *hkil* with (*h*-*k*) divisible by 3 are at least 100 times as intense as those for which (*h*-*k*) is not divisible by 3. It is safe to infer that the heavy cerium and calcium atoms do not contribute to the weak reflections and are therefore responsible for the pseudo-H-centering of the cell, which gives rise to the pronounced pseudo-period a', common to all four species. In other words, for every cerium or calcium atom in any site x, y, z, there must be two other atoms of the same metal at $x+\frac{2}{3}$, $y+\frac{1}{3}$, z and $x+\frac{1}{3}$, $y+\frac{2}{3}$, z. The structure thus contains horizontal layers of cations. Substitution of calcium and cerium for each other is ruled out because it would result in an increased intensity of the weak reflections. The pronounced pseudo-period c' indicates that the heavy atoms repeat along the z axis at intervals close in length to c'. In consequence the number of cerium atoms and that of calcium atoms in the pseudo-cell ac' must be multiples of 3.

The possibility must be considered that roentgenite and synchisite might be polymorphic forms of parisite, so that their compositions would

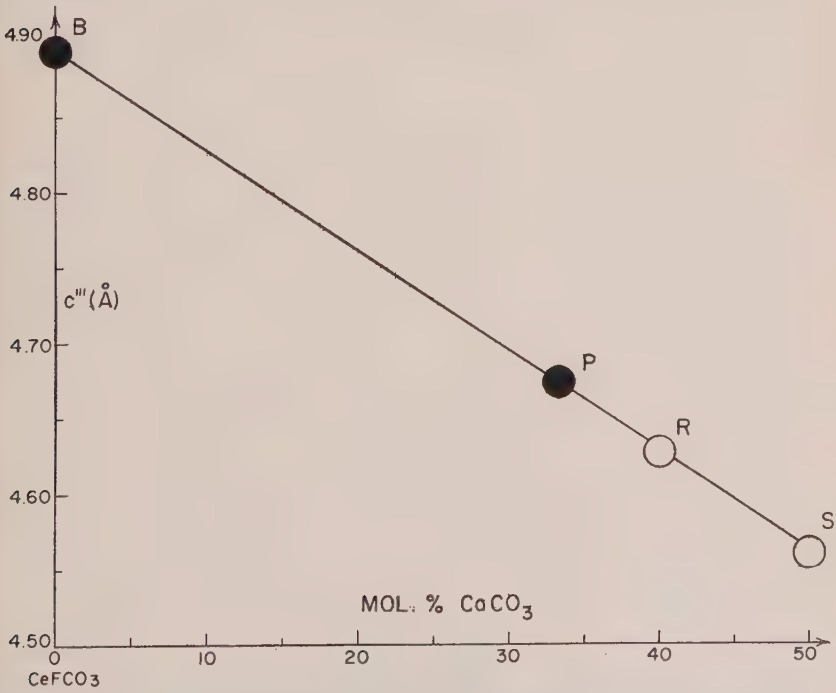

FIG. 7. Pseudo-period c'''(Å) plotted against composition expressed in mol. % $CaCO_3$. Black circles used to construct line; size of circles gives uncertainty of measurements.

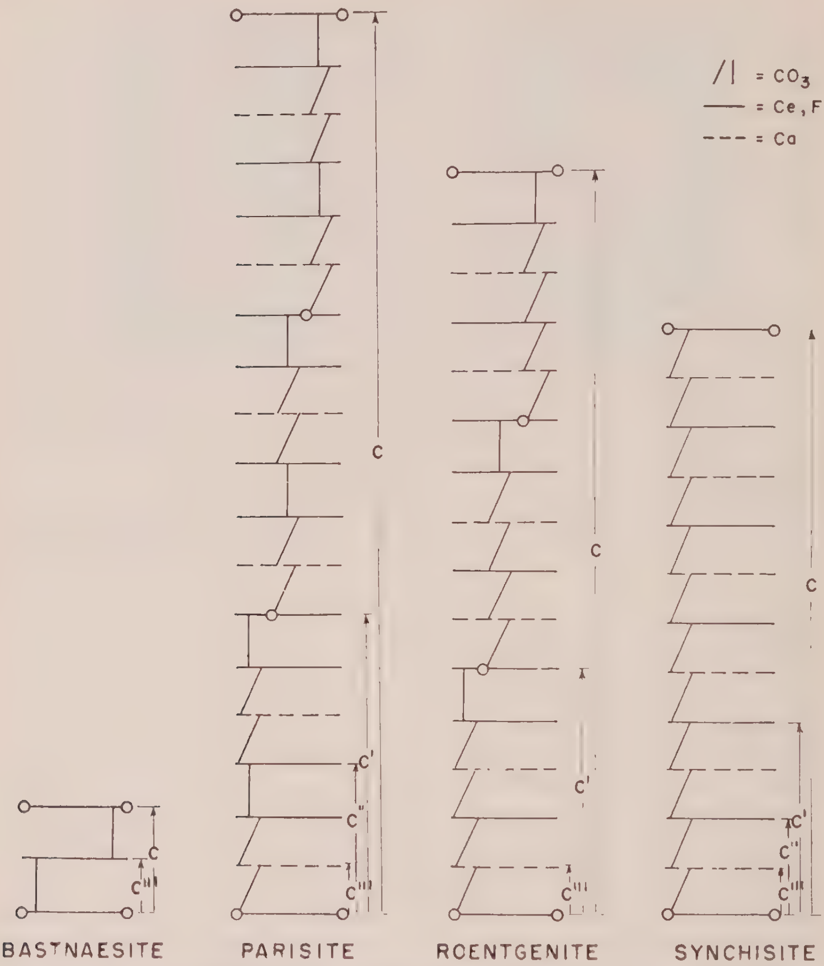

FIG. 8. Schematic representation of crystal structures. Rhombohedral lattice points are shown along diagonal of the rectangle.

be $Ce_2CaF_2(CO_3)_3$ or very close to it. With the measured specific gravities (Table 1), the contents of the cell ac' turn out to be $Ce_{10}Ca_5F_{10}(CO_3)_{15}$ for roentgenite and $Ce_8Ca_4F_8(CO_3)_{12}$ for synchisite. Neither 10, nor 5, nor 8, nor 4 is a multiple of 3! The hypothesis of polymorphism is thus ruled out.

How does the cell volume vary with composition? The smallest cell, namely $a'c'''$, is used as it probably contains the same number of cations in every species. The variation in a' from mineral to mineral is insignificant but that of c''' is not. Consequently c''' is plotted against composition, the latter being expressed in mol. % $CaCO_3$ (Fig. 7). A straight line is drawn through the two known points corresponding to bastnaesite and parisite. The observed c''' value of roentgenite, when placed on this line, gives a composition of 40.0 mol. % $CaCO_3$; that of synchisite gives 50.0% $CaCO_3$. In order to check the integral values found graphically, c''' values for these compositions are calculated from the equation of the line. For $3CeFCO_3 \cdot 2CaCO_3$ the calculated c''' is 4.629 Å as compared with the observed value of 4.627±0.015 Å; the calculated c''' value for $CeFCO_3 \cdot CaCO_3$ is 4.563 Å as compared with 4.560±0.015 Å.

The contents of the ac' cells calculated with the formulas thus obtained lead to 5 layers, 3 of cerium and 2 of calcium, in roentgenite; and 4 layers, 2 of cerium and 2 of calcium, in synchisite (Fig. 8). The observed pseudo-periods c' are thus explained, a fact which in itself is a confirmation of the chemical formulas. The chemical formulas are further supported by the excellent agreement between calculated and observed indices of refraction (to be discussed below). The comparison of observed and calculated specific gravities, commonly used to check the composition, cannot be relied on, because specimens large enough to be weighed on the Berman balance are likely to be polycrystals. The wide range of densities reported for bastnaesite and parisite (Table 1) bears out this statement.

Crystal Structure

The structural scheme of bastnaesite, parisite, and synchisite was predicted by Oftedal (1931a, b), and our structural hypothesis is essentially in agreement with his. He refers bastnaesite to the true cell ac and gives the correct space group $C\bar{6}2c$, which is derived from the morphological point group $\bar{6}2m$ and the space group extinctions ($hh\overline{2h}l$ absent when l

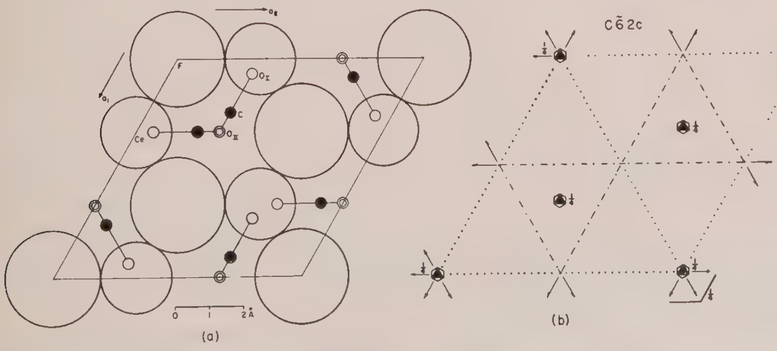

FIG. 9. (a) Fluorine-cerium layer at levels 0 and $\frac{1}{2}$ schematically showing positions of carbonate groups at heights $\frac{1}{4}$ (faint line) and $\frac{3}{4}$ (heavy line). (b) Space-group symmetry of $C\bar{6}2c$.

is odd). He refers parisite and synchisite to pseudo-cells, namely cells $a'c'$, but he does not specify the space groups.

In all four species cerium and fluorine ions alternate at the vertices of regular hexagons (Fig. 9). With the radii given in the literature, $r(Ce^{3+}) = 1.02$ Å (Zachariasen, 1948) and $r(F^-) = 1.36$ Å (Wells, 1950, p. 70), the side of the hexagon has length $1.02+1.36=2.38$ Å and the predicted cell edge a is $3\times 2.38=7.14$ Å. The observed a ranges from 7.11 ± 0.02 Å for synchisite to 7.18 ± 0.02 Å for parisite. In the crystal structures of parisite, roentgenite, and synchisite, calcium layers alternate with cerium-fluorine layers in various proportions (Fig. 8). Calcium ions are placed above cerium ions. The disordered crystal structures of parisite (Fig. 4) and of the parisite-roentgenite polycrystal result from irregularities in the sequence of these layers. The decreased a value of the disordered parisite may be ascribed to a slight displacement of fluorine and cerium with respect to each other, so they no longer lie in one horizontal plane. Bastnaesite cannot show disorder of this kind as it contains only cerium-fluorine layers. In synchisite the disordered form would have to contain calcium layers adjacent to each other; the nearly vertical positions of the carbonate groups between the layers (see below) makes such an arrangement very unlikely.

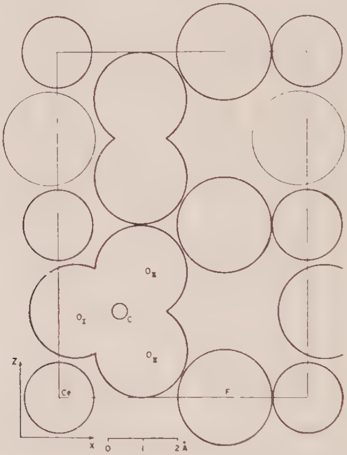

FIG. 10. Vertical section of bastnaesite structure by plane $y=\frac{1}{3}$. Light circles show neighboring oxygen atoms.

Oftedal refers the crystal structure of parisite to a pseudocell (a', $c'/2$) that contains one formula unit of $2CeFCO_3 \cdot CaCO_3$. He states (1931b, p. 448, last line) that calcium at the origin is the only choice permitted by all possible space groups: $C\bar{6}m2(D_{3h}^1)$, $C\bar{6}2m(D_{3h}^3)$, $C6mm$

(C_{6v}^1), C622(D_6^1), and C6/*mmm*(D_{6h}^1). He overlooks the fact that $C\bar{6}m2$ offers the one-fold position 1(*c*): $\frac{1}{3}$, $\frac{2}{3}$, 0. He places cerium (not fluorine) above the origin, at 00*u* in parisite, at 00$\frac{1}{4}$ in synchisite. In his paper on bastnaesite he stated that interchanging the cerium and the fluorine ions would not appreciably alter his proposed structure (1931a, p. 469). We are very grateful to H.T. Evans, of the Geological Survey, for pointing out to us that the two resulting structures differ radically. Indeed with cerium above the origin no structure will give acceptable interatomic distances for any of the species, whereas with fluorine above the origin the intensities of medium-strong and strong reflections are accounted for and reasonable interatomic distances are obtained (Table 3). The frequent occurrence of intergrowths also supports the identical choice of origin in the four crystal structures, because with this choice a number of cerium-fluorine layers can extend throughout the polycrystal (Fig. 6).

TABLE 2. ATOMIC PARAMETERS PREDICTED FOR BASTNAESITE
Space Group $C\bar{6}2c$ (D_{3h}^4); 6$CeFCO_3$ per Cell

Atom	Position	Atomic sites	Atomic parameters	
			Oftedal	Donnay
F	2(*a*)	0, 0, 0; 0, 0, $\frac{1}{2}$	—	—
F	4(*f*)	$\frac{1}{3}, \frac{2}{3}, z; \frac{2}{3}, \frac{1}{3}, \bar{z}; \frac{2}{3}, \frac{1}{3}, \frac{1}{2}+z; \frac{1}{3}, \frac{2}{3}, \frac{1}{2}-z.$	$z\approx 0$	$z\approx 0$
Ce	6(*g*)	$x, 0, 0; 0, x, 0; \bar{x}, x, 0;$ $x, 0, \frac{1}{2}; 0, x, \frac{1}{2}; \bar{x}, \bar{x}, \frac{1}{2}.$	$x=\frac{1}{3}$	$x=0.333$
C	6(*h*)	$x, y, \frac{1}{4}; \bar{y}, x-y, \frac{1}{4}; y-x, \bar{x}, \frac{1}{4};$ $y, x, \frac{3}{4}; \bar{x}, y-x, \frac{3}{4}; x-y, \bar{y}, \frac{3}{4}.$	—	$x=0.245; y=0.333$
O_I	6(*h*)	as above	—	$x=0.067; y=0.333$
O_{II}	12(*i*)	$x, y, z; \bar{y}, x-y, z; y-x, \bar{x}, z;$ $x, y, \frac{1}{2}-z; \bar{y}, x-y, \frac{1}{2}-z; y-x, \bar{x}, \frac{1}{2}-z;$ $y, x, \frac{1}{2}+z; \bar{x}, y-x, \frac{1}{2}+z; x-y, \bar{y}, \frac{1}{2}+z;$ $y, x, \bar{z}; \bar{x}, y-x, z; x-y, \bar{y}, \bar{z}.$	—	$x=0.333; y=0.333$ $z=0.138$

As the symmetry of bastnaesite is such that, with the help of known ionic radii, one can predict the coordinates of *all* the atoms (Table 2), we shall discuss this structure in detail. There are six formula units of $CeFCO_3$ per cell. Fluorine ions are placed at 2(*a*):0, 0, 0 and 4(*f*): $\frac{1}{3}$, $\frac{2}{3}$, *z*, with $z=0.0$ (Int. Tab. 1935, I,279); cerium ions are in position 6(*g*):*x*, 0, 0 with $x=0.333$. The three oxygen atoms of the carbonate group are assumed to be at the vertices of an equilateral triangle, with carbon at the center and the carbon-oxygen distance d_{C-O} equal to 1.27 Å (Zachariasen, 1933). The six carbon atoms and six of the oxygen atoms, referred to as O_I's, can only be placed in positions 6(*h*):*x*, *y*, $\frac{1}{4}$, on the horizontal mirrors. The remaining twelve oxygen atoms lie in 12 (*i*):*x*, *y*, *z*. Let us

TABLE 3. INTERATOMIC DISTANCES PREDICTED FOR BASTNAESITE

(Lengths in Å units)

Ce–F	2.39
Ce–O_I	2.49
Ce–O_{II}	2.74
F–O_{II}	2.74
C–O_I or $_{II}$ (intra-ionic)	1.27
O_{II}–O_I or $_{II}$ (intra-ionic)	2.19
O_{II}–O_{II} (inter-ionic)	2.70

The same distances are also predicted for corresponding layers in the structures of parisite and roentgenite.

call them O_{II}. From the size of the carbonate group, their z parameter is fixed at 0.13_8. O_{II} is placed on the vertical line through the center of the hexagon outlined by fluorine and cerium (Fig. 10), namely at $x=0.333$, $y=0.333$, $z=0.138$, O_{II} is thus at a distance of 2.74 Å from each of the three fluorine ions. Using the fluorine radius of 1.36Å, the oxygen radius found by subtraction is 1.38 Å, a value that falls well within the range reported in the literature (Evans, 1946, p. 171, gives 1.32 Å; Wells, 1950, p. 70, gives 1.40 Å, for the radius of $O^=$ in 6-fold coordination). Any displacement of O_{II} in x or y would decrease one of the fluorine-oxygen distances, but any distance smaller than 2.74 Å is unlikely. The O_{II}'s should thus lie on (or very nearly on) the c glide plane. As far as they are concerned, the glide reduces to a translation $c/2$. In consequence the O_{II}'s will not contribute to reflections *hkil* with l odd; only O_I and carbon are responsible for these reflections. This conclusion agrees with the observation that the ratio of faint to strong intensities is considerably smaller for bastnaesite than for the other species, in which some of the O_{II}'s do contribute to the faint reflections. Equating the height of the carbonate group to the pseudo-period c''' yields an oxygen radius for O_{II} equal to 1.35 Å (Fig. 10).

The distance between O_{II} and Ce is, of course, the same as between O_{II} and F, namely 2.74 Å. This is a large value, as the sum of the ionic radii of $O^=$ and Ce^{3+} is only 2.40 Å. The bonds Ce$-O_{II}$ must therefore be weak ones; to a first approximation, they may be neglected. Ce is thus left with two positive charges after we subtract the three bonds of strength $\frac{1}{3}+$ each, which go to the neighboring fluorine ions. Cerium can therefore be expected to attract O_I as close to itself as possible. In other words C and O_I will, in horizontal projection, lie on a straight line $O_{II}-$Ce.

There are three such lines: two of them parallel to the cell edges and the third one coincident with the trace of the *c* glide plane. Placing the carbonate group on the *c* glide plane would mean that it would be repeated, by translation *c*/2, in the upper half of the cell. The cell height would then have to be *c*/2 instead of *c*, which would be contrary to fact. The carbonate group will, therefore, be projected on a line parallel to a cell edge; another carbonate group, related to the first one by a glide-reflection, will be projected parallel to the other cell edge. C is placed at $x=0.245$, $y=0.333$, $z=\frac{1}{4}$ and O_I at $x=0.067$, $y=0.333$, $z=\frac{1}{4}$. The $\text{Ce}-\text{O}_\text{I}$ distance is 2.49 Å. The $\text{Ce}-\text{O}_\text{I}$ bonds form vertical zigzag chains: one in the plane $y=\frac{1}{3}$, others in the planes symmetrical to it (Fig. 10). Again ignoring the bonds $\text{Ce}-\text{O}_\text{II}$, each Ce gives two bonds, each of strength 1+, to the O_I's, and each O_I receives two such bonds. Thus the total charge on the carbonate group is neutralized. The strength of these vertical bonds accounts for the observed lack of cleavage (0001). It was not possible to check by structure-factor calculations the proposed orientation of the carbonate groups because the reflections *hkil* with *l* odd are barely visible and the contributions of C and O_I to the other reflections

TABLE 4. ATOMIC PARAMETERS PREDICTED FOR PARISITE AND ROENTGENITE
space groups R3 (C_3^4): 18,[$2\text{CeFCO}_3\cdot\text{CaCO}_3$] per unit cell of parisite;
9[$3\text{CeFCO}_3\cdot2\text{CaCO}_3$] per unit cell of roentgenite

Atom	Position	Atomic sites ($0, 0, 0; \frac{1}{3}, \frac{2}{3}, \frac{2}{3}; \frac{2}{3}, \frac{1}{3}, \frac{1}{3}$)+	Atomic parameters	
			Parisite	Roentgenite
F	3(a)	$0, 0, z$.	$z=0$; 0.333; 0.667; 0.108; 0.441; 0.775; 0.167; 0.500; 0.834; 0.275; 0.608; 0.942.	$z=0$; 0.333; 0.667; 0.131; 0.464; 0.798; 0.263; 0.596; 0.930.
Ce	9(b)	x, y, z; $\bar{y}, x-y, z$; $y-x, \bar{x}, z$.	$x=0.333, y=0, z=0$; $x=0.333, y=0, z=0.108$; $x=0.333, y=0, z=0.167$; $x=0.333, y=0, z=0.275$.	$x=0.333, y=0, z=0$; $x=0.333, y=0, z=0.131$; $x=0.333, y=0, z=0.263$.
Ca	9(b)	x, y, z; $\bar{y}, x-y, z$; $y-x, \bar{x}, z$.	$x=0.333, y=0, z=.054$; $x=0.333, y=0, z=0.221$.	$x=0.333, y=0, z=0.066$; $x=0.333, y=0, z=0.197$.
C	9(b)	x, y, z; $\bar{y}, x-y, z$; $y-x, \bar{x}, z$.	$x=0.245, y=0.333, z=0.138$; $x=0.245, y=0.333, z=0.304$; x_n, y_n, z_n; $n=1$ to 4.	$x=0.245, y=0.333, z=0.298$; x_n, y, z_n; $n=1$ to 4.
O	9(b)	x, y, z; $\bar{y}, x-y, z$; $y-x, \bar{x}, z$.	$x=0.067, y=0.333, z=0.138$; $x=0.067, y=0.333, z=0.304$; $x=0.333, y=0.333, z=0.124$; $x=0.333, y=0.333, z=0.151$; $x=0.333, y=0.333, z=0.291$; $x=0.333, y=0.333, z=0.317$; x_n, y_n, z_n; $n=1$ to 12.	$x=0.067, y=0.333, z=0.298$; $x=0.333, y=0.333, z=0.282$; $x=0.333, y=0.333, z=0.314$; x_n, y_n, z_n; $n=1$ to 12.

are insignificant as compared with the contributions of cerium.

For the same reason it is impossible to determine all the atomic coordinates in the three remaining structures. In the cases of parisite and roentgenite, the true space group can be derived as follows. The Laue class is $\bar{3}$ and the diffraction aspect R**. The atomic arrangements in the cerium-fluorine layer, in the calcium layer, and in the interlayer rule out the center of symmetry. The space group is uniquely determined as R3.

For the crystal structures of parisite and roentgenite, the atomic coordinates of fluorine, cerium, calcium, and those carbonate groups that lie between two cerium-fluorine layers can be predicted (Table 4). If the distance between cerium-fluorine layers in bastnaesite, equal to 4.89 Å, is assumed to hold true for parisite, roentgenite, and synchisite, the calculated distance between cerium-fluorine layer and calcium layer is 4.56 Å in all three structures. The normal to the plane of a carbonate group between two chemically different layers must therefore make an angle of about 79° with the vertical ($\sin 11° \approx 4.56/4.89$).

Considering the structural scheme of these minerals, $m\mathrm{CeFCO_3} \cdot n\mathrm{CaCO_3}$, one can see no reason why values of m/n different from ∞, 2, $\frac{3}{2}$, and 1 cannot exist. Even solid solution resulting in a disordered crystal structure can be envisioned. There exists, however, no x-ray evidence of more than four species. Compositions richer in calcium than synchisite with analogous crystal structures are not to be expected. Their structures would have to contain adjacent calcium layers, and with the nearly vertical arrangement of the carbonate groups, the calcium coordination number would be too low. Carbonate groups parallel to the calcium layers, as for example in calcite, would be predicted.

CRYSTAL MORPHOLOGY

Now that the four species can be unequivocally referred to their true cells by x-rays, it is possible in each case to ascertain which cell governs the morphological development. The goniometric data of Palache and Warren (1911) are interpreted in Table 5. The polycrystals they measured did not contain any bastnaesite, but their measured angles are found among the calculated angles of all three remaining species. In view of the difficulties encountered in measurement, the agreement between their measured angles and our calculated angles is truly remarkable. It bears witness to the skill and accuracy of these old-time crystallographers.

Bastnaesite

The morphology is controlled by the true cell *ac* and has point-group symmetry $\bar{6}2m$. Most crystals are tabular on c {0001}. One crystal from

Gaines Mountain, Muzo, Colombia (Harvard Museum No. 11019), is short prismatic in habit, with a large trigonal prism *a* $\{2\bar{1}\bar{1}0\}$, a small hexagonal prism *m* $\{10\bar{1}0\}$, and three hexagonal dipyramids: *q* $\{10\bar{1}1\}$, *p* $\{10\bar{1}2\}$, *t* $\{10\bar{1}3\}$. Measurements from excellent reflections give $\rho\ (10\bar{1}1) = 57°42'$ and $\rho\ (10\bar{1}2) = 38°19'$, from which we calculate $c/a = 1.369$, in agreement with 1.367, the ratio of the cell edges obtained by *x*-rays.

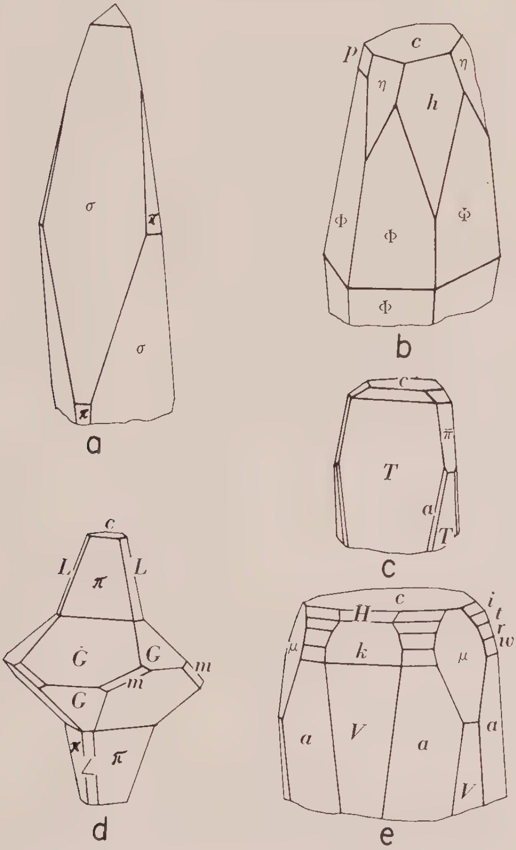

FIG. 11. (a) Parisite (after Palache and Warren, 1911).—(b) Parisite (after Cesàro, 1907).—(c) Roentgenite (after Palache and Warren, 1911).—(d) Intergrowth: synchisite between roentgenite tips (Flink, 1901).—(e) Synchiste (after Palache and Warren, 1911).

The morphological space group is $C\bar{6}2c(D_{3h}^4)$, found as follows: the lattice cannot be rhombohedral because the dipyramids violate the R-criterion, "$(-h+k+l)$ divisible by 3"; the *c* glide plane is required by the form *s* $\{11\bar{2}2\}$, which is reported in the literature and obeys the *L*-criterion, "*l* even." Palache *et al* (1951, p. 289) erroneously gives $C\bar{6}c2$ (D_{3h}^2) as the space group, with $\bar{6}m2$(?) as the point group.

Parisite

There is no obvious morphological feature that would necessitate lowering the point-group symmetry below $\bar{3}2/m$. The morphology is *not* controlled by the true cell *ac*; the morphological axial ratio is either $\frac{1}{2}\,c/a$ or $\frac{1}{4}\,c/a$. In each case the indices can be made to obey the R-criterion. The series of forms obtained with $\frac{1}{2}\,c/a$ (see Table 5) contain several forms that have not been reported by Palache and Warren (1911). The alternate axial ratio, $\frac{1}{4}\,c/a$, would bring about some simplification, but it is difficult to decide between the two. Tentatively we have adopted $\frac{1}{2}\,c/a$. The rhombohedra that are positive with the ratio c/a or $\frac{1}{4}\,c/a$ must become negative with the ratio $\frac{1}{2}\,c/a$ in order to obey the R-lattice criterion (see Table 5). For example: h $\{10\bar{1}4\}$ or $\{10\bar{1}1\}$ becomes $\{01\bar{1}2\}$.

A typical parisite crystal from Quincy Mass. (Fig. 11a), is reproduced from Palache and Warren (1911). Its dominant rhombohedron should be lettered σ $\{10\bar{1}1\}$. The parisite crystal from Muzo (Fig. 11b) described by Cesàro (1907) can be indexed as follows: ϕ $\{22\bar{4}3\}$, h $\{01\bar{1}2\}$, η $\{20\bar{2}5\}$, σ $\{10\bar{1}1\}$, c $\{0003\}$, p $\{11\bar{2}3\}$.

The dominant rhombohedron of a crystal from Narsarsuk, Greenland (Harvard Museum No. 84233) gave a ρ angle of 73°38′. It should be indexed h $\{01\bar{1}2\}$. It yields an axial ratio equal to $\frac{1}{2}\times 11.796$, as compared with 11.722 and 11.807, found by *x*-rays for the ordered and the disordered form, respectively, which correspond to ρ angles of 73°32′ and 73°39′. We checked by *x*-rays that the symbol of this rhombohedron would be $\{10\bar{1}4\}$ if it were referred to the structural c/a.

This parisite specimen is twinned by reticular merohedry. The twinned crystal consists of at least three horizontal slices intercalated in the main crystal. The composition surface is planar, parallel to the base. The rhombohedron σ $\{10\bar{1}1\}$, with measured ρ of 81°35′, is brought in zone with h $\{01\bar{1}2\}$ by twinning.

Roentgenite

The rhombohedral lattice obtained by *x*-rays manifests itself in the morphology. Referred to the true cell *ac*, determined by *x*-rays, the forms are: T $\{1011\}$ dominant, π $\{01\bar{1}2\}$, c $\{0001\}$ subordinate. These forms obey the R-criterion, "$(-h+k+l)$ divisible by 3," provided the base is written $\{0003\}$, as it should be, in view of its relatively small size. This indexing of forms is compatible with the diffraction aspect R**.

The same relative importance of the forms could, however, also be expressed by indexing them as follows: T $\{01\bar{1}2\}$, π $\{10\bar{1}4\}$, c $\{0006\}$, and by doubling the axial ratio. In this case the aspect would have to be R**c*.

The morphological *c* cannot be twice the structural *c*, because crystal

Measured ρ angles and no. of crystals (Palache and Warren, 1911)	Calculated ρ angles							
	Bastnaesite		Parisite		Roentgenite		Synchisite	
	$\frac{c}{a}=1.369$		$\frac{1}{2}\left(\frac{c}{a}\right)=\frac{11.722}{2}$ to $\frac{11.807}{2}$		$\frac{c}{a}=9.732$		$\frac{c''}{a'}=2.223$	
A 29° 9′(57′–35′) 4			$1.1.\bar{2}.21$	29°10′	$0.1.\bar{1}.20$	29°20′	A $11\bar{2}8$	29° 5′
β 30°44′(28′–56′) 8					$1.1.\bar{2}.33$	30°32′		
B 30°34′(24′–49′)11					B $1.0.\bar{1}.19$	30°36′		
C 31°41′(30′–50′) 9			C $0.1.\bar{1}.11$	31°36′–47′				
γ 32°29′(20′–41′) 8							γ $11\bar{2}7$	32°25′
							$10\bar{1}4$	32°41′
					$1.1.\bar{2}.30$	32°59′		
			$1.1.\bar{2}.18$	33° 7′–16′				
D 33°36′(20′–51′) 4					D $0.1.\bar{1}.17$	33°28′		
δ 33°45′(22′–34′)19			δ $1.0.\bar{1}.10$	34° 5′–17′				
	$11\bar{2}4$	34°25′						
E 34°57′(20′–80′)10					E $1.0.\bar{1}.16$	35° 5′		
					$1.1.\bar{2}.27$	35°48′		
F 36°54′(......) 3							F $11\bar{2}6$	36°33′
			$1.1.\bar{2}.15$	38° 0′–13′				
	$10\bar{1}2$	38°20′						
ε 38°47′(25′–62′)23					ε $0.1.\bar{1}.14$	38°45′		
					$1.1.\bar{2}.24$	39° 3′		
d 40° 2′(53′–21′) 1			d $01\bar{1}8$	40°13′–27′				
G 40°48′(40′–56′) 6					G $1.0.\bar{1}.13$	40°51′	G $10\bar{1}3$	40°33′
H 41°40′(25′–58′) 8							H $11\bar{2}5$	41°39′
	$11\bar{2}3$	42°24′						
					$1.1.\bar{2}.21$	42°50′		
			$10\bar{1}7$	44° 2′–13′				
			$1.1.\bar{2}.12$	44°20′–33′				
					$0.1.\bar{1}.11$	45°37′		
b 45°47′(......) 1							b $20\bar{2}5$	45°45′

TABLE 5. (*Continued*)

	Measured ρ angles and no. of crystals (Palache and Warren, 1911)	Calculated ρ angles							
		Bastnaesite		Parisite		Roentgenite		Synchisite	
		$\frac{c}{a}=1.369$		$\frac{1}{2}\left(\frac{c}{a}\right)=\frac{11.722}{2}$ to $\frac{11.807}{2}$		$\frac{c}{a}=9.732$		$\frac{c''}{a'}=2.223$	
		$20\bar{2}3$	46°31′						
						1.1.2.18	47°15′		
e	48° 4′(54′–14′) 5							*e* *ζ* $11\bar{2}4$	48° 2′
ζ	47°54′(47′–60′) 5								
						1.0.1.10	48°20′		
i	52°10′(45′–36′)18			*i* $11\bar{2}9$	52°30′–42′	*i* 1.1.$\bar{2}$.15	52°21′	*i* $10\bar{1}2$	52° 5′
				$01\bar{1}5$	53°33′–45′				
		$11\bar{2}2$	53°52′						
θ	54°35′(13′–52′) 4					*θ* $01\bar{1}8$	54°35′		
								$11\bar{2}3$	55°59′
l	57°33′(30′–43′) 4			*l* 2.2.$\bar{4}$.15	57°24′–36′				
		$10\bar{1}1$	57°42′						
I	58°21′(18′–24′) 5					*I* $10\bar{1}7$	58° 5′		
n	58°23′(11′–36′) 9					*n* 1.1.$\bar{2}$.12	58°21′		
f	59°44′(. . . . . .) 3			*f* $10\bar{1}4$	59°24′–36′				
t	59°45′(34′–60′)10							*t* $20\bar{2}3$	59°42′
J	62°54′(43′–58′) 3			*J* $02\bar{2}7$	62°39′–49′				
q	62°47′(. . . . . .) 4			*q* $11\bar{2}6$	62°54′–64′				
		$40\bar{4}3$	64°38′						
u	65°14′(11′–18′) 2					*u* $11\bar{2}9$	65°11′		
g	65°53′(48′–57′) 3					*g* $01\bar{1}5$	66° 1′	*g* $11\bar{2}2$	65°47′
		3032	67° 8′						
r	68°48′(36′–60′)10			*r* $22\bar{4}9$	69° 0′– 8′			*r* $10\bar{1}1$	68°43′
η	69°47′(42′–52′) 1			*η* $20\bar{2}5$	69°44′–52′				
		$11\bar{2}1$	69°57′						
L	70°22′(56′–40′) 5					*L* $10\bar{1}4$	70°25′		

Measured ρ angles and no. of crystals (Palache and Warren, 1922)	Bastnaesite $\frac{c}{a}=1.369$		Parisite $\frac{1}{2}\left(\frac{c}{a}\right)=\frac{11.722}{2}$ to $\frac{11.807}{2}$		Roentgenite $\frac{c}{a}=9.732$		Synchisite $\frac{c''}{a'}=2.223$	
M 71°23′(10′–35′) 2							*M* $22\bar{4}3$	71°21′
	$20\bar{2}1$	72°28′						
v 72°58′(48′–64′) 6					*v* $11\bar{2}6$	72°52′		
h 73°35′(27′–45′) 6			*h* $01\bar{1}2$	73°32′–39′				
p 75°21′(59′–43′) 3			*p* $11\bar{2}3$	75°39′–45′				
	$50\bar{5}2$	75°48′						
N 76°18′(13′–28′) 6	$33\bar{6}2$	76°19′						
k 77°27′(14′–35′)10					*k* $20\bar{2}5$	77°27′	*k*, *μ* $11\bar{2}1$	77°19′
μ 77°23′(0′–60′)10								
	$30\bar{3}1$	78° 6′						
w 79° 1′(48′–23′) 9							*w* $20\bar{2}1$	78°59′
π 80° 2′(45′–25′)16	$22\bar{4}1$	73°39′	*π* $04\bar{4}5$	79°32′–37′	*π* $01\bar{1}2$	79°54′		
P 80°52′(50′–54′) 4							*P* $44\bar{8}3$	80°25′
	$40\bar{4}1$	81° 1′			$11\bar{2}3$	81°14′		
S 81°40′(32′–51′) 4							*S*, *σ* $33\bar{6}2$	81°29′
σ 81°42′(24′–55′)11			*σ* $10\bar{1}1$	81°35′–39′				
Q 82°17′(4′–25′) 5							*Q* $5.5.\overline{10}.3$	82°18′
o 82°30′(......) 2							*o* $30\bar{3}1$	82°37′
φ 82°55′(53′–58′) 2	$50\bar{5}1$	82°48′	*φ* $22\bar{4}3$	82°42′–46′				
	$33\bar{6}1$	83° 4′						
R 83°32′(22′–45′) 8							*R*, *ρ* $22\bar{4}1$	83°35′
ρ 83°22′(23′–48′) 4								
T 84°53′(34′–69′)14					*T* $10\bar{1}1$	84°55′	$40\bar{4}1$	84°26′
ψ 84°36′(17′–50′) 5					*ψ* $03\bar{3}3$	84°55′		
V 85°39′(21′–58′) 6			*V* $02\bar{2}1$	85°46′–48′			*V*, *ω* $33\bar{6}1$	85°43′
ω 85°38′(5′–60′) 3								
							$44\bar{8}1$	86°47′
					$02\bar{2}1$	87°27′		
			$40\bar{4}1$	87°53′–54′				

structure restricts symmetry more—not less—than crystal morphology. It is difficult to see, from the structural scheme considered above, how $a/2$ could be a pseudo-period. It follows that the morphological c/a is the same as the structural c/a. The series of forms obtained with the structural c/a (Table 5) are satisfactory.

The angle measurement on a crystal from Narsarsuk (U. S. National Museum No. R 2613) were poor on T faces, good on π faces. Whereas the axial ratio $c/a = 9.733$ obtained by x-rays requires ρ $(01\bar{1}2)$ to be 79°54′, the measured value is equal to $79°55\frac{1}{2}' \pm 2'$. The corresponding morphological ratio is 9.749 ± 0.033. The value of ρ $(10\bar{1}1)$, calculated from $c/a = 9.733$ is 84°55′.

One of the crystal drawings of Palache and Warren (1911), reproduced here as figure 11c, shows a specimen that is essentially roentgenite, with T $\{10\bar{1}1\}$ dominant, truncated by π $\{01\bar{1}2\}$ and a $\{11\bar{2}0\}$.

The two ends of the peculiar "crystal" of Flink (1901), reproduced as figure 11d, consist of roentgenite. The three forms called γ $\{03\bar{3}1\}$, α $\{30\bar{3}2\}$, y $\{03\bar{3}4\}$ by Flink should be interpreted as referring to the ratio $5c'''/a = 3.244$ of roentgenite, not to $3c'''/a' = 3.365$ of parisite. The confusion is easily explained—$a = a'\sqrt{3}$, so that $3c'''/a' = (3\sqrt{3})c'''/a = 5c'''/a$, since $3\sqrt{3}$ is equal to 5 within 4 percent. When γ, α, and y are referred to the structural ratio $c/a = 15\,c'''/a$ of roentgenite, they become after interchanging the signs of the rhombohedra, T $\{1011\}$, π $\{0112\}$ L $\{10\bar{1}4\}$.

Ungemach (1935b) predicted a new species, which he called parisite β, with an axial ratio of 10.094, that is to say $9c'''/a'$. Parisite β is therefore roentgenite.

The point group cannot be determined from morphology alone as no doubly terminated single crystal has been found, and it is therefore impossible to decide whether $\{1011\}$ and $\{0112\}$ are rhombohedra or trigonal pyramids.

The apparent point-group symmetry, $\bar{6}m2$, of some of the "crystals" is incompatible with the rhombohedral lattice that is clearly indicated by the morphology. The symmetry $\bar{6}m2$ is obviously that of a twin, in which reflection in (0001) is the twin operation. As the lattice is rhombohedral, we are dealing with twinning by reticular merohedry. What information does twinning yield on the point-group symmetry? If the point group were $3\ 2/m$, it would give the twin symmetry $6/m\ 2/m\ 2/m$. This is contrary to fact, and point group $\bar{3}\ 2/m$ is ruled out. If the point group were 32, $3m$, or $\bar{3}$, the same twin reflection would lead to the following twin symmetry: $\bar{6}2m$, $\bar{6}m2$, or $6/m$, respectively. On this basis, only one of the three hemihedries, namely $3m$, is a possible point group. Finally, if the point group were 3, twinning by reflection in (0001) would lead to $\bar{6}$ as symmetry of the twin. Further twinning could raise the twin symmetry to $\bar{6}m2$. Point group 3 is also possible on this count.

Evidence of striations or other surface features that would rule out the mirrors of $3m$ was looked for under the binocular microscope at high magnification, but to no avail. The distinction between $3m$ and 3 must rest on the Laue class determined by x-rays.

Synchisite

Although synchisite has been found by x-rays to have lower symmetry, it is markedly pseudo-hexagonal. Its morphology is controlled by the pseudo-cell $a'c''$ (see under unit-cell dimensions, above), with axial ratio $c''/a' = 2.223$. The series of forms are satisfactory (Table 5), judging from the data taken from Palache and Warren (1911). These authors give a crystal drawing (Fig. 11e) that shows only synchisite forms, namely: $c, a, k, \mu, V, H, r, w, i, t$. This crystal looks orthorhombic. If one wishes to refer synchisite to the orthorhombic system, the transformation 100/120/001 must be applied to the hexagonal indices (third index omitted). The $\{h.h.2\bar{h}.l\}$'s become $\{2h.0.l\}$'s and $\{h.3h.l\}$'s; the $\{h0\bar{h}l\}$'s become $\{hhl\}$'s and $\{0.2h.l\}$'s. The orthorhombic lattice is C-centered, with axial ratios

$$a_{\text{or}}:b_{\text{or}}:c_{\text{or}} = a':a:c'' = \frac{1}{\sqrt{3}}:1:\frac{2.223}{\sqrt{3}} = 0.577:1:1.283.$$

One intergrowth from Muzo (U. S. National Museum No. 106295) gave good measurements on faces of the synchisite "dipyramids" o $\{30\bar{3}1\}$ and Q $\{5.5.\overline{10}.3\}$, namely: 82°33′ to 82°37′ (82°37′, calc.) and 82°17′ (82°18′, calc.). Two crystals of synchisite found on this intergrowth are turned 30° with respect to each other around the c axis, as shown by the following readings.:

ϕ:	20°35′,	50°38′,	80°30′,	140°30′,	200°35′,
ρ:	82°33′,	82°33′,	82°17′,	82°36′,	82°37′.

This is, however, the only example we found of this phenomenon. None of the polycrystals examined by x-rays shows it.

Morphology of the intergrowths

The following relationship has been established: the a-axes of two intergrown species are rigorously parallel within the limits of observation, but they are not in every case directed in the same sense. As mentioned above, x-rays show that they are directed in opposite senses in a roentgenite-parisite polycrystal from Narsarsuk. On such an edifice positive rhombohedra of roentgenite occur in zone with negative rhombohedra of parisite and *vice versa*.

When synchisite occurs with either parisite or roentgenite, the $\{h.h.\overline{2h}.l\}$'s of synchisite referred to c''/a' occur in zone with the $\{h0\bar{h}l\}$'s and the $\{0h\bar{h}l\}$'s of the other species, whose indices are referred to the axes c and a. The arrangement in columns of Table 5 is intended to bring out tautozonal faces of the polycrystals. Occasionally twinning introduces additional complication.

The central part of Flink's intergrowth (Fig. 11d) could be synchisite showing G $\{10\bar{1}3\}$ and m $\{11\bar{2}0\}$, in which case the a' axes of synchisite would parallel the a axes of roentgenite.

CRYSTAL OPTICS

The indices of refraction of the four species were measured by H. Jaffe on small grains identified by x-rays. Indices of refraction were calculated in two ways: (1) from ionic refractivities; (2) from form birefringence.

Ionic refractivities

The following equations, which are known to be fair approximations for ionic structures, are used to calculate the indices of refraction;

$$\frac{\epsilon^2 - 1}{\epsilon^2 + 2} \cdot \frac{MW}{G} = \sum_i (R_\epsilon)_i n_i \qquad (1)$$

$$\frac{\omega^2 - 1}{\omega^2 + 2} \cdot \frac{MW}{G} = \sum_i (R_\omega)_i n_i \qquad (2)$$

n_i is the number of atoms of the ith element in the molecule, R_ϵ and R_ω are the ionic refractivities. They are given by Bragg (1939) for all but the cerium ion (Table 6). For the carbonate ion the refractivities are referred to vibration directions parallel and perpendicular to the plane of the ion, $R_\parallel = 11.32$ and $R_\perp = 8.38$. In bastnaesite R_ϵ equals $R_\parallel$, because all carbonates are parallel to c and are therefore parallel to the vibration direction of ϵ. In all other structures this same value of R_ϵ was used as a first approximation. To obtain the value of $R_\omega = 9.58$, we assume elliptic variation of refractivity with vibration direction, and calculate the average radius vector of the ellipse whose half-axes are $R_\parallel$ and $R_\perp$.

TABLE 6. IONIC REFRACTIVITIES

Ion	$R\omega$	$R\epsilon$	Source
Ce^{+3}	5.51	5.55	Calculated
Ca^{++}	1.99	1.99	Bragg, 1939, p. 185
F^-	2.20	2.20	Bragg, 1939, p. 182
$CO_3^=$	9.58	11.32	$R\omega$ calculated from $R_\perp = 8.38$, $R_\epsilon = R_\parallel$, Bragg, 1939, p. 185

The refractivities of cerium are obtained by substituting the observed indices of refraction of bastnaesite into equations (1) and (2) and solving for $(R_\epsilon)_{Ce^{+3}}$ and $(R_\omega)_{Ce^{+3}}$. Bastnaesite was chosen because, having the highest indices of the four species, the highest reliable indices reported for it in the literature were likely to be those of single crystal grains. With $\epsilon_{bast.} = 1.8242$ and $\omega_{bast.} = 1.7225$ (Geijer, 1921), R_ϵ and R_ω of cerium are calculated to equal 5.55 and 5.51, respectively. These refractivities together with those of the other ions lead to calculated refractive indices of parisite, roentgenite, and synchisite in good agreement with observed values. The latter were obtained by H. Jaffe, of the Geological Survey, on grains previously identified by *x*-rays (Table 7). Contrary to custom the calculated and observed birefringences are not listed, because they are not computed directly. Any systematic error in calculated values of ϵ and ω would cancel in the expression $\epsilon - \omega$. Good agreement in birefringences could therefore be misleading.

Form birefringence

The crystal structures of the four species can be visualized (Fig. 12) as consisting of two kinds of "slabs" stacked in different proportions: bastnaesite slabs (B) and synchisite slabs (S).

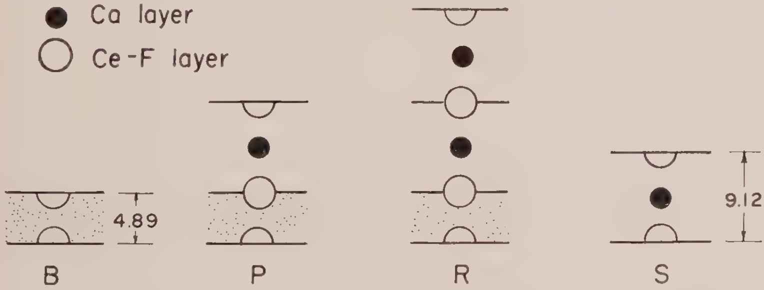

FIG. 12. Stacking of slabs in crystal structures: Bastnaesite = B = $CeFCO_3$, parisite = B.S., roentgenite = B.2S, synchisite = S = $CeFCO_3 \cdot CaCO_3$.

Crystals of parisite or of roentgenite and polycrystals of any two species may be considered *mixed bodies*, in Wiener's sense (1912), for slab thicknesses are smaller than the wavelength of light. Let v_1 and v_2 be the volume fractions of the two constituents ($v_1 + v_2 = 1$). Let ϵ_1, ω_1 be the indices of refraction of bastnaesite; ϵ_2, ω_2 those of synchisite. The stack of slabs is optically uniaxial and its indices *e*, *o* are given by Wiener's formulas for negative form birefringence (see, for instance, Ambronn and Frey, 1926, or Donnay, 1936, 1945):

$$e^2 = \frac{\epsilon_1^2 \epsilon_2^2}{v_1 \epsilon_2^2 + v_2 \epsilon_1^2}, \qquad o^2 = v_1 \omega_1^2 + v_2 \omega_2^2.$$

TABLE 7. INDICES OF REFRACTION AND SPECIFIC GRAVITY

No.	Locality	ϵ	ω	λ	Observer	Reference	G
Bastnaesite							
1	Bastnäs, Sweden	1.8242	1.7225		Geijer ('21)	Glass & Smalley ('45)	4.93
	Bastnäs, Sweden	1.8235	1.7220		Glass	Glass & Smalley ('45)	
2	Belgian Congo	1.823	1.722		Glass	Glass & Smalley ('45)	*ca.* 5
3	Gallinas, N. Mex.	1.819	1.718		Glass	Glass & Smalley ('45)	4.99
4	Narsarsuk, Greenld.	1.818	1.718	(Na)	Jaffe	Jan. 23, 1953 (pr. com.)	
5	Pikes Peak, Colo.	1.818	1.717		Larsen and Berman	Larsen and Berman (1934)	
	Pikes Peak, Colo.	1.818	1.717		Glass	Glass & Smalley ('45)	
6	Madagascar	1.818	1.717		Glass	Glass & Smalley ('45)	4.948
7	Jamestown, Colo.	1.817	1.716		Glass	Glass & Smalley ('45)	
8	Belgian Congo	*ca.* 1.815	*ca.* 1.713		Buttgenbach	('47)	
Parisite							4.36 4.42
9	Narsarsuk, Greenld.	1.7701	1.6742		Flink ('01)	in Palache, *et al.* (1951)	
10	Narsarsuk, Greenld.	1.7690	1.6730	(589)	Quercigh ('12)	in Palache, *et al.* (1951)	
11	Muzo, Colombia	1.7712	1.6717	(589)	Quercigh ('12)	in Palache, *et al.* (1951)	
12	Narsarsuk, Greenld.	1.765 (±5)	1.670 (±2)	(Na)	Jaffe	Jan. 16, 1953 (pr. com.)	
	($2CeFCO_3 \cdot CaCO_3$)	1.768	1.667		Calcd. from ionic refractivities		4.29
Roentgenite							
13	Narsarsuk	1.756	1.662	(Na)	Jaffe	Jan. 23, 1953 (pr. com.)	
	($3CeFCO_3 \cdot 2CaCO_3$)	1.755	1.654		Calcd. from ionic refractivities		4.19
Synchisite							
14	Narsarsuk, Greenld.	1.745 (±5)	1.650 (±2)	(Na)	Jaffe	Jan. 16, 1953 (pr. com.)	
15	Switzerland	>1.74	1.649		Parker *et al.* ('39)		3.94
16	Transvaal	1.744	1.644		Söhnge ('44)	in Palache, Berman and Frondel (1951)	3.90
	($CeFCO_3 \cdot CaCO_3$)	1.744	1.641		Calcd. from ionic refractivities		3.99

The height of the B slab, obtained by *x*-rays, is $h_1 = 4.89$ Å; that of the S slab, $h_2 = 9.12$ Å. Because the unit mesh in the basal plane has the same area in each case, the volume fractions are proportional to the height fractions. The general formula $Bn_1\,Sn_2$ of a polycrystal corresponds to the chemical composition (n_1+n_2) $CeFCO_3 \cdot n_2CaCO_3$. The volume fractions are

$$v_1 = n_1h_1/(n_1h_1+n_2h_2), \quad v_2 = n_2h_2/(n_1h_1+n_2h_2).$$

For pure parisite $n_1 = n_2 = 1$ and $v_2 = 0.6508$; for pure roentgenite $n_1 = 1$, $n_2 = 2$, and $v_2 = 0.7885$.

The highest values on record for the indices of refraction of bastnaesite are those obtained by Geijer (1921) on material from the type locality: $\epsilon_1 = 1.8242$, $\omega_1 = 1.7225$. It is difficult to decide which measured values to use for the synchisite indices. Söhnge's values (Palache, Berman and

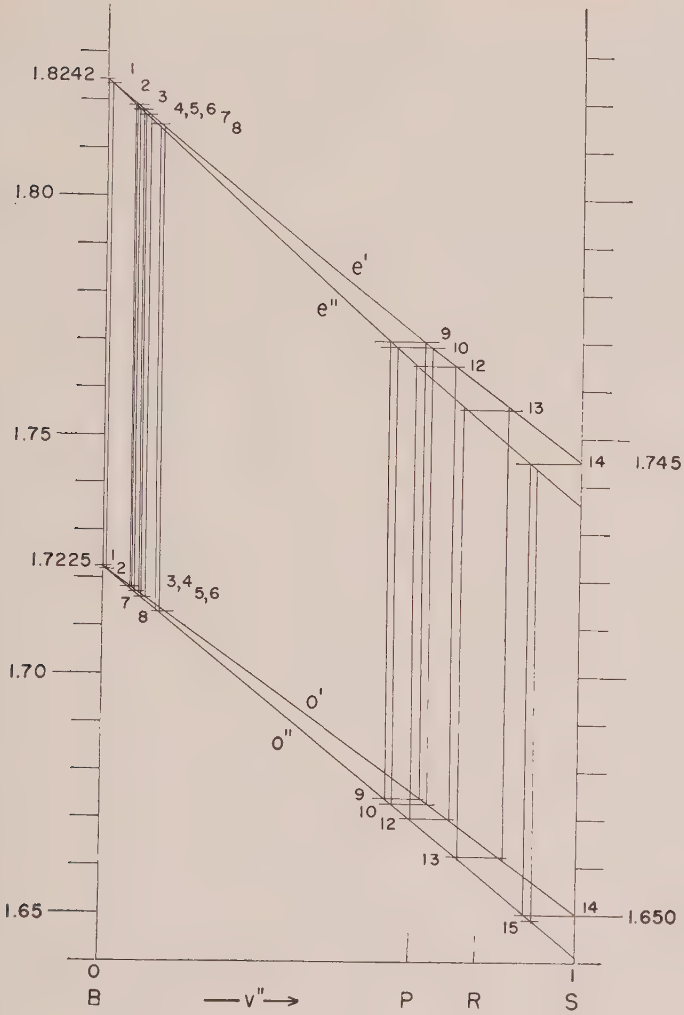

FIG. 13. Indices of refraction vs. composition expressed as volume fraction of S slabs. Curves $e'o'$ obtained from Wiener's formula with Geijer's values for the indices of bastnaesite and Jaffe's values for those of synchisite. Curves $e''o''$ obtained with the same indices for bastnaesite and Jaffe's values for parisite.

Frondel, 1951, p. 287), $\epsilon_2 = 1.744$, $\omega_2 = 1.644$, were tried first. They give *e* and *o* curves which account fairly well for the experimental data. But the measurements that H. Jaffe made on our material, $\epsilon_2 = 1.745$, $\omega_2 = 1.650$, give better curves (e' and o', Fig. 13) on which measured indices of various sources (numbered in Table 7) can be seen to lie vertically above each other, each pair (ϵ_i, ω_i) corresponding to one and the same abscissa. The parisite values (Nos. 9–12), however, all fall to the right of the theoretical composition; likewise the roentgenite indices (No. 13) fall to the right of their abscissa. This lack of agreement in position is taken as an indication that the indices used for synchisite were not measured on pure synchisite.

By assuming that the indices measured on our parisite (No. 12) by H. Jaffe are those of pure parisite, we can calculate much lower indices for pure synchisite, namely 1.736 and 1.641. The corresponding curves (e'' and o'', Fig. 13) likewise show that any pair of measured indices lie on a vertical line. Now, however, the roentgenite pair falls to the left of its composition and the group of parisite values (other than No. 12) also falls to the left of the parisite composition. The correct curves should probably lie between e' and e'' and between o' and o''. Such uncertainties will not be resolved until the indices can be measured on two crystals of known compositions. From the e and o curves that could then be drawn, it would be possible to read the composition corresponding to any pair of measured indices.

The variations observed in the indices of the bastnaesite specimens (Nos. 1 to 8) indicate the presence of some S slabs, either as part of a little intercalated parisite or roentgenite or as intersitial S slabs that do *not* constitute synchisite crystals. In the first case the specimen is a polycrystal. In the second case we are dealing with a special kind of solid solution in which not random isolated atoms but whole structural layers at a time substitute for each other. For a given composition the type of disorder observed by x-rays, namely faults in the stacking of layers, should not affect the indices of refraction.

REFERENCES

AMBRONN, H., AND FREY, A. (1926), Das Polarisationsmikroskop—Leipzig.

BRAGG, W. L. (1939), The Crystalline State, Vol. 1, A General Survey—London.

BUTTGENBACH, H. (1947), Les Minéraux de Belgique et du Congo Belge—Paris-Liége.

CESÀRO, G. (1907), Contribution à l'étude des minéraux: *Bull. Acad. Roy. Belgique Cl. Sc.*, No. **4**, 313–338.

DONNAY, GABRIELLE (1953a), The "polycrystal," a product of syntaxic intergrowth (abstract): *A.C.A. meeting, Ann Arbor, Mich., June* 22–26, 1953.

——— (1953b), Roentgenite, a new mineral from Greenland: *Am. Mineral.*, **38**, 868–870.

DONNAY, J. D. H. (1936a), La biréfringence de forme dans la vaterite: *Ann. Soc. géol. Belgique*, **59**, B 215–222.

——— (1936b), La biréfringence de forme dans la calcédoine: *ibid.*, **59**, B 289–302.

——— (1945), Form birefringence of nemalite: *Univ. Toronto Studies, Geol. Ser.*, No. **49**, 5–15.

———, AND DONNAY, GABRIELLE (1952), Syntaxic intergrowth in the andorite series (abstract): *A.C.A. meeting, Tamiment, Pa., June 16–20, 1952.*

EVANS, R. C. (1946), An Introduction to Crystal Chemistry—Cambridge.

Flink, G. (1901), On the minerals from Narsarsuk on the Firth of Tunugdliarfik in southern Greenland: *Meddelelser om Grönland*, **24**, 9–213. (For parisite see pp. 29–42 and plate II.)

Geijer, P. (1921), The cerium minerals of Bastnäs at Riddarhyttan: *Sveriges geologiska Undersökning*, Årbok **14** (1920), No. 6, 1–24.

Glass, J. J., and Smalley, R. G. (1945), Bastnäsite: *Am. Mineral.*, **30**, 601–615.

International Tables for the Determination of Crystal Structures (1935), Vol. **1**—Berlin.

Jagodzinski, H. (1949), Eindimensionale Fehlordnung in Kristallen und ihr Einfluss auf die Röntgeninterferenzen. I. Berechnung des Fehlordnungsgrades aus den Röntgenintensitäten: *Acta Cryst.*, **2**, 201–207.

Larsen, E., and H. Berman (1934), The Microscopic Determination of the Nonopaque Minerals, *U. S. Geol. Survey Bull.* **848**, Washington, D. C.

Oftedal, I. (1931a), Zur Kristallstruktur von Bastnäsit: *Zeits. Krist.*, **78**, 462–469.

——— (1931b), Über Parisit, Synchisit und Kordylit: *ibid.*, **79**, 437–464.

——— (1931c), Über die Parallelvierwachsung von Tysonit und Bastnäsit: *Norsk. Geol. Tidsskr.*, **12**, 459–467.

Palache, C., Berman, H. and Frondel, C. (1951), Dana's System of Mineralogy, Vol. II, John Wiley and Sons, New York, N. Y.

Palache, C., and Warren, C. H. (1911), The chemical composition and crystallization of parisite and a new occurrence of it in the granite-pegmatites at Quincy, Mass., U.S.A.: *Am. Jour. Sci.*, **31**, 533–557.

Parker, R. L., de Quervain, F., and Weber, F. (1939), Über einige seltene Mineralien der Schweizeralpen: *Schweiz. Mineral. und Petr. Mitt.*, **19**, 293–306.

Strunz, H. (1949), Mineralogische Tabellen, 2nd edition—Leipzig.

Ungemach, H. (1935a), Sur certains minéraux sulfatés du Chili: *Bull. Soc. fr. Min.*, **58**, 97–221.

——— (1935b), Sur la syntaxie et la polytypie: *Zeits. Krist.*, **91**, 1–22.

Wells, A. F. (1950), Structural Inorganic Chemistry, 2nd edition—Oxford.

Wiener, O. (1921), Die Theorie des Mischkörpers für das Feld der stationären Strömung: *Abh. math.-phys. Klas. sächs. Ges. Wiss.*, **32**, 507–604.

Zachariasen, W. H. (1933), The crystal lattice of sodium bicarbonate, $NaHCO_3$: *J. Chem. Phys.*, **1**, 634–639.

——— (1948), Crystal radii of the heavy elements: *Phys. Rev.*, **73**, 1104–1105.

FAUSTITE, A NEW MINERAL, THE ZINC ANALOGUE OF TURQUOIS*

Richard C. Erd, Margaret D. Foster, *U. S. Geological Survey, Washington, D. C.*, and Paul D. Proctor,
Brigham Young University, Provo, Utah.

Abstract

The name faustite is given to a new mineral having the formula $(Zn_{.8}Cu_{.2})Al_6(PO_4)_4(OH)_8 \cdot 5H_2O$, the zinc analogue of turquois. It occurs as an apple-green vein filling in altered shales at Copper King mine, Maggie Creek district, Eureka County, Nev., intimately associated with a montmorillonitic clay. Pale greenish-white vein fillings in the same locality consist predominantly of montmorillonitic clay. Although *x*-ray powder patterns of turquois and faustite are similar, the two minerals may be distinguished by the identification of their dissociation products upon ignition. The specific gravity of faustite is 2.92; mean index of refraction is 1.613. The isomorphous relations with turquois are discussed.

Introduction

A zinc aluminum phosphate recently discovered has proved to be a new mineral, the zinc analogue of turquois. This new mineral, $(Zn_{.8}Cu_{.2})Al_6(PO_4)_4(OH)_8 \cdot 5H_2O$, is named faustite in honor of George T. Faust of the United States Geological Survey. This discovery not only adds a new member to the turquois group but suggests a new isomorphous series of turquois minerals having varying proportions of CuO and ZnO, ranging from turquois with one CuO to faustite with one ZnO. This is the second known phosphate of zinc and aluminum, the first being the mineral kehoeite, which was described by Headden in 1893.

The first specimen of this new mineral was collected by one of us (P. D. P.) at Copper King mine, Maggie Creek district, Eureka County, Nev., and was sent to the U. S. Geological Survey for mineralogic study in August 1952. *X*-ray study showed the mineral to be similar to turquois, but microchemical tests indicated the presence of considerable zinc.

Geological Occurrence

The Copper King mine in which faustite is found is in the Maggie Creek (also known as Susie Creek or Schroeder) district which is located in the Tuscarora Mountains about 10 miles northwest of Carlin, Eureka County, Nev. The district has been mined for lead, silver, gold, antimony, and copper. Barite has also been mined in considerable quantity a few miles to the southeast. The mine is in sedimentary rocks of Paleozoic age that dip to the northwest at 45° to 50°; the rocks are thin-bedded cherts with interbedded shales and minor amounts of limestone. Conspicuous shears have developed along the bedding planes, probably as a result of compressional forces acting on the beds. An oxide ore body, consisting of chrysocolla, malachite, azurite, and cuprite, is localized in the limestone beds. As far as could be determined there is no primary copper mineralization visible in the mine. Directly down the rake of the main ore shoot on the 100-foot level the only sign of mineralization is a small veinlet of pale-green montmorillonite. Apparently the copper solutions, moving either from the sides or from above, encountered a favorable structural trap in the intensely sheared limestone which was also a more favorable rock for stratigraphic control than the thin-bedded cherty shales.

---

* Publication authorized by the Director, U. S. Geological Survey.

Faustite occurs on the main level of the mine as apple-green veinlets up to $\frac{1}{4}$-inch wide cutting through altered wall rock, which is chiefly argillized cherts and shales. It is intimately associated with montmorillonitic clay of various colors from white to dark green. Most of the faustite found in the veins is enclosed by a light- to dark-green montmorillonitic clay. It also occurs as nuggets or nodules which have roughly polygonal shape and which are enclosed by a montmorillonitic clay of an olive-green color. In both types of occurrence the interface between the green montmorillonitic clay and faustite is marked by a thin film of pure white montmorillonite. Montmorillonite is also admixed with the faustite and constitutes about 20 per cent of the sample analyzed. The altered wall rock consists chiefly of quartz and kaolinite, and in places alunite occurs in veinlets.

The origin of faustite is a matter of conjecture. The source of the zinc is not known with certainty, as no zinc minerals were noted in the mine; however, nearby lead-silver veins carry small amounts of sphalerite. The other ingredients are readily available. There is abundant apatite in the montmorillonitic clay to provide the phosphate, the source of the aluminum would appear to be in the shales, and the copper mineralization has already been mentioned.

The nearest occurrence of turquois is in the Eight mine in the Lynn district, 12 miles to the northwest.

X-RAY POWDER DATA

Faustite, magnified 27,000 times by electron micrographs (taken by E. J. Dwornik and C. Davis), is seen only as irregular masses. This extremely fine particle size limits crystallographic studies to an examination of the *x*-ray diffraction data. As may be seen in Table 1, the powder patterns of faustite and turquois are nearly identical, showing that the minerals are isostructural. The powder data for turquois given by Gra-

TABLE 1. *X*-RAY POWDER DATA FOR FAUSTITE AND TURQUOIS

1. Faustite. Eureka County, Nev. (Fe/Mn radiation; $\lambda=1.9373$ Å)		2. Turquois. Campbell County, Va. (Cu/Ni radiation; $\lambda=1.5418$ Å)		3. Turquois. Campbell County, Va. (Graham, 1947) (Fe/Mn radiation)			
d (meas.) Å	Intensity	*d* (meas.) Å	Intensity	*d* (meas.) kX	Intensity	*d* (graph) kX	Indices *hkl*
9.03	5	9.09	5	9.35	1	8.98	010
6.70	7	6.73	5	6.69	2	6.71	001
6.14	7	6.17	7	6.14	3	6.14 6.14	$0\bar{1}1$ $\bar{1}\bar{1}1$
5.98	4	6.00	4				
5.80	2	5.77	2				
4.81	5	4.80	6	4.78	4	4.83 4.82	011 $1\bar{1}0$
4.61	2	4.65	2				
4.48	2	4.49	1				
4.19	2	4.18	1				
4.05	4	4.06	1	4.05	2	4.09 4.05	$\bar{1}11$ 101
3.68	10	3.68	10	3.67	10	3.73 3.72 3.70	$\bar{2}\bar{1}1$ $1\bar{1}1$ 111
3.50	1	3.51	1				
3.44	6	3.44	7	3.43	3	3.46 3.41	$\bar{2}01$ $\bar{2}\bar{2}1$
3.28	6	3.28	7	3.27	2	3.32 3.31 3.30 3.30	210 $\bar{1}20$ 021 $\bar{1}\bar{3}1$
3.08	4	3.10	4	3.09	0.5		
3.03	2	3.05	2				
2.99	2	3.00	2	2.99	0.5		
2.92	6	2.91	8	2.90	9		
2.89	8	2.89	1				
2.79	1	2.84	2				
2.70	1	2.74	2				
2.60	1	2.62	1				
2.56	1	2.58	1				
2.52	4	2.52	4	2.52	2		
2.47	2	2.47	2				
2.42	2	2.44	1	2.45	1		
2.40	2	2.40	2	2.40	1		
2.35	4	2.35	4	2.34	1		
2.31	2	2.32 2.29	4 Broad	2.30	2		
2.29	4						
2.23	4	2.23	4	2.23	2		
2.18	2	2.19	2	2.14	1		
2.12	4	2.12	4	2.11	2		
2.05	7	2.07	5	2.06	2		

Table 1—*(continued)*

1. Faustite. Eureka County, Nev. (Fe/Mn radiation; $\lambda=1.9373$ Å)		2. Turquois. Campbell County, Va. (Cu/Ni radiation; $\lambda=1.5418$ Å)		3. Turquois. Campbell County, Va. (Graham, 1947) (Fe/Mn radiation)			
d (meas.) Å	Intensity	*d* (meas.) Å	Intensity	*d* (meas.) kX	Intensity	*d* (graph) kX	Indices *hkl*
2.02	5	2.02	6	2.01	5		
1.994	1	1.994	1				
1.970	1	1.966	1				
1.946 1.928	0.05	1.934	2				
1.900	4	1.903	4	1.90	3		
1.850	4	1.845	4	1.84	4		
1.830	4	1.824	4				
1.807	2	1.814	1	1.81	4		
1.783	2	1.784	2	1.78	2		
1.718	2	1.727	2	1.72	1		
1.682	1	1.677	2				
1.665	1	1.672	2	1.67	1		
1.645	2	1.639	4	1.64	3		
1.610	2	1.607	2	1.61	1		
1.578	2	1.582	2	1.58	1		
1.565	2	1.567	2	1.57	1		
1.550	2	1.548	2 Broad	1.54	2		
1.527	1	1.529	1				
1.517	2	1.511	2	1.51	1		
1.491	2	1.494	2	1.49	1		
1.472 1.468	1	1.471	1	1.48	1		
1.454	1	1.452	2				
1.445	2	1.438	2				
1.421	4	1.426	2				
1.397	1	1.395	1	1.39	2		
1.373	1	1.376	1				
1.353	2	1.349	2				
1.331	2	1.333	2				
1.316	1	1.320	1				
1.302	1	1.307	1				
1.283	1	1.284	1				
1.268	1	1.266	2				
1.261	3	1.258	2				
1.226	2	1.227	2 Broad				
1.221	2	1.220	2 Broad				
1.207	2	1.204	2				
1.194	2	1.193	1				
1.158	1	1.154	1				
1.152	1	1.153	2				
1.117	1	1.112	1				
1.093	1	1.093	1				

ham (1947) with the spacings in kX units and partly indexed are given for comparative purposes. The most noticeable difference between the patterns, easily detected by the unaided eye, is in the separation of the 2.05–2.02 Å spacings of faustite and of the 2.07–2.02 Å spacings of turquois. The slightly lower *d* values for faustite indicate that it has a somewhat smaller unit cell than turquois.

PHYSICAL PROPERTIES

Faustite occurs as hard compact masses with a smooth feel and with a slightly conchoidal to smooth fracture. The mineral is brittle; the hardness is $5\frac{1}{2}$. A slight correction in the determined hardness, and in some of the other measured physical and optical properties of faustite, might be necessary owing to the 20 per cent of montmorillonite present. The specific gravity, as determined with a Berman microbalance, is 2.76. As determined using an Adams-Johnston pycnometer of fused silica, the specific gravity is 2.791 at 4° C., measured on a 1.162 g sample. If the admixed montmorillonite is assumed to have a specific gravity of 2.25, the recalculated value for faustite would be 2.92. This compares with the calculated value of 2.91 for turquois. The agreement is what would be expected, as zinc and copper have nearly identical atomic weights and constitute only a small part of the structure. The substitution of zinc for copper increases the formula weight by 0.2 per cent.

OPTICAL PROPERTIES

The material on which the chemical analysis was made is apple green in color, with a waxy to somewhat dull luster. Associated material, which contains a greater percentage of copper and may be intermediate between faustite and turquois, has a distinctly bluish cast. Faustite compared with various specimens of "green" turquois was seen to have more yellow in its color; presumably the pure zinc end member, free of copper and iron, would be white or colorless. In transmitted light the color is brown with a slight greenish cast. The powdered mineral is yellow green and the streak is white to pale yellow green. Faustite is opaque except on thin edges. It is not fluorescent.

In thin section the mineral is extremely fine grained, and no crystal outlines could be found. The surfaces of the aggregate grains are marked by shatter cracks, similar to those of opal or halloysite, which probably represent a slight contraction of the material in drying. A complete determination of the optical properties of faustite could not be made owing to the small particle size. The mean index of refraction, determined using sodium light and standard immersion media, is 1.613; the birefringence is medium and appears to be about the same or slightly less than that of fine-grained turquois with which it was compared.

CHEMICAL PROPERTIES

Pyrognostics

In a closed tube faustite decrepitates rather strongly, loses water, and turns a light clove brown. The mineral does not fuse before the blowpipe and leaves the flame uncolored; the residue is colored clove brown. As insufficient material was available for study by differential thermal analysis, small (2 to 5 mg.) grains of faustite were heated on an electric hot plate at various temperatures and for varying lengths of time in order to study the products of dehydration. Faustite dried at 110° C. for 60 hours faded slightly in color; heated at 210° C. for 30 hours, it faded to a light brownish gray. The structure is not destroyed, however, as shown by *x*-ray diffraction patterns, until a temperature of 400° C. is reached. These data agree with the findings of Schaller (1912) for turquois. Faustite held at 400° C. for 60 hours turned dark clove brown in color and gave an *x*-ray pattern with two broad and diffuse bands at 4.5 Å and 12 Å. A few spotty lines of the pattern of berlinite ($AlPO_4$, quartz type) are also present, but the material is chiefly amorphous and has an index of refraction of 1.568. When faustite was strongly heated (above 900° C.) in a crucible or before the blowpipe, the residue was found to consist of gahnite and aluminum phosphate ($AlPO_4$, cristobalite type). In samples insufficiently heated, the tridymite-like polymorph of $AlPO_4$ is also present (Manly, 1950).

The residue of turquois, ignited for comparison, was found to consist of oxides of copper and, again depending upon the degree of heating, of either or both of the high temperature polymorphs of $AlPO_4$. As faustite yields a spinel on extreme heating, *x*-ray study of the ignition products (Foster, 1952) provides an easy method of distinguishing faustite from turquois.

Ground faustite is very slowly soluble in cold concentrated acids but is much more soluble after ignition to about 400° C. The solubility is not increased by heating beyond this point, which presumably marks the destruction of the crystal structure. Faustite is readily soluble without heating in warm 1*N* orthophosphoric acid. The color is unaffected by ammonia, in which the mineral is no more than slightly soluble.

Chemical analysis and composition

X-ray examination showed that faustite was intimately associated with a clay of the montmorillonite type. In order to allocate properly the common constituents Al_2O_3, Fe_2O_3, and H_2O between faustite and the clay present, it was necessary to know the composition of the clay. *X*-ray examination showed that a pale greenish-white vein filling in the same locality was predominantly a montmorillonitic clay. As the greenish-white material and the green material containing, and admixed with, faustite occurred under similar conditions, it seemed probable that the montmorillonitic clay, which was the dominant mineral in the greenish-white material, would have approximately the same composition as the montmorillonitic clay in the green material. An analysis of the greenish-white material is given in Table 2. As *x*-ray examination showed the greenish-white vein material to contain some apatite, we are justified in removing CaO (except for exchangeable CaO in the clay), and P_2O_5 from the analysis of the greenish-white material in order to arrive at the composition of the clay. And as treatment with 0.5*N* NaOH (Foster, 1953) showed the material to contain 1.27 per cent free Al_2O_3, this also may be subtracted from the Al_2O_3 found to obtain the Al_2O_3 content of the clay. The 1.3 per cent CuO found, together with the 0.23 per cent CO_2, may indicate the presence of a small amount of malachite, an amount, however, too small to be detected in the *x*-ray diffraction pattern. The ZnO found is, on the other hand, considered to be in the clay, as zinc is known

TABLE 2. ANALYSIS OF GREENISH-WHITE VEIN FILLING[1]

	Greenish-white material	Apatite	Malachite	Free Al_2O_3	Clay	Clay Calculated to 100%
SiO_2	39.67	—	—	—	39.67	47.48
Al_2O_3	19.27	—	—	1.27	18.00	21.54
Fe_2O_3	0.66	—	—	—	0.66	0.79
CuO	1.30	—	1.30	—	—	—
ZnO	0.30	—	—	—	0.30	0.36
CaO	8.87[2]	7.27	—	—	1.60	1.92
MgO	2.72[3]	—	—	—	2.72	3.26
P_2O_5	5.91	5.91	—	—	—	—
H_2O^-	8.40	—	—	—	8.40	10.05
H_2O^+	12.20	—	—	—	12.20	14.60
CO_2	0.23	—	0.23	—	—	—
Total	99.53					100.00

Cation exchange—milliequivalents 0.78.

[1] Margaret D. Foster, analyst.

[2] Exchangeable CaO, 1.60 per cent.

[3] Exchangeable MgO, 0.42 per cent.

to enter the montmorillonite structure (Ross, 1946). With these adjustments, and calculating the remaining constituents to 100 per cent, the composition of the clay is that of a typical montmorillonite (Table 2). Assuming the clay in the green vein filling (admixed with faustite) to be of similar composition and taking the silica found in the green material as indicating the amount of clay in the material, the composition of faustite, calculated to 100 per cent, is shown in Table 3. Thus faustite may be considered the zinc analogue of turquois and near the zinc end member of a possible isomorphous series of which turquois is the copper end member.

TABLE 3. ANALYSIS OF GREEN VEIN FILLING AND COMPOSITION OF FAUSTITE[1]

	Green vein filling	Clay	Faustite	Calculated to 100%	Ratios		
SiO_2	8.63	8.63	—	—	—		
Al_2O_3	33.10	3.39	29.19	35.31	0.3463	0.3571	1.01×3
Fe_2O_3	1.57	0.14	1.43	1.73	0.0108		
CuO	1.33	—	1.33	1.61	0.0202	0.1153	0.98×1
ZnO	6.40	—	6.40	7.74	0.0951		
CaO	0.40	0.40	—	—	—		
MgO	0.56	0.56	—	—	—		
P_2O_5	28.79	—	28.79	34.83		0.2453	1.04×2
H_2O^-	0.70	0.70	—	—	—		
H_2O^+	18.17	2.65	15.52	18.78		1.0422	0.98×9
Total	99.65			100.00			

Sp. Gr. 2.791

Formula of faustite $(Zn_{.8}Cu_{.2})O \cdot 3Al_2O_3 \cdot 2P_2O_5 \cdot 9H_2O$ or, in more condensed form, $(Zn_{.8}Cu_{.2})Al_6(PO_4)_4(OH)_8 \cdot 5H_2O$.

A spectrographic analysis by Janet D. Fletcher, U. S. Geological Survey, gives the following results for faustite, in per cent:

X0.0	Al, P
X.0	Zn, Cu, Fe, Si
0.X	Ca, Mg, Ba, V
0.0X	Cr, Ti
0.00X	Co, Ni, Sc, Zr, Sr
0.000X	Mn, Be

Elements looked for but not found were: Ag, Au, Pb, Bi, Pt, Mo, W, Ge, Sn, As, Sb, Cd, Tl, Ga, Y, Yb, La, Tb, Nb, Ta, U, and B.

---

[1] Margaret D. Foster, analyst.

The turquois-faustite series

The discovery of a zinc member of the turquois group raises the question as to whether other samples of turquois, in which the amount of CuO present is considerably less than the theoretical amount, may not contain some zinc. In the analysis of turquois, zinc is not ordinarily determined and may, therefore, have been missed. Re-examination of samples of turquois may show some to be intermediate between turquois and faustite. To pursue this point, qualitative microchemical tests were made on 15 samples of turquois from England, France, Chile, and Cuba and from Arizona, California, Nevada, and New Mexico. Weak to moderate (less than 1 per cent) tests for zinc were obtained on all but 3 of the samples; however, all the samples are close to the turquois end member and give a strong test for copper. These tests were also applied to some minute grains of faustite that had a bluer color than the analyzed apple-green material, and these contained slightly more copper than type faustite. These tests indicate that intermediate members of the series may be present.

ACKNOWLEDGMENTS

The authors are grateful for the help provided by Janet D. Fletcher, who made the spectrographic analysis; for the assistance of George Switzer, of the U. S. National Museum, who loaned the turquois specimens; and for the many helpful suggestions and advice from Waldemar T. Schaller. Donald H. Richter was especially helpful in many ways.

REFERENCES

FOSTER, MARGARET D. (1953), Geochemical studies of clay minerals, III. The determination of free silica and free alumina in montmorillonites: *Geochim. et Cosmochim. Acta*, **3**, 143–154.

FOSTER, WILFRID R., (1952), Blowpipe petrography: *Am. Mineral.*, **37**, 758–763.

GRAHAM, A. R. (1947), X-ray study of chalcosiderite and turquois: *Univ. Toronto Studies, Geol. Ser.*, **52**, 39–53.

HEADDEN, W. P. (1893), Kehoeite, a new phosphate from Galena, Lawrence Co., S. D.: *Am. Jour. Sci.*, 3d ser., **46**, 22–25.

MANLY, R. L., JR. (1950), The differential thermal analyses of certain phosphates: *Am. Mineral.*, **35**, 108–115.

ROSS, C. S. (1946), Sauconite—a clay mineral of the montmorillonite group: *Am. Mineral.*, **31**, 411–424.

SCHALLER, W. T. (1912), Crystallized turquoise from Virginia: *Am. Jour. Sci.*, 4th ser., **33**, 35–40.

STEVENSITE, REDEFINED AS A MEMBER OF THE MONTMORILLONITE GROUP*

George T. Faust and K. J. Murata, *U. S. Geological Survey, Washington, D. C.*

Abstract

Stevensite, a hydrous magnesium silicate, typically pseudomorphous after pectolite in basalt, has been restudied. *X*-ray diffraction analysis, staining tests, and differential thermal analysis all indicate that the mineral is a member of the montmorillonite group of clay minerals.

Stevensite differs from saponite in lacking essential amounts of aluminum and from hectorite in lacking lithium and fluorine. As is indicated by its formula, $[Mg_{2.88}Mn_{.02}Fe_{.02}][Si_4]O_{10}[OH]_2x_{.15}$, stevensite has an abnormally low base-exchange capacity compared with the average value for montmorillonite of 0.37 equivalent per formula weight. This low capacity is believed to be due to the unique and probably restricted manner in which the charge deficiency apparently originates in the mineral—namely, through a deficiency in the total number of ions in positions of octahedral coordination. Multivalent ions, whose higher charge would compensate for the deficiency in number, as in sauconite, are practically absent in stevensite.

History of Stevensite and Its Synonyms

Professor Albert R. Leeds, of the Stevens Institute of Technology, Hoboken, New Jersey, in 1873 published a description and analysis of a mineral which he called talc pseudomorphous after pectolite. An examination of his paper (Leeds, 1873) shows, however, that he was not convinced of the interpretation of his analysis, for he writes (p. 24):

> "While closely approaching talc in its physical properties this pseudomorph after pectolite is near sepiolite in its chemical composition."

The mineral which he analyzed was found "in veins of calcite which traverse the trap rock in the vicinity of Bergen Hill Tunnel, Hoboken, New Jersey." His analysis, Table 1, shows that his sample was nearly but not quite pure.

According to Chester (1896) the name stevensite was subsequently proposed by Leeds in 1873 in honor of E. A. Stevens, the founder of the Stevens Institute of Technology. Chester (p. 257) describes the naming as follows: "This name was suggested in 1873 at a meeting of the N. Y. Lyceum of Natural History, but not published though soon after used on labels." Chester cites a reference to a note by Leeds published in "The Naturalists Leisure Hour" for 1889, but a search of two copies of this publication (from the Library of Congress and the American Museum of

---

* Publication authorized by the Director, U. S. Geological Survey.

TABLE 1. CHEMICAL ANALYSES OF STEVENSITE, PECTOLITE, AND OF NATURAL MIXTURES

Analysis No.	1	2	3	4	5	6	7	8	9
Name	Stevensite	Stevensite	Stevensite	Stevensite +pectolite	Magnesium-pektolith	Walkerite	Pectolite	Pectolite	"Stevensite"
Locality	Springfield, N. J.	Bergen Hill Tunnel, Hoboken, N. J.	Hartshorn Quarry Springfield Twp., N. J.		Burg Herborn, Germany	Corstorphine Hill, Scotland	Paterson, N. J.	Theory	Jersey City, N. J.
	U.S.N.M. R4719								Selfridge No. 51
SiO_2	57.30	60.55	58.03	53.84	56.22	52.20	53.80	54.2	57.24
Al_2O_3	None	1.02	0.37	1.18	0.67	—	0.00	—	None
Fe_2O_3	0.32	—				—	0.00	—	1.14
FeO	None	0.72	—	—	—	1.33	1.00	—	0.12
MnO	0.21	0.65	0.03	0.13	—	—	0.12	—	0.75
MgO	27.47	26.56	27.66	9.81	5.76	5.12	0.00	—	27.89
CaO	0.97	1.41	1.61	22.59	24.72	28.64	33.20	33.8	0.38
Na_2O	0.03	—	3.73	5.59	6.89	6.50	9.01	9.3	—
K_2O	0.03	—	—	—	0.21	0.85	0.00	—	—
H_2O^+	7.17	9.30	8.45	6.76	5.53	5.28	2.94	2.7	7.69
H_2O^-	6.69		*	*	*	*		—	4.76
F	None	—	—	—	—	—	—	—	None
	100.19	100.21	99.88	99.90	100.00+	99.92	100.07	100.0	99.97
Analyst	K. J. Murata	A. R. Leeds (1873)	M. L. Glenn (1916)		M. Dittrich (Reuning, 1907)	M. F. Heddle (1880)	F. A. Gonyer (Peacock, 1935)		K. J. Murata

* Sample dried at 110° C. before analysis.

Natural History) failed to reveal any mention of the naming of this mineral. Chester also cites the erroneous usage of stevenite for stevensite.

After Leeds' work was published two other closely related magnesium silicates were described. Heddle (1880) named a magnesium silicate from Corstorphine Hill, Scotland, walkerite. Walkerite (not walkererde of Hintze = walkerite of Dana's System of Mineralogy, 1892) contains 5.12 per cent MgO. (See Table 1.) Reuning (1907) described a mineral which he called magnesiumpektolith (magnesium pectolite) from the diabase at Burg bei Herborn, Driesdorf, Germany.

Valiant (1904) included stevensite in his list of New Jersey mineral localities.

The problem of the character and composition of stevensite was reopened by Glenn (1916). He made an analysis of stevensite and of a partly altered specimen of pectolite from the Hartshorn quarry in Springfield Township, Essex County, New Jersey. From a study of these two analyses he concluded that walkerite and magnesiumpektolith were mixtures of stevensite and pectolite.

Hilgard (1916) found a peculiar clay at Hacienda Santa Lucia near Mexico City which on analysis showed 17.10 per cent MgO. He named this mineral lucianite.

Rogers (1917) in a review of the status of amorphous minerals suggested that (1) "stevensite . . . is probably the amorphous equivalent of crystalline talc" and (2), referring to lucianite, Hilgard's clay, "This substance . . . is probably a synonym of stevensite."

The occurrence of stevensite at nine localities in the Watchung basalt of New Jersey is given by Manchester (1931), who considered it to be a variety of talc.

Lorent (1933) in studying the hydrothermal alteration of the limburgite of Sasbach in the Kaiserstuhl discovered a gel-like substance which he called a "magnesiumsilikatgel." Analysis of a sample weighing only 0.3793 gram showed it to consist of 46.1 per cent H_2O; 26.7 SiO_2, 2.8 Al_2O_3, 0.6 CaO and 24.7 MgO; sum = 99.7 per cent. The ratio of MgO to SiO_2 shows that this mineral, if homogeneous, is not stevensite.

Stevensite was reported in the matrix of the Mayville iron ore of Wisconsin by Hawley and Beavan (1934), who identified it by optical and microchemical tests.

Selfridge (1936) included some data on stevensite in his paper on the serpentine minerals. He listed stevensite with deweylite and commented as follows (p. 484): "No explanation could be found for the higher indices of No. 51. Duplicate x-ray patterns show that it is deweylite. Optically it approaches serpentine," and (on p. 500) "The deweylite pattern of Specimen No. 51, which displayed optical characters similar to those near the low index of serpentine, indicates the need for further study between deweylite and serpentine."

The most detailed description of stevensite appeared in the Ergänzungsband of Hintze's Handbuch der Mineralogie (1936–1937), where two pages (649–650) are devoted to the description of this mineral and its synonymy.

Strunz (1941) in his Mineralogische Tabellen considered stevensite to be talc pseudomorphous after pectolite; walkerite to be weathered pectolite; and lucianite to be stevensite (amorphous talc?).

Ross and Hendricks (1945) in their paper on the minerals of the montmorillonite group observed that the lucianite of Hilgard is "essentially similar to saponite and differs only in being a little higher in calcium oxide and lower in magnesia than most saponites."

Hey (1950) in his book, An index of mineral species and varieties, lists stevensite as "talc pseudomorphous after pectolite"; walkerite as a variety of pectolite, and gives as a synonym magnesium-pectolite. He also interprets lucianite as "probably an impure saponite."

Descriptions of the Specimens Studied

Stevensite No. 1. Locality: Springfield, New Jersey (U.S.N.M. R4719). Pseudomorphous after pectolite. Pink masses. Analysis 1, Table 1.

Stevensite No. 2. Locality: Jersey City, New Jersey (Selfridge No. 51). Deweylite, "Serpentine after pectolite." Amber masses. Analysis 9, Table 1.

Stevensite No. 3. Locality: Paterson, New Jersey (F-1104). Pseudomorphous after pectolite. Buff, in part resinous in appearance.

Pectolite No. 1. Locality: Paterson, New Jersey (F-1103). White, radiating needles.

X-ray Powder Diffraction Study

X-ray powder diffraction patterns of stevensite, saponite, and pectolite, made from spindles prepared with Duco cement or cellulose acetate dissolved in toluene as the binder, were obtained using filtered copper radiation. Indices were assigned to stevensite on the basis of the work of Faust (1951) on the related mineral sauconite.

The data in Table 2 show that the *x*-ray powder diffraction data for stevensite are practically identical with those of the montmorillonite mineral saponite.

The measurements in Table 2 were made on stevensite No. 1 dried at room temperature. A small amount of stevensite was treated with ethylene glycol, and it was found that (001) advanced from 14± Å to 15.1 Å.

Stevensite No. 3, from Paterson, New Jersey, yielded a pattern showing (001), for air-dried material mounted in ethyl cellulose in toluene, to be 16± Å.

TABLE 2. *X*-RAY POWDER DATA FOR STEVENSITE, SAPONITE, AND TALC DRIED AT ROOM TEMPERATURE

(Cu/Ni; λ=1.5418 Å)

Stevensite No. 1 Springfield, New Jersey				Saponite, Cathkin near Glasgow, Scotland				Talc Brindley (1951)	
U.S.N.M. R4719 Miller Indices	d(Å)	I	Notes	Miller Indices	d(Å)	I	Notes	d(kX)	I
(001)	14.±	s	Shows a "tail"	(001)	14.8	vs			
				(002)	7.71	m	Broad	9.4	8
	5.14	s	Center of Duco band	(003)	5.14	m	Broad		
								4.69	4
(110)(020)	4.55	s		(110)(020)	4.59	ms	Broad		
					4.34	vvf			
				(004)	3.79	vw		3.88	1b
(005)?	3.20	m		(005)	3.09	m		3.37	3
								3.11	10
(130)	2.63	m	Not a good separation		2.613	m		2.70	1
								2.59	2
(200)	2.53	w-m		(200)	2.545	m	Diffuse		
								2.47	5
(220)(040)	2.284	vw	Diffuse					2.32	1
					1.852	vvf		2.20	3
								2.09	2
(240)	1.722	w		(150)	1.747	w		1.92	½
				(310)	1.703	w		1.86	3
(060)	1.526	s		(060)	1.543	s	Broad	1.725	2
					1.498	vvvf		1.67	4
					1.458	vvvf		1.652	1−
(260)(170)	1.315	mw		(260)	1.327	m	Broad	1.632	1b
(400)	1.265	vw		(400)	1.278	vvvf	Broad	1.55	3
					0.999	vvvf	Diffuse	1.52	4
(290)(460)	0.990	vvw						1.501	2
(380)(520)								1.461	1
(480)	0.879	vvw		(550)(390)	0.890	vvvf	Broad	1.446	½
								1.405	2
								1.390	3b
								1.330	2
								1.315	2
								1.291	2

Stevensite No. 2, which is part of the material studied by Selfridge (1936) and which he called deweylite No. 51, was chemically analyzed and the data are recorded in Table 1. Microscopic examination of some acid-treated material showed the presence of a little quartz. *X*-ray study suggests that this material is a mixture of talc and stevensite.

X-ray examination of the material produced by the dissociation of stevensite in the differential thermal analysis study, record C-123, showed it to consist of enstatite.

Physical Properties

Specific gravity

The specific gravity of stevensite as reported in the literature is given in Table 3.

Table 3. Specific Gravity of Stevensite, Talc, Saponite and Montmorillonite

Species	Locality	Specific gravity	Reference
Stevensite	Bergen Hill Tunnel, Hoboken, N. J.	2.565	Leeds (1873)
Stevensite	Hartshorn quarry, Springfield Township, Essex County, N. J.	2.15–2.20	Glenn (1916)
Talc	Various	2.7–2.8	Dana-Ford (1932)
Talc	Theoretical (x-ray)	2.824	Gruner (1934)
Montmorillonite, variety: saponite		2.26±	Larsen and Berman (1934)
Montmorillonites, various		2.04–2.52	Rosenholtz and Smith (1931)

An examination of these data shows that the specific gravity range reported for stevensite is within the commonly accepted range of values given for montmorillonite and is definitely lower than that of talc.

Hardness

The hardness determination made on nearly pure material by Leeds (1873) is 2.5. Glenn (1916) confirmed this for his specimens. Rogers (1917) and others ignored this property in relegating stevensite to the status of an amorphous equivalent of talc.

Swelling characteristics

Glenn (1916) noted, "In H_2O some pieces crumble and give off air bubbles with a crackling sound." A small fragment of stevensite No. 3 when dropped in water gives off air bubbles but shows no easily detectable swelling.

Staining relations

Stevensite was examined by the staining tests devised by Faust (1940) for differentiating the clay minerals of the montmorillonite group from those of the kaolinite group. Briefly, the method is as follows: a small pinch of the ground mineral is placed on a microscope slide. The fragments are covered with a drop of the staining solution, such as malachite green dissolved in nitrobenzene. A cover glass is placed over the preparation and it is then examined under the microscope. This shows whether the fragments have been stained, and if so the color of the stained fragments is normally emerald green. A small amount of the mineral in its natural state is ground and then heated with a 10 per cent solution of hydrochloric acid. The acid-treated mineral is washed by decantation until it is free of acid, and then dried on a steam bath. This material is then stained as described above. If the mineral is a member of the montmorillonite group the fragments are stained yellow, if of the kaolinite group they are emerald green.

Stevensite No. 1 stained deep emerald green in a solution of malachite green dissolved in nitrobenzene. The acid-treated stevensite stained a very pale yellow.

The reaction of stevensite with an aqueous solution of benzidine was also investigated. It was found that the instantaneous reaction between stevensite and benzidine solution produced a light-green coloration. This green deepened in tone after 2 hours of contact, and after 18 hours the color changed to a light powder blue. Stevensite thus behaves like a montmorillonite in forming a colored reaction product with benzidine. The mechanism of this rearrangement of benzidine by montmorillonites has been discussed by Hendricks and Alexander (1940).

CHEMISTRY

Methods of chemical and spectrographic analysis

A 1-gram sample of stevensite No. 1 and a half-gram sample of stevensite No. 2 were first dried to constant weight at 110° C. and then ignited at 900° C. in order to determine H_2O- and H_2O+. During ignition the color of stevensite No. 1 changed from pink to black and finally to white, as was noted by Leeds (1873) with his sample. The ignited materials were fused with three times their weight of sodium carbonate and the subsequent chemical analysis done by conventional methods (Hillebrand, 1919). Ferrous iron was determined on separate half-gram portions of the original samples. A qualitative test for fluorine, based on the color change of the zirconium-alizarin lake and sensitive to 0.02 per cent F, was negative. The results of the chemical analyses are given in Table 1.

A semiquantitative spectrographic analysis of stevensite No. 1 was also made in order to determine the minor elements. Twenty-five milligram duplicate samples were loaded into graphite electrodes, ignited over a Meker burner, and excited by means of the d-c arc. The spectrographic equipment, the general procedure, and the comparison standards used were the same as those described in Gordon and Murata (1952). The orders of magnitude of the various elements were estimated by visual comparison with previously exposed spectrograms of pegmatite base standards. Besides the elements reported in the chemical analysis, the following were determined in the spectrograms of stevensite No. 1: 0.0X per cent B, Al; 0.00X per cent Sr; 0.000X per cent Cu; elements looked for but not detected were Ag, As, Ba, Be, Bi, Cd, Co, Cr, Ga, Ge, In, La, Li, Mo, Nb, Ni, P, Pb, Sb, Sc, Sn, Ti, Tl, V, W, Y, Yb, Zn, and Zr.

Base-exchange capacity

After stevensite had been found by other techniques to be a member of the montmorillonite group, closely allied to saponite, it became desirable to determine its base-exchange capacity and the ratios of the exchangeable bases present. M. D. Foster, of the Geological Survey, kindly determined these values for us. Her report is given in Table 4.

TABLE 4. BASE-EXCHANGE RELATIONS OF STEVENSITE NO. 1

[Determinations by M. D. Foster]

Locality		Exchangeable bases					Total exchangeable bases determined	Total base-exchange capacity
		CaO	MgO	ZnO	Na_2O	K_2O		
Springfield, New Jersey	%	0.93	0.25	0.00	0.03	0.03		
U.S.N.M. R4719	milli-equiv./g	0.33	0.13	0.00	0.00	0.06	0.46	0.36

The sum of the exchangeable bases is larger than the determined exchange capacity. This may be explained by the presence of about a half per cent of fine-grained calcite in the sample, which could not be removed, and which would appear as excess calcium in the base-exchange solution. In all of the calculations reported later in the paper, the determined capacity was used rather than the sum of the bases. The exchange capacity of 0.36 milliequivalent per gram is considerably lower than the mean value of 0.95 found by Foster (1951) for 14 montmorillonitic clays. The low exchange capacity of stevensite is probably due to the unusual way in which the charge deficiency originates in the mineral, as discussed in the following section.

Formula

Two previously established magnesium-rich members of the montmorillonite group of minerals are saponite and hectorite. Stevensite differs from them by not containing essential amounts of aluminum, lithium, or fluorine.

In the absence of aluminum, the tetrahedral positions in the structure of stevensite must be filled solely by silicon. The formula of stevensite No. 1 has been calculated according to the method outlined by Ross and Hendricks (1945, p. 42). A preliminary calculation indicated a slight excess of silica. Although no separate silica phase was noticed in this material, a small amount of quartz was observed microscopically in stevensite No. 2, analysis 9 of Table 1.

Y, Ross and Hendrick's notation for the number of aluminum atoms in tetrahedral positions, becomes zero when 1 per cent excess silica is assumed to be present in stevensite No. 1. The formula calculated under this assumption is as follows:

$$[Mg_{2.88}Mn_{.02}Fe_{.02}][Si_4]O_{10}[OH]_2x_{.15}$$

In the absence of aluminum, no deficiency of charge can arise in the tetrahedral Si positions; therefore, the charge deficiency equal to the exchange capacity must originate in the octahedral Mg positions. An example of such an origin of charge deficiency is found in hectorite, whose formula may be written

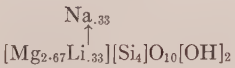

$$[Mg_{2.67}\overset{\overset{Na_{.33}}{\uparrow}}{Li}_{.33}][Si_4]O_{10}[OH]_2$$

In hectorite the octahedral positions are completely filled ($\sum = 3.00$), and the charge deficiency is due to the substitution of monovalent Li for divalent Mg. In stevensite, the octahedral positions are not completely filled ($\sum = 2.92$), and the charge deficiency is to be ascribed to an insufficiency of ions in these positions. Perhaps only a limited amount of charge deficiency can arise in this manner, resulting in a low base-exchange capacity for the mineral.

Incompletely filled octahedral positions ($\sum = 2.70$–2.90) have been noted in sauconite (Ross, 1946). However, in this mineral, the presence of substantial amounts of trivalent aluminum and iron substituting for bivalent zinc and magnesium, produces an excess of charge rather than a deficiency in the octahedral positions. Nevertheless, the example of sauconite is valuable in showing that incompletely filled octahedral positions are possible in trioctahedral clay minerals. In stevensite, an insufficiency of magnesium ions leads directly to a charge deficiency because trivalent ions are virtually absent. Such an origin for charge deficiency has not been hitherto recognized, and should be looked for in other trioctahedral clay minerals that are low in multivalent ions.

A comparison of the formula of stevensite with those of other saponites, taken from the paper of Ross and Hendricks, arranged according to increasing alumina, is given to show the relationship among them. A recent formula (No. 4) of Schmidt and Heystek (1953) was added after this paper was prepared.

1. 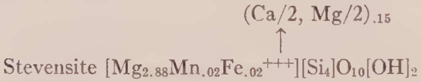
$\text{Stevensite } [\mathrm{Mg}_{2.88}\mathrm{Mn}_{.02}\overset{\overset{(\mathrm{Ca}/2,\ \mathrm{Mg}/2)_{.15}}{\uparrow}}{\mathrm{Fe}_{.02}^{+++}]}[\mathrm{Si}_4]\mathrm{O}_{10}[\mathrm{OH}]_2$
(New Jersey)

2. 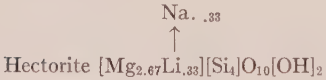
$\text{Hectorite } [\mathrm{Mg}_{2.67}\overset{\overset{\mathrm{Na}._{.33}}{\uparrow}}{\mathrm{Li}_{.33}}][\mathrm{Si}_4]\mathrm{O}_{10}[\mathrm{OH}]_2$
(California)

3. 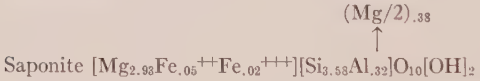
$\text{Saponite } [\mathrm{Mg}_{2.93}\mathrm{Fe}_{.05}^{++}\mathrm{Fe}_{.02}^{+++}][\mathrm{Si}_{3.58}\overset{\overset{(\mathrm{Mg}/2)_{.38}}{\uparrow}}{\mathrm{Al}_{.32}}]\mathrm{O}_{10}[\mathrm{OH}]_2$
(Montreal)

4. 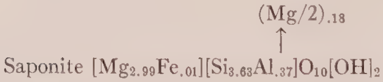
$\text{Saponite } [\mathrm{Mg}_{2.99}\mathrm{Fe}_{.01}][\mathrm{Si}_{3.63}\overset{\overset{(\mathrm{Mg}/2)_{.18}}{\uparrow}}{\mathrm{Al}_{.37}}]\mathrm{O}_{10}[\mathrm{OH}]_2$
(Transvaal)

5. 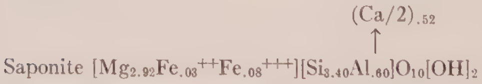
$\text{Saponite } [\mathrm{Mg}_{2.92}\mathrm{Fe}_{.03}^{++}\mathrm{Fe}_{.08}^{+++}][\mathrm{Si}_{3.40}\overset{\overset{(\mathrm{Ca}/2)_{.52}}{\uparrow}}{\mathrm{Al}_{.60}}]\mathrm{O}_{10}[\mathrm{OH}]_2$
(Kearsarge mine, Michigan)

Interpretation of the chemical analyses of stevensite and related minerals

Stevensite is commonly derived by the action of magnesium-bearing solutions on pectolite, and as a result pectolite laths may be present as an impurity. This genetic relationship has been observed for much of the stevensite in the Watchung basalt of New Jersey, for the magnesiumpektolith from Germany, and for the walkerite from Scotland. A graphical study of analyses 1 through 8 of Table 1 is presented in Figure 1. Calcium oxide was selected as the constituent for the primary location of the analysis on the line stevensite-pectolite. It is probably the most reliable index, although a very small amount of the calcium reported in the

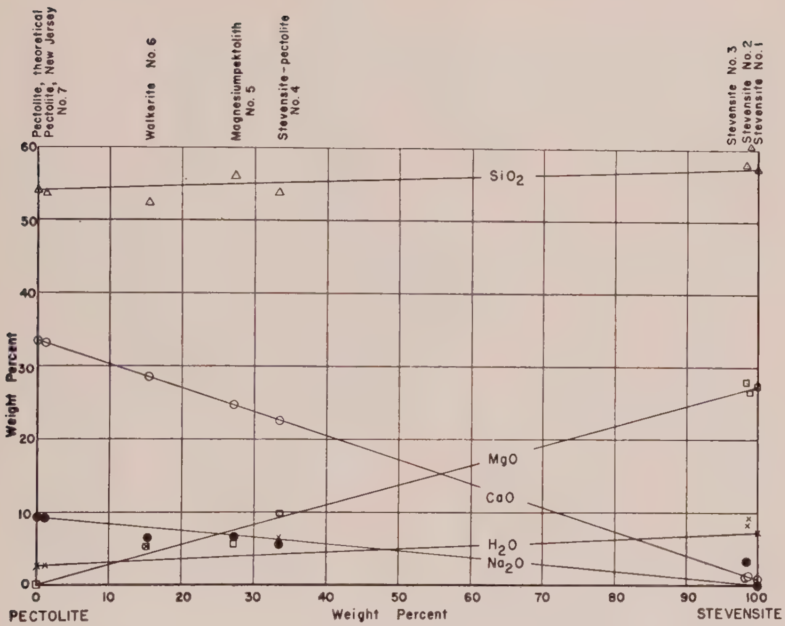

FIG. 1. A graphical study of chemical analyses of stevensite and of natural mixtures of stevensite and pectolite. The ordinate represents the percentage of a given constituent in each analysis. The abscissa gives the compositions of the natural mixtures.

analysis is actually base-exchangeable and a still smaller amount may be present as calcite. The value of H_2O- was ignored. Within the limitations of the data, the graphical relationships support the interpretations of the chemical analyses in terms of two phases, stevensite and pectolite.

Differential Thermal Analysis

A differential thermal analysis was made on part of the tube sample of stevensite No. 1, used for the analytical studies, and the results are shown in Figure 2. Differential thermal analysis curves are given for saponite, talc, and the serpentine minerals chrysotile and antigorite. The data obtained from these curves are summarized in Table 5.

Comparison of these curves shows clearly that stevensite is a member of the montmorillonite group and is definitely not talc or a serpentine mineral. The curve of stevensite is very closely related to that of saponite.

Notes on Some Supposed Hydrated Talcs

The possibility that stevensite might be a hydrated form of talc such as described by Foshag and Wherry (1922) was considered. Differential

TABLE 5.—OBSERVATIONS ON THE THERMAL CURVES OF STEVENSITE, SAPONITE, TALC, CHRYSOTILE AND ANTIGORITE

Mineral	Record no.	Temperature of peaks (° C.)								Locality	Weight of sample used (gram)
		Low temperature		Intermediate temperature		High temperature					
		Endo-thermic	Exo-thermic	Endo-thermic	Exo-thermic	Endothermic			Exo-thermic		
Stevensite No. 1	C-123	152	420	639	583	805	865	—	—	Springfield, N. J. (U.S.N.M. R4719)	0.4762
Saponite	C-185	159	400	562		—	840	—	—	Truckee River Canyon, about 20 miles east of Reno, Nev. (on U. S. Highway 40)	0.5177
Talc	C-130	—	—	—	—	—	—	999	—	Balsam Gap, N. C.	0.4828
Chrysotile	C-489	—	—	670	—	—	—	—	807	Synthetic, T2-29C (Bowen and Tuttle)	0.2382
Antigorite	C-64	—	—	—	—	774	845	1003	—	Antigoro Valley, Italy (U.S.N.M. 96,917)	0.4613

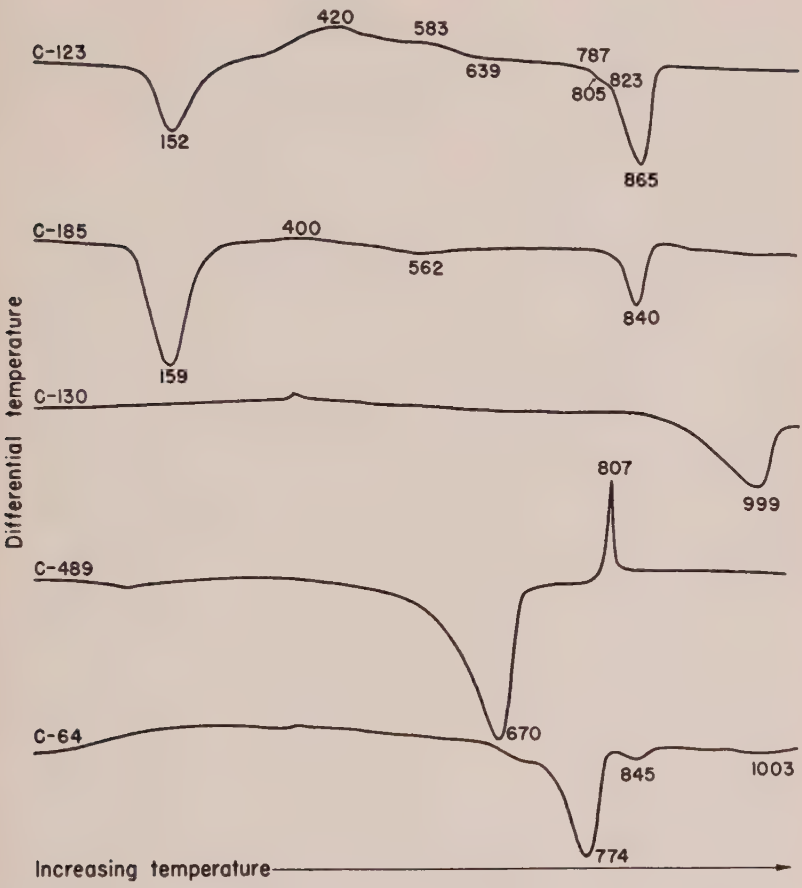

FIG. 2. Differential thermal analysis curves for stevensite No. 1, Springfield, New Jersey, C-123; saponite, Truckee Canyon, near Reno, Nevada, C-185; talc, Balsam Gap, North Carolina, C-130; chrysotile, synthetic, Bowen and Tuttle preparation T2-29C, C-489; and antigorite, Antigoro Valley, Italy, C-64.

All temperatures are given in degrees Centigrade. These curves were all obtained with a resistance of 600 ohms in the galvanometer circuit.

thermal analysis curves of material studied by Foshag and Wherry were obtained and they indicated mixtures of talc and serpentine.[1]

Strunz (1941) in his Tabellen lists "talkhydrat" as brucite and hydrotalc as penninite.

Bowen and Tuttle (1949) in their study of the system $MgO-SiO_2-H_2O$ found no place in the system for a hydrous form of talc. They made a specific point of studying the variability in the composition of talc and found none. They write:

---

[1] Faust, George T., Unpublished data.

"The water content is also in accord with that formula, $\{Mg_3Si_4O_{10}(OH)_2\}$ analysis of our product showing 4.6 per cent H_2O. The theoretical value is 4.75 per cent."

REFERENCES

BOWEN, N. L., AND TUTTLE, O. F. (1949), The system MgO-SiO_2-H_2O: *Geol. Soc. Am. Bull.*, **60,** 439–460.

BRINDLEY, G. W., editor, (1951), *X*-ray identification and crystal structures of clay minerals: London, Mineral. Soc. (See p. 311.)

CHESTER, A. H. (1896), Dictionary of the names of minerals including their history and etymology, 1st ed., 320 pp., New York, John Wiley & Sons.

DANA, E. S. (1892), System of mineralogy, 6th ed., New York, John Wiley & Sons, (See p. 374.)

DANA, E. S., revised by Ford, W. E. (1932), Textbook of mineralogy, New York, John Wiley & Sons, (See p. 677).

FAUST, GEORGE T. (1940), Staining of clay minerals as a rapid means of identification in natural and beneficiated products. (With a general discussion on staining technique): *U. S. Bur. Mines Rept. Inv.* **3522,** 21 p.

——— (1951), Thermal analysis and *x*-ray studies of sauconite and of some zinc minerals of the same paragenetic association: *Am. Mineral.*, **36,** 795–822.

FOSHAG, W. F., AND WHERRY, E. T. (1922), Notes on the composition of talc: *Am. Mineral.*, **7,** 167–171.

FOSTER, M. D. (1951), Importance of the exchangeable magnesium and cation-exchange capacity in the study of montmorillonitic clays: *Am. Mineral.*, **36,** 717–730.

GLENN, M. L. (1916), A new occurrence of stevensite, a magnesium-bearing alteration product of pectolite: *Am. Mineral.*, **1,** 44–46.

GORDON, MACKENZIE, AND MURATA, K. J. (1952), Minor elements in Arkansas bauxite: *Econ. Geol.*, **47,** 169–179.

GRUNER, JOHN W. (1934), The crystal structure of talc and pyrophyllite: *Zeitschr. Kristallographie*, **88,** 412–419.

HAWLEY, JAMES E., AND BEAVAN, A. P. (1934), Mineralogy and genesis of the Mayville iron ore of Wisconsin: *Am. Mineral.*, **19,** 493–514. (See page 503.)

HEDDLE, M. F. (1880), Preliminary notices of substances which may prove to be new minerals. Part 2: *Mineralogical Mag.*, **4,** 117–123. (See p. 121.)

HENDRICKS, STERLING B., AND ALEXANDER, LYLE T. (1940), A qualitative color test for the montmorillonite type of clay minerals: *Jour. Am. Soc. Agronomy*, **36,** 455–458.

HEY, MAX H. (1950), An index of mineral species and varieties arranged chemically. 609 pp., London, British Museum (Natural History).

HILGARD, EUGENE W. (1916), A peculiar clay from near the City of Mexico: *Nat. Acad. Sci. Proc.*, **2,** 8–12.

HILLEBRAND, W. F. (1919), Analysis of silicate and carbonate rocks: *U. S. Geol. Survey Bull.* **700,** 285 p.

HINTZE, CARL (1936 1937), Handbuch der Mineralogie, Ergänzungsband (Neue Mineralien). Lieferung I–IV, 760 pp., Berlin und Leipzig, Walter de Gruyter and Co.

LARSEN, ESPER S., AND BERMAN, HARRY (1934), The microscopic determination of the nonopaque minerals: 2d ed., *U. S. Geol. Survey Bull.* **848,** 266 pp. (See p. 80.)

LEEDS, ALBERT R. (1873), Contributions to mineralogy: *Am. Jour. Sci.*, 3d ser., **6,** 22–26.

LORENT, GUIDO (1933), Der Limburgit von Sasbach am Kaiserstuhl und seine Hydrothermale Mineralführung: *Berichten der Naturforschenden Gesellschaft zu Freiburg in Breisgau.* **32,** 1–48.

MANCHESTER, JAMES G. (1931), The minerals of New York City and its environs: *Bull. New York Mineralogical Club*, **3,** 186 pp., New York.

PEACOCK, MARTIN A. (1935), On pectolite: *Zeitschr. Kristallographie*, Abt. A., **90,** 97–111.

RUENING, ERNST (1907), Über ein Vorkommen von Magnesiumpektolith aus dem grobkörnigen hornblende und glimmerführenden Diabas zu Burg bei Herborn: *Centralbl. Mineralogie*, 739–741.

ROGERS, AUSTIN F. (1917), A review of the amorphous minerals: *Jour. Geology*, **25** 515–541. (See p. 537.)

ROSENHOLTZ, JOSEPH L., AND SMITH, DUDLEY T. (1931), Tables and charts of specific gravity and hardness for use in the determination of minerals: Rensselaer Polytech. Inst. Eng. and Sci. Ser. 34, 83 pp., Troy, New York.

ROSS, C. S. (1946), Sauconite—a clay mineral of the montmorillonite group: *Am. Mineral.*, **31,** 411–424.

ROSS, CLARENCE S., AND HENDRICKS, STERLING B. (1945), Minerals of the montmorillonite group: *U. S. Geol. Survey Prof. Paper* **205-B,** 79 pp.

SCHMIDT, E. R., AND HEYSTEK, H. (1953), A saponite from Krugersdorp district, Transvaal: Abstract of a paper presented at the June 11, 1953 meeting of the Mineralogical Society (Great Britain) and published in Notice No. 82 of the Society.

SELFRIDGE, GEORGE C., JR. (1936), An *x*-ray and optical investigation of the serpentine minerals: *Am. Mineral.*, **21,** 463–503.

STRUNZ, HUGO (1941), Mineralogische Tabellen. 287 pp., Leipzig, Akad. Verlags, Becker und Erler, Kom.-Ges. (See section entitled: Ausgeschiedene Mineralnamen und Register.)

VALIANT, WILLIAM S. (1904), New Jersey mineral localities: *The Mineral Collector*, **11,** 123–125; 137–141; 150–154.

THE BAVENITE PROBLEM*

MICHAEL FLEISCHER, *U. S. Geological Survey, Washington, D. C.*

AND

GEORGE SWITZER, *Smithsonian Institution, Washington, D. C.*

ABSTRACT

Published analyses of bavenite, beryllium calcium aluminosilicate, indicate a wide range of BeO content, but it is probable that all of the early analyses of bavenite gave incorrect figures for the BeO content. A new chemical analysis of bavenite from California shows 7.66 per cent BeO, in good agreement with the analysis of duplexite by Rowledge and Hayton; duplexite is bavenite.

INTRODUCTION

Rowledge and Hayton (1948) described two new beryllium calcium aluminosilicate minerals, named by them duplexite and bowleyite, from the Londonderry feldspar quarry near Coolgardie, Western Australia. Study of their data and of the data in the literature indicated that duplexite is closely related to bavenite, as Rowledge and Hayton suggested, or identical with it.

Further study of these minerals by spectrographic and *x*-ray methods was therefore made. The mechanism of substitution in beryllium-bearing silicates is very imperfectly understood, and it seemed likely that useful data might be obtained from a study of the bavenite-duplexite series, in which the BeO content was reported to range from 2.48 to 7.72 per cent. As reported below, however, it turned out that the BeO content is much less variable than had been reported.

Bowleyite and bityite (the latter described from Madagascar by Lacroix, 1908) are also closely related, but preliminary work has indicated the need for a new chemical analysis of bityite, and single crystal *x*-ray study of both. This work is being continued and will be reported on at a later date.

THE BAVENITE PROBLEM

Bavenite was first described from Baveno, Italy, by Artini (1901), but the presence of beryllium was overlooked by him. Schaller and Fairchild (1932) described bavenite from the Himalaya mine, Mesa Grande, California; Fairchild's analysis gave BeO 2.67 per cent, and spectrographic study by George Steiger on two samples from Baveno is cited as indicating that the Italian bavenite contained fully as much BeO as the California material. Schaller and Fairchild deduced the

---

* Publication authorized by the Director, U. S. Geological Survey, and the Secretary, Smithsonian Institution.

TABLE 1. ANALYSES OF BAVENITE

	1	2	3	4	5	6	7	8	9
SiO_2	56.93	58.40	56.19	57.40	57.11	57.25	58.92	59.13	57.64
Al_2O_3	15.42	12.16	12.49	12.08	9.60	9.89	6.88	7.00	6.46
Fe_2O_3	—	0.10	—	—	0.11	0.10	0.07	none	—
BeO	—	2.67	3.12	2.48	6.60	6.33	7.72	7.14	7.66
CaO	24.47	23.73	25.12	25.76	24.30	24.35	23.26	23.90	23.96
MnO	—	—	—	—	—	—	0.01	0.01	—
MgO	0.12	—	—	—	—	—	0.13	0.05	—
Na_2O	0.29	—	—	—	—	—	0.44	0.10	—
H_2O+	2.49	2.90	2.74	3.00	1.87	1.90	2.41	2.46[a]	3.56[b]
H_2O-	—	—	—	—	—	—	0.06	0.06	0.32
Other	—	—	—	—	0.31[c]	0.31[c]	0.04[d]	0.16[e]	—
	99.72	99.96	99.66[f]	100.72	99.90	100.13	99.94	100.01	99.60
Sum Al_2O_3+ Fe_2O_3+BeO	15.42	14.93	15.61	14.56	16.31	16.32	14.67	14.14	14.12

1. Artini (1901), from Baveno, Italy; Artini, analyst.
2. Schaller and Fairchild (1932), from Mesa Grande, Calif.; Fairchild, analyst.

3, 4. Grill (1941), from Baveno; 3. G. Pagliani, analyst; 4. T. Bianchi, analyst.

5, 6. Kutukova (1946) from Malshevsky mine; 5. V. S. Saltukova, analyst; 6. M. E. Kazakova, analyst.

7, 8. Rowledge and Hayton (1948), from Londonderry; W. Australia; Hayton, analyst.

9. From Mesa Grande, Calif. M. K. Carron, analyst; new analysis on same sample as No. 2 above; analysis corrected by spectrographic determination, by Janet D. Fletcher, of Be in $AlPO_4$ and Al in BeO (USNM 104299).

[a] Ignition loss minus 0.06 per cent H_2O-, Cl 0.02; CO_2 0.03, C 0.11 per cent.

[b] Ignition loss minus H_2O-.

[c] B_2O_3 0.31 per cent.

[d] K_2O 0.04 per cent.

[e] Cl 0.02, CO_2 0.03, C 0.11 per cent.

[f] Given in original as 99.47 per cent.

formula $Ca_4Al_2BeSi_9O_{25}(OH)_2$. This was confirmed by two new analyses from Baveno, published by Grill (1941), and was shown by Ksanda and Merwin (1933) to fit satisfactorily the orthorhombic unit cell they found for bavenite, calculation giving $Z=1.004$ molecules of the above formula in the unit cell. Claringbull (1940) found that the unit cell of bavenite had a volume exactly four times as great as that given by Ksanda and Merwin. He states, "Carbon arc spectra of the type material from Baveno and that from Muotta Nera (Switzerland) indicate the presence of similar quantities of beryllium in each."

Thus the composition of bavenite seemed to be well established. In 1946, however, Kutukova published two analyses showing 6.60 and 6.33 per cent BeO, and later Rowledge and Hayton (1948) published two analyses showing 7.72 and 7.14 per cent BeO on material from the Londonderry quarry, Western Australia, to which they gave the name duplexite. They called attention to the close resemblance in optical properties to bavenite, but, apparently unaware of the work of Kutukova, thought the composition sufficiently different to justify a new name.

TABLE 2. OPTICAL PROPERTIES OF BAVENITE

	1	2	3	4	5	6	7	8	9	10
α	—	1.578	1.580	1.580	1.579	1.580	1.583–1.584	1.583	1.586	1.582
β	1.580	1.579	1.582	—	1.581	—	1.585	—	1.588	1.584
γ	—	1.583	1.590	1.588	1.589	1.587	1.590	1.589	1.593	1.593
$\gamma-\alpha$	—	0.005	0.010	0.008	0.010	0.007	0.006–0.007	0.006	0.007	0.011
2V	47°	Small	—	—	—	58°	—	—	60°	22°
Sign	+	+	+	. . .	+	+	+	+	+	+
Elong.	—	—	Neg.	Neg.	Neg.	Neg.	—	—	Pos.	Neg.
Ext.	2°	Very small	—	—	2°	—	0°	—	—	2–5°
Sp. Gr.	2.72	—	—	—	—	—	2.74_5	2.74	2.733	2.71

1. Artini (1901), from Baveno, Italy.
2. Larsen (1921), from Baveno.
3. Schaller and Fairchild (1932), from Baveno.
4. Schaller and Fairchild (1932), fibers from Mesa Grande, Calif.
5. Schaller and Fairchild (1932), crystals from Mesa Grande.
6. Ross quoted by Schaller and Fairchild (1932), fibers from Mesa Grande.
7. Ksanda and Merwin (1933), crystals from Baveno.
8. Claringbull (1940), from Muotta Nera and Val Casaccia, Switzerland.
9. Kutukova (1946), from Malshevsky emerald mine.
10. Rowledge and Hayton (1948), from Londonderry, W. Australia.

The analyses are compiled in Table 1; in analyses 2 to 8, the BeO content ranges from 2.48 per cent to 7.72 per cent, a very large range for a constituent with so low a molecular weight; the sum of Al_2O_3+BeO does not, however, vary greatly. The optical data, as shown in Table 2, show but little variation, and this seems to be random and not closely related to the apparent differences in composition.

It seemed desirable to check the apparent variation. Selected small samples including one from a new locality, Amelia, Virginia, were analyzed in the spectrographic laboratory of the U. S. Geological Survey with the results shown in Table 3.

In view of these results, a new sample was prepared from the specimen studied by Schaller and Fairchild. Its analysis by M. K. Carron of the Geological Survey is given in Table 1, column 9. The analysis was made by the method of Stevens and Carron (1946), and the weights of the precipitates of $AlPO_4$ and BeO were checked by spectrographic determi-

TABLE 3. SPECTROGRAPHIC DETERMINATIONS OF BERYLLIUM IN BAVENITE

Locality	Per cent BeO	Analyst
Baveno, Italy (USNM R-4158)	5.4±0.5	E. L. Hufschmidt
Mesa Grande, Calif. (USNM 104299)	7.8	J. D. Fletcher
Rutherford mine, Amelia, Va. (USNM 106718)	8.0	J. D. Fletcher

nation of Be in the $AlPO_4$ and of Al in the BeO. The analysis agrees very well with the analyses by Rowledge and Hayton, who used the 8-hydroxyquinoline method to separate beryllium and aluminum. Kutukova does not state what methods were used in the analyses of the Russian material, but does state that the purity of the BeO and Al_2O_3 weighed were checked spectrographically.

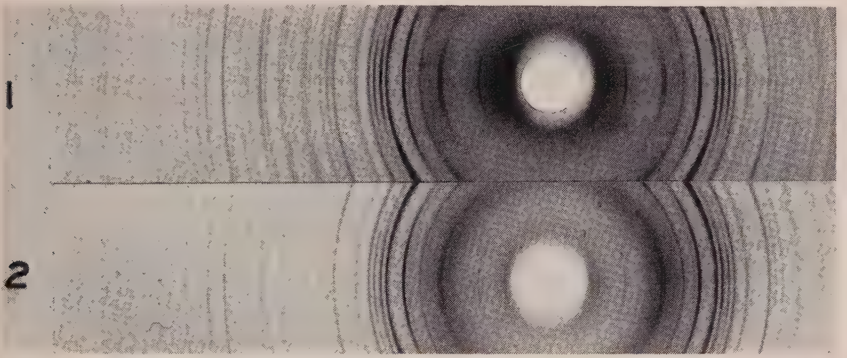

FIG. 1. 1. Duplexite, Coolgardie, Western Australia. USNM 105929.
2. Bavenite, Baveno, Italy. USNM C 3475.

It seems probable that all of the early analyses are in error, part of the BeO being reported as Al_2O_3. A new analysis of Baveno material is highly desirable to check the figure for BeO given in Table 3. The data available suggest that there is not a great range in BeO content and that bavenite contains about as much BeO as the material from Australia named duplexite. *X*-ray powder photographs of bavenite and duplexite, as shown in Figure 1, are identical. The latter name should therefore be dropped.

Recalculation of analyses 8 and 9, table 2, gave the following results:

Anal. 8 (Hayton) $Ca_{3.87}Be_{2.57}Al_{1.24}Si_{8.88}O_{26} \cdot 1.23H_2O$
Anal. 9 (Carron) $Ca_{4.11}Be_{2.95}Al_{1.22}Si_{9.22}O_{26} \cdot 1.90H_2O$

If the specific gravity is assumed to be 2.73, the unit cell determined by Claringbull contains 4.06 formula weights of the formula above derived from analysis 8, 3.91 formula weights of the formula above derived from analysis 9. If one assumes 4 formula weights in the unit cell, the calculated specific gravity is 2.69 for analysis 8, 2.79 for analysis 9.

X-ray powder data for bavenite (duplexite) from Australia, measured by Dr. K. Norrish, are given in Table 4.

Bavenite from Amelia, Va.—A single specimen of bavenite from the Rutherford mine, Amelia, Va., was collected by Ned Blandford of McLean, Va. The optical properties and *x*-ray powder pattern of the

TABLE 4. *X*-RAY POWDER DATA BY K. NORRISH

Bavenite (duplexite)		
d/n	I	hkl
11.46	m	010
7.36	m	110
4.86	w.d.	120, 200, 001
4.32	vw	210
4.14	m-S	111
3.81	vw	021, 030
3.701	m-S	220
3.332	S	211
3.180	m	300
3.062	vw	310, 031
2.992	m-S	230, 221
2.826	w	320, 040
2.716	vw	301
2.632	vw	311
2.538	m-S	002
2.457	vw	102, 321, 330, 240
2.394	w	400, 112
2.271	m	050, 122
2.223	w	241, 331, etc.
2.147	vw	401
2.072	w.m.d.	250, 222, 132
1.965	w	341, 312
1.926	w	500, 232
1.862	w	142, 350
1.810	vw	520
1.755	m	161
1.730	m	441
1.695	vvw	003
1.655	m	450, 113
1.615	w	170
1.562	w-m	071, 361
1.530	vw	062, 302, 133
etc.		

Virginia material are identical with those from Mesa Grande, Calif.; its BeO content, determined spectrographically, is given in Table 3. The bavenite was found as rosettes of thin, colorless plates, having a maximum size of 0.5 mm. in a small cavity in albite (cleavelandite). Emplanted on the bavenite are a few minute crystals of bertrandite.

ACKNOWLEDGMENTS

We thank Dr. K. Norrish for the use of his data and H. P. Rowledge, Director, Government Chemical Laboratories, Western Australia, for supplying a copy of Dr. Norrish's report and granting permission to quote from it. We thank M. K. Carron, U. S. Geological Survey, who made the chemical analysis of bavenite from California, and K. J. Murata, Janet D. Fletcher, and Elizabeth L. Hufschmidt, all of the U. S. Geological Survey, who made spectrographic analyses. Ned Blandford kindly granted permission for the removal of part of the bavenite on his specimen from Amelia for analysis. It is a special pleasure to acknowledge our debt to W. T. Schaller for many suggestions.

References

Artini, Ettore (1901), Di una nuova specie minerale trovata nel granito di Baveno: *Atti (Rend.) reale accad. Lincei, Classe sci. fis., mat. e nat.*, **10,** 139–145.

Claringbull, G. F. (1940), Occurrences of bavenite in Switzerland: *Mineralog. Mag.*, **25,** 495–497.

Grill, E. (1941), Bavenite: composizione, chimica, diffusiona: *Rend. soc. mineral. Ital.*, **1,** 97–107.

Ksanda, C. J., and Merwin, H. E. (1933), Bavenite: Symmetry, unit cell: *Am. Mineral.*, **18,** 341–344.

Kutukova, E. (1946), Bavenite from the emerald mines: *Doklady Akad. Nauk S.S.S.R.*, **54,** 725–728. (in Russian).

Lacroix, Alfred (1908), Les mineraux des filons de pegmatite a tourmaline lithique de Madagascar: *Bull. soc. franc. mineral.*, **31,** 218–247; on bityite, 241–244.

Larsen, E. S. (1921), The microscopic determination of the nonopaque minerals: *U. S. Geol. Survey Bull.* **679,** 44.

Larsen, E. S., and Berman, Harry (1934), The microscopic determination of the nonopaque minerals: 2d ed. *U. S. Geol. Survey Bull.* **848,** 177.

Rowledge, H. P., and Hayton, J. D. (1948), Two new beryllium minerals from Londonderry: *J. Roy. Soc. Western Australia*, **33,** 45–52.

Schaller, W. T., and Fairchild, J. G. (1932), Bavenite, a beryllium mineral, pseudomorphous after beryl, from California: *Am. Mineral.*, **17,** 409–422.

Stevens, R. E. and Carron, M. K. (1946), Determination of beryllium in ores: *U. S. Geol. Survey Bull.* **950,** 91–100.

GEOCHEMICAL STUDIES OF CLAY MINERALS: II—RELATION BETWEEN IONIC SUBSTITUTION AND SWELLING IN MONTMORILLONITES*†

Margaret D. Foster, *U. S. Geological Survey, Washington, D. C.*

Abstract

The swelling of Na-saturated montmorillonites from 12 different localities was determined after the clays were separated from associated minerals. The degree of swelling, which ranged between 21 and 66 ml. per gram of sample, showed no correlation with cation-exchange capacity or with tetrahedral charge but did show a correlation with octahedral substitution, in the direction of decrease in swelling with increase in octahedral substitution. Substituted Fe^{+2} had a greater depressing effect on swelling than Fe^{+3}, which in turn appeared to have about the same depressing effect as Mg^{+2}.

Swelling, considered as an osmotic property of montmorillonites, is affected by degree of dissociation. The greater the dissociation the greater the swelling, and vice versa. It is suggested that substitutions in the montmorillonite structure affect the energy relationships of the structural constituents and hence the degree of dissociation of the montmorillonite in water. The decrease in swelling found to accompany increase in octahedral substitution seems to indicate that the effect of substitution of Mg and Fe for Al is in the direction of decrease in the degree of dissociation of the montmorillonite.

Introduction

Studies on the swelling of montmorillonite have given much more attention to the effect of the exchangeable cation than to the effect of the composition although Grim (1935) pointed out, some years ago, that the physical properties of clays may be ascribed to the two factors—the character of the exchangeable cation and the composition of the clay mineral. By composition Grim referred to the make-up of the clay mineral, particularly with regard to substitutions within the structure. "Two montmorillonites, identical except for differences in Mg^{+2} replacements of Al^{+3} in gibbsite positions, may be expected to impart different physical properties to clays containing them. In other words the properties depend not only on the presence of montmorillonite, but on the composition of the particular montmorillonite."

Differences in the physical properties of two montmorillonites identical in composition except for differences in Mg^{+2} replacements of Al^{+3} in gibbsite positions might be attributed to differences in cation-exchange capacity. However, Kelley (1943) pointed out that, although swelling of soil colloids seems to increase as the base-exchange capacity increases, different soil colloids having equal exchange capacity may swell very differently and that the swelling of Na-saturated montmorillonite samples from different sources is not always proportional to the base-exchange capacity.

---

* Publication authorized by the Director, U. S. Geological Survey.

† The term "montmorillonite" as used in this paper refers specifically to the mineral montmorillonite and not to the group unless so designated.

The difference in swelling between a montmorillonite and a beidellite (an aluminian montmorillonite) of equal exchange capacity has been attributed by Marshall (1936) to the fact that in the one mineral the seat of the charge is in the Al layer and in the other it is in the Si layers. An excess negative charge originating in the outer Si layers is presumed to be strong enough to hold the units closely together and to prevent the entrance of water and expansion. An excess negative charge originating in the Al layer is, on the other hand, generally thought to have the strength to hold exchangeable cations but not the strength necessary to hold the units closely together and prevent expansion and the entrance of water. Interpreted osmotically, the cations associated with a charged Al layer are presumed to be more easily dissociated than the cations associated with a charge originating in the Si layers, since they are physically separated from the seat of the charge by the Si layers and are consequently less strongly held. The degree of dissociation of a montmorillonite and consequently the swelling would, therefore, be expected to be greater than that of a beidellite having the same charge.

On the presumption that the difference in swelling between a beidellite and a montmorillonite is due to the source of the charge, whether on the Al layer or the Si layers, two montmorillonites of equal exchange capacity but differing in the proportion of the charge originating in the Al and Si layers would also be expected to swell differently. And two montmorillonites with equal exchange capacity originating to the same degree in the Al and Si layers would be expected to swell to the same degree. Thus the composition of a montmorillonite, especially with respect to substitutions in the structure that contribute to total charge and to the relative distribution of the charge between the outer and inner layers, would be expected to have a significant influence on the swelling volume. As Fe^{+3} substituted for Al^{+3} does not change the charge on the inner layer, it would not be expected to affect the swelling volume.

The purpose of the present study was to determine whether and to what extent the swelling volume of montmorillonite is affected by composition. The 12 samples of montmorillonite used in the study differed considerably in the extent of Fe and Mg substitution in the Al layer, in total exchange capacity, and in the relative distribution of charge between the Al and Si layers. In order to hold constant the second factor mentioned by Grim—character of exchangeable cation—all the specimens were converted to the Na form at the beginning of the investigation.

TABLE 1. ANALYSES OF BENTONITES AND PEGMATITE CLAYS

	1	2	3	4	5	6	7	8	9	10	11	12
SiO_2	54.58	54.28	53.35	54.07	58.31	52.09	54.28	58.13	57.80	51.50	51.29	51.72
Al_2O_3	16.44	22.94	17.53	21.07	20.20	18.98	17.92	15.96	17.06	19.44	15.96	17.24
Fe_2O_3	2.59	.24	2.25	2.45	3.26	.06	3.88	.84	1.71	.10	2.46	5.30
FeO	.11	Tr.	—	.74	.55	—	—	—	—	—	.14	.37
TiO_2	.18	.06	—	.14	.11	none	.20	.07	.15	none	.18	.69
CaO	.72	3.18	.91	.55	.25	3.28	1.80	1.35	1.65	.48	2.21	.72
MgO	4.90	2.92	.354	1.92	2.50	3.80	3.76	3.72	3.01	5.07	3.95	2.50
Na_2O	3.02	.08	—	2.35	2.35	—	.10	.10	.05	.20	.05	.09
K_2O	.81		—	.40	.15	—	.25	.04	.02		.13	1.04
MnO	—	—	—	.01	—	.06	—	—	—	—	.00	—
SO_3	.03	none	—	.17	.30	none	.01	none	none	—	none	.01
H_2O^-	11.10	7.82	—	11.60*	6.65*	14.75	10.84	—	—	14.50	18.00*	15.65*
H_2O^+	5.49	8.70	—	4.89	5.15	7.46	7.32	—	—	8.04	5.37	4.66
Total	99.97	100.22	—	100.36	99.78	100.48	100.36	—	—	99.33	99.74	99.99
Total cation exchange per gram	1.110	1.029	.805	.860	.877	.980	.856	.833	.810	.975	.900	.665
Associated minerals	.50	3.49	1.81	7.33	8.85	.18	.94	8.65	4.41	.22	2.04	7.55
Excess SiO_2	none	none	2.80	2.18	1.91	none	none	10.85	7.97	none	none	
Excess Al_2O_3	none	2.25	none	none	none	.90	none	none	none	none	.39	

1. Amargosa Valley, Calif.—J.G.Fairchild[1]
2. Greenwood, Maine.—J. G. Fairchild[1]
3. Fort Steel, Wyo.—M. D. Foster
4. Belle Fourche, S. D.—M. D. Foster
5. Upton, Wyo.—M. D. Foster
6. Tatatila, Mex.—K. J. Murata[1]
7. Nieder-Bayern, Germany—J. G. Fairchild[1]
8. Rideout, Utah—M. D. Foster
9. San Antonio, Tex.—M. D. Foster
10. Santa Rosa, Mex.—J. G. Fairchild[1]
11. Burns, Miss.—M. D. Foster
12. Aberdeen, Miss.—M. D. Foster

* H_2O- at 300° C.

[1] Same sample as described by Ross and Hendricks. (1945)

PREPARATION AND ANALYSES OF SPECIMENS

Many of the specimens of montmorillonite used in this study were used by Ross and Hendricks (1945) in their investigation of the minerals of the montmorillonite group and by the author (1951)* in her study of exchangeable magnesium and cation-exchange capacity in montmorillonites. For these specimens analyses and cation-exchange data were available. The specimens from Mississippi, South Dakota, and Upton, Wyoming, were collected and analyzed by the author. Analyses of the bentonites and pegmatite clays used in the study are given in Table 1. Also included are data on cation-exchange capacity, associated minerals, and soluble or excess SiO_2 and Al_2O_3. Free SiO_2 and free Al_2O_3 were obtained by digesting the clay in $0.5N$ NaOH. The details of this procedure will be described in a forthcoming paper.

TABLE 2. ANALYSES OF CLAY (MONTMORILLONITE) FRACTIONS
(Sample numbers same as in Table 1)
M. D. Foster, analyst

	1	2	3[1]	4[1]	5[1]	6[2]	7	8[1]	9[1]	10	11	12
SiO_2	56.56	55.56	59.09	54.07	57.50	52.78	57.78	57.44	58.19	56.60	57.74	55.68
Al_2O_3	17.18	22.48	18.86	21.02	20.59	17.91	18.64	19.40	19.91	21.24	17.38	19.42
Fe_2O_3[3]	2.80	.20	2.08	3.72	3.94	.06	4.18	1.10	2.22	2.0	3.11	6.51
TiO_2	.16	.00	.20	.14	.11	—	.16	.14	.22	.00	—	.80
MgO	4.85	3.30	4.20	2.09	2.45	3.56	3.37	3.85	3.04	3.46	4.25	2.30
Na_2O	3.58	3.68	3.10	2.84	2.87	3.19	3.03	3.39	3.13	3.71	3.35	2.48
MnO	.02	.08	.00	—	—	—	—	.01	.00	.01	—	.01
Cation exchange per gram	1.11	1.14	.96	.88	.89	.99	.94	1.05	.97	1.15	1.04	.77
Excess SiO_2	—	—	3.2	2.18	1.91	—	—	7.00	7.10	—	—	—
Excess Al_2O_3	—	—	—	—	—	1.30	—	—	—	—	—	—

[1] Values adjusted to correct for free SiO_2.
[2] Values adjusted to correct for free Al_2O_3.
[3] Total Fe as Fe_2O_3.

In order that the results of the swelling tests should represent the swelling of the actual montmorillonites in the bentonites and pegmatite clays used, the clays, after conversion to the Na form, were separated by suspension from associated minerals—feldspar, quartz, etc. The supernatant liquid containing the clay fraction was then siphoned off, evaporated to dryness, and the clay crushed. One gram of material passing 20 mesh but retained on 40 mesh was set aside for the swelling test; the remainder of the material was crushed to pass 80 mesh and used for analysis of the clay fraction of the samples and for redetermination of free SiO_2 and free Al_2O_3 in the clay fraction of those specimens that had

---

* This paper was No. I of the series "Geochemical Studies of Clay Minerals."

Table 3. Formulas from Clay Fractions for Montmorillonites
(Sample numbers the same as in table 1)

No.	Locality	Formulas	Swelling volume, ml.
1.	Amargosa Valley, Calif.	$[\mathrm{Al}^{+3}_{1.37}\mathrm{Fe}^{+3}_{.15}\mathrm{Mg}^{+2}_{.50}][\mathrm{Si}^{+4}_{3.96}\mathrm{Al}^{+3}_{.04}]\mathrm{O}_{10}[\mathrm{OH}]_2\ \mathrm{x}_{.47}$	21
2.	Greenwood, Maine	$\mathrm{Al}^{+3}_{1.66}\mathrm{Fe}^{+3}_{.01}\mathrm{Mg}^{+2}_{.34}][\mathrm{Si}^{+4}_{3.83}\mathrm{Al}^{+3}_{.17}]\mathrm{O}_{10}[\mathrm{OH}]_2\ \mathrm{x}_{.47}$	50
3.	Fort Steel, Wyo.	$[\mathrm{Al}^{+3}_{1.49}\mathrm{Fe}^{+3}_{.10}\mathrm{Mg}^{+2}_{.43}][\mathrm{Si}^{+4}_{3.98}\mathrm{Al}^{+3}_{.02}]\mathrm{O}_{10}[\mathrm{OH}]_2\ \mathrm{x}_{.39}$	35
4.	Belle Fourche, S.D.	$[\mathrm{Al}^{+3}_{1.60}\mathrm{Fe}^{+3}_{.19}\mathrm{Mg}^{+2}_{.22}][\mathrm{Si}^{+4}_{3.84}\mathrm{Al}^{+3}_{.16}]\mathrm{O}_{10}[\mathrm{OH}]_2\ \mathrm{x}_{.38}$	43.5
5.	Upton, Wyo.	$[\mathrm{Al}^{+3}_{1.55}\mathrm{Fe}^{+3}_{.20}\mathrm{Mg}^{+2}_{.25}][\mathrm{Si}^{+4}_{3.90}\mathrm{Al}^{+3}_{.10}]\mathrm{O}_{10}[\mathrm{OH}]_2\ \mathrm{x}_{.36}$	35
6.	Tatatila, Mexico	$[\mathrm{Al}^{+3}_{1.58}\mathrm{Fe}^{+3}_{.00}\mathrm{Mg}^{+2}_{.40}][\mathrm{Si}^{+4}_{3.99}\mathrm{Al}^{+3}_{.01}]\mathrm{O}_{10}[\mathrm{OH}]_2\ \mathrm{x}_{.45}$	43
7.	Nieder-Bayern, Germany	$[\mathrm{Al}^{+3}_{1.45}\mathrm{Fe}^{+3}_{.21}\mathrm{Mg}^{+2}_{.34}][\mathrm{Si}^{+4}_{3.95}\mathrm{Al}^{+3}_{.05}]\mathrm{O}_{10}[\mathrm{OH}]_2\ \mathrm{x}_{.39}$	23
8.	Rideout, Utah	$[\mathrm{Al}_{1.55}\mathrm{Fe}_{.06}\mathrm{Mg}_{.39}][\mathrm{Si}_{3.97}\mathrm{Al}_{.03}]\mathrm{O}_{10}[\mathrm{OH}]_2\ \mathrm{x}_{.44}$	32.5
9.	San Antonio, Tex.	$[\mathrm{Al}^{+3}_{1.57}\mathrm{Fe}^{+3}_{.12}\mathrm{Mg}^{+2}_{.30}][\mathrm{Si}^{+4}_{3.99}\mathrm{Al}^{+3}_{.01}]\mathrm{O}_{10}[\mathrm{OH}]_2\ \mathrm{x}_{.38}$	43
10.	Santa Rosa, Mexico	$[\mathrm{Al}^{+3}_{1.63}\mathrm{Fe}^{+3}_{.01}\mathrm{Mg}^{+2}_{.36}][\mathrm{Si}^{+4}_{3.90}\mathrm{Al}^{+3}_{.10}]\mathrm{O}_{10}[\mathrm{OH}]_2\ \mathrm{x}_{.48}$	66
11.	Burns, Miss.	$[\mathrm{Al}^{+3}_{1.41}\mathrm{Fe}^{+3}_{.16}\mathrm{Mg}^{+2}_{.43}][\mathrm{Si}^{+4}_{3.99}\mathrm{Al}^{+3}_{.01}]\mathrm{O}_{10}[\mathrm{OH}]_2\ \mathrm{x}_{.43}$	26
12.	Aberdeen, Miss.	$[\mathrm{Al}^{+3}_{1.44}\mathrm{Fe}^{+3}_{.34}\mathrm{Mg}^{+2}_{.24}][\mathrm{Si}^{+4}_{3.86}\mathrm{Al}^{+3}_{.14}]\mathrm{O}_{10}[\mathrm{OH}]_2\ \mathrm{x}_{.32}$	23

been found to contain several per cent of these impurities before the separation of associated minerals. As shown in Table 2, the clay fraction of some of the specimens contained several per cent of free or soluble SiO_2. *X*-ray examination of these clay fractions showed this free SiO_2 to be present predominantly as cristobalite, with a trace of quartz.

Formulas derived from the analyses of the clay fractions are given in Table 3. These formulas were calculated according to the method of Ross and Hendricks, after correcting for free SiO_2, if present, and exchangeable Mg, and using the determined cation-exchange value. The determined cation-exchange capacity ranged between 0.77 and 1.15 milliequivalents per gram (the mean value being 0.97), indicating a 50 per cent difference among the specimens in the extent to which the structure was unbalanced. Substitution of Fe^{+3} for Al^{+3} ranged from none up to 0.34, substitution of Mg^{+2} for Al^{+3} ranged between 0.22 and 0.50, and total substitution of Al^{+3} in the octahedral layer by Fe and Mg ranged between 0.35 and 0.65. There were several specimens in which all, or very nearly all, of the unbalance in the structure was in the octahedral layer, as several specimens had little or no substitution of Al^{+3} for Si^{+4} in the tetrahedral layer. In others, however, almost half of the unbalance of the structure was in the tetrahedral layer. In only one sample, however, was the substitution due entirely to one element, Mg. This was the Tatatila specimen, with no substitution of Fe^{+3} for Al^{+3} in the octahedral layer and only $0.01Al^{+3}$ substituted for Si^{+4} in the tetrahedral layer. Thus the specimens used in the study varied widely in type and amount of replacement, in total cation-exchange capacity, and in the distribution of charge between the Al and Si layers.

Determination of Swelling

The procedure used for the determination of swelling was as follows: One gram of air-dried material, crushed to pass 20 mesh but to be retained on 40 mesh, was added, in divided portions, to 100 ml. of distilled water contained in a 100-ml. graduate. Montmorillonite aggregates of this grain size are just heavy enough to sink of their own weight in water. Each portion added amounted to 0.10 to 0.15 gram of material, which was gently tapped from the end of a small spatula blade into the water. Addition of similar portions was repeated at 5-minute intervals until the whole sample had been added. Twenty-four hours after the last portion had been added the volume of the gel was measured on the graduate.

This method for measuring free swelling is capable of giving results that are comparable if the samples are prepared under uniform conditions of room temperature and humidity and if they are added to the water at the same rate.

The results of the swelling tests are given in Table 3.

Discussion of Results

The variation in swelling volume between 21 and 66, a more than three-fold difference, strongly supports the assumption that the swelling of montmorillonites is greatly influenced by factors other than the effect of the exchangeable cation, which was the same, i.e. Na, in all the specimens. As the amount of Na present varied with the total cation-exchange capacity, it seemed possible that the differences in swelling volume might be due to differences in the amount of Na present, i.e. to differences in total exchange capacity. However, comparison of cation-exchange capacity with swelling volume (Fig. 1) indicated that, although the Santa Rosa sample, which had the highest cation-exchange capacity, had also the highest swelling volume and the Aberdeen sample, which had the lowest exchange capacity, had the lowest swelling volume, a more detailed examination showed certain discrepancies. For example, the Aberdeen, Nieder-Bayern and Amargosa Valley samples, which had quite dif-

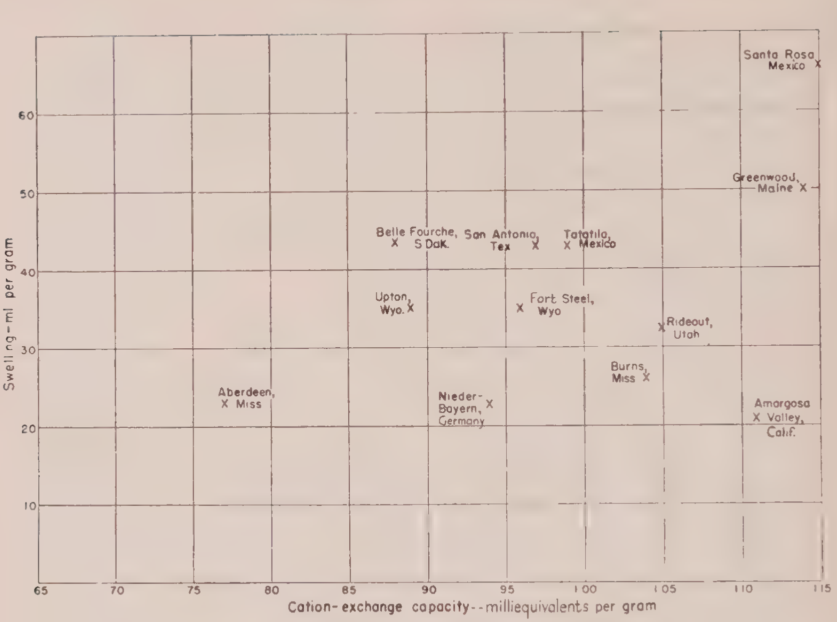

FIG. 1. Relation between swelling and cation-exchange capacity.

ferent exchange capacities, 0.77, 0.94, and 1.11 respectively, had approximately the same swelling volumes, 23, 23, and 21 mls., respectively. On the other hand, the Amargosa Valley and Greenwood samples had almost the same exchange capacities, 1.11 and 1.14, but their swelling volumes were quite different, 21 and 50 mls., respectively.

As an excess negative charge originating in the outer tetrahedral layers is presumed to be stronger and more adequate to hold the units together and prevent expansion in water than an excess charge originating in the octahedral layers, it would be expected that of two samples having the same total charge, one in which the charge originated almost wholly in the octahedral layer would swell more than one in which a considerable part of the charge originated in the tetrahedral layers. The samples from Fort Steel (No. 3, Table 3) and Belle Fourche (No. 4, Table 3) have almost the same total charge, 0.39 and 0.38 respectively. In the Fort Steel sample this charge originates almost wholly in the octahedral layer; in the Belle Fourche sample almost half the charge originates in the tetrahedral layers. Yet the Belle Fourche sample had a swelling volume of 43.5 ml., while the Fort Steel sample swelled to only 35 ml. Similarly the Amargosa Valley and Greenwood samples had the same total charge, 0.47, but the Greenwood sample, with 0.17 tetrahedral charge, swelled more than the Amargosa Valley sample with only 0.04 tetrahedral charge.

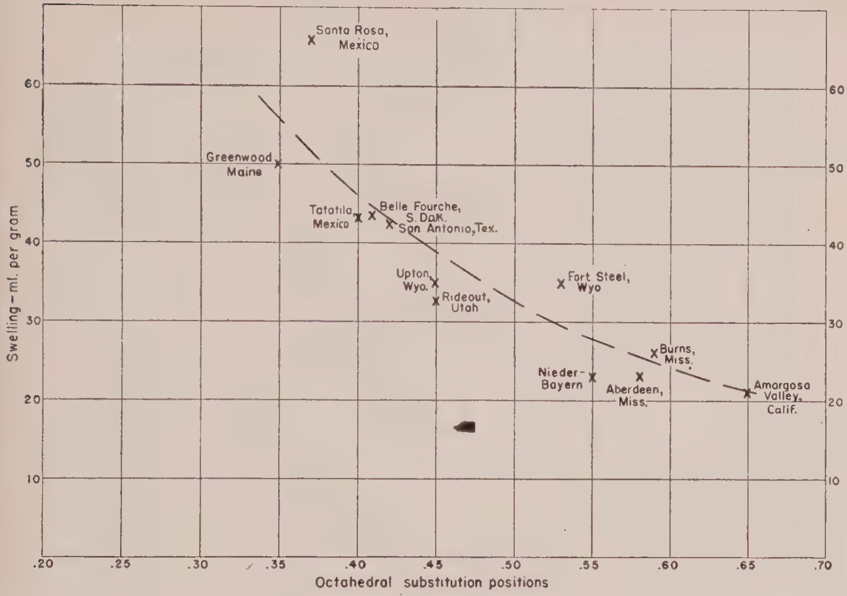

FIG. 2. Relation between swelling and octahedral substitution.

Other samples with the same total charge and the same tetrahedral charge, as, for example the Nieder-Bayern and San Ontario samples, had quite different swelling volumes. These examples indicate that neither total charge nor tetrahedral charge has, apparently, much influence on the swelling volume.

Inspection of the formulas of the last-mentioned pair of samples—Nieder-Bayern and San Antonio—shows that although the total charge and the tetrahedral charge, or substitution of Al^{+3} for Si^{+4}, is the same in both samples, the amount of substitution in the octahedral layer is quite different, being 0.55 and 0.43 respectively, and that the sample with the greater octahedral substitution has the lower swelling volume. Examination of the other pairs of samples cited above shows the same relationship. In each pair the sample with the higher octahedral substitution has the lower swelling volume.

When the swelling volume of each specimen is plotted against octahedral substitution (Figure 2) there is apparent a much closer relationship than when swelling is plotted against cation-exchange capacity (Figure 1). The Burns and Aberdeen samples, with quite different cation-exchange capacities (1.04 and 0.77, respectively) have almost the same amount of octahedral substitution and almost the same swelling volumes. Similarly Tatatila and Belle Fourche have very different cation-exchange capacities but the same amount of octahedral substitution and the same swelling volumes.

The fact that Fe^{+3} substitution has a significant effect on swelling is apparent when the formulas and swelling volumes of the Tatatila, Fort Steel, and Burns samples are compared.

		Swelling volume ml.
Tatatila	$[Al^{+3}_{1.58}Fe^{+3}_{.00}Mg^{+2}_{.40}][Si^{+4}_{3.99}Al^{+3}_{.01}]O_{10}[OH]_2\ X_{.45}$	43
Fort Steel	$[Al^{+3}_{1.49}Fe^{+3}_{.10}Mg^{+2}_{.42}][Si^{+4}_{3.99}Al^{+3}_{.01}]O_{10}[OH]_2\ X_{.39}$	35
Burns	$[Al^{+3}_{1.41}Fe^{+3}_{.16}Mg^{+2}_{.43}][Si^{+4}_{3.99}Al^{+3}_{.01}]O_{10}[OH]_2\ X_{.43}$	26

In these samples the amount of Fe^{+3} substitution increases from 0.00 in the Tatatila sample to 0.16 in the Burns sample and the swelling volume decreases from 43 ml. for the Tatatila sample to 26 ml. for the Burns sample. As the make-up of the tetrahedral layers is the same and the amount of Mg^{+2} substitution in the octahedral layers is essentially the same in all three samples, it seems reasonable to conclude that the differences in Fe^{+3} substitution are responsible for the differences in swelling volume. For these three samples an increase of 0.16 in Fe^{+3} substitution was accompanied by a decrease of 17 ml. in swelling volume. The Belle Fourche and Aberdeen samples similarly show a decrease in swelling volume with increase in Fe^{+3} substitution, other substitutions remaining essentially constant.

		Swelling volume, ml.
Belle Fourche	$[Al^{+3}_{1.60}Fe^{+3}_{.19}Mg^{+2}_{.22}][Si^{+4}_{3.84}Al^{+3}_{.16}]O_{10}[OH]_2\ X_{.38}$	43.5
Aberdeen	$[Al^{+3}_{1.44}Fe^{+3}_{.34}Mg^{+2}_{.24}][Si^{+4}_{3.86}Al^{+3}_{.14}]O_{10}[OH]_2\ X_{.32}$	23

In this pair of samples an increase of 0.15 in Fe^{+3} substitution is accompanied by a decrease of 20.5 ml. in swelling.

The effect of Fe^{+3} substitution on swelling volume is similar to that of Mg^{+2} substitution. Between the San Antonio and Amargosa samples there is a difference of 22 ml. in swelling volume corresponding to a difference of 0.19 in Mg^{+2} substitution, all other substitutions remaining the same.

		Swelling volume, ml.
San Antonio	$[Al^{+3}_{1.56}Fe^{+3}_{.12}Mg^{+2}_{.31}][Si^{+4}_{3.96}Al^{+3}_{.04}]O_{10}[OH]_2\ X_{.40}$	43
Amargosa	$[Al^{+3}_{1.37}Fe^{+3}_{.15}Mg^{+2}_{.50}][Si^{+4}_{3.96}Al^{+3}_{.04}]O_{10}[OH]_2\ X_{.47}$	21

Thus Fe^{+3}, although it does not contribute to the charge on the structure or to cation-exchange capacity, appears to have much the same effect on the swelling property as Mg^{+2}, which does contribute to the charge and cation-exchange capacity.

On the other hand, differences in the amount of Al^{+3} substituted for Si^{+4} in the tetrahedral layer apparently have little effect on the swelling volume. For example, in the Belle Fourche and Tatatila samples, the tetrahedral substitution of Al^{+3} for Si^{+4} differs considerably, being 0.16 and 0.01 respectively, but they had the same swelling volume; they also have essentially the same amount of octahedral substitution. The Aberdeen and Burns samples also differ considerably in tetrahedral substitution, but they, too, have essentially the same octahedral substitution and nearly the same swelling volume. Thus, Al^{+3} substituted for Si^{+4} appears to have little effect on the swelling volume although it does contribute to cation-exchange capacity, and gives rise to an excess negative charge on the outer layers of the structure, where it would be expected to have more effect in preventing expansion than substitution in the middle layer.

RELATIVE EFFECT OF Fe^{+2} AND Fe^{+3} ON SWELLING

The examples cited indicate that Fe^{+3} in octahedral positions affects the swelling to about the same extent and in the same way as Mg^{+2} even though it does not affect the charge on the layer. The effect of Fe^{+2} relative to Fe^{+3} is shown by comparing the swelling volumes of two specimens of bentonite identical in chemical composition except for the proportionate amounts of Fe^{+2} and Fe^{+3} present.

In natural exposures and near the surface the bentonite commonly known as the "Wyoming" bentonite is pale olive green or cream in color. However, under a few feet of cover many of the blocks, into which the bentonite has cracked due to drying and shrinkage, have a small central core of blue-gray material. With greater depths under cover the proportion of blue-gray to olive-green material increases and under 40 feet or more of cover the blocks are, as a rule, wholly made up of blue-gray material. Analyses (Table 4) of the blue-gray and olive-green phases of the same block, and the derived formulas, show that the two-color phases are essentially identical in chemical composition except for the state of oxidation of the iron. The total iron content of the two phases is the same but in the blue-gray phase two-thirds of the iron is present as Fe^{+2}, and in the olive-green phase two-thirds is present as Fe^{+3}. Swelling tests showed that the blue-gray phase had a swelling volume only two-thirds as great as that of the olive-green phase (Table 4).

Nine months after the first examination, a redetermination of the FeO content of the blue-gray material from block No. 1 showed a decrease of

Table 4. Analyses of Blue-gray and Olive-green "Wyoming" Bentonite, Belle Fourche, South Dakota

	Bicolored block No. 1		Bicolored block No. 2	
	Blue-gray phase	Olive-green phase	Blue-gray phase	Olive-green phase
SiO_2	54.34	54.62	54.34	54.07
Al_2O_3	19.92	20.08	20.12	20.24
Fe_2O_3	1.11	2.36	1.13	2.45
FeO	2.17	1.03	2.06	.74
TiO_2	.11	.11	.14	.14
CaO	.33	.40	.53	.55
MgO	2.21	2.15	2.02	1.92
Na_2O	2.65	2.26	2.44	2.35
K_2O	.45	.35	.49	.40
MnO	.01	.01	.01	.01
SO_3	.18	.16	.15	.17
H_2O- (300° C.)	11.73	11.78	12.18	11.90
H_2O+	4.50	4.58	4.62	4.89
Total	99.71	99.89	100.23	99.83

	Formulas	Swelling volume, ml.
Blue-gray (No. 1)	$[\mathrm{Al}^{+3}_{1.60}\mathrm{Fe}^{+3}_{.06}\mathrm{Fe}^{+2}_{.13}\mathrm{Mg}^{+2}_{.22}][\mathrm{Si}^{+4}_{3.91}\mathrm{Al}^{+3}_{.09}]\mathrm{O}_{10}[\mathrm{OH}]_2\,\mathrm{x}_{.41}$	39.5
Olive-green (No. 1)	$[\mathrm{Al}^{+3}_{1.61}\mathrm{Fe}^{+3}_{.13}\mathrm{Fe}^{+2}_{.06}\mathrm{Mg}^{+2}_{.20}][\mathrm{Si}^{+4}_{3.92}\mathrm{Al}^{+3}_{.08}]\mathrm{O}_{10}[\mathrm{OH}]_2\,\mathrm{x}_{.36}$	60
Blue-gray (No. 2)	$[\mathrm{Al}^{+3}_{1.62}\mathrm{Fe}^{+3}_{.06}\mathrm{Fe}^{+2}_{.13}\mathrm{Mg}^{+2}_{.20}][\mathrm{Si}^{+4}_{3.92}\mathrm{Al}^{+3}_{.08}]\mathrm{O}_{10}[\mathrm{OH}]_2\,\mathrm{x}_{.38}$	40
Olive-green (No. 2)	$[\mathrm{Al}^{+3}_{1.62}\mathrm{Fe}^{+3}_{.13}\mathrm{Fe}^{+2}_{.05}\mathrm{Mg}^{+2}_{.19}[\mathrm{Si}^{+4}_{3.90}\mathrm{Al}^{+3}_{.10}]\mathrm{O}_{10}[\mathrm{OH}]_2\,\mathrm{x}_{.37}$	60

one percent—2.17 to 1.17—and the swelling volume had increased from 39.5 to 48 ml. Eleven months after the first determination of FeO in this specimen, the FeO content had decreased to 1.05 per cent—as compared with 1.03 per cent FeO in the olive-green phase at the start of the tests—and the swelling volume was 66 ml. as compared with 60 ml. for the olive-green material at the start. During this 11-month period the color of the blue-gray material when wet had changed from blue-gray to olive-green. The blue-gray material from block No. 2 showed a similar increase in swelling volume with decrease in FeO content.

These data suggest that there is a close relationship between the state of oxidation of iron and the swelling volume and that Fe^{+2} in octahedral positions has a greater depressing effect than Fe^{+3} on the swelling volume.

Interpretation of Results

It is apparent from this comparison of the swelling volumes of 12 samples of Na-saturated montmorillonite that there is a significant relation between the composition and the swelling volume of montmorillonite. A montmorillonite that has a relatively high degree of octahedral substitution has, for example, a lower swelling volume than one that has a relatively low degree of octahedral substitution. The effect on the swelling volume is not limited to those substitutions that induce a charge on the structure, such as the substitution of Mg^{+2} or Fe^{+2} for Al^{+3}. Substitution of Fe^{+3} for Al^{+3} seems to have about the same effect on the swelling volume as substitution of Mg^{+2} for Al^{+3}. Apparently, therefore, the effect of substitutions of other atoms for Al is not necessarily related to the charge induced by the substitution, but rather to some other change in the structural relations brought about by the substituted atoms.

Hartley (1935) differentiated charged colloids into two classes: (1) those of which the bulk of the particle is made up of insoluble material in regard to which there is no equilibrium and whose charge is due chiefly to preferential adsorption of foreign ions and (2) those of which the particle is made up of a definite ionizing compound with regard to which there is true equilibrium and whose charge is due to ionization of this compound. The term "colloidal electrolytes" may be applied to this second class. From structural considerations Marshall (1936) concludes that the clays of the montmorillonite group may be placed in the second class and may be looked upon as colloidal electrolytes. The substitutions found in the montmorillonite structure result in a net negative charge on the ultimate clay particle, which is balanced by cations held by electrostatic attraction. When such a particle is dispersed in water, these cations dissociate to a greater or less degree. Thus a suspension of montmorillonite in water may be likened to a dissociated electrolyte, one of whose ions falls within the colloidal range of dimensions.

Dissociation of the exchangeable cations leaves some of the structural units of montmorillonite negatively charged. Thus charged, the units have a tendency to repel one another, and the montmorillonite appears to swell. The more complete the dissociation and the greater the number of units carrying a charge, the greater is the swelling; the less complete the dissociation, the fewer are the units carrying a charge and the less is the swelling. The greater swelling of Na-montmorillonite as compared with Ca-montmorillonite may be reasonably explained, therefore, by the greater dissociation of Na-montmorillonite, by which a greater number of structural units are left with a negative charge.

The greater dissociation of exchange cations associated with a charge on the Al layer as compared with cations associated with a charge on the

Si layer as an explanation of the swelling relationships of montmorillonite and beidellite has already been mentioned.

If swelling is thus assumed to be related to dissociation, the decrease in swelling found to accompany increase in the amount of substitution of iron and magnesium for aluminum in gibbsite positions suggests that these substitutions affect in some way the degree of dissociation of the exchangeable cations, even though, as in the replacement of Al^{+3} by Fe^{+3}, the charge on the layer may not be affected. Because of their lesser polarizing power as compared with Al^{+3}, the substitution of these atoms for Al^{+3} may be accompanied by a change in the polarization of neighboring atoms, which is reflected throughout the structure, thus altering the energy relationships of the whole structure. The more extensive the substitution, the more the internal energy relationships of the structure will be affected. Such an alteration in the energy relationships of the structure may well affect the bonding energy and hence the degree of dissociation of the exchangeable cations on dispersion of the montmorillonite in water. The decrease in swelling found to accompany increase in octahedral substitution seems to indicate that the effect of the substitution is in the direction of decrease in the degree of dissociation of the montmorillonite. Although a colloidal electrolyte like montmorillonite cannot be strictly compared with a soluble electrolyte, the change in the strength of acetic acid brought about by the substitution of one or more of the H atoms by positive or negative atoms or groups—such as Cl, OH or CH_3—and the increase in the strength of ammonium hydroxide caused by the substitution of one or more of the H atoms by CH_3 groups are examples of the way in which the degree of dissociation of a compound can be changed by substitutions.

This interpretation of the decreased swelling found to accompany increase in substitution in the octahedral group in montmorillonite is, admittedly, speculative, and further work is required to clarify the relation between substitutions in the montmorillonite structure and swelling.

REFERENCES

FOSTER, MARGARET D. (1951), The importance of exchangeable magnesium and cation-exchange capacity in the study of the montmorillonite clays: *Am. Mineral.*, **36,** 717–730.

GRIM, R. E. (1935), Properties of clay, *in* Recent marine sediments, Thos. Murby & Co., London, 466–495.

HARTLEY, G. S. (1935), Application of the Debye-Hückel theory to colloidal electrolytes: *Trans. Faraday Soc.*, **31,** 68.

KELLEY, W. P. (1943), Mattson's papers on "the laws of soil colloidal behavior"—Review and comments: *Soil Science*, **56,** 443–456.

MARSHALL, C. E. (1936), Soil science and mineralogy: *Soil Sci. Soc. America Proc.* **1,** 23–31.

MARSHALL, C. E., AND KRINBILL, C. A. (1942), The clays as colloidal electrolytes: *Jour. Phys. Chem.*, **46,** 1077–1090.

ROSS, C. S., AND HENDRICKS, S. B. (1945), Minerals of the montmorillonite group: *U. S. Geol. Survey Prof. Paper* **205-B,** 23–79.

HYDROXYL SUBSTITUTION IN THORITE AND ZIRCON*

Clifford Frondel, *Harvard University, Cambridge Massachusetts.*

Abstract

The ill-defined thorite-like minerals thorogummite, nicolayite, hydrothorite, maitlandite, mackintoshite and hyblite are found to be minor chemical variants of a single phase, for which the name thorogummite has priority. Thorogummite is isostructural with thorite and has virtually the same unit-cell dimensions. It differs from thorite in being secondary in origin, in being formed by the alteration of primary thorium minerals including thorite itself, in occurring as fine-grained aggregates that are not metamict but crystalline, and in containing essential water. Chemically, thorogummite seems to be a hydroxyl-containing variant of thorite, $ThSiO_4$, in which there is a serial substitution of $(OH)_4$ for (SiO_4) with the formula $Th(SiO_4)_{1-x}(OH)_{4x}$.

Cyrtolite apparently stands in an analogous relation to zircon.

Introduction

Thorite, like zircon, is surrounded by a diffuse nomenclatural halo of ill-defined minerals. These minerals approximate in composition hydrous thorite, and like thorite often contain uranium, lead, rare earths or other elements in variable and sometimes large amounts in substitution for thorium. Because of their composition and the occasional evidence of tetragonal crystal form, they are commonly listed in textbooks as synonyms or varieties of thorite. Table 1 lists these minerals, and notes are made therein of authentic specimens that were available for the present study.

There are features of occurrence and composition that make the identification of these minerals as thorite seem doubtful or unusual. Thorite hitherto has been known only as a primary mineral. It occurs chiefly in pegmatites, but also in small amounts in hydrothermal deposits formed probably at moderate temperature. Hence it is of interest to find that many of the thorite-like substances listed in Table 1 clearly are of secondary origin. The thorogummite from Japan is a yellow earthy alteration product of yttrialite. Both the thorogummite (nicolayite) and hydrothorite from Wodgina, Western Australia, occur as yellow earthy nodules in the weathered outcrops of pegmatites and have been derived by the alteration of primary thorium silicates—sometimes observed as black residuals within the nodules. The thorogummite from Easton, Pennsylvania, is a secondary product formed by the alteration of thorianite, apparently during serpentinization of the matrix. Hyblite, from Hybla, Ontario, is an alteration of thorite itself. It occurs as white crusts in cracks

---

* Publication authorized by the Director, U. S. Geological Survey.

Table 1. Thorite-like Minerals

Auerlite *Hidden and Mackintosh* (Am. Jour. Sci. 36, 461, 1888). Henderson County, North Carolina.

Calciothorite *Brögger* (Geol. fören. Förh. 9, 258, 1887). Langesund Fiord, Norway.

Chlorothorite *Hidden* (New York Acad. Sci. Trans. 8, 185, 1889). Baringer Hill, Texas. [Name intended as a synonym of thorogummite.]

Enalite *Kimura and Miyako* (Chem. Soc. Japan Jour. 53, 93, 1932). Naegi, Japan.

Eucrasite *Paijkull* (Geol. fören. Förh. 3, 350, 1877). Langesund Fiord, Norway.

Ferrothorite *Lacroix* (Min. de Madagascar 3, 309, 1923). Befarita, Madagascar. [Name given to a supposed ferroan variety of thorite.]

Freyalite *Esmark* cited in *Damour* (Soc. Franç. Miner. Bull. 1, 33, 1878). Langesund Fiord, Norway.

*Hyblite *Ellsworth* (Am. Mineralogist 12, 368, 1927). Two types were distinguished, called alpha- and beta-hyblite. Harvard specimen verified personally by Ellsworth in 1952.

*Hydrothorite *Simpson* (Royal Soc. Western Australia Jour. 13, 27, 1927). Wodgina, Western Australia. Harvard specimen labelled as a gift from Simpson.

*Mackintoshite *Hidden and Mackintosh* (Am. Jour. Sci. 46, 98, 1893). Baringer Hill, Texas. A supposed later occurrence described by Simpson, Geol. Surv. Western Australia Bull. 48, 1912, and Nat. History Soc. Western Australia Jour. 4, 1912, from Wodgina, Western Australia [see also maitlandite]. A U. S. National Museum specimen answering description, but without direct evidence of authenticity.

*Maitlandite *Simpson* (Royal Soc. Western Australia Jour. 16, 33, 1930). Wodgina, Western Australia. [Name applied to material earlier described under the name mackintoshite.] U. S. National Museum specimen originally obtained from Simpson.

*Nicolayite *Simpson* (Royal Soc. Western Australia Jour. 16, 25, 1930). Wodgina, Western Australia. [Name applied to material earlier described under the name thorogummite.]

*Pilbarite *Simpson* (Chem. News 102, 283, 1910). Wodgina, Western Australia. U. S. National Museum specimen originally from Simpson, and a specimen from the O. I. Lee collection originally from the Government Museum, Western Australia. These specimens gave unlike *x*-ray patterns, and neither mineral was found to be related to thorite.

*Thorium gummite *Wells, Fairchild and Ross* (Am. Jour. Sci. 26, 45, 1933). Easton, Pennsylvania. Commonly called thorogummite. Thorogummite, uranophane and two unidentified minerals, all alterations of thorianite, were found in a suite of 60 specimens from the locality. None of these minerals could be identified with certainty with the analyzed material of Wells, Fairchild and Ross, as the several substances very closely resemble each other; none of analysis material is extant (C. S. Ross, personal communication, 1952).

*Thorogummite *Hidden and Mackintosh* (Am. Jour. Sci. 38, 480, 1889); also mentioned by Hidden and Hillebrand, Am. Jour. Sci. 46, 98, 1893, and Hidden, Am. Jour. Sci. 19, 425, 1905. Baringer Hill, Texas. Three later occurrences were described by Iimori and Hata, Tokyo Inst. Phys. Chem. Res., Sci. papers 34, 447, 1938, from Iisaka, Japan; by Simpson, Geol. Surv. Western Australia Bull. 48, 1912 and Nat. History Soc. Western Australia Jour. 4, 1912, from Wodgina, Western Australia [see also nicolayite]; and by Henmi, Geol. Soc. Japan Jour. 57, 345, 1951, from South Manchuria. The material available here included a Harvard specimen from Iisaka labelled as a gift from Iimori; a Harvard specimen and a U. S. National Museum specimen from Wodgina, the latter a gift from Simpson; and four specimens from the Harvard and O. I. Lee collections from Baringer Hill, Texas, all of which answered the description but none of which is known to be type material.

---

* Material examined in the present study.

between uranoan thorite and the weathered feldspathic matrix, and locally grades into the glassy black thorite from which it has been derived. The thorogummite from Baringer Hill, Texas, is found as dull gray-green pseudomorphs after thorite and locally encloses glassy residuals of metamict black thorite. The thorogummite from Manchuria also seems to be a pseudomorph after thorite. Metamict thorite from Jamestown, Colorado, has altered to a weakly birefringent, hydrated substance that was tentatively identified by Phair and Shimamoto (1952) as hydrothorite, and a similar alteration has been observed in metamict thorite from California (George, 1951) and other places.

X-RAY AND OPTICAL DATA

All of the thorite-like substances listed in Table 1 for which specimens were available, except pilbarite, were found to give an identical *x*-ray pattern for unheated material. This pattern is virtually identical with that of tetragonal $ThSiO_4$, thorite. The $ThSiO_4$ samples used for comparison were prepared by sintering coprecipitated ThO_2 and SiO_2 with NaCl in air at 1000° C., and by heating coprecipitated ThO_2 and SiO_2

TABLE 2. *X*-RAY POWDER SPACING DATA FOR THOROGUMMITE. BARINGER HILL, TEXAS. INDEXING FOR TETRAGONAL CELL WITH $a_0=7.068$ Å, $c_0=6.260$ Å, $c_0/a_0=0.8857$. COPPER RADIATION, NICKEL FILTER. CORRECTED FOR FILM SHRINKAGE

I	d(meas.)	d(calc.)	hkl	I	d(meas.)	d(calc.)	hkl
9	4.695	4.686	011	2	1.379	1.379	431
10	3.537	3.534	200	3	1.326	1.326	224
4	2.821	2.821	121	2	1.267	1.267	152
6	2.653	2.653	112	4a	1.172	1.171	044
3	2.499	2.499	220	1a	1.130	1.130	532
½	2.336	2.343	022	2	1.112	1.112	244
4	2.203	2.205	031	½a	1.088	1.087	541
4	2.000	2.001	013	½a	1.055	1.052	622
3	1.869	1.871	321	½a	1.039	1.039	631
6	1.818	1.819	312	1b	1.021 to 1.013	1.011	415
1	1.767	1.767	400	3a	0.976	0.976	444
1	1.740	1.741	123	2b	0.953 to 0.951	0.952	552
1	1.653	1.653	411	3a	0.908	0.909	624
1	1.582	1.580	420	a	0.888	0.884	800
1	1.565	1.565	004	c	0.833	0.831	644
2	1.469	1.470	332	c	0.807	0.805	662
3	1.431	1.431	024	c	0.791	0.790	840

a = diffuse line; b = diffuse line, possibly a doublet; c = broad bands centering as given, relative intensity uncertain.

with ThF_4 and water in a steel bomb at 240° C. The pattern of the natural thorite-like minerals was completely indexed in terms of a tetragonal cell identical with that of $ThSiO_4$ and with almost the same cell dimensions. The *x*-ray powder data are given in Table 2. Similar cell dimensions have been obtained by others on natural, nonmetamict thorite, as shown in Table 3.

Four specimens of ordinary, coarsely crystallized isotropic thorite from pegmatites also were examined by *x*-rays. Unheated samples of the Hybla material described by Ellsworth (1927) gave a few very faint and diffuse thorite lines, and two different specimens from Arendal, Norway, gave no pattern at all. Glassy yellow crystals from Ambatofotsikely, Madagascar, gave no pattern; but yellow, opaque material veining the crystals gave a sharp thorite pattern for unheated material. Pabst (1952) also has noted that an unheated thorite from Madagascar gave an *x*-ray pattern. The behavior of these metamict thorites on heating is described below. The very faint diffraction patterns given by some isotropic, glassy, pegmatitic thorite (and zircon) crystals are conventionally attributed to residual order.

TABLE 3. TETRAGONAL UNIT CELL DIMENSIONS OF THORITE AND THOROGUMMITE

a_0 (Å)	c_0 (Å)	Material	Locality	Reference
7.03	6.25	Thorite	Nettuno, Sicily	Bonatti and Gallitelli (1951)
7.08	6.28	Thorogummite	Manchuria	Henmi (1951)
7.12	6.32	Uranothorite	New Zealand	Pabst (1951)
7.068	6.260	Thorogummite	Texas	Present study
7.117	6.295	$ThSiO_4$	Synthetic	Present study

None of the substances listed in Table 1 had to be heated in order to give a good *x*-ray pattern. The thorogummite from Baringer Hill, Easton, and Wodgina was seen under oil immersion to be microcrystalline. Most of the material is barely resolved as formless birefringent specks, but some minute rods that have parallel extinction can be distinguished. Hyblite, hydrothorite, and the Japanese thorogummite were sensibly isotropic, although some grains of hyblite showed weak birefringence presumably due to strain or to parallel aggregation of submicroscopic crystallites. The thorogummite from Manchuria is described by Henmi (1951) as birefringent in part. The mean index of refraction of all samples was low and variable but increased when the samples were heated, presumably due to loss of water. Similar observations have been made by others (Pabst, 1952; Larsen, 1921) both on supposed thorite proper and on alteration products.

CHEMISTRY

The pertinent chemical analyses are listed in Table 4. The empirical formulas derived by the original authors are given in Table 5. The ratio of

TABLE 4. CHEMICAL ANALYSES OF THOROGUMMITE AND RELATED SUBSTANCES

	1	2	3	4	5	6	7	8
ThO_2	41.44	24.46	25.05	57.79	45.30	24.72	21.20	
ZrO_2			4.78		0.88		0.05	47.82
UO_3	22.43	37.33	7.91	2.98			18.63	
UO_2					22.40	35.60		
$(Ce, La)_2O_3$	6.69	0.12	0.57	0.24	tr.	0.10	0.08	1.42
$(Y, Er)_2O_3$		0.32	12.19	0.73	1.86	0.25	9.47	
CaO	0.41	1.62	0.95	1.65	0.59	1.28		4.72
MgO		0.16		0.60	0.10	0.15		0.17
PbO	2.16	7.78	tr.	1.25	3.74	7.90	0.17	
Al_2O_3	0.965		2.22	0.88			8.84	0.71
Fe_2O_3	0.845		8.67				2.84	1.56
SiO_2	13.085	15.30	21.10	15.77	13.90	16.19	14.43	28.84
P_2O_5	1.19		1.77	1.33	0.67		2.63	
H_2O+	7.88	8.37	10.80	6.06	4.31	12.04	7.82	1.56
H_2O-	1.23	4.19		9.12	0.50	0.88	5.61	8.52
Rem.		0.40	4.48	1.50	2.25	0.94	8.28	4.69
Total	98.325	100.05	100.49	99.90	96.50	100.05	100.05	100.01
Sp. gr.	4.43–4.54	4.13	3.26–3.31		5.361–5.438	4.31–4.45		3.76

1. Thorogummite, Baringer Hill, Texas. Hidden and Mackintosh (1889). Atomic weight of rare earths given as 135.
2. Thorogummite (nicolayite). Wodgina, Western Australia. Simpson (1930). Remainder is $(Nb, Ta)_2O_5$ 0.40.
3. Thorogummite, Iisaka, Japan. Iimori and Hata (1938). Remainder is $(Nb, Ta)_2O_5$ 0.40, BeO 0.40, MnO 0.35, $(As, Sb)_2O_5$ 0.32, CO_2 3.01.
4. Hydrothorite, Wodgina, Western Australia. Simpson (1927). Remainder is CO_2 1.50.
5. Mackintoshite, Baringer Hill, Texas. Hidden and Hillebrand (1893). Remainder is K_2O 0.42, $(Na, Li)_2O$ 0.68, FeO 1.15.
6. Maitlandite, Wodgina, Western Australia. Simpson (1930). Remainder is $(Nb, Ta)_2O_5$ 0.67, MnO 0.07, FeO 0.20. Another partial analysis is cited by Simpson.
7. Thorogummite, Haicheng Prefecture, South Manchuria. Yosimura and Yamada analysis in Henmi (1951). Remainder is BeO 0.16, SnO_2 0.31, Nb_2O_5 7.81.
8. Zircon (cyrtolite), Karelia, U.S.S.R. Kostyleva (1946). Remainder is TiO_2 0.02, HfO_2 1.70, U_3O_8 1.27, MnO 0.11, Na_2O 0.59, K_2O 0.28, SO_3 0.72.

TABLE 5. FORMULAS OF THORITE-LIKE MINERALS

Analysis no.	Oxide ratios of original authors	Atomic ratios referred to thorite-type formula
1	$3ThO_2 \cdot UO_3 \cdot 3SiO_2 \cdot 3H_2O$	$[Th_{1.94}\overset{6}{U}_{0.97}Ce_{0.52}Al_{0.23}\overset{3}{Fe}_{0.13}Ca_{0.09}Pb_{0.12}]_4[(SiO_4)_{2.69}(PO_4)_{0.21}((OH)_4)_{1.31}]_{4.21}$
2	$3ThO_2 \cdot 4UO_3 \cdot 2(Pb, Ca)O \cdot 8SiO_2 \cdot 21H_2O$	$[Th_{1.25}\overset{6}{U}_{1.75}Ce_{0.01}Y_{0.04}Ca_{0.39}Mg_{0.05}Pb_{0.47}Nb_{0.04}]_4[(SiO_4)_{2.43}((OH)_4)_{0.99}]_{4.42}$
3	$(ThO_2, UO_3, Y_2O_3, \text{etc.}) \cdot SiO_2 \cdot 2H_2O$	
4	$ThO_2 \cdot SiO_2 \cdot 4H_2O$	$[Th_{2.79}\overset{6}{U}_{0.13}Ce_{0.02}Y_{0.08}Ca_{0.37}Mg_{0.32}Pb_{0.07}Al_{0.22}]_4[(SiO_4)_{3.34}(PO_4)_{0.24}((OH)_4)_{0.09}]_{3.67}$
5	$3ThO_2 \cdot UO_3 \cdot 3SiO_2 \cdot 3H_2O$	$[Th_{1.96}\overset{4}{U}_{0.90}Zr_{0.08}Y_{0.19}Ca_{0.12}Mg_{0.03}\overset{2}{Fe}_{0.18}Pb_{0.19}K_{0.10}Na_{0.25}]_4[(SiO_4)_{2.64}(PO_4)_{0.11}((OH)_4)_{0.71}]_{3.46}$
6	$3ThO_2 \cdot 4UO_2 \cdot 2(Pb, Ca)O \cdot 8SiO_2 \cdot 23H_2O$	$[Th_{1.28}\overset{4}{U}_{1.71}Ce_{0.01}Y_{0.03}Ca_{0.31}Mg_{0.05}\overset{2}{Fe}_{0.04}Pb_{0.49}\overset{2}{Mn}_{0.01}Nb_{0.07}]_4[Si(O, OH)_4]_{3.70}$
7		$[Th_{0.63}\overset{6}{U}_{0.51}Zr_{0.003}Sn_{0.02}Nb_{0.46}Y_{0.66}Ce_{0.003}Al_{1.37}\overset{3}{Fe}_{0.23}Pb_{0.01}Be_{0.05}]_4[(SiO_4)_{1.90}(PO_4)_{0.29}((OH)_4)_{2.07}]_{4.26}$

SiO_2 to the sum of RO_2, R_2O_3, etc., ranges from virtually 1:1 to about 3:4, with water regarded as essential in all instances. As the *x*-ray work shows that all of the substances are isostructural with anhydrous $ThSiO_4$, with $SiO_2:RO_2=1:1$, the departure from the ideal thorite formula must be explained on crystallochemical grounds. The principal problem is to account for the presence of water and for the diminished ratio of SiO_2. It may be assumed that the apparent deficiency of Si is due to a substitution of $(OH)_4$ for (SiO_4). To test this, the cations were calculated to a total of 4, the ideal unit cell contents of thorite being $Th_4(SiO_4)_4$. Enough O was then assigned to Si to make SiO_4 and to P or S (when present) to make PO_4 or SO_4, and $(OH)_4$ was then calculated in the amount needed to balance the remaining charge of the cations. The test of agreement with the thorite type of formula is that the sum of SiO_4, PO_4, SO_4, and $(OH)_4$ is 4, or that $(OH)+O=16$. This is a stringent test because all of the analytical error is thrown into the (OH). The atomic ratios derived in this way are given in Table 5.

Analyses 1 and 2 are the best of those available. The calculated cation to anion ratios are 1:1.05 and 1:1.12, respectively, indicating that these substances conform to a thorite-type formula in which an omission of $(SiO_4)^{-4}$ is balanced by a substitution of $(OH)_4^{-4}$. The mechanism of compositional variation may be formulated in terms of the ideal unit cell contents as

$$4[Th(SiO_4)_{1-x}(OH)_{4x}]$$

with $x=1.31$ in the Baringer Hill material of analysis 1 and $x=0.99$ in the Wodgina material of analysis 2. This general mechanism has already been identified in the so-called hydrogarnets by Flint and others (1941), Pabst (1942), and Hutton (1943), in which an isostructural series conforming to the formula

$$Ca_3Al_2(SiO_4)_{3-x}(OH)_{4x}$$

extends from grossularite, $Ca_3Al_2(SiO_4)_3$, through hibschite to calcium aluminate, $Ca_3Al_2(OH)_{12}$. Griphite is a phosphate that shows the same mechanism (McConnell, 1942).

In both analyses 1 and 2 only part of the available $H_2O+(110°)$ is required for valence compensation. The water content of the derived formulas (Table 5) is 4.11 and 2.95 per cent, respectively. The point +110° is a wholly arbitrary limit for essential water. The thermal data described below indicate that a considerable amount of water is lost at not much higher temperatures and this may well be nonessential. The large and variable content of nonessential water and the fine-grained to earthy nature of some of the substances make the measured specific gravities uncertain; the calculated values are higher.

The remaining analyses conform to a thorite-type formula, but less closely. Analysis 3 has been disregarded because the large content of CO_2 and other evidence indicates that the sample contains much impurity. The material of analysis 4 was stated to contain about 10 per cent impurities; here only the CO_2 was disregarded. Analysis 7 probably contained admixed fergusonite, $YNbO_4$, according to Henmi (1951). Analysis 5 has a very low summation. Both analyses 5 and 6 show an anion deficiency after valence compensation of the cations is effected, and in analysis 6 not only is no $(OH)_4$ required but a small amount of (OH) must be calculated as $Si(O, OH)_4$. The anion deficiency of these analyses would be remedied if a small amount of the U reported as U^4 were present as U^6. It also may be noted that the requirement of $(OH)+O=16$ is satisfied if $(H_2O)_4$ is assigned to the vacant anion positions.

The substitution of (PO_4) for (SiO_4) in the thorite structure type is well known, with $Si:P=1:0.8$ in the auerlite variety of thorite and $Si:P=1:0.2$ in the yamaguchilite variety of zircon. Xenotime, YPO_4, an isotype of thorite, has been reported to contain (SO_4); and the unanalyzed hyblite of the present study was found qualitatively by Ellsworth (1927) to contain (SO_4).

Roughly four dozen analyses of thorite have been reported in the literature. It is frequently impossible to tell from the description whether the material was the original (metamict) thorite or a crystalline alteration product like that discussed here. Most analyses show a deficiency of Si together with more than enough water to effect the mechanism $(SiO_4) = (OH)_4$. The question whether primary thorite may contain essential (OH) remains open.

THERMAL DATA

Thermal study indicates that the $H_2O+(110°)$ reported in these thorite-like minerals is, at least in part, essential and is retained presumably as (OH) until it reaches high temperatures. Simpson (1927) found that the hydrothorite of analysis 4 lost 9.12 per cent H_2O at 100°, about 5 per cent H_2O at 600°, and the remaining 1.06 per cent H_2O at about 800°. Differential thermal analysis of the Baringer Hill thorogummite showed a gradual loss of water at about 150° and an exothermic peak at 750°, with no further change to 1050°. Separate samples heated in air for 60 minutes at 110°, 470°, and 610° gave a thorite x-ray pattern, as did unheated material, and the 1050° DTA sample gave a thorite pattern plus distinct lines of ThO_2. The thermal break at 750° is interpreted as loss of (OH) with accompanying recrystallization to a mixture of $ThSiO_4$ and ThO_2, as follows

$$Th_4(SiO_4)_{4-x}(OH)_{4x} \rightarrow (4-x)ThSiO_4 + xThO \ + 2xH_2O$$

Another sample of Baringer Hill thorogummite that differed from typical material in its wholly isotropic nature and yellow color gave a DTA curve with a low broad exothermic peak at about 575° instead of 750°. Samples of hydrothorite and thorogummite from both Wodgina and Baringer Hill showed a mixture of tetragonal $ThSiO_4$ and ThO_2 when heated for 30 minutes in air at 1000°. The hydrothorite that has the lower content of $(OH)_4$ showed the less amount of ThO_2.

Differential thermal analyses also were made of two metamict thorite crystals from Arendal and of one from Hybla. These all showed a gradual loss of water at 100° to 225° and a sharp single exothermic break at 875° to 880° due to crystallization. Separate samples of these proved to be still metamict when heated in air at 470° and 610°, but at 920° a faint ThO_2 pattern appeared. The 1050° DTA samples gave patterns with lines of both ThO_2 and the monoclinic polymorph of $ThSiO_4$, huttonite. Normal crystalline $ThSiO_4$ and $ZrSiO_4$ gave DTA graphs without breaks. Microcrystalline thorogummite and metamict thorite react differently when heated to 1000°; the former develops the tetragonal, the latter the monoclinic polymorph of $ThSiO_4$. ThO_2 also is formed in both cases. It is formed in relatively larger amounts when metamict thorite is heated, and here too it may be ascribed to crystallization from a (SiO_4)-deficient matrix. The Hybla material, for which a superior analysis is available (Ellsworth, 1927), has a cation to Si ratio of 1:0.945. The conventional explanation for the appearance of ThO_2 or ZrO_2 on heating metamict thorite or zircon is that an equivalent amount of SiO_2 remains unreacted and amorphous and does not give an x-ray pattern.

ZIRCON

Zircon is isostructural with thorite and, at least in synthetic material made at a high temperature by sintering the mixed oxides with SiO_2, forms a complete series with that substance. Zircon often alters chemically, especially when it contains U, Th, Pb, and cations of valence lower than four. It is then characterized by the presence of 10 to 12 per cent of water and by a deficiency of silica. These features provide grounds for suspecting the existence of an $(OH)_4=(SiO_4)$ substitution such as that indicated for thorite. It also is found that many altered zircons, especially the reddish-brown crystals with curved faces commonly termed cyrtolite, are microcrystalline, pseudomorphous, recrystallization products of metamict zircon. George (1949) has noted the microcrystalline granular to fibrous structure of cyrtolite. A cauliflower-like aggregate of cyrtolite crystals from a pegmatite at Hybla, Ontario, was examined here in some detail. The outer parts of the crystals are dull and are composed of an aggregate of microscopic crystalline grains with a variable amount of an isotropic groundmass. This material grades inwardly into veins between residual areas of clear metamict zircon on both a macroscopic and a microscopic scale. It locally follows lineage boundaries or cracks, as shown in Figure 1, and sometimes particular growth zones are strongly affected. Unheated samples of the recrystallized portions gave a strong *x*-ray pattern of zircon. A DTA curve of material containing about 15 per cent of metamict material showed a gradual loss of water at 100° to 225°, a broad exothermic peak at 460° to 550°, and a single sharp peak at 880° due to crystallization of the metamict material. Kulp, Volchok, and Holland (1952) obtained a similar curve on metamict zircon from Hybla and Bedford, N. Y., except that, as in other metamict zircons examined by them, they obtained a distinct double peak at 890° to 910°.

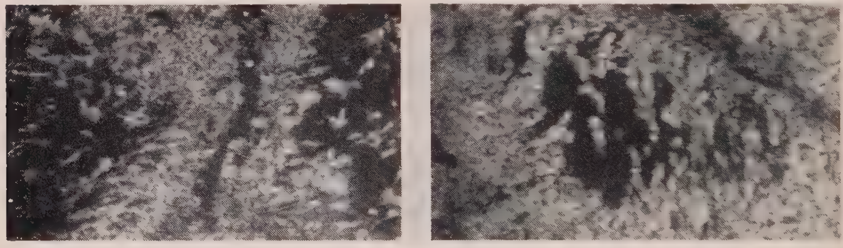

FIG. 1. Thin sections of Hybla cyrtolite crystals showing secondary zircon developed along an open crack and embaying a residual area of metamict zircon. Crossed nicols, ×60. The dark isotropic areas are metamict. The recrystallized areas are a mosaic of isolated grains of irregular and sometimes elongate or vermicular shape. These areas extinguish uniformly, but *x*-ray Laue photographs taken through them show disorientation effects.

The only metamict zircon for which an analysis and *x*-ray, dehydration, and thermal data are available is a cyrtolite from northern Karelia described by Kostyleva (1946) (analysis 8, Table 4). This material had $a_0 = 6.455$ Å, $c_0 = 5.938$, and sp. gr. 4.14 after ignition (3.76 unheated). The dehydration curve showed a gradual loss of 5.22 per cent H_2O up to 200°, where there was a slight inflection, a gradual loss of 4.78 per cent H_2O from 200° to 600° where there was a slight inflection, and a gradual loss of the remaining 1 to 1.5 per cent H_2O from 600° to 1000°. The DTA curve showed a single recrystallization break at 860°. Above 600° the water is regarded by Kostyleva as essential and required for valence compensation in the structure. If the 1.27 per cent U_3O_8 is disregarded as due to admixture, and if Al, Fe, and S are reckoned in four-coordination with Si, then (Zr, Hf, RE, Ca, Mg, Mn, Na, K):(Si, Al, Fe, S) = 1:1 and a substitution of (OH) for O in the (XO_4) tetrahedra is required. Each (OH) would nullify a Si-O-cation bond and, as Kostyleva recognizes, make the crystal prone to metamictization. If the Al and Fe are reckoned with the cations then there is a deficiency of (XO_4); a small substitution of (OH) as $Si(O, OH)_4$ is still required but no $(OH)_4$, and the summation of (XO_4) is only 3.55. Possibly $(H_2O)_4$ is present in the 0.45 anion vacancies, and the formula then becomes:

$$[Zr_{2.82}Hf_{0.06}Al_{0.09}Fe_{0.13}RE_{0.09}Mn_{0.01}Ca_{0.61}Mg_{0.03}Na_{0.13}K_{0.03}]_4$$
$$[(Si(O_{3.98}(OH)_{0.02})_4)_{3.48}(SO_4)_{0.07}((H_2O)_4)_{0.45}]_4$$

This formula gives a total water content of 5.27 per cent, 0.18 from $Si(O, OH)_4$ and 5.09 from $(H_2O)_4$. If the U is regarded as essential then $(OH)_4$ is required.

The water characteristically present in metamict substances is generally disregarded as nonessential and due to alteration, but it now seems that its role might be fundamental. This matter and that of the natural recrystallization of metamict material, as in thorogummite and cyrtolite, with its implication of the readjustment of the original composition, also bear on the use of thorite and zircon in geologic age studies by thermal, *x*-ray and chemical methods.

ACKNOWLEDGMENTS

The writer wishes to express his appreciation to Dr. Arthur Montgomery of Lafayette College, Dr. S. E. Clabaugh of the University of Texas, and the late Mr. O. I. Lee of Jersey City, N. J., for the loan of specimens. This work was done on behalf of the Division of Raw Materials of the U. S. Atomic Energy Commission.

REFERENCES

BONATTI, S., AND GALLITELLI, P. (1951), Sulla torite di Nettuno (Roma): *Soc. Toscana Sci. Nat. Atti Mem.*, ser. A, **57**, 182–183.

ELLSWORTH, H. V. (1927), (I) Uranothorite from the MacDonald mine, Hybla, Ontario; (II), Alpha and beta hyblite, new sulphatic alteration products of the Hybla thorite: *Am. Mineral.*, **12**, 368–372.

FLINT, E. P., MCMURDIE, H. F., AND WELLS, L. S. (1941), Hydrothermal and *x*-ray studies of the garnet-hydrogarnet series and the relationship of the series to hydration products of Portland cement: *Natl. Bur. Standards Jour. Research*, **26**, 13–33.

GEORGE, D. R. (1949), Mineralogy of uranium and thorium bearing minerals: U. S. Atomic Energy Comm. Pub. RMO 563, 198 p.

——— (1951), Thorite from California, a new occurrence and variety: *Am. Mineral.*, **36**, 129–132.

HENMI, K. (1951), Rare element minerals produced in Hai-cheng hsien, southern Manchuria (abstract): Geol. Soc. Japan, Jour., **57**, 345–346. (In Japanese).

HUTTON, C. O. (1943), Hydrogrossular, a new mineral of the garnet-hydrogarnet series: *Royal Soc. New Zealand, Trans. and Proc.*, **73**, 174–180.

KOSTYLEVA, E. E. (1946), Metamict alteration of minerals of the zircon group: *Akad. Nauk SSSR, Fersman Memorial Volume*, 27–35. (In Russian).

Kulp, J. L., Volchok, H. L., and Holland, H. D. (1952), Age from metamict minerals: *Am. Mineral.*, **37**, 709–718.

Larsen, E. S., Jr. (1921), The microscopic determination of the nonopaque minerals: *U. S. Geol. Survey Bull.* **679**, 294 p.

McConnell, D. (1942), Griphite, a hydrophosphate garnetoid: *Am. Mineral.*, **27**, 452–461.

Pabst, A. (1942), Re-examination of hibschite: *Am. Mineral.*, **27**, 783–792.

——— (1951), *X*-ray examination of uranothorite: *Am. Mineral.*, **36**, 557–562.

——— (1952), The metamict state: *Am. Mineral.*, **37**, 137–157.

Phair, G., and Shimamoto, K. O. (1952), Hydrothermal uranothorite in fluorite breccias from the Blue Jay mine, Jamestown, Boulder County, Colorado: *Am. Mineral.*, **37**, 659–666.

Simpson, E. S. (1927), Contributions to the mineralogy of Western Australia: *Royal Soc. Western Australia Jour.*, **13**, 37–48.

STUDIES OF URANIUM MINERALS (XII): THE STATUS OF BILLIETITE AND BECQUERELITE*

JUDITH W. FRONDEL AND FRANK CUTTITTA, *U. S. Geological Survey.*

ABSTRACT

Billietite ($BaO \cdot 6UO_3 \cdot 11H_2O$), originally described from Katanga by Vaes (1947), is a valid species isostructural with becquerelite ($7UO_3 \cdot 11H_2O$).

New chemical analyses and Weissenberg *x*-ray studies on two specimens of billietite from Katanga gave: (1) BaO 6.88, UO_3 82.76, H_2O 8.97, SiO_2 0.76, CaO 0.30, total 99.67; a_0 14.25 Å, b_0 12.04, c_0 15.06, with four formula units per unit cell; α 1.730, β 1.810, γ 1.815; sp. gr. 5.32 (meas.), 5.33 (calc.); (2) BaO 7.41, UO_3 84.39, H_2O 8.68, total 100.48; a_0 13.98 Å, b_0 12.08, c_0 15.06; α 1.725, β 1.780, γ 1.790; sp. gr. 5.36 (meas.), 5.40 (calc.). Space group *Pmma.* Billietite is orthorhombic with 2V $(-)\sim 35°$; X pale yellow, Y and Z deep golden yellow. The unit cell differs from that of Brasseur (1949) in that the a-axis is doubled.

A new analysis and *x*-ray study of becquerelite from Katanga gave UO_3 89.53, H_2O 8.95, SiO_2 1.82, total 100.30; a_0 13.92 Å, b_0 12.45, c_0 15.09; α 1.730, β 1.805, γ 1.820; sp. gr. $\sim$5.3 (meas.), 5.60 (calc.). From this new analysis the old formula for becquerelite ($2UO_3 \cdot 3H_2O$) has been revised to $7UO_3 \cdot 11H_2O$, analogous to the formula for billietite, and there are four formula units per unit cell. Space group *Pmma.* Becquerelite is orthorhombic, 2V $(-)\sim 30°$; X yellow, Y and Z deep golden yellow.

BILLIETITE

New chemical analyses and Weissenberg *x*-ray studies indicate that the hydrated barium uranium oxide, billietite, is a valid mineral species isostructural with the hydrated uranium oxide, becquerelite.

In the original description of becquerelite (Schoep, 1922) the chemical analysis showed about 5.25 per cent of PbO, which at that time was considered an impurity. Later, Schoep and Stradiot (1948) described becquerelite without lead and suggested that in the lead variety there was a substitution of some Pb for U. Vaes (1949), however, considered the original analyses to be in error in that the Pb was actually Ba. He believed that the original becquerelite actually was the more recently described mineral, billietite (Vaes, 1947), a hydrated barium-uranium oxide. He proposed that the name becquerelite be retained for the mineral without lead or barium and that the name billietite be reserved for the mineral with barium. There exist, then, to date, no authenticated specimens of lead-becquerelite.

Optically billietite and becquerelite are very similar (Table 1), except that twinning, common in billietite, has not been observed in becquerelite. Both minerals are orthorhombic and are holohedral. They are yellow to golden yellow and have a distinct pleochroism, with X colorless or pale yellow, and Y and Z deep golden yellow. The 2V of becquerelite is

---

* Publication authorized by the Director, U. S. Geological Survey.

TABLE 1. OPTICS OF BILLIETITE AND BECQUERELITE

	Billietite			Becquerelite	
	1	2	3	4	5
	(Na)				
α	1.730	1.730	1.725	1.725	1.730
β	1.822	1.810	1.780	1.82	1.805
γ	1.829	1.815	1.790	1.83	1.820
2V	∼47°	∼35°	∼35°	∼30°	∼30°
X	Colorless	Pale yellow	Pale yellow	Colorless	Pale yellow
Y	Greenish yellow	Deep golden yellow	Deep golden yellow	Yellow	Deep golden yellow
Z	Deep yellow	Deep golden yellow	Deep golden yellow	Yellow	Deep golden yellow

1. Brasseur (1949).
2. No. 104456, Katanga specimen from Spence collection of uranium minerals at Harvard University.
3. No. 104455, Katanga specimen sent by Vaes to Harvard University.
4. Brasseur (1949).
5. No. 104454, Katanga specimen obtained from Trace Elements Section Washington Laboratory, U. S. Geological Survey.

TABLE 2. CHEMICAL ANALYSES OF BILLIETITE AND BECQUERELITE

	Billietite				Becquerelite		
	1	2	3	4	5	6	7
UO_3	83.86	82.76	84.39	83.08	90.09	89.53	89.66
BaO	6.95	6.88	7.41	7.38			
H_2O	10.49	8.97	8.68	9.54	9.91	8.95	10.34
SiO_2		0.76				1.82	
CaO		0.30					
Total	101.30	99.67	100.48	100.00	100.00	100.30	100.00

1. Vaes (1949).
2. No. 104456. Analyst, Frank Cuttitta.
3. No. 104455. Analyst, Frank Cuttitta.
4. $BaO \cdot 6UO_3 \cdot 11H_2O$.
5. Schoep and Stradiot (1948).
6. No. 104454. Analyst, Frank Cuttitta.
7. $7UO_3 \cdot 11H_2O$.

about 30° and of billietite about 35°. The reported indices of refraction of the two minerals overlap. Both billietite and becquerelite have a perfect cleavage on (001) and their optic orientation is the same. The plane of the optic axes is (100), with Y = a, Z = b, and X = c. In Vaes' original description of billietite (1947) he made the cleavage plane (010). Thoreau (1948) reoriented the mineral, with his *abc* = Vaes' *cab*. This orientation was followed by Brasseur (1949) and is used in the present study. The distinction of billietite and becquerelite is difficult; it is best to use *x*-ray powder photographs together with qualitative chemical tests for Ba and Pb.

TABLE 3. CELL CONSTANTS[1] AND SPECIFIC GRAVITIES OF BILLIETITE AND BECQUERELITE

	Billietite			Becquerelite
	Brasseur (1949)	No. 104456	No. 104455	No. 104454
a_0	7.11	14.25	13.98	13.92
b_0	12.08	12.04	12.08	12.45
c_0	15.09	15.06	15.06	15.09
sp. gr. (meas.)	5.28	5.32[2]	5.36[2]	5.3 (approx.)[3]
sp. gr. (calc.)	—	5.33	5.40	5.60

[1] All measurements are ±0.005 Å.

[2] Specific gravities determined with Berman balance on 10 to 12 mg. of sample.

[3] Sample too small for accurate determination of specific gravity.

In the past two years the Harvard University mineral collection acquired two specimens of billietite from Katanga. One was sent by Vaes. The other was in the Spence collection of uranium minerals. Both specimens have been analyzed chemically, and the results agree closely with those of Vaes' analysis (Table 2). Vaes proposed the formula $BaO \cdot 6UO_3 \cdot 10H_2O$. The new chemical analyses are represented better by the formula $BaO \cdot 6UO_3 \cdot 11H_2O$, suggested by Brasseur (1949). A Weissenberg *x*-ray study, using copper radiation ($\lambda = 1.5418$ Å), was made of both analyzed specimens. The unit cell differs from that of Brasseur (1949) in that the a-axis is doubled (Table 3). It is possible that Brasseur missed the odd orders in his rotation photograph about the a-axis, as he used molybdenum radiation and the unit cell is large. There are, then, four formula units per unit cell, rather than two. Plots of the zero, first, and second layer Weissenberg photographs about all three axes gave:

(hkl) all orders present,
(hk0) present only with h = 2n,

(h0l) all orders present,
(0kl) all orders present.

The space group, therefore, is *Pmma*. The crystal forms observed by Thoreau (1948) as referred to the unit of the *x*-ray cell are given in table 4, and show that billietite is holohedral. The calculated specific gravities, 5.33 and 5.40, are close to the two measured values, 5.32 and 5.36, respectively. The specific gravities were measured with a Berman balance on about 10 to 12 milligrams of sample.

Table 4. Crystallographic Forms of Billietite

Thoreau (1948)			J. W. Frondel		
Form	ϕ	ρ	Form	ϕ*	ρ*
001	0°	0°	001	0°	0°
011	0°	51°48′45″	011	0°	51°16′
021	0°	68°31′52″	021	0°	68°12′
010	0°	90°00′	010	0°	90°
101	90°00′	—	201	90°	64°41′
110	58°55′10″	90°00′	210	59°22′	90°
111	58°55′10″	—	211	59°22′	67°50′
223	58°55′10″	58°39′18″	423	59°22′	58°35′
			New Forms Observed		
			232	29°23′	65°06′
			212	59°22′	50°55′

* Angles calculated from cell constants $a_0=14.25$ Å, $b_0=12.04$, and $c_0=15.06$, giving $a=1.184$, $c=1.251$, $p_0=1.057$, and $q_0=1.251$.

Becquerelite

A new chemical analysis and a Weissenberg *x*-ray study were made on a Katanga specimen of becquerelite obtained several years ago by the Trace Elements Section Washington Laboratory of the U. S. Geological Survey. The analysis agrees closely with that of Schoep and Stradiot (1948) on lead-free material (Table 2). The old formula of becquerelite ($2UO_3 \cdot 3H_2O$) is here replaced by $7UO_3 \cdot 11H_2O$, as this formula fits the analysis quite well and is analogous to the billietite formula. The cell constants are close to those of billietite (Table 3), and there are, similarly, four formula units per unit cell. The space group is *Pmma*. The calculated specific gravity is 5.60; the measured value is approximately 5.3. The measurement was made with a micropycnometer on a very small sample and may be in error. The attempt to make the two formulas analogous is justified because the near coincidence in dimensions and

Table 5. Interplanar Spacings of Billietite and Becquerelite from *X*-ray Powder Patterns (Å) Cu/Ni Radiation = 1.5418 Å

Billietite No. 104455		Becquerelite No. 104454	
d	I*	d	I*
—	—	8.51	1
7.53	10	7.50	10
—	—	6.63	2
—	—	6.24	1
—	—	5.63	1
4.59	2	4.71	6
—	—	4.31	1
3.77	9	3.75	8
3.54	5	3.56	8
—	—	3.48	2
—	—	3.39	2
3.17	8	3.22	9
3.02	1	3.13	1
2.89	1	2.97	2
2.79	2	2.88	3
—	—	2.73	1
2.56	3	2.58	7
2.49	4	2.47	2
—	—	2.44	2
—	—	2.38	2
2.30	2	2.31	3
2.19	1	2.21	1
2.10	3	2.11	2
—	—	2.07	3
2.03	6	2.04	4

* Intensities estimated visually.

intensities of the single crystal and powder photographs (Table 5) of billietite and becquerelite indicates that these minerals are isostructural. It is presumed that one Ba^{2+} substitutes for one U^{6+}. If the role of water in the structure were understood, it might be possible to explain the necessary valence compensation for such a substitution by the O to (OH) ratio in each mineral. Though no specimen of lead-bearing becquerelite is at hand, the authors believe that for crystallo-chemical reasons such a mineral may exist. It also may be noted that the closely related hydrous uranium oxide, schoepite ($UO_3 \cdot 2H_2O$), can contain up to 4.56 per cent PbO (Schoep, 1924). Should re-examination and chemical analyses of museum specimens indicate the presence of such a mineral, or if the original analyses of becquerelite containing lead are presumed to be correct, then a general formula for becquerelite, lead-becquerelite, and billietite might be written:

$$[U^{6+}_{1-x}(Ba, Pb)^{2+}_{x}]U^{6+}_{6}O_{20-4x}(OH)_{2+4x}\cdot(10\text{-}2x)H_2O$$

ACKNOWLEDGMENTS

This work was completed as a part of a program undertaken by the U. S. Geological Survey on behalf of the Atomic Energy Commission. The authors wish to thank Dr. Clifford Frondel, of Harvard University, for his assistance in the interpretation of results.

REFERENCES

BRASSEUR, H. (1949), Étude de la billietite: *Acad. royale Belgique Bull., Cl. Sci.*, **35,** 793–804.

SCHOEP, A. (1922), Sur la becquerelite, nouveau minéral radioactif: *Acad. sci. Paris Comptes rendus*, **174,** 1240.

——— (1924), Recherches sur la becquerelite et la schoepite: *Soc. franç. Minéralogie Bull.*, **47,** 147–157.

SCHOEP, A., AND STRADIOT, S. (1948), Additional data on the properties of becquerelite and billietite: *Am. Mineral.*, **33,** 503–507.

THOREAU, J. (1948), Caractères cristallographiques de la billietite et de la vandendriesschéite: *Soc. Géol. Belgique Bull.*, **71,** 76–78.

VAES, J. F. (1947), Six nouveaux minéraux d'urane provenant de Shinkolobwe (Katanga): *Soc. Géol. Belgique Bull.*, **70,** 212–225.

——— (1949), Becquerelite ou billietite (À propos d'un article de MM. Schoep et Stradiot): *Soc. géol. Belgique Bull.*, **72,** 237–248.

THE MAYODAN METEORITE, ROCKINGHAM COUNTY, NORTH CAROLINA*

Edward P. Henderson and Stuart H. Perry,
U. S. National Museum, Washington, D. C.

Abstract

A new hexahedrite from North Carolina is analyzed and described. The orientation of the inclusions, the Neumann lines, and the granules of kamacite were measured and are discussed. These structures are assumed to be in effect primary and a theory is given for their origin.

Introduction

In September, 1950, Mr. James E. Beaver of High Point, N. C., submitted to the U. S. National Museum a small fragment for identification which he thought might be a meteorite. Having read in the September issue of *Science Digest* a description of a meteorite and of the interest that this Museum has in them, he asked us to investigate a sample that for years had been considered by his family to be an iron meteorite.

The sample proved to be an iron meteorite. In response to our request for permission to see the main mass, Mr. Beaver sent it for examination and supplied the historical information about its discovery. In a letter dated September 18 he wrote:

> "This meteorite was discovered in 1920 near our farm in Rockingham County, N. C. Back in those days the upkeep of the roads was the responsibility of each county and it was the practice of the few neighbors to get together and repair the section of the road that passed by their property. It was while working with a few of his neighbors in repairing one of these roads that my father discovered this meteorite (embedded) in the road. They thought at first that it was just another rock, but when one of them lifted it to carry it (out of the road) they found that it was much too heavy to be an ordinary rock, so my father carried it home with him, where it remained for 30 years as an object of curiosity and conjecture. However, my father suspected that it was a meteorite, in fact we have been calling it a meteorite ever since I can remember. He sent a sample of it to an iron smelting concern and they replied that it was of no value." (Portions enclosed in parentheses were corrected in the next letter.)

The meteorite, as received, weighed 34 pounds and was an altered irregular mass with none of the original flight surfaces preserved. The loosely attached oxide scales on the surface suggested that this meteorite contained lawrencite and perhaps would be difficult to preserve. Mr. Beaver when asked to furnish the exact location of this find kindly sent a map on which the place of discovery was marked.

The nearest town to that place is Mayodan, the name selected for this

---

* Publication authorized by the Secretary of the Smithsonian Institution.

meteorite. The latitude and longitude of the place of discovery are 36°23′ N. and 79°52′ W. respectively.

Mr. Beaver in a letter dated September 24 added the following facts that corrected the statements enclosed in parentheses which were given in his former letter:

> "This meteorite was not embedded in the road itself as was my original impression, but was in the bank of the road and was uncovered when the road was being widened by men using plow, picks and shovels. The meteorite was definitely not hauled to that point from another location when the road was built or repaired, as no material was ever brought from a distant point for this purpose.
>
> "During the 30 years since this meteorite was discovered it has been exposed to the weather part of the time, and part of the time it has been completely protected from the weather. For two or three years it was out of doors and was completely exposed to the weather and then for several years it was stored in a building where it was completely protected from the weather. During all the rest of the time it was kept in an old building with a leaky roof, and the meteorite would get wet every time it rained.
>
> "While making this investigation, I uncovered some more information that will probably be of interest to you. About 30 years before this meteorite was discovered several people reported seeing and hearing a meteorite fall somewhere in the general locality where this meteorite was found. Some of them said they heard the sound it made while falling through the air, while others said they heard the sound and also saw the flash of light that accompanied the fall.
>
> "Of course I do not definitely know that this was the same meteorite that was discovered, but everyone presumed it to be. From the information the date of fall would be somewhere around 1890."

The information about the possible date of this fall is given for what interest it may have, but as Mr. Beaver stated, we can not be certain this is the date of fall for this meteorite.

It is perhaps fortunate that this iron was stored as Mr. Beaver described, since storage for 30 years in a well-roofed building and consequent accumulation of corrosive iron chloride on the surface might have caused even more extensive alteration. Probably the frequent wetting removed much of the corrosive agent and thus helped to preserve the specimen.

Chemical Analysis

The pieces selected for analysis were placed in a flask, covered with dilute hydrochloric acid ($1\ HCl+2\ H_2O$) and the gas given off was passed through a solution of lead acetate. The lead sulfide was recovered, converted to lead sulfate, and the sulfur content calculated.

The acid which dissolved the sample was not heated above the minimum temperature needed to make it react with the sample. Cold acid will attack the metal at first, but soon all action practically stops. When the flask is heated by suspending it in hot water, the sample again started to dissolve. After everything that would dissolve had gone into solution in the hydrochloric acid, some rhabdite needles and a few rectangular plates remained. There also was a small amount of black particles which were non-magnetic and had a density only slightly higher than that of the acid solution. By attaching a magnet on the bottom of the flask, the metallic portion was retained in the flask while the dark non-magnetic inclusions were separated by washing with dilute acid, filtered off, dried and weighed as carbon.

The magnet was removed and the magnetic residue was dried quickly within the flask, brushed out, and weighed. It made up 0.53% of the sample and consisted of essentially two different types of crystals.

This residue was separated into two portions by handpicking. Both portions were *x*-rayed and found to be identical schreibersite. The portion consisting of the needles was dissolved and found to contain 33.6% Ni. This is more nickel than usually is found in schreibersite, but agrees with the nickel-poor rhabdites reported by Farrington (1915).

There were not enough of the rectangular plates to make a reliable nickel determination, but the tests made gave 25.1% Ni. This value is only useful in showing that the larger phosphide inclusions contain less nickel than the needles. This is consistent with existing information. The needles which are the last of the phosphide to separate apparently always contain more nickel.

These rectangular bodies required about 30 hours to dissolve in aqua regia. The needles dissolved much more rapidly. However they have a

TABLE 1. COMPOSITION OF THE MAYODAN, ROCKINGHAM COUNTY, N. C., METEORITE
E. P. Henderson, analyst

	1 Composition of the portion sol. in HCl	2 Composition corrected for inclusions, see text
Fe	93.42*	93.70*
Ni	5.48	5.63
Co	0.48	0.49
P	0.09−	0.17
C	0.003	0.003
S	0.003	0.003
Phosphides residue	0.53	
Total	100.006	99.996
Mol. Ratio $\frac{\text{Fe}}{\text{Ni+Co.}}$ =	16.55	16.28

* By difference.

much higher ratio of surface to mass and it may be that these two types of inclusions actually dissolved at about the same rate.

The composition of the Mayodan meteorite reported in column 1, Table 1, was determined on the portion which was soluble in dilute HCl, and does not include the composition of the insoluble phosphides. The phosphorus contents of schreibersite and rhabdite have been determined several times in these laboratories and elsewhere and average between 15 and 15.5%, hence it is possible to calculate the phosphorus content of this meteorite.

The sulfur reported was determined on a 14-gram sample. The piece selected contained no appreciable inclusions of troilite so that the sulfur content of the meteorite is somewhat but not much higher. The nickel, cobalt, and iron determinations given in column 1, Table 1, do not include the percentage of these elements from the insoluble phosphide. Column 2 has been corrected for the estimated composition of the phosphide inclusions.

DESCRIPTION

This meteorite is a hexahedrite. The two distinct sets of Neumann lines shown in Fig. 1 intersect at an angle slightly more than 37° as measured on the polished surface. The theoretical angle between the trace of the $1\bar{2}1$ and the $2\bar{1}1$ faces on the 001 face should be 36°52′. Thus these two sets of Neumann lines are parallel to the trace of these two trapezohedral faces. More conspicuous than the Neumann lines are the two sets of straight lines which intersect at right angles. These are the traces of the cleavage of kamacite. Hexahedrites often show a tendency to separate along these cubic planes.

The small fragment of this meteorite which Mr. Beaver first sent for examination apparently was broken from the main mass by a hammer. It had two flat surfaces which were at right angles to each other and on these surfaces a few silvery rectangular plates were noticed. These were later identified as rhabdites.

Oxides occur within some of the cleavage planes of the first two slices cut from this iron, but these are weathering products. Small beads of lawrencite developed along these cleavages when the specimen was exposed to the humid atmosphere for several days.

The dark irregular area at the center of Fig. 1 is iron oxide, the result of weathering penetrating into the meteorite. This slice was cut parallel to a relatively flat surface on the main mass, but just deep enough to pass below the lowest depression on that surface. By good fortune the slice removed happened to be parallel to the 001 direction, a cleavage plane. Thus at some time this mass may have been cleaved from another, possibly during flight through the atmosphere.

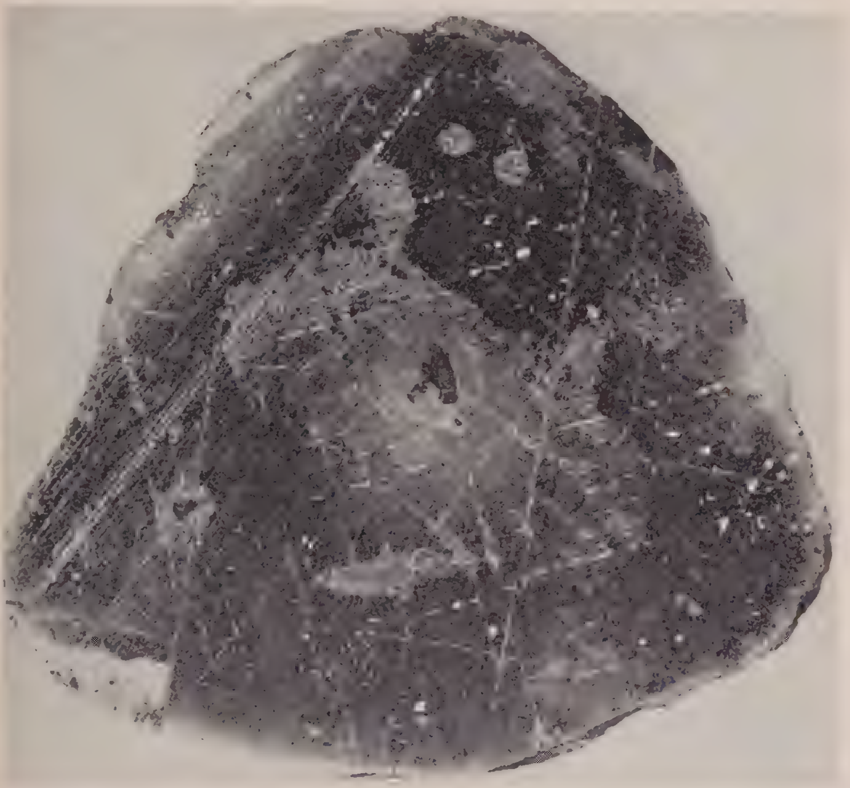

FIG. 1. Etched section of the Mayodan, N. C., meteorite. Note the orientation of the small light colored kamacite granules and their relationship with the Neumann lines, cleavage planes and phosphide inclusions. The prominent lines at right angles to each other are cleavage planes. The dark area at the center represents the penetration of alteration from the outside. The gray inclusions, lower center and upper right, are troilite. About $\frac{2}{3}$ natural size.

The specific gravity of this iron was determined on two pieces. The portion from near the surface, although it appeared to the eye to be fresh, gave a density of 7.82 which is lower than the density of a hexahedrite should be. The density measured on a piece selected from nearer the center of the mass, far below the zone of alteration, gave a density of 7.910.

The troilite has a peculiar grayish-black color because it contains carbon. Some phosphides occur around the edges of the troilite inclusions. In most meteorites the troilite and its enclosing zone of schreibersite form rounded inclusions but in this meteorite many of the troilite masses have an irregular outline because small prongs extend into the surrounding metal.

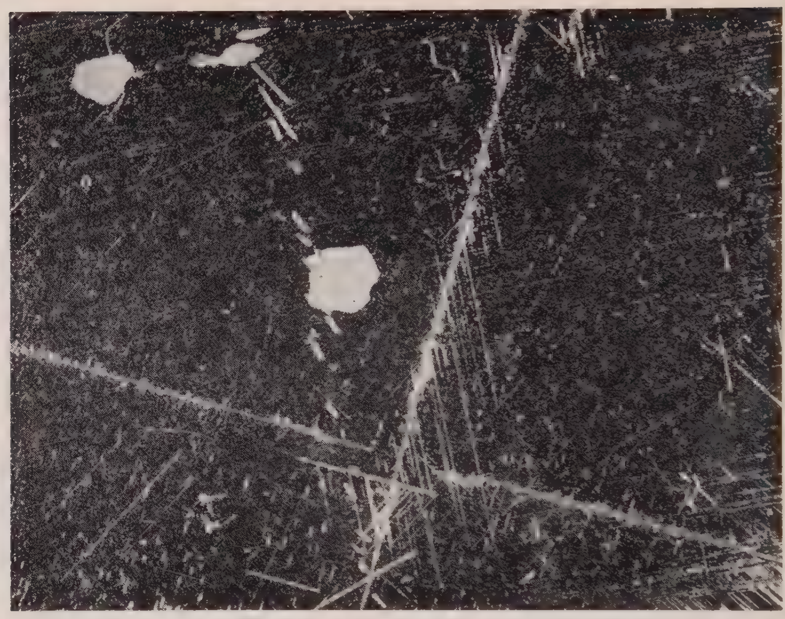

FIG. 2. An area near the lower edge of Figure 1. Rhabdite rods lie en echelon roughly parallel to each other and form rows. Occasionally rhabdites penetrate one of the kamacite granules, which sometimes are bounded by straight edges. The two lines at right angles are cleavages and lie parallel to the cube face, hence it was easy to orient the Neumann lines. ×5.

The iron surrounding many of the larger troilite inclusions (Fig. 1) appears to contain brilliant needle-like inclusions, but when these are examined more closely they are found to be Neumann lines that are more deeply etched out. Thus the brilliant lines around the troilite inclusions are not phosphide bodies but reflections from the sides of deeply etched Neumann lines.

There are two types of phosphide inclusions in the Mayodan meteorite. One type is rectangular or rod shaped (Fig. 2) and the other, not visible in Figure 1, occurs in delicate needles. These needles should be called rhabdites and perhaps the larger rectangular inclusions would be called schreibersite, but because they have a more symmetrical outline than most observed schreibersite, rhabdites seem to be a better name.

A feature of this meteorite is the alignment of the rectangular phosphide inclusions (Figs. 1–4 and 7–9). In many places these rod-like inclusions are aligned in rows. Each single inclusion seems to lie roughly parallel to the others in a given row, and at an angle to the direction the row makes across the surface.

The direction of both the Neumann lines and the rows of these phosphide inclusions was determined by assuming the two right angle cleavages (Figs. 1–2), are parallel to 100 and 010. The rows of phosphide inclusions are essentially parallel to $1\bar{2}1$ and $2\bar{1}1$ directions. The Neumann lines in these two plates closely parallel the $2\bar{1}1$ and $1\bar{2}1$ directions. The measurements of the Neumann lines from these plates are not in perfect agreement with the theoretical directions of $2\bar{1}1$ and $1\bar{2}1$ lines, because the plane of the section is not exactly parallel to the 001 face and the sample was slightly inclined to the axis of the camera when the picture was made. Yet the agreement in the direction of these Neumann lines and the orientation of the rows of inclusions so closely parallel the trace of the $1\bar{2}1$ and $2\bar{1}1$ faces on the 001 face that it can be assumed they are aligned along those directions.

The rectangular phosphide bodies which remained as a residue when the sample was dissolved in dilute hydrochloric acid, vary in size (Figs. 1–3 and 7). Many of the particles shown in Figure 6 may be fragments of the longer ones which were broken in the process of separating them from the matrix. The dimensions of the fragments of inclusions determined from Figure 6, range between 0.2 and 0.3 mm. in width and the maximum length is 1 mm. However an average of 10 measurements made on the polished surface gave 3.6 mm. as the average length of these phosphides. The maximum length was 7 mm.

Many of the schreibersite bodies show minute holes, usually about midway of the width of the inclusion. Such minute holes, or islands of kamacite in phosphide inclusions, have been observed in other hexahedrites (see Fort Duncan, Plate 56, in The Metallography of Meteoric Iron by S. H. Perry, U. S. Natl. Museum Bull. 184 (1944)).

Another feature of this meteorite is the small light-colored areas shown in Figure 1, which resemble inclusions. These are kamacite. Their long direction lies parallel to a set of Neumann lines. In other words the kamacite granules and the Neumann lines are aligned parallel to the trapezohedral directions. These small and irregular granules occur rather closely spaced along these directions. Their longest dimensions range between 3 and 4 mm. and their shorter dimensions are about half of that distance.

Commonly these kamacite inclusions consist of 2 or 3 granules. Generally there are some differences in the orientation of these granules but the difference between the group and the groundmass is more conspicuous. No taenite occurs between these granules or around them, a significant point discussed elsewhere in this paper by Dr. H. H. Uhlig. These granules interrupt Neumann lines. A few needle-like rhabdites extend from the groundmass into the granule without a break in the rhabdite. Because of this we suggest the granule formed after the rhabdite was in place. Whatever produced these granules did not exert enough force to break a rhabdite needle.

Some small phosphides are uniformly oriented within these kama-

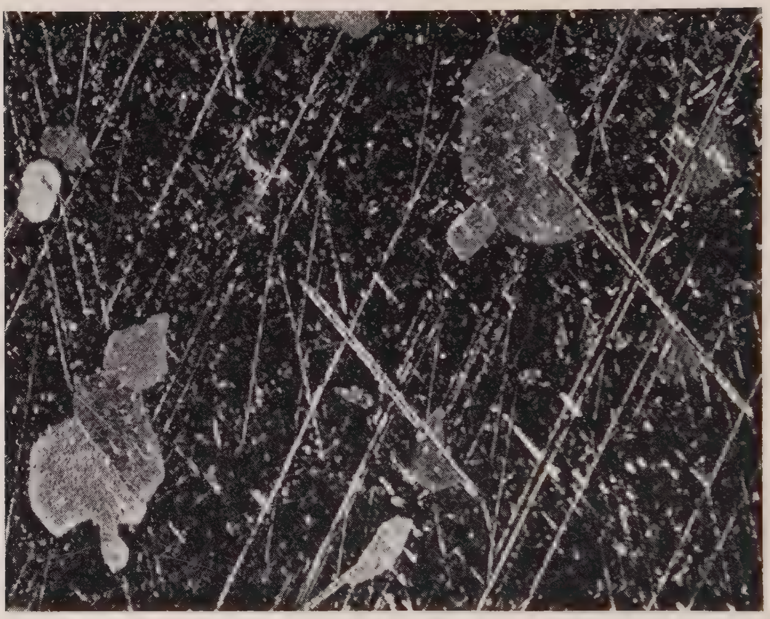

FIG. 3. The groundmass is kamacite containing kamacite granules many of which are aggregates of smaller granules. These apparently crystallized due to some mechanical working but the secondary crystallization did not disturb the orientation of the included rod-like phosphide bodies because they have about the same orientation as the rods in the groundmass. ×9.

cite granules (Fig. 3). Commonly these granules have a flat side which parallels a Neumann line or a rhabdite inclusion. Since the kamacite inclusions in the groundmass are distributed along a direction of one of the trapezohedral faces and the Neumann lines are always so aligned the kamacite granules and the Neumann lines must be related. Any explanation for one must account for the other.

The close relationship between these features suggests that both are primary structures. It seems more logical to consider the Neumann lines as primary structures than to assign their origin to a shock which occurred during the flight of the meteor. Before attempting an explanation of the granules or Neumann lines, the composition of this iron should be considered in reference to the nickel-iron diagram, Fig. 10.

OBSERVED RELATIONS IN THE LIGHT OF THE IRON-NICKEL DIAGRAM

The cut through the Mayodan iron by good fortune paralleled the 001 direction, so it provided an excellent opportunity to observe many relationships about the features in hexahedrites. The points considered were the sulfides, phosphide inclusions, Neumann lines and the separately oriented granules of kamacite within the groundmass of the hexahedrite. All of these except the troilite, and carbon occurring within the troilite, seem to have formed at a time when they were controlled by the lattice structure of the kamacite. The troilite separates from the melt in particles that coalesced into round masses which solidified before the beginning of the gamma-alpha transformation and therefore are older than any structure in the meteorite.

No sizable inclusions of schreibersite were found, and the limited amount of phosphide which is present may be close to the limit of the solubility of schreibersite in meteoritic iron of this composition. As the temperature is lowered, more and more phosphide separates. The larger rods, which we regard as the first generation of phosphide, contain less nickel than the small needles. These minute needles separate at lower temperatures, hence had more time to become enriched in nickel. Since rhabdites are orientated in hexahedrites as well as in the kamacite in octahedrites, we infer that these phosphides, if given a chance, will take a position parallel to one of the trapezohedral directions.

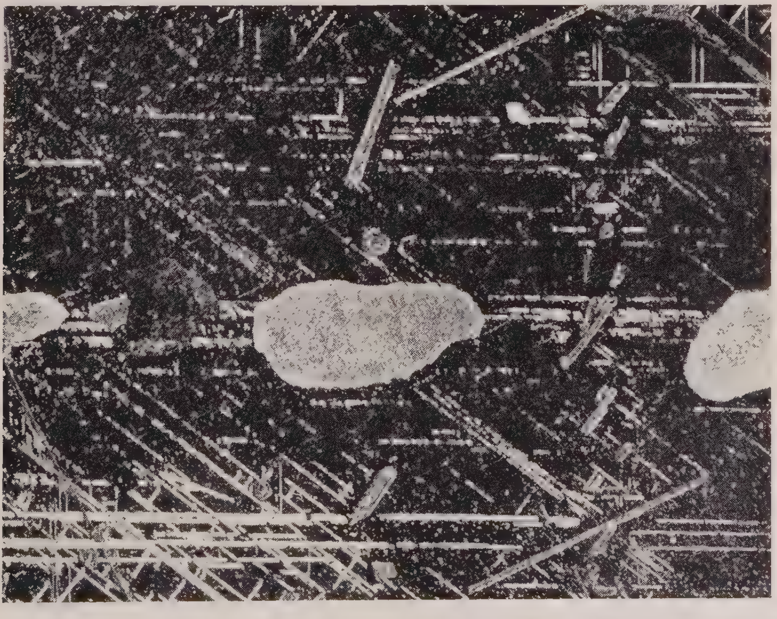

FIG. 4. The kamacite granules, Neumann lines and the vertical row of phosphide inclusions, at the right, are parallel to one of the directions of the trapezohedron. The rather indistinct diagonal line extending from below left center towards the bottom, is a cubic cleavage. The sizable granules across the center are not perfectly parallel, but deviate by a few degrees from paralleling a trapezohedron face; rather than regard them as aligned along some complex form they are assumed to parallel the trapezohedron. ×8.

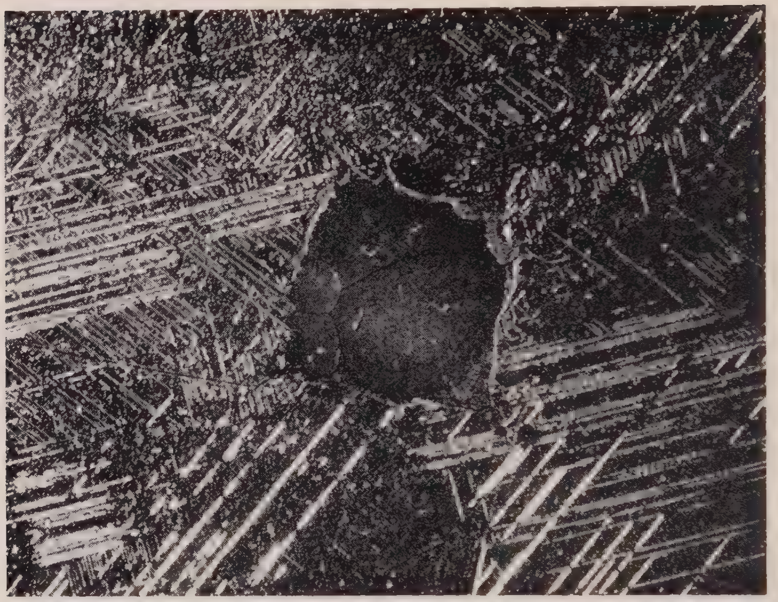

FIG. 5. The troilite and the smaller amount of phosphide that surrounds the FeS are not oriented, but all the other inclusions in this iron are. We believe the FeS separated from the iron-nickel alloy at relatively high temperatures and remained in the same relative position ever since. Many of the troilites are darkened by carbon. The phosphide around some of the troilite inclusions extend as prongs into the groundmass which gives an unusual outline to some of these bodies. ×8.

As the iron cooled along its composition line (Fig. 10), a normal hexahedrite would have formed because this line enters the single phase area at approximately 450° C. However something further must have happened before the metal was cooled to room temperature. This event, in our opinion, took place before either the Neumann lines or the granules of kamacite were formed.

Probably many theories could be proposed to explain the origin of the granules of kamacite, but two new possibilities are offered in the hope of stimulating others to discuss this important point.

Cooling took place along a composition line of 5.6% Ni which corresponds to the Mayodan meteorite. On the Owen and Liu (1949) diagram (Fig. 10) this line enters the mixed phase at about 760° C. Here the kamacite will contain slightly more than 2% Ni while the taenite will carry about 6%. As the temperature drops the Ni content of the kamacite separating increases until at 450° C. it contains about 5.6% Ni.

Assuming that the metal cooled slowly a logical assumption if it was part of a large mass—there is ample time for one continuous kamacite crystal to form. Yet if the smaller quantities of mixed phases, which are

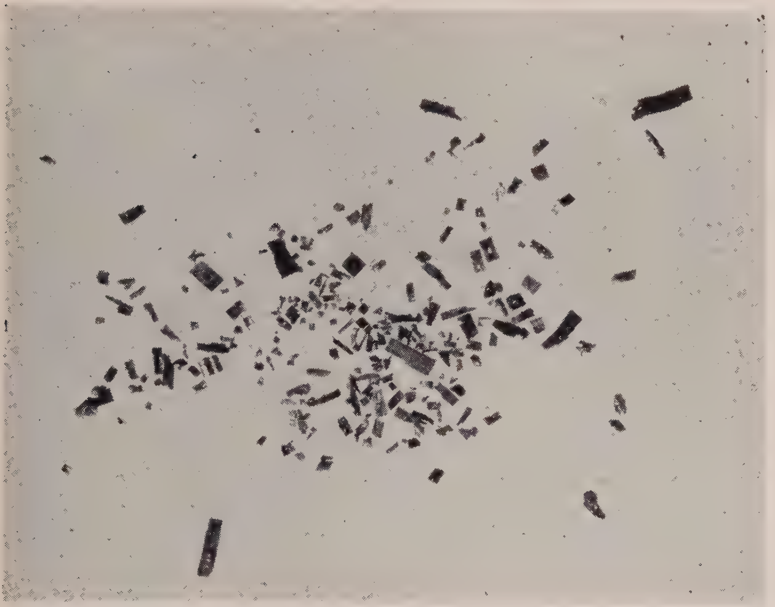

FIG. 6. Most of the rhabdites have holes midway of their width. The large pieces average between 0.2 and 0.3 mm. wide; the longest one shown is 1 mm., but longer ones can be seen in Figure 4. Although many of the smaller pieces may be fragments, made during the process of recovery, the analytical data show there is a difference in the nickel content of the coarse and fine material. ×8.

essentially kamacite, had separated at various places throughout the metal, and if the temperature was sustained between 400 and 450° C. for a long time, these incipient quantities of mixed phases could migrate and coalesce into small areas within the groundmass. However, since each area was essentially kamacite at the time of its formation, it would ultimately appear as kamacite if the cooling rate was accelerated.

An accelerated cooling rate or anything which will reduce the molecular mobility would freeze these areas into their position before they could be assimilated by the groundmass. The very limited amount of taenite which could be present should lie at the boundary of the granules where it could be most readily assimilated when the temperature went lower than 450° C. because the composition line then enters the single phase area.

The above interpretation is based on the temperatures above 450° C. and rigidly following the iron-nickel diagram in Fig. 10. However in the earlier diagram of Owen & Sully (3) the kamacite at 400° C. contained the same percentage of nickel as shown in Fig. 10, only the line AB bent slightly to the left below 400° C. so that at 300° C. kamacite contained 5.5% Ni. The recent diagram indicates no such curve to the left; unless that curve is there or the line AB is moved to the left, the Owen and Liu diagram fails to explain the structures in iron meteorites.

If those granules of kamacite, Figure 1, formed between temperatures of 760–450° C. and if Figure 10 faithfully tells what takes place, there should be decreasing amounts of taenite formed around the granules as the temperature is lowered. The quantity of taenite decreases because, as the diagram shows, the nickel content of the taenite increases rapidly as the temperature is lowered.

Thus, taenite should not occur around kamacite islands in a hexahedrite because at 450° C. such an alloy as the Mayodan iron enters into the kamacite area. As the Mayodan iron has no taenite around these kamacite granules, it indicates either that Owen and Sully erred in indicating the kamacite boundary curved towards the left or that this meteorite has yet to reach equilibrium.

The Owen and Liu diagram fails to explain the composition and structures found in iron meteorites because the kamacite at 400° C. or lower would contain between 6 and 7.5% Ni and no hexahedrite with such a nickel percentage has been found although about 60 hexahedrites are

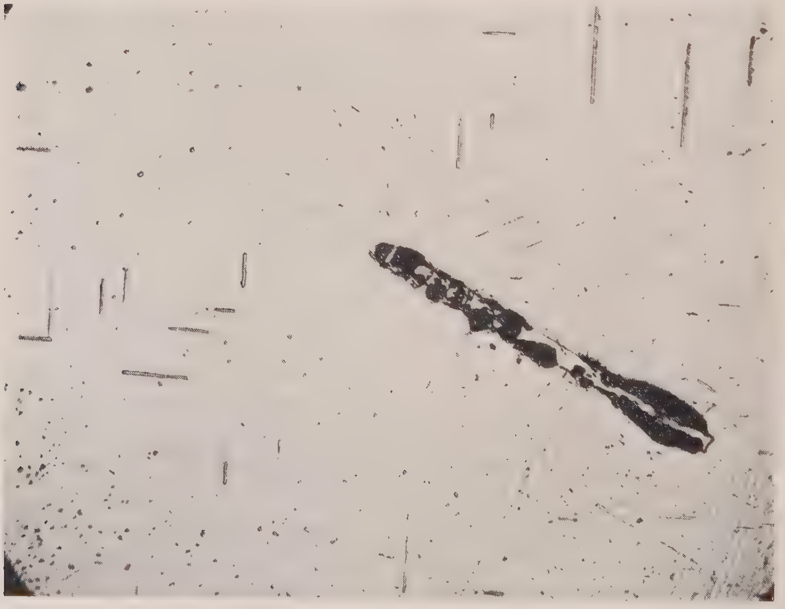

FIG. 7. The big inclusion is rhabdite, perhaps large enough to be called schreibersite, the dark spots are due to chipping in the preparation of the surface. If the plane of the picture is parallel to 001, the small rhabdites at right angles to each other lie along the cube face and the large phosphide body and the other rhabdites are parallel to trapezohedral faces. ×40.

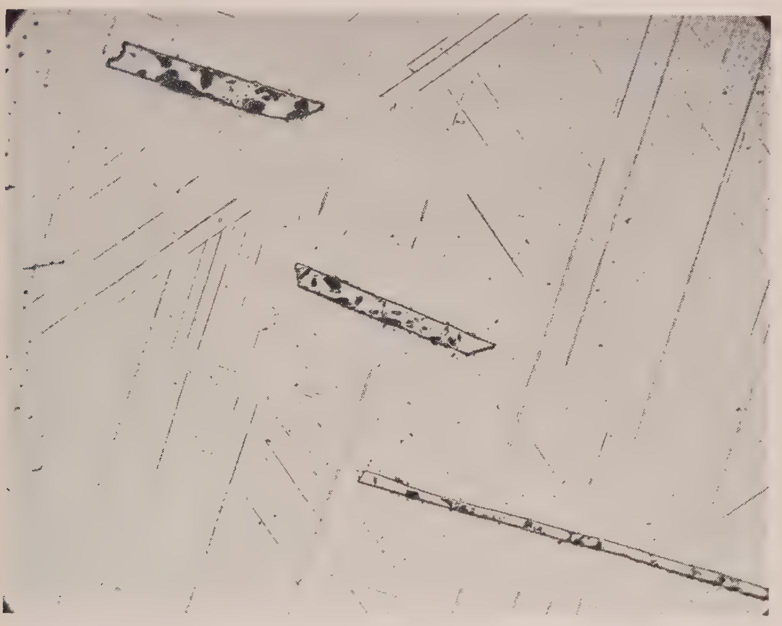

FIG. 8. The large inclusions are phosphide, dark spots due to chipping. There are 4 sets of Neumann lines in the kamacite, but as usual they terminate a short distance from the phosphide bodies. ×40.

known. Meteorites with nickel between 6 and 7.5 are usually coarse octahedrites.

Through informal communications regarding this point, Dr. Uhlig reports that he regards Owen and Liu's work as representing the conditions of normal pressure and since meteorites fail to agree with their diagram, it is likely they formed under different conditions,—most likely higher pressures.

It has been repeatedly proved that Neumann lines in artificial irons are a product of shock or sudden stress and these lines may have been produced in meteorites by the stress of extreme air pressure, by disruption in the air, or possibly in some cases by the impact of the meteorite on a hard surface. Furthermore it seems reasonable to assume that if a planet-like body with a cooling core of iron, should disrupt or explode, the fragments would be subjected to such shock and stress as to develop Neumann lines. In such a case the lines might fairly be termed a primary structure.

On that theory, it seems necessary to relate the kamacite granules and the Neumann lines in the Mayodan iron and to conclude that they were produced simultaneously. Dr. Uhlig has offered the following explanation, which has merit because all the steps take place at moderate tem-

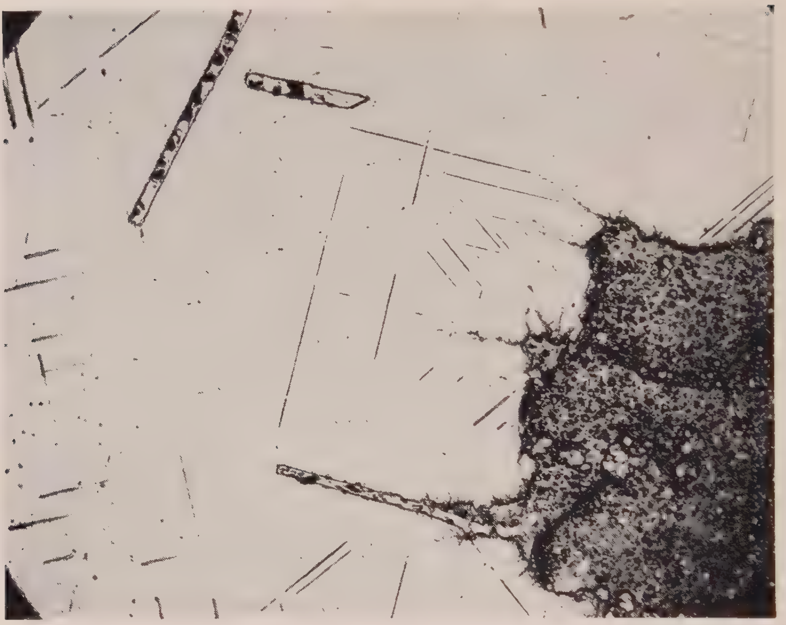

FIG. 9. The troilite at lower right is darkened by carbon, lacks a sharp border, and occasionally phosphide rods extend as prongs from the edges of the FeS. Four sets of Neumann lines are shown in the kamacite. ×40.

peratures and are those which would have occurred if the mass came from a planet-like body which fragmented.

The temperature of the metal was probably below 450° C. when an explosion separated the mass into smaller fragments and produced numerous Neumann bands. These Neumann bands are mechanical twins and therefore produce a certain amount of what the metallurgist calls "cold working." Cold working an alloy produces nuclei for new crystals ot grow and these have a different orientation from the background material. Since mechanical twinning occurs along the 211 planes, the cold-work nuclei also occur along these planes, because under terrific stress or impact these apparently are the only planes that take part in mechanical deformation. Therefore until the alloy cools to room temperature, these nuclei grow and would consist of kamacite of identical composition with the background but with a different orientation. There would be no taenite in these granules if this mechanism is correct, and in fact none is observed.

ACKNOWLEDGMENTS

The authors desire to express appreciation to the following persons for their part in this study: Dr. L. J. Spencer of the British Museum to

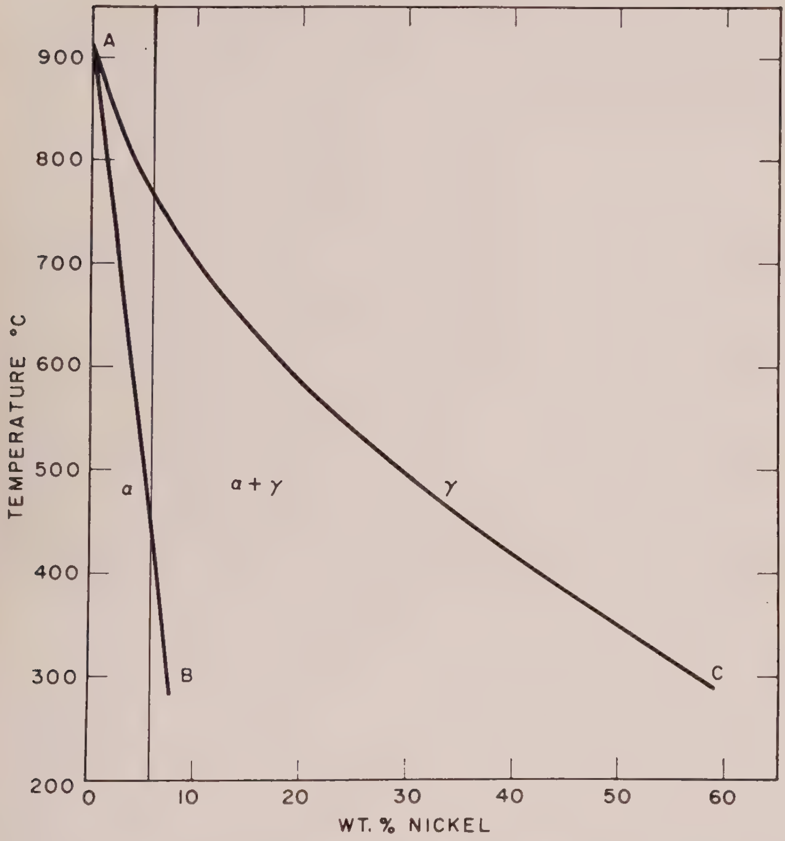

FIG. 10. Phase diagram for iron-nickel alloys at one atmosphere. (Owen and Liu, 1949.)

whom some of these plates showing the included minerals were sent; E. John Long, a science writer who prepared the popular magazine article on meteorites which, when read by James E. Beaver, prompted him to communicate with the Museum. Drs. H. H. Uhlig of Massachusetts Institute of Technology for his suggestions and to Walter Curvello, Museu Nacional, Rio de Janeiro, Brazil, who was visiting this laboratory during this investigation and took an active interest in discussing the results.

REFERENCES

FARRINGTON, O. C. (1915), Meteorites, 233 p. Chicago. Privately printed.

OWEN, E. A. AND LIU, Y. H. (1949), Further x-ray study of the equilibrium diagram of the iron-nickel system, *Jour. Iron & Steel Inst.*, **163**, 132–137.

OWEN, E. A. AND SULLY, A. H. (1939), Equilibrium diagram of iron-nickel alloys, *Phil. Mag. & Jour.*, **27**, no. **184**, 614–636.

TWO URANIUM-BEARING PEGMATITE BODIES IN SAN BERNARDINO COUNTY, CALIFORNIA*

D. F. Hewett and Jewell J. Glass, *U. S. Geological Survey, Washington, D. C.*

Abstract

Two uranium-bearing pegmatite bodies have been discovered recently in San Bernardino County, California. Examination shows that each one contains small amounts of some uncommon minerals that are composed largely of titanium, niobium, and uranium. However, the mineral assemblages are different for each. One body, in the Cady Mountains, contains, in addition to the common feldspars and quartz, the rare minerals betafite, niobian anatase, and cyrtolite. This is the first known occurrence of betafite in California. From the Pb^{206}/U^{238} ratio of betafite, the geologic age of the pegmatite has been determined as 155 million years or Middle Jurassic.

The other pegmatite body, at Pomona Tile quarry near Rock Corral, 40 miles southwest of the one in the Cady Mountains, contains euxenite and an unidentified uranium-bearing mineral, as well as the rare-earth minerals monazite and allanite and several common minerals. Euxenite is described for the first time from California. According to the lead-uranium ratio of the euxenite the age of this pegmatite is 150 million years or Middle Jurassic. The isotopic composition of lead in the euxenite has not yet been determined, so the amount of original lead is unknown.

Introduction

As a result of the widespread interest in uranium and thorium many persons, mostly prospectors and amateur mineralogists, are searching the Mojave Desert for radioactive minerals, and some have been successful. The Cady Mountains pegmatite was brought to the attention of D. F. Hewett by Oscar Hoerner, who lives 6 miles southeast of Newberry Station on the Atchison, Topeka & Santa Fe Railroad, and by Ralph W. Ross, of South Pasadena. These two were very helpful in guiding Hewett to the pegmatite during February 1950. The Pomona Tile Quarry pegmatite was found by Hewett in February 1951 during a reconnaissance in the Rock Corral area.

The descriptions of the geologic features and relations of both pegmatite bodies presented here are based on field work by D. F. Hewett, who collected numerous specimens. The minerals were determined by Jewell J. Glass, who also organized the laboratory work. Spectroscopic analyses of the numerous specimens were made by K. J. Murata, *x*-ray work was done by J. M. Axelrod and F. A. Hildebrand; all are members of the staff of the U. S. Geological Survey.

Locality and Accessibility

The Cady Mountains pegmatite here named is at the top of one of the highest peaks of the Cady Mountains (Fig. 1), a rugged area that lies about 35 miles east of Barstow, between the Union Pacific Railway and U. S. Highway 91 on the north, and the Atchison, Topeka and Sante Fe Railroad and U. S. Highway 66 on the south. It is accessible from Hector, on the Santa Fe Railroad, by a fairly good desert road, as follows:

---

* Publication authorized by the Director, U. S. Geological Survey.

1. From Hector, N. 20° E., about 2 miles.
2. Due east on section line about 4 miles.
3. Northeast up wash into canyon about 2½ miles.
4. Northwest up wash to base of mountain about half a mile.
5. From this point a trail leads westward up the mountain slope to the pegmatite, which lies about 750 feet above the wash.

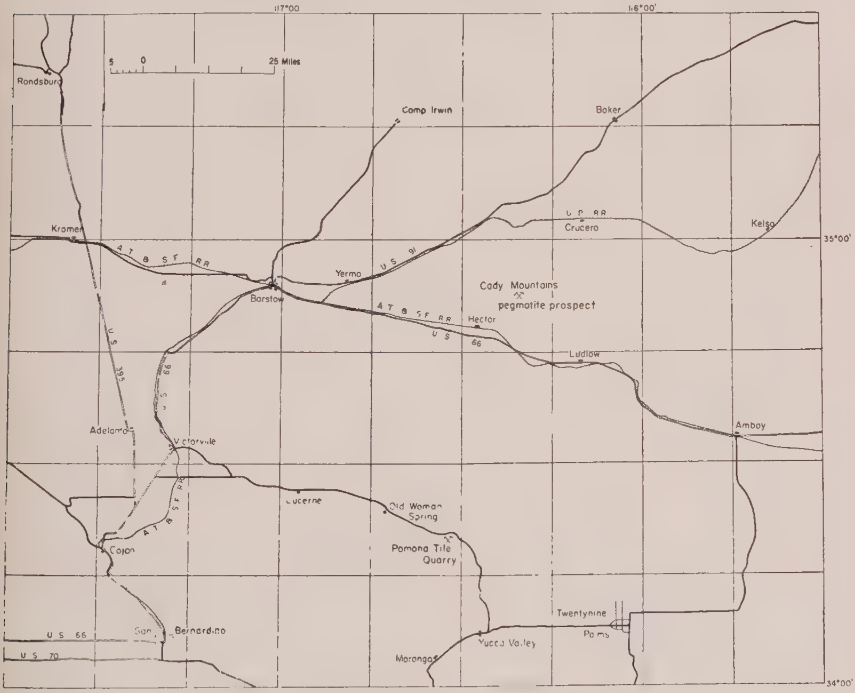

FIG. 1. Sketch map of part of San Bernardino County, California, showing location of pegmatite prospects.

The Pomona Tile Quarry pegmatite here named is about 19 miles northwest of Yucca Valley, a settlement on the paved State highway that extends from the vicinity of Whitewater, on U. S. Highway 70-60-99, up Morongo Valley to Twentynine Palms. From a point on this highway a mile east of Yucca Valley, a graded desert road leads northwest 16 miles to a spur that extends to Rancho Roqueño. The Pomona Tile

Co. quarry road from this spur turns west 1.8 miles from the junction with the road from Yucca Valley. The Pomona Tile Co. quarry lies on the crest of a prominent ridge $2\frac{1}{2}$ miles from the Yucca Valley road. Rock Corral, a well-known watering trough, is 2 miles west of the quarry. The Pomona Tile Co. quarry is about 40 miles S. 10° W. from the Cady Mountains pegmatite.

Geology of the Cady Mountains Pegmatite Area

The host rock of the pegmatite body is a type of quartz monzonite that is common in the eastern Mojave Desert. There is no record that more than a small part of the rocks of the Cady Mountains has ever been studied or mapped. During 1930–31 Dion L. Gardner (1940) mapped about two-thirds of the area between longitude 116° and 117° W. and latitude 34°30′ and 35°00′ N. Gardner, however, did not study or map the rocks of the Cady Mountains. In 1945 Cordell Durell (1953) mapped the eastern part of the Cady Mountains in connection with a study of the celestite deposits along the south slope. Durell has been kind enough to give a copy of his map to the writers. This map shows that the southeastern part of the Cady Mountains is wholly Tertiary volcanic rocks; there are basalt flows at the base of the section, overlain by andesite flows, and these by rhyolite tuffs and playa deposits, which contain the beds of celestite. The map shows a small area of granite (monzonite) in the saddle that separates the main mass of the Cady Mountains from the lower hills to the southeast. This granite (monzonite) appears to form most of the higher part of the Cady Mountains in which the pegmatite is found.

Near the Cady Mountains pegmatite body, the monzonite is coarsely crystalline; the feldspar crystals range from 3 mm to 1 cm in diameter; the grains of quartz and biotite are smaller. Thin sections show orthoclase and microcline, about 35 per cent; plagioclase (andesine), 25 per cent. In the vicinity of the pegmatite are numerous dikes of similar rock of finer grain. A thin section shows orthoclase and microcline, 30 per cent; plagioclase and microperthite, 25 per cent; quartz, 35 per cent; magnetite, 5 per cent; biotite, 3 per cent; and sphene, 2 per cent. These dikes trend northwest roughly parallel to the trend of the pegmatite. The monzonite lacks any layering or foliation, but several systems of joints are present.

Gardner's map shows large bodies of such monzonite, to which he assigned a Late Jurassic age, in the mountains that are 10 to 25 miles east, southwest, and west of the Cady Mountains. Also, this monzonite closely resembles the Cactus granite of Vaughan (1922) mapped by Gardner in the eastern part of the Newberry Mountains. The type locality of

Vaughan's Cactus granite is Cactus Flat, on the north slope of the San Bernardino Mountains, 60 miles south of the Cady Mountains.

The Cady Mountains pegmatite body is small and is simple in form and structure. It is in the central part of a large mass of quartz monzonite that underlies the Cady Mountains. In addition to orthoclase, quartz, and albite, which form most of the pegmatite, it contains small masses within which the following minerals have been found; biotite, muscovite, albite, betafite, cyrtolite, and niobian anatase.

Cady Mountains Pegmatite Body

As there is no cover of vegetation, the borders and extent of the pegmatite are well exposed. In plan, the body is roughly elliptical, about 100 feet long and 25 feet wide at the widest part. The contact that separates the pegmatite from the enclosing monzonite is definite and sharp. The longer axis of the pegmatite strikes about N. 10° W. and the body seems to dip about 65° W. The ends are distinctly round rather than wedge-shaped. The internal arrangement and relations of the minerals that make up the pegmatite are well shown in an open cut on the east slope of the peak; it is about 40 feet long, about 10 feet deep, and the face is 15 feet high.

Mineral arrangements. As exposed in the open cut, the pegmatite is roughly separable into two parts or longitudinal zones. The lower or eastern zone is about 12 feet thick and is made up largely of light reddish-brown feldspar, minor amounts of quartz, magnetite, and pale greenish mica. This zone shows a faint layering, which is not noticeable in the upper zone. The upper zone, also about 12 feet thick, contains large irregular masses of white quartz; these masses of quartz seem to replace the feldspar.

Coarsely crystalline, pale reddish-brown orthoclase is the most abundant mineral in the lower zone. No terminated crystals were found but some cleavage faces are several inches in diameter. This feldspar is replaced sporadically by large areas of feathery white albite. There are also small pipelike bodies of clear, glassy quartz whose longer axes are normal to the footwall; these are a few inches in diameter and 6 to 15 inches long. The reddish orthoclase of the lower zone also contains isolated small rounded lumps of magnetite, as much as 2 inches long; these show no radioactivity, therefore contain no inclusions of uranium-bearing minerals.

Within the lower zone there are several round masses of loosely coherent material, pale yellowish green in color; one of these is a few inches in diameter and 10 inches long. This material disintegrates readily in water, and after the coarse fragments of feldspar are panned and screened out the residue is composed of three minerals—flakes of pale greenish mica (muscovite), small crystals of quartz, and flat tetragonal crystals of niobian anatase. This residue shows slight radioactivity. Nothing resembling these masses is found in the upper zone. In the lower zone, also, there are a few rosettes of biotite plates 15 to 20 inches in diameter; thin plates of biotite 5 to 8 inches long radiate outward from centers. The plates of biotite contain sparse, small crystals of cyrtolite.

The upper zone contains much more quartz than feldspar, which it seems to replace. The masses of quartz do not contain any other minerals. A single lens of dark minerals about 36 inches long and about 20 inches thick occurs with the reddish-brown orthoclase. The lens is made up of thin plates of biotite 1.5 mm to 3 mm thick and as much as 6 inches long; between these biotite plates, layers 6 mm to 2.5 cm thick composed of magnetite, reddish orthoclase, and albite have formed. Pseudohexagonal crystals of cyrtolite (metamict zircon) occur on the borders of the biotite zone, and octahedrons of betafite are found enclosed in the magnetite masses and in the feldspar. After some 25 pounds of the dark minerals from the lens were crushed and examined carefully, about 25 grams of betafite crystals were recovered. It is possible that the entire lens would yield about 100 grams of this mineral.

The common and abundant minerals that make up the pegmatite are orthoclase, microcline, plagioclase (albite), microperthite, quartz, magnetite, biotite, and muscovite. Only the uncommon and relatively sparse minerals betafite, cyrtolite, and anatase are here described in detail.

Betafite. Betafite is a niobate and titanate of uranium. Special interest is attached to this mineral because it seems to be very uncommon in American pegmatites. A sufficient amount of the mineral has been recovered from the pegmatite here described to permit the determination of its age. Except for a few grains observed in the midst of albitized orthoclase, this mineral forms perfect octahedrons. Most of the crystals are either embedded in the magnetite or lie between plates of magnetite and feldspar that are themselves enclosed within layers of biotite. Thus far, the largest crystal found is about 6 mm in diameter, but most of the crystals range from 2 to 4 mm in diameter. All of the crystals of betafite show an outer zone of pale yellowish, fine-grained material, the nature of which has not been determined. It probably represents an alteration of the betafite that forms the core of each crystal. The unaltered core of betafite is pale yellowish brown, in part slightly greenish, is transparent, and the luster ranges from vitreous to resinous. It shows conchoidal fracture but no cleavage; hardness is about 3. Immersed in index media, the fragments are pale greenish yellow, isotropic, and have an average index of refraction of 1.910. The shell or alteration product is too fine-grained to be determined.

Table 1 presents spectrographic analyses of betafite, cyrtolite, and niobian anatase.

TABLE 1. QUALITATIVE SPECTROGRAPHIC ANALYSES OF BETAFITE, CYRTOLITE (METAMICT ZIRCON), AND NIOBIAN ANATASE FROM CADY MOUNTAINS, SAN BERNARDINO COUNTY, CALIFORNIA

K. J. Murata, analyst

Percentage	Constituents		
	Betafite	Cyrtolite (metamict zircon)	Niobian anatase
>5	Nb, U, Ti	Zr, Si	Ti
1–5	Ca	Th	Fe, Si
0.X	La, Fe, Si, Ba, Sr, Ta, Th	U, Y, Fe, Ti, La, Nb	Nb, Ta, Mn, La
0.0X	Pb, Mn, Zr, Y, Sn, B, (As?)	Ca, Ba	Pb, Al, Zr, Y, Ca, Sn, Ba
0.00X	Be, Al	Be, Pb, Mn, Cu, Al, B	V, Cu
0.000X	—	Sr	Be
Not found in sample	Cu, V	V, As, Ta, Sn	U, Sr, Th, B, As, Sn

Not found in any sample: Ag, Bi, Mo, Sb, Ga, W, Ge, Zn, Cd, In, Tl, Ni, Co, Cr, P, and Na.

In order to determine the age of betafite, the unaltered portions were separated and submitted to Harry Levine, of the U. S. Geological Survey, for analysis for uranium, thorium, and lead. The results obtained are as follows: U 10.68 per cent, ThO_2 4.22 per cent, and PbO 0.63 per cent. In addition, the lead present in betafite was separated and subjected to isotopic analysis. We are indebted to Lorin Stieff, U. S. Geological Survey, for the following calculations of age based on the chemical and isotopic analyses:

"The lead extracted from the betafite was prepared as the iodide. This iodide was analyzed by the Assay Laboratory Department, Carbide and Carbon Chemicals Co., Y-12 Plant, Oak Ridge, Tennessee. The abundance of the lead isotopes in atom per cent in the betafite is given below:

Pb^{204}	Pb^{206}	Pb^{207}	Pb^{208}
0.717	50.691	13.095	35.495

"Four separate age calculations on the betafite have been made. These ages are shown in the following table.

Calculated ages of betafite to nearest 5 million years

Pb^{206}/U^{238}	Pb^{207}/U^{235}	Pb^{207}/Pb^{206}	Pb^{208}/Th
155	165	300	285

Isotopic analysis of the lead for the betafite indicated that the sample contained approximately 52 per cent original lead. In the absence of any isotopic analyses of lead from the Cady Mountains we have assumed that the original lead in the betafite is similar in isotopic composition to lead from vanadinite from the Tucson Mountains in Arizona, analyzed by Nier (1938).

"Of the four ages the Pb^{206}/U^{238} (155) is probably the nearest to the actual age of the betafite. The relatively high Pb^{207}/Pb^{206} age of 300 million years probably reflects the errors introduced by assuming the original lead in the betafite to be similar to the lead from the Tucson Mountains. An analysis of common lead from the vicinity of the Cady Mountains would undoubtedly permit a more accurate age determination. In addition, a Pb^{207}/Pb^{206} age is not very reliable in the 0–500 million year range. The similarity between the thorium age and the Pb^{207}/Pb^{206} age is probably fortuitous. A more judicious choice of common lead might lower the thorium age, and the Pb^{207}/Pb^{206} age would be expected to drop radically. A selective loss of thorium from the sample would not be expected but might possibly account for the older thorium age. A selective loss of lead from the sample does not seem probable because the uranium ages are younger than the thorium ages."

Cyrtolite (*metamict zircon*). Cyrtolite is a name applied by some authors to metamict zircon. Crystals of this mineral are very common in the large lens of magnetite, feldspar, and biotite in the upper zone of the pegmatite and are less common in the rosettes of biotite in the lower zone. Most of the crystals range from 2 to 3 mm in diameter. The color is pale grayish red. A few crystals show tetragonal symmetry, but most of them are flattened or otherwise distorted; some are roughly triangular or pseudohexagonal in outline. The hardness is about 7; the luster is vitreous. In the large magnetite lens, the crystals are concentrated in the layers of biotite.

In thin section the mineral is transparent, but it contains minute grains of hematite that may account for the pale reddish color. The central part of the crystals is isotropic, that is, the mineral is metamict, and has an index of refraction of about 1.825. The borders of the crystals are anisotropic and are deeply stained; no optical figure could be obtained. The mean index of refraction is about 1.890.

The metamictic condition of the Cady Mountains uranium- and thorium-bearing cyrtolite may be explained (Table 1) on the basis of work on zircon and cyrtolite by Kostyleva (1946) establishing the conclusion that metamictic disintegration is the result of the destruction of bonds in the lattice produced by alpha-radiation from the radioactive elements present.

Niobian anatase (*octahedrite*). This mineral forms myriads of perfect tetragonal crystals of pyramidal habit, few of which are as much as 0.5 mm in diameter. They are included in the small masses of muscovite that occur in the lower zone of the pegmatite. Some of the crystals show a combination of pyramid, prism and base. The masses of muscovite, quartz, and anatase disintegrate readily in water.

The crystals are transparent and deep green in transmitted light; thin fragments are pale yellowish green. The mineral is uniaxial negative; ϵ is near 2.45. Interference colors in thin section are sapphire blue, purple, and reddish yellow; hardness is about 5. Spectrographic analysis of the mineral is shown in Table 1.

Geology of the Pomona Tile Quarry Pegmatite Area

The general geology of the area between Rancho Roqueño and Rock Corral, within which the Pomona Tile Quarry body is found, has been studied and mapped by Vaughan (1922). Later Woodford (Woodford and Harris, 1928) restudied a part of the area near Blackhawk Canyon and revised some of Vaughan's conclusions. In the northeastern part of the San Bernardino Mountains, Vaughan recognized three major geologic units: 1) heterogeneous plutonic rocks; 2) Cactus granite (thought by Woodford to be nearer to quartz monzonite) intrusive into the older plutonic rocks; 3) undifferentiated schists into which the foregoing rocks were intruded.

A reconnaissance of several square miles around the Pomona Tile Quarry pegmatite indicates that the three major rock units recognized by Vaughan are present. Probably the most abundant rock in this area is a light-colored quartz monzonite (Cactus granite of Vaughan) in which the pegmatite is found. This intrudes a darker gneissic granite, abundant near Rock Corral, in which large white orthoclase crystals are embedded in a dark matrix, largely quartz and biotite. Several miles east of the pegmatite body, the young quartz monzonite (Vaughan's Cactus granite) intrudes an earlier quartz monzonite that is characterized by large, flat crystals of orthoclase. The third group of rocks in this area includes sporadic blocks of dark rocks that range from several tens of feet to several hundreds of feet in diameter; most of these blocks have flat bases and rest on the above-described intrusive rocks. All of these blocks show foliation, now in diverse attitudes. The dark color of these blocks is due largely to abundant biotite. Some specimens show small amounts of quartz and orthoclase; several contain abundant cordierite and sillimanite. These blocks of dark foliated rocks are regarded as remnants of roof pendants on the underlying intrusive rocks. Almost all of the blocks examined show noticeable radioactivity, which seems to be due to thorium-bearing cyrtolite (metamict zircon).

Pomona Tile Quarry

Pegmatite body. Six open cuts and trenches reveal several flat-lying tabular bodies of pegmatite within an area of several acres along the crest of a prominent ridge. The uppermost and largest body strikes about N. 70° E. and dips 5 to 10° NW. and is 10 to 15 feet thick. This body has yielded all of the uncommon minerals that are described herein. Four other open cuts show masses of gray glassy quartz and pale reddish coarsely crystalline feldspar,—orthoclase, and microcline. These explorations do not show the exact shape or size of any pegmatite body. The explored bodies seem to be tabular lenses that form a zone in the quartz monzonite.

The largest trench on the crest of the ridge shows one large and several small concentrations of uncommon minerals in the midst of the feldspar and quartz that form most of the tabular body. In this, as in other lenses of pegmatite on the ridge, there seems to be no simple form of the masses of quartz and feldspar, nor any simple arrangement of the masses. There is no layering or zoning whatsoever.

The largest concentration of uncommon minerals is in and around the border of a nucleus of quartz from which thin plates of ilmenite 1 to 5 mm thick radiate outward as much as 3 feet. In the nucleus the plates are wholly embedded in gray glassy quartz, but beyond the nucleus they are wholly in reddish microcline. The other uncommon minerals are dispersed as grains and crystals in or near the nucleus of quartz; none is found in the outer zone of ilmenite plates. Two other small areas of radiating plates of ilmenite lie about 50 and 75 feet southwest of the largest body, but these contain only very small amounts of the uncommon minerals.

The following minerals have been found in the Pomona Tile Quarry pegmatite: albite, allanite, epidote, biotite, hematite, magnetite, monazite, rutile, sphene, euxenite, and an unidentified uranium-bearing mineral; other minerals, probably products of weathering of some of the minerals listed above, are: kaolinite, leucoxene, limonite, manganese oxide, and fluorescent hyalite. Only the uranium-bearing minerals will be described.

Euxenite. Euxenite is a niobate and titanate of yttrium, erbium, cerium, and uranium. Numerous small tabular crystals, dark brown in color, 3 to 8 mm in maximum diameter were found wholly in the reddish feldspar near the nucleus of the pegmatite body; these crystals are shown by spectrographic analysis to be euxenite (Table 2). This analysis was confirmed by x-ray determination made by F. A. Hildebrand. The mineral is isotropic (metamict), has a mean index of refraction of 2.25, and a hardness of about 6.

TABLE 2. QUALITATIVE SPECTROGRAPHIC ANALYSIS OF TWO METAMICT EUXENITES FROM POMONA TILE QUARRY PEGMATITE, SAN BERNARDINO COUNTY, CALIFORNIA

K. J. Murata, analyst

Percentage	Constituents
>10	Nb, Ti, Y
1–10	U, Fe, Th, Yb
0.X	Ta, Ca, Pb, Mn, La
0.0X	Mg, Si, Al, Sc

Not found in samples: B, Be, As, Sb, Sn, Bi, Cu, Ag, Ge, Ga, Tl, In, Zn, Cd, Mo, W, Cr, V, Co, Ni, Sr, Ba, Na, Pt, P.

The analysis above applies to both samples.

Lead, uranium, and thorium determinations on euxenite from Pomona Tile Quarry pegmatite were made by Paul Scott, Rivers A. Powell, and Glen Edgington, analysts on the staff of the U. S. Geological Survey. The percentage determinations are U = 13.9, 14.5; Pb = 0.30, 0.30, 0.29; and Th = 2.51. These values were used in calculating the geologic age of the Pomona Tile Quarry pegmatite.

Computations for the age determination were made by Dr. John Putnam Marble, Chairman, Committee on measurement of geologic time, National Research Council. A summary of his report is quoted below:

"Using the simplest age formula:

$\text{Age} = 7600\left[\frac{\text{Pb}}{\text{U}+0.36\text{Th}}\right]$ million years, which is good enough for the present purposes, especially in view of the spread in the U determinations quoted, the age works out to be 149.7 million years. The data do not really indicate anything closer than, say, 145–155 million years.

"The calculations are summarized as follows:
Average per cent Pb = 0.297; U = 14.2; Th = 2.51
$0.297/14.2+0.36\times 2.51 = 0.297/14.2+0.90 = 0.297/15.10 = 0.0197$
$0.0197\times 7600 = 149.7$."

The lead from euxenite has not yet been analyzed isotopically, so the amount of ordinary lead is not known. Therefore the age obtained above by means of the simplest age formula may be subject to some revision when the results of the isotopic analysis become available.

An unidentified uranium-bearing mineral. A few grains of a highly splendent black mineral occur in the feldspar remote from the quartz nucleus. The material has been analyzed spectrographically (Table 3). The composition is similar to that of davidite (Bannister and Horne, 1950). An *x*-ray powder diffraction pattern obtained by F. A. Hildebrand shows an unidentified mineral. Some similar grains of this mineral were

TABLE 3. QUALITATIVE SPECTROGRAPHIC ANALYSIS OF AN UNIDENTIFIED URANIUM-BEARING MINERAL FROM POMONA TILE QUARRY PEGMATITE, SAN BERNARDINO COUNTY, CALIFORNIA

K. J. Murata, Analyst

Percentage	Constituents
>10	Ti, Fe
6–10	U
1–5	Th, Si, Y, Ca
0.X	Nb, Yb, La, Zr
0.0X	Mg, Al, Ba, V, Pb
0.00X	B

Not found: Cu, Bi, Ag, Au, Pt, Mo, W, As, Sb, Sn, Cd, Ga, In, Tl, Co, Ni, Cr, Sc, Na, P, Be, Zn, and Sr.

found in the midst of masses of microcline unaccompanied by any of the other minerals found near the nucleus of the pegmatite body, as much as 25 feet distant from the largest concentration of the rare minerals. This mineral attracted attention because it exhibits unusually strong radioactivity.

REFERENCES

BANNISTER, F. A., AND HORNE, J. E. T. (1950), A radioactive mineral from Mozambique related to davidite: *Mineral. Mag.*, **29**, 101–112.

DURELL, CORDELL (1953), Geological investigations of strontium deposits: *California Dept. Nat. Res. Spec. Rept.* **32,** 48 p.

GARDNER, D. L. (1940), Geology of the Newberry and Ord Mountains, San Bernardino County, California: *California Jour. Mines and Geology*, **36,** 257–292.

KOSTYLEVA, E. E. (1946), Metamict alteration of minerals of the zircon group: *Fersman Memorial Vol., Akad. Nauk SSSR*, 27–35.

NIER, A. O. (1938), Variations in the relative abundance of isotopes of common lead from various sources: *Jour. Amer. Chem. Soc.*, **60,** 1571.

VAUGHAN, F. E. (1922), Geology of the San Bernardino Mountains north of San Gorgonio Pass: *University of California, Bull. Dept. of Geologic Sciences*, **13,** 319–411.

WOODFORD, A. O., AND HARRIS, T. F. (1928), Geology of Blackhawk Canyon, San Bernardino Mountains, California: *University of California, Bull. Dept. of Geologic Sciences*, **17,** 265–304.

MINIMIZING THE EFFECTS OF PREFERRED ORIENTATION IN *X*-RAY POWDER DIFFRACTION PATTERNS*

Fred A. Hildebrand, *U. S. Geological Survey, Washington 25, D.C.*

Abstract

A number of techniques to reduce preferred orientation in samples for *x*-ray powder diffraction patterns were studied. Minerals were mounted in ethyl cellulose spindles and spheres, on greased Lindemann glass rods, and in nylon tubes. Gross differences in intensities of diffraction lines are demonstrated on films showing random and preferred orientation of fibrous pectolite and platy paragonite mica. The sphere-mount method was shown to be the most successful and convenient method for achieving random orientation and thus for obtaining more nearly correct intensities of diffraction lines.

Introduction

It has long been known that fine-grained aggregates of fibrous and platy minerals when dispersed in liquids and dried or when subjected to mild pressures tend to form oriented aggregates. Rod-shaped particles tend to align their long axes parallel and platy minerals tend to lie on their platy surfaces and form matted layers of overlapping flakes.

Several fibrous and platy minerals were studied by various methods in an attempt to reduce preferred orientation in *x*-ray powder diffraction mounts. Among these, fibrous pectolite and platy paragonite mica were chosen for further tests because optical examination showed that they retain their fibrous and platy character even when ground extremely fine. The platy character of several micas was found to diminish with decreasing particle size because the thickness of the plates increased relative to the dimensions across the flakes. Hence the effects of preferred orientation in the powder diffraction patterns of paragonite are not as great as in those of pectolite.

Preparation of Sphere Mounts

The production of spheres in which preferred orientation in powder patterns of fibrous or platy minerals can be reduced to a minimum is an outgrowth of a method of preparing spindle mounts that was developed in the *x*-ray laboratory of the U. S. Geological Survey by several technicians over a period of about 12 years.

In this method, a small quantity of the mineral is finely powdered with a glass rod in a depression of a standard spot plate. A 10 per cent solution of granular, low-viscosity ethyl cellulose dissolved in toluene is used as a binder. A little xylene may be added when the amount of ma-

---

* Publication authorized by the Director, U. S. Geological Survey.

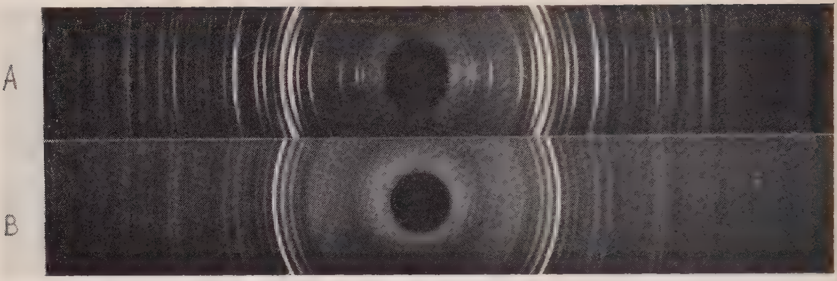

FIG. 1. Pectolite, Bergen Hill, New Jersey, USNM. 82452. A. Ethyl cellulose spindle 0.15 mm. in diameter showing preferred orientation, B. Ethyl cellulose sphere 0.29 mm. in diameter showing minimized preferred orientation.

terial is extremely small, in order to avoid too rapid drying. A very small amount of the binder is taken up on the end of a sewing needle and is thoroughly mixed with the powder until the mixture is no longer sticky, and a plastic, workable ball is obtained. This ball is quickly placed between a plate glass surface and a microscope slide and is rolled between the two pieces of glass in a circular motion, with the microscope slide resting on the edge of the glass plate as a pivot line. Whereas spindle type mounts conventionally used in powder diffraction cameras can easily be rolled to an optimum diameter of 0.10 mm. to 0.15 mm. because the excess material can squeeze out in the direction of the spindle length, the ultimate diameter of a spherical mount is determined by the initial amount of material used. It was found that the smallest spheres that could conveniently be made by rolling were 0.25 mm. to 0.30 mm. in diameter.

A sphere produced by this rolling technique is cemented to the end of an ethyl cellulose binder spindle simply by dipping the end of the spindle in toluene and touching it while still wet to the sphere. The spindle is then mounted in the camera in standard fashion, care being taken to project only the sphere into the collimating tube field.

OTHER METHODS INVESTIGATED

Three other sample-mounting techniques investigated to minimize preferred orientation were as follows:

1) A short cylindrical section of the spindle used in preparing the pattern shown in Figure 1 A was cemented to the end of a binder spindle with its cylindrical axis normal to this supporting spindle. The mount was then placed in the camera in the same fashion as a sphere mount. The resulting diffraction pattern indicated that preferred orientation had been appreciably decreased, but not so strikingly as with sphere mounts.

TABLE 1. *X*-RAY DIFFRACTION DATA FOR PECTOLITE

d(Å, meas.)	A	B
	Figure 1 A film 6509	Figure 1 B film 6994
	I	I
7.83	7	5
7.03	7	5
5.50	7	5
4.98	3	1
4.55	1	1
4.00	2	2
3.90	8	6
3.77	2	2
3.52	8	5
3.43	1	4
3.33	9	6B
3.28	9	
3.16	4	5
3.10	10	8
2.921	6	10
2.739	8	6
2.637	1	—
2.600	8	6
2.495	3	—
2.430	3	5
2.368	4	—
2.338	6	5
2.298	9	6
2.270	2	—
2.227	3	2
2.191	6	6B
2.166	2	
2.090	5	2
2.053	2	3B
2.002	4	
1.945	5	2
1.926	5	4
1.877	2	4
1.831	6	4
1.781	3	3
1.752	7	6
1.716	5	6
1.675	6	2
1.661	7	4
1.603	3	4
1.570	6	2
1.554	5	5
1.521	2	2
1.490	8	5
1.475	5	5B
1.465	2	
1.431	4	2
1.393	6	2
1.377	6	4
1.356	6	3
1.329	1	1
1.312	1	1
1.299	6	2
1.285	5	1
1.265	2	1
1.245	3	2B
1.220	2	1B
1.180	3	—
1.169	5B	4
1.149	2	2
1.136	2	4
1.114	2	1
1.105	5	5
1.093	5	2
1.084	2	1
1.065	2B	1B
1.052	2B	—
1.043	3	2
1.032	1	1
0.999	4	2

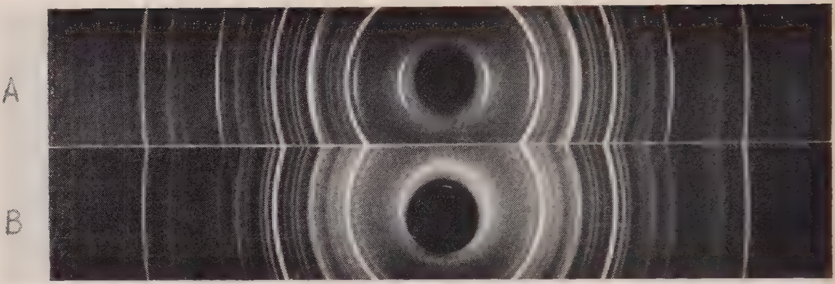

FIG. 2. Paragonite mica, Monte Campione, Switzerland, USNM. R4414, W. T. Schaller No. 19, D-1432-Pa 1. A. Ethyl cellulose spindle 0.16 mm. in diameter showing preferred orientation. B. Ethyl cellulose sphere 0.30 mm. in diameter showing minimized preferred orientation.

2) Lindemann glass rods 0.12 mm. in diameter coated with "celloseal" grease were dipped into the powdered mineral and mounted like a spindle in the camera. The resulting diffraction patterns of these also indicated that preferred orientation had been appreciably decreased. This method is probably not so advantageous as other methods not only because of the additional materials required for the sample mount but also because it is difficult to coat the greased rod uniformly with the powdered mineral and prevent broad bands contributed by the glass from showing up in the diffraction pattern.

3) A nylon tube with an inner diameter of 0.33 mm. was loosely filled with the mineral and mounted like a spindle in the camera. In the resulting pattern many strong broad bands contributed by the nylon almost completely obliterated the diffraction lines of the mineral, so that the method was not practical. A repetition of this test with a slightly larger nylon tube also gave unsatisfactory results. Nylon tubes with smaller diameters were not available.

X-RAY DATA

In Figure 1 A, the diffraction pattern of pectolite made with a spindle, preferred orientation is best shown by unequal intensities of the diffraction lines along their arcs. In Figure 1 B, the diffraction pattern of a portion of the same mixture used in the spindle of Figure 1 A but rolled into a sphere, preferred orientation has been appreciably reduced, with a leveling off of the line intensities along their arcs as well as relative to each other. In Table 1, a comparison of the measured intensities of the two patterns of pectolite in Figure 1 shows the gross differences in intensities of identical diffraction lines. The line intensities shown by the sphere mount, Table 1 B, are the more nearly correct intensities for pectolite. Likewise, Figure 2 and Table 2 demonstrate preferred orientation in

TABLE 2. *X*-RAY DIFFRACTION DATA FOR PARAGONITE

d(Å, meas.)	A	B	d(Å, meas.)	A	B
	Figure 2 A film 7026	Figure 2 B film 7002		Figure 2 A film 7026	Figure 2 B film 7002
	I	I		I	I
9.7	9	8	1.834	3B	3B
4.96	2	6B	1.774	2B	2B
4.85	7		1.728	2B	1B
4.44	7	10	1.687	4B	5B
4.27	4	4	1.658	2	2
4.15	2	2	1.639	2	2
4.06	4	6	1.616	6B	6B
3.97	2	—	1.583	2B	3B
3.87	2	—	1.549	2B	2B
3.79	4	6	1.514	2B	2B
3.68	4	6	1.486	7B	8B
3.56	2	—	1.459	1	—
3.48	3	2	1.427	2	2
3.39	4	5	1.410	2	2
3.30	5	5	1.384	4	3
3.22	10	6	1.349	3B	4B
3.18	5	5	1.315	4B	4B
3.03	1	—	1.296	2	—
2.979	3	—	1.284	4	5
2.921	6	7	1.265	3B	3B
2.831	6	7	1.238	3B	4B
2.772	1	—	1.211	3	2
2.706	5	6	1.199	2	2
2.571	6	6	1.176	3B	3B
2.536	8	9	1.150	2	1
2.430	7	8	1.136	2	2
2.356	5B	6B	1.118	1B	2B
2.222	3	3	1.094	2B	2B
2.186	5	6B	1.049	2B	2B
2.146	1B	2B	1.025	2B	1B
2.103	6B	6B	1.013	1B	1B
2.067	2	2	0.985	2B	2B
2.027	3	3	0.969	2B	2B
1.989	5	3	0.961	3B	2B
1.965	2	—	0.9022	3B	2B
1.933	8	6	0.8577	2B	2B
1.895	2	2			

paragonite, and Table 2 B shows the more nearly correct line intensities for paragonite.

Examination of Figure 1 shows that there is more broadening of lines in the sphere pattern than in the spindle pattern. Whether the greater diameter of the sphere is responsible for this broadening can not be established with certainty. Some of the other methods used to minimize preferred orientation also resulted in patterns in which there was broadening of lines with some loss of resolution. The best example of this was method (1) described under the heading "other methods investigated," where a very short section of the same spindle used to produce the pattern in Figure 1 A was mounted on a binder spindle. The resulting pattern showed more random orientation but also broadening of lines and poorer resolution. In view of the many factors involving both technique and instrumentation in the production of powder diffraction patterns, it is difficult to attribute broadening of lines and loss of resolution to any one factor.

In the patterns produced from sphere mounts it was noted that virtually all the lines except a few very weak ones were measurable both as to position and as to intensity in spite of broadening of lines and that these measurements agreed admirably with those made from patterns produced from spindle mounts although the spindle-mount patterns showed better resolution.

The diffraction patterns shown in Figures 1 and 2 were taken with North American Philips Debye-Scherrer powder cameras (114.59 mm. diameter) using the Straumanis and Wilson techniques with $CuK\alpha$ (Ni filter), $\lambda = 1.5418$ Å.

ACKNOWLEDGMENTS

The need for investigating new techniques for minimizing preferred orientation in powder diffraction films was pointed out by C. L. Christ, and an investigation of the problem was strongly urged by W. T. Schaller in connection with his studies of fibrous minerals. The minerals used in the tests described here are from Dr. Schaller's collection. Some of the grease-dipped rods were made by J. M. Axelrod in the early stages of the investigation.

GIANT AMYGDULES IN ANDESITE FROM THE SOUTHERN QUITMAN MOUNTAINS, TEXAS*

EARL INGERSON, *U. S. Geological Survey, Washington, D. C.*

ABSTRACT

The volcanic rocks of Tertiary age of the southern Quitman Mountains in Hudspeth County, Texas, contain some rather unusual amygdules. The cavity fillings are mostly varieties of silica, but one zone has much calcite, and there are minor amounts of iron and manganese oxides, montmorillonite, and saponite. The individual amygdules range in size from microscopic to some eight inches in diameter. Previously these volcanic rocks have been lumped as "rhyolitic volcanics," but more detailed study shows them to range from rhyolite and rhyolite tuff through trachyte to andesite. The amygdules are confined to the andesite. The amygdules appear to be confined to the neighborhood of highly jointed zones that provided access for later hydrothermal solutions, which altered the andesite and deposited the minerals of the amygdules.

INTRODUCTION

Location of area

The Quitman Mountains form one of the northwest-trending ranges of trans-Pecos Texas. Starting at the pass on the Southern Pacific Railroad 10 miles west of the town of Sierra Blanca, they extend in a southeasterly direction for a distance of 35 miles. Their southern end is on the Rio Grande, between Indian Hot Springs and the mouth of Quitman Arroyo. The area covered in this report is shown by diagonal lines on Figure 1.

Previous work

The northern part of the Quitman Mountains, down to Quitman Gap, has been mapped and described in detail by Huffington (1943). The southern part of the range is much less completely known. Von Steeruwitz (1890, p. 680), from the disturbed structural condition of the area and the presence of hot springs, assumed that there were igneous rocks present, but apparently he did not find them. He gave an account of the geology of much of the trans-Pecos country, but he did not prepare a geologic map.

Baker (1927) mapped the Quitman Mountains on a scale of 4 miles to the inch. His map shows two areas of "rhyolitic volcanics" on the eastern flank of the range from about 3 to 10 miles from its southern extremity. The general geologic relations shown in Figure 2 are after Baker's map.

Taff (1890, Pl. 27) shows a structure section across the southern part of the range in the neighborhood of Quitman Gap, where there are no

---

* Publication authorized by the Director, U. S. Geological Survey.

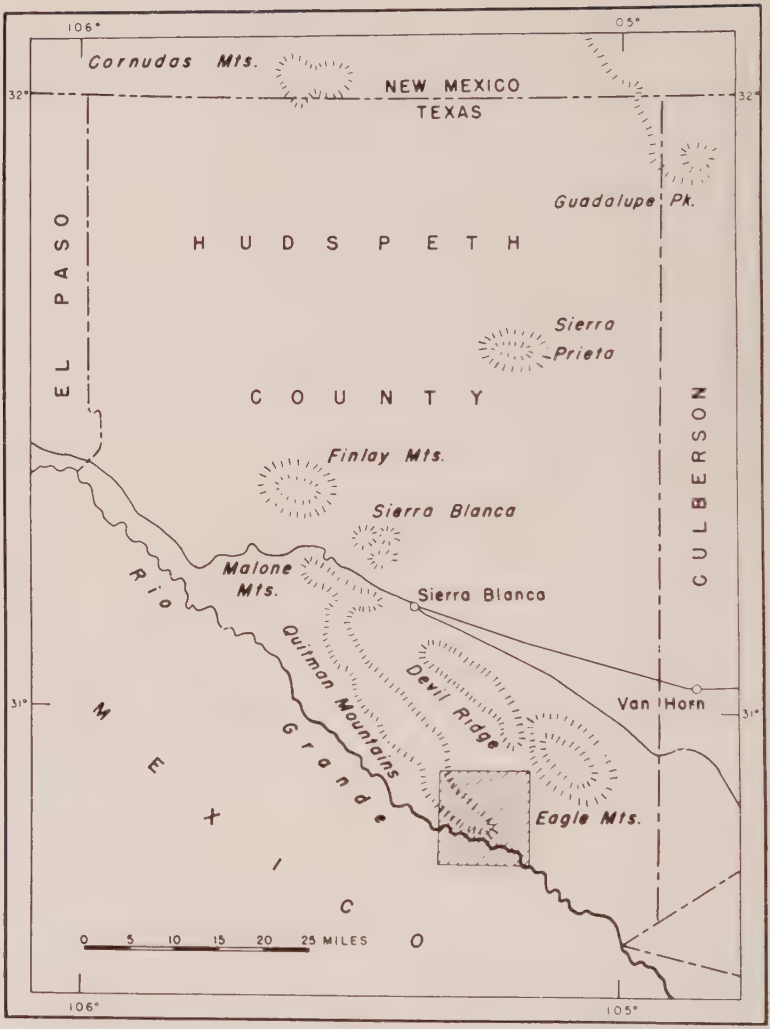

FIG. 1. Index map showing the location of the area described.

volcanics. Baker (1927, 1934) has given more details of the structure, including recognition of a thrust fault and location of the major fold axes.

VOLCANIC ROCKS

Baker's map shows two areas of volcanic rocks separated by alluvium and sedimentary rocks of Cretaceous age. It is possible that a cross fault is covered by the alluvium. Although there are many local irregularities in the structure, the dips in the northern area are steeper and the strikes

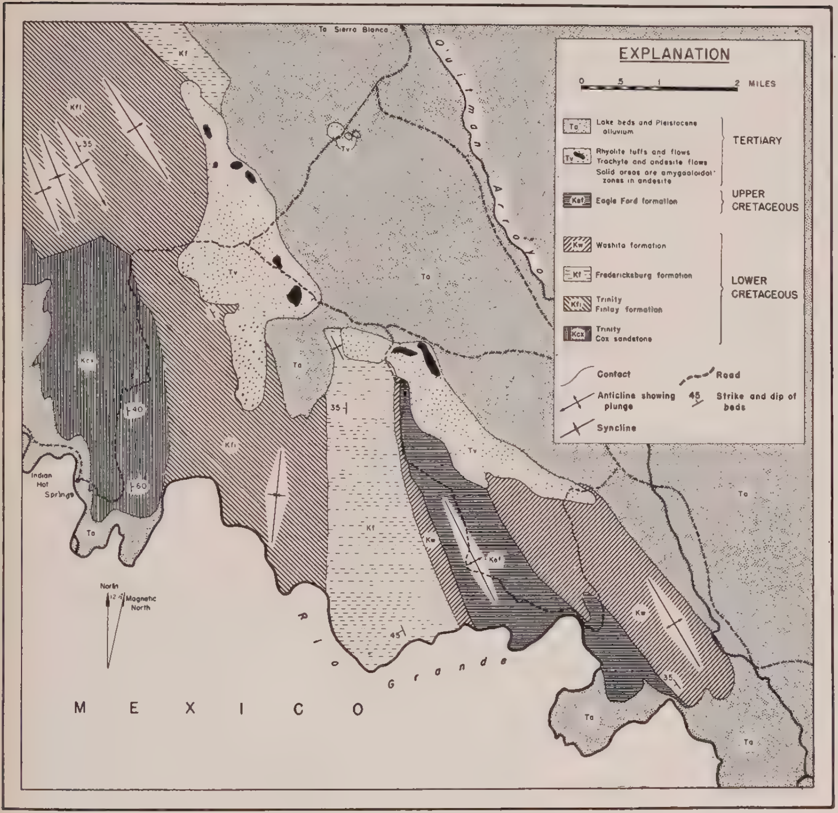

FIG. 2. Geology of the southern tip of the Quitman Mountains, adapted from Baker (1927). Distribution and structure of the sedimentary rocks after Baker (1927). Distribution of volcanic rocks modified from Baker (1927). Distribution of amygdaloidal areas (solid black) mapped by present author.

are more nearly northward than those of the southern area.

There is a third outcrop of volcanic rocks not shown on Baker's map. It is smaller than either of the other two and is located on the Sierra Blanca-Indian Hot Springs road about 1.8 miles northeast of where the road enters the northernmost of the two areas of volcanic rocks shown on Baker's map. This area is composed of red trachytic, nonamygdaloidal rocks. It may be connected with the other area(s) under the alluvial cover. The three areas of volcanic rocks and the associated sedimentary rocks are shown on the geologic map, Figure 2.

In the two areas shown by Baker, rhyolitic rocks probably predominate, although in the northernmost area trachytic to andesitic rocks are about as abundant as rhyolites. In the northern third of the southern area trachytes and andesites predominate, but the rest of the area, where a much thicker section is exposed, consists almost entirely of rhyolites and rhyolite tuff.

The entire thickness of the volcanic rocks is nowhere exposed, because the eastern edge of the areas is covered by the alluvium that laps onto the eastern flank of the mountains from Quitman Arroyo.

AMYGDULES IN ANDESITE

General

For many years inhabitants of the Sierra Blanca area have collected rounded to elongate agate and quartz masses in the southern part of the Quitman Mountains. The locality is referred to as the "geode bed," and many of the specimens do resemble geodes, being cavities lined with chalcedony and quartz crystals (Fig. 4).

In the fall of 1951 the writer spent several days in the area. The "geodes" turned out to be amygdules, some of remarkable size, in reddish andesite. Plate I A and Figure 3, top-center, show the manner of occurrence in the andesite. In the short time available it was not possible to do more than map the zone in which they occur and to collect speci-

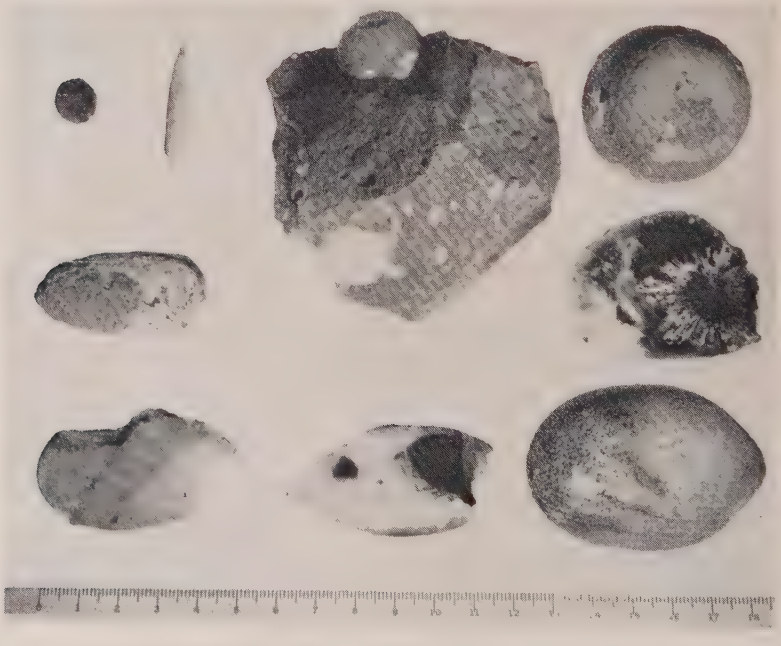

FIG. 3. Group of amygdules showing variations in size and shape. Note zeolite-like mineral in right center specimen. Scale is in centimeters.

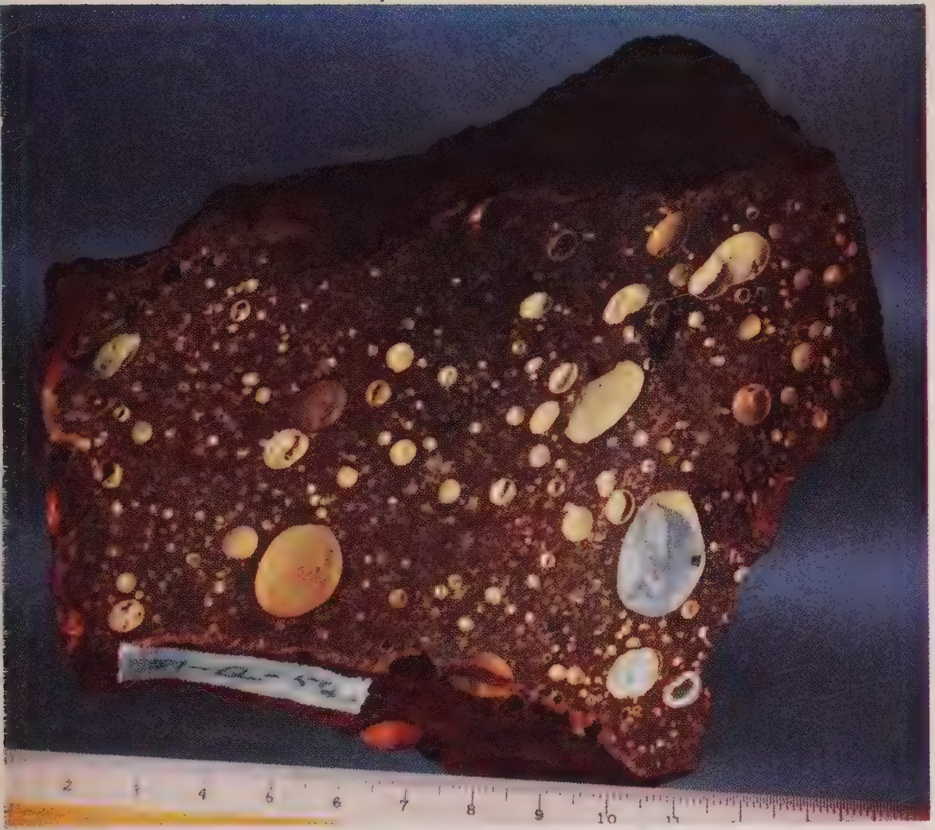

Plate I A. Color photo showing manner of occurrence of the amygdules in andesite. Scale is in centimeters.

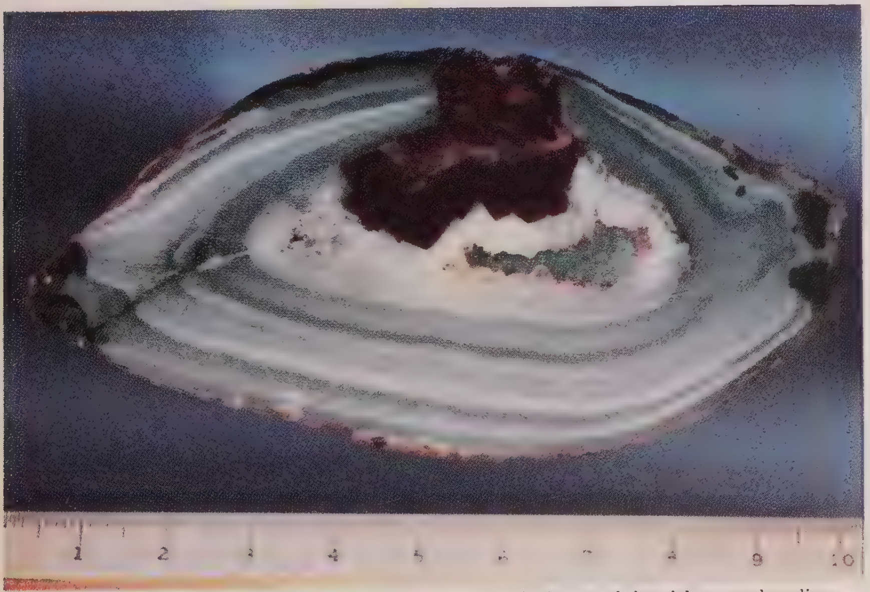

Plate I B. Color photo showing cross section of typical amygdule with agate banding around the periphery and quartz crystals in the interior.

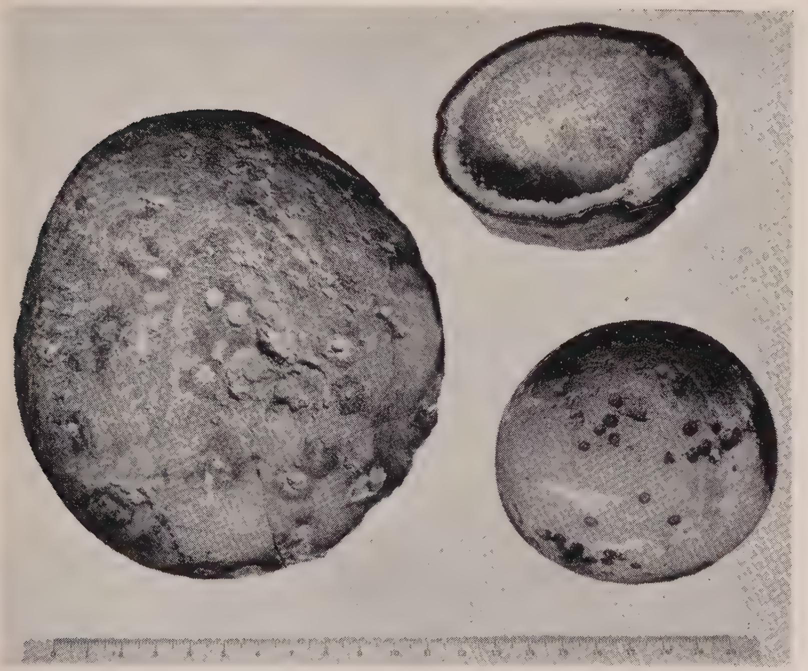

FIG. 4. Two larger amygdules showing near-spherical shape of those in this size range. Scale is in centimeters.

mens of the amygdules, the andesite that contains them, and the associated volcanic rocks.

Figure 2 shows the areas (solid black) in which the amygdules were found. These areas are zones in andesite; no amygdules were found in the associated rhyolites or trachytes. There are also areas in the andesite where the vesicles are not filled. The amygdules appear to be related to cross faults or highly jointed zones.

Size

The amygdules range in size from microscopic up to several inches in diameter. The largest one found thus far is almost 8 inches in diameter; sizes up to 3 inches are common.

Shape

The largest amygdules are all more or less spheroidal, probably because large gas cavities are unstable under differential motion of the containing lava. The smaller ones range from spherical to highly elongate and flattened, depending on the shapes of the vesicles at the time the lava ceased its motion. The most highly elongate one collected measures 35×6×4 mm. Figures 3 and 4 show something of the range in size and shape.

Structure

Typically the vesicles are filled more or less completely with silica. In general the larger ones are less completely filled than the smaller ones, although a few as much as 4 inches in diameter are completely filled, and some hollow ones only a few millimeters in diameter have been found. Commonly there is a banded rim around the outside, and the interiors are filled to varying degrees with quartz. The thickness of the banded rim may be only a few per cent of the diameter of the cavity, or may constitute almost the entire filling. Plate I B shows a typical amygdule of medium size with agate around the periphery and quartz crystals projecting into a central cavity.

Mineralogy

The mineralogy of most of the amygdules is very simple. The banded rim is "agate," chalcedony with or without intercalated layers of opal and/or quartz.

The quartz of the central cavities varies from paper-thin layers of very fine crystals to massive fillings with the largest crystals up to half an inch long and an eighth of an inch in diameter. The quartz crystals are roughly proportional in size to the size of the cavity or amygdule that contains them. They tend to grow with their *c*-axes normal to the cavity walls.

Many of the amygdules contain rounded black masses embedded in the siliceous filling. (See Pl. I B and Fig. 3.) They are, for the most part, so thoroughly impregnated (partly replaced) by silica that optical and *x*-ray methods fail to differentiate their substance from the matrix. In cavities where the material is still partly friable it consists of a mixture of manganese and iron oxides.

In some of the amygdules there are radiating masses that very much resemble zeolites in structure and cross section of individual blades (Fig. 3, right-center). They are so thoroughly impregnated and replaced with silica, however, that no mineral other than silica can now be identified.

Near the northwest tip of the more northwesterly of the two areas of amygdules in the southern patch of volcanics, there is a zone in which the mineralogy of the amygdules is quite different. In this zone most of the amydules are filled with coarse-grained calcite; a few cavities are entirely filled by a single anhedron.

Montmorillonitic and saponitic clay is associated with the calcite, as cavity linings outside of the calcite, as rounded masses enclosed by carbonate, and as irregular intergrowths with the calcite. The montmorillonite is flesh colored to pink, and the saponite is yellowish green.

There are also silica-filled amygdules in and near this zone. Many of them are coated and/or intergrown with saponite, and a few were found in which calcite crystals rest on the quartz lining.

Origin

All of the areas of amygdules appear to be associated with cross faults or zones of shearing where the rock is highly jointed. This is particularly true of the area where the fillings are largely of calcite. Here the structure of the andesite strikes approximately eastward and dips some 25° N. The calcite-clay amygdules are related to a prominent zone of closely spaced cross joints that strikes N. 25° E. and is almost vertical. In addition to the amygdules there are abundant joint fillings and coatings and irregular masses of calcite at intersections of joints.

The vesicles were probably filled under near-surface conditions by means of low temperature hydrothermal solutions. The association of saponite, montmorillonite, calcite, opal, chalcedony, zeolites(?), and low-temperature quartz suggests temperatures not much in excess of 100° C. There is a possibility that much of the deposition was accomplished below 100° C. Several samples of the largest quartz crystals were studied carefully for liquid inclusions, but none could be identified with certainty. Some of the crystals contain planes of very small inclusions with about the right index of refraction for aqueous solutions, but no vapor bubbles could be identified even with a high-power objective. If these inclusions are liquid this observation is consistent with a low temperature of formation.

It is probable that these rocks have never been buried to depths of more than several hundred to a few thousand feet. Skees (1953) gives a column of volcanic rocks of Tertiary age in the Chinati Mountains (80 miles to the southeast of this area) totaling about 2400 feet in thickness. In that area, where the rocks are much less disturbed, and the sequence can be determined readily, the youngest rock is a basalt flow some 300 feet thick. There is evidence that a similar basalt flow capped the series in the southern Quitman Mountains; there is a great deal of basalt float, but none was found in place. It has either been completely removed or the remnants are buried under the alluvium to the east.

It is very unlikely that the solutions that deposited the fillings of the vesicles were derived from any of the volcanic rocks, because great quantities of silica have been transported and deposited and large volumes of andesite altered. There was probably an intrusion of silica-rich magma whose crystallization produced the effective solutions. The pluton of the northern Quitman Mountains (Huffington, 1943) has given rise to numerous quartz veins, and solutions from it have produced large amounts of silicate minerals in the contact zone.

Three components comprise practically all of the material deposited in the vesicles: 1) silica, 2) calcium carbonate, and 3) manganese and iron oxides. The silica was probably derived from a crystallizing subjacent pluton. The solutions almost certainly had to traverse limestone areas on the way up and could have picked up the calcium carbonate from them. The ferromagnesian minerals of the andesite in the amygdaloidal zones have been almost completely altered, probably by the solutions that filled the vesicles. This would provide a logical and sufficient source for the iron and manganese oxides.

Acknowledgments

Thanks are due to J. B. Carson of Sierra Blanca for aid in the mapping and collecting. Charles Milton and J. M. Axelrod, of the U. S. Geological Survey, identified the fine-grained clay minerals and oxides; J. A. Denson, of the Geological Survey, took the pictures of specimens; and Harry B. Groom, also of the Geological Survey, drafted the maps for publication. David B. Stewart, of the Geological Survey, prepared the base map for Figure 2 from aerial photographs.

References

Baker, C. L. (1927), Exploratory geology of a part of southwestern trans-Pecos Texas: *Texas Univ., Bull.* **2745,** 1–68.

———, (1934), Major structural features of trans-Pecos Texas, *in* The geology of Texas, Vol. 2, Structural and economic geology: *Texas Univ., Bull.* **3401,** 137–214.

Huffington, R. M. (1943), Geology of the northern Quitman Mountains, trans-Pecos Texas: *Geol. Soc. Amer., Bull.*, **54,** 987–1048.

Skees, Wm. (1953), Tertiary volcanics of southeastern Presidio County, Texas: W. Tex. Geol. Soc. Spring Field Trip to the Chinati Mountains, Presidio, County, West Texas, May 28–30, 1953, Guidebook, 55–59.

Taff, J. A. (1890), The Cretaceous deposits, *in* Report on the geology and mineral resources of trans-Pecos Texas: *Texas Geol. Survey*, **2nd Ann. Rept.,** 714–738.

Von Streeruwitz, W. H. (1890), Report on the geology and mineral resources of trans-Pecos Texas: *Texas Geol. Survey*, **2nd Ann. Rept.,** 669–713.

AMYGDULAR CAMPTONITE DIKES FROM MOUNT JO, MOUNT MARCY QUADRANGLE, ESSEX COUNTY, NEW YORK*

HOWARD W. JAFFE, *U. S. Geological Survey, Washington 25, D. C.*

ABSTRACT

Three small, amygdular camptonite dikes intrude the Marcy anorthosite in Mount Jo, Mount Marcy quadrangle, Essex County, N. Y. They show a northeasterly strike, 80° to 90° dip, and are 13 to 20 inches thick. They are similar to the post-Ordovician camptonite dikes from the Lake Champlain valley. Three modal analyses, one chemical analysis, one spectrographic analysis, and optical properties of the individual minerals are presented. The dikes are porphyritic, with phenocrysts of olivine, zoned augite-pigeonite, brown hornblende, and magnetite in a holocrystalline groundmass composed essentially of plagioclase, An_{22-35}. Modal analyses show 75 per cent of mafic minerals, 23 per cent of plagioclase, and 2 per cent of amygdular calcite. The norm shows 45 per cent of salic minerals composed of albite, anorthite, orthoclase, and nepheline. The poor agreement between mode and norm is due to the presence of major amounts of the abnormative minerals, augite and hornblende. The dikes may be classified as camptonite (family 3216H, Johannsen), sub-basalt (DVMγ-75, Shand), or CIPW III.5.3.4 (Washington). Formation of the camptonites is attributed to the injection of crystals of olivine, augite, and alkalic liquid as small dikes into cold anorthosite under conditions of low pressure and moderate to high temperature.

INTRODUCTION

Camptonite dikes from the northeastern Adirondack region have been described by Kemp and Marsters (1889 and 1893), Kemp (1921), Hudson and Cushing (1931), and Buddington (1939 and 1941). Detailed modes of these rocks are lacking, and the only two chemical analyses in the literature are those of Kemp and Marsters (1889 and 1893) and Leeds (1878) cited by Kemp (1921). Five camptonite dikes reported by Kemp (1921) from the Mount Marcy Quadrangle, Essex County, N. Y. (Fig. 1) were only briefly described. In the summer of 1949 the author found three additional camptonite dikes in the quadrangle. These were investigated in detail and this report gives data on their geological occurrence, mineralogy, and chemistry.

OCCURRENCE

Three camptonite dikes, DMJ-1, 2, and 3, intrusive into the Marcy anorthosite, are exposed near the summit of Mount Jo near Heart Lake in the northwestern part of the Mount Marcy quadrangle, Essex County, N. Y. (Fig. 1). The summit of Mount Jo can be reached in less than half an hour by means of a good trail leading from the Adirondack Loj at Heart Lake. The lake is 9 miles by road from the village of Lake Placid,

---

* Publication authorized by the Director, U. S. Geological Survey.

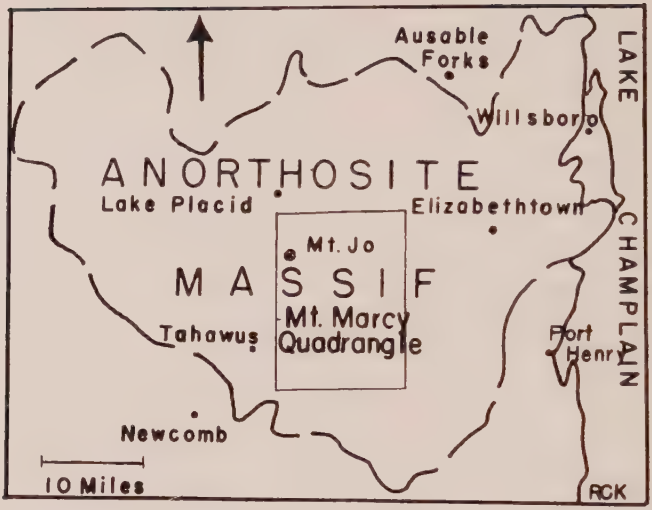

FIG. 1. Index map of the Adirondack region, New York.
(Anorthosite massif after Balk, 1931.)

N. Y. The strike, dip, and thickness of the three dikes are compared in Table 1 with the camptonite dikes reported by Kemp (1921) from the Mount Marcy quadrangle.

Dikes DMJ-1 and 2 (Table 1) have been considerably eroded away from the anorthosite, forming two steep-sided erosional slots. All of the dikes in the Mount Marcy quadrangle are less resistant than the essentially monomineralic anorthosite host rock, and many of the numerous small waterfalls in the quadrangle are located on eroded post-anorthosite dikes. Dikes DMJ-1 and 2 show parallel strike and dip, N. 31° E., 80° S.E., and discordantly cut the Marcy anorthosite. A marked foliation in the anorthosite, enhanced by large plagioclase crystals, strikes N. 78° W.

TABLE 1. CAMPTONITE DIKES, MOUNT MARCY QUADRANGLE, ESSEX COUNTY, NEW YORK

Location	Strike	Dip	Thickness
1. DMJ-1, Mount Jo	N. 31° E.	80° S.E.	13 inches
2. DMJ-2, Mount Jo	N. 31° E.	80° S.E.	20 inches
3. DMJ-3, Mount Jo	N. 52° E.	90°	15 inches
4. E. br. Ausable R.	N. 75° W.	90°	5 to 6 feet
5. E. br. Ausable R.	East	90°	5 feet
6. John's Brook	N. 27° E.	—	1 to 3 feet
7. John's Brook	N. 67° E.	—	1 to 3 feet
8. John's Brook	N. 62° E.	—	1 to 3 feet

Dike DMJ-3 outcrops in the trail about a quarter of a mile below the summit of Mount Jo. It shows a more easterly strike, N. 52° E., and has a vertical dip.

TEXTURE

In the field the dark, dense camptonite dikes may be readily mistaken for the abundant diabase dikes of the quadrangle, which also have a northeasterly strike. With the aid of a hand lens, observation of the small, round, white amygdules characteristic of the camptonites serves to distinguish them from the diabase. Weathered portions of the camptonite show pitting due to the removal of calcite from the amygdules. In thin section the camptonite and diabase show different textures. The diabase shows an ophitic texture with rudely oriented laths of andesine-laboradorite, and interstitial augite, the latter extensively altered to serpentine and calcite. The camptonite is porphyritic and amygdular, showing abundant phenocrysts of olivine and clinopyroxene, and round amygdules in a groundmass of sodic plagioclase containing laths and microlites of brown hornblende, biotite, and pyroxene (Fig. 2). Only the mafic minerals olivine and augite, and to a lesser extent hornblende and magnetite, form phenocrysts. The camptonite is much fresher than the diabase.

Hudson and Cushing (1931) describe a camptonite dike from the Lake Champlain area as follows: "Abundant large phenocrysts of augite, which is nearly colorless in thin section, but with lilac-colored borders

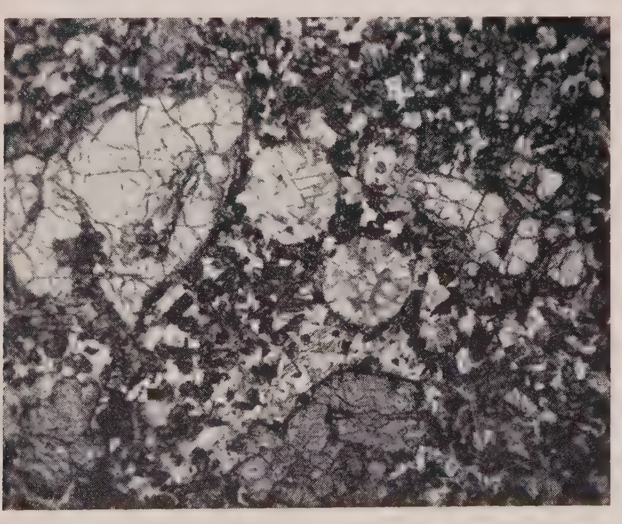

FIG. 2. Camptonite dike, DMJ-3, showing phenocrysts of olivine (white), clinopyroxene (gray, near bottom of photograph), and two calcite-filled amygdules (center of photograph) in a groundmass of plagioclase, hornblende, clinopyroxene, and magnetite. (Plane polarized light ×25.)

and crammed full of inclusions, in part arranged zonally. A few small, rotted olivines. Groundmass of feldspar laths, small augites and magnetite and some apparently devitrified glass base. Some calcite-filled amygdules." Buddington (1941) has also noted similar amygdular camptonite dikes in the Willsboro quadrangle, N. Y., near Lake Champlain. Both Hudson and Cushing (1931) and Buddington (1941) consider these camptonites to be post-Ordovician rocks. In all probability the Mount Jo camptonite dikes are of the same age. It is interesting to note that the late Pleistocene camptonite dikes near Boulder Dam, Arizona, described by Campbell and Schenk (1950), also contain amygdules.

MINERALOGY

Modes of the three camptonite dikes, DMJ-1, 2, and 3, are given in Table 2. The modal analyses were made of thin sections, using the point counter mechanical stage described by Chayes (1949). The three dikes are similar in mineralogy. Although the pyroxene and hornblende percentages are variable, in each dike their sum is almost 50 per cent. Amygdules (0.1 to 0.5 mm. in diameter) form 1 to 3 per cent of the rock and are always completely filled with calcite and sodic plagioclase. Dike DMJ-3 contains 2.7 per cent of amygdules represented in Table 2 by 1.8 per cent of modal calcite and 0.9 per cent of modal plagioclase.

TABLE 2. MODES* OF THREE CAMPTONITE DIKES FROM MOUNT JO, ESSEX COUNTY, N. Y.

	DMJ-1	DMJ-2	DMJ-3
Olivine†	12.5	14.2	10.8
Augite+pigeonite	32.3	16.0	28.0
Brown hornblende	16.8	32.5	23.2
Biotite	2.0	3.1	2.0
Magnetite	10.2	14.2	8.4
Plagioclase (An_{22-35})	24.0	18.0	25.8
Calcite	2.2	2.0	1.8
Apatite	Trace	Trace	Trace
	100.0	100.0	100.0

* All percentages by volume.

† Includes some secondary serpentine and talc.

Data on the optical properties and the habits of the individual minerals are given in the following paragraphs. The minerals are discussed in their probable order of crystallization.

Olivine forms the largest phenocrysts, showing average grain diameters of 1.×0.5 mm. and maximum grain diameters of 2.×1. mm. Many of the phenocrysts are euhedral and remarkably fresh. They commonly show fresh cores with marginal corrosion and alteration to a mixture of fine-grained serpentine, talc, and magnetite. The mineral is colorless with $\alpha = 1.660$, $\beta = 1.679$, $\gamma = 1.700$, $2V = 88°(+)$, indicating a composition near forsterite—85 per cent: fayalite—15 per cent (Larsen and Berman, 1934).

Clinopyroxene forms euhedral, equant cross sections (0.25–0.5 mm.), stout prisms (0.1×0.5 mm.), and smaller narrow laths. Phenocrysts occur isolated or in clusters sometimes mantling olivine. Virtually all of the pyroxenes show marginal opaque corrosion or rims of brown hornblende. All of the pyroxenes are intricately zoned, many showing well-developed hourglass structure (Fig. 3). Concentric zoning, observed on euhedral cross sections, shows cores of augite, succeeded by a narrow zone of pigeonite, a second zone of augite, and finally, pigeonite rims. Axial angles measured by Norman Herz with a Universal stage showed cores with a $2V = 53°$ and rims with a $2V = 28°$. Pigeonite rims show marked anomalous blue interference colors, and the optic axis emerging in {001}

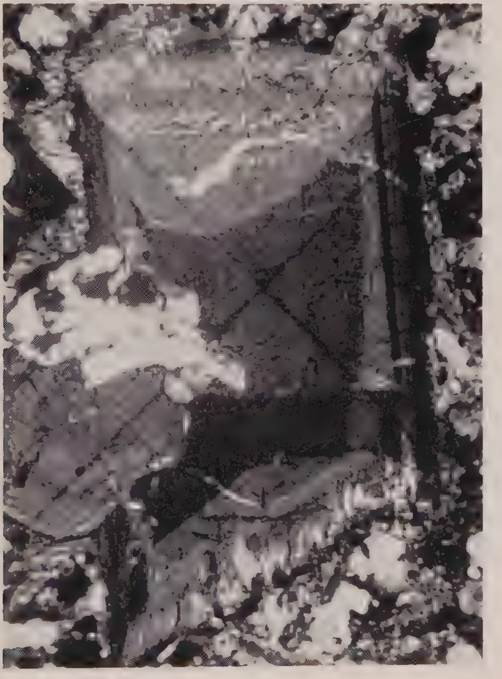

FIG. 3. Hourglass structure in clinopyroxene. (Crossed nicols ×150.)

shows strong dispersion with r > v. Augite cores show weak to moderate dispersion, r > v, of the corresponding optic axis. Dispersion of the optic axis emerging in {100} is reversed for both minerals with v > r, weak. Extinction angles were difficult to measure accurately because of the zoning. Longitudinal grains show maximum extinction angles, $Z \wedge c = 51°$ for pigeonite rims and 44° for augite cores. Because of the intricate zoning and frayed crystal margins, all of the indices of refraction could not be measured. Index of refraction measurements for pigeonite gave $\beta = 1.732$ and $\gamma = 1.752$, indicating an abnormally high iron content. Variable measurements were obtained on the augite, which may indicate a continuous compositional change within this pyroxene. Poldervaart and Hess (1951) suggest a continuous reaction series from magnesian augite to ferroaugite in basaltic rocks and a discontinuous reaction series from magnesian olivine through orthopyroxene to pigeonite. As both minerals become enriched in iron they may react with the liquid to form hornblende.

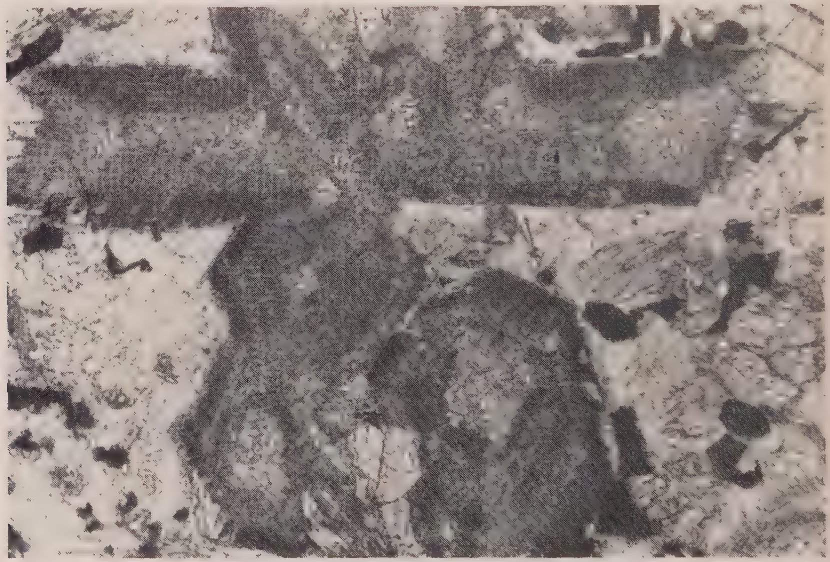

Fig. 4. Ghost pyroxenes showing relict hourglass structure (elongate grain) and relict augite pigeonite zoning (equant cross-sections). The pyroxenes are completely replaced by serpentine and talc (light zones were augite) and magnetite, hornblende, and biotite (dark zones were pigeonite). (Plane polarized light ×175.)

In thin section the pyroxene is feebly pleochroic from pale grayish green to pale brown, with many of the grains showing a purplish tinge presumably due to titanium (Hess, 1949). Where hourglass structure is present the hourglass centers show a lighter color and a lower index of refraction than the sides of the grain. Alteration of these grains produces ghost pyroxenes (Fig. 4) with light-colored centers of serpentine and talc bounded on both sides by fine-grained magnetite, which is in turn bounded by a narrow rim of hornblende or biotite. In altered cross sections of the zoned pyroxenes, the zonal structure may persist (Fig. 4), augite being replaced by serpentine and pigeonite replaced by fine opaque material, presumably magnetite. Some of the basal sections show simple contact twins with a {100} composition plane. Cruciform twinning, relatively uncommon in clinopyroxene, is illustrated in Figure 5.

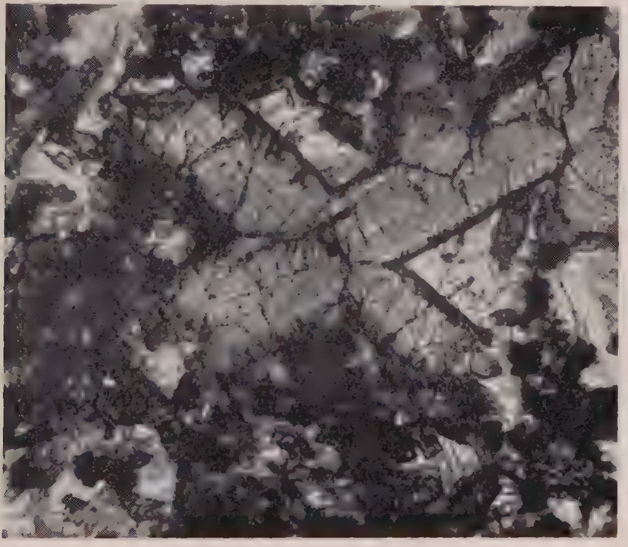

FIG. 5. Cruciform twinning in clinopyroxene. (Plane polarized light ×125.)

Magnetite occurs in small euhedral and skeletal grains less than 0.1 mm. in diameter. Some very fine grained magnetite is exsolved from the alteration of pyroxene and olivine.

Brown hornblende occurs in laths with maximum grain dimensions of 0.02×0.15 mm. and may occasionally show basal sections. It commonly forms narrow rims around pyroxene phenocrysts, presumably the result of reaction of lime-poor pigeonite rims with the liquid. The mineral is strongly pleochroic with $\alpha=1.678$ (yellow), $\beta=1.700$ (red-brown), $\gamma=1.708$ (dark red-brown), $2V=62°$ $(-)$, dispersion $v>r$ moderate, and $Z\wedge c=9°$. The optical properties are similar to those reported for brown hornblende, "kaersutite," from the camptonite near Bounder Dam (Campbell and Schenk, 1950). The latter has $\alpha=1.670$, $\beta=1.692$,

$\gamma = 1.701$, $Z \wedge c = 8°–10°$, and $2V = 81°$. If these indices of refraction are correct, the value for 2V is in error and should be 64° (−) rather than 81° (−).

The groundmass is birefracting and is composed essentially of plagioclase An_{30-35}. The feldspar occurs in simple laths and felted aggregates showing poorly developed albite twinning. Plagioclase An_{22} occurs in small laths as projections into amygdules (Fig. 6) and as radial groups in amygdules. An *x*-ray powder diffraction pattern of feldspar concentrated from the rock showed the spacing 3.01, which is diagnostic of high-temperature albite (Tuttle and Bowen, 1950). The concentrate was submitted to Tuttle for further examination. Tuttle (personal communication, 1950) could not decide whether high- or low-temperature plagioclase was present because it is difficult to distinguish between them in the range An_{30-35}. The spacing 3.01 may be due to an impurity. He confirmed the presence of two feldspars, one with $\beta = 1.550$, $2V = 70°$ (−), An_{30-35}, high- or low-temperature, and another with $\beta = 1.540$, An_{22}, low-temperature. Although the feldspars are unaltered, the presence of very fine laths of augite, hornblende, and biotite in the groundmass made it impossible to obtain a feldspar concentrate of high purity.

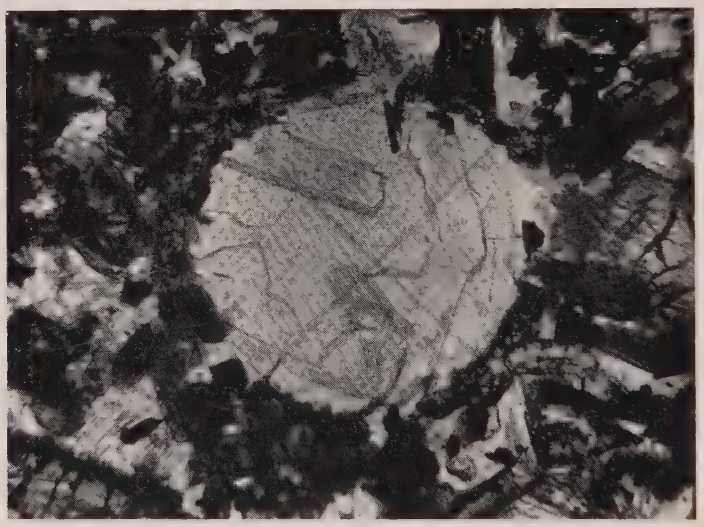

Fig. 6. Plagioclase laths and calcite in an amygdule. (Plane polarized light ×150.)

Calcite, $\omega = 1.658$, occurs as well-developed grains completely filling amygdules or filling feldspar interstices in the amygdules (Fig. 6).

Serpentine, talc, and fine-grained magnetite are alteration products of olivine and pyroxene.

ANALYSIS AND CLASSIFICATION

A chemical analysis of one of the camptonite dikes (DMJ-3) is given in Table 3. The CIPW norm, modal analysis, and spectrographic analysis are also compared in the same table. Table 4 compares analyses of camptonites and olivine diabases. The poor agreement between mode and norm is due to the presence of large amounts of the abnormative minerals augite and hornblende and some biotite. Orthoclase and nepheline were looked for in numerous immersions but could not be identified. In all probability, the brown hornblende contains an appreciable amount of the alkalies indicated by the normative orthoclase and nepheline. Biotite makes up only 1.9 per cent of the rock and could account for a maximum of 0.2 per cent K_2O. Brown hornblende ("kaersutite") from the camptonite near Boulder Dam (Campbell and Schenk, 1950), with similar optical properties contains 1.72 per cent K_2O and 2.29 per cent Na_2O. Horn-

TABLE 3. CHEMICAL, SPECTROGRAPHIC, NORMATIVE, AND MODAL ANALYSES OF CAMPTONITE DIKE, DMJ-3, MOUNT JO, MOUNT MARCY QUADRANGLE, ESSEX COUNTY, N. Y.

Chemical analysis*		Spectrographic analysis†	Norm		Mode		
						Volume	Weight
SiO_2	42.58	>10.0	Orthoclase	7.78	Plagioclase (An_{22-35})	25.8	20.8
TiO_2	3.38	0.3–3.0	Nepheline	1.99	Olivine	10.8	11.1
ZrO_2		0.01–0.1	Albite	21.48	Augite Pigeonite	28.0	29.4
Al_2O_3	12.00	>10.0	Anorthite	13.62	Hornblende	23.2	22.7
Fe_2O_3	5.09	>10.0	Olivine	18.28	Biotite	2.0	1.9
FeO	8.82		Diopside	15.87	Magnetite	8.4	12.6
Cr_2O_3		0.01–0.1	Magnetite	7.42	Apatite	Trace	Trace
Ga_2O_3		<0.01	Ilmenite	6.38	Calcite	1.8	1.5
Sc_2O_3		<0.01	Apatite	1.34		——	——
V_2O_5		0.02–0.2	Calcite	2.84		100.0	100.0
MnO	0.40	0.02–0.2	Water	2.02			
MgO	10.44	>10.0		——			
CaO	9.21	>10.0		99.02			
BaO		0.1–1.0					
NiO		0.005–0.05					
CuO		<0.01					
PbO		0.002–0.02					
Na_2O	2.98	0.5–5.0					
K_2O	1.34	0.5–5.0					
Li_2O		0.008–0.08					
H_2O-	0.23				CIPW—III.5.3.4		
H_2O+	1.79						
CO_2	1.25						
P_2O_5	0.62						
	——						
	100.13						

* Ruth Holzinger, analyst.
† M J. Peterson, analyst.

TABLE 4. ANALYSES OF CAMPTONITES AND OLIVINE DIABASE

	A	B	C	D	E	F	G
SiO_2	42.58	42.26	43.41	41.00	41.94	40.70	48.54
TiO_2	3.38	3.18	0.35		4.15	3.86	1.31
Al_2O_3	12.00	14.61	19.42	21.36	15.36	16.02	15.24
Fe_2O_3	5.09	5.38	5.72	13.44	3.27	5.43	3.06
FeO	8.82	4.56	6.69		9.89	7.84	8.88
MnO	0.40	0.05			0.25	0.16	0.21
MgO	10.44	6.12	5.98	3.85	5.01	5.43	8.08
CaO	9.21	9.40	9.11	10.40	9.47	9.36	9.38
BaO		0.16					
Na_2O	2.98	2.64	4.39	2.86	5.15	3.23	2.69
K_2O	1.34	1.48	0.47	1.31	0.19	1.76	0.98
H_2O-	0.23	2.72					
H_2O+	1.79	3.93	3.00	5.00	3.29	2.62	1.35
CO_2	1.25	2.99	2.00		2.47	2.97	
P_2O_5	0.62	0.62				0.62	0.28
S		0.09					
	100.13	100.19	100.54	99.22	100.44	100.00	100.00

A. Camptonite, DMJ-3, Mount Jo, Mount Marcy quadrangle, Essex County, N. Y., Ruth Holzinger, analyst.

B. Camptonite, 8 miles south of Boulder Dam, Ariz., F. A. Gonyer, analyst (Campbell and Schenk, 1950).

C. Camptonite, Mount Marcy quadrangle, Essex County, N. Y., A. B. Leeds' analysis, 1876, cited by Kemp (1921).

D. Camptonite, Whitehall, Washington County, N. Y., Kemp and Marsters (1889 and 1893).

E. Camptonite, Campton, N. H., original camptonite, G. W. Hawes, analyst (1879)

F. Daly's average of 15 camptonites (1933).

G. Daly's average of 12 olivine diabases (1933).

blende would also account for the excess of normative anorthite and probably some of the normative ilmenite. The brown hornblende from the camptonite near Boulder Dam contains 5.70 per cent TiO_2. The purplish tinge on some of the pyroxene phenocrysts suggests that this mineral is also enriched in titanium (Hess, 1949).

Finally, the most serious shortcoming of the norm is that it shows 45 per cent of salic minerals, whereas the mode shows only 20 per cent. Thus, a camptonite cannot be distinguished from many diabases and gabbros by the CIPW classification. The CIPW classification of the Mount Jo camptonite is camptonose: class III, order 5, rang 3, subrang 4, the same as that obtained from the analyses of many diabases. Using Johannsen's system (1937), the rock would be classified as camptonite, family No. 3216H. Using Shand's classification (1943), the rock would be categorized as sub-basalt, DVMγ (75). This category includes rocks that have been classed as camptonites, a name firmly entrenched in the literature.

Regardless of which name is used, the Mount Jo dikes, classified as DVMγ (75) after Shand, would meet the following requirements:

D—The rock has crystallized rapidly under conditions of low pressure and moderate to high temperature. This is confirmed by the presence of zoned pyroxene and the fine-grained groundmass.

V—The alkalies are saturated with respect to silica and no feldspathoids are present. Conversely, the dark minerals are unsaturated, as indicated by the presence of essential amounts of magnesian olivine.

M—The molecular proportion of Al_2O_3 exceeds that of Na_2O and K_2O combined but is less than that of Na_2O, K_2O, and CaO combined. Some alumina may enter the dark silicates and usually there are non-aluminous dark silicates present with aluminous dark silicates. In this case olivine occurs with zoned augite mantled with brown hornblende.

γ—The character of the feldspar must be $An > Or$ and $Ab > An$.

(75)—The rock contains 75 per cent of dark minerals.

This provides a much more accurate description of the rock than the CIPW normative classification, which indicates only 50 per cent of dark minerals and an exceedingly poor agreement between norm and mode.

PETROGENESIS

The three camptonite dikes in Mount Jo are in every way typical of rocks generally classed as lamprophyres, a term that has had a diversity of usage. The Mount Jo dikes are lamprophyres in the sense of Bowen (1928): "characteristically porphyritic rocks, the porphyritic elements highly femic (olivine, hornblende, mica) and the groundmass notably alkalic." The Mount Jo dikes also conform to Grout's usage (1932): "rocks that are dark, basic, mostly of sugary texture and mostly occurring in dikes"; Johannsen (1937) notes further that characteristically only the dark minerals form phenocrysts, feldspar being almost wholly limited to the groundmass. Bowen (1928) states that there is no evidence for the existence of a liquid of the total composition of the olivine-bearing lamprophyres. He suggests that these rocks may be formed by the injection of crystals of olivine and augite in an alkalic liquid. This femic-alkalic association of crystals and liquid may result from fractional resorption of complex minerals, notably hornblende and biotite. Injection of the olivine, augite, and alkalic liquid as small dikes into cold anorthosite would produce rapid cooling and the formation of the Mount Jo camptonites. The rock contains 75 per cent of femic minerals and only

25 per cent of sodic plagioclase (An_{22-35}). Magnesian olivine is mantled by zoned augite, with iron-rich pigeonite rims, which is in turn mantled by brown hornblende. The brown hornblende, presumably rich in alkalies, continued to crystallize as fine needles with plagioclase (An_{30-35}) until crystallization was nearly completed. Near-surface conditions of injection permitted separation of a vapor phase, giving rise to the formation of amygdules containing projections of plagioclase (An_{22}) and cores of calcite. Alteration of olivine and pyroxene to serpentine, talc, and magnetite accompanied the formation of the amygdules. Each amygdule shows a narrow halo of intensely altered ghost pyroxenes. The preservation of the perfectly round, calcite-filled amygdules in dikes only 1 to 2 feet thick in massive anorthosite is indicative of the absence of significant deformation since the emplacement of the dikes. Hudson and Cushing (1931) describe deformed amygdules from the camptonites of the Lake Champlain valley. They state that these dikes were emplaced below 4000 feet of beds of Chazy age and that the amygdules therefore cannot be explained on the basis of near-surface intrusion. They ascribe the amygdules to a sudden widening of tension fissures filled with partly crystallized magma. Relief of pressure and gas expansion permitted formation and localization of amygdules at viscous dike centers. Amygdules in the Mount Jo dikes are not localized and need have had no such origin but probably formed because of near-surface intrusion. Mount Jo is situated in the core of the Adirondack anorthosite massif, which is believed never to have been covered with sediments since its intrusion into the Grenville series.

ACKNOWLEDGMENTS

The author is indebted to O. F. Tuttle of the Geophysical Laboratory for making optical and *x*-ray studies of two plagioclase feldspars separated from one of the camptonite dikes.

REFERENCES

BALK, R. (1931), Structural geology of the Adirondack anorthosite: *Min. u. Petrog. Mitt.*, **XLI,** 308–434.

BOWEN, N. L. (1928), The evolution of the igneous rocks, Princeton Univ. Press, Princeton, N. J.

BUDDINGTON, A. F. (1939), Adirondack igneous rocks and their metamorphism: *Geol. Soc. Amer., Mem.* **7,** 191–194.

——— (1941), Geology of the Willsboro quadrangle: *N. Y. State Mus. Bull.* **325,** 80–86.

CAMPBELL, I. AND SCHENK, E. T. (1950), Camptonite dikes near Boulder Dam, Arizona: *Am. Mineral.*, **35,** 671–692.

CHAYES, F. (1949), A simple point counter for thin-section analysis: *Am. Mineral.*, **34,** 1–11.

DALY, R. A. (1933), Igneous rocks and the depths of the earth, New York, McGraw-Hill Book Co., Inc., p. 28.

GROUT, F. F. (1932), Petrography and petrology, New York, McGraw-Hill Book Co., Inc., pp. 121–125.

HAWES, G. W. (1879), On a group of dissimilar eruptive rocks in Campton, N. H.: *Am. Jour. Sci.*, (3), **17**,150.

HESS, H. H. (1949), The optical properties and chemical composition of common clinopyroxenes: *Am. Mineral.*, **34**, 621–666.

HUDSON, G. H., AND CUSHING, H. P. (1931), The dike invasions of the Champlain Valley, N. Y.: *N. Y. State Mus. Bull.* **286**, 81–112.

JOHANNSEN, A. (1937), A descriptive petrography of the igneous rocks, Univ. Chicago Press, Chicago, Ill., Vol. IV.

KEMP, J. F. (1921), Geology of the Mt. Marcy quadrangle, N. Y.: *N. Y. State Mus. Bull.* **229–230**, 51–59.

——— AND MARSTERS, V. F. (1889), Camptonite dikes near Whitehall, Washington County, N. Y.: *Am. Geol.*, **4**, 97–102.

——— (1893), The trap dikes of the Lake Champlain region: *U. S. Geol. Survey Bull.* **107**, 11–62.

LARSEN, E. S. AND BERMAN, H. (1934), The microscopic determination of the nonopaque minerals: *U. S. Geol. Survey Bull.* **848**, 239.

LEEDS, A. B. (1878), Notes on the lithology of the Adirondacks: *N. Y. State Mus., 30th Ann. Rpt.*, 102.

POLDERVAART, A. AND HESS, H. H. (1951), Pyroxenes in the crystallization of basaltic magma: *Jour. Geol.*, **59**, 472–489.

SHAND, S. J. (1943), Eruptive rocks, 2d ed., London, Murby & Co.

TUTTLE, O. F. AND BOWEN, N. L. (1950), High temperature albite and contiguous feldspars: *Jour. Geol.*, **58**, 572–583.

WASHINGTON, H. S. (1917), Chemical analyses of igneous rocks: *U. S. Geol. Survey Prof. Paper* **99**, 1210 p.

THE GENESIS OF PEGMATITES

II. QUANTITATIVE ANALYSIS OF LITHIUM-BEARING PEGMATITE, MORA COUNTY, NEW MEXICO

RICHARD H. JAHNS, *California Institute of Technology, Pasadena, California.*

CONTENTS

Abstract 1078
Introduction 1079
The pegmatite area 1081
Description of the Pidlite pegmatite 1083
  General features 1083
  Structure 1083
  Zones 1086
  Composite units 1087
  Mineralogy 1089
Quantitative analysis of the Pidlite pegmatite 1094
  General methods 1094
  Modal analyses 1096
  Chemical composition 1099
Analysis of the replacement features 1101
  The general problem 1101
  Quantitative relations 1104
  Discussion and conclusions 1108
References 1110

ABSTRACT

The Pidlite dike, one of several lithium-bearing pegmatite bodies in the Precambrian terrane of the Sangre de Cristo Range, lies in southwestern Mora County, New Mexico. Its major part, which is well exposed in surface and underground mine workings, has the form of a discoidal lens whose longest axis is essentially vertical. The dike consists of seven readily distinguishable types of pegmatite, four of which form typical zones that have a concentric arrangement. The other three rock types form units that are similar to the zones in shape and disposition, but are distinguished by their content of minerals that appear to have been developed by replacement of earlier pegmatite minerals.

The outer zones are granitoid aggregates of quartz, albite, perthite, and muscovite, and are relatively thin and continuous. The inner zones, which are lenticular to pod like, are much coarser grained and consist mainly of quartz and perthite. The other three units show greater textural irregularity, and are characterized by an abundance of highly sodic albite, lepidolite, and white to pink muscovite. Additional minerals in the dike include amblygonite, apatite, beryl, betafite, bismuth, bismutite, columbite-tantalite, cyrtolite, fluorite, gahnite, hatchettolite, loellingite, magnetite, microlite, monazite, pyrite, spessartite, spodumene, topaz, and tourmaline (varieties elbaite and schorl).

The mineralogic and chemical composition of the Pidlite pegmatite was determined quantitatively by means of dimensional measurements of the zones and other units, megametric analyses of their mineral content, and chemical and optical analyses of representative samples of the major minerals. The calculated bulk composition of the dike is remarkably similar to that of at least two other lepidolite-bearing pegmatites in the southwestern United States, and is not much different from that of Daly's average granite.

The amount of mineral replacement in the dike was estimated by means of detailed measurements of recognizable pseudomorphs and distribution of residual masses of earlier minerals. These data indicate that the dike, if formed mainly by crystallization from a pegmatite magma, must have been at least 75 per cent consolidated prior to the major stage of mineral replacement. The net amount of material transfer involved in the replacements need not have been very great, and can be accounted for quantitatively in terms of reactions between earlier-formed minerals and residual fluids derived from sources within the dike.

On the basis of their distribution, as well as their structural, textural, and compositional relations, the zones in the Pidlite dike are thought to have been developed by fractional crystallization of a pegmatite magma under essentially closed-system conditions. The younger minerals appear to have been developed in part through replacement of earlier-formed zonal material by residual fluid, and in larger part by direct crystallization from the fluid, beginning mainly at a time when this highly reactive residuum constituted 15 per cent to 25 per cent of the dike. Conditions may well have approached those of a closed system until consolidation of the pegmatite was virtually complete.

The possibility of late-stage replacement under open-system conditions, involving more dilute solutions derived from sources outside the dike, cannot be ruled out entirely. All the evidence at hand, however, suggests that the lepidolite and other late-stage minerals are products of replacement by, and direct crystallization from, residual fluid that was generated wholly within the dike.

INTRODUCTION

The widespread development of some pegmatite minerals by corrosion and replacement of other pegmatite minerals has been noted and described by hundreds of competent investigators, and plainly is a characteristic feature of pegmatites in general. However, the quantitative significance of such replacement varies considerably from one body of pegmatite to another, and in most of them the process appears to have played only a minor part in the formation of the minerals that can be observed. Other pegmatite bodies, and particularly those of highly complex mineralogy, show impressive evidence of mineral replacement on larger scales, and have provoked much discussion as to the nature and source of the fluids that were involved.

Most investigators recognize two major kinds of pegmatite bodies—those formed mainly by replacement of non-pegmatitic country rock, and those formed wholly or in part by crystallization from a mechanically injected fluid, or magma. Commonly included in the latter group are pegmatite bodies that are internally zoned, i.e., that comprise lithologically distinctive units that are more or less concentrically disposed within a given pegmatite body and reflect, at least to some degree, its general shape and structure. A magmatic stage in the formation of these and many other pegmatites ordinarily is adduced on the basis of structural relations between pegmatite and country rock, as well as structural, textural, and compositional relations within each pegmatite body. Most of the critical features have been summarized and discussed by Kemp

(1924), Johannsen (1932, pp. 74–84), Landes (1933, pp. 41–56), Cameron, *et al.* (1949, pp. 97–106), Flawn (1951, pp. 180–190), and many others.

Replacement phenomena within pegmatite bodies of magmatic origin, though readily identified in most occurrences, commonly are interpreted in different ways by different observers. In particular, opinions differ widely concerning the nature and amount of material that was replaced, the stage or stages during which replacement was active, and the effects of the replacement on the composition of the system as a whole. These factors are of prime importance in any attempt to establish the source of the replacing solutions, or to determine whether or not the replacement proceeded under open-system conditions. Unfortunately, however, they rarely have been assessed quantitatively or in detail. In discussing the origin of replacement material in pegmatites, for example, Cameron, *et al.* (1949, p. 106) remark that "it is worthwhile to remember that we have little data on what changes, if any, in the bulk composition of whole pegmatites have been effected during replacement. Most of the data and observations available apply only to limited portions of pegmatite bodies, and information regarding the more completely exposed pegmatites is mostly qualitative, not quantitative."

Anyone who attempts to determine the bulk chemical or mineralogical composition of entire pegmatite bodies soon recognizes the serious difficulties imposed by the characteristic variations in their texture and structure. Most bodies are so coarsely and irregularly crystallized that ordinary methods of sampling do not yield acceptable results, and few bodies are well enough exposed in three dimensions to permit meaningful determinations by any method of sampling. Discouraging as these factors may be, however, the great need for more complete and quantitative data on pegmatite composition remains as a stimulus to investigators, whether they are interested primarily in the commercial aspects of certain pegmatite minerals or solely in theoretical questions of pegmatite genesis.

This paper presents a brief description of mineralogically complex pegmatites from northern New Mexico, as well as the results of quantitative analysis of one small pegmatite body that is particularly well exposed. The field work on which the paper is based was done during 1946 and 1947, and both it and supplementary laboratory studies were supported by a research grant from the California Institute of Technology. The investigations were facilitated considerably by E. P. Chapman and John A. Wood of the Hayden Mining Company, who permitted access to mine workings and provided a useful map of the principal pegmatite dike. Valuable assistance in the mapping of the pegmatite bodies was given by Don M. George, Jr., Lauren A. Wright, and Arthur Montgomery. The writer also is indebted to Rudolf von Huene, who built the measuring device that was used for megametric analysis of the pegmatite in the field, to Mrs. Charlotte Bjornsson, who drafted two of the illustrations for this paper, and to Mrs. Florence Wiltse, who aided in preparation of the manuscript.

THE PEGMATITE AREA

Numerous masses of lithium-bearing pegmatite are exposed high on the east slope of the Sangre de Cristo Range near and along the south edge of western Mora County, New Mexico. Most of them lie at distances of 4 to 7 miles west and northwest of Lower Rociada, a village that in turn is 24 miles by road northwest of Las Vegas. The southern part of the pegmatite area can be reached by road and trail from Lower Rociada via Sparks Creek and Maestas Creek, and the northern part is served by a steep road that extends northwestward up Sparks Creek, and thence westward into the higher country south of the creek. This road ends at the Pidlite lithia mine, approximately 5½ miles from Lower Rociada.

The pegmatite area is elongate, and trends in a northerly direction for a distance of at least 2 miles across rough, heavily timbered country in which altitudes range from 8200 to about 9800 feet. It appears to be underlain chiefly by Precambrian metamorphic rocks that are concealed in many places by a thick mantle of soil and vegetation. These rocks include medium- to coarse-grained amphibolite and amphibole schist, biotite-bearing schist and gneiss, and coarse-grained quartz-muscovite gneiss, in all of which a very steeply dipping planar structure trends northeast to east. Beginning a short distance west of the pegmatite area, generally less than a mile, the Precambrian rocks are overlain by sandy to shaly limestone of Pennsylvanian age.

The pegmatite bodies occur as irregular dikes and discordant lenses that trend northerly and appear to have prevailingly steep dips. They range in breadth from a few inches to 22 feet, and few exceed 150 feet in maximum dimension. As exposed in low outcrops and several small prospect openings, they are mainly medium- to very coarse-grained aggregates of quartz, perthite, and albite, with subordinate muscovite and lepidolite. The principal accessory constituents are apatite, beryl, spessartite, tantalum-niobium minerals, and topaz. Spodumene and amblygonite are present in some of the pegmatite bodies. Tourmaline, though rare in the pegmatites, is abundant in the immediately adjacent country rock.

Most of the pegmatite bodies are distinctly zoned. Typically they comprise outer zones with granitoid texture, and irregular, pod-like inner

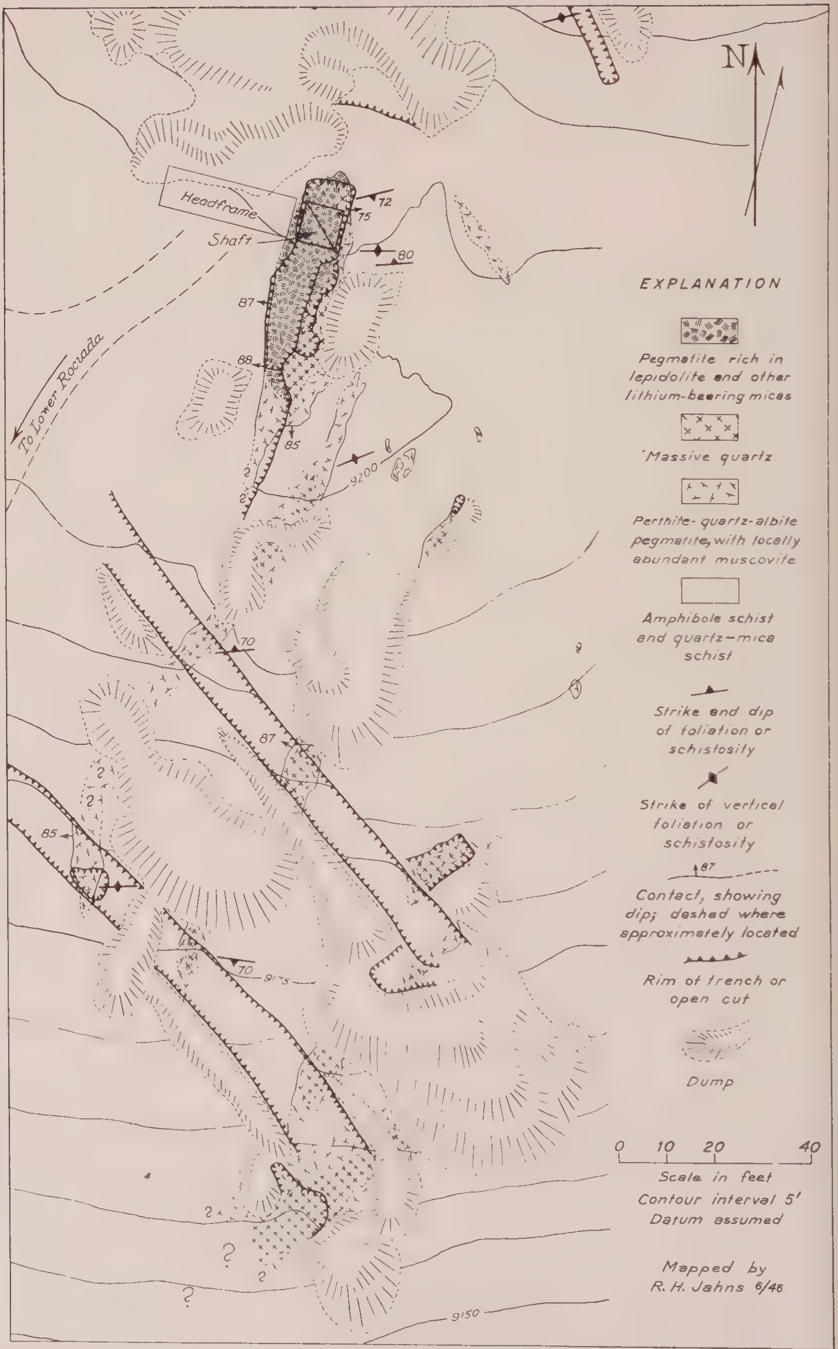
N
Headframe
Shaft
72
75
80
87
88
85
To Lower Rociada
9200
70
87
85
70
9175
9150
EXPLANATION
Pegmatite rich in lepidolite and other lithium-bearing micas
Massive quartz
Perthite-quartz-albite pegmatite, with locally abundant muscovite
Amphibole schist and quartz-mica schist
Strike and dip of foliation or schistosity
Strike of vertical foliation or schistosity
87
Contact, showing dip; dashed where approximately located
Rim of trench or open cut
Dump
0 10 20 40
Scale in feet
Contour interval 5′
Datum assumed
Mapped by R. H. Jahns 6/46

FIG. 1. Geologic map of the Pidlite mine area, Mora County, New Mexico.

zones in which very coarse-grained, anhedral quartz and large, euhedral crystals of perthite are most conspicuous. In addition, some of them also contain aggregates of quartz, cleavelandite, lepidolite, and muscovite that form veinlets, stockworks, and larger, lens-like masses with poorly defined margins.

DESCRIPTION OF THE PIDLITE PEGMATITE

General features

The Pidlite pegmatite lies at the crest of a prominent ridge between the headwaters of Sparks and Maestas creeks. It is a nearly vertical dike about 75 feet long and 18 feet in maximum exposed breadth, and was first prospected for lithium minerals at least two decades ago. It was stripped by means of a bulldozer in November 1945 largely on the basis of several inconspicuous showings of lepidolite-rich pegmatite, and was mined by open-cut methods early in the following year. Underground operations, conducted during 1946 and 1947 by the Hayden Mining Company, led to development of a 55-foot shaft and appended drifts in the northern part of the dike (Fig. 1). Small quantities of microlite and a modest tonnage of lepidolite constitute the commercial output from the deposit.

The locality was visited briefly by the writer in July 1943, and was studied and mapped in June 1946, April 1947, and July 1947, when mining operations yielded successively larger and more complete exposures of the pegmatite. It also was visited in 1948 by Page and McKinley (1950, p. 21), who prepared a sketch map of the dike, and in 1951 by Heinrich (1953, pp. 31–32), who devoted particular attention to the micas in the pegmatite.

The dike strikes north-northeast, and in most places is very sharply bounded from the adjacent country rock (Fig. 2), here mainly a fine-grained amphibole schist. It tapers abruptly southward, as shown in Figure 1, to form a 20-foot "tail" that is only 2 feet to 4 feet thick. About 10 feet of schist separates this thin part of the dike from the northeastern part of a second, nearly parallel dike that is 130 feet long and 3 feet to 10 feet thick. Farther southeast are at least four other subparallel, pinching-and-swelling dikes, which are exposed mainly in test pits and two exploratory trenches (Fig. 1). All these dikes in the mine area dip very steeply, and are arranged en echelon to form a north-trending pegmatite belt that is about 100 feet wide.

Structure

Excepting its relatively thin "tail," the Pidlite dike has the form of a discoidal lens whose major axes are essentially horizontal and vertical,

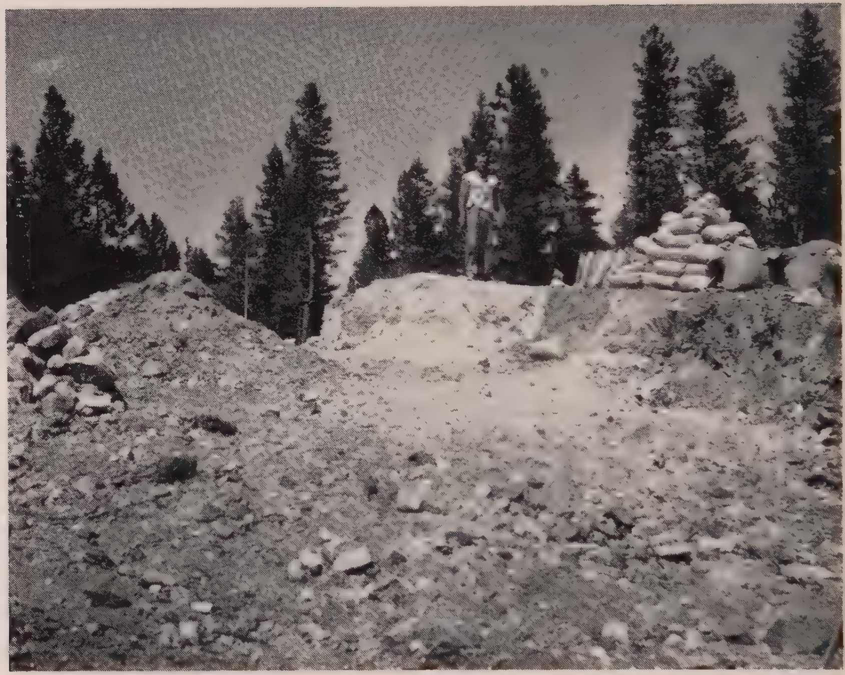

FIG. 2. View of main open cut, Pidlite mine, looking northeast. Note sharp contact between pegmatite and country rock in wall of cut immediately to left of the sacked lepidolite. Man is standing on contact between rib-like mass of quartz (at left) and perthite-quartz-albite pegmatite (at right).

respectively. As traced downward from its outcrop, it has a slight but prevailing hade to the east-southeast, and this is accentuated by a pronounced bend in both walls about 35 feet beneath the surface (Fig. 3). A second, much sharper jog in the opposite direction at the 55-foot level reflects a 10-foot to 12-foot displacement along a gently dipping fault. The north edge of the lens is fluted, and has a very steep northward plunge. The fluting is broadly expressed at and near the surface as three rounded bulges, and at greater depths it appears as more elongate projections (Fig. 3). The south edge of the lens, at the base of the "tail" of the dike, has a similar shape but appears to plunge less steeply northward and to become somewhat less well defined with depth.

The dike consists of seven readily distinguishable types of pegmatite, four of which form typical zones (Cameron *et al.*, 1949, pp. 13–24). As shown in Figure 4 I, these zones have a broadly concentric arrangement, and hence reflect the general shape of the pegmatite body. The other three rock types, which are most extensively developed in the northern and western parts of the dike, form units that are similar to the zones in

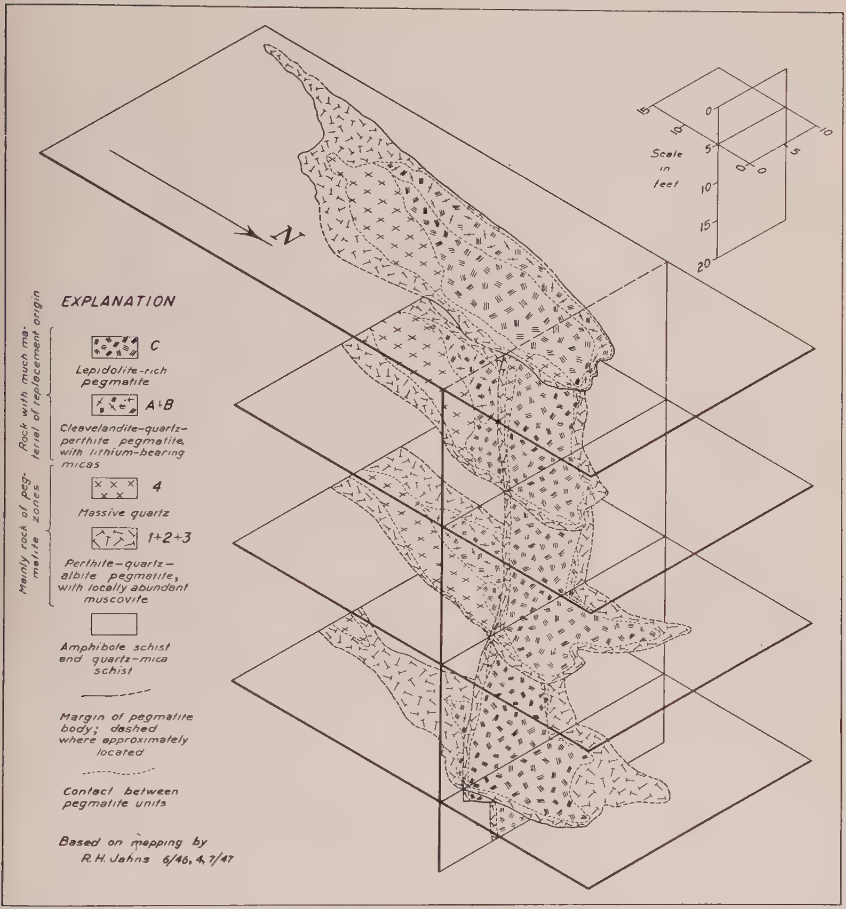
N
Scale in feet
0
5
10
15
20
EXPLANATION
Rock with much material of replacement origin
C
Lepidolite-rich pegmatite
A+B
Cleavelandite-quartz-perthite pegmatite, with lithium-bearing micas
Mainly rock of pegmatite zones
4
Massive quartz
1+2+3
Perthite-quartz-albite pegmatite, with locally abundant muscovite
Amphibole schist and quartz-mica schist
Margin of pegmatite body; dashed where approximately located
Contact between pegmatite units
Based on mapping by R.H. Jahns 6/46, 4, 7/47

FIG. 3. Isometric plate diagram of the Pidlite pegmatite body, showing distribution of major units in the dike.

shape and disposition, but are distinguished by their content of minerals that appear to have been developed by replacement of earlier pegmatite minerals. It is with the origin of these units that much of this paper is concerned.

The surface distribution of all the pegmatite units is indicated in Figure 4-I. Their distribution in three dimensions is shown in more generalized form by the diagram in Figure 3, and they are further generalized on the map of the mine area (Fig. 1).

The outer zones of the dike are relatively thin and continuous, and thus form envelopes around the lenticular to pod-like inner units. The inner units are present only in the thick part of the dike, where they form

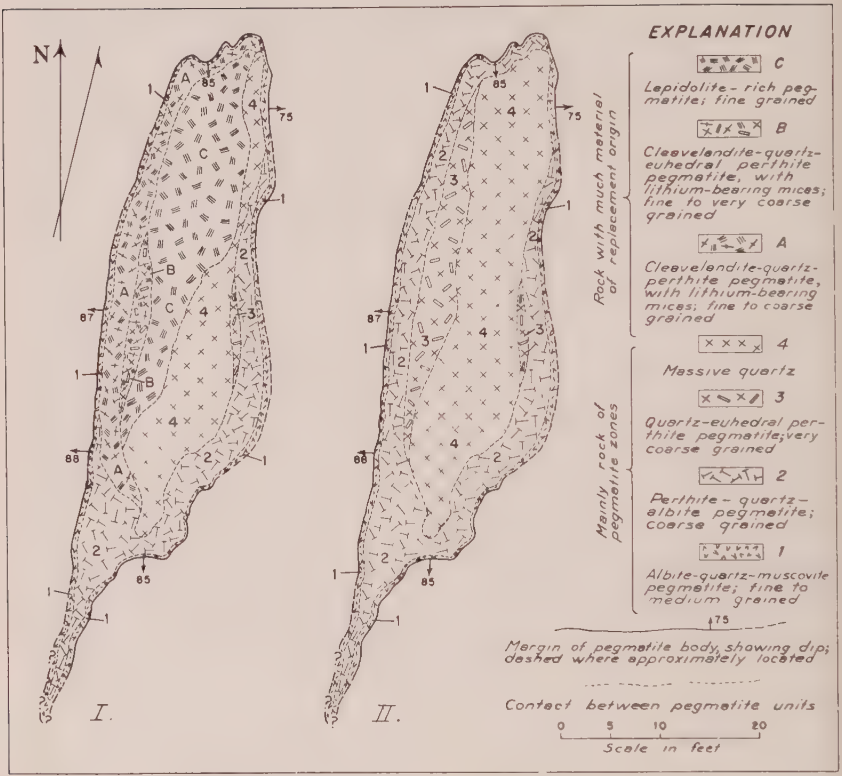
N
I.
II.
A
B
C
1
2
3
4
85
75
87
88
EXPLANATION
C
Lepidolite-rich pegmatite; fine grained
B
Cleavelandite-quartz-euhedral perthite pegmatite, with lithium-bearing micas; fine to very coarse grained
A
Cleavelandite-quartz-perthite pegmatite, with lithium-bearing micas; fine to coarse grained
Rock with much material of replacement origin
4
Massive quartz
3
Quartz-euhedral perthite pegmatite; very coarse grained
2
Perthite-quartz-albite pegmatite; coarse grained
1
Albite-quartz-muscovite pegmatite; fine to medium grained
Mainly rock of pegmatite zones
75
Margin of pegmatite body, showing dip; dashed where approximately located
Contact between pegmatite units
0
5
10
20
Scale in feet

FIG. 4. Surface plan of Pidlite dike, showing distribution of pegmatite units. I. Distribution of units as they now exist. II. Possible distribution of zones, had there been no development of the composite units.

more than half of its outcrop breadth. As they are traced downward beneath the outcrop, their major horizontal axes decrease in length, evidently in response to the slight downward convergence of the ends of the main, thick part of the dike (Fig. 3).

Zones

The border zone of the dike (unit 1 in Fig. 4) is a fine- to medium-grained selvage, 3 inches to 2 feet thick. It consists of calcic to median albite, quartz, and muscovite, with minor perthite and accessory apatite, beryl, fluorite, spessartite, and schorl. The immediately adjacent wall zone (unit 2, Fig. 4), which is about 2 feet in average thickness, is a coarse-grained, granitoid aggregate of perthite, quartz, and median albite, with minor muscovite and a suite of accessory minerals similar to that of the border zone. It also contains irregular masses of quartz and fine-grained greenish muscovite, as well as scattered veinlets and fist-sized pods of cleavelandite and pink muscovite.

An intermediate zone of very coarse-grained quartz-euhedral perthite pegmatite (unit 3, Fig. 4) forms a thin lens on the east side of the dike. It contains accessory beryl and spessartite, and is cut by numerous veinlets and irregular aggregates of coarse-grained cleavelandite and muscovite. This zone is grouped with the border zone and the wall zone in the diagram of Figure 3.

The most conspicuous zone in the dike consists chiefly of very coarse-grained, anhedral quartz (unit 4, Fig. 4), and crops out as a bulbous to rib-like mass that is sharply bounded from the adjacent more feldpathic pegmatite (Figs. 2, 5). Some apophyses of quartz extend outward from this unit into the earlier-formed zones that flank it.

In the outer parts of the fourth zone are scattered crystals of perthite, and in its inner parts are a few prisms of topaz and numerous lath-shaped crystals of spodumene. At least three zones could be distinguished and mapped on the basis of the presence or absence of these other minerals, but for simplicity they are grouped together as one quartz-rich unit. Cleavelandite, muscovite, and lepidolite occur in the quartz as irregular bunches and lenses, and as stockworks of fracture-controlled veinlets. Locally these late-stage minerals constitute as much as one-third of the rock.

The other dikes in the mine area show similar zonal structure, except that in many places the border and wall zones constitute the entire thickness of exposed pegmatite. The cores of these dikes consist mainly of massive quartz, and occur as lens-like segments 2 inches to 10 feet thick and 15 inches to about 50 feet long (Fig. 1). Locally they are flanked by thin, discontinuous intermediate zones of quartz-euhedral perthite pegmatite.

Composite units

The other three units of the dike plainly are composite, in the sense that they contain two well defined generations of minerals. One of these units (A, Fig. 4), a thin, curving mass near the west wall of the dike, is a fine- to coarse-grained aggregate of cleavelandite, quartz, perthite, median albite, lepidolite, and white to pink muscovite. The micas and cleavelandite vein and corrode the other minerals, and appear to have been developed largely at their expense. This unit grades southward into the granitoid wall zone described above, and contains the same suite of accessory minerals as the wall zone.

A second, much smaller composite unit (B, Fig. 4), is analogous to the quartz-euhedral perthite zone on the opposite side of the dike, but is

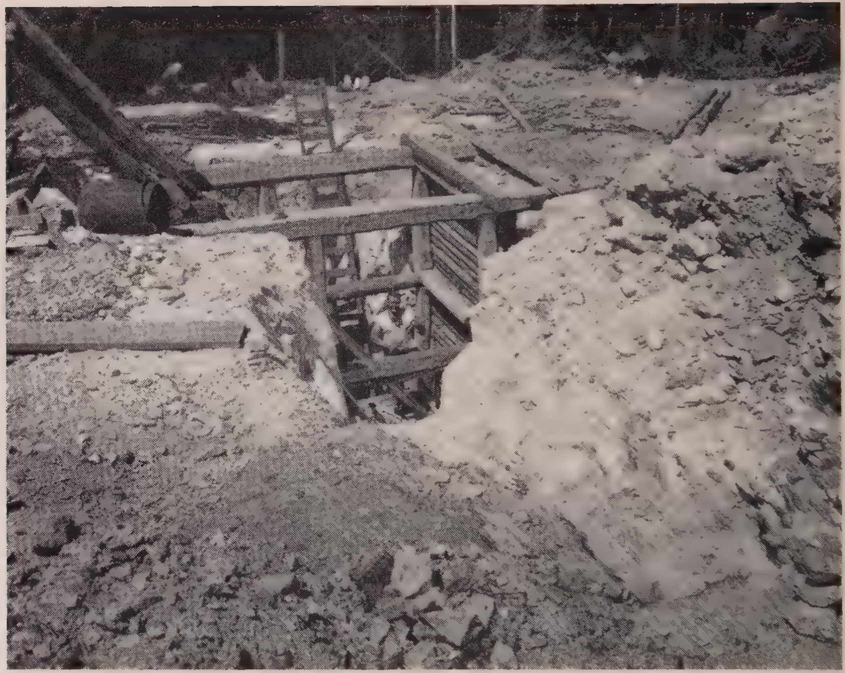

FIG. 5. View of shaft and part of main open cut, Pidlite mine, looking northeast. The openings are in lepidolite-rich pegmatite. Massive quartz with blocky fracture is exposed high on wall of cut at right.

characterized by abundant albite, muscovite, and lepidolite that transect and corrode the earlier crystals of quartz and potash feldspar. All stages in the replacement of perthite by sodic albite can be observed, and numerous pseudomorphs of cleavelandite and of fine-grained, sugary albite after perthite are present. The micas appear to have replaced quartz along fractures and crystal boundaries, and pseudomorphs of muscovite and lepidolite after topaz and spodumene also can be recognized.

The third composite unit (C, Fig. 4) consists mainly of lepidolite. As shown in Figures 3, 4, and 5, it is a bulbous, centrally disposed mass that is thickest in the northern part of the dike. It grades westward and northward into the composite units described immediately above, and eastward and southward into the zone that is rich in massive quartz. In its outer parts are conspicuous evidences of replacement of quartz, potash feldspar, spodumene, and topaz by sodic albite and micas, but its inner parts, which are composed almost wholly of fine-grained lepidolite (Fig. 6) with minor albite and tantalum-niobium minerals, show no such evidences of replacement. As pointed out later on, the total *amount* of de-

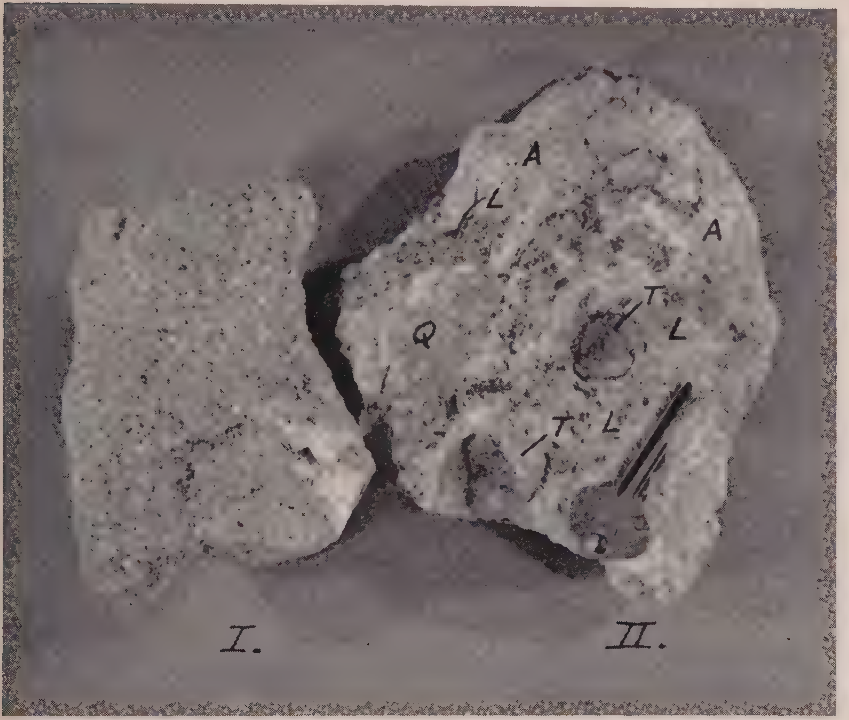

FIG. 6. Lepidolite-bearing pegmatite, Pidlite dike. I. Fine-grained lepidolite from inner part of unit C. II. Crystals of topaz (T) and residual mass of quartz (Q) in aggregate of lepidolite (L) and sodic albite (A), in rock from outer part of unit C.

monstrable replacement in this unit is not as great as one might estimate from a casual inspection of the rock, in which *qualitative* evidence for corrosion and replacement is both impressive and widespread.

No similar large composite units are definable within the other dikes of the mine area. Cleavelandite, lepidolite, and pink muscovite do occur, however, as irregular veinlets and pods in parts of several quartz-rich core segments, where they resemble units A and B of the main dike. None of these is large enough to be represented separately on the map in Figure 1.

Mineralogy

The Pidlite dike contains an assemblage of minerals strikingly similar to those of the Harding pegmatites (Jahns, 1951, pp. 52–53) farther north in New Mexico, the Brown Derby pegmatites (Eckel, 1933; Landes, 1935, p. 333; Hanley *et al.*, 1950, pp. 68–74), in Gunnison County, Colorado, the Stewart pegmatite (Jahns and Wright, 1951, pp. 30–42, 57–61), in San Diego County, California, and to those of several other lithium-bearing pegmatites in the United States. These masses of rock are essentially granitic in composition, and consist chiefly of perthite, quartz, and sodic plagioclase. All of those specifically mentioned contain abundant lepidolite, and all but the Brown Derby pegmatites contain spodumene and small quantities of lithium-bearing phosphate minerals, as well. The similarities of their accessory-mineral suites, as indicated in Table 1, testify to a consistent occurrence of beryllium, bismuth, boron, columbium (niobium) and tantalum, fluorine, manganese, and rare-earth elements.

TABLE 1. ACCESSORY MINERALS OF THE PIDLITE PEGMATITE AND OTHER LITHIUM-BEARING PEGMATITES IN THE SOUTHWESTERN STATES

Mineral	Pidlite pegmatite, Mora County, New Mexico	Harding pegmatite, Taos County, New Mexico	Brown Derby pegmatite, Gunnison County, Colorado[a]	Stewart pegmatite, San Diego County, California[b]
Apatite	x	x	x	x
Beryl	x	x	x	x
Betafite	x	—	x	—
Beyerite	—	x	—	x
Bismite	—	x	—	x
Bismuth	x	x	—	x
Bismuthinite	—	x	—	x
Bismutite	x	x	—	x
Chalcocite	—	x	—	x
Columbite-tantalite	x	x	x	x
Cyrtolite	x	—	—	—
Elbaite	x	—	x	x
Fluorite	x	x	x	—
Gahnite	x	x	x	x
Hatchettolite	x	x	x	—
Lithiophilite	—	x	—	x
Loellingite	x	x	—	x
Magnetite	x	x	x	x
Microlite	x	x	x	x
Monazite	x	x	x	x
Pyrite	x	x	—	x
Schorl	x	x	x	x
Spessartite	x	x	x	x
Topaz	x	x	x	—
Zinnwaldite	—	—	x	x

[a] List furnished by J. B. Hanley, U. S. Geological Survey.

[b] Jahns, R. H., and Wright, L. A., 1951, pp. 30–42.

The major minerals of the Pidlite dike, as traced from its borders inward to its center, show many of the variations that are characteristic for zoned pegmatites in general. The perthite, for example, becomes progressively coarser, and ranges in color from medium tan and flesh through pale buff to gray. The contained lamellae of albite also become coarser, as well as increasingly sodic, toward the center of the dike. The characteristic plagioclase of the border zone is gray albite in the Ab_{90-95} range, whereas that of the wall zone is whiter and has the composition Ab_{94-97}. The albite of the inner pegmatite units is extremely sodic, and occurs both as lustrous, white, sugary aggregates and as sheaves and clusters of white to dark pearly gray cleavelandite. Most of the cleavelandite blades are 1 inch to 6½ inches long, and typically are curved and bent. The coarsest crystals are mottled white to medium bluish gray.

Spodumene, which occurs mainly with quartz in the central part of the dike, forms chunky prismatic crystals one-half inch to 14 inches in maximum dimension. These are white to greenish gray, and have a dull to waxy luster. Most are partly altered to very fine-grained albite, micas, and clay minerals, and resemble the altered crystals described, for example, from lithium-bearing pegmatite in Colorado (Hanley *et al.*, 1950, p. 13), Arizona (Jahns, 1953), southern California (Jahns and Wright, 1951, pp. 36–37), and the Black Hills region of South Dakota (Schwartz and Leonard, 1926). In addition, some of the crystals are veined and partly replaced by coarser-grained aggregates of white to pink muscovite and lithium-bearing micas; where replacement has been complete, the mica pseudomorphs retain the crystal outlines and even traces of the prismatic cleavage of the original spodumene.

Topaz occurs as white to gray prisms that are characteristically rhombic in cross section (Fig. 6–II). Most are cigar shaped, and are 1 inch to 5 inches long. The crystals are somewhat rounded, and are sheathed with flaky to waxy aggregates of white and pale pink muscovite and paragonite. In addition, many of them are rimmed, veined, and otherwise partly replaced by micas of varying coarseness (Fig. 7). The fresh topaz has the following optical properties: $\alpha=1.616$, $\beta=1.618$, $\gamma=1.625$, all ± 0.002; 2V approximately 60°. These data suggest the presence of 10 to 15 mol. per cent of the hydroxyl-bearing member in the formula for this material (Winchell and Winchell, 1951).

Beryl is present in nearly all the pegmatite units. It forms white to gray anhedral crystals in the outer zones, very pale pinkish, nearly equant subhedral crystals in the inner zones, and rare white, tabular euhedral crystals in the lepidolite-rich units. None of the observed crystals is greater than 3 inches in maximum dimension, and most are less than an inch. The ω index of refraction of this mineral ranges from 1.583

for some crystals in the border zone to 1.595 for several of those in the central units. This indicates a relatively high content of alkali elements (Schaller, oral communication), particularly cesium and sodium, in all of the beryl, as well as a progressive increase in the proportions of these elements as the mineral is traced from the margins of the dike inward to its center. This consistent trend in alkali content seems to be a widespread characteristic of the beryl in zoned pegmatite bodies (see, for example, Cameron *et al.*, 1949, pp. 69, 99; Fersman, 1931; Heinrich, 1952; Jahns and Wright, 1951, pp. 37-38; Jahns and Adams, 1953; Landes, 1925, p. 374), and constitutes a strong argument for crystallization of this mineral from a magma during successive development of the zones in a given pegmatite body.

The most widespread accessory constituents of the outer pegmatite zones are pale to bluish gray apatite, colorless to gray fluorite, lustrous red spessartite, and minor schorl in small prisms and needles. Tiny crystals of cyrtolite are present as inclusions in scattered small books of biotite, which are present only at the borders of the dike. White to pale bluish amblygonite occurs sparingly with spodumene and topaz in the inner part of the quartz-rich zone. Associated accessory constituents, present mainly in the massive quartz, include apatite, beryl, bismuth minerals, columbite-tantalite, gahnite, spessartite, and sulfides. These minerals, together with betafite, fluorite, and monazite, also occur in the wall zone, where they represent an association very similar to that reported from the Brown Derby pegmatites in Colorado (Page, 1950, p. 30).

Three generations of micas can be recognized in the Pidlite dike. Pale yellowish green and green muscovite is a minor constituent of the pegmatite zones, and is most abundant in the outer part of the dike, where it forms foils and thin plates $\frac{1}{16}$ inch to about 3 inches in diameter. It is associated with a little biotite in the border zone. A younger generation of mica is represented by lepidolite, which is widely distributed, as already noted, and is particularly abundant in the central parts of the dike. Most of it forms dense aggregates of small, thick, crystals (Fig. 6), which range in color from pinkish gray through lilac and pale lavender to pale purple. Other crystals are much coarser, and thin plates 2 inches to 5 inches in diameter form fringes around rosettes of cleavelandite blades in the outer composite units of the dike.

Similar coarse books form a relatively high proportion of the lepidolite in the other dikes of the mine area, in which they are closely associated with albite, and especially with the cleavelandite variety. The lepidolite commonly veins and corrodes the albite in detail, and on a larger scale replaces other, earlier minerals in the pegmatite.

The youngest micas in the main dike are white to pale pink muscovite

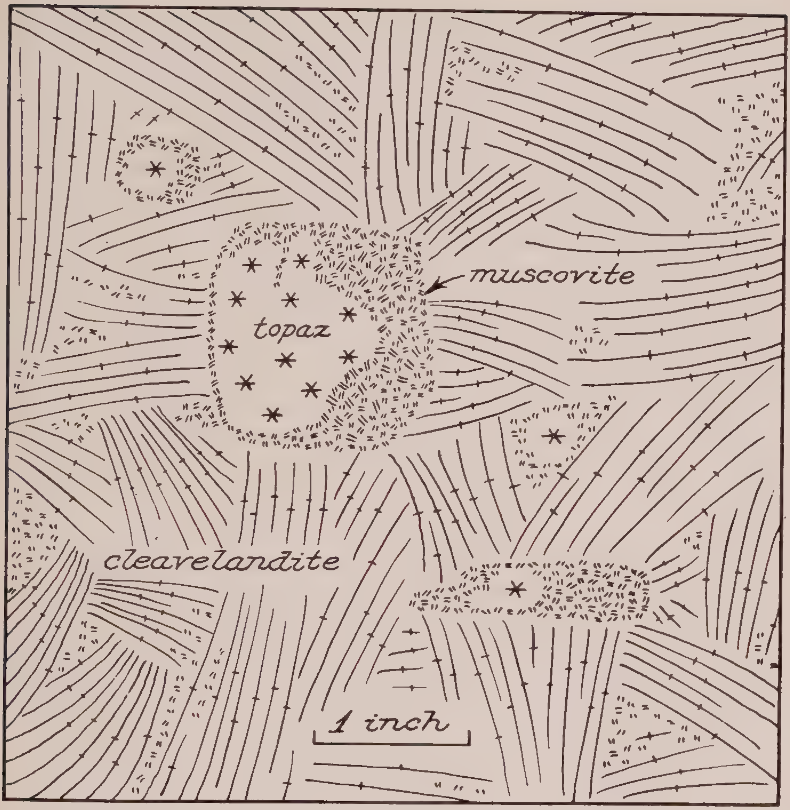

FIG. 7. Peripheral replacement of topaz crystals by pink muscovite, outer part of Unit C, Pidlite dike.

and paragonite, which form waxy to finely crystalline aggregates that are most abundant in the pegmatite immediately adjacent to the lepidolite-rich unit (C, Figs. 3, 4). As pointed out by Heinrich and Levinson (1953, pp. 31–32), these aggregates are interstitial to blades of cleavelandite as elongate or irregular pods, generally an inch or less across. They also form irregular veinlets in aggregates of lepidolite and sugary albite, and in individual crystals of apatite, beryl, quartz, potash feldspar, and other earlier minerals. In addition, they form jackets around crystals of elbaite, spodumene, and topaz (Fig. 7). Some of these jackets contain individual flakes $\frac{1}{8}$ inch to $\frac{1}{2}$ inch in diameter, and resemble the aggregates of pink muscovite that replace spodumene in the Harding pegmatite (Heinrich and Levinson, 1953, pp. 29–31 and Plate I; Jahns, 1951, p. 53).

A few rough, opaque prisms of pale green to pink elbaite, $\frac{1}{4}$ inch to 2 inches long, are scattered through some of the quartz-albite-lepidolite pegmatite in the inner part of the dike. This tourmaline also forms small, distinctly flattened inclusions in some of the coarsest crystals of lepidolite. A little deep purple fluorite, in anhedral crystals $\frac{1}{2}$ inch or less in maximum dimension, occurs with albite in the largest masses of lepidolite. Associated with it are small tabular crystals of monazite and columbite-tantalite.

Microlite is scattered through the lepidolite-rich unit in the northern part of the dike, and several concentrations of this and other tantalum-columbium minerals were encountered in the mine workings at about the 30-foot level. The microlite forms microscopic grains and honey-yellow to pale yellowish brown octahedral crystals $\frac{1}{32}$ inch to $\frac{3}{8}$ inch in diameter. Many of the crystals are zoned, with pale centers and dark-colored rims. Nearly all of the microlite has a specific gravity greater than 6.00 and an index of refraction above 2.00, as determined by immersion in selenium melts, and evidently is characterized by a high tantalum-niobium ratio.

Hatchettolite, the uranian microlite, also is present in the aggregates of lepidolite, where it forms small, roughly faced crystals with waxy to brightly resinous luster. They are dark mahogany brown to black, and are surrounded by haloes of discoloration in the enclosing lepidolite. In general appearance they resemble the hatchettolite of the Harding pegmatites and the uranian microlite of the Brown Derby pegmatites (Hanley *et al.*, 1950, pp. 72–73).

QUANTITATIVE ANALYSIS OF THE PIDLITE PEGMATITE

General methods

The mineralogic and chemical composition of the Pidlite pegmatite was determined quantitatively by a simple, though indirect, method. The difficulties of collecting representative composite or bulk samples of all the pegmatite units (or a single sample of the dike as a whole) for microscopic or chemical analysis were regarded as prohibitive, and hence the determinations were based instead upon three general types of data:

1. Dimensional measurements of pegmatite units, obtained directly in the field and indirectly from 23 detailed plans and sections of the pegmatite body.
2. Proportions of major minerals in each pegmatite unit, determined by measurements along closely spaced linear traverses.
3. Average composition of individual mineral species, obtained directly by chemical analyses of representative material and indirectly by means of optical data.

Mapping of the dike at the surface was done with plane table and telescopic alidade at a scale of 10 feet = 1 inch, and supplementary control was set in by means of tape-triangulation and by tape-measured offsets from previously established lines. Additional direct measurements with a yardstick were used wherever needed to define irregularities in the contacts between pegmatite units, or between pegmatite and country rock. Similar techniques were used in the preparation of the subsurface plans and cross sections, except that a simple sight alidade was used with the plane table.

Areas of all pegmatite units were determined on each plan and section by means of a transparent measuring grid ruled in twentieths of an inch. The areas were converted to volumes by the so-called cross-section method, first by using successive plans as sections of the dike and then by using successive cross-sections as the sections. The results were found to be in close agreement (Table 2). Calculations were based on the end-area formula:

TABLE 2. VOLUMES AND TONNAGES OF PEGMATITE UNITS IN THE PIDLITE DIKE

Unit	Volume (cubic feet)			Amount (short tons)
	Determined from successive plans of dike	Determined from successive cross-sections of dike	Average	
Zones 1+2+3	16,172	16,138	16,155	1,353.1
Zone 4	7,568	7,552	7,560	633.1
Composite units A+B	3,834	3,852	3,843	321.9
Composite unit C	9,301	9,419	9,360	783.9
Total dike to 55-foot level (by summation)	36,875	36,961	36,918	3,092.0
Total dike to 55-foot level (by direct measurement)	37,007	36,919	36,963	3,095.7

$$V = 1/2H(A_1 + 2A_2 + 2A_3 + \cdots + 2A_{n-1} + A_n),$$

where V is the volume of the solid, H is the distance between the parallel sections that form its ends, and A_1, A_2, A_3, etc. are the areas of equally spaced parallel sections of the solid. The more general prismoidal formula was used as a check, and yielded very similar results. All volumes were converted to masses on the basis of a density factor of 11.94 cubic feet per ton of pegmatite.

Modal analyses of the pegmatite units were made megametrically by the Wentworth method. Measurements of mineral intercepts were made in the field along linear traverses spaced one foot apart, and two sets of these traverses, at right angles to each other, covered each exposure of pegmatite. The respective intercepts were converted to volume proportions of minerals, and then to weight proportions. Most of the measuring was done with a 5-inch wheel mounted on the end of a rod. As the wheel was rolled along a given line on a rock exposure, its revolutions were recorded by means of an attached counter. A second counter, which could be engaged or disengaged by means of a clutch, was used to record the intercepts of a given mineral. The traverse was repeated for each of the other minerals exposed along the line. Direct measurements with a steel tape were made on a few irregular walls in the underground workings, where the mechanical device was limited in its usefulness.

Data on average composition of the muscovite, lepidolite, paragonite, and spodumene were obtained from chemical analyses of one or more composite samples of each species. The proportions of alkalies in the feldspars were estimated on the basis of partial chemical analyses of five composite samples. Perthites from two analyzed samples were examined in thin section, and the proportions of intergrown albite, as determined micrometrically, were found to be compatible with the proportions of K_2O and Na_2O indicated by the chemical analyses. Further micrometric work was done to check the proportions of perthitic albite in fourteen other samples, in order to broaden the basis for estimating the average composition of perthite in the dike.

Modal analyses

Two major simplifications in the modal analyses of the dike and its component parts were made in order to save time without sacrificing accuracy or essential detail. First, although areas of all the pegmatite units were determined in the surface exposures and in several subsurface exposures of the dike, some of these units were grouped together, as shown in Figure 3, for the final calculation of modes. The border zone, wall zone, and quartz-euhedral perthite intermediate zone (Zones 1, 2, and 3) were considered together, as were two of the composite units (A and B). Second, none of the minor accessory minerals in the pegmatite was considered in the measurements, which were confined to quartz, perthite, calcic to median albite, cleavelandite and other highly sodic albite, muscovite and minor paragonite, lepidolite, spodumene, and topaz.

Table 2 shows the respective volumes and tonnages of the units that were measured. These represent the part of the dike that lies between the surface and a level 55 feet beneath the collar of the shaft. The chief source of error in the figures is the possible occurrence of major irregularities in the subsurface disposition of the units at points where no exposures are provided by mine workings. Owing to this factor, it seemed unwise to attempt more elaborate methods for estimating the volumes. In the words of Jackson and Knaebel (1932, p. 117), "Somewhat intricate calculations involving higher mathematics have sometimes been advocated for making tonnage estimates, but since the basic data usually are not exact and often speculative it is questionable whether such refinements in calculation are warranted." Another source of error, plainly of much lesser import, is the application of a single conversion factor for calculating tonnage from the volumes of units that differ from one another in composition.

The linear-traverse method of analysis under the microscope has been so thoroughly discussed in the geologic literature (Chayes, 1946, 1949, 1951; Lincoln and Reitz, 1913; Thomson, 1930) that its megametric analogue, used in the present investigation, needs no elucidation here. The chief source of error in the mineral measurements almost certainly is one of sampling, and stems in large part from incomplete exposure of the dike in three dimensions, and from the markedly uneven distribution of certain mineral constituents in the rock. The proportion of exposed pegmatite, however, was unusually large, and fortunately the exposures

TABLE 3. MODES OF PEGMATITE UNITS IN THE PIDLITE DIKE

Mineral	Zones 1+2+3		Zone 4		Composite Units A+B		Composite Unit C	
	Proportion	Amount (short tons)	Proportion	Amount (short tons)	Proportion	Amount (short tons)	Proportion	Amount (short tons)
Quartz	29.8	403.2	87.3	552.7	19.5	62.8	9.6	75.2
Perthite	42.2	571.0	2.3	14.5	15.3	49.3	3.4	26.7
Albite: calcic to median	22.6	305.8	—	—	—	—	—	—
Albite: highly sodic	—[a]	—	5.0	31.7	38.1	122.6	21.5	168.5
Muscovite and minor paragonite	5.4	73.1	2.7	17.1	14.7	47.3	4.8	37.6
Lepidolite	Tr.	—	1.1	7.0	12.2	39.3	60.4	473.5
Spodumene	—	—	1.6	10.1	Tr.	—	Tr.	—
Topaz	—	—	Tr.	—	0.2	0.6	0.3	2.4
Total	100.0	1,353.1	100.0	633.1	100.0	321.9	100.0	783.9
Total traverse length (feet)	4,840.7		2,077.0		1,464.4		3,916.2	

[a] Cleavelandite and other highly sodic albite are present, but were grouped together with median albite in measurements of these zones.

were most nearly complete in those units with the coarsest and most irregularly distributed minerals.

The modes of the pegmatite units are recorded in Table 3. The total length of traverses in each unit was sufficiently great to insure a reasonably small analytical, or precision, error, and comparison of different sets of traverses within each unit indicated only a modest scattering in the proportions of individual minerals. No attempt was made to apply shape-factor corrections, as the only major minerals with markedly platy or elongate habit occur principally as aggregates of diversely oriented crystals.

The data in Tables 2 and 3 were used to calculate the mode of the entire mass of pegmatite between the surface and the 55-foot level, and the results appear in Table 4. Although a large proportion of the dike was available for study, it cannot be denied that significant error might well attend any assumption that the composition of its exposed parts is the same as its true bulk composition, either mineralogically or chemically. Unfortunately, there is no satisfactory means for determining the amount or composition of the pegmatite that lies beneath the deepest mine workings, or of the pegmatite that has been eroded from points above the present outcrop. On the basis of comparisons with numerous other, more fully exposed pegmatites with zonal structure and pod-like form, however, it might be assumed that the distribution of rock units along the vertical axis of the Pidlite dike is not fundamentally different from that along its major horizontal axis. If this assumption is correct, the mode of the entire dike cannot differ greatly from that recorded in Table 4, particularly with respect to quartz and feldspars. The proportion

TABLE 4. MODE OF THE PIDLITE DIKE

Mineral	Units in which mineral occurs in more than trace amounts	Amount (short tons)	Proportion
Quartz	All	1,093.9	35.4
Perthite	All	661.5	21.4
Albite: calcic to median	1+2+3	305.8	9.9
Albite: highly sodic	4+A+B+C	322.8	10.4
Muscovite and minor paragonite	All	175.1	5.7
Lepidolite	4+A+B+C	519.8	16.8
Spodumene	4	10.1	0.3
Topaz	A+B+C	3.0	0.1
Total		3,092.0	100.0

Table 5. Composition of Major Minerals in the Pidlite Dike

	Quartz	Perthite[a]	Albite[b] (calcic to median)	Albite[c] (highly sodic)	Muscovite[d] (and minor paragonite)	Lepidolite[e]	Spodumene[f]	Topaz[g]
SiO_2	100.0	65.0	67.1	68.3	45.4	50.8	53.5	32.7
Al_2O_3	—	18.8	20.5	19.7	37.7	26.6	29.9	55.5
CaO	—	0.3	1.2	0.3	0.1	—	1.2	—
Na_2O	—	2.0	10.7	11.4	2.5	2.7	4.3	—
K_2O	—	13.9	0.5	0.3	9.8	10.5	3.4	—
Li_2O	—	—	—	—	—	4.3	4.6	—
H_2O	—	—	—	—	4.5	2.0	3.1	1.2
F	—	—	—	—	—	5.4	—	18.2
Total	100.0	100.0	100.0	100.0	100.0	100.0[h]	100.0	100.0[i]

[a] Based on average composition of 16.5 per cent pure albite, 1.5 per cent pure anorthite, and 82.0 per cent pure microcline, as estimated from two partial chemical analyses and optical data.

[b] Based on average composition of 91.0 per cent pure albite, 6.0 per cent pure anorthite, and 3.0 per cent pure microcline, as estimated from two partial chemical analyses and optical data.

[c] Based on average composition of 97.0 per cent pure albite, 1.5 per cent pure anorthite, and 1.5 per cent pure microcline, as estimated from a partial chemical analysis and optical data.

[d] Weighted average of two chemical analyses.

[e] Weighted average of four chemical analyses.

[f] Based on two partial chemical analyses of altered crystals, one partial analysis of a fresh crystal, and modal determinations of the ratio of fresh to altered material in the dike.

[g] Based on composition of 12 mol. per cent of $[Al(OH)]_2SiO_4$ and 88 mol. per cent of $(AlF)_2SiO_4$, as estimated from optical data.

[h] Includes—2.3 correction for O equivalent to F.

[i] Includes—7.6 correction for O equivalent to F.

of lepidolite, however, would be appreciably smaller, and perhaps would amount to 12 or 13 per cent.

Chemical composition

The composition of each major mineral in the dike is shown in Table 5, and the sources of the data are summarized in the footnotes. The figures should be regarded as approximate, even though an attempt was made to reduce sampling errors through the use of composite samples and by petrographic examination of specimens obtained from all parts of the dike. Where chemical analyses were available for different varieties of a

TABLE 6. BULK COMPOSITION OF THE PIDLITE DIKE, COMPARED WITH OTHER LITHIUM-BEARING PEGMATITE BODIES AND WITH GRANITES

	Pidlite dike, Mora County, New Mexico[a]	Main Harding dike, Taos County, New Mexico[b]	Main bulge of Stewart dike, San Diego County, California[a]	Granite of all geologic periods, average of 546 chemical analyses[c]	"Alkaline" granite, average of 12 chemical analyses[c]	Pre-cambrian granites of Colorado and New Mexico, average of 23 chemical analyses
SiO_2	74.5	75.43	74.9	70.18	73.30	74.81
Al_2O_3	14.8	14.66	14.9	14.47	12.33	13.30
CaO[d]	0.2	0.23	0.1	2.87	0.72	0.75
Na_2O	3.3	4.13	3.6	3.48	4.55	3.44
K_2O	5.4	3.01	5.2	4.11	4.20	5.42
Li_2O	0.7	0.76	0.7	—[e]	—[e]	Tr.
H_2O	0.6[f]	0.43[g]	0.4[f]	0.84[g]	0.86[g]	0.73[g]
F	0.9	0.55	0.4	—[e]	—[e]	0.19
XO[h]	n.d.	0.88	n.d.	4.05	4.04	1.37
	100.4	100.08	100.2	100.00	100.00	100.01
Correction for O equivalent to F	0.4	0.23	0.2	—	—	0.1
Total	100.4	99.85	100.0	100.00	100.00	100.00

[a] Analysis calculated from the mode. Accessory minerals and minor chemical constituents are neglected.

[b] Chemical analysis of composite sample from cores of 39 diamond-drill holes in thickest part of the dike. Eileen H. Oslund and Samuel S. Goldich, analysts; Li_2O determined by R. B. Ellestad.

[c] Quoted from Daly, R. A., 1933. Igneous rocks and the depths of the earth, pp. 9–10, McGraw-Hill Book Company, Inc., New York.

[d] Includes small amounts of MgO.

[e] Not included in calculations.

[f] Represents OH in micas, topaz, and altered spodumene.

[g] Includes H_2O+ and H_2O-.

[h] Includes Fe_2O_3, FeO, MnO, CO_2, TiO_2, and P_2O_5, wherever respectively determined.

given mineral as, for example, green and pink muscovite—their averages were weighted in accordance with the respective abundance of each variety in the pegmatite. The data thus are thought to constitute a reasonably satisfactory basis for calculating the bulk composition of the exposed pegmatite, and it seems evident that further refinements not only would necessitate many additional analyses, but probably would be limited in value by the degree to which the available exposures reflect the true composition of the pegmatite units.

The bulk composition of the Pidlite dike, as calculated from the data in Tables 4 and 5, is given in Table 6, which also shows analyses of the lepidolite-rich parts of the main Harding dike, about 30 miles to the northwest, and the Stewart dike, in southern California. The similarities in composition are evident. It should be noted that the analyses of the Pidlite and Stewart dikes were obtained by means of modal determinations, whereas that of the Harding was obtained chemically from one very large composite sample.

The composition of the Pidlite pegmatite does not differ greatly from that of Daly's average granite (Table 6), although the granite does contain considerably more total iron (included in XO, Table 6) and calcium. Daly's average, however, includes calcalkaline rocks, as well as some rocks that many geologists would regard as more nearly granodioritic than strictly granitic. The composition of the pegmatite even more closely resembles that of Daly's average "alkaline" granite, as well as that of average granite from the Precambrian terranes of Colorado and New Mexico, as calculated by the writer from 23 published analyses. The most notable differences in the constituents listed in Table 6 reflect a distinct concentration of lithium and fluorine in the pegmatites, and a higher proportion of mafic minerals in the granites.

It is not the purpose of this paper to discuss the implication of the figures in the table, but it seems worth while to emphasize the essentially normal granitic composition, in terms of all major constituents, of three pegmatites that are not likely to appear "normal" to the casual observer in the field. In particular, large masses of quartz in these and many other pegmatite bodies give an understandably exaggerated impression of the SiO_2 content of such bodies, and the occurrence of large crystals or crystalline aggregates of the less common minerals often gives a similar impression. Further, there has been a tendency among a few geologists to consider the genesis of pegmatites, and especially of zoned pegmatites, solely in terms of the composition of individual minerals or of restricted mineral groups. This approach can be misleading, especially if it is used as a measure of the composition of presumed fluids from which the minerals were formed. It would seem to be much more desirable first to approach the problem in terms of the composition of pegmatite zones and other units, as well as the bulk composition of entire pegmatite bodies.

Analysis of the Replacement Features

The general problem

Despite a few firmly expressed opinions to the contrary (for example, Barth, 1952; Higazy, 1949), pegmatite zones commonly are regarded as products of fractional crystallization from a magma, or melt, with incomplete reaction between successive crops of crystals and rest-liquid (for example, Cameron *et al.*, 1949, pp. 79–106; Flawn, 1951, pp. 183–190; Jahns and Wright, 1951, pp. 44–45). This thesis has impressed many investigators as the most satisfactory means for explaining the structure, texture, and mineralogy of zones, as well as the chemical trends and age relations within and between such pegmatite units.

Nearly all zoned pegmatite bodies exhibit widespread evidences of replacement, and many contain masses of rock that appear to have been formed, wholly or in large part, at the expense of earlier pegmatite minerals. Such masses, or units, have been termed replacement bodies by Cameron, *et al.* (1949, pp. 84–85), who attempt to restrict the term to those units "formed by replacement at a stage following the complete crystallization of the parts of the pegmatite body affected by replacement." They point out, however, that such units are not always readily distinguished from those in which replacement took place prior to complete consolidation.

Replacement of one mineral by another can occur at various stages during crystallization of the pegmatite magma under conditions approaching those of a closed system. Widespread reaction between crystals and rest-liquid, especially during the early stages, can be characterized as magmatic or late-magmatic, depending, perhaps, upon the extent to which the initial pegmatite magma itself reflects differentiation from a "normal" granitic magma. During a later stage, when residual liquid has been largely concentrated in the central part of the pegmatite body and in pores and other openings in its almost wholly crystallized outer parts, the effects of replacement can be characterized as post-magmatic (Chayes 1950, p. 36), high-temperature hydrothermal (Shand, 1944, p. 350), or simply as deuteric. The effects of replacement during this stage are gradational from those of the earlier stages, except that hydroxyl-bearing silicates commonly are more abundant and the effects of replacement tend to be much more localized.

As the more volatile constituents in the residual liquid are increasingly concentrated by crystallization of minerals that do not contain these constituents, or contain them only in small proportions, a second fluid phase may separate, either as a liquid saturated with alkali salts (Shand, 1944, p. 348) or as a vapor. This second phase can react with previously formed crystals, and, if it leaves the residual fluid as a vapor that condenses elsewhere in the pegmatite body, the condensate can be highly reactive (Bowen, 1933, pp. 124–125). Mineral replacements accomplished by this second phase, which is relatively rich in water and other volatile constituents, ordinarily are referred to as hydrothermal. The reacting fluid commonly appears to have been controlled in its distribution by fractures in the earlier-formed rock, and it is largely to masses of pegmatite formed by this type of fracture-controlled replacement that Page (1950, pp. 15–23), for example, restricts the term replacement body.

Alternative mechanisms for explaining the replacement features in pegmatites bespeak open-system conditions, and commonly involve the introduction of hydrothermal fluids from sources outside the pegmatite bodies. According to one possible mechanism, solid pegmatite first is formed by a magmatic process, and then, as described by Schaller (1926, p. 59), is acted upon hydrothermally in an open system, with "much material moving, coming in, and going out." An alternative mechanism, advocated in various forms by Andersen (1931), Quirke and Kremers (1943), and others, involves deposition of successive layers of pegmatite from solutions traveling along a channelway. The deposition is accompanied, under these open-system conditions, by various mineral replacements. Still other investigators make no specific suggestion as to the immediate source of the replacing fluids, although it is clear that they recognize two stages in the development of certain pegmatite bodies. Björlykke (1937, p. 244), for example, notes that some granitic pegmatites in southern Norway "were subsequently influenced by solutions and gases following cracks in the already congealed magmatic pegmatite, thus forming deposits of hydrothermal-pneumatolytic origin. . . ."

As pointed out by Cameron, *et al.* (1949, p. 105), the development of some replacement bodies can be correlated with development of an inner zone in the same pegmatite body, and the source of the material thereby established. Consistencies in distribution, age relations, and trends in mineralogy and composition of replacement units in many pegmatite bodies have impressed some investigators as evidences of closed-system, or restricted-system, conditions during development of these pegmatites. Further, many replacement units occur as apophyses that extend outward from the central, or youngest, parts of the containing pegmatite body, suggesting development from a source within the body, perhaps under deuteric conditions.

A major question often is raised concerning the amounts of material involved in replacement reactions within a given pegmatite body. If the replacement minerals are small in amount, as compared with the earlier-formed magmatic pegmatite, it seems reasonable to regard them as the products of residual solutions accumulated during final consolidation of the pegmatite body. On the other hand, numerous investigators have pointed out (Cameron *et al.*, 1949, p. 106) that "where the volume of replacement material is great in proportion to the total volume of pegmatite . . . an appeal to solutions from outside the pegmatite becomes more attractive." Unfortunately, however, little is known about the quantitative relations of replacement, and especially about the net gains and losses of elements during replacement, in the very pegmatite bodies that contain the most conspicuous evidences of this process.

Evidences of replacement are so well developed in the Pidlite dike that no observer would deny the widespread occurrence of replacement minerals, especially in the units that contain large proportions of cleavelandite, lepidolite, and pink to white muscovite. The quantitative relations in these composite units, however, are considerably less obvious. An attempt was made to evaluate them by means of detailed measurements, in the hope that they might be useful in connection with the problems discussed above.

Quantitative relations

The texture and mineralogy of the outer composite unit (A) of the Pidlite dike indicate that it comprises minerals of the wall zone (Zone 2) and minerals formed mainly by replacement of typical wall-zone constituents. Similarly, the middle composite unit (B) evidently was developed by widespread partial replacement of a segment of the quartz-euhedral perthite intermediate zone (Zone 3) and a marginal part of the massive-quartz zone (Zone 4). The lepidolite-rich composite unit (C) clearly was developed in part from the massive-quartz zone and in small part from the quartz-euhedral perthite zone, but much of its inner portion, though composed of late-stage minerals, shows no evidences of a replacement origin. Figure 4-II indicates what the zonal structure of the dike might have been, had there been no development of the composite units. By analogy with other zoned pegmatites in which no lepidolite-rich units are present, the central zone probably would have consisted mainly of very coarse-grained, anhedral quartz.

All exposures of the composite units were studied in detail, in order to determine the minimum amounts of earlier minerals that were present before partial replacement by later minerals. The original outlines of earlier crystals, now wholly or in part replaced by albite and micas, were restored as accurately as possible, chiefly on the basis of recognizable pseudomorphs and the distribution of residual masses of the earlier material (Fig. 8). These outlines were sketched in with crayon on the exposed surfaces of rock, and the total proportion of material whose existence prior to replacement could be thus demonstrated was determined megametrically by means of linear traverses. By this means, it was found that the rock in units A and B must have been at least 95 per cent solid prior to corrosion and replacement by albite and micas, and the rock in unit C must have been at least 22 per cent solid prior to attack of its early-formed constituents. It should be noted that these are minimum esti-

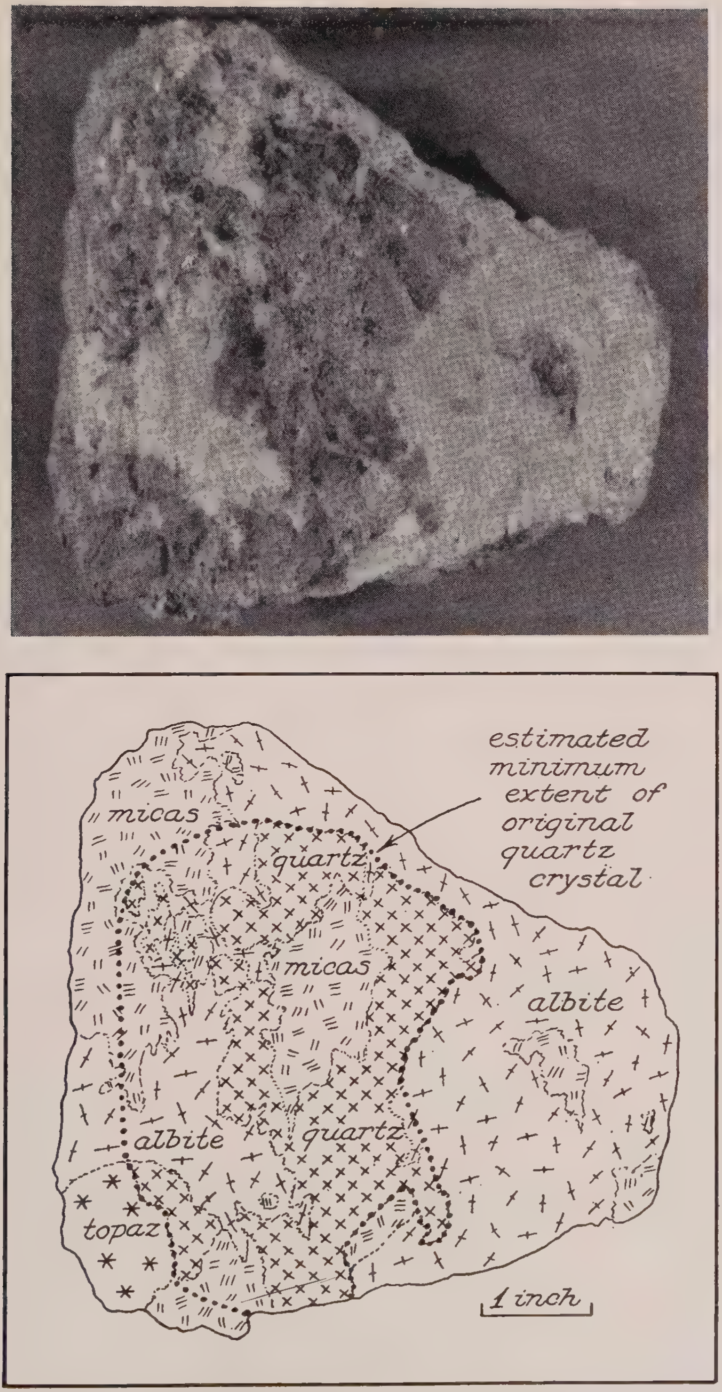

FIG. 8. Specimen of complex pegmatite from outer part of unit C, Pidlite dike, showing general method used to estimate the amount of quartz removed through replacement by albite and micas.

mates, and that much additional solid material may have been removed completely during development of the composite units, without leaving recognizable evidence of its former presence.

Analysis of mineral distribution in the composite units, as determined by study of the exposures in the field, indicates that the rock of units A+B was derived from a volume of material whose composition can be represented as follows:

		Per cent	*Short tons*
Material X, which yielded Units A+B =	Zone 2	63.5	204.4
	Zone 3	20.0	64.4
	Zone 4	11.5	37.0
	Not accounted for (=fluid?)	5.0	16.1
		100.0	321.9

Similarly, unit C appears to have been derived from earlier material of the following composition:

		Per cent	*Short tons*
Material Y, which yielded Unit C =	Zone 3	1.0	7.8
	Zone 4	21.0	164.6
	Not accounted for (=fluid?)	78.0	611.5
		100.0	783.9

No change of weight is assumed in comparing units A, B, and C with their antecedents, materials X and Y. The compositions of X and Y, converted in part to proportions and amounts of contained minerals, are as follows:

Material X			*Material Y*		
	Per cent	*Short tons*		*Per cent*	*Short tons*
Quartz	42.5	136.8	Quartz	20.8	162.6
Perthite	41.6	133.9	Perthite	0.7	5.5
Albite (calcic to median)	9.0	29.0	Spodumene	0.5	4.3
Muscovite	1.4	4.5	Not accounted for (=fluid?)	78.0	611.5
Spodumene	0.5	1.6			
Not accounted for (=fluid?)	5.0	16.1			
	100.0	321.9		100.0	783.9

The processes involved in converting material X to units A and B and converting material Y to unit C, considered together in quantitative terms, resulted in net losses of 161.4 tons of quartz, 63.4 tons of perthite, 29.0 tons of calcic to median albite, and 5.9 tons of spodumene, together with disappearance of pegmatite fluid or fluids and possibly of additional solid material for whose existence there is no present evidence. Attending these losses were net gains of 291.1 tons of sodic albite, 80.4 tons of muscovite, 512.8 tons of lepidolite, and 3.0 tons of topaz. These figures of course apply only to the composite units, and the relatively minor replacement features within the units mapped as true zones (Figs. 3, 4) are neglected in this approximate analysis.

The net losses noted above represent minerals that were eliminated, as such, through replacement by younger minerals, but not all of the younger minerals in the composite units need have been formed by replacement. Indeed, the net gain of 3 tons of topaz does not appear to represent replacement at all, as this mineral is an early-stage constituent of the composite units, and is partly replaced by the lepidolite and cleavelandite. It is younger, however, than most of the mineral constituents of materials X and Y. With regard to the lepidolite, if as much as half of the large central mass of this mineral were formed by replacement, substantial quantities of the earlier minerals must have disappeared without a trace.

TABLE 7. MINIMUM GAINS AND LOSSES OF OXIDES IN DEVELOPMENT OF COMPOSITE UNITS A, B, AND C FROM THEIR IMMEDIATE ANTECEDENTS, MATERIALS X AND Y

	Gain (From development of minerals by replacement and by direct crystallization from fluids) (Short tons)	Loss (From removal of solid material from X and Y by reaction and replacement) (Short tons)	Loss (Representing contributions from other parts of X and Y: fluid material and/or other replaced solid material) (Short tons)
SiO_2	496.8	225.2	271.6
Al_2O_3	225.7	19.6	206.1
CaO	1.0	0.6	0.4
Na_2O	49.0	4.6	44.4
K_2O	62.6	9.2	53.4
Li_2O	22.1	0.3	21.8
H_2O	13.9	0.2	13.7
F	27.8	0.0	27.8
	898.9	259.7	639.2[a]

[a] Discrepancy between this sum and 627.6, the sum of the "not-accounted-for" portions of Materials X and Y, represents the correction for O equivalent to F.

The net amount of material transfer involved in the mineral replacements was of course considerably less than the losses and additions of mineral species as such. The K_2O liberated during the albitization of potash feldspar, for example, was available for development of muscovite and lepidolite, and the Li_2O derived from spodumene was available for the development of lepidolite. The minimum gains and losses of oxide constituents are shown in Table 7, the right-hand column of which represents the bulk composition of the materials needed for net conversion of demonstrably solid parts of materials X and Y to the composite units A, B, and C.

The composition of these materials is expressed as proportions of oxide constituents in Table 8. This would be an approximation of the actual composition of fluids plus any earlier-formed solids, if the entire process of transfer took place under essentially closed-system conditions. On the other hand, if open-system conditions prevailed, much material probably would have been added to the system, and appropriate amounts of material would have escaped; in this case the figures in Table 8 would represent the effective composition of the materials that actually took part in final development of the composite units.

TABLE 8. COMPOSITION OF FLUID AND/OR SOLID MATERIAL NEEDED FOR NET CONVERSION OF THE DEMONSTRABLY SOLID PARTS OF MATERIALS X AND Y TO THE COMPOSITE UNITS A, B, AND C

SiO_2	43.3
Al_2O_3	32.8
CaO	0.1
Na_2O	7.1
K_2O	8.5
Li_2O	3.5
H_2O	2.2
F	4.4
	101.9
Correction for O equivalent to F	1.9
	100.0

Discussion and conclusions

Whether or not the composite units were formed under open-system conditions, it is interesting to compare the net composition of the very late-stage materials with the bulk composition of the dike (Tables 6 and 8). The dike as a whole is markedly richer in SiO_2, but poorer in almost all other constituents. It should also be noted, however, that the concentrations of Li_2O, H_2O, and F in the late-stage fluids (and solids, if present) need not have been as great as one might expect from casual observation of the inner units of the dike.

It has been emphasized that, although evidences of mineral replacement are widespread in the dike, the *amount* of demonstrable replacement material is relatively small as compared with the bulk of the pegmatite. Even in the lepidolite-rich composite unit, it cannot be proved that more than 22 per cent of the present space was occupied by solid material prior to the attack of this material by replacing fluids. For purposes of discussion, however, let it be assumed that as much as 85 per cent of this space actually was occupied by crystallized pegmatite prior to replacement, and that the replacement thus was much more extensive than is indicated by any evidence now available. The solid material probably would have consisted mainly of quartz and some potash feldspar and spodumene, as previously noted, and hence probably would have contained at least 630 tons of SiO_2. Inasmuch as the entire unit, as now exposed, contains only about 465 tons of SiO_2, at least 165 tons necessarily would have been expelled preferentially from the space now occupied by this rock.

There is little evidence for such wholesale expulsion of silica at a late stage in the development of the Pidlite dike. Indeed, the late-stage replacement in its outer parts, much of which seems best attributed, on structural grounds, to fluids that were ejected from its innermost parts, testifies to a large-scale introduction of Al, Na, H_2O, and F, but not of silica. The mineral replacements noted on earlier pages plainly involved reductions, rather than increases, in the proportion of SiO_2 during development of the final products.

It might be argued, to be sure, that silica was expelled from the dike as a whole, and was fixed in silicate minerals within the surrounding country rock. This may well have happened on a small scale. Granting that much larger quantities could be disposed of in this way without effecting marked changes in the rock, no evidence of such major transfer could be found, despite the most careful search. A few veinlets of quartz do occur in the wallrock, but their total volume in the mine area is trivial. The only noteworthy change in the rock adjacent to the pegmatite body is the conversion of hornblende to biotite, and this almost certainly involves no increase in silica; moreover, it appears to be associated with the earlier, rather than the later, stages in the history of the dike. It can only be concluded that if large amounts of SiO_2 were introduced into the country rock during development of the composite pegmatite units, their effects on the rock were too subtle to be recognized by ordinary examination in the field or under the microscope.

The quantitative analyses of pegmatite units and of replacement features in the dike indicate that all the observed relations can be accounted for if the zones were developed by fractional crystallization of a pegmatite magma, and if the composite units were developed in part by replacement of earlier-formed zonal material and in larger part by direct crystallization from residual fluid or fluids, especially if the period of major replacement began when 15 per cent to 25 per cent of the dike still was fluid. The general conditions would approach those of a closed system, with emphasis on transfer of materials within the pegmatite body during the latest stages of its development, rather than on introduction of some materials from sources outside the pegmatite body, accompanied by the escape of others into the enclosing country rock. That the dike actually did develop in this way is suggested by the textural, structural, compositional, and age relations of the different units, as well as by their disposition within the dike.

There is no positive evidence to indicate that the central part of the dike, now occupied mainly by lepidolite, was composed largely of solid material prior to development of lepidolite and other minerals by replacement of still earlier minerals. If it were, it would be difficult to account for the implied removal of SiO_2 in large quantities by fluids whose sources lay wholly within the dike. The ratio of expelled silica to fluids available for carrying this silica would be very high, and the effects of deposition from such concentrated solutions should be evident within or adjacent to the dike.

More dilute solutions presumably could have removed the silica and distributed it through large volumes of country rock, but the source of such solutions necessarily would lie outside the margin of the dike, owing to the large amounts of fluid material required. This in turn bespeaks open-system conditions during the end stages of the pegmatite formation, for which there is little evidence in the Pidlite dike. It seems best, therefore, to regard development of the lepidolite as involving both replacement of earlier minerals and direct crystallization from residual pegmatite fluid.

References

Andersen, Olaf (1931), Discussion of certain phases of the genesis of pegmatites: *Norsk. Geol. Tidsskrift*, **7**, 1–56.

Barth, T. F. W. (1952), Theoretical petrology, pp. 218–224, 317–320, John Wiley and Sons, Inc., New York.

Björlykke, Harald (1937), The granite pegmatites of southern Norway: *Am. Mineral.*, **22**, 241–255.

Bowen, N. L. (1933), The broader story of magmatic differentiation, briefly told, in Ore deposits of the Western States, pp. 106–128, *Am. Inst. Min. Met. Eng.*, New York.

Cameron, E. N., Jahns, R. H., McNair, A. H., and Page, L. R. (1949), Internal structure of granitic pegmatites: *Econ. Geol., Mon.* **2**, 115 pp.

Chayes, Felix (1946), Linear analysis of a medium-grained granite: *Am. Mineral.*, **31,** 261–275.

——— (1949), A simple point counter for thin-section analysis: *Am. Mineral.*, **34,** 1–11.

——— (1950), On a distinction between late-magmatic and post-magmatic replacement reactions: *Am. Jour. Sci.*, **248,** 22–36.

——— (1951), A cooperative investigation of precision and accuracy in chemical, spectrochemical, and modal analyses of silicate rocks. Part 5. Modal analyses of the granite and diabase test rocks: *U. S. Geol. Survey, Bull.* **980,** 59–68.

Eckel, E. B. (1933), A new lepidolite deposit in Colorado: *Amer. Ceramic Soc., Jour.*, **16,** 239–245.

Fersman, A. E. (1931), The pegmatites: *Acad. Sci., U.R.S.S.*; Translated from the Russian into French under the direction of R. du Trien de Terdonck and J. Thoreau, 422–423, 535–536, 556, Univ. of Louvain, Belgium, 1951.

Flawn, P. T. (1951), Pegmatites of the Van Horn Mountains, Texas: *Econ. Geol.*, **46,** 163–192.

Hanley, J. B., Heinrich, E. W., and Page, L. R. (1950), Pegmatite investigations in Colorado, Wyoming, and Utah: *U. S. Geol. Survey, Prof. Paper* **227,** 125 pp.

Heinrich, E. W. (1952), Chemical differentiation of multi-generation pegmatite minerals (abstract): *Geol. Soc. Amer., Bull.*, **62,** 1261.

Heinrich, E. W., and Levinson, A. A. (1953), Studies in the mica group; mineralogy of the rose muscovites: *Am. Mineral.*, **38,** 25–49.

Hess, F. L. (1925), The natural history of the pegmatites: *Eng. and Min. Jour.*, **120,** 289–298.

Higazy, R. A. (1949), Petrogenesis of perthite pegmatites in the Black Hills, South Dakota: *Jour. Geol.*, **57,** 555–581.

Jackson, C. F., and Knaebel, J. B. (1932), Sampling and estimation of ore deposits: *U. S. Bur. Mines, Bull.* **356.**

Jahns, R. H. (1946), Lithium-tantalum pegmatites in Mora County, New Mexico (abstract): *Geol. Soc. Amer., Bull.*, **57,** 1208.

——— (1951), Geology, mining, and uses of strategic pegmatites: *Am. Inst. Min. Met. Eng., Trans.*, **190,** 45–59.

——— (1953), Pegmatite deposits of the White Picacho district, Maricopa and Yavapai Counties, Arizona: *Arizona Bur. Mines, Bull.*, **162.**

Jahns, R. H., and Adams, J. W. (1953), Beryl deposits in the Harding pegmatites, Taos County, New Mexico (abstract): *Econ. Geol.*, **48,** 328–329.

Jahns, R. H., and Wright, L. A. (1951), Gem- and lithium-bearing pegmatites of the Pala district, San Diego County, California: *California Div. Mines, Spec. Rept.* **7-A,** 72 pp.

Johannsen, Albert (1932), A descriptive petrography of the igneous rocks, Vol. II, The quartz-bearing rocks, The University of Chicago Press, Chicago, Illinois.

Kemp, J. F. (1924), The pegmatites: *Econ. Geol.*, **19,** 697–723.

Landes, K. K. (1925), The paragenesis of the granite pegmatites of central Maine: *Am. Mineral.*, **10,** 355–411.

——— (1933), Origin and classification of pegmatites: *Am. Mineral.*, **18,** 33–56, 95–103.

——— (1935), Colorado pegmatites: *Am. Mineral.*, **20,** 319–333.

Lincoln, E. C., and Reitz, H. L. (1913), The determination of the relative volumes of the components of rocks by mensuration methods: *Econ. Geol.*, **8,** 120–139.

Montgomery, Arthur (1950), Geochemistry of tantalum in the Harding pegmatite, Taos County, New Mexico: *Am. Mineral.*, **35,** 853–866.

Page, L. R. (1950), Uranium in pegmatites: *Econ. Geol.*, **45,** 12–34.

Quirke, T. T., and Kremers, H. E. (1943), Pegmatite crystallization: *Am. Mineral.* **28,** 571–580.

Schaller, W. T. (1925), The genesis of lithium pegmatites: *Am. Jour. Sci., 5th ser.*, **10,** 269–279.

—— (1926), Mineral replacements in pegmatites: *Am. Mineral.*, **12,** 59–63.

——— (1933), Pegmatites, in Ore deposits of the Western States, 144–151, *Am. Inst. Min. Met. Eng.*, New York.

Schwartz, G. M., and Leonard, R. J. (1926), Alteration of spodumene in the Etta mine, Black Hills, South Dakota: *Am. Jour. Sci., 5th ser.*, **11,** 257–264.

Shand, S. J. (1944), The terminology of late-magmatic and post-magmatic processes: *Jour. Geol.*, **52,** 342–350.

Thomson, Ellis (1930), Quantitative microscopic analysis: *Jour. Geol.*, **38,** 193–222.

Winchell, A. N., and Winchell, Horace (1951), Elements of optical mineralogy. Part II. Descriptions of minerals (Fourth ed.), p. 510.

CLINTONITE AS A CONTACT-METASOMATIC PRODUCT OF THE BOULDER BATHYLITH, MONTANA

ADOLPH KNOPF, *Stanford University, Stanford, California.*

ABSTRACT

The brittle mica clintonite occurs with grossularite, hydrogrossular, vesuvianite, blue spinel, and other minerals in a pyrometasomatically altered limestone xenolith enclosed in granodiorite of the Boulder bathylith south of Helena, Montana.

It occurs also at other places in the contact zone of the main bathylith or in those of its satellitic stocks, generally associated with black spinel. Specially fine material was found in the famous old mining camp of Elkhorn, on the east border of the bathylith, and xanthophyllite, a member of the clintonite group, has been reported by Felts (1947) to occur at the southern border of the bathylith.

CLINTONITE NEAR HELENA, MONTANA

A striking association of minerals occurs in a xenolith of limestone near the head of Dry Gulch, 5 miles south of Helena, Montana. The xenolith is enclosed in basic granodiorite ($d=2.79$) near diorite in composition, which constitutes the earliest plutonic mass in the sequence of intrusions that makes up the great composite body known as the Boulder bathylith. The xenolith is situated 300 feet from the contact with the late Mesozoic rocks that the bathylith here intrudes. The xenolith is a slab 30 or more feet long and 5 feet thick, trending N. 30° E. and dipping 70° S. It has been explored by a prospect adit, and because azure-blue spinel is a conspicuous constituent of the deposit, the prospect will here be referred to as the Blue Spinel prospect.

The deposit, or mass of tactite, is made up largely of four minerals: vesuvianite, a pale-green, nearly white grossularite, hydrogrossular, and calcite. The brittle mica clintonite, in pearly white plates, and blue spinel are the most striking constituents. Vesuvianite of pale greenish yellow color is probably the dominant mineral. Subordinately occur diopside, calcic plagioclase, scapolite, pale blue tourmaline, epidote, phlogopite, muscovite, chlorite, calcite, and stilbite. The mass manifestly represents a deposit that was formed at high temperature and was somewhat altered by retrograde changes during the stage of falling temperature.

The granodiorite is cut by narrow dikes of aplite, which is essentially a panidiomorphic aggregate of microcline and quartz, with more or less micropegmatite. Both the granodiorite and aplite adjacent to the xenolith have locally been altered; the granodiorite by epidotization and the aplite by the metasomatic introduction of diopside, epidote, and sphene. Hence the alteration of the xenolith to tactite took place after the aplite dikes had been injected.

The white grossularite, which rarely shows crystal forms, has an index of refraction of 1.739, being therefore close in composition to the ideal mineral ($n=1.734$); it is absolutely colorless in oils and is completely isotropic. On further investigation, some of the white vitreous supposed grossularite was found to have an index of refraction of approximately 1.725. This low value suggested that the mineral is hydrogrossular (Hutton, 1943). Dr. C. O. Hutton very kindly established that the mineral is hydrogrossular: 1, by determining that magnesium is absent, thereby ruling out the possibility that the low index is the result of pyrope in solid solution with the grossularite; and 2, by determining that water is present in considerable amount. An unsolved problem is whether the hydrogrossular thus found was developed by the hydration of earlier formed grossularite. The grossularite and possibly the diopside are the oldest minerals in the deposit. They were subsequently fractured, and a succession of minerals was deposited. The paragenetic sequence appears to be: 1, grossularite and diopside; 2, vesuvianite; 3, clintonite and blue spinel; 4, calcic plagioclase (bytownite); 5, scapolite; 6, epidote; 7, phlogopite; 8, muscovite; 9, chlorite; 10, calcite; and 11, stilbite. Near the end of the period of the formation of the minerals, removal of material outstripped deposition. Small open channel-ways were formed and were partly filled by spherules and radiating groups of stilbite.

The blue spinel occurs in irregular masses and sporadically as perfectly-formed octahedrons, up to 5 mm. in length. The finest of these octahedrons is embedded in vesuvianite. In oils, the spinel is colorless, and its index of refraction is 1.72, indicating nearly pure $MgAl_2O_4$($n=1.715$). The calcite in the deposit is mostly white, but some is sky blue. Under the microscope the calcite is biaxial, 2E being about 20°. Scapolite is a minor constituent of the deposit, though in places it is megascopically visible as columnar aggregates as much as 3 cm. long. It is a sodic scapolite, $\omega=1.556$ and $\epsilon=1.544$, indicating that its composition is $Ma_{70}Me_{30}$.

Diopside is abundant in some thin sections, and the strong dispersion $r>v$ on the optic axis B indicates an aluminous, fassaitic pyroxene.

The clintonite occurs as fan-shaped groups of snow-white color and pearly luster. The maximum size is 1.5 cm. across. It is embedded either in vesuvianite or in calcite, and may have blue spinel associated with it. Under the microscope the clintonite is colorless. Because of the high index of refraction, basal sections show shagreened surfaces. These sections give a uniaxial or nearly uniaxial negative interference figure. Some of the clintonite is interleaved with a colorless phlogopite and partly replaced by it; and in places both the clintonite and phlogopite have been altered to white chlorite, probably leuchtenbergite.

Dr. Horace Winchell has kindly made precise determinations of some of the properties of the clintonite. The density is 3.03. The γ index of refraction, is 1.6591 for sodium light. The dispersion of that index is rather high—$F-C=0.0451$. α is probably about 1.646. The birefringence is therefore 0.013. *X*-ray patterns of the clintonite were taken at Yale University by Mr. James W. Clarke, and of seybertite from the type locality in New York (Brush Collection No. 3965) and of xanthophyllite from Crestmore, California (Brush Collection No. 5910). All three patterns are closely similar, but the clintonite from Montana corresponds most nearly with the seybertite from New York. As the type seybertite is known to contain 1.26 per cent of fluorine, it seemed desirable to test the Montana mineral for fluorine. A qualitative test by Dr. C. O. Hutton showed that fluorine is present.

In view of the present knowledge of this group of brittle micas the name clintonite appears to be the most appropriate for the Montana mineral. According to Koch (1935), who has done the most careful work on this group in recent years, in fact supplying four new analyses made on centrifuged material: "the warrant for grouping together the brittle micas clintonite [seybertite], xanthophyllite, and brandisite under the name clintonite is clear from the analyses and optical data of these minerals. The identity in crystallographic and chemical properties is so close that a single name must be considered as fully justified." Winchell and Winchell (1951) voice the same opinion: "xanthophyllite, brandisite, and seybertite are sometimes considered varieties of clintonite; they are almost identical." However, more work on the clintonite group (as used in the restricted sense of comprising xanthophyllite, brandisite, and seybertite) is clearly desirable.

When Eakle in 1916 described xanthophyllite as a product of contact metamorphism occurring at Crestmore, California, associated with blue calcite and monticellite, he commented on the fact that the two previously recorded occurrences of xanthophyllite were in schists—talc schist and chlorite schist. However, the original "clintonite" discovered by Finch, Mather, and Horton in 1828 at Amity, New York (which name became according to Dana (1892) a *nomen nudum* because of prior publication of the name seybertite by Clemson in 1832) is a contact-metamorphic mineral in limestone associated with amphibole, spinel, graphite, and leuchtenbergite (Tschermak and Sipöcz, 1879). Brandisite also is a contact-metamorphic mineral, doubtless pyrometasomatic, occurring in the Fassatal, Tyrol, in limestone in association with the aluminous pyroxene fassaite and black spinel.

The clintonite found by Laitakari (1921) at three localities in the Parainen (Pargas) district, Finland, occurs in parageneses very similar to those around the Boulder bathylith. It occurs in limestone with pargasite, sky-blue spinel, and phlogopite. In Tenby the clintonite is associated with scapolite, grossularite, vesuvianite, and diopside. The clintonite is either colorless or very pale green. The largest individual was 4 cm. in diameter.

CLINTONITE AT OTHER LOCALITIES

Tactite containing clintonite occurs along the border of the granodiorite stock northwest of the trestle of the Northern Pacific Railway across Greenhorn Gulch. This stock is 1 mile north of the Boulder bathylith and is 0.4 square mile in area. It is intrusive into early Paleozoic formations ranging from the Meagher limestone of Middle Cambrian age to the Jefferson formation of late Devonian age. The tactite consists, in descending order of abundance, of diopside, serpentinized forsterite, biaxial calcite, clintonite, and phlogopite. Some of the clintonite incloses minute octahedrons of spinel. The clintonite as seen in hand specimens is vitreous with bronzy metallic reflections. In thin section it is faintly pleochroic, being brownish rose transverse to the cleavage and showing maximum absorption in that position—a feature found to be a valuable diagnostic aid in distinguishing clintonite from other minerals.

Clintonite was recognized to occur in the Marysville district (Knopf, 1950), where it replaces the diopside, in the superb scapolite-diopside hornfelses that make up Drumlummon Hill.

A tactite containing clintonite occurs in the Madison limestone on the border of the Spring Hill granodiorite stock, 5 miles southwest of Helena. It is S. 30° E. of the summit of Spring Hill. The tactite consists of vesuvianite, calcite, black spinel, and clintonite. The clintonite is more or less filled with octahedrons of spinel. It is weakly pleochroic: nearly colorless parallel to Z and brownish yellow parallel to X, the maximum absorption being perpendicular to the elongation and cleavage.

In the contact zone of a small diorite stock ($d = 2.81$) west of Holmes Gulch, which is a few miles southeast of Helena, is a blackish rock containing innumerable minute octahedrons (1 mm. or less in size) of black spinel in a poikilitic matrix of calcite and clintonite. As seen under the microscope, the spinel is green, with strong central pigmentation and the borders nearly colorless. A strange feature is that countless minute octahedrons are juxtaposed around large crystals of spinel. About half the tactite consists of spinel. The clintonite, which occurs as rather large metacrysts, is crowded with euhedral spinel. The only other constituent is the white chlorite leuchtenbergite in small amount.

Clintonite, so far as now known, occurs at two localities at Elkhorn on the eastern margin of the Boulder bathylith. It was recognized by the writer to occur as a minor constituent in a specimen collected by Barrell in 1899 (Yale University Petrographic Coll. No. 3289). This tactite has a density of 3.15 and is made up chiefly of vesuvianite and clinopyroxene, with 15 per cent of calcite. The clintonite in this rock also is faintly pleochroic. Geologically, the tactite occurs in the contact zone of the gabbro mass of Black Butte.

The finest clintonite-spinel tactite was found to occur in a small prospect pit on the divide between Elkhorn and Queen gulches. The rock is nearly black because of the prevalence of closely crowded minute octahedrons of black spinel, and is more or less spangled with plates of clintonite. As found microscopically, the tactite is made up dominantly of green spinel and clintonite in lamellar-radiate groups, with subordinate colorless phlogopite and diopside, probably fassaitic, as it shows strong dispersion $r>v$ on the optic axis B.

Xanthophyllite has been reported by Felts (1947) to occur at the south end of the Boulder bathylith. It is associated with grossularite, diopside, vesuvianite, forsterite, and calcite; much of the forsterite and diopside are now serpentine.

In conclusion, clintonite has been shown to occur from the contact zone of the Marysville granodiorite stock on the north, 6 miles north of the Boulder bathylith, to the southern end of the bathylith. It generally has spinel occurring with it, in places abundantly so, an association that harmonizes with the fact that clintonite is low in silica (18 per cent) and high in alumina (40 per cent).

REFERENCES

Dana, J. D. (1892), System of Mineralogy, 6th ed., 638–639.

Eakle, A. S. (1916), Xanthophyllite in crystalline limestone: *Washington Acad. Sci. Jour.*, **6**, 332–335.

——— (1917), Minerals associated with the crystalline limestone at Crestmore, Riverside County, California: *Univ. California Dept. of Geology Bull.* **10**, no. 19, 341–342.

Felts, W. M. (1947), Xanthophyllite near Butte, Montana: *Geol. Soc. Amer. Bull.* **58**, 1179 (abstract).

Forman, S. A. (1951), Xanthophyllite: *Am. Mineral.*, **36**, 450–457.

Hutton, C. O. (1943), Hydrogrossular, a new mineral of the garnet-hydrogarnet series: *Roy. Soc. New Zealand Trans. Proc.* **43**, 49–51.

Knopf, Adolph (1950), The Marysville granodiorite stock, Montana: *Am. Mineral.*, **35**, 834–844.

Koch, G. (1935), Chemische und physikalisch-optische Zusammenhänge innerhalb der Sprödglimmergruppe: *Chemie der Erde*, **9**, 458–461.

Laitakari, A. (1921), Ueber die Petrographie und Mineralogie des Kalksteinlagerstätten von Parainen (Pargas): *Comm. Geol. Finlande Bull.*, **54**, 87–89.

Stevens, R. E. (1946), A system for calculating analyses of micas and related minerals to end members: *U. S. Geol. Survey Bull.* **950**, 113.

Tschermak, G., and Sipöcz, L. (1879), Die Clintonitgruppe: *Ztschr. Krist.*, **3**, 496–515.

Winchell, A. N., and Winchell, Horace (1951), Elements of optical mineralogy, Part II, 391.

ZONED ZIRCON FROM OKLAHOMA*

Esper S. Larsen, Jr., C. L. Waring, and Joseph Berman
U. S. Geological Survey, Washington, D. C.

Abstract

Large zircon crystals from a pegmatite body in the Wichita Mountains, Oklahoma, are zoned with fresh and metamict zircon. The metamict zircon is chiefly isotropic $n=1.82$; some is uniaxial positive, $\omega=1.85$, $\epsilon=1.86$. The change from fresh to metamict zircon seems to be an abrupt and not a gradual one.

The age of the zircon is determined as 635 million years from α determinations and 641 million years from chemical determinations of uranium and thorium.

Introduction

The zircon described is from the collections of the U. S. National Museum; similar specimens from the same locality are on deposit in many museums. This zircon is from a pegmatite body that cuts the Quanah granite of Shannon (1917) (sec. 21, T. 3 N., R. 15 W., Comanche County, Okla.) in Quanah Mountain, in the Wichita Mountains of Oklahoma. The pegmatite is the youngest pre-Cambrian rock of the area. The zircon is rather abundant in the pegmatite and forms stout brown crystals some of which are more than 30 mm. long. The crystals show recurrent zones of fresh and metamict zircon.

The fresh zircon is shattered and along the fractures has a little dust of reddish-brown material. It has the properties of nearly all the fresh zircon we have studied and is uniform, $\omega=1.918$, $\epsilon=1.971$. The main part of the metamict zircon is tough, hornlike, and isotropic with $n=1.82$. It is cut by a network of tiny veinlets of material that is moderately birefracting and extinguishes as a unit in any crystal along with the fresh zircon. Its form indicates that it is not fresh zircon but an alteration product, probably formed during or after the isotropic material.

Powdered crystals of the zircon show a small amount of metamict zircon that is weakly magnetic, uniaxial positive, with ω about 1.85, ϵ 1.86. This material is present in some zones of the zircon and it extinguishes with the fresh zircon.

This study is part of a program undertaken by the U. S. Geological Survey on behalf of the Division of Research of the Atomic Energy Commission.

Chemical Analyses

The first crystals furnished by Frank L. Hess of the U. S. Bureau of Mines were studied by E. S. Larsen, Jr., and R. C. Wells in 1922. The crystal selected for analysis had a large core of shattered fresh zircon, an intermediate zone of compact, firm, metamict zircon, and a pale outer skin that was metamict (Wa, Wb, and Wc respectively of Table 1). The three zones were sharply separated by rough crystal faces. The shattered inner fresh zircon was picked out with a needle, and separates were cleaned by hand-picking. The analyses of the three zones, made by Wells, are shown in Table 1.

---

* Publication authorized by the Director, U. S. Geological Survey.

TABLE 1. ANALYSES OF THREE ZONES FROM ZIRCON CRYSTALS

(R. C. Wells, analyst)

	Wa	Wb	Wc	Theoretical $ZrSiO_4$	Average
SiO_2	25.9	30.2	28.4	32.7	31.2
Fe_2O_3	3.8	3.2	1.2		2.6
Al_2O_3		0.7			Trace
CaO		0.4			0.3
Rare earths	0.6	3.9	1.6		3.5
ZrO_2	67.6	60.3	66.4	67.3	60.2
H_2O					1.5
					99.3

Wa—Hand-picked from the shattered core of a large crystal of about 98 per cent fresh zircon ($\omega=1.918$, $\epsilon=1.971$) and 2 per cent isotropic metamict zircon ($n=1.82$).

Wb—Compact, metamict material forming main part of the crystal. About 90 per cent isotropic ($n=1.82$).

Wc—Outer metamict skin of crystal. Isotropic ($n=1.82$) and weakly birefracting (uniaxial positive, $\omega=1.86$, $\epsilon=1.87$).

Average is analysis of whole crystal.

Analysis Wc is fairly near the composition of theoretical zircon but is 4 per cent low in SiO_2. Analysis Wb is about 6 per cent low in ZrO_2+HfO_2 and $2\frac{1}{2}$ per cent low in SiO_2. It is high in rare earths and Fe_2O_3. In general the fresh zircon is much poorer in U, Th, and Pb than the metamict part. It is poorer in the rare earths, especially Dy and Yb, and is somewhat richer in Hf. In 1952, new separates were made on several crystals with the Frantz isodynamic separator. The three separates were analyzed spectrographically by Waring, with the results given in Table 2. The data given in Table 2 for fresh zircon (Sa) are for material that is only 94 per cent fresh zircon. Calculations from this and from the data for the metamict zircon indicate only approximately 0.04 per cent Th and 0.006 per cent U in the fresh zircon.

TABLE 2. SPECTROGRAPHIC ANALYSIS OF FRESH AND METAMICT ZIRCON

(C. L. Waring, analyst)

	Fresh	Metamict	
	Sa	Sb	Sc
Fe	1.6	1.8	2.0
Al	0.6	0.4	0.2
Ca	0.2	0.3	0.1
Th	0.08	0.6	0.8
Nb	<0.01	<0.01	<0.01
Pb	0.0045	0.034	0.036
Hf	0.9	0.7	0.5
B	0.01	0.01	0.02
Mg	0.008	0.01	0.02
Ba	0.02	0.01	0.01
Mn	0.007	0.007	0.01
Cu	0.008	0.01	0.005
V	0.004	0.009	0.009
Sn	0.001	<0.001	0.006
Ti	0.004	0.005	0.005
Sr	0.001	0.002	0.001
Cr	0.001	0.001	0.001
Dy[1]	<0.04	0.2	0.2
Y	0.7	0.9	0.9
Yb	0.09	0.4	0.4
Ce	0.01	0.01	0.01
Ra	0.01	0.01	0.01
Er[2]	0.1 to 1.0	0.1 to 1.0	0.1 to 1.0
Tm	0.01 to 0.1	0.1 to 1.0	0.1 to 1.08
Lu	0.01 to 0.1	0.1 to 1.0	0.1 to 1.0
Ho	<0.01	0.01 to 0.1	0.01 to 0.1
U[3]	0.013	0.117	0.165
Loss on ignition 1 hr. at 1000 C.		0.96	1.17

Sa—Nonmagnetic fresh zircon 94 per cent ($\omega=1.92$), 2 per cent isotropic material ($n=1.82$), 2 per cent weakly birefracting ($\omega=1.85$), and 2 per cent cloudy.

Sb—Weakly magnetic (1.5 A), 88 per cent isotropic (n near 1.82), 10 per cent weakly birefracting ($\omega=1.86$), 2 per cent fresh zircon.

Sc—Weakly magnetic (1.0 A) 87 per cent isotropic, 10 per cent weakly birefracting, 3 per cent fresh zircon.

[1] Rare earths were determined spectrographically by a chemical concentration method (Waring and Mela, 1953).

[2] This group of rare earths was tested semiquantitatively, as no pure chemicals were available for preparation of quantitative standards.

[3] U determined by fluorescent method by Frank Cuttitta.

TABLE 3. AGE OF OKLAHOMA ZIRCON FROM α-COUNTS AND FROM SPECTROGRAPHICALLY DETERMINED Pb

Number	Per cent fresh zircon	Pb ppm	α c/mg/hr	Age (million years)
Z 61	96	43	168	575
1	98	88	326	621
3	97	41	150	628
Sa (no acid)	98	45	170	609
Sa (acid)			152	
Z 61A	96		160	
2	5	290	1103	605
2a (no acid)	5	352	1380	587
2a (acid)		350	1292	623
4	10	335	1220	632
4a	10	380	1270	699
Sb (no acid)	11	340	1180	663
Sb (acid)			1050	
Sc (no acid)	5	360	1230	673
Sc (acid)			1210	
Z 63	3	343	1190	663
Z 63 (acid)		339	1168	664

AGE

The Oklahoma zircons were used to test the suitability of using zircon for age determination. Determinations on 13 samples were made by the ratio of α-counts as measured with a Geiger counter and Pb as determined by the spectrograph (Larsen *et al.*, 1952). The approximate formula for this measurement is $T(MY) = aPb/\alpha$ where a is 1990 for Th alone and 2680 for U alone. An average value for the Oklahoma zircons is 2300. The results are given in Table 3. Four of these samples (1, 2, 3, 4) are quoted from Larsen, Keevil, and Harrison (1952) after correcting for the ratio of 100 U/eU as 44 for these zircons. The age determinations range from 576 to 699 million years and average 635 million years. In the course of our study, data for U and Th were secured on six of the samples used for α counting, and the ages determined for these six samples are given in Table 4.

$$T(MY) = \frac{7230\ \mathrm{Pb}}{\mathrm{U} + (0.322\ \mathrm{Th})}.$$

The standard deviation, the average value, and the probable range within which nine out of ten measurements should fall for the four measurements of fresh zircon, nine of metamict zircon, all thirteen measurements of zircon (fresh and metamict), and the six determinations of zircon by chemical methods are given in Table 5.

TABLE 4. AGE OF OKLAHOMA ZIRCON FROM Pb DETERMINED BY THE SPECTROGRAPH, FROM U DETERMINED BY THE FLUORESCENT METHOD, AND FROM Th DETERMINED CHEMICALLY AND SPECTROGRAPHICALLY

Number	Per cent fresh zircon	U	Th	Pb	Age (million years)
		(parts per million)			
2a	5	1800	7000±	352	630
4a	10	2300[1]	6130[1]	380[2]	643
Sb	11	1170[3]	6000[4]	340	790
Sc	5	1650[3]	8000[3]	360	615
Z 61	96	296	810[5]	43	572
Z 63	3	1650	7600[5]	343	615
					Average = 644

Using formula $\text{Age} = \dfrac{7230\ \text{Pb}}{\text{U} + 0.322\ \text{Th}}$

[1] Determined chemically by Robert G. Milkey.

[2] Pb determined chemically by Harry Levine.

[3] Determined by Frank Cuttitta.

[4] Determined spectrographically by Waring.

[5] Determined by John Rosholt.

TABLE 5. STATISTICAL DATA ON MEASUREMENTS OF AGE OF ZIRCON

Type	Number of measurements	Average age value (MY)	Standard deviation	Limits for 9 out of 10 measurements
Fresh zircon	4	608	23.8	±28
Metamict	9	645	39.0	±24.7
All α-measurements	13	635	31.0	±16
Chemical	6	641	74	±60

X-RAY DATA

X-ray spectrometer patterns were made of the three different types of Oklahoma zircon described above. The three separates are designated as fresh zircon (61A), weakly birefringent zircon (62), and isotropic and weakly birefringent zircon (63).

The fresh zircon (61A) produced a good x-ray pattern with fairly sharp diffraction lines in the forward 2 θ or larger interplanar spacing region and comparatively weak and diffuse lines in the smaller interplanar spacing region (greater than 90° 2 θ). The separate that is weakly birefringent (62) and the one that contains some isotropic zircon (63) produced almost

Table 6. X-ray Data for Zircon

Oklahoma zircon-"Fresh" #61A mostly crystalline not ignited		Oklahoma zircon #61A ignited to ca 1000° C. ± 25° C. in air		Oklahoma zircon #62 partly metamict not ignited		Oklahoma zircon #62 ignited to ca 1000° C. in air		Oklahoma zircon #63 mostly metamict not ignited		Oklahoma zircon #63 ignited to ca 0000° C. in air		Indian zircon Fresh		Brazilian zircon Fresh		Brazilian zircon heated to ca 1000° C. in air		Cyrtolite Hybla, Ontario, heated to 1000° C.		Cyrtolite Hybla, Ontario, not heated	
d-(Å)^{o}	I*	d-(Å)	I*	d-(Å)	I*	d-(Å)	I*	d-(Å)	I*	d-(Å)	I*	d-(Å)	I*	d-(Å)	I*	d-(Å)	I*	d-(Å)	I*	d-(Å)	I*
4.44	50	4.42	70	4.44	1	4.44	20	4.43	1	4.44	20	4.43	60	4.43	50	4.43	70	4.42	60	4.45B	15
3.31	80	3.30	100	3.30	15	3.30	60	3.30	20	3.30	50	3.30	100	3.30	100	3.30	100	3.30	95	3.32B	50
						2.96^{a}VB	20			2.96^{a}B	20							2.96^{a}	3		
2.653	5	2.644	10			2.64B	1			2.64B	1	2.65	10	2.65	20	2.64	15	2.64	5		
2.528	40	2.515	50	2.52	1	2.52	20	2.52VB	1	2.52 2.51	20	2.517	40	2.517	40	2.514	60	2.515	70	2.54B	10
																				2.51B	5
2.340	10	2.333	30			2.335	1			2.335 2.331	1	2.333	20	2.328	20	2.333	20	2.333	10		
2.222 2.217	8	2.214	20			2.222 2.215	1			2.215	1	2.216	10	2.213	10	2.216	10	2.215	5		
2.067	20	2.065	50			2.067	5			2.063	2	2.063	40	2.065	50	2.064	50	2.062	20	2.07B	Nil
1.916 1.912	8	1.908	15			1.910 1.903	2			1.903	1	1.907	10	1.909	10	1.907	20				
						1.810^{a}VB	5			1.82^{a}B	5							1.82^{a}	Nil		
										1.81^{b}B	5										
1.755 1.751	8	1.750	20			1.752	1			1.751	1	1.750	20	1.750	20	1.750	30	1.748	10		
1.715	60	1.711	60			1.712	15			1.711	15	1.712	70	1.712	70	1.712	70	1.711	40	1.72B	10
1.651	60	1.650	50			1.652	2			1.649	2	1.650	40	1.650	40	1.650	40	1.650	20		
1.549	2	1.546 1.543	5			1.544VB	2			1.543VB	2	1.546	10	1.545	5	1.546	5	1.548	Nil		
1.502	5	1.494	3									1.498	Nil	1.497B	2	1.495	Nil	1.494	Nil		
1.478	8	1.476	3			1.479	2			1.477B	2	1.476	20	1.476	15	1.476	20	1.477	5		
1.382	5	1.380	20			1.380B	1			1.380	2	1.380	20	1.380	15	1.381	20	1.380	5		
1.365B	2	1.361	8			1.364B	1			1.360	1	1.363	5	1.362	5	1.362	10	1.362	3		
1.291	2	1.289	8									1.289	10	1.290	5	1.289	10	1.289VB	10		
1.261	2	1.259	10			1.260B	Nil			1.259	1	1.260	5	1.260 1.259	3	1.259	5	1.258	3		
1.251B	Nil									1.249	3			1.249	3	1.249	Nil				
1.191	3	1.188	25									1.188	10	1.188	15	1.188	Nil	1.188VB	5		
1.188	5																				
1.169	2	1.167	5									1.168	3	1.168	2	1.167	2				
1.166	1																				
		1.108	5									1.1083	5	1.110	5	1.108	3	1.109VB	Nil		
														1.103	5						
1.102	20	1.100	20									1.1001	10	1.101	8	1.101	10	1.101VB	Nil		
		1.068	2									1.0680	3	1.069	5	1.068	2				

TABLE 6—(*continued*)

Oklahoma zircon-"Fresh" #61A mostly crystalline not ignited		Oklahoma zircon #61A ignited to ca 1000° C. ± 25 C. in air		Oklahoma zircon #62 partly metamict not ignited		Oklahoma zircon #62 ignited to ca 1000° C. in air		Oklahoma zircon #63 mostly metamict not ignited		Oklahoma zircon #63 ignited to ca 1000° C. in air		Indian zircon Fresh		Brazilian zircon Fresh		Brazilian zircon heated to ca 1000° C. in air		Cyrtolite Hybla, Ontario, heated to 1900° C.		Cyrtolite Hybla, Ontario, not heated	
d-(Å)[c]	I*	d(Å)	I*	d (Å)	I*	d-(Å)	I*	d (Å)	I*	d (Å)	I*	d-(Å)	I*	d (Å)	I*	d (Å)	I*	d (Å)	I*	d-(Å)	I*
1.061	3	1.059	20			1.062B	1			1.060VB	1	1.0590	5	1.060	10	1.059	10				
1.051VB	3	1.0505	15			1.050B	1			1.051VB	2	1.0503	5	1.0515	10	1.0507	10	1.051B	3		
1.046VB	3	1.0441	3							1.045VB	2	1.0437	5	1.0447	10	1.0443	5	1.041B	3		
1.005B	Nil	1.0011	2									1.0020	Nil	1.003B	Nil	1.002B	Nil				
														1.9769B	5						
0.9745	2	0.9746	2									0.9752	Nil	0.9759	5	0.975B	3				
0.9720	3	0.9714	2									0.9712	2	0.9720	8	0.971B	3				
												0.9586	Nil	0.9593B	Nil	0.959B	Nil				
0.9544B	Nil	0.9538	2									0.9534	2	0.9542	5	0.954B	3				
														0.9438	2						
0.9317B	Nil	0.9318B	Nil									0.9316	Nil	0.9325	2	0.933B	2				
		0.9200	2									0.9200	Nil	0.9205	2	0.9203B	2				
0.9166	2	0.9155	1									0.9157	Nil			0.9159B	10				
		0.8995	3									0.9000B	Nil			0.8996B	3				
		0.8977	3																		
												0.897B	Nil	0.898 0.987 B	2						
		0.8947	Nil													0.8949	Nil				
0.8921B	3	0.8913	15									0.8915	10	0.8920	20	0.8918	20				
												0.8867	2	0.8871	3	0.8867	5				
		0.8863	3									0.8564	3	0.8567	5	0.8563	10				
0.8572B	3	0.8562	3													0.8399B	2				
0.8559	5B	0.8396B	1									0.8328	5	0.8333	15	0.8330	20				
0.8337		0.8328	3									0.8256	3	0.8261	5	0.8257	5				
		0.8254	3													0.8206	Nil				
		0.8207B	1									0.8117	2	0.8122	2	0.8117	5				
		0.8116	3									0.8010	3	0.8013	3	0.8010VB	5				
		0.8008	3									0.7907	3	0.7909	3	0.7900	10				
0.7906B	1	0.7901	8									0.7885	2								
		0.7811	5									0.7811	10	0.7813	2	0.7812	20				

B = broad.
VB = very broad.
* Based on Brazilian zircon with d-distance of 3.30 = intensity of 100.
[a] Cubic ZrO_2.
[b] Some impurity.
[c] All d-distances calculated from 2θ measured with a spectrometer—silicon used as a standard, $\lambda = 1.5405$ Å (copper radiation with nickel filter).

identical poor x-ray patterns with weak, broad, and diffuse diffraction lines. Only the diffraction lines corresponding to the strong lines of fresh zircon appeared. As the zircons become more metamict and consequently more disordered, the x-ray diffraction patterns have weaker, broader, and more diffuse lines, which are difficult to measure accurately. However, the tables of d-spacings (Table 6) indicate that there are only small measurable differences in the d-spacings between the partly metamict zircon and the same specimen after it has been well crystallized by ignition at elevated temperatures.

The x-ray powder patterns indicate that all of the Oklahoma zircons examined show some degree of disorder. Even though the material may look fresh and unchanged optically, the fact that the diffraction lines become broader and more diffuse with increasing 2θ suggests that there exists considerable short-range disorder in the fresh zircon, even though the long-range order is essentially maintained. For purposes of comparison of x-ray data some well-crystallized, well-ordered zircon as well as some nearly completely metamict zircon (cyrtolite) are included in the tables. In order to study these zircons further they were heated to sufficiently high temperatures to cause an ordered crystalline structure. It is observed that different metamict and partly metamict zircons heated to identical temperatures have slightly different lattice parameters. It is reasonable to assume that these differences are due to compositions of the zircons studied.

X-ray data disclose that the Oklahoma zircons here studied occur in different gradations of metamictization. If slightly metamict zircons are heat-treated they readily revert to well-crystallized zircon. The more metamict zircons require higher temperatures and relatively greater time to crystallize. In fact some of the more metamict material crystallizes to zirconium dioxide with amorphous silica. This reaction indicates that the metamict condition in these samples has resulted in some complete disruption of the original zircon structure.

REFERENCES

LARSEN, E. S., JR., KEEVIL, N. B., AND HARRISON, H. C. (1952), Method for determining the age of igneous rocks using the accessory minerals: *Geol. Soc. Am. Bull.*, **63**, 1045–1052.

SHANNON, C. W., AND OTHERS (1917), Petroleum and natural gas in Oklahoma, Part II; A discussion of the oil and gas fields, and undeveloped areas of the state, by counties: *Oklahoma Geol. Survey Bull.* **19**, pl. 12.

WARING, CLAUDE L., AND MELA, HENRY, JR. (1953), Method for determination of small amounts of rare earths and thorium in phosphate rocks: *Anal. Chemistry*, **25**, 432–435.

MORAESITE, A NEW HYDROUS BERYLLIUM PHOSPHATE FROM MINAS GERAIS, BRAZIL*

M. L. Lindberg, W. T. Pecora, *U. S. Geological Survey, Washington, D. C.*

AND

A. L. de M. Barbosa, *Escola de Minas, Ouro Preto, Minas Gerais, Brazil.*

Abstract

Moraesite, a new hydrous beryllium phosphate from the Sapucaia pegmatite mine, Minas Gerais, Brazil, has the composition $Be_2PO_4(OH)\cdot 4H_2O$. It occurs in spherulitic masses, as distinct crystals, and as crusts with a coarse fibrous structure. Crystals are singly terminated needles, acicular [001] with forms {100} and {130} and faces (131) and $(1\bar{3}1)$. Moraesite is monoclinic domatic (m, Cc), or prismatic (2/m, C_{2h}). The specific gravity is 1.805 (measured), 1.806 (calculated). It is biaxal negative, $2V = 65°$; $\alpha = 1.462$, $\beta = 1.482$, $\gamma = 1.490$; $Z = b$, $Y \wedge c = 11°$. Chemical analysis gives P_2O_5 34.76, BeO 25.28, Fe_2O_3 0.11, Al_2O_3 none, H_2O 39.80, insol 0.30, total 100.25%. Possible space groups are $C2/c$ (C^6_{2h}) or Cc (C^4_s). Unit cell dimensions are $a_0 = 8.55$, $b_0 = 36.90$, $c_0 = 7.13$ Å; $\beta = 97°41'$; volume $= 2229$ Å^3; $Z \approx 12$. Moraesite has a superstructure, with a pseudocell in which $b_0 = 12.30$ Å.

The mineral is named in honor of Dr. Luciano Jacques de Moraes, Brazilian geologist.

Introduction

This paper presents a detailed mineralogical description of moraesite, a hydrous beryllium phosphate, the third new mineral from the Sapucaia pegmatite mine, Minas Gerais, Brazil. The first two new minerals, frondelite and faheyite, have been described in earlier papers (Lindberg, 1949; Lindberg and Murata, 1953). These published accounts are preliminary to a more complete description, now in preparation, of the structure and mineralogy of this pegmatite.

The Sapucaia pegmatite mine is in the municipio of Galilea, formerly a part of the municipio of Conselheiro Pena, in the Rio Doce valley region of eastern Minas Gerais. This mine, a substantial producer of mica and beryl, was one of a great number in the mica belt of Minas Gerais under investigation in the period 1942–45 by joint field parties of the U. S. Geological Survey and the Departamento Nacional da Produção Mineral (D.N.P.M.) of Brazil. A suite of mineral specimens from this property, collected intermittently during that period by W. T. Pecora and A. L. de M. Barbosa and examined in preliminary fashion by them in Rio de Janeiro, was turned over to M. L. Lindberg for complete identification and description. The original suite has been augmented by welcomed additions in the period 1950–53, from E. R. Swoboda, Robert Green-

---

* Publication authorized by the Director, U. S. Geological Survey.

wood, Sumner Anderson, and Emerson I. Brown. The authors are particularly grateful to Mr. Greenwood for six hand specimens of excellently developed moraesite.

Moraesite is named after Dr. Luciano Jacques de Moraes, well-known Brazilian geologist, whose original geological investigations have added much to the knowledge of the geology of his beloved state of Minas Gerais. In his role of onetime Director of the D.N.P.M., he gave enthusiastic support to a program of collaboration between his bureau and the U. S. Geological Survey that has since produced a number of geological reports in Portuguese and in English.

The prototype specimens of moraesite have been deposited in the U. S. National Museum (USNM 106,577), Washington, D. C., and in the Museu Nacional, Rio de Janeiro.

OCCURRENCE

Phosphate minerals are most abundant in the central part of the granitic pegmatite at the Sapucaia mine, where they are associated with quartz, beryl, perthite, and muscovite. The pegmatite is oval-shaped in outcrop and internally well zoned (Pecora, *et al.*, 1950, p. 254). Large masses of triphylite and heterosite are the principal phosphate minerals, and individual masses of these minerals up to several tons in weight are not uncommon. In addition to moraesite, other phosphate minerals in-

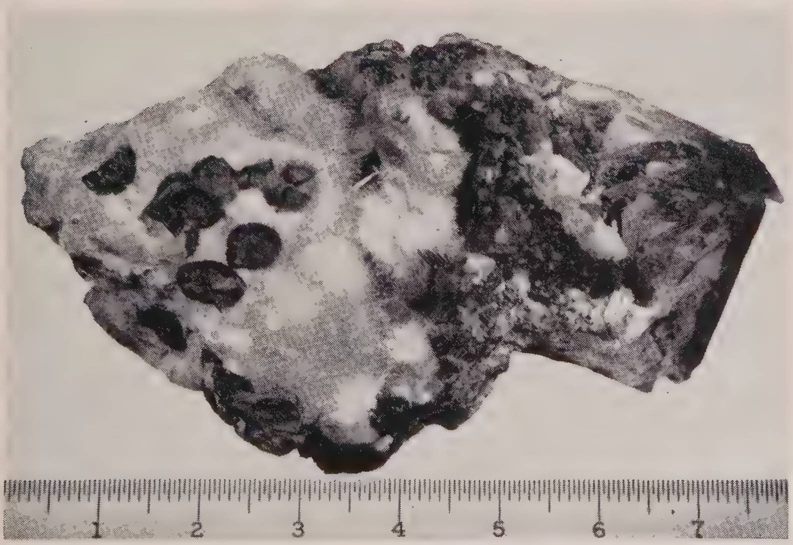

FIG. 1. Moraesite (white needles in crusts and radiating fibers) enclose spherulites of brown frondelite (on left) and are associated with books of muscovite (on right).

clude frondelite, faheyite, hureaulite, childrenite, apatite, roscherite, vivianite, and variscite.

Moraesite occurs in tufted or radial aggregates, in fibrous coatings, or in spherulitic masses on the walls of vugs that have developed in or adjacent to beryl, and on surfaces of albite, quartz, and muscovite (Fig. 1). Growths of moraesite frequently occur on the botryoidal surfaces of frondelite and contain unaltered fragments of beryl. On free surfaces, individual crystals form a fragile and delicate assortment of needles that grade into crusts with a coarse fibrous structure.

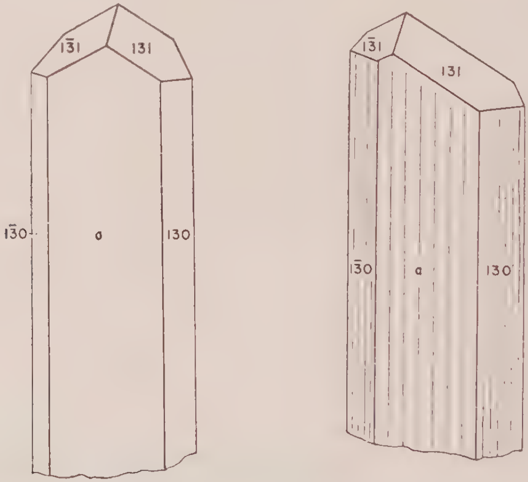

FIG. 2. Moraesite, idealized (left) and natural (right) habit of typical crystals of moraesite.

CRYSTALLOGRAPHY

Crystals are minute singly terminated needle-like laths, acicular parallel to the c-axis [001], and tabular parallel to the orthopinacoid {100}. The pyramid face (131)[1] is usually better developed than ($1\bar{3}1$) and in some crystals gives the general appearance of a basal plane of a triclinic mineral. The faces (130) and ($1\bar{3}0$) are better developed than ($\bar{1}30$) and (130). The orthopinacoid and prism faces of the forms {100} and {130} are striated parallel to the c-axis. Figure 2 shows the idealized and natural habits of crystals. The dimensions of a typical crystal measured parallel to the crystal axes are (|| to c) = 1.0 mm., (|| to a) = .05 mm., (|| to b) = .02 mm.

[1] The {131} and {130} forms are so indexed on the basis of x-ray data which gives the length of the b-axis as 36.9 Å in the true cell. Moraesite has a superstructure, with a smaller pseudocell in which b = 12.3 Å. In this pseudocell the pyramid and prism become {111} and {110}.

The small number of crystal faces observed makes determination of the crystal class uncertain. *X*-ray data indicate a choice of classes: monoclinic, prismatic or domatic. Crystallographic data confirm a plane of symmetry, as indicated by the presence of pairs of faces (131) $(1\bar{3}1)$, (130) $(1\bar{3}0)$, and $(\bar{1}30)$ $(\bar{1}\bar{3}0)$. A two-fold axis would give as possible crystal faces the pairs (131) $(\bar{1}3\bar{1})$, $(1\bar{3}1)$ $(\bar{1}\bar{3}\bar{1})$, (130) $(\bar{1}30)$, and $(1\bar{3}0)$ $(\bar{1}\bar{3}0)$. Crystals of moraesite are singly terminated, and the pyramid faces $(\bar{1}3\bar{1})$ and $(\bar{1}\bar{3}\bar{1})$ have not been observed. However, all four faces of the form $\{130\}$ are present, although not equally well developed. The $(\bar{1}30)$ and $(\bar{1}\bar{3}0)$ faces may be related to the (130) and $(1\bar{3}0)$ faces by a twofold axis (prismatic class), or they may be independently developed (domatic class).

The morphological data determined from measuring 20 crystals on the goniometer are summarized in Table 1. Owing to the small number of forms observed, and the poor quality of the reflections from the striated faces of the prism zone, it became necessary to make use of *x*-ray data to identify the crystal forms observed and to calculate the morphological

TABLE 1. MORPHOLOGICAL DATA

Form	No. of Times Observed	Quality	ϕ		ρ	
			Range	Average	Range	Average
100	25	Poor	88°38′–90°45′	89°38′	89°28′–90°16′	89°51′
160	2	Poor	36°14′–36°28′	36°21′	89°55′–90°04′	90°00′
130	40	Fair	54°47′–56°09′	55°34′	89°41′–90°14′	89°57′
133	1	Fair		65°30′		25°00′
131	30	Fair-Good	59°00′–60°17′	59°22′	48°05′–49°20′	48°35′

TABLE 2. CRYSTALLOGRAPHIC ELEMENTS AND ANGLE TABLE
(Calculated from *x*-ray data)

Monoclinic; prismatic —$2/m$ (C_{2h}) or domatic m (C_s)

$a:b:c=0.2317:1:0.1932;\ \beta=97°41'$
$p_0:q_0:r_0=0.8339:0.1915:1$
$r_2:p_2:q_2=5.222:4.355:1;\ \mu=82°19'$
$p_0'=0.8415;\ q_0'=0.1932;\ x_0'=0.1349$

Forms:	ϕ	ρ	ϕ_2	$\rho_2=B$	C	A
100	90°00′	90°00′	0°00′	90°00′	82°19′	0°00′
160	35 58	90 00	0 00	35 58	85 30	54 02
130	55 26	90 00	0 00	55 26	83 40	34 34
133	65 04	24 37	67 27	79 53	26 31	67 48
131	59 18	48 38	45 41	67 28	42 10	49 49

elements and angle table given in Table 2. Measured values for ϕ and ρ (Table 1) agree closely with the values calculated from x-ray data (Table 2).

PHYSICAL PROPERTIES

Moraesite is white. Some samples have a light-brown coating of iron oxide. Moraesite has two excellent cleavages, the traces of which on $\{100\}$ are parallel to the b- and c-axes. The specific gravity, as measured on the sample used for analysis by means of an Adams-Johnston pycnometer of fused silica, is 1.805. That calculated from x-ray data is 1.806. The streak is white. The small size and perfect cleavage of the fibers made determination of the hardness impracticable.

Moraesite is biaxial negative, with $2V=65°$. Indices of refraction are: $\alpha=1.462$, $\beta=1.482$ and $\gamma=1.490$. The optical orientation is: $Z=b$, $Y \wedge c=11°$.

CHEMICAL PROPERTIES

Moraesite is a hydrous beryllium phosphate with formula $Be_2(PO_4)(OH) \cdot 4H_2O$. The analysis is given in Table 3. The presence of 0.11 per cent Fe_2O_3 is probably due to the small amount of iron staining and is excluded in calculating the ratios. Al_2O_3 was not found even though it was tested for by the fluorometric method (Weissler and White, 1946) which would have detected 0.01 per cent Al_2O_3.

TABLE 3. CHEMICAL COMPOSITION OF MORAESITE

	Analysis	Recalcd. to 100% after deducting insol. and Fe_2O_3	Ratios	Equivalents	Atoms per* unit cell
Insol.	0.30				
P_2O_5	34.76	34.82	0.2453	Be 1.0124	24.5
BeO	25.28	25.32	1.0124	P 0.4906	11.9
Fe_2O_3	0.11			O 4.4509	107.9
Al_2O_3	none			H 4.4240	107.2
H_2O	39.80	39.86	2.2120		
	100.25	100.00			

USNM 106,577
M. L. Lindberg, analyst.
Formula $Be_2PO_4(OH) \cdot 4H_2O$, $Z=12$.

---

* Obtained by multiplying equivalents by $.01 \times 2423$, the weight of unit cell on a chemical scale in which $O=16$.

Moraesite is soluble in dilute HCl, HNO_3, and H_2SO_4. When heated, it decrepitates, giving off water, but does not fuse into a globular mass.

X-RAY CRYSTALLOGRAPHY

Moraesite has no apparent structural relationship to any known phosphate mineral. *X*-ray rotation and Weissenberg pictures for the 0-, 1-, and 2-levels were taken, with [100] and [001] as rotation axes; also rotation and 0-level pictures were taken about [010]. The plane net patterns and reflections observed[2] indicate a centered monoclinic lattice with choice of space groups C2/c(C_{2h}^6) or C-c(C_s^4).

Examination of the Weissenberg pictures taken about the c-axis shows that strong, medium, and weak spots occupy positions indicating a large diamond-shaped reciprocal pseudocell; additional weak spots occupy positions indicating a smaller true reciprocal cell, also diamond shaped, in which the length of the a*-axis remains unchanged, and the length of the b*-axis is one-third that of the larger reciprocal pseudocell. The same relations (thirding of the b*-axis) are observed in pictures taken about the a-axis, except that the plane net pattern is rectangular. The rotation picture about the b-axis gives strong 0, 3, 6, 9, 12, and 15 layers, with scattered spots on the in-between levels barely visible.

In Table 4 are given the cell dimensions determined from single crystal data and the powder-diffraction data including calculated spacings for the various planes observed in the Weissenberg photograph. Calculations were made only for planes observed, i.e., planes for which either h or $l = <2$ or $k = 0$ although other planes may have contributed to the intensity of some reflections. Similarly, calculations were made only for hkl planes in which the k index was 0 or divisible by 3, since the intensity of reflections from other planes is too weak to consider that they form a major contribution to the d-spacings measured on the powder photograph. A rotation picture of a needle [001] was taken in the powder camera, and the hk0 reflections were scaled off on the powder photograph as an additional aid to indexing.

PARAGENESIS

Moraesite formed late in the mineral sequence at the Sapucaia granitic pegmatite mine. Early minerals to form include quartz, albite, perthite, beryl, muscovite, and triphylite. Hydrothermal fluids generated within the pegmatite produced a large variety of secondary minerals, which have been deposited as spherulitic masses, fibers, needles, and equant crystals in cavities, in or adjacent to quartz, beryl, muscovite, triphylite, and other minerals.

---

[2] Reflections observed on hkl:h+k even, l even or odd; on hol:h even and l even; on okl:k even, l even or odd; on oko:k divisible by 6 only.

Table 4. *X*-ray Diffraction Data for Moraesite
Iron Radiation, Manganese Filter

Single Crystal Data
$a_0=8.55\pm.04$ Å; $b_0=36.90\pm.18$ (true cell), $12.30\pm.06$ Å (pseudocell);
$c_0=7.13\pm.04$ Å; $\beta=97°41'\pm15'$; volume=2229 Å^3; cell contents
12 $Be_2PO_4(OH)\cdot 4H_2O$; cell weight=2433

Powder Diffraction Data

I	d meas. Å	Index	d calc. Å	I	d meas. Å	Index	d calc. Å	I	d meas. Å	Index	d calc. Å
10	7.00	130	6.98	1	2.116	400	2.118	½	1.512	264	1.511
4	6.15	060	6.15			$\bar{2}$.12.2	2.115	1	1.492	3.21.0	1.492
3	5.28	$\bar{1}$31	5.26	4	2.050	0.18.0	2.050	½	1.472	4.18.0	1.473
6	4.24	200	4.24			$\bar{2}$63	2.056			$\bar{4}$.18.1	1.470
½	3.69	190	3.70			$\bar{3}$92	2.049	2	1.440	2.24.0	1.445
1	3.54	002	3.54	3	1.998	460	2.002			$\bar{1}$.15.4	1.441
1	3.49	260	3.49			$\bar{1}$.15.2	1.999			532	1.440
½	3.34	$\bar{1}$91	3.35	2	1.964	0.18.1	1.969			3.21.1	1.439
9	3.278	$\bar{2}$61	3.273			2.12.2	1.963	1	1.409	600	1.411
3	3.198	191	3.195	2	1.937	193	1.936			$\bar{3}$.21.2	1.411
3	3.071	0.12.0	3.075			$\bar{4}$02	1.934			0.24.2	1.410
		062	3.066	1	1.870	0.12.3	1.870			$\bar{1}$.21.3	1.408
6	3.023	132	3.022	½	1.843	$\bar{4}$62	1.845	1	1.396	5.15.0	1.395
½	2.910	$\bar{2}$02	2.913			2.18.0	1.845	1	1.378	065	1.378
6	2.819	0.12.1	2.819	½	1.813	$\bar{2}$.18.1	1.811	½	1.359	$\bar{2}$.24.2	1.360
3	2.753	330	2.753	3	1.757	3.15.1	1.756	½	1.341	5.15.1	1.341
½	2.685	$\bar{3}$31	2.678			$\bar{1}$34	1.760			3.21.2	1.341
1	2.631	$\bar{2}$62	2.632	½	1.738	4.12.0	1.744			$\bar{6}$62	1.340
		$\bar{1}$92	2.630			$\bar{4}$.12.1	1.736			0.18.4	1.339
1	2.479	192	2.482	½	1.720	1.21.0	1.721	½	1.333	*	
		2.12.0	2.488	½	1.677	$\bar{5}$31	1.684	½	1.316		
1	2.459	331	2.458			$\bar{1}$.21.1	1.682	½	1.307		
1	2.405	2.12.1	2.407			$\bar{2}$.18.2	1.676	½	1.289		
2	2.354	1.15.0	2.362	1	1.651	462	1.655	½	1.274		
		262	2.357			4.12.1	1.652	½	1.262		
4	2.325	390	2.326	2	1.639	1.15.3	1.638	½	1.251		
		$\bar{3}$32	2.323			$\bar{4}$.12.2	1.637	1	1.245		
		0.12.2	2.320	½	1.586	531	1.586	½	1.229		
½	2.288	2.12.1	2.291	½	1.571	$\bar{5}$91	1.570	2	1.220		
		$\bar{3}$91	2.285			590	1.566	½	1.190		
2	2.141	391	2.141			1.21.2	1.564	1	1.183		
				½	1.560	204	1.559				

Accuracy of reading: lines with intensity ½ ± .2 mm; lines with intensity >1 ± .1 mm

* These lines have not been indexed because the large number of choices made results meaningless.

Conditions of formation of moraesite were such as to effect a simple separation of this hydrous beryllium phosphate from other constituents present in the hydrothermal solutions attacking beryl and other pegmatite minerals. Additional elements in the hydrothermal solutions, principally iron, manganese, and aluminum, were combined to form other secondary minerals of complex composition. It is noteworthy that such a distinct and pure mineral of as simple a composition as moraesite could be formed under these conditions.

ACKNOWLEDGMENTS

The authors wish to acknowledge colleagues in the U. S. Geological Survey whose work suggested this mineral as a new species before the detailed investigations by Mrs. Lindberg. Particular acknowledgment is made to Fred Hildebrand for an *x*-ray powder photograph; to W. T. Schaller for reconnaissance optical study; and to Janet Fletcher and K. J. Murata for a qualitative spectrographic analysis.

REFERENCES

LINDBERG, MARIE LOUISE (1949), Frondelite and the frondelite-rockbridgeite series: *Am. Mineral.*, **34,** 541–549.

LINDBERG, MARIE LOUISE, AND MURATA, K. J. (1953), Faheyite, a new phosphate mineral from the Sapucaia pegmatite mine, Minas Gerais, Brazil: *Am. Mineral.*, **38,** 263-270.

PECORA, W. T., KLEPPER, M. R., LARRABEE, D. M., BARBOSA, A. L., AND FRAYHA, R. (1950), Mica deposits in Minas Gerais, Brazil: *U. S. Geol. Survey Bull.*, **964-C,** 205–305.

WEISSLER, ALFRED, AND WHITE, C. E. (1946), Fluorometric determination of aluminum in steels, bronzes, and minerals: *Ind. and Eng. Chemistry*, **18,** 530–534.

THE WEBSTER-ADDIE ULTRAMAFIC RING, JACKSON COUNTY, NORTH CAROLINA, AND SECONDARY ALTERATION OF ITS CHROMITE*

Roswell Miller III, *Drakes Corner Road, Princeton, N. J.*

Abstract

The structure of the Webster-Addie ultramafic ring in Jackson County, North Carolina, is discussed briefly. The ultramafic ring is almost everywhere concordant with the enclosing and enclosed gneiss and is thought to have been intruded as a sheet-like mass and subsequently deformed.

The mineralogy of the dunite, websterite, and enstatite pyroxenite is discussed. A table is presented showing that the Fe_2SiO_4 content of nine olivines from the ultramafic ring varies only $1\frac{1}{4}\%$ and shows no "trend" across three quarters of the thickness of the mass. Chemical analyses are given for the two types of enstatite from the enstatite pyroxenite, and for two chromite samples and one kammererite sample. The hydrothermal alteration of chromite to kammererite is described and photomicrographs presented to illustrate the progression of this reaction toward an ideal chromite-magnetite solid solution.

General Geology

The Webster-Addie ultramafic ring lies in Jackson County, North Carolina, fifty miles southwest of Asheville. The ring, comprised of dunite, websterite, and enstatite pyroxenite, is an ellipse with a maximum dimension of six miles and a minimum dimension of three and a half miles. The greatest width of outcrop of the ultramafic rocks, just south of the town of Addie, is a little under four tenths of a mile.

Except for very local areas, the Webster-Addie ultramafic rocks are concordant with the enclosing and enclosed gneiss. The gneiss forms a dome on the flanks of which lies the thin band of dunite (Fig. 1). The position of the dome itself probably was determined by original structures in the Carolina gneiss, and its present form was brought about by the interaction of lateral compression and vertical uplift during recurring periods of deformation in Paleozoic time. The dip of the gneiss and ultramafic rocks varies from 23 degrees near the center of the dome to vertical at several localities on the flanks of the dome, but in general it is steeper away from the long northeast-southwest axis (Fig. 2).

The extreme granulation of the dunites in the Webster-Addie ring and the prevalent faulting along dunite-country rock contacts indicates great post-intrusion deformation. The actual magnitude of this deformation cannot be determined because of the recurrent character of the deformation and the impossibility of dating precisely the ultramafic rocks them-

---

* Submitted in partial fulfillment of the requirements for the degree of Ph.D. at Princeton University.

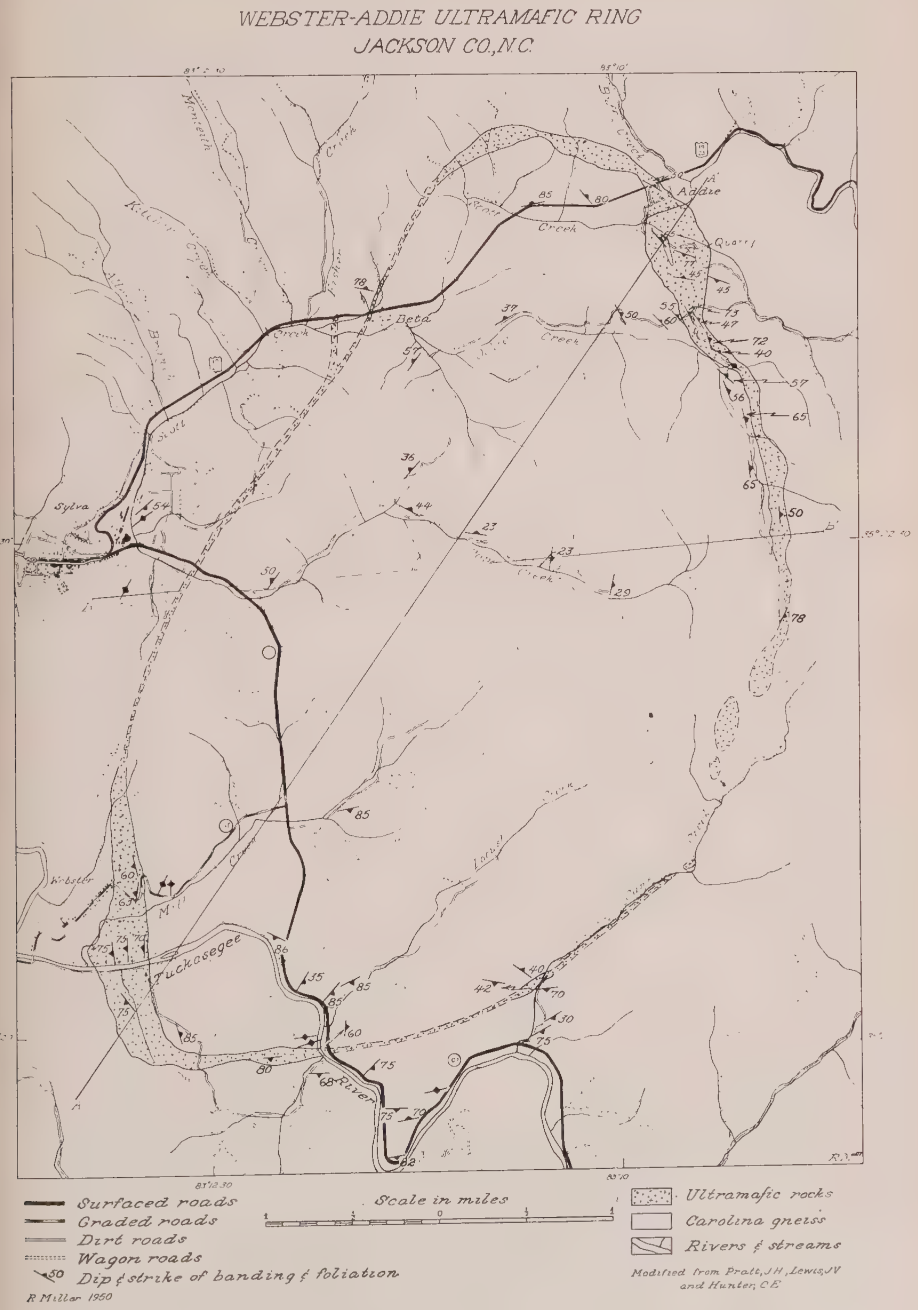
WEBSTER-ADDIE ULTRAMAFIC RING
JACKSON CO, N.C.
83°10'
Addie
Quarry
Scott Creek
Creek
Beta
Sylva
Monteith
Kitchin Cr.
Fisher
Webster
Mill Creek
Tuckasegee
River
Laurel
A'
B'
A
B
35°12'30"
83°12'30"
83°10'
Surfaced roads
Graded roads
Dirt roads
Wagon roads
Dip & strike of banding & foliation
Scale in miles
Ultramafic rocks
Carolina gneiss
Rivers & streams
Modified from Pratt, J.H., Lewis, J.V. and Hunter, C.E.
R Miller 1950

FIG. 1

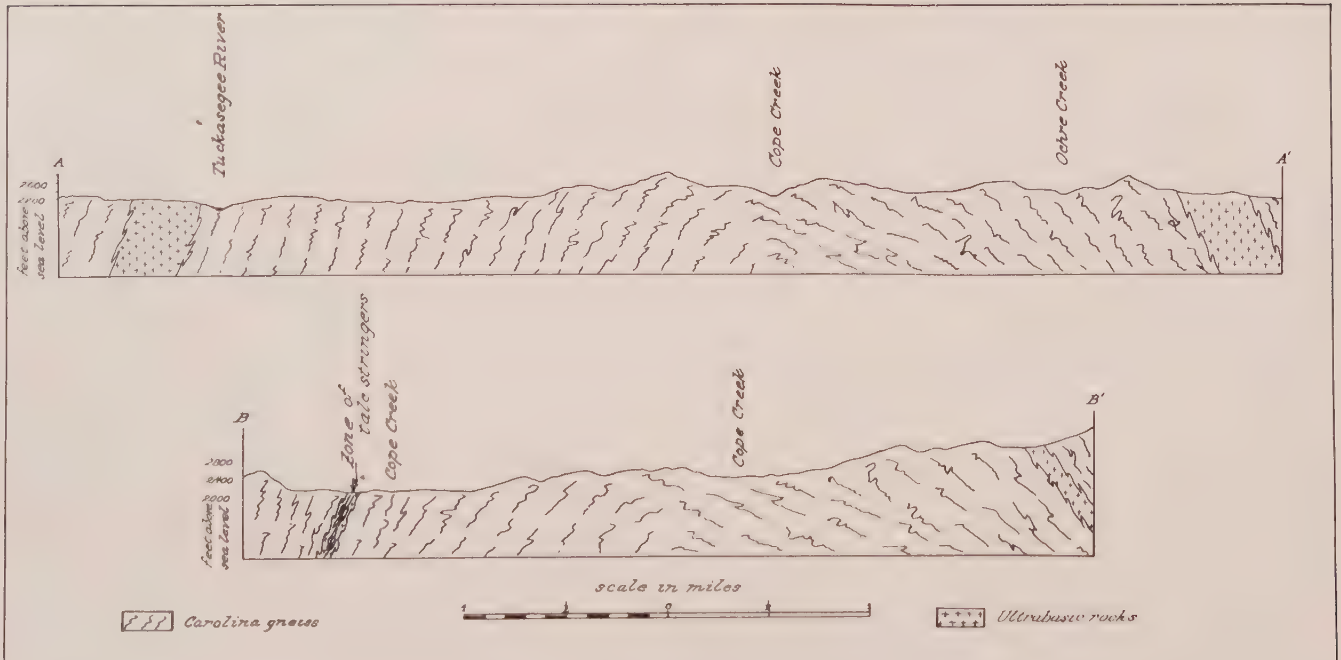

Fig. 2 Cross sections of Webster-Addie ring along lines A-A', B-B', Fig 1

FIG. 2

selves. If the magma had been intruded up the flanks of a dome which even approached the steepness of the Webster-Addie dome, it is suggested that the outline of the ultramafic ring might have been highly irregular. Such extreme doming would be likely to cause fractures in the country rock which would have been zones of weakness. Since the ultramafic rocks are concordant with the gneiss and essentially regular in outline, it is thought that no such fractures existed at the time of intrusion. However, it is not possible to say that the mass was intruded horizontally. The thickening at the ends of the long diameter certainly suggests a phacolithic type of intrusion. The most important point is that the Webster-Addie ultramafic rocks were intruded as a sheet-like mass (the term "sheet," as opposed to "sill," has been used advisedly), and that their present elliptical outcrop and steep dip is the result of post-emplacement doming of the gneiss into which they were intruded.

No contact metamorphism is at present observable in the gneiss either inside or outside of the Webster-Addie ring. However, the gneiss itself, since it contains garnets, indicates a moderately high temperature environment. At every locality where the dunite-gneiss contact is exposed, a six inch to three foot zone of vermiculite is present in the gneiss. This zone has been caused by later hydrothermal solutions which came up along the contacts and obliterated any narrow contact metamorphosed zone which may have existed.

DUNITE

The ultramafic rocks of the Webster-Addie ring fall into three groups; dunite, websterite, and enstatite pyroxenite. Dunite is far more abundant than the other two. In this paper dunite is defined as containing ninety per cent or more of olivine. Under this classification there is no harzburgite in the Webster-Addie ring, although in almost all hand specimens occasional grains of enstatite can be seen.

The least altered dunite of the Webster-Addie ring consists of medium to coarse, allotriomorphic olivine together with very minor amounts of accessory minerals. It is worthy of note that none of the four and six inch giant olivine crystals found at Balsam Gap, $3\frac{1}{2}$ air miles east of Addie, have been found in the dunites of the Webster-Addie ring. Under the microscope the olivine is colorless, transparent and has the typical optical properties of high index of refraction, high birefringence, and an optic angle approaching 90 degrees. The grains are often transected by uneven fractures and/or imperfect cleavage parallel to [010]. Most grains are free of inclusions, but occasionally "dusty" brown chromite is present along cleavage traces.

The maximum amount of replacement of olivine by serpentine noted by this writer in any of the Webster-Addie dunites is in the neighborhood of forty per cent. Serpentinization begins first along grain boundaries, cleavage traces, and fractures in the olivine grains. Where serpentinization has progressed to a considerable extent, the olivine grains become rounded and there is noticeable development of iron oxides concentrated along their peripheries. No iron oxides form where only small amounts of serpentine are present.

The beta index of refraction was measured on oriented grains of olivine from nine dunite specimens from the Webster-Addie ring. Seven of these were samples taken across the large outcrop near Webster; the other two were from the quarry at Addie. Their indices and corresponding content of the Fe_2SiO_4 molecule are given in Table 1. The figures for the molecular Fe_2SiO_4 content were taken from Poldervaart's chart (1950, p. 1073). It will be noted from Table 1 that the maximum variation in the Fe_2SiO_4 content for the specimens tested is $1\frac{1}{4}$ per cent for all the samples. Furthermore, the seven Webster olivines show no "trend" in composition across twelve hundred feet or about three quarters of the thickness of the mass.

TABLE 1. THE BETA INDEX OF REFRACTION AND MOLECULAR PER CENT Fe_2SiO_4 OF NINE OLIVINE SAMPLES FROM THE WEBSTER-ADDIE DUNITES

Specimen	Beta	Distance from footwall contact (feet)	Molecular Fe_2SiO_4 (%)
W-39	1.6669	90	7.5
W-41	1.6657	210	6.75
W-43	1.6670	430	7.5
W-45	1.6671	730	7.75
W-46	1.6681	770	8.0
W-47	1.6660	860	7.0
W-51	1.6671	1175	7.75
A-13	1.6660		7.0
A-5	1.6651		6.5

WEBSTERITE

The type locality of websterite lies in the large dunite mass southeast of the town of Webster. It lies wholly within the dunite in a zone with a maximum exposed width of about 260 feet on the north bank of the Tuckasegee River, and from this locality extends about one half mile to the north and one half mile to the south, parallel to the general strike of the dunite mass. Its position within the dunite is slightly below the center of the body, being about 900 feet from the hanging wall contact and only 430 feet from the footwall contact. Under the microscope websterite is an allotriomorphic aggregate of enstatite and diopside. These minerals have a tendency to form bands and "nests," and crystals of both many times larger than the average are common. The websterite has been considerably less altered than the surrounding dunite, there being almost no serpentine visible in thin section. A few small chromite grains are scattered through the rock, and tiny irregular magnetite (?) specks are common. The latter occur either interstitially or along cleavage traces in the pyroxenes. Small, rounded, translucent, greenish brown picotite grains commonly occur in the larger plates of pyroxene. They are usually arranged parallel to the cleavage.

Hess has given a chemical analysis and the optical properties of the fine grained diopside from this rock (Hess, 1949, p. 645). The maximum index of refraction and the optic angle were measured by this writer on one of the large diopside crystals in the websterite. The optic angle was essentially the same as that given by Hess for the fine-grained type. The average beta index, however, was determined to be 1.6880 with a range of plus or minus .0003, or .0098 higher than that given by Hess. Using his chart (Hess, 1949, p. 634) this difference indicates about a three per cent increase in iron and a very small increase in calcium in the coarse-grained over the fine-grained diopside.

The enstatite from the websterite was also analysed by Hess and Phillips (Hess and Phillips, 1940, p. 276). Their sample had a molecular $MgSiO_3$ content of 89.60 per cent. (Hess and Phillips, 1940, plate 1). In the present investigation the gamma index of refraction was measured for two samples of enstatite from websterite, one fine grained and one coarse. These indices were 1.6780 and 1.6755 (average), respectively, with a range in each case of plus or minus .0004. Using Hess' chart (Hess, 1952, Figure 2), these indices indicate a molecular $MgSiO_3$ content of $89\frac{1}{2}$ per cent for the fine-grained variety and $90\frac{1}{2}$ per cent for the coarse-grained variety.

ENSTATITE PYROXENITE

Two types of this rock are found on the north bank of the Tuckasegee River southeast of Webster. A bright green coarsely crystalline rock made up almost entirely of interlocking grains of enstatite occurs as a lense or pod within the websterite zone. This lens or pod is roughly twenty feet wide and probably not more than one hundred feet long. In thin section the prevalence of strain banding, wavy extinction, and interstitial small grains of grass green amphibole suggest crushing and some later hydrothermal action. A brown variety of enstatite pyroxenite occurs as boulders at the same locality. This rock shows less strain banding, wavy extinction, and green amphibole than the green variety, suggesting a greater resistance to granulation.

Diopsidic lamellae occur in both the green and brown enstatite, but are very much more common in the latter. They are best seen under crossed nicols in sections containing Y and Z. The lamellae are parallel to the optic plane. Individual lamellae vary in width from too narrow to be measured under the ordinary petrographic microscope up to 0.003 mm. There is also a great variation in the number of lamellae per millimeter. Generally, the larger grains contain many more lamellae per millimeter than the small ones. Counts show about ten lamellae per millimeter as the maximum concentration, but in adjacent grains of the same size one may have this concentration and the other be completely free of lamellae. There is no apparent relationship between the width and the spacing of the lamellae.

In addition to the lamellae there are occasionally irregular grains or blebs of the same material associated with the lamellae. These have their long axis parallel to the long axis of the lamellae, and are apparently oriented the same way as they extinguish simultaneously. They are generally tabular in form; up to 0.01 mm. in width; and have straight, parallel sides and highly irregular ends. A lamellae-free area is common at the

TABLE 2. ANALYSES OF ENSTATITE

	1	2
SiO_2	56.59	57.73
Al_2O_3	1.42	0.95
Fe_2O_3	0.71	0.42
FeO	7.14	3.57
MgO	33.22	36.13
CaO	0.57	0.23
H_2O+	0.28	0.52
H_2O-	0.04	0.04
TiO_2	0.05	0.04
Cr_2O_3	0.42	0.46
MnO	0.18	0.08
NiO	0.07	0.35
Total	100.69	100.52
Density	3.303	3.249
$MgSiO_3$ (Molecular)	87.50	94.50
Gamma Index	1.6702	1.6776

1. Brown enstatite from enstatite-pyroxenite, Webster, N. C., Analyst L. C. Peck.
2. Green enstatite from enstatite-pyroxenite, Webster, N. C., Analyst L. C. Peck.

ends of the blebs, but no such impoverishment is present along their sides (i.e. parallel to their long axis), lamellae often almost touching them. There is no "gradational" form between the lamellae and the blebs, even where they occur in the same grain. Both lamellae and blebs only rarely reach the periphery of the host grain, but tend to be concentrated near the center. A very pronounced concentration of lamellae is often present at the junction of two strain bands in an enstatite grain. Tiny grains of picotite are also arranged along some of these planes but seem to occur wholly within the enstatite rather than in the lamellae. Where individual lamellae transect these strain planes they are either bent at a slight angle or offset. The amount of offset is difficult to measure because of the previously mentioned concentration of lamellae along the planes, but it was never measured with certainty to be more than one or two hundredths of a millimeter.

The presence and concentration of the lamellae and blebs are reflected by the CaO content of the analyzed specimens in Table 2. No lamellae were noted in the enstatites in any of the dunites, even when they were properly oriented on a universal stage.

CHROMITE

Chromite occurs in the ultramafic rocks of the Webster-Addie ring as sparsely scattered grains or more rarely as bands made up of small to medium size grains. The concentration of chromite grains in these bands varies from being almost imperceptible to almost solid chromite. Likewise the width of the bands varies from merely a series of closely spaced small grains to bands an inch or more in width. Under the microscope these chromite bands show alternating coarse uncrushed layers and finer grained highly sheared layers identical in appearance with the layering in the dunites. Thus any grain-size sorting which may have existed in the chromite has been obscured by post-emplacement shearing. However, similar bands of chromite have been described from areas where shearing has been less pronounced, and E. Sampson says that: "They (the bands) appear to represent crystal settling, the banding in many cases probably being accentuated by flowage during consolidation" (Sampson, 1942, p. 110). There is no available evidence in the Webster-Addie area to support an opinion as to when (i.e., pre- or post-intrusion) the chromite was concentrated in these bands. This question can only be answered by a fuller understanding of the temperature and physical characteristics of ultramafic masses during intrusion.

Ross (1929) has presented evidence that at least some of the chromite in the Webster-Addie ring is later than the surrounding silicates; the relation of the chromite to shear planes in dunite and its occurrence as

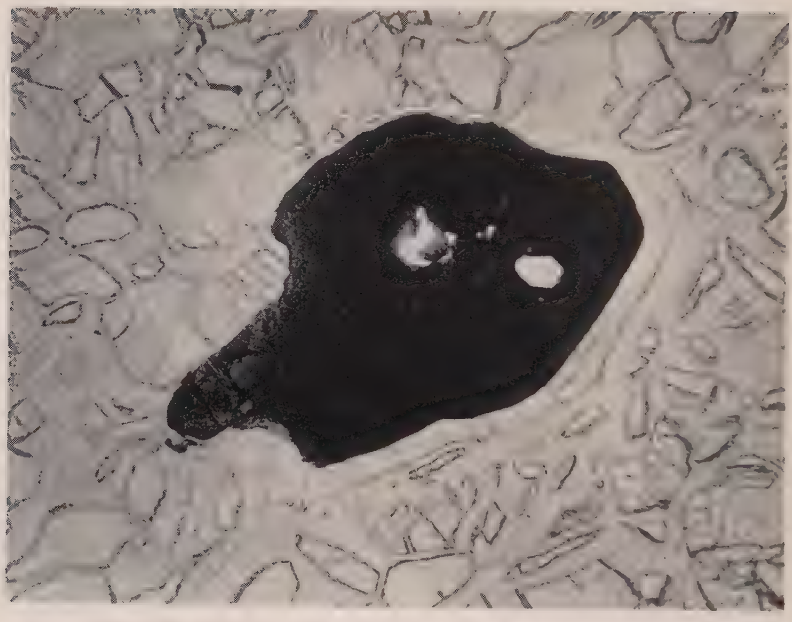

FIG. 3. Unaltered chromite grain surrounded by serpentine. ×70.

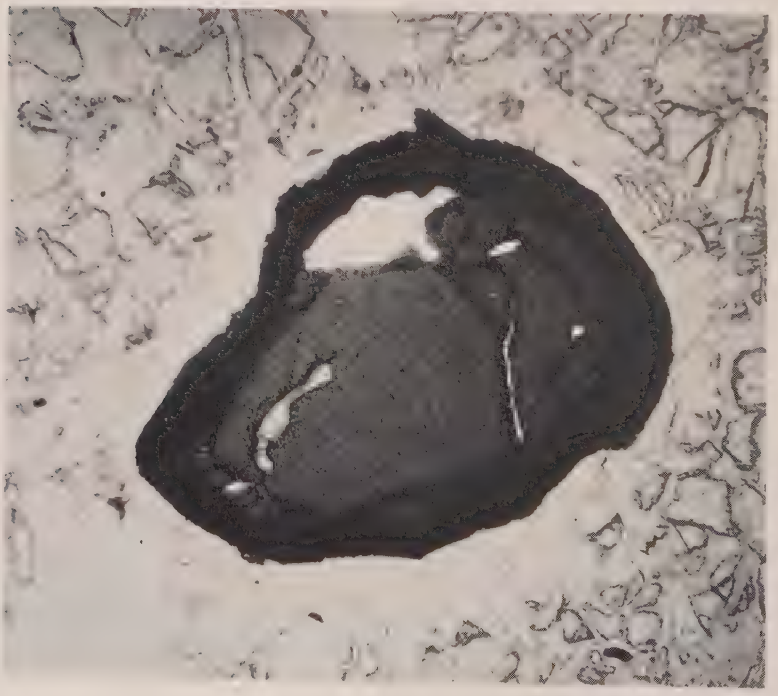

FIG. 4. Chromite grain surrounded by chlorite and partially altered to black opaque material. ×60

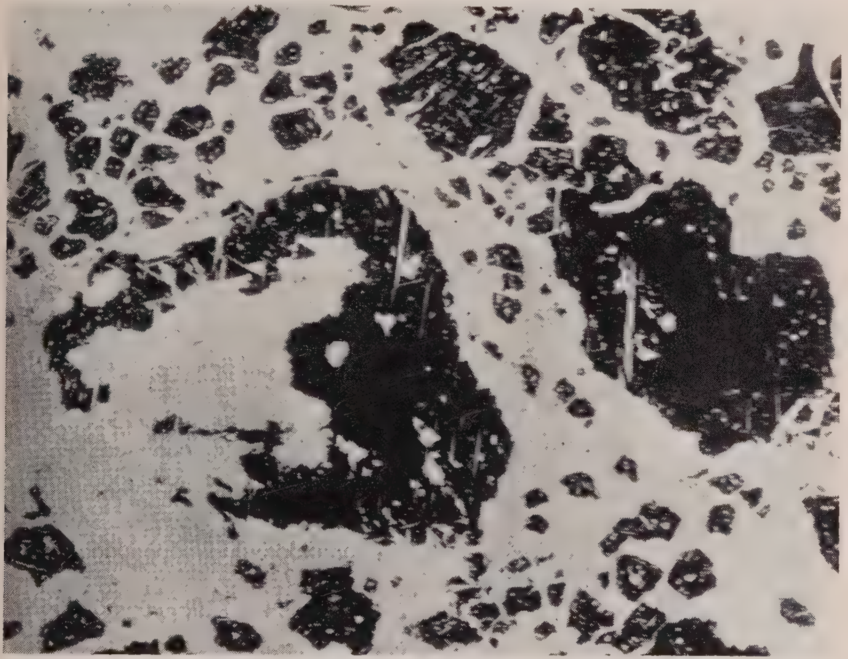

FIG. 5. Chromite grains with primary cores and alteration zones of opaque chromite (black) and kammererite (white). ×25

"vein-like" masses where it is associated with chrome-bearing hydrothermal minerals. The occurrence has been noted of small unaltered olivine grains in chromite grains in highly serpentinized (for the Webster area) dunite. It is unlikely that these olivine grains are merely irregularities in the chromite grains which on slicing appear as inclusions, because in the Webster dunites serpentinization always starts along contacts between grains. Such inclusions are considered evidence that some of the chromite is later than the olivine. A further line of evidence is supplied by the distinct interstitial relationship which some of the fine-grained chromite bears to the olivine.

During serpentinization chromite develops chlorite aureoles and a rim of black opaque material forms around the periphery of the chromite grain (Fig. 4). As this reaction progresses, parting develops in the opaque material allowing the chlorite to "eat" into the center of the grain until none of the typical brown non-opaque chromite is left. Figures 5, and 6 show this reaction. In some cases the chromite grain becomes a mass of tiny, rounded globules of the opaque material (Fig. 7). These are gradually replaced by the chlorite until almost no trace of the original chromite grain is left (Fig. 8). It is believed that knots of chlorite that show no

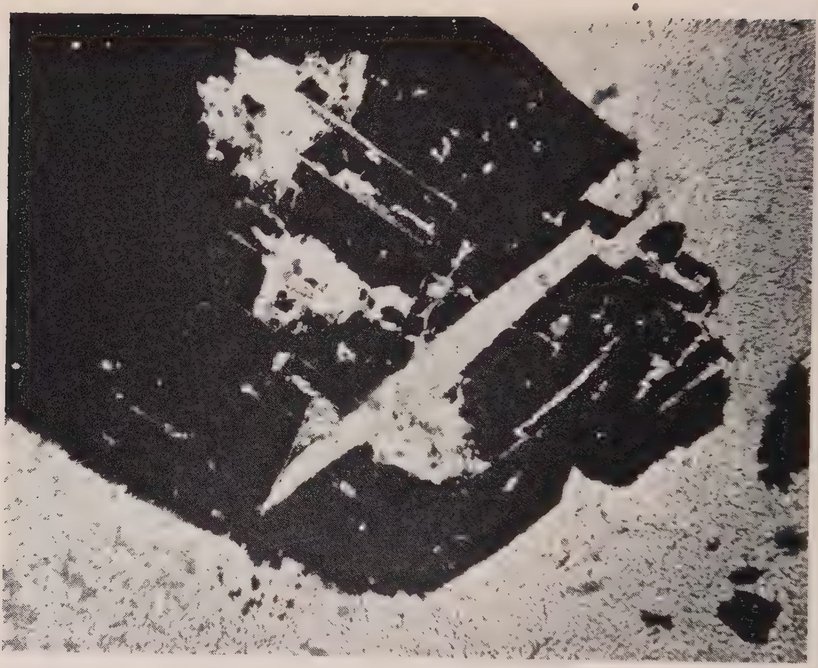

FIG. 6. Same as Fig. 5. ×75

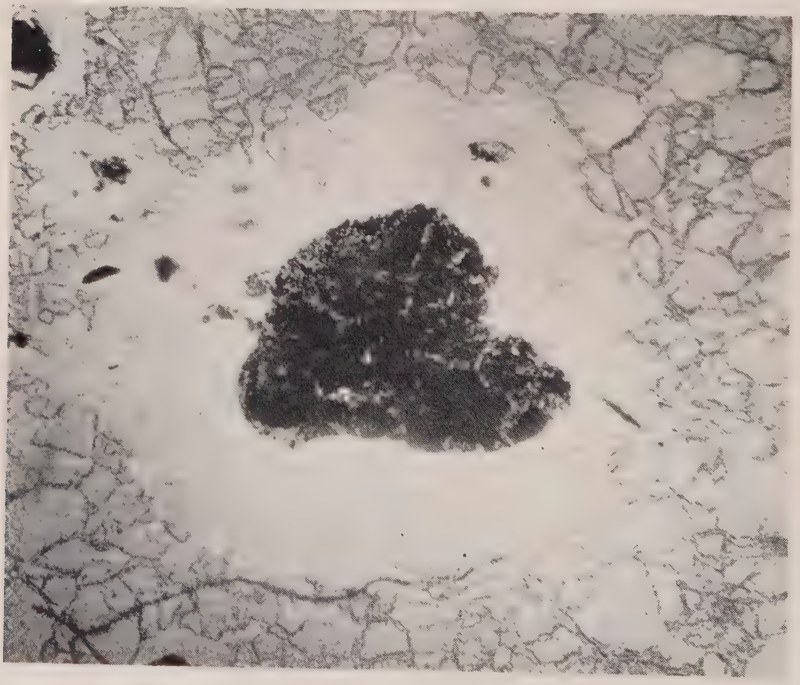

FIG. 7. Altered chromite grain in kammererite "knot." In this case the black opaque chromite is in the form of tiny rounded grains. ×37

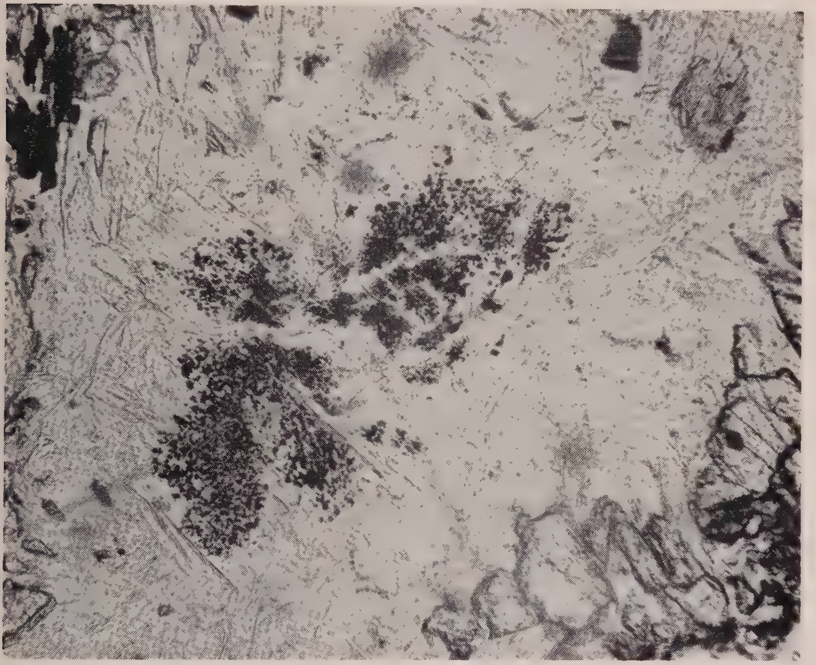

FIG. 8. Partial replacement of black opaque grains by kammererite. ×144

remnants of chromite are places where the reaction has progressed to the point where all of the chromite has been replaced. The chlorite is a kammererite as shown in Table 4.

An effort was made to separate the black opaque material from unaltered chromite for chemical analysis. This was not entirely successful as the two apparently have almost the same magnetic susceptibility and specific gravity. Two samples were analyzed, one of which showed about 80 per cent of black opaque material and the other in which the chromite was unaltered. These samples were from the same locality (Table 3, columns 1 and 2).

The specimen of altered chromite which was analyzed was known to contain some kammererite which was impossible to separate even by fine crushing. The analysis shows this impurity in the figure for SiO_2 and water. Assuming that the SiO_2 content is all in the form of kammererite, 6.31% of this mineral was subtracted from the altered chromite analysis. In this calculation the analysis of kammererite given in Table 4 was used. The resulting material was further estimated to contain about 20% of unaltered chromite in the cores of the grains. Using column 1 of Table 3

TABLE 3. ANALYSES OF UNALTERED AND ALTERED CHROMITE

	1	2	3
SiO_2	0.82	2.06	0.00
Al_2O_3	10.97	4.59	2.41
Fe_2O_3	3.62	10.92	13.62
FeO	19.68	20.58	21.74
MgO	9.52	7.65	5.87
CaO	0.31	0.34	0.35
H_2O (tot.)	0.21	1.12	0.34
TiO_2	0.26	0.32	0.30
Cr_2O_3	54.49	52.06	54.84
MnO	0.29	0.38	0.44
NiO	0.05	0.11	0.09
Total	100.22	100.13	100.00

1. Unaltered chromite. Analyst L. C. Peck.
2. Altered chromite. Analyst L. C. Peck.
3 Altered chromite recalculated after removal of 6.31% kammererite and 20% unaltered chromite.

Using Thayer's method (1946) the ratio $RO/R_2O_3=1.03/1$, and the composition of the unaltered chromite in molecular percentages of RO and R_2O_3 is $Cr_{73}Al_{22}(Mg_{46})$. The necessary R″ ions were subtracted to balance the small amount of silica assumed to be an impurity.

TABLE 4. ANALYSIS OF KAMMERERITE

Analyst, L. C. Peck

Specimen W-31 Kammererite	Weight Per cent	Molecular Ratios	Atomic Ratios			Cations to 18 O·(OH)		Theoretical
SiO_2	31.95	532	Si	532	167			
Al_2O_3	13.94	139	Al	278		Z	3.99	4.00
Cr_2O_3	3.90	26	Cr	52	111			
Fe_2O_3	0.22	1	Fe‴	3		X	6.04	6.00
FeO	1.83	25	Fe″	25				
MnO	0.01	—	Mg	865		(OH)	7.97	8.00
MgO	34.87	865	Ni	3				
NiO	0.21	3	Ca	3				
CaO	0.18	3						
H_2O+	12.61	700	OH	1400				
H_2O-	0.13	7				2V=20°		
Na_2O	0.00	—				optic sign (+)		
K_2O	0.04	1				$\beta=1.5855$ (range $=\pm.0005$)		
TiO_2	0.02	—				dispersion v>r weak		
P_2O_5	0.00	—						
	99.91							

this was also removed and the results are given in column 3 of Table 3. This material, the calculated black opaque, has a ratio $RO/R_2O_3 = 1/1.01$. Using Thayer's method (1946) the composition in molecular percentages of RO and R_2O_3 is $Cr_{77}Al_5(Mg_{34})$. The foregoing calculations indicate that as the reaction progresses there is a tendency toward the abstraction $MgO \cdot Al_2O_3$ and an increase of $FeO \cdot Fe_2O_3$. In addition some Cr_2O_3 is being lost to the kammererite. The end product of the reaction theoretically would be an ideal chromite ($FeCr_2O_4$)—magnetite solid solution.

Acknowledgments

The writer wishes to express his gratitude to Dr. H. H. Hess for his unfailing interest and guidance in the writing of this paper. Discussions with Drs. J. C. Maxwell, A. F. Buddington, and E. Sampson relating to various parts of the work were of great value and were much enjoyed and appreciated.

Dr. C. S. Ross and Robert L. Smith of the U. S. Geological Survey were kind enough to spend two days in the field with the writer. Their interest and help in the project is hereby gratefully acknowledged.

References

Hess, H. H. (1949), Chemical composition and optical properties of common clinopyroxenes; Part I: *Am. Mineral.*, **34,** 621–666.

——— (1952), Orthopyroxenes of the Bushveld type, ion substitutions and changes in unit cell dimensions: Bowen Volume, *Am. Jour. Sci.*, 173–187.

Hess, H. H., and Phillips, A. H. (1940), Optical properties and chemical composition of magnesian orthopyroxenes: *Am. Mineral.*, **25,** 271–285.

Poldervaart, A. (1950), Correlation of physical properties and chemical composition in the plagioclase, olivine, and orthopyroxene series: *Am. Mineral.*, **35,** 1067–1079.

Ross, C. S. (1929), Is chromite always a magmatic segregation product?: *Econ. Geol.*, **24,** 641–645.

Sampson, E. (1942), Chromite deposits *in* Ore deposits as related to structural features, p. 110–125, Princeton Univ. Press, Princeton, N. J.

Thayer, T. P. (1946), Preliminary chemical correlation of chromite with the containing rocks: *Econ. Geol.*, **41,** 202–219.

THE IDENTITY OF TINZENITE WITH MANGANOAN AXINITE*

C. Milton, F. A. Hildebrand, and A. M. Sherwood,
U. S. Geological Survey, Washington, D. C.

Abstract

Tinzenite, described in 1923 as a new mineral of formula $2CaO \cdot Mn_2O_3 \cdot Al_2O_3 \cdot 4SiO_2$, is shown by x-ray, chemical, physical, and optical data to be manganoan axinite. More than 5% B_2O_3 was overlooked in all of the previous seven analyses of tinzenite. The existence of such axinite with CaO content greatly lower than previously known shows that the formula of axinite, usually written $HCa_2(Fe, Mn)Al_2BSi_4O_{16}$, is better written $H(Ca, Fe,Mn)_3Al_2BSi_4O_{16}$.

History of Tinzenite

Tinzenite was described by Jakob (1923) from Tinzens, Canton Graubünden, Switzerland, as a new species, with the formula, based on two analyses, $2CaO \cdot Mn_2O_3 \cdot Al_2O_3 \cdot 4SiO_2$. The mineral was described as yellow, fibrous to platy, with monoclinic symmetry, with cleavage perfect on {100}, optic plane parallel to {010}, Z=c; indices of refraction 1.693, 1.701, 1.704, with corresponding pleochroism, weak yellow green, weak green, colorless; density 3.286.

In abstracting the paper, Foshag (1925) commented that the formula given by Jakob did not include the water content, which may be essential; that recalculation of Jakob's analysis led to a formula closer to $2CaO \cdot 3(Al,Mn)_2O_3 \cdot 6SiO_2$; that the purity of the analyzed specimens was not stated; and that the exact character of this mineral (tinzenite) must be considered doubtful.

Jakob (1926) replied to this criticism by stating that the analyzed material was microscopically pure; the water (and alkalies) was not extraneous, but belonged in the constitution of the mineral; that low summations (in two of four analyses) resulted solely from the smallness of the samples analyzed; the water, most of which required strong heating to drive off, must, with the alkalies, be considered as replacing CaO, and not, as Foshag suggested, be disregarded. Jakob believed that variability in color of tinzenite, from citron yellow to orange red, is not caused by superficial alteration, but that it may be found in perfectly fresh material. Two new analyses by P. Esenwein are similar to the two made by Jakob. He concludes that variability in color may be related to oxidation states of the manganese, which present analytical methods cannot precisely define.

Tinzenite was also identified from Cassagna in Liguria, Italy, by Pelloux (1934) in material which he had described some years earlier (Pelloux, 1919).

---

* Publication authorized by the Director, U. S. Geological Survey.

Sanero (1936) studied Pelloux's tinzenite, giving two new analyses of the Italian mineral that closely agree with the four previous analyses of tinzenite from Switzerland.

Jakob (1933) reviewed the mineralogy, especially the chemistry of tinzenite, with a fifth analysis of rose red material (formula $2CaO \cdot Mn_2O_3 \cdot Al_2O_3 \cdot 4SiO_2$), which agrees well with previous analyses of citron yellow to orange red tinzenite. He also mentions that tinzenite had been erroneously identified as zoisite (Müller, 1916; Arbenz and Tarnuzzer, 1923). This fifth analysis made on adequate "absolutely pure" material, and stated to be "absolutely reliable" (absolut zuverlässig), is cited below in analysis A, Table 2.

Winchell (1951) also refers to tinzenite as "closely related to thulite in composition and properties," and ascribes a formula $H_2Ca_3Al_4Mn_4Si_8O_{32}$.

The morphology of tinzenite has been investigated recently by Parker (1948) and Waldmann (1948), who found a triclinic symmetry and who mentioned a crystal setting showing some relation to axinite.

Strunz (1949) lists tinzenite as monoclinic with the formula $Ca\,Mn'''Al(SiO_4)_2$, with structure undetermined.

It seems strange that in all these analyses no test for boron was made, notwithstanding the close similarity of properties of the so-called tinzenite with those of axinite. The low summation in Jakob's analyses should have indicated an undetermined constituent. Jakob's interpretation of the state of oxidation of the manganese as trivalent gave him a better summation, but so much Mn_2O_3 (20%+) would hardly yield a yellow mineral with weak yellow green, weak greenish, to colorless pleochroism. One is reminded of the deep color and strong pleochroism of piedmontite with much less Mn_2O_3. It may be that the rose red and orange red varieties of the so-called tinzenite contain a small amount of Mn_2O_3.

The Identity of Tinzenite with Manganoan Axinite

The validity of tinzenite as a species was not seriously questioned until 1952, when, in the course of a study of manganese ore from Aroostook County, Maine, a special study was made of the rare manganese silicate ganophyllite, which had been found there. Among the comparative material investigated was ganophyllite from Franklin, New Jersey, which occurred in close association with a manganoan axinite, described by Palache (1935), who noted its yellow color as characteristic of axinite from this locality. He also noted a pale rose colored variety, as well as yellowish green and colorless. We prepared x-ray diffraction patterns of the yellow Franklin axinite (U.S.N.M. 95339) and axinite from Dauphin,

TABLE 1. *X*-RAY DIFFRACTION DATA FOR AXINITE AND TINZENITE = MANGANOAN AXINITE

Axinite*		Tinzenite = manganoan axinite†		Axinite*		Tinzenite = manganoan axinite†	
d(Å, meas.)	I	d(Å, meas.)	I	d(Å, meas.)	I	d(Å, meas.)	I
		8.83	3	2.526	3		
6.30	7	6.30	7	2.489	2		
5.87	½	5.90	2	2.474	2	2.474	3
5.15	½	5.12	2	2.444	5		
4.99	1	4.94	2	2.424	5	2.424	3
4.80	2	4.78	3			2.400	3
4.53	3	4.55	3	2.396	1		
3.99	2	3.96	3			2.368	3
		3.87	1	2.363	5		
3.80	3					2.323	2
3.68	6	3.66	3	2.318	½		
3.46	8	3.46	8	2.292	1		
3.42	½	3.42	4	2.271	3		
3.39	½					2.254	1
3.28	6	3.28	6	2.250	3		
3.23	½			2.226	1		
3.19	½					2.210	1
3.16	9	3.14	7	2.206	3		
3.08	4B	3.06	4	2.190	6		
3.02	5	3.01	5	2.179	2	2.179	4
2.998	6	2.975	7	2.163	7		
2.968	5					2.152	7
2.931	3			2.134	3B		
		2.881	6			2.126	2
2.874	3			2.060	5	2.060	4
2.839	4			2.040	5		
2.812	10	2.812	10			2.033	3
2.792	4			2.014	3B		
		2.766	2			2.008	7B
2.760	4			1.998	3B		
		2.734	2	1.989	5	1.990	2
2.667	4			1.973	½		
		2.661	3			1.967	3
2.643	4B			1.955	4		
		2.620	2			1.940	2
2.575	5			1.926	5		
2.564	6					1.923	3B
		2.553	6B	1.895	1B		

TABLE 1—(*continued*)

Axinite*		Tinzenite = manganoan axinite†		Axinite*		Tinzenite = manganoan axinite†	
d(Å, meas.)	I	d(Å, meas.)	I	d(Å, meas.)	I	d(Å, meas.)	I
		1.870	2B	1.426	3		
		1.818	2	1.420	3		
1.808	2			1.405	5B	1.403	3B
1.788	4	1 791	4B	1.374	2B		
1.744	1			1.359	4		
1.732	3	1.732	2			1.355	3
1.721	3			1.348	1B		
1.704	2	1.706	2			1.343	1
1.691	1	1.693	2			1.331	5
1.680	1			1.327	5		
1.668	4	1.668	2	1.323	3		
1.652	4	1.650	2	1.314	1B		
1.636	5					1.307	1B
		1.630	4	1.301	1		
1.623	3			1.296	1		
		1.617	3	1.288	1		
1.608	2					1.280	1B
1.597	3	1.597	3	1.273	1VB		
1.580	4			1.256	1VB		
1.570	2	1.570	3	1.242	2	1.241	2B
1.538	3			1.233	2	1.230	2B
		1.526	2B	1.225	1VB		
1.516	2B			1.215	1		
		1.505	1	1.211	1		
1.495	3					1.205	1
		1.490	2			1.195	1
1.478	2			1.190	1B		
		1.463	2B	1.175	1		
1.460	4B			1.166	1		
		1.449	2B	1.135	1B		
1.442	1			1.127	1B		
1.435	1			1.120	1B		
		1.430	2				

* Axinite from Bourg d'Oisans, Dauphine, France (U.S.N.M. C-3141) (film 7051).

† Tinzenite = manganoan axinite from Tinzens, Switzerland (U.S.N.M. R-6433) (film 6987) (analyzed sample).

France (U.S.N.M. C-3141), obtained through George Switzer, of the U. S. National Museum, and noted the evident similarity of the pattern recorded for tinzenite from Switzerland (Geiger, 1948). Thereupon we also obtained from the U. S. National Museum some type Swiss material and verified the similarity of the *x*-ray patterns of minerals from the

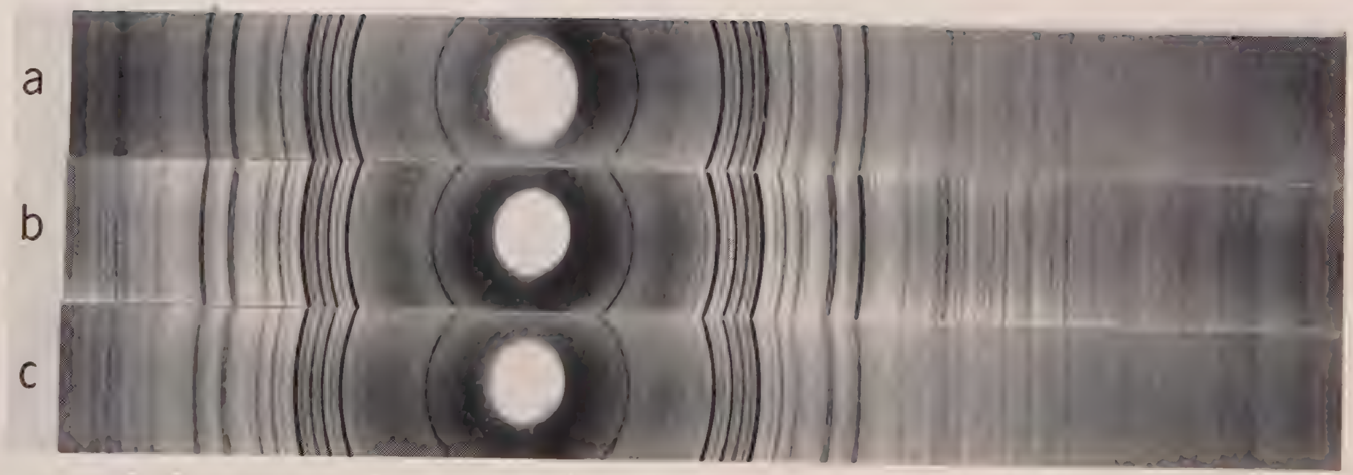

FIG. 1. a. Tinzenite = manganoan axinite from Tinzens, Switzerland (film 7077) b. Manganoan axinite from Franklin, New Jersey (film 7070) and c. Axinite from Dauphine, France (film 7067). The broken line in this pattern is attributed to a small amount of quartz.

Franklin and the Tinzens localities (Fig. 1, a, b and c). Our suspicion that a single mineral, not two, was in question was quickly verified when qualitative chemical tests, soon confirmed by spectrographic study (by E. L. Hufschmidt, of the Geological Survey), showed substantial boron in tinzenite. The complete analysis of the Tinzens mineral showed that tinzenite is manganoan axinite, and that all previous analyses of tinzenite were in error in that 5 per cent or more of B_2O_3 was overlooked. It was also an error to assume trivalent, not divalent, manganese; the oxygen assumed in this erroneous calculation masked the absence of boron, one of the major constituents. If Jakob's formula for tinzenite, $2CaO \cdot Mn_2O_3 \cdot Al_2O_3 \cdot 4SiO_2$, is doubled, and the Mn_2O_3 converted to $2MnO$, and one molecular proportion of B_2O_3 and of H_2O added, it gives the accepted formula of axinite, $4CaO \cdot 2(Mn, Fe, Mg)O \cdot 2Al_2O_3 \cdot B_2O_3 \cdot 8SiO_2 \cdot H_2O$, as suggested by Schaller (1911).

In addition to the diffraction patterns shown in Figure 1, patterns of axinite from the Toroku mine, Miyazaki Prefecture, Japan (U.S.N.M. 105575) (no chemical analysis), and "tinzenite" from the Huachuca Mountains, Arizona (U.S.N.M. 102822) (no chemical analysis), were also obtained. The patterns indicate that all five minerals are isostructural but not identical because of small differences in chemical composition. The patterns of axinite from Bourg d'Oisans, Dauphine, France, and the Toroku mine, Japan, are identical. The patterns of tinzenite from Arizona and manganoan axinite from Franklin, New Jersey, are identical and so similar to patterns of the axinites from France and Toroku mine, Japan, that measurement of their lines was not deemed necessary. X-ray diffraction data for axinite from Dauphine, France, and tinzenite = manganoan axinite from Tinzens, Switzerland, are shown in Table 1.

All diffraction patterns were made with North American Philips Debye-Scherrer powder cameras (114.59 mm. diameter) using the Straumanis and Wilson techniques with FeKα (Mn filter), $\lambda = 1.9373$ Å.

Calculation of the molecular ratios of Sherwood's analysis (Table 2, analysis B) gives

B_2O_3	0.96
SiO_2	8.05
Al_2O_3, Fe_2O_3	2.00
MnO, MgO, CaO, Na_2O, K_2O	6.27
H_2O+	0.97

These percentages are in fair accord with the accepted formula of axinite. (The small iron content has been assigned to R_2O_3, rather than RO, arbitrarily; but even if this were not done the ratios would still be much the same.) It may also be noted that these ratios are much closer to whole numbers than those computed from Jakob's analysis (Table 2, analysis A).

TABLE 2. ANALYSES OF TINZENITE, MANGANOAN AXINITE, AND AXINITE

	Tinzenite, Tinzens J. Jakob, analyst (Jakob, 1933)		Manganoan axinite (tinzenite) Tinzens A. Sherwood, analyst	Axinite Radautal, Harz (Fromme, 1909)	Axinite yellow, brown, Obira, Japan (Ford, 1903)		Axinite Franklin, N. J., W. E. Ford, analyst (Palache, 1935)	Axinite Kristiania, Norway (Goldschmidt, 1911)	Axinite Bourg d'Oisans Dauphine, France (Ford, 1903)
	A		B	C	D		E	F	G
B_2O_3	—		5.65	6.31	5.61		5.10	5.13	6.12
SiO_2	40.65		40.80	41.74	41.80		42.77	41.99	42.78
TiO_2	0.00		—	—	—		—	—	—
Al_2O_3	18.31		16.23	17.08	17.15		16.73	16.32	17.67
Fe_2O_3	0.03		1.59	1.87	1.11		1.03	1.62	0.99
FeO	—		—	1.35	2.84		—	—	6.02
Mn_2O_3	24.87		—	—	—		—	—	—
MnO		(22.38)	21.19	11.54	10.71		13.69	12.86	2.99
MgO	0.00		0.17	0.34	0.21		0.23	0.07	2.41
CaO	13.50		12.51	18.65	19.51		18.25	20.14	20.16
Na_2O	0.58		0.27	—	—	(CuO	0.12)	—	—
K_2O	0.48		0.13	—	—	(PbO	—)	—	—
						(ZnO	1.48	0.12)	—
H_2O+110°	1.47		1.20	1.81	1.22		1.29	1.87	1.40
H_2O−110°	0.10		0.10	—	—		—	—	—
	99.99	(97.50)	99.84	100.69	100.16		100.69	100.12	100.54
Sp. Gr.	3.286			3.313	3.302		3.358	3.334	3.287

Optical properties of four of the minerals whose analyses are given in Table 2 are tabulated in Table 3.

Table 2 gives Jakob's analysis (1933) of tinzenite from Tinzens, Switzerland (A), followed by Sherwood's analysis of another specimen (U.S.N.M. R6433) of the same material from the U. S. National Museum collection (B). Analyses C, D, E, and F are of manganoan axinites from the literature, G is a low-manganese axinite.

The analyzed Tinzens tinzenite was first cleaned from a thin adherent film of dark-brown or black manganese dioxide by treatment with dilute nitric acid and hydrogen peroxide. This manganese mineral could not be identified from its diffraction pattern, which shows that it is poorly crystalline with broad lines at approximately 9.4 Å, 7.2 Å, 4.7 Å, 3.9 Å, and 2.2 Å.

The analysis of the Tinzens specimen was supplemented by spectrographic determinations by Helen W. Worthing, of the U. S. Geological Survey, as follows:

More than 10%	Al Mn Si
1.0–10%	Ca B
0.1–10%	Fe Mg
0.01–0.1%	Ni Sr Ba
0.001–0.01%	Ga V Ti Y Zr Cr Cu
0.0001–0.001%	Be Yb

Table 3. Comparison of Optical Properties of Tinzenite with Those of Manganoan Axinite

	Tinzenite	Manganoan axinite			
	A (B)	C	D	E	F
α	1.693	1.681	(No optics recorded by Ford)	1.684	1.679
β-α	0.008	0.007		0.008	0.006
β	1.701	1.688		1.692	1.685
γ-β	0.003	0.003		0.004	0.013
γ	1.704	1.691		1.696	1.698
γ-α	0.011	0.010		0.012	0.019
2V	63°				
Color	yellow		yellow brown	yellow	yellow

The indices of refraction of tinzenite are slightly higher than those reported for any axinite, as would be expected because of the lower CaO content and higher MnO content. Winchell (1951) cites as maximum values for the indices of refraction of axinite 1.690, 1.698 and 1.704.

Composition of Axinite

W. T. Schaller (whose interest in this study is gratefully acknowledged) suggested (Schaller, 1911) that the amount of CaO in axinite may be constant because most of the analyses depart but slightly from 20 per cent CaO, regardless of considerable reciprocal variation in percentages of FeO and MnO. Those analyses, made prior to 1911, in which the percentages of CaO departed considerably from 20 per cent were rejected at that time by Schaller as being of questionable accuracy. However, his suggestion is invalidated by recognition of the identity of tinzenite, which contains much less than 20 per cent CaO, with axinite.

Likewise Gädeke (1938), in discussing the relations of iron and manganese in axinite, states that the manganese almost entirely ("fast ausschliesslich") replaces divalent iron and not calcium. He plots the variations of the mean refractive index (the average of the three) for five selected axinites that contain from 0.33 per cent to 12.86 per cent of MnO. The graph shows a linear variation. However, tinzenite so plotted does not fall on his curve at all, but this variation may be ascribed to the low CaO.

A tabulation of 53 analyses of axinite (all that have been recorded, including those of tinzenite) shows (Fig. 2) that there is a serial variation in CaO extending from 12 to perhaps 30 per cent, with a very marked clustering close to 20 per cent. Nearly two-thirds of all the analyses lie between 19 and 21 per cent CaO. The range, however, is both below and above 20 percent.

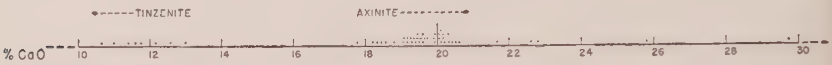

FIG. 2. Serial variation in CaO content of axinite (including tinzenite, i.e., manganoan axinite).

The formula of axinite, therefore, should not be written as $HCa_2(Fe, Mn)Al_2BSi_4O_{16}$, with calcium constant, but as $H(Ca, Fe, Mn)_3Al_2BSi_4O_{16}$. Whether a calcium-free axinite or an iron- and manganese-free axinite will be found remains to be seen.

Peacock (1937) made an exhaustive study of the crystallography of axinite, in which he assigned as the contents of the unit cell 2 moles of composition $HBAl_2Ca_2(Mn, Fe)Si_4O_{16}$. He also accepts the established formula of axinite with Ca in fixed ratio, and assumes that Mn and Fe are present in equal atomic proportions, to give a molecular weight of 569.5. Of course, he was not concerned in the problem under consideration.

The crystal structure of axinite has been worked out by Ito and Takeuchi (1952) on axinite from Obira, Japan, with composition given as $H(Fe_{0.3}Mn_{0.7})Ca_2Al_2BSi_4O_{16}$.

A recent paper by Simonen and Wiik (1952) describes two axinites, one from Jokoinen, southwest Finland, and the other from Petsamo, U.S.S.R. that are remarkably high in FeO (9.36% and 9.56% respectively) and notably low in MnO (0.69% and 0.75% respectively); MgO on the other hand is very high for axinite (1.59% and 1.19%). These writers accept Peacock's unit-cell content $H_2B_2Al_4Ca_4(Mn, Fe)_2Si_8O_{32}$ and give a triangular diagram of the FeO:MnO:MgO ratios of some 19 axinites. They show that whereas pure Mg-axinite does not exist, Fe- and Mn-axinites do. By pure, however, they signify a molecule with 4 fixed atoms of Ca and 2 of Fe+Mn. However, as we have shown, considering tinzenite as manganoan axinite broadens the picture considerably, and the variation to be considered is not Simonen and Wiik's ternary, but a fourfold Ca-Fe-Mn-Mg.

There are two analyses reported in the literature with extremely high CaO content, 25.84 per cent and 29.70 per cent. Both have questionable features and probably should not be accepted as valid. The first one, of a Swedish axinite cited by Hintze (1897), was made by Hisinger in 1826 and is obviously defective. No B_2O_3 or ferrous iron is determined. In view of the inadequacy of analytical methods 130 years ago with regard to complex borosilicates, we may well disregard this analysis.

The second more recent analysis, of axinite from Radautal, Harz, was published by Luedecke (1889); Dana (1892) gives the same analyses with, however, a somewhat different set of figures (i.e., CaO 30.21%). Confusion arises in Dana's using Luedecke's calculated, not actually determined, composition. Luedecke noted that the formula based on his analysis departs widely from formulas of all previously identified axinite. One may infer that the axinite was imperfectly separated from other calcium silicate minerals—augite, garnet, and wollastonite—accompanying it.

These uncertainties, however, do not exist in the low CaO (tinzenite) range, where the analyzed material was sufficiently homogeneous and the critical analysis dependable.

References

Arbenz, P., and Tarnuzzer, Ch. (1923), Die Eisen und Manganerze der Schweiz, Die Manganerze in Radiolarenhornstein in Mittelbünden: *Beitr. Geologie der Schweiz., Goetech. Ser.* **13**, Pt. 1, 253–277.

Dana, E. S. (1892), System of Mineralogy, 6th Ed., 529.

Ford, W. E. (1903), On the chemical composition of axinite: *Am. Jour. Sci.*, (4)**15**, 195–201.

Foshag, W. F. (1925), New minerals—doubtful species: *Am. Mineral.*, **10**, 108.

Fromme, J. (1909), *Min. Petrog. Mitt.*, **28**, 305.

Gädeke, Rudolf (1938), Die gesetzmässigen Zusammenhänge und Anomalien in der Vesuviangruppe und einigen anderen Kalksilikaten: *Chemie der Erde* (Linck), **11**, 592–636.

Geiger, Th. (1948), Manganerze in den Radiolariten Graubündens: *Beitr. Geologie der Schweize*, Geotech. Ser. Lieferung, **27**, 1–89.

Goldschmidt, V. M. (1911), Die Kontaktmetamorphose in Kristianiagebiet: *Vid. Skrift. 1 Mat. Naturw. Kl.* No. 1, 448–466.

Hintze, C. (1897), Handbuch der Mineralogie, **2**, 508–509.

Ito, T., and Takeuchi, Y. (1952), The crystal structure of axinite: *Acta Crystallographica*, **5**, 202–208.

Jakob, Johann (1923), Vier Mangansilikate aus den Val d'Err (Kanton Graubünden): *Schweiz. Min. Petrog. Mitt.*, **3**, 227–236.

——— (1926), Die Tinzenite-Varietäten aus dem Val d'Err (Graubünden): *Schweiz. Min. Petrog. Mitt.*, **6**, 200–202.

——— (1933), Die Manganerzlagerstätten zwischen Val d'Err und Roffna (Oberhalbstein), ihre Begleitminerale und ihre Genesis: *Schweiz Min. Petrogr. Mitt.*, **13**, 17–39.

Luedecke, O. (1889), *Zeitschr. f. Naturw.*, **62**, 14.

Müller, F. P. (1916), Über einiger Mineralien aus dem Manganerz-Lagerstätten des Oberhalbstein (Graubünden, Schweiz): *Centralbl. Mineral. Geol., Palaeontol. A*, 457–459.

——— (1916), Die Manganerzlagerstätten des Oberhalbstein (Graubünden, Schweiz): *Zeitschr. Prakt. Geol.*, **24**, 219–228.

Palache, Charles (1935), The Minerals of Franklin and Sterling Hill, Sussex County, New Jersey: *U. S. Geol. Survey Prof. Paper* **180**, 99–100.

Parker, Robert L. (1948), Zur Krystallographie von Tinzenit: *Schweiz. Min. Petrog. Mitt.*, **28**, 475–492.

Peacock, M. A. (1937), On the crystallography of axinite and the normal setting of triclinic crystals: *Am. Mineral.*, **22,** 588–620.

Pelloux, A. (1919), Mem. Soc. Lunigianese "Giovanni Cappelini," Vol. 1, No. 1.

——— A. (1934), Tinzenite e Parsettensite della miniera di Cassagna (Liguria): *Boll. Soc. Geol. Ital.*, **53,** 235–238.

Sanero, Eduardo (1936), Richerche chimiche sulla tinzenite e parsettensite della miniera di Cassagna (Liguria): *Periodico Miner.*, **7,** 123–132.

Schaller, W. T. (1911), Mineralogical Notes, Series I, Axinite from California: *U. S. Geol. Survey Bull.* **490,** 37–47.

Simonen, Ahti, and Wiik, H. B. (1952), The axinites from Jokoinen and Petsamo: *Bull. Comm. Geol. de Finlande* **No. 157,** 1–6.

Strunz, H. (1949), Mineralogische Tabellen—2d ed., p. 185, Akad. Verlag., Leipzig.

Waldmann, Hans (1948), Uber die Krystalloptik von Tinzenit: *Schweiz. Min. Petrog. Mitt.*, **28,** 493–501.

Winchell, A. N., and Winchell, H. W. (1951), Elements of Optical Mineralogy, Vol. II, 4th ed., John Wiley and Sons, N. Y.

STUDIES OF URANIUM MINERALS (XIII): SYNTHETIC URANOSPINITES

MARY E. MROSE,† *State Teachers College, Salem, and Harvard University, Cambridge, Massachusetts*

ABSTRACT

Compounds having the formula $A(UO_2)_2(AsO_4)_2 \cdot 8H_2O$, where $A = Ca$, H_2, Na_2, or $(NH_4)_2$, have been synthesized, the last two by base exchange with hydrogen-uranospinite, $H_2(UO_2)_2(AsO_4)_2 \cdot 8H_2O$. Synthetic calcium-uranospinite and hydrogen-uranospinite crystals are thin tablets flattened on {001} with {010} and {110}. *X*-ray single crystal study by the Weissenberg method indicated tetragonal symmetry and gave the space group P4/nmm, if holohedral symmetry is assumed. Calcium-uranospinite has cell dimensions a_0 7.19 Å, c_0 8.81 (a_0:c_0=1:1.225). Specific gravity 3.65 (calc.). Color lemon yellow. Perfect cleavage {001}. Optically anomalously biaxial negative (−) with α 1.591 (nearly colorless), β 1.619 (pale lemon yellow), γ 1.621 (pale lemon yellow); 2V variable, 0°–5°; $r>v$, moderate. Hydrogen-uranospinite has cell dimensions a_0 7.16 Å, c_0 8.80 (a_0:c_0=1:1.230). Specific gravity 3.55 (meas.), 3.55 (calc.). Color lemon yellow. Perfect cleavage {001}. Optically uniaxial negative (−) with ω 1.612 (pale lemon yellow), ϵ 1.584 (nearly colorless). Sodium-uranospinite has cell dimensions a_0 7.12 Å, c_0 8.70 (a_0:c_0=1:1.222), obtained by the powder method. Specific gravity 3.80 (calc.). Optically uniaxial negative (−) with ω 1.617 (pale yellow), ϵ 1.586 (colorless). Ammonium-uranospinite has cell dimensions a_0 7.21 Å, c_0 8.85 (a_0:c_0=1:1.227), obtained by the powder method. Specific gravity 3.60 (calc.). Optically uniaxial negative (−) with ω 1.611 (pale yellow), ϵ 1.601 (colorless). All fluoresce bright lemon yellow in long-wave ultraviolet light and less brightly in short-wave ultraviolet light. Natural troegerite, supposedly $(UO_2)_3(AsO_4)_2 \cdot 12H_2O$, is a member of the metatorbernite group and probably has the composition $H_2(UO_2)_2(AsO_4)_2 \cdot 8H_2O$.

INTRODUCTION

Uranospinite, a hydrated arsenate of calcium and uranium, $Ca(UO_2)_2(AsO_4)_2 \cdot nH_2O$, was originally found in 1871 at the Weisser Hirsch mine at Neustädtel, near Schneeberg, Saxony, Germany, and was first named and described by Weisbach (1873). The mineral occurred there in association with other secondary uranium minerals—zeunerite, walpurgite, uranospherite, and troegerite. Since then the mineral has been reported from only one other locality—near Pahreah, Kane County, Utah (Butler, *et al.*, 1920).

The only available analysis of the Schneeberg material, made by Winkler (1873), established the composition at that time as $Ca(UO_2)_2(AsO_4)_2 \cdot 8H_2O$, though Church (1877) states that Winkler's analysis does not conclusively prove it to contain only 8 molecules of water and suggests that the water may correspond to 10 molecules instead of 8.

---

† Present address: U. S. Geological Survey, Washington, D. C.

Winkler (Weisbach, 1873) successfully obtained minute yellow crystals of uranospinite by adding a solution of uranyl nitrate to a solution of lime in excess arsenic acid. His analysis of this synthetic material showed it to be in close agreement with the Schneeberg uranospinite (Table 3).

Uranospinite from Schneeberg was described by Weisbach (1873, 1877) as siskin green in color, occurring in thin tabular crystals {001}, square to rectangular in outline. Cleavages {001} perfect, {100} distinct; hardness 2–3; specific gravity 3.45; pearly luster on {010}. On the basis of the biaxial optical character Weisbach considered the mineral to be orthorhombic, but possessing pseudo-tetragonal symmetry. The forms *c*{001}, *q*{1.0.10}, *y*{102}, *r*{101}, and *x*{012} were identified by goniometric measurements by Weisbach (1877) who obtained, as a result, the axial ratio a:b:c = 1 (approx.):1:2.9123.

Goldschmidt (1899), on the other hand, considered the mineral as possessing tetragonal symmetry as a result of optical studies he made on Winkler's synthetic uranospinite and Weisbach's natural uranospinite. Winkler's material was found to be uniaxial negative; the Schneeberg material, anomalously biaxial negative. Neither Goldschmidt nor Weisbach, however, recorded the indices of refraction for the natural or synthetic uranospinite. Goldschmidt (1923) observed the forms *c*{001}, *q*{105}, *d*{011}, and *r*{021} on uranospinite crystals and obtained, as a

TABLE 1. OPTICAL PROPERTIES AND UNIT CELL DIMEN-

	Synthetic Hydrogen-uranospinite	Synthetic Calcium-uranospinite (C. Frondel)			
	Air-dried at room temp.	Air-dried at room temp.	Heated to 110°	Heated to 1000°	Hydrated in H_2O for 1 week
Anal. No.	2	5			
Sign	(−)	(−); anomalously biax.	(−)	(−)	(−)
Indices					
α or ε	1.584±0.003	1.591±0.003	1.615±0.003	1.765±0.003	1.562±0.003
β		1.619±0.003			
γ or ω	1.612±0.003	1.621±0.003	1.637±0.003	1.778±0.003	1.589±0.003
Opt. Orient.	X=c	X=c	X=c	X=c	X=c
Dispersion		r>v, moderate			
Pleochroism					
X or E	nearly colorless	nearly colorless	nearly colorless	pale yellow brown	nearly colorless
Y		pale lemon yellow			
Z or O	pale lemon yellow	lemon yellow	pale lemon yellow	yellow brown	pale lemon yellow
2V	0°	variable, 0°–5°	0°	0°	0°
Space Group	P 4/nmm	P 4/nmm			
a_0	7.16 Å±0.02	7.19 Å±0.02			
c_0	8.80 ±0.02	8.81 ±0.02			
$a_0:c_0$	1:1.230	1:1.225			

result, the axial ratio a:c = 1:1.4561, which is one-half the *c* value obtained by Weisbach (1877).

Numerous specimens labelled uranospinite and troegerite from Schneeberg, Saxony, were examined by means of optical and *x*-ray methods in the attempt to identify the presence of these two uranium minerals. A wide variation in optical data and *x*-ray powder patterns was obtained for materials supposedly uranospinite and troegerite. Since in every instance the limited amount of material on the specimens precluded the possibility of chemical analysis as a certain means of identification, it was decided to pursue the problem with the use of synthetic materials.

Syntheses of Uranospinites

Crystals of synthetic uranospinite, $Ca(UO_2)_2(AsO_4)_2 \cdot 8H_2O$, prepared by Dr. Clifford Frondel, were available for study. At the same time, because of the possibility that material labelled uranospinite and troegerite might actually be the hydrogen, sodium, or ammonium analogues of $Ca(UO_2)_2(AsO_4)_2 \cdot 8H_2O$, crystals of these compounds were synthesized. Hydrogen-uranospinite, $H_2(UO_2)_2(AsO_4)_2 \cdot 8H_2O$, was the first to be prepared, by the method described below; sodium- and ammonium-uranospinite were obtained by base exchange with hydrogen-uranospinite.

sions for Synthetic and Natural Uranospinites

Natural Uranospinite (Larsen, 1921)			Synthetic Sodium-uranospinite	Synthetic Ammonium-uranospinite
Schneeberg	Schneeberg	Schneeberg	Air-dried at room temp.	Air-dried at room temp.
			9	11
(−)	(−)	(−)	(−)	(−)
1.560±0.003	1.560±0.01	1.55 ±0.01	1.586±0.003	1.601±0.003
1.582±0.003		1.567±0.003		
1.587±0.003	1.586±0.003	1.572±0.003	1.617±0.003	1.611±0.003
X=c				
r>v, rather strong				
nearly colorless	nearly colorless	colorless	colorless	colorless
pale canary yellow		pale yellow		
pale canary yellow	pale yellow	pale yellow	pale lemon yellow	pale lemon yellow
46°	0°	62°±3°	0°	0°
			7.12 Å±0.02	7.21 Å±0.02
			8.70 ±0.02	8.85 ±0.02
			1:1.222	1:1.227

Synthesis of Calcium-uranospinite

Uranospinite, $Ca(UO_2)_2(AsO_4)_2 \cdot 8H_2O$, was precipitated at room temperature as a flocculent lemon-yellow precipitate by reaction in water solution of calcium chloride, uranyl nitrate, and monohydrogen sodium arsenate in molar ratio of 1:2:2. The precipitate was then heated in the mother solution, which had an acid reaction, for five months at 50° C. In this time the original precipitate recrystallized into thin lemon-yellow plates, square to rectangular in outline, up to 0.5 mm. on an edge.

Syntheses of Hydrogen-, Sodium-, and Ammonium-uranospinite

Several methods were employed in the effort to synthesize measurable crystals of hydrogen-uranospinite, $H_2(UO_2)_2(AsO_4)_2 \cdot 8H_2O$. The following method yielded best results: 6.04 g arsenic acid were dissolved in 400 cc hot water and then brought to the boiling point. To this a hot solution of uranyl nitrate (10.1 g $(UO_2)(NO_3)_2 \cdot 6H_2O$ in 80 cc. hot water) was slowly added. The resultant solution was allowed to boil vigorously for 20 minutes. When allowed to cool to room temperature at this stage, distinct but very small crystals averaging less than 0.01 mm. on an edge were precipitated. Large crystals, up to 1.5 mm. on an edge, were obtained by placing the boiling solution in an oven at 100° C., filtering the solution at the end of four days, then placing the filtrate in a flask sealed except for a small capillary tube set into the cork and allowing this to cool slowly by lowering the oven temperature 5° per day. When the oven temperature was lowered from 35° to 30°, large crystals were precipitated.

Sodium- and ammonium-uranospinite were synthesized by base-exchange with hydrogen-uranospinite. Sodium-uranospinite, $Na_2(UO_2)_2(AsO_4)_2 \cdot 8H_2O$, was obtained by immersing small crystals of hydrogen-uranospinite in a 1N water solution of sodium chloride for two weeks at room temperature. Ammonium-uranospinite, $(NH_4)_2(UO_2)_2(AsO_4)_2 \cdot 8H_2O$, was similarly obtained, using ammonium chloride.

OPTICAL PROPERTIES

The optical properties of synthetic and natural uranospinites are summarized in Table 1. The indices of refraction for the air-dried synthetic uranospinites are somewhat different from those reported for natural uranospinite. It may be noted in Table 1 that the only synthetic preparation whose indices of refraction approach those of the natural material is the Ca member after it had been immersed in water at room temperature for one week. With the apparent increase in water content, there was an accompanying decrease in indices of refraction. On the other hand, the loss of water by dehydration of synthetic $Ca(UO_2)_2(AsO_4)_2 \cdot 8H_2O$ at 110° C. and at 1000° C. (Table 1) caused a considerable increase in both ω and ϵ. The decrease and increase in indices of refraction are consistent with the *x*-ray data which show changes in crystal structure at these stages in the dehydration process. Though it seems apparent that the natural material may be a higher hydrate than the $8H_2O$ hydrate obtained by synthesis, no conclusive statement can herewith be made concerning the optical relationships between the two, since chemical analyses are lacking for the natural material described optically by Larsen (1921).

Numerous specimens labelled uranospinite and troegerite were examined optically during the course of this study. Only two specimens contained material whose optics were in close agreement with those reported for uranospinite by Larsen (1921). The crystals on both specimens were siskin green in color, rectangular in outline, and fluoresced bright lemon yellow in long-wave and short-wave ultraviolet light. The optical data for these are as follows (all values ±0.003):

	"Troegerite" Schneeberg, Saxony (C 4394)	"Uranospinite" Spanish Fork, Utah (USNM 94665)	Pleochroism	
α	1.560	1.560	X nearly colorless	Biaxial neg. (−)
β	1.581	1.584	Y pale lemon yellow	2V∼45°
γ	1.585	1.586	Z pale lemon yellow	r>v, moderate

The *x*-ray powder patterns of the two specimens, however, differed from each other. The unanalyzed "troegerite" from Schneeberg gave a pattern identical with the meta-I hydrate of the torbernite group, while the unanalyzed "uranospinite" from Spanish Fork, Utah, corresponded to the fully hydrated phase. However, in neither case was sufficient material available for quantitative or qualitative analyses. Several other specimens labelled uranospinite and troegerite were later proven to be saléeite and novacekite. Some still remain unidentified.

Qualitative analyses were made by Forrest A. Gonyer on eight specimens labelled troegerite. Four of these were reported to contain As and P together with Mg. These were subsequently proven by chemical analyses to be saléeite and novacekite (Frondel, 1951b). The other four were reported to have an excess of As over P but without either Ca or Mg. It was hoped that these might prove to be hydrogen-uranospinite, believed to exist in nature as troegerite. The optical data for these four samples are as follows (all values ±0.003):

	Schneeberg (H 15781)*	Schneeberg (H 665)*	Schneeberg (Y 1016)†	Joachimsthal (H 977)*	Pleochroism
Sign	(−)	(−)	(−)	(−)	
α	1.600	1.600	1.600	1.584	X nearly colorless
β	1.629	1.628	1.628	1.620	Y pale lemon yellow
γ	1.631	1.630	1.630	1.623	Z pale lemon yellow
Opt. Orient.	X=c	X=c	X=c	X=c	
Dispersion	r>v, mod.	r>v, perc.	r>v, mod.	r>v, perc.	
2V	0°–40°	∼15°	∼30°	∼20°	

* Harvard specimen number.

† Yale specimen number.

They show three to be in close agreement with each other while the fourth (Joachimsthal) is in fair agreement with the data listed by Larsen (1921) for troegerite.

The x-ray powder photographs of the three specimens of "troegerite" from Schneeberg are very similar to those of sabugalite, an aluminum-autunite (Frondel, 1951a) and resemble but are distinct from both fully-hydrated autunite and meta-autunite. Qualitative analyses and optical data, however, eliminate this mineral (sabugalite) as a possibility. The Joachimsthal specimen afforded a pattern similar to that of novacekite; the optical data are in good agreement. However, the qualitative analysis eliminates this mineral as novacekite.

CRYSTALLOGRAPHY

Only the crystals of synthetic hydrogen-uranospinite were large enough to afford accurate goniometric measurements. Examination of numerous crystals indicated the presence of two habits; the smaller crystals were, for the most part, square in outline with only the forms {001} and {010} present; the larger crystals, on the other hand, were eight-sided with {001} and {010} truncated by {110}. Because of the absence of inclined forms, it was impossible to derive a linear axial ratio based on the morphology.

The morphological development of the synthetic Ca, Na, and (NH_4) compounds was observed only under the microscope. The forms noted were the same as found on the crystals of synthetic hydrogen-uranospinite.

Single crystal x-ray work was done on the synthetic calcium-uranospinite and hydrogen-uranospinite crystals. The x-ray rotation and Weissenberg films conclusively proved that both synthetic compounds possess tetragonal symmetry. The space group established by the diffraction effects is P 4/nmm, if holohedral symmetry is assumed. Unit cell dimen-

TABLE 2. *X*-RAY POWDER SPACING DATA FOR SYNTHETIC URANOSPINITES
Copper radiation, nickel filter, in Å (λ=1.5418)

Hydrogen-uranospinite		Calcium-uranospinite				Sodium-uranospinite		Ammonium-uranospinite	
d(meas.)	I*	Air-dried d(meas.)	I*	Heated to 1000° d(meas.)	I*	d(meas.)	I*	d(meas.)	I*
8.59	10	8.85	10	7.20	2	8.42	10	9.26	10
5.50	7	5.57	6	6.46	2	5.44	7	5.72	7
5.04	4	5.10	7	5.10	7	5.01	6	5.14	4
4.35	7	4.40	2	4.82	8	4.27	5	4.54	6
3.79	9	3.74	5	4.06	7	4.09	½	4.30	½
3.56	6	3.59	9	3.58	10	3.93	½	3.86	9
3.30	8	3.34	8	3.29	9	3.63	9	3.60	6
3.14	½	3.02	4	2.96	2	3.55	7	3.36	8
2.99	5	2.81	1	2.87	1	3.27	8	3.20	½
2.76	2	2.68	1	2.77	6	2.97	6	3.04	5
2.70	7	2.55	5	2.69	3	2.74	2	2.80	7
2.59	3	2.44	4	2.53	5	2.64	6	2.63	5
2.53	6	2.29	3	2.42	5	2.56	4	2.55	3
2.43	5	2.20	2	2.23	6	2.52	4	2.46	6
2.30	2	2.16	2	2.15	3	2.49	5	2.33	2
2.26	3	2.10	2	2.12	4	2.41	5	2.28	7
2.19	7	2.00	1	2.01	5	2.29	4	2.22	7
2.16	4	1.945	1	1.933	3	2.27	4	2.18	2
2.10	5	1.845	½	1.863	5	2.18	4	2.14	4
2.01	7	1.804	5	1.841	1	2.14	5	2.07	7
1.931	3	1.755	1	1.821	3	2.08	5	1.961	2
1.873	2	1.704	1	1.784	5	1.977	6	1.928	1
1.845	3	1.642	3	1.749	5	1.926	3	1.890	3
1.807	4	1.608	3	1.667	5	1.834	4	1.863	1
1.787	4	1.575	3	1.629	1	1.797	4	1.828	6
1.752	4	1.499	½	1.600	5	1.781	4	1.801	3
1.705	1	1.414	½	1.568	4	1.740	3	1.770	3
1.685	½	1.384	½	1.499	4	1.722	2	1.713	7
1.658	7	1.361	½	1.453	2	1.692	1	1.670	3
1.643	2			1.433	4	1.670	½	1.633	3
1.613	3			1.397	3	1.626	7	1.608	7
1.598	3			1.377	2	1.598	4	1.589	3
1.576	7			1.365	2	1.561	6 (broad)	1.518	3
1.541	½			1.347	2	1.517	½	1.486	4
1.508	½			1.337	3	1.495	1	1.456	3
1.492	1			1.288	2	1.478	2	1.422	8
1.473	½			1.278	2	1.453	1	1.401	½
1.462	1			1.251	2	1.421	½	1.373	4
1.437	4			1.222	3	1.408	5	1.361	2
1.427	4			1.188	4	1.384	1	1.321	½
1.388	6			1.148	4	1.370	5	1.304	2

* Intensities estimated visually.

sions for the synthetic uranospinites are cited in Table 1; those given for sodium- and ammonium-uranospinite were obtained by indexing the powder photographs in terms of the hydrogen-uranospinite cell. *X*-ray powder spacing data are given in Table 2.

The *x*-ray ratio for calcium-uranospinite ($a:c=1:1.225$) and the morphological ratio obtained by Goldschmidt (1923) on natural crystals ($a:c=1:1.4561$) are not in good agreement. The unit of the *x*-ray cell for hydrogen-uranospinite ($a:c=1:1.230$) differs from the morphological unit of Goldschmidt (1899) on natural troegerite in that the *c*-axis is halved ($a:c=1:2.16$); the agreement in ratios is not close.

CHEMISTRY

Chemical analyses of the various synthetic uranospinites (cited in Table 3) indicate the general formula of the compounds to be $A(UO_2)_2(AsO_4)_2 \cdot nH_2O$, where $A=H_2$, Ca, Na_2 or $(NH_4)_2$.

The analysis of synthetic hydrogen-uranospinite is cited in column 2. The measured specific gravity of this compound is 3.55, representing an average of five different measurements made on the Berman microbalance. Using this value as the density, the analysis of column 2, and the unit cell dimensions obtained by single crystal *x*-ray study, the molecular weight of the unit cell was found to be 965. The calculated cell contents approach closely the formula

$$H_2(UO_2)_2(AsO_4)_2 \cdot 8H_2O.$$

The calculated specific gravity is 3.55. The analysis of troegerite, given in column 3 probably natural hydrogen-uranospinite—indicates somewhat lower water content than that of the synthetic material.

The percentage of CaO in the analysis made on C. Frondel's calcium-uranospinite (column 5, Table 3) is low as compared with that reported by Winkler for his synthetic material (column 6, Table 3). The *x*-ray powder photograph of Frondel's material, however, is in agreement with that given by synthetic calcium-uranospinite, prepared by Fairchild's salting-out method, furnished the writer by Mr. K. J. Murata of the United States Geological Survey, when both materials were brought into equilibrium with each other. The deficiency in calcium is probably due to a partial substitution of H_2 for Ca, in a series toward hydrogen-uranospinite. A similar situation is known in synthetic meta-autunite (Beintema, 1938).

The small size and fragility of the crystals of calcium-, sodium-, and ammonium-uranospinite precluded making specific gravity measurements. Assuming $Ca(UO_2)_2(AsO_4)_2 \cdot 8H_2O$ as the formula for calcium-uranospinite and the cell dimensions obtained by single crystal *x*-ray study (Table 1), the calculated specific gravity is 3.65. Using the cell

TABLE 3. CHEMICAL ANALYSES OF URANOSPINITES

	1	2	3	4	5	6	7	8	9	10	11
CaO				5.60	3.10	5.62	5.47				
Na_2O								6.15	5.90		
$(NH_4)_2O$										5.22	5.11
UO_3	59.34	59.26	63.76	57.09	58.56	59.01	59.18	56.75	58.68	57.32	59.70
As_2O_5	23.84	23.70	19.64	22.93	23.54	23.01	19.37	22.80	22.86	23.02	23.14
H_2O	16.82	17.09	14.81	14.38	14.60	14.27	16.19	14.30	12.69	14.44	12.13
Total	100.00	100.05	98.21	100.00	99.80	101.91	100.21	100.00	100.13	100.00	100.08
G (meas.)		3.55									
G (calc.)		3.55		3.65				3.80		3.60	

1. $H_2(UO_2)_2(AsO_4)_2 \cdot 8H_2O$. Theoretical weight percentages.
2. Hydrogen-uranospinite. Synthetic (Mrose). Gonyer, analyst, 1950.
3. Troegerite. Schneeberg, Saxony (Winkler, 1873).
4. $Ca(UO_2)_2(AsO_4)_2 \cdot 8H_2O$. Theoretical weight percentages.
5. Uranospinite. Synthetic (C. Frondel). Gonyer, analyst, 1950.
6. Uranospinite. Synthetic (Winkler, 1873).
7. Uranospinite. Schneeberg, Saxony (Winkler, 1873).
8. $Na_2(UO_2)_2(AsO_4)_2 \cdot 8H_2O$. Theoretical weight percentages.
9. Sodium-uranospinite. Synthetic (Mrose). Gonyer, analyst, 1950.
10. $(NH_4)_2(UO_2)_2(AsO_4)_2 \cdot 8H_2O$. Theoretical weight percentages.
11. Ammonium-uranospinite. Synthetic (Mrose). Gonyer, analyst, 1950

dimensions obtained by the powder method (Table 1) and assuming $Na_2(UO_2)_2(AsO_4)_2 \cdot 8H_2O$ as the formula for sodium-uranospinite and $(NH_4)_2(UO_2)_2(AsO_4)_2 \cdot 8H_2O$ as the formula for ammonium-uranospinite, the calculated specific gravities are 3.80 and 3.60, respectively.

Dehydration Data

X-ray powder photographs of synthetic air-dried hydrogen-, calcium-, sodium-, and ammonium-uranospinite were of the meta-autunite I type of structure, and each pattern probably represents material containing 8 molecules of water. The spacing data for these patterns are listed in Table 2.

No structural change was produced by heating hydrogen-uranospinite at 90°, but an unidentified phase was formed between 90° and 200°. Frondel's synthetic calcium-uranospinite lost 11.3% of zeolitic (?) water when heated to 110°, the indices of refraction increased to ω 1.637, ϵ 1.615 with 2V 0°, and the color changed from lemon yellow to martius yellow (Ridgway, 1912). When exposed to air at room temperature the material regained most of its water (8.3%) and the indices decreased. The water content of this phase thus varies zeolitically over a wide range. The same material when immersed in water at room temperature converted to the fully hydrated phase with ω 1.589, ϵ 1.562, 2V 0° and when exposed again to air reverted to the meta-I hydrate with $\sim 8H_2O$. A sample heated to 1000° changed in color from lemon yellow to old gold (Ridgway, 1912), and afforded an entirely new pattern unlike that of the meta-I or meta-II hydrates of torbernite that probably represents the anhydrous phase CaU_2O_7; it was uniaxial negative with ω 1.778, ϵ 1.765.

Fluorescence varies with water content. All the synthetic uranospinites ($\sim 8H_2O$) fluoresce bright lemon yellow in both short-wave and long-wave ultraviolet radiation; calcium-uranospinite when reduced in water content by heating to 110° fluoresces weak olive green; the same synthetic material heated to 1000°, clove brown. The intensity of the fluorescence in all instances is somewhat greater in long-wave than in short-wave radiation.

The status of natural uranospinite and troegerite is still problematic and further work on these minerals is desirable, provided sufficient material is available for chemical analyses.

ACKNOWLEDGMENTS

The author wishes to express her gratitude to Dr. Clifford Frondel of the Department of Mineralogy and Petrography, Harvard University, for his suggestion of the study and direction of the research; to Mr. K. J. Murata of the United States Geological Survey, for making available his preparation of synthetic uranospinite for comparative purposes; and to Dr. George Switzer of the United States National Museum and Dr. Horace Winchell of Yale University for the loan of specimens for use in this study.

REFERENCES

BEINTEMA, J. (1938), On the composition and the crystallization of autunite and the meta-autunites: *Rec. Trav. Chim. Pays-Bas*, **57**, 155.

BUTLER, B. S., LOUGHLIN, G. F., HEIKES, V. C., AND OTHERS (1920), The ore deposits of Utah: *U. S. Geol. Surv., Prof. Paper* **111**, 115.

CHURCH, A. H., (1877), Note on Uranocircite: *Min. Mag.*, **1**, 236.

FRONDEL, C. (1951a), Studies of uranium minerals (VIII); Sabugalite, an aluminum-autunite: *Am. Mineral.*, **36**, 671–679.

— (1951b), Studies of uranium minerals (IX); Saléeite and Novacekite: *Am. Mineral.*, **36**, 680–686.

GOLDSCHMIDT, V. (1899), Ueber Trögerit und künstlichen Uranospinit: *Zeit. Krist.*, **31**, 468–478.

——— (1923), Atlas der Krystallformen, **9**, 41.

LARSEN, E. S., AND BERMAN, H. (1921), *U. S. Geol. Survey Bull.* **679**, 145–146, 150–151.

PALACHE, C., BERMAN, H., AND FRONDEL, C. (1951), "Dana's System of Mineralogy," 7th ed., vol. II, 966–967, 990–991, John Wiley & Sons, New York.

RIDGWAY, R. (1912), Color Standards and Color Nomenclature. Washington, D. C.

WEISBACH, A. (1873), *Neues Jahrb. f. Min.*, 314.

——— (1877), *Berg- u. hüttenm. Jahrb. Leoben*, **42**, 53.

WINKLER, C. (1873), *Jour. prakt. Chem.*, **7**, 11.

BURBANKITE AND CALKINSITE, TWO NEW CARBONATE MINERALS FROM MONTANA*

W. T. PECORA AND JOE H. KERR†, *U. S. Geological Survey, Washington 25, D. C.*

ABSTRACT

Burbankite and calkinsite, two new rare-earth-bearing carbonates, have been discovered in veins in the Bearpaw Mountains of Montana. Burbankite is an anhydrous carbonate with the general formula $Q_6(CO_3)_5$, where Q represents Na, Ca, Sr, Ba, and rare earths. Calkinsite is a hydrous carbonate with the formula $(RE)_2(CO_3)_3 \cdot 4H_2O$, where RE represents the summation of the rare earths. Burbankite is unlike any other carbonate, and calkinsite resembles lanthanite but has less water.

The physical properties of burbankite are: Hexagonal; color, grayish yellow; H, $3\frac{1}{2}$; Sp. gr., 3.50; uniaxial (−); ω, 1.627; ϵ, 1.615; cleavage, prismatic. The physical properties of calkinsite are: Orthorhombic; color, pale yellow; H, $2\frac{1}{2}$; Sp. gr., 3.28; habit, platy, {010}; biaxial (−); 2V, 57.2°; α, 1.569; β, 1.657; γ, 1.686; cleavage, {010}, perfect, {101} distinct; parting (?), {001}.

X-ray crystallographic data for burbankite: $a_0 = 10.53$ Å ± 0.05 Å, $c_0 = 6.47$ Å ± 0.02 Å, space group $P6_3/mmc$ or D_6^4h, number of formula units in the unit cell is 2. *X*-ray crystallographic data for calkinsite: $a_0 = 9.57$ Å ± 0.02 Å, $b_0 = 12.65$ Å ± 0.08 Å, $c_0 = 8.94$ Å ± 0.02 Å, space group $P2_1\,22_1$ or $D_2{}^3$, number of formula units in the unit cell is 4; a:b:c = 0.757 :1:0.707. Morphological crystallography for calkinsite: $p_0:q_0:r_0 = 0.934:0.707:1$; forms c {001}, b {010}, a {100}, d {102}, q {122}, r {132}; twinning plane {101}; crystal class, probably P 2/m 2/m 2/m.

Burbankite occurs with intimately intergrown ancylite as irregular masses or veinlets younger than calcite, and as separate crystals in calcite, in hydrothermal deposits composed essentially of silicates, carbonates, and sulfides. Calkinsite is a late mineral associated with barite in vugs and associated with lanthanite, barite, and goethite in porous areas of weathered burbankite and ancylite.

The minerals are named after W. S. Burbank and F. C. Calkins, of the U. S. Geological Survey.

INTRODUCTION

A number of rare-earth-bearing carbonates have been identified during the study of a group of silicate-carbonate-sulfide deposits in the Bearpaw Mountains of Montana. Two among them are recognized as new minerals and their description is the purpose of this paper. The deposits themselves will be described in a later publication as another of a series developing from current geological investigations in the Bearpaw Mountains. The two new minerals, *burbankite* and *calkinsite*, are named after W. S. Burbank and F. C. Calkins, geologists of the U. S. Geological Survey, in recognition of their contributions to the geology of mineral deposits of the Western States.

Both burbankite and calkinsite are well-defined minerals for which the

---

* Publication authorized by the Director, U. S. Geological Survey.

† Deceased Sept. 11, 1953, while on field duty.

optical and x-ray data that have been determined have a high order of reliability. Very fine grained intergrowths with other minerals, unfortunately, have not permitted satisfactory purification of samples for an equally reliable interpretation of chemical analysis. The type material has been deposited in the U. S. National Museum, Washington, D. C.

LOCATION

The deposits containing burbankite and calkinsite are located in southeastern Hill County, Montana, at the head of Big Sandy Creek in sec. 19, T. 28 N., R. 16 E. The group of prospects, locally known as "Vermiculite Prospects," are in the Rocky Boy's Indian Reservation and can be reached from the town of Boxelder on U. S. Highway 87 by traveling eastward about 24 miles, and from the city of Havre on U. S. Highway 2 by traveling southward about 30 miles.

GEOLOGICAL OCCURRENCE

The mineral deposits at the Vermiculite Prospects occur in shonkinite, mafic monzonite, and syenite that are a part of the Rocky Boy composite stock, briefly described by Pecora (1942, p. 398) and correlated with

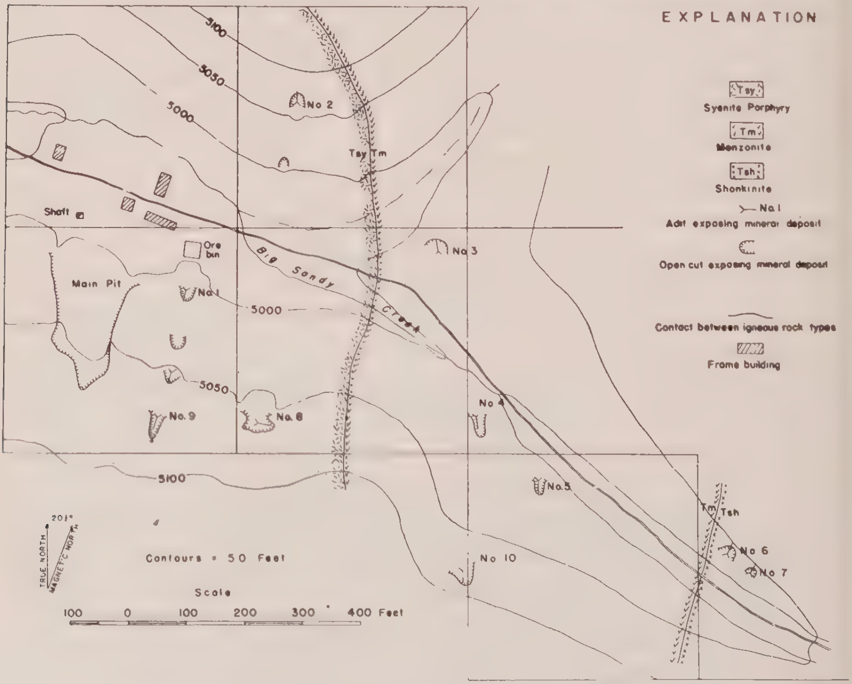

FIG. 1. Sketch map of the Vermiculite Prospects on Big Sandy Creek.

volcanic rocks of Eocene age (Brown and Pecora, 1950). Six minerals in varying abundance essentially make up these deposits; they are sanidine, biotite, aegirite, calcite, pyrite, and pyrrhotite. The two most easterly prospects on Big Sandy Creek, numbered 6 and 7 in Figure 1, have more burbankite and calkinsite than any of the others.

Specimens from prospect number 6 provided the material prepared for chemical analysis. At this locality, shonkinite is irregularly fractured and is host to a random network of interconnecting veins that define a fracture zone about 12 feet wide. The veins range in thickness from a fraction of an inch to 8 inches. Calcite is the dominant mineral of the vein material; and the other minerals, in addition to burbankite and calkinsite, include sanidine, biotite, aegirite, pyrrhotite, pyrite, chalcopyrite, galena, tetrahedrite, ilmenite, barite, ancylite, lanthanite, and a number of unidentified alteration products. A crude zoning is apparent in some of the veins, with sanidine and aegirite concentrated at their margins; and a streaked or banded feature is apparent in others and is suggestive of reopened fractures.

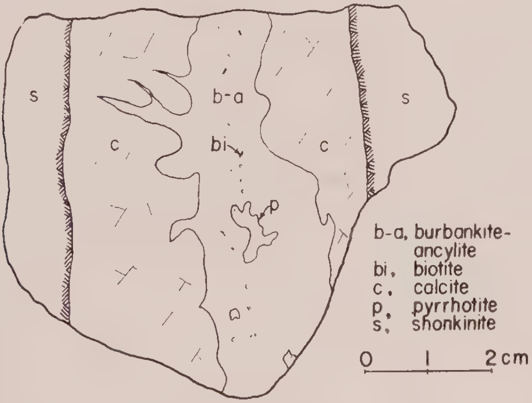

Fig. 2. Sketch of carbonate vein in shonkinite showing distribution of the principal minerals associated with burbankite.

Irregular stringers and patches, as much as 5 cm. wide, within the calcite-rich vein material (Fig. 2) are composed almost entirely of rare-earth-bearing minerals or their weathering products. In unweathered specimens these portions of the veins are essentially burbankite that is intricately veined by very fine grained ancylite and subordinate amounts of calcite and biotite. The largest burbankite crystals are 3 cm. across. Burbankite is also disseminated in calcite as anhedral crystals commonly less than 0.02 mm. in largest dimension.

As a result of weathering, the burbankite-ancylite intergrowth is altered to a porous, flaky, powdery material containing plates of calkinsite and lanthanite, fine-grained barite, goethite, and some other unidentified, fine-grained minerals. Calkinsite is most abundant in the partly altered area adjacent to unweathered burbankite; and lanthanite and barite are most abundant in completely altered material. Both calkinsite and barite are present also in rare vugs that show no evidence of weathering. The plates of calkinsite are less than 1 mm. in maximum dimension and their average maximum dimension is is about 0.2 mm.

BURBANKITE

Physical Properties

Powdered burbankite has a grayish-yellow color. In freshly broken hand specimens, the burbankite-rich material has a pale-yellow color. Burbankite effervesces strongly in cold dilute (1:5) HCl, has a hardness of about $3\frac{1}{2}$, and a specific gravity (pycnometer method) of 3.50. Its cleavage is prismatic, $\{100\}$, distinct to imperfect. Its optical properties, compared with those of associated ancylite, are given in Table 1.

TABLE 1. OPTICAL PROPERTIES OF BURBANKITE AND ANCYLITE FROM THE BEARPAW MOUNTAINS

	Burbankite	Ancylite
Indices of refraction	$\left.\begin{matrix}\omega=1.627\\ \epsilon=1.615\end{matrix}\right\}$ Na ±0.001	$\left.\begin{matrix}\alpha=1.615\\ \beta=1.695\\ \gamma=1.730\end{matrix}\right\}$ Na ±0.003
Birefringence	0.012	0.115
Optical character	(−)	(−)
Optic angle		70°±5°
Dispersion		$r<v$
Crystal system	Hexagonal	Orthorhombic

The very low birefringence (0.012) for burbankite is noteworthy in view of its composition. Winchell (1931, p. 204) records a birefringence as low as 0.050 for some synthetic carbonates of the alkalies and alkaline earths. No carbonate is known analogous to burbankite in composition that has so low a birefringence.

Chemical Composition

Purity of the analyzed sample: The sample of powdered burbankite prepared for chemical analysis was determined by grain counts in immersion to contain about 96 per cent burbankite, 3 per cent ancylite, and one per cent biotite, sulfides, and other minerals. It was prepared from 30 grams of hand-picked fragments that were crushed, sieved, washed, and purified by means of methylene iodide and the Frantz isodynamic separator. This method removed most of the impurities but unfortunately also concentrated admixed ancylite. Despite repeated heavy liquid separations and some 400 passes in the Frantz separator, at different settings, it was impossible to improve the purity of the final sample in the size range of 200–400 mesh beyond 96 per cent burbankite.

Chemical analysis: The chemical analysis of the original sample of burbankite by M. K. Carron is given in Table 2, column 1, and a recalcu-

TABLE 2. CHEMICAL ANALYSIS OF BURBANKITE

M. K. Carron, Analyst

	1 Original sample	2 Recalculated to 100% pure		3 Moles	4 Cation ratios		5 Atoms based on $5CO_3$ and 6 cations
CO_2	32.55	33.39		0.7587	0.7587		
CaO	13.46	13.68		0.2439	0.2439		1.611 Ca
SrO	19.42	19.70		0.1901	0.1901		1.255 Sr
BaO	13.56	14.02		0.0914	0.0914		0.603 Ba
La_2O_3		2.34		0.0072	0.0144		0.095 La
Ce_2O_3		4.65		0.0142	0.0284		0.188 Ce
Pr_2O_3		0.37		0.0011	0.0022	0.09086	0.015 Pr
Nd_2O_3	9.48	1.40	9.04	0.0042	0.0084		0.055 Nd
Sm_2O_3		0.10		0.0003	0.0006		0.004 Sm
Gd_2O_3		0.08		0.0002	0.0004		0.003 Gd
Y_2O_3		0.10		0.0004	0.0008		0.005 Y
Na_2O	9.69	10.17		0.1640	0.3280		2.166 Na
K_2O	0.15	100.00					6.000
SiO_2	0.16						
Al_2O_3	0.25						
Fe_2O_3	0.03						
MgO	0.14						
P_2O_5	0.12						
$H_2O\pm$	0.18						
S	0.24						
	99.43						
Less $O=S$	0.12						
	99.31						

Na_2O and K_2O by flame photometer by E. A. Nygaard.
Rare-earth distribution by spectrograph by H. J. Rose.

lation to 100 per cent purity by allowance for the impurities is given in column 2. The alkalis were determined by E. A. Nygaard on a part of the original sample and the distribution of the rare-earth elements was determined by H. J. Rose on the precipitate of the total rare earths. The mean index of refraction calculated from the chemical composition and density after the Law of Gladstone and Dale is 1.632. This is in close agreement with the mean index of 1.625 calculated from the measured indices of refraction.

Formula of burbankite: As shown by the data listed in Table 2, columns 3, 4, and 5, the ratio of cations to CO_3 is 6:5 and the calculated cation formula is $(Na_{2.17}Ca_{1.61}Sr_{1.26}Ba_{0.60}RE_{0.36})(CO_3)_5$, where RE is the total of the rare earths. The general formula may be thus expressed as $Q_6(CO_3)_5$, where Q is the summation of the cations. The corresponding chemical formula weight is 658, or about one-half the unit cell weight (1310) that is calculated from cell dimensions and density.

The total positive charge of the cations, as stated above, slightly exceeds the negative charge of the CO_3. If, as is possible, the given amount of rare earths is too high and sodium too low, the general formula could be expressed as $Na_2R_4(CO_3)_5$, where R is Ca, Sr, Ba, and rare earths, and an amount of Na equal to the amount of rare earths.

X-ray Crystallography

Powder pattern: X-ray powder data for burbankite are given in Table 3. The calculated interplanar spacings are based on cell dimensions: $a_0 = 10.53$ Å ± 0.05 and $c_0 = 6.47$ Å ± 0.02, which were determined from the indexing of an *x*-ray powder photograph taken with Fe radiation and an Mn filter. These values are in close agreement with those determined in the later single crystal work, and they are probably more accurate because the powder photographs were corrected for film shrinkage by use of the back reflections. The cell volume calculated from the above cell dimensions is 621 Å^3. If two or more planes contribute to a line on the powder photograph, all are listed in Table 3.

Single crystal data: An anhedral crystal of burbankite measuring $0.5 \times 0.3 \times 0.3$ mm. was oriented with the *c* crystal axis ($c = E$ vibration direction) parallel to the goniometer axis. Orientation was completed by taking *x*-ray oscillation photographs. A rotation photograph and Weissenberg photographs (zero, first, and second layers) were then taken in this orientation. The rotation photograph permitted the determination of a c_0 cell dimension of 6.48 Å ± 0.03; and an a_0 cell dimension of 10.46 Å ± 0.08 was determined from the zero layer Weissenberg photograph. A primitive hexagonal lattice is indicated by these photographs.

The only systematic omission noted is $h\,h\,l$, where l is odd. This makes

TABLE 3. INDEXED *X*-RAY POWDER LINES WITH OBSERVED AND CALCULATED INTERPLANAR SPACINGS FOR BURBANKITE

Cu/Ni Radiation U.S.G.S. Film #9105		Fe/Mn Radiation U.S.G.S. Film #3943		d Å Calculated	Probable *hkl*
I	*d* Å	I	*d* Å		
2	9.10	2	9.16	9.12	100
5	5.26	7	5.28	5.28	101
				5.27	110
1	4.55	1	4.56	4.56	200
5	3.719	6	3.729	3.728	201
1	3.431	1	3.442	3.447	210
2	3.240	3	3.246	3.237	002
6	3.034	8	3.041	3.043	211
				3.040	300
3	2.748	3	2.758	2.758	112
				2.752	301
10	2.630	10	2.639	2.640	202
				2.633	220
½	2.524			2.530	310
1	2.350	1	2.358	2.360	212
				2.356	311
1	2.272	½	2.281	2.280	400
1	2.213	½	2.218	2.216	302
5	2.145	7	2.150	2.151	401
				2.158	003
1	2.100	1	2.107	2.100	103
				2.093	320
2	2.040	2	2.045	2.043	222
2	1.986	2	1.990	1.990	410
				1.991	321
2	1.951	2	1.956	1.951	203
½	1.895			1.902	411
1	1.860	1	1.864	1.864	402
½	1.827			1.829	303
				1.824	500
3	1.754	2	1.757	1.757	322
½	1.691			1.695	412
3	1.662	2	1.664	1.666	421
½	1.640			1.638	510
				1.641	313
½	1.619			1.618	004
1	1.585	½	1.588	1.588	511
1	1.566	½	1.569	1.567	
½	1.525	½	1.530	1.525	
1	1.518	1	1.519	1.520	
½	1.499				
1	1.458				
½	1.422				
½	1.380				
½	1.376				
1	1.346				
½	1.314				
½	1.282				
½	1.277				
½	1.248				
½	1.238				
½	1.231				
½	1.217				
1	1.208				
½	1.178				
½	1.166				
½	1.128				
½	1.121				

the space group $P6_3/mmc$ or D_{6h}^4. The symmetry requirements of this space group do not allow all the CO_3 groups to occupy similar positions. The low birefringence of burbankite, moreover, would suggest that the CO_3 groups are not coplanar.

CALKINSITE

Physical Properties

Calkinsite is pale yellow and has a typical platy habit parallel to {010}. The plates are commonly twinned, compound, and elongate parallel to the *a* axis (Figs. 3 and 4). The mineral effervesces strongly in cold dilute (1:5) HCl. Its hardness is about 2½, and its specific gravity (pycnometer method) is 3.28±0.01. The optical and cleavage data for calkinsite are given in Table 4. Lanthanite, which occurs with calkinsite, has many similar physical properties but can be readily distinguished from it by the indices of refraction obtainable on the cleavage plates (see Table 4), as well as by its powder pattern. Lanthanite also has a lower specific gravity and higher water content than calkinsite.

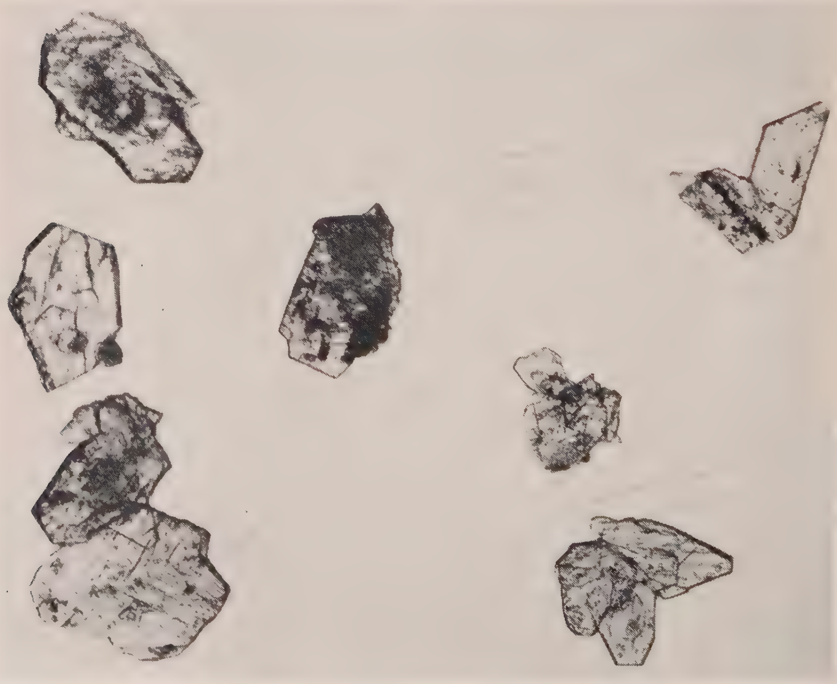

FIG. 3. Photomicrograph (×110) of calkinsite crystals in immersion, showing variation in crystal habit.

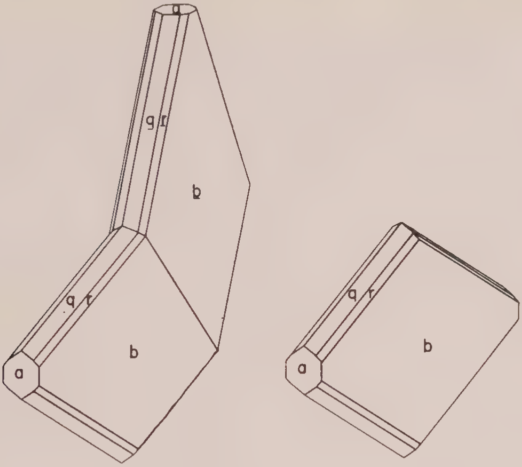

FIG. 4. Clinographic projection of twinned (left) and untwinned (right) crystals of calkinsite.

TABLE 4. OPTICAL DATA FOR CALKINSITE AND LANTHANITE FROM THE BEARPAW MOUNTAINS, MONTANA

	Calkinsite	Lanthanite
Indices of refraction	$\alpha=1.569$	
	$\beta=1.657$	1.587
(na ±0.002)	$\gamma=1.686$	
2V (Universal stage)	54°, (−)	
(Calculated)	57.2°, (−)	
(Estimated)		60°, (−)
Dispersion	r<v, perceptible	r<v, perceptible
Crystal system	Orthorhombic	Orthorhombic
Cleavage	{010}, perfect {101}, distinct {001}, parting (?)	{010}, perfect {101}, distinct
Twin plane	{101}	{101}
Orientation and pleochroism	X=b (yellow) Y=c (colorless) Z=a (colorless)	X=b Y=c Z=a

Chemical Composition

Purity of the analyzed sample: A sample of 1.4 grams containing at least 85 per cent calkinsite was submitted for chemical analysis. This was recovered from an original hand-selected sample of 50 grams of powdery material that contained less than 5 per cent of calkinsite; the treatment included gentle crushing, sieving, riffling on sheet stationery, and repeated treatment in the Frantz isodynamic separator. The identified impurities include burbankite, ancylite, lanthanite, barite, biotite, calcite, and some unidentified sulfate mineral. Heavy liquids were not used because of the potential danger of decomposition.

Chemical analysis: The chemical analysis of the impure sample of calkinsite is given in Table 5, column 1, and approximate recalculation to 100 per cent purity by estimating the per cent and composition of the impurities is given in column 2. The alkalies and the rare earths were

TABLE 5. CHEMICAL ANALYSIS OF CALKINSITE

	1 Original sample	2 Recalculated to 100% pure		3 Moles		4 Mole ratios	5 Theoretical analysis	
La_2O_3	54.42	19.82	62.73	0.608	0.1909	1	19.48	61.69
Ce_2O_3		32.05		0.0976			31.51	
Pr_2O_3		2.89		0.0088			2.86	
Nd_2O_3		7.97		0.0237			7.84	
CO_2	22.40	23.93		0.5437		2.85	24.78	
H_2O	12.00	13.34		0.7405		3.88	13.53	
		100.00					100.00	
MgO	0.96							
CaO	1.46							
SrO	0.54							
BaO	4.23							
Fe_2O_3	0.47							
MnO	0.08							
Al_2O_3	0.97							
SiO_2	0.92							
Na_2O	0.26							
K_2O	0.18							
SO_3	1.58							
	100.47							

M. K. Carron, Analyst.
Na_2O and K_2O by flame photometer by E. A. Nygaard.
Rare-earth distribution by spectrograph by H. J. Rose.

Table 6. Indexed *X*-ray Powder Lines (with Estimated Intensities and Interplanar Spacings) for Calkinsite

Cu/Ni radiation film 9158		Fe/Mn radiation film 9185	Calculated *d* Å	Probable hkl
I	Measured *d* Å			
10 broad	6.54	6.52β 6.57	6.32	020
4	4.78	4.77β 4.76	4.78	200
4	4.49	4.47β 4.45	4.47	002
½	4.24	4.27	4.22	030
			4.22	012
2	3.87	3.87	3.86	112
			3.82	220
2	3.71	3.71	3.65	022
5	3.27	3.27β 3.26	3.27	202
1 broad	3.17	3.16	3.16	040
			3.16	212
			3.16	230
½		3.02	3.03	140
			3.00	301
3 broad	2.931	2.940	2.981	041
			2.923	311
			2.921	132
2	2.897	2.899	2.902	222
½	2.713	2.708	2.714	321
½	2.654	2.650	2.638	240
1	2.595	2.596	2.595	123
			2.582	042
			2.582	232
½	2.433		2.434	033
½	2.393	2.393	2.392	400
			2.402	322
½	2.338	2.336	2.359	133
½	2.281	2.283	2.272	242
			2.273	411
1	2.248	2.245	2.238	420
			2.235	004
			2.246	340
½	2.207		2.201	014
			2.211	332
½	2.179	2.181	2.176	104
			2.178	341
			2.171	421
			2.169	043
			2.169	233
3	2.128	2.127	2.145	114
			2.146	313
3	2.115	2.113	2.109	402
			2.108	060
			2.107	024

TABLE 6—(*continued*)

Cu/Ni radiation film 9158		Fe/Mn radiation film 9185	Calculated *d* Å	Probable hkl
I	Measured *d* Å			
			2.115	143
3	2.074	2.070	2.052	061
			2.059	160
			2.059	323
			2.081	412
			2.081	430
			2.058	124
½	2.029	2.028	2.025	204
			2.027	431
3	2.009	2.008	2.001	422
			2.000	214
			2.006	161
			2.007	342
½	1.985		1.975	034
			1.975	243
3	1.945	1.944	1.934	134
			1.935	333
1	1.925	1.921	1.929	224
2	1.902	1.899	1.908	440
			1.907	062
1 broad	1.840	1.835	1.830	304
			1.846	413
1	1.786	1.785	1.793	144
			1.794	343
			1.789	423
½		1.762	1.755	442
			1.758	324
			1.759	360
1 broad	1.634	1.634	1.633	404
½		1.626		
1	1.591	1.591		
½	1.570	1.568		
½	1.548	1.550		
½	1.527	1.531		
1	1.502	1.502		
1	1.466	1.463		
1	1.421	1.422		
1 broad	1.357			
½	1.319			
1	1.300			
½	1.262			
½	1.221			
½	1.176			

determined in the same manner as for burbankite. The mean index of refraction calculated by the Law of Gladstone and Dale is 1.619, and that calculated from the indices of refraction is 1.636.

Formula of calkinsite: As shown by the data in Table 5, column 4, the chemical formula derived from the mole ratios can be expressed as $(RE)_2(CO_3)_3 \cdot 4H_2O$. Recalculating the chemical analysis from theoretically perfect ratios would yield the weight per cents listed in column 5, which, in comparison with those in column 2, lends more credibility to the probable composition of pure calkinsite. The chemical formula can be given as $(La_{0.64}Ce_{1.02}Pr_{0.09}Nd_{0.25})(CO_3)_3 \cdot 4H_2O$. The calculated chemical formula weight is 533, which is almost exactly one-fourth the unit cell weight of 2140. Four formula units per unit cell are thus indicated. Lanthanite is chemically very closely related to calkinsite but is an octahydrate with the formula $(RE)_2(CO_3)_3 \cdot 8H_2O$.

X-ray Crystallography

Single crystal data: Single crystals of calkinsite suitable for *x*-ray study were initially mounted with the aid of a binocular microscope and oriented by successive oscillation photographs. Unfortunately, none of these crystals exceeds 0.1 mm. in maximum dimension. Rotation photographs were taken about the *a* and *c* axes on two different crystals; and zero, first, and second layer Weissenberg photographs were obtained in these orientations. The photographs, although imperfect, showed calkinsite to be orthorhombic. The cell dimensions obtained are: $a_0 = 9.57$ Å ± 0.02; $b_0 = 12.65$ Å ± 0.08; and $c_0 = 8.94$ Å ± 0.02. The cell volume is 1083 Å^3. The only systematic omissions were *h00* and *00l*, in which *h* and *l* are odd. This indicates the space group $P2_1\,22_1$ or D_2^3.

Powder pattern data: *X*-ray powder pattern data for calkinsite are given in Table 6. All of the lines on the photographs are indexed by use of the cell dimensions obtained from the single crystal study. The good agreement of the calculated and observed interplanar spacings for {030}, {040}, and {060} support a satisfactory value for the b_0 cell dimension. The poor agreement shown for {020} can perhaps be explained by absorption. Beta lines observed in the *x*-ray powder photograph taken with Fe radiation are due to a weak Mn filter.

Morphological Crystallography

Goniometric measurements were made on both crystals of calkinsite which were mounted for *x*-ray study with (001) and (100) polar. A third crystal was mounted with (010) polar and its faces were similarly measured. Because of the small size of the crystals and imperfection of the crystal faces, the signals were poor. Several forms were observed under

TABLE 7. MORPHOLOGICAL DATA FOR CALKINSITE (ORTHORHOMBIC, DIPYRAMIDAL, PROBABLY P2/m 2/m 2/m)

Calculated ratios $a:b:c = 0.757:1:0.707$ $p_0:q_0:r_0 = 0.934:0.707:1$
$q_1:r_1:p_1 = 0.757:1.071:1$ $r_2:p_2:q_2 = 1.414:1.321:1$

Calculated angles

Form	ϕ	$\rho = C$	ϕ_1	$\rho_1 = A$	ϕ_2	$\rho_2 = B$
c {001{[1]	—	0°	0°	90°	90°	90°
b {010}	0°	90°	90°	90°	—	0°
a {100}[1]	90°	90°	—	0°	0°	90°
d {102}[1]	90°	25°02′	0°	64°58′	64°58′	90°
q {122}	33°28′	40°18′	35°16′	69°09′	64°58′	57°23′
r {132}	23°45′	49°14′	46°38′	72°14′	64°58′	46°08′
{101} (cleavage)	0°	43°03′	0°	46°57′	46°57′	90°

Measured angles

Form (faces)	Quality	ϕ	ρ	ϕ_1	ρ_1	ϕ_2	ρ_2
b {010} 2	Fair	89°57′–89°55′	0°	89°54′–90°12′	89°36′–90°00′		0°06′
q {122} 7	Poor	34°54′	40°16′	34°18′–38°40′	69°11′–71°25′	64°11′–66°43′	58°37′–60°00′
r {132} 3	Poor			44°35′	72°45′	66°24′–68°15′	47°05′–47°45′
{101}[2] (cleavage)		(90°)	42°30′				

[1] Forms observed on many crystals but not measurable in goniometric work.

[2] Measured with a petrographic microscope.

the microscope which could not be verified by goniometric measurements. Variation in crystal habit is shown in Figure 3 and clinographic projections are shown in Figure 4. The twinning and composition plane is {101}. The crystallographic data are summarized in Table 7. All the crystals observed appear to have full orthorhombic symmetry belonging to the class P2/m 2/m 2/m.

ORIGIN

In the sequence of mineral development, burbankite is younger than most of the calcite. Ancylite was formed locally by a reaction on burbankite by a hydrothermal solution. In this reaction burbankite, an anhydrous complex carbonate, contributed to form a hydrous complex carbonate richer in rare earths. Both of these complex carbonates were decomposed to contribute to the formation of calkinsite and lanthanite, two hydrous simple carbonates richer still in rare earths. This final decomposition most probably was effected by weathering and further resulted in local deposition of barite, goethite, and an unidentified sulfate. Such decomposition by weathering of the vein material could provide sufficient sulfate radical by alteration of the sulfide minerals, particularly pyrrhotite, to lower the pH of the environment and to combine with barium and other cations released by the carbonates or other minerals. The occurrence of coarse barite and calkinsite in isolated vugs may possibly indicate the development of some or all of the calkinsite under late hydrothermal conditions, but the lanthanite certainly resulted from weathering alone.

ACKNOWLEDGMENTS

K. J. Murata made several reconnaissance spectrographic analyses early in the study that led to an appreciation of the problem of chemical composition of these minerals, and Fred Hildebrand made several powder photographs for comparison. The junior author, who made the *x*-ray and morphology studies, acknowledges the guidance given by M. L. Lindberg. Howard Jaffe furnished unpublished *k* values for the rare earths. Thanks are due M. K. Carron for his determinations of the specific gravity of both minerals by the pycnometer method. The authors are indebted to a number of other colleagues for critical suggestions throughout this investigation, particularly to Howard Evans, D. H. Richter, D. B. Stewart, and Michael Fleischer.

REFERENCES

BROWN, R. W., AND PECORA, W. T. (1950), Paleocene and Eocene strata in the Bearpaw Mountains, Montana: *Science*, **109**, 487–489.

PECORA, W. T. (1942), Nepheline syenite pegmatites, Rocky Boy stock, Bearpaw Mountains, Montana: *Am. Mineral.*, **27**, 398–400.

WINCHELL, A. N. (1931), The microscopic characters of artificial inorganic solid substances, or artificial minerals, 2d ed., John Wiley & Sons, New York.

PREPARATION OF ROCK THIN SECTIONS*

FRANK S. REED AND JOHN L. MERGNER, *U. S. Geological Survey, Washington, D. C.*

CONTENTS

Abstract 1184
Introduction 1184
Equipment 1185
  Grinding motors and laps 1185
  Diamond saw 1186
  Mounting table 1187
  Band saw 1188
Standard rock thin sections 1189
Mounting and impregnating media 1192
  Canada balsam 1192
  Kollolith 1193
  Glycol phthalate 1193
  Bakelite varnish 1194
Method of applying the abrasive 1194
Repairing damaged thin sections 1195
Materials requiring special treatment 1196
  Clays 1196
  Water-soluble minerals and those decomposed by water 1198
  Gypsum 1199
  Coal 1201
Acknowledgments 1203
References 1203

ABSTRACT

A firm rock or mineral of which a thin section is to be made must first be sawed to obtain a slice approximately $\frac{1}{8}$ in. thick. This is then cemented to a numbered glass slide with Canada balsam, pressing the slice at an oblique angle against the glass slide to eliminate bubbles. The slice is then ground on a rotating lap using 1F silicon carbide and finally on a similar lap using #600 silicon carbide until the standard thickness of 0.03 mm is obtained, when the cover glass is cemented firmly to the section.

Friable rocks such as sandstones, clays, and shales must first be impregnated with Canada balsam or some other medium before sawing and grinding. Coals are treated with a mixture of two parts of Canada balsam and one part of marine glue. Kollolith and glycol phthalate are also used to cement the rock slice to the glass slide. Very friable rocks are impregnated with Bakelite varnish.

INTRODUCTION

The U. S. Geological Survey is occasionally requested to furnish information concerning the techniques employed in the preparation of rock thin sections. To make such information readily available, this paper describes the procedures involved in making thin sections of ordinary, firm, non-friable materials as well as clays, coals, gypsum, water-soluble minerals, and minerals decomposed by water.

---

* Publication authorized by the Director, U. S. Geological Survey.

The preparation of thin sections, which was described by Sorby (1882), was well developed by 1860. A clear presentation of the techniques involved was published by Vogelsang (1867). Vogelsang's paper contains the fundamentals of methods for preparing thin sections. The history of the development of thin section technique is treated by Holmes (1923) and Johannsen (1918). In recent years the methods of preparing standard thin sections have been described by Milner and Part (1916), by Head (1929), and by Rogers and Kerr (1942). A paper by Mary G. Keyes (1925) describes in part the techniques developed in the Geological Survey laboratories. The following treatment gives the methods in use in the Geological Survey laboratory in greater detail and includes the developments of the past quarter of a century.

Equipment

Grinding motors and laps

Thin sections require several stages of grinding on steel laps driven by $1\frac{1}{2}$-hp. vertical motors (Fig. 1). There are three such laps in the Geological Survey laboratory used for rough, medium, and fine grinding. The motors are driven at a speed of 1150 rpm. Each motor rests on a cast-iron stand 2 ft. 11 in. high. The laps on which the grinding is done are made of milled forged steel. They are 13 in. in diameter and 1 in. thick when new. The hub is 2 in. long and the outer diameter $2\frac{1}{4}$ in. The laps become concave with use and should be resurfaced as soon as a straightedge shows a slight concavity. This is especially necessary for the fine-grinding lap, for if this lap becomes too concave the preparation of a uniform thin section is impossible. Lead-lined boxes for catching and holding the abrasive as it flies from the rotating lap rest on top of cast iron stands. A framed glass case, with one end open to permit the entrance of the hands during grinding, rests on the lead-lined box. This aids further in minimizing the amount of abrasive that flies from the box and serves as a safety measure so that the operator will not inhale too much abrasive. The abrasive used for the three stages of grinding is #120 silicon carbide for rough-grinding, #1F silicon carbide for medium-grinding, and #600 silicon carbide for fine-grinding.

In connection with the description of the grinding motors and laps, mention must be made of hand-grinding on plate glass. A piece of plate glass about 8 in. square and $\frac{1}{4}$ in. thick is a very convenient size for this operation. No. 600 optical alundum is used for this grinding.

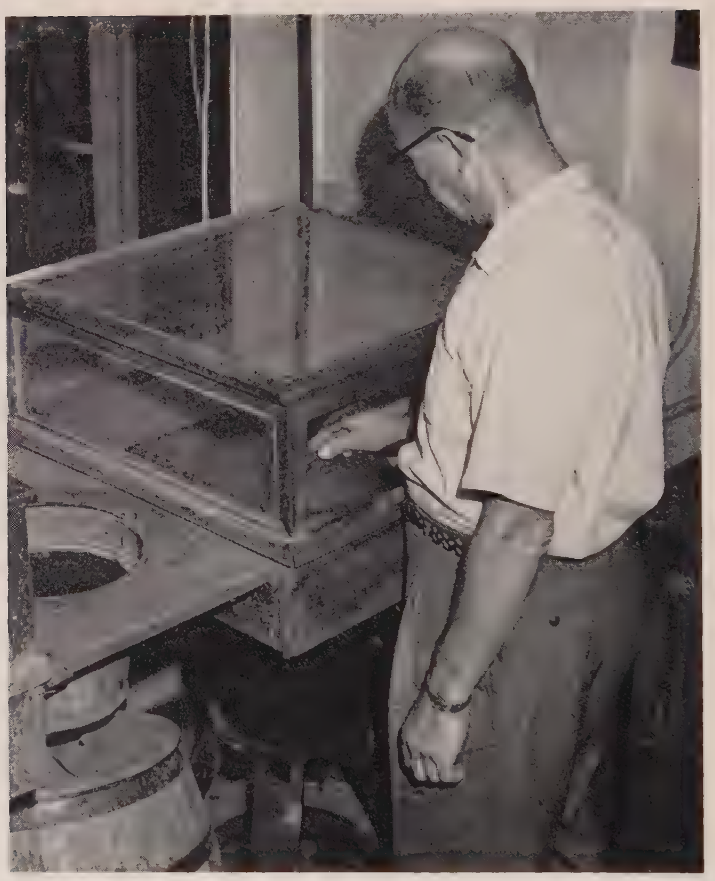

FIG. 1. Grinding unit with horizontal steel lap.

Diamond saw

A rotary diamond saw is a most helpful and necessary piece of equipment for the thin-section laboratory. A rock slice of uniform thickness can be cut very rapidly and much time saved thereby as contrasted with the slower method of breaking small chips from the hand specimen with a square sharp-edged trimming hammer. A blade 8 in. in diameter has proved to be the most practical for general use in the laboratory.

The first blades used were made of copper. However, contamination of copper was occasionally detected in the thin section being studied under the petrographic microscope. This led to the adoption of a steel blade. Surprisingly, the blade proved most efficient, cutting much faster and binding very much less than the copper blade when it neared the point when the diamond abrasive was about gone. This sawing machine is

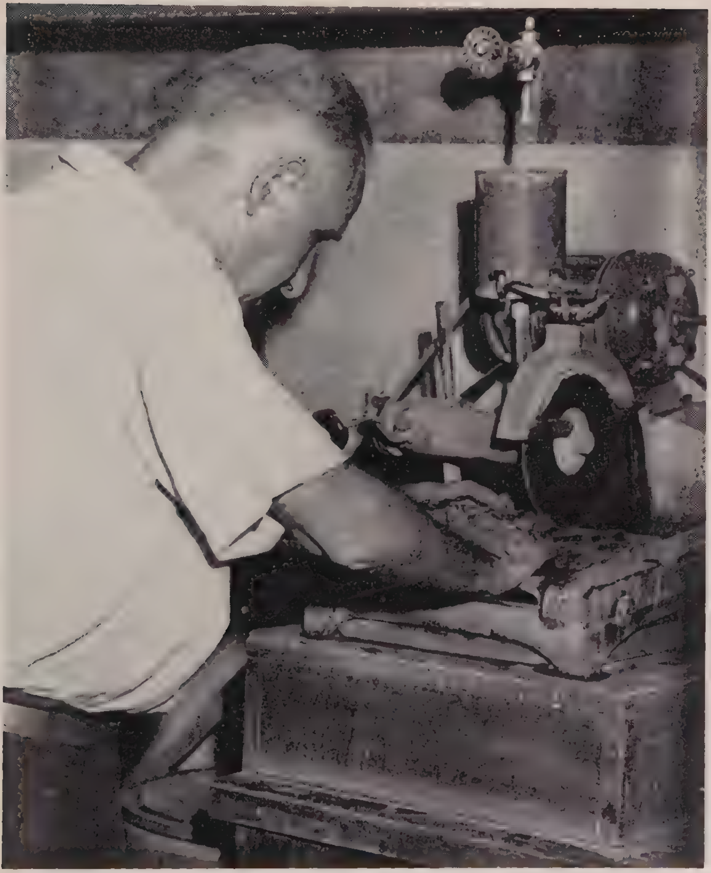

FIG. 2. Use of diamond saw.

driven by a $\frac{1}{2}$-hp motor at a speed of 1425 to 1475 rpm. Water or kerosene can be used as a lubricant. In the Survey laboratory, a soapy-water solution has been found to be a very satisfactory lubricant for sawing. Use of the diamond saw is illustrated in Figure 2.

Mounting table

The table on which the rock slices are mounted to the glass slides is brass $18\times5\frac{1}{4}\times\frac{1}{4}$ in. and supported on four legs 8 in. long (Fig. 3). The table holds 20 rock slices and their corresponding numbered slides. It is heated to a temperature of approximately 100° C. by a Bunsen burner. Reference numbers are cut on the glass slides with a diamond point mounted in a holder $5\frac{1}{2}$ in. long and $\frac{5}{16}$ in. in diameter. Canada balsam is used for cementing the rock slices to the glass slides. A mounting rod

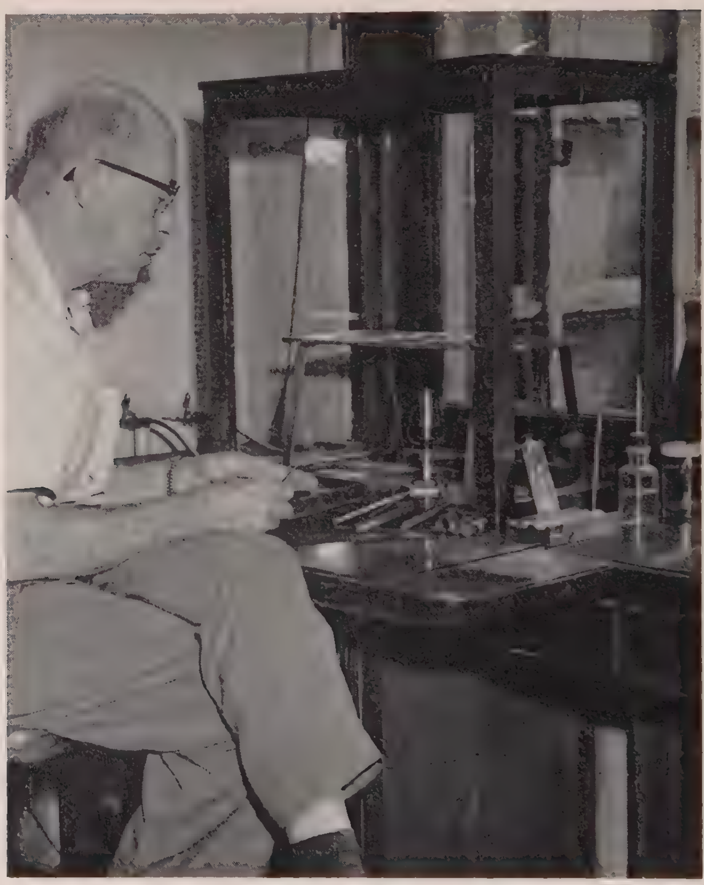

FIG. 3. Brass mounting table heated by a Bunsen burner.

8 in. long and ½ in. in diameter has one end bluntly pointed, and this end is heated sufficiently so that it can be pushed into a lump of hard-cooked balsam. When cool the lump of balsam is held firmly.

Band saw

An ordinary wood-cutting band saw with few modifications is made serviceable for stone cutting (Fig. 4). The rock specimen to be sawed is clamped to a sliding platform that is guided by two tracks. There are a sufficient number of threaded bore holes cut into the platform so that specimens of various sizes and shapes may be clamped. Five or six iron rods threaded at both ends and ranging from 6 in. to 12 in. in length, a channeled crossbar, and iron weights or wooden blocks comprise the equipment for clamping the rock to the platform. A glass container is filled with #120 silicon carbide abrasive. The flow of abrasive is controlled

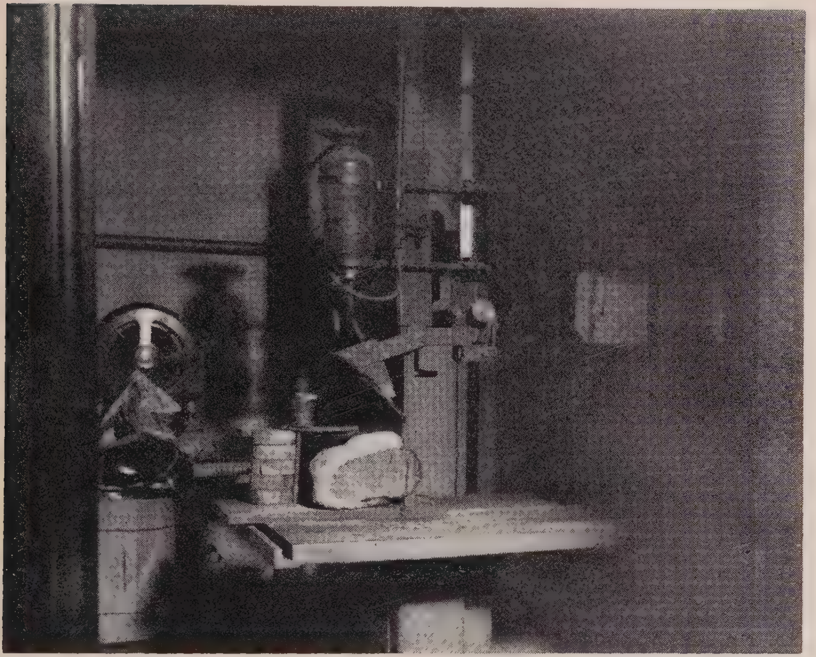

FIG. 4. Band saw modified for cutting rocks.

by a petcock cemented at the bottom of the container. The abrasive drops into a metal box and is flushed onto the saw with water. A piece of leather belting that ends in a point is attached to the metal box with rubber bands to direct the flow of the abrasive onto the edge of the saw. The upper wheel of the saw has an attachment for moving the band against or away from the rock. Obviously, the band must come into contact with the rock specimen. The wheels are set so as to provide pressure of the band against the specimen.

When a rock specimen has been securely clamped to the platform, the silicon carbide and water are turned on, adjusted to the proper flow, and the motor started. The specimen is slowly and carefully pushed to the edge of the saw band to allow the band gradually to cut its way into the rock. As the sawing progresses the platform is moved forward, about half an inch at a time, to keep the saw and rock in contact. A slow speed is best for this type of sawing. The motor is geared for a band speed of about 150 feet per minute.

STANDARD ROCK THIN SECTIONS

For the ordinary firm rock thin section, a slice approximately $\frac{1}{8}$ in. thick is cut from the specimen with the diamond saw. This slice is first ground on the rough-grinding lap. Very little grinding is needed to remove saw marks, but a uniform thickness should be maintained to facilitate the elimination of air bubbles when the chip is cemented to the glass slide.

The rock chip, after having been "roughed down," is transferred to the fine-grinding lap and one of the faces given a smooth, flat, scratch-free surface. Any convexity of this surface must be avoided. The chip should be held firmly and evenly against the lap during grinding and not be permitted to "rock," and the fine-grinding lap must be free from concavity. The tendency of the laps to become concave can be lessened by grinding the chip with a circular motion from the center of the lap to the edge and back again to the center. Also, in fine-grinding the surface of the rock chip, a flat surface is best obtained if, when the chip is ground nearly flat, it is held firmly in one place near the center of the lap for approximately the last half minute of grinding.

After the rock slice has been rough- and fine-ground, it is ready for cementing to the glass slide with Canada balsam. Both chip and numbered slide are placed on the mounting table and heated until the hardened balsam applied with the mounting rod spreads easily when applied to the slide and chip, both of which are to be coated with balsam. The slide is taken up with the fingers and pressed down on the chip, beginning at one side of the chip and pressing down at an oblique angle toward the opposite side, to eliminate air bubbles. After the slide is firmly pressed onto the chip, excess balsam and air bubbles, if any remain, are removed by moving the slide in a circular motion while exerting pressure from the mounting rod.

The mounted chip is then ground on the lap with No. 1F silicon carbide, which is the most suitable abrasive for this first grinding of the mounted chip. It allows grinding down to a point where the section becomes sufficiently translucent to transmit light with a minimum of strain and scratching of the slide. The section is then ground on the fine lap. Here #600 silicon carbide is used, and the rock section is ground down until it reaches the standard thickness (0.03 mm.). Most of the thin sections made from ordinary firm rock material can be finished on the rotating lap. Some thin sections show signs of fraying at the edges; and then it is necessary to continue the grinding by hand on a piece of plate glass with #600 optical alundum.

The ability to decide when the thin section has been ground to the proper thickness is a matter of experience. The thickness of a thin section may be very accurately judged by means of the birefringence exhibited by certain standard minerals, as shown under the petrographic microscope. The following suggestions should, however, prove helpful to beginners. Quartz and feldspar are common minerals in most igneous rocks, and their birefringences are similar. As a consequence of this phenomenon, grains in a position of maximum birefringence may be safely used as indicators of the proper thickness of a section. The birefringence of these minerals is given in the following table:

Table of birefringence

Quartz	0.009
Orthoclase	0.006
Microcline	0.007
Plagioclase	0.007–0.012

Charts relating birefringence to thickness for crystalline substances are contained as colored plates in many books on optical mineralogy or petrography (Iddings, 1911; Rogers and Kerr, 1942).

By consulting such charts it is possible to determine under crossed nicols the proper interference color that the grains should exhibit when the thin section is ground to the proper thickness, namely, 0.03 mm. Thus, for quartz, orthoclase, and some of the plagioclases the maximum color shown by any grains of these minerals is pure white; and for the very calcic plagioclases, the proper color may be pale yellow. Some of the other common rock-forming minerals, such as the amphiboles, pyroxenes, and olivine, show a considerable variation in birefringence with crystallographic orientation and require more knowledge on their use as indicators than do the minerals referred to above. The experienced worker, by noting the interference colors of these minerals when associated with the standard minerals, should be able to use them as guides in such rocks as dunites, pyroxenites, and amphibolites, in which the light-colored minerals are commonly absent.

Most sedimentary and metamorphic rocks carry some of the minerals listed above, and in addition they frequently contain calcite or dolomite. The interference colors of calcite in a thin section of standard thickness are referred to as "whites of high order." Actually, when the calcite is examined closely in polarized light, and under crossed nicols, this "white" is seen to be made up of an intricate pattern of tiny pale-colored areas that blend to give the impression of white light. An altered igneous rock that has been ground to the proper thickness as judged by the standard minerals and that contains calcite serves well as a reference for the carbonates.

The next operation is the mounting of the cover glass. The balsam still clinging to the slide is chipped away with a small sharp steel knife to within $\frac{1}{16}$ in. around the edge of the entire section. Then the slide is gently washed with a fine camel's-hair brush dipped in turpentine. This washing removes any particles of silicon carbide that may have become embedded in the balsam surrounding the section or in holes or cracks in the section itself. Turpentine is used because it has a slight solvent action on the balsam. The film of turpentine remaining on the slide is blotted off with newspaper or paper hand towel, and the lint from the paper that clings to the slide is removed by gently rubbing the slide over the palm of the hand. Most thin sections of common rocks are sufficiently coherent so that they will not tend to part along grain boundaries during the mounting of the cover glass. A small amount of uncooked Canada balsam is now placed on the thin section, the amount sufficient to cover the area of the section. It is very important to have the mounting table just barely warm when the thin section is placed upon it for cover-glass mounting. If it is too hot, bubbles form immediately. The gas burner is then turned up enough to heat the mounting table to about 90° C. The thin section with its fresh coating of uncooked Canada balsam should be heated long enough so that the balsam will be hard but not brittle when cool. If the balsam is too brittle, the cover glass tends to work loose from the slide before long. Sufficient cooking is tested by removing a small globule of balsam from the thin section with a mounting needle and pressing it lightly against the finger nail. If it does not stick to the finger nail, the balsam has been sufficiently hardened and the thin section is ready for the cover glass to be placed upon it. The cover glass is held in a pair of forceps and slightly heated in the flame of the Bunsen burner, then placed at one side of the slide and drawn at an oblique angle slowly over the thin section to the opposite side. This procedure helps to eliminate air bubbles. Excess balsam is pressed from between the slide and cover glass with the mounting needle. The contact between the cover glass and the thin section must be as close and even as possible to permit petrographic examination under the highest-power objectives. All excess balsam around the edges of the cover glass is cut away with a hot knife. This knife is an ordinary bread knife squared by cutting off the rounded end. The remaining thin film of balsam on the slide is washed off with alcohol and the slide immersed in a pan of water to prevent the alcohol from eating under the edges of the cover glass. If the rock is so friable that there is danger of its parting along grain boundaries, the surface should be given a thin coating of collodion before the cover glass is applied. The collodion, which is applied with a fine camel's-hair brush, is colorless and does not affect the relations between the indices of refraction of the minerals and the mounting balsam.

Mounting and Impregnating Media

Canada balsam

Canada balsam is the most satisfactory mounting medium for most common rocks except coal. For coal the combination of two parts Canada balsam and one part marine glue is better than Canada balsam alone. The index of refraction of Canada balsam (1.54) approximates the index of quartz, thus making it very useful in the microscopic determination of the minerals in thin sections. The balsam is easy to prepare and serves to cement both the ground chip to the glass slide and the cover glass to the thin section. It remains workable long enough to eliminate bubbles. Furthermore, less heat is required than for other media. The hard-cooked balsam used for cementing the ground chips to the slides is prepared by pouring the desired amount into a procelain dish and cooking slowly on an electric hot plate until a globule of it on the end of the mounting needle will not stick when pressed against the thumbnail. Care must be taken to guard against overcooking, which causes the balsam to become brittle. Should this happen, serious difficulty will be encountered in the final stages of grinding the thin section. When the section is approaching the proper thinness, the brittle balsam will break away from the slide and pull portions of the section with it.

Canada balsam also serves very well as an impregnating medium for friable rocks. The friable chip is placed in a container with some lumps of the hard-cooked balsam and allowed to cook slowly on an electric hot plate for about 10 minutes or until all the pores of the chip are thoroughly impregnated. After this impregnation the chip can be sawed or rough-ground. Large chips may have to be impregnated twice.

Kollolith

The compound Kollolith is similar to Canada balsam as a medium for cementing rock slices to slides and the mounting of cover glasses. When obtainable it can be had in tubes in both the liquid and the hardened state. It differs from Canada balsam in having a slightly lower index of refraction. Long-continued heating of friable rocks impregnated with it does not cause appreciable darkening of the material.

Glycol phthalate

Glycol phthalate is a hard and tough compound that is not satisfactory for most types of thin-section work, but it has the special advantage of adhering to the glass slide with much greater tenacity than balsam. It requires a much higher temperature than balsam for melting, and this high temperature causes bubbles to develop in great numbers; also the material hardens so quickly that difficulty is experienced in trying to squeeze out the bubbles. Owing to the high viscosity at lower temperatures, greater pressure is required to squeeze out the bubbles; and this pressure tends to cause the thin section to separate along crystal boundaries. It is used most effectively in making polished thin sections, which require no cover glasses. The technique of the preparation of polished thin sections has been worked out in this laboratory and has been described by Kennedy (1945).

Bakelite varnish

The greatest usefulness of bakelite is in the impregnation of particularly friable materials preparatory to making thin or polished sections (see section on impregnation). Overnight heating in the electric oven, with a temperature of 70° C. is required to harden it sufficiently. For the preparation of thin sections of small grains or fragments bakelite varnish is desirable.

In preparing thin sections of rock fragments or grains, first cut a piece of glass about $\frac{3}{4}$ in. square from a slide, then spread a thin layer of grains over the entire area or as many of the small rock fragments as it will hold. Next dilute the bakelite varnish with acetone until it is of the consistency of thin syrup. Then drop the thinned bakelite on the grains or fragments until they are completely covered. After an hour or so the excess of acetone will have evaporated; place the glass slide holding the grains or fragments in the electric drying oven overnight at a temperature of 70° C. By morning the bakelite varnish will have been cured, i.e., polymerized. The grains or fragments thus cemented to the glass are ground on the fine lap until a smooth scratch-free surface has been obtained. From here on the method for making the thin section follows the same procedure as that of the ordinary rock thin section. The bakelite has a high index of refraction (1.63) and a pale amber color, which may be objectionable. The one who is to use the thin section should be told that bakelite has been used if he himself has not suggested its use.

METHOD OF APPLYING THE ABRASIVE

The abrasive, a silicon carbide and water mixture, is scooped from a container with the fingers onto the rotating lap for the rough-grinding of the chip. The lap must be sufficiently charged with the abrasive during the grinding. For the final grinding of both the unmounted and the mounted chip the abrasive is applied in the same manner as in the preceding grindings. The abrasive should be of such consistency that, when applied to the lap, it will not be thrown off too fast because of its wetness or not be so thick as to impede its spreading over the lap evenly. Some practice will be necessary, however, before the technician learns how much and how often to apply the different abrasives to the laps in the several stages of grinding.

Repairing Damaged Thin Sections

If a thin section is dropped, it may be shattered beyond repair, but more commonly the damage is a sprung cover glass or a broken corner. Sometimes the thin section clings to the cover glass instead of to the slide. A sprung cover glass may show only slight strains in the Canada balsam and exhibit an iridescent effect. Also, if a thin section gets too hot, as, for example, if it is left near a window in direct sunlight, it may develop bubbles.

When the damage is slight, such as a few strained areas in the balsam appearing between the cover glass and the slide, repair is simple. If the slide is held in a pair of forceps and passed gently through the flame of a Bunsen burner several times, the balsam will soften enough to eliminate the strained areas. Caution should be exercised to avoid overheating, because this may produce bubbles. If this happens, the cover glass must be removed and the thin section remounted. The same treatment is used for a cover glass that has completely sprung from the slide or for one held only by a small area of balsam. When numerous bubbles have formed between the cover glass and the slide, from overheating in the attempt to remove strains, the cover glass is removed by holding the slide in the forceps and passing it through the flame until the cover glass can be moved rather freely with the mounting needle. Then it is pushed to one end of the slide and removed with the fingers. If the balsam begins to stiffen before the cover glass has been pushed out to a little beyond the end of the slide, reheating is necessary.

A cover glass held only by a small area of balsam can be pried loose by inserting the edge of a razor blade between it and the slide and giving it a quick flip. The balsam still adhering to the slide need not be washed away if it has not become discolored or too hard. The chief trouble encountered when balsam has hardened too much because of age is that the thin section cannot be moved about on the slide for the removal of bubbles, should they be present between thin section and slide. Under these circumstances, the thin section is transferred to another slide. The slide is heated on the mounting table until the thin section can be gently pushed from the old slide onto the new one. This same method is used also when the thin section clings to the cover glass. Where there is no discoloration or extra hardness in the balsam, a small amount of uncooked Canada balsam is deposited on the thin section as in the procedure described in the section on standard rock thin sections. Occasionally, however, balsam becomes so tough that it is risky to heat the slide with the intention of transferring the thin section to a new slide. When this happens, the thin section slide is immersed in a suitable receptacle containing turpentine. The balsam dissolves overnight. If the receptacle has not been disturbed, the thin section will be found to be resting on the slide. The slide is carefully removed from the container with forceps and the thin section gently pushed onto the new slide, upon which has been deposited a small amount of uncooked Canada balsam. Then an additional amount of balsam is applied to the thin section, and the previously described standard procedure followed. Such transfers are successful only if the material of the thin section is very coherent. If it has been previously coated with collodion, however, the chances are that it will withstand transfer. Transfer of a thin section from a broken slide to a new one is comparatively simple if the thin section is sound. All that has to be done is to remove the cover glass, heat the slide over the Bunsen burner until the balsam is soft, and, with the aid of the mounting needle, gently push the thin section onto the new slide.

MATERIALS REQUIRING SPECIAL TREATMENT

At one time petrographic studies were confined largely to crystalline rocks and a few sedimentary rocks, such as sandstones and limestones. More recently geologists have become increasingly interested in the more friable rocks, including shales, bentonites, poorly consolidated volcanic materials, slightly indurated sands or gravels, bauxites, coals, ceramic materials, and a large variety of clays and soils. To prepare usable thin sections of this variety of materials necessitated the devising of new mounting media and section-making techniques that were not necessary in the old days. However, the materials and textures range over such wide limits that procedures can not be standardized. Each lot of specimens must be evaluated individually and the most suitable method devised.

Ross (1926) was the first to suggest a suitable method. Ahrens and Weyland (1928) and later Schaffer and Hurst (1938) have also described satisfactory methods for the preparation of thin sections of friable rocks. The methods given here are essentially those of Ross. Some of these materials have to be ground without the use of water; heating to the lowest possible temperature when mounting chips on the glass slides is another requisite in the process of making thin sections of friable material.

The preparation of coal thin sections has been studied by Thiessen and associates (1938).

Clays

For clays, a slice is cut from the sample with a fine-toothed hacksaw or, if available, a jewelers hacksaw. If the sample is comparatively free from quartz, a motor-driven circular carborundum saw permits one to cut a slice from the sample quickly with less danger of breakage than if the sample is held by the fingers and cut with the hacksaw. No water is used with the carborundum saw. The equivalent of rough-grinding on the sawed clay slice is done on a 12-in. flat "bastard" file. The chip is rubbed forward and backward over the file to eliminate saw marks. Deep scratches must be avoided, for they cause a distortion of the clay chip that results in birefringent striae in the thin section. If such scratches are formed an appreciable thickness of the clay material underlying the scratch must be removed. This can be done on the same file or, if preferred, a 12-in. flat "smooth" file may be used. With a little practice, the proper feel or touch is developed. Samples of nearly pure clay materials, or shales or related material containing mineral grains with a diameter less than the thickness of the finished thin section, present a minimum of difficulties. If coarser grains are present, impregnation permitting wet grinding is commonly advisable. Some samples become checked after the moisture dries out, others become friable, so that impregnation is necessary before they can be sawed and rubbed on the file. Kollolith or Canada balsam is used. After a reasonably smooth surface has been obtained by rubbing on the file, further grinding is continued on plate glass with mineral oil and #600 optical alundum. Liquid petrolatum (light) mineral oil is recommended for the mixture because this does not rapidly dissolve the balsam. The chip is rubbed firmly and gently over the plate glass until the remaining fine traces of the file marks are removed. If there are quartz grains present, some will break loose, and they will gouge deep lines into the clay slice. Impregnation with balsam or Kollolith helps to overcome this obstacle if the clay is not too compact. By impregnating the slice, penetration is deep enough to hold the quartz grains. On the other hand, when the specimen is very compact and impregnation is more or less ineffective, a fair result is obtained by gently rubbing the clay slice on the plate glass in a thick paste of alundum and oil. When mounting the clay slice on the slide, care must be exercised to avoid too rapid heating and overheating. If this should happen, the ground surface becomes checkered with numerous cracks, preventing good mounting. In most cases, however, only a few cracks develop in the clay slices during mounting. After the clay slice has been cemented to the slide with Canada balsam, it is ground or rubbed down on the file until it becomes translucent. The final grinding of the section to the proper thickness is completed on the plate glass. Number 600 optical alundum and the mineral oil serve for this grinding. Despite the fine, even-grained texture of this grade of alundum, some fine scratches will be found in the thin section. In thin sections they are quite numerous and rather coarse, if fine grains of quartz break loose. Further grinding on the plate glass to reduce them is useless. Dipping the forefinger into some of the oil and alundum, and then rubbing rather firmly forward and backward over the thin section helps to reduce the number of scratches and to decrease their coarseness.

The mounting of the cover glass follows the procedure for other friable rock thin sections. However, care must be exercised to avoid washing away the clay when the old balsam is removed with turpentine. The technique of reducing scratches by rubbing with the forefinger is effective also with such soft waxlike minerals as talc, gypsum, alunite, and serpentine.

Water-soluble minerals and minerals decomposed by water

The following methods have been used successfully on shortite, halite, sylvite, and polyhalite.

A piece is cut from the sample with a hack saw having 14 teeth to the inch. The chip is roughed down on the flat "bastard" file on both sides until it is as close to 3 mm. thick as possible. The use of water is not permissible in any of the grinding operations. Instead of proceeding with the fine-grinding on the plate glass with oil and optical alundum, grinding of the chip surface is resumed on the fine rotating lap charged with a mixture of #600 silicon carbide and alcohol, to provide a finished surface for mounting on the glass slide. Ordinarily, a suitably fine-ground surface can be obtained on the rotating lap. If not, the finishing touches are applied by grinding on plate glass with #600 optical alundum and alcohol. The silicon carbide that clings about the edges of the chip is washed away with a stiff-bristled hand brush and alcohol. Chips of these minerals are mounted in the same way as those of the ordinary rock thin sections with the exception of minerals that lose water readily when heated. Here the least possible amount of heat must be used.

After the chips have been mounted on the glass slides, grinding is resumed on the file until the chips are cut down to the balsam or farther, if they will stand it, which saves time in the final preparation. After the section has been ground down on the file, final grinding to the proper thickness is done by hand on the plate glass with # 600 optical alundum and oil. Oil is substituted here for alcohol, which would dissolve the balsam holding the thin section to the slide. Except for minerals decomposed by heat, the cover glasses are mounted in the same manner as those for friable rock thin sections. For minerals decomposed by heat, however, a somewhat different method of cover-glass mounting is employed. The thin section of a mineral that is broken down by heating should have its cover-glass mounted with xylol-balsam, a cold mount, following the procedure for friable rock thin sections. By handling carefully, a thin section so mounted can be examined under the microscope without getting either the hands or the microscope sticky. However, the thin section can be dried in an electrical oven overnight at a temperature not above 40° C. With a little experience one can learn to mount with just enough xylol-balsam so that the balsam flows to the edges of the cover glass and no farther. Also, with practice, one can learn to place the cover glass on the section so as to prevent the forming of bubbles altogether.

Gypsum

The procedure employed in cutting thin sections of gypsum follows the same general pattern as that of ordinary rock thin sections, but the softness of the mineral and the low temperature at which it tends to undergo a transition to the hemihydrate present unusual difficulties.

A slice is cut from the hand specimen or drill core on the diamond saw. With this soft mineral grinding on the rough lap is not necessary. The first grinding takes place on the medium lap with #1F silicon carbide to remove saw marks and to cut the slice down uniformly to about $\frac{1}{8}$ in. in thickness. If $\frac{1}{8}$ in. can be achieved, very little grinding on the medium lap is necessary to remove saw marks. Soft minerals like gypsum require special care in getting a fine-ground surface prior to mounting on the glass slide. This operation is thus a critical one in the procedure. Number 600 silicon carbide serves as the grinding abrasive on the fine-grinding lap. Grinding on the fine lap is continued until further grinding does not improve the smoothness. Scratches and also a finely pitted surface develop during this grinding. To remove them, grinding is resumed on the plate glass with #600 optical alundum. The key to producing a smooth, scratch-free surface is the pasty consistency of the mixture of the alundum and water. If the mixture is too watery, the grains of alundum flow too freely and form scratches even though this abrasive is very fine and of even texture. By a gentle, steady rubbing forward and backward on the glass plate, a smooth, scratch-free surface is obtained. A little practice is necessary to get the best results.

The gypsum slice is next mounted on the glass slide with Canada balsam. As gypsum loses part of its water of crystallization and water absorbed between cleavage planes at a low temperature, bubbles are readily formed and must be guarded against. Therefore chips are not heated but are allowed to dry overnight at room temperature before being cemented to slides.

For mounting, the slide and chip are heated on the brass mounting table just enough so that the hard-cooked Canada balsam will flow fairly easily and allow pressing the slide down on the chip and squeezing out excess balsam. Keeping the temperature low prevents the formation of bubbles (as mentioned above). But difficulty will be experienced in getting a good mount the first time because the balsam, while flowing fairly easily, is not as fluid as it would be at a higher temperature. Generally the operation has to be repeated several times before all bubbles are removed. After the chip is cemented to the glass slide, grinding is resumed on the medium lap. Number 1F silicon carbide serves as the abrasive for this grinding. For good results the gypsum chip is ground down no thinner than $\frac{1}{32}$ in. The next and final grinding on the revolving lap follows the usual procedure in the preparation of ordinary rock thin sections. Here it is well to grind down the section until the gypsum shows a bright-yellow interference color under crossed nicols. An attempt to secure a thinner section might result in the complete grinding away of the section. Final grinding is done on plate glass with # 600 optical alundum until the required thinness is obtained. It may not always be possible to cut the section down to a thinness to permit gray to show under the crossed nicols because of a tendency for the section to fray at the edges. Usually gypsum sections show pale yellow under crossed nicols by the time fraying begins. Once fraying begins, it progresses rather rapidly, and therefore grinding must be stopped before the section becomes very small or is lost entirely. A pasty mixture of water and alundum is necessary to prevent scratches when a fine surface is to be ground on the mounted gypsum chip.

The cover glass is mounted after the various stages of grinding are completed. This proceeds partly along the same lines as in the preparation of ordinary rock thin sections. As mentioned before, the use of minimum heat is an important factor. To avoid any danger of overheating, the cover glass is mounted by cold mounting, as described above. The slide is placed in the electric oven at 50° C. and allowed to remain overnight, so that the balsam becomes hardened about the edges of the cover glass. The excess balsam around the edges is removed with a knife, just hot enough to permit the scraping away of the balsam. If too hot, it causes sufficient melting of the balsam to form bubbles under the cover glass. It is necessary, after the first scraping, to place the slide in the oven again overnight at the same temperature to allow the balsam under the cover glass to harden to a greater depth from the edges inward. On removing the slide from the oven this second time, a little more balsam will be found to have oozed from under the cover glass. This is also scraped away with a hot knife. In most cases the balsam under the cover glass has had sufficient volatile matter driven off so that it is hard enough to permit washing off of the remaining film of balsam adhering to the slide. Only experience enables one to determine how far this procedure should be carried. The slide is washed in alcohol with a hand brush and quickly immersed in water to prevent the alcohol from eating under the edges of the cover glass, after which it is dried with a soft cloth. As a safeguard against the possibility that the balsam is not sufficiently hard and to prevent stickiness about the edges of the cover glass, it is a good plan to place the slide back in the oven for another night.

Coal

Thin sections of coal are more difficult to prepare than any material previously described. Some of the difficulties are due to friability, the danger of burning and checking of the fine-ground surface with the application of too much heat, and the fact that the thin sections of coal must be thinner than other thin sections. The sample of coal from which the thin section is to be cut is impregnated with paraffin overnight in the electric oven at a temperature of 70° C. The sample is placed in a white enameled pan with enough paraffin when melted to cover it. In this way it is made strong enough to permit the sawing off of a piece for a thin section. Also, a lower temperature can be used than would be possible if Canada balsam or some other impregnating medium were used. Next morning the sample is taken from the oven and placed on a mat of paper hand towels or newspapers so that excess paraffin drains off. When cool a piece is cut from the sample with the diamond saw, or, as a second choice, with a hack saw. During mounting to the slide, which requires a moderate amount of heat, the impregnated coal has a tendency to warp. This may be prevented by cutting a rather thick slice—5 mm. or more, depending on the soundness of the sample. The first grinding takes place on the medium lap with #1F silicon carbide, for the removal of saw marks, after which grinding continues on the fine lap with #600 silicon carbide. This is followed by hand grinding with #600 optical alundum on the plate glass until a smooth, scratch-free surface is obtained. Coal sections differ from most other sections in that a polished surface is necessary. Before mounting on the glass slide, the smoothly ground surface is polished on a cloth-covered 6-in. rotating lap with tin oxide or chromic oxide until all traces of scratches and pits are removed. The cloth used in covering the lap should not be coarse, but a fine-grade cotton material. The chromic oxide or tin oxide is placed in a container with water and applied to the revolving lap with a camel's-hair brush. Manipulation by the fingers of the coal slice in a circular movement from the center of the lap to the edge prevents furrows from developing.

The Canada balsam used in mounting the polished coal slice on the slide should be cooked only to the degree of hardness that will permit pressing the fingernail into it with slight effort. It is then soft enough to give a cushioning effect to the chip during the grinding of the slide. If a very slight fluidity of the mounting medium is not objectionable, a mixture of one-third by volume of marine glue and two-thirds uncooked Canada balsam answers very well. This mixture is prepared by cooking the balsam and the marine glue to a consistency that, when cool, can be dented easily with the fingernail. The cushioned effect created by the marine glue mixture or the not-too-hard cooked balsam aids considerably by preventing the thin section of coal from fraying away at the edges. By allowing the chip to dry thoroughly overnight, the tendency to form bubbles is reduced. The chip is mounted on the slide in the same way as a chip of gypsum. However, after the coal chip has been firmly mounted on the slide and all bubbles eliminated, it is a good plan to maintain pressure on the slide with the mounting rod until the balsam has set.

Grinding is resumed on the medium rotating lap with #1F silicon carbide until the coal section is approximately 0.25 mm. thick, and then continued on the fine lap with #600 silicon carbide. This grinding is continued until the section becomes slightly translucent at the edges. Commonly the section starts to fray a little at the edges before it shows any sign of translucency. When this happens, it is time to discontinue the lap grinding. Grinding is continued by hand on the plate glass with #600 optical alundum, but a close watch is kept for signs of fraying at the edge of the section. A slight fraying away is not dangerous and happens with most coal sections. The last operation, in which the coal thin section is ground down to the proper thinness, is done on a 6-in. cloth-covered lap with #600 optical alundum. The cloth used here is of the same type as that for polishing the surface of the unmounted chip. Alundum and water are applied to the rotating lap with the fingers. The lap must be kept moist to prevent scorching of the section. The slide is moved slowly with the fingers in complete circles from the center of the lap toward the edge and back until the section is thin enough. Throughout this polishing the slide should be held firmly against the lap and not be permitted to rock from one side to the other. This ensures uniform thinness. Sometimes further polishing and grinding, using the forefinger, is necessary to finish the section. By applying a pasty mixture of water and alundum to the section of coal and rubbing it with a firm forward and backward motion with the forefinger, the proper thickness can be attained. If there are several coal sections to be ground, the forefinger may become sore and tender. A cork big enough to cover the thin section and worked in the same manner as the forefinger can be substituted. The probable advantage of the forefinger is that a sense of feel is present. This operation, whether performed with the forefinger or the cork, is somewhat tedious, but with care and patience excellent results can be obtained.

The cover glass is mounted as for thin sections of gypsum. However, one may risk mounting of the cover glass by the procedure for standard friable sections. If heating is carefully controlled, very little scorching will develop. The cleansing of the slide proceeds in the manner described for both the cold and the hot mountings.

ACKNOWLEDGMENTS

In the preparation of this paper, we owe much to Dr. Clarence S. Ross of the Geological Survey. During the many years of close association with him, he has also helped us in many other ways. His encouragement, assistance, and inspiration has made our work a pleasure. Dr. W. T. Schaller and Professor Esper S. Larsen, Jr., have also aided us with their many suggestions.

REFERENCES

AHRENS, W., AND WEYLAND (1928), Die Herstellung von Dunnschliffen aus locherem Material für petrographische Untersuchungen: *Centralbl. Mineralogie*, **1928,** Abt. A., 370–375.

HEAD, R. E. (1929), The technique of preparing thin sections of rock: *Utah Eng. Exper. Sta.*, **Tech. Paper 8.**

HOLMES, ARTHUR (1923), Petrographic methods and calculations, London, Thomas Murby & Co., Pt. 2, 231–249.

IDDINGS, J. P. (1911), Rock minerals, 2d ed., New York, John Wiley & Sons.

JOHANNSEN, ALBERT (1918), Manual of petrographic methods, New York, McGraw-Hill Book Co., 2d ed., 572–602.

KENNEDY, GEORGE C. (1945), The preparation of polished thin sections: *Econ. Geol.*, **40,** 353–360.

KEYES, M. G. (1925), Making thin sections of rocks: *Am. Jour. Sci.*, 5th ser., **10,** 538–550.

MILNER, H. B., AND PART, G. M. (1916), Methods in practical petrology, London, Thomas Murby & Co., 1–14.

ROGERS, A. F., AND KERR, P. F. (1942), Optical mineralogy, 2d ed., New York, McGraw-Hill Book Co.

ROSS, C. S. (1926), Methods of preparation of sedimentary material for study: *Econ. Geol.*, **21,** 454–468.

SCHAFFER, R. J., AND HURST, P. (1930), The preparation of thin sections of friable and weathered materials by impregnation with synthetic resin: *Geologists' Assoc. Proc.*, London, **41,** 32–43.

SORBY, H. C. (1882), Preparation of transparent sections of rocks and minerals: *Northern Microscopist*, London, **2,** 137.

THIESSEN, R., SPRUNK, G. C., AND O'DONNELL, H. J. (1938), Preparation of thin sections of coal: *U. S. Bur. Mines Inf. Circ.* **7021,** 1–18.

VOGELSANG, H. (1867), Philosophie der geologic und mikroscopische Gesteinsstudien, Bonn. 225–228.

THE LEONA RHYOLITE, ALAMEDA COUNTY, CALIFORNIA*

G. D. Robinson, *U. S. Geological Survey, Denver, Colo.*

Abstract

The Leona rhyolite crops out discontinuously for 21 miles along the front of the hills from Berkeley to a point 4 miles southeast of Hayward, Calif. Long ago, A. C. Lawson and C. W. Clark agreed that it represents a single extensive lava flow of late Tertiary, probably Pliocene age. Because so many large rhyolite extrusive rocks are being interpreted nowadays as welded tuffs, re-examination of the Leona is timely.

In its southern half, recently studied, the rhyolite belt exhibits continuous groundmass fabric with unfragmented phenocrysts and practically lacks pyroclastic debris, suggesting origin as lava. However, downward extension of several broad hill cappings into narrow feeder-like masses, the presence of rhyolite dikes, and other features suggest extrusion as a series of domes and short flows rising more or less simultaneously along subsidiary shears in a major fault zone rather than as a single flow.

Commonly, the rock is a weathered mixture of iron oxide-stained quartz and argillized feldspar. Where fresh, it typically contains a few corroded phenocrysts of sodic plagioclase and quartz in spherulitic glass or in a felted microcrystalline groundmass of quartz and albite. A little chlorite and altered biotite are the only ferromagnesian minerals. Pyrite crystals, many of them rounded but not altered chemically, are abundant in fresh rhyolite but extremely rare in the underlying rocks; the pyrite appears to be primary.

In previous descriptions, orthoclase and oligoclase have been identified as major components, and albite has not been reported. Despite the modified mineralogy, the name soda rhyolite, originally assigned by Lawson, still seems appropriate.

The formation is little deformed and thus apparently is younger than the intense regional post-Pliocene orogeny; it is overlain by Pleistocene sedimentary rocks. This and other indirect evidence favor emplacement of the rhyolite rather early in the Pleistocene. Since then, it has played an important role in the geomorphic development of the east side of San Francisco Bay.

Introduction

The hills that rise abruptly on the east side of San Francisco Bay are discontinuously capped with distinctive light-colored pyritic soda rhyolite. Lawson (1914) named the formation Leona rhyolite, from its impressive exposures at Leona Heights in Oakland, and concluded that it is the eroded remnant more than 21 miles long of a single great lava flow of late Tertiary, probably Pliocene age. Clark (1917) studied the formation shortly afterward and reached similar conclusions. Nowadays, many workers doubt that rhyolitic lava ever flows more than a few miles; an increasing number of rhyolitic rocks once thought to be extensive lava flows are turning out, upon close examination, to be welded tuffs. This doubt has originated perhaps, from recognition of the high viscosity of rhyolitic melts both in the field and in the laboratory. Restudy of the Leona may, then, be of interest. The southern half of the rhyolite belt

---

* Publication authorized by the Director, U. S. Geological Survey.

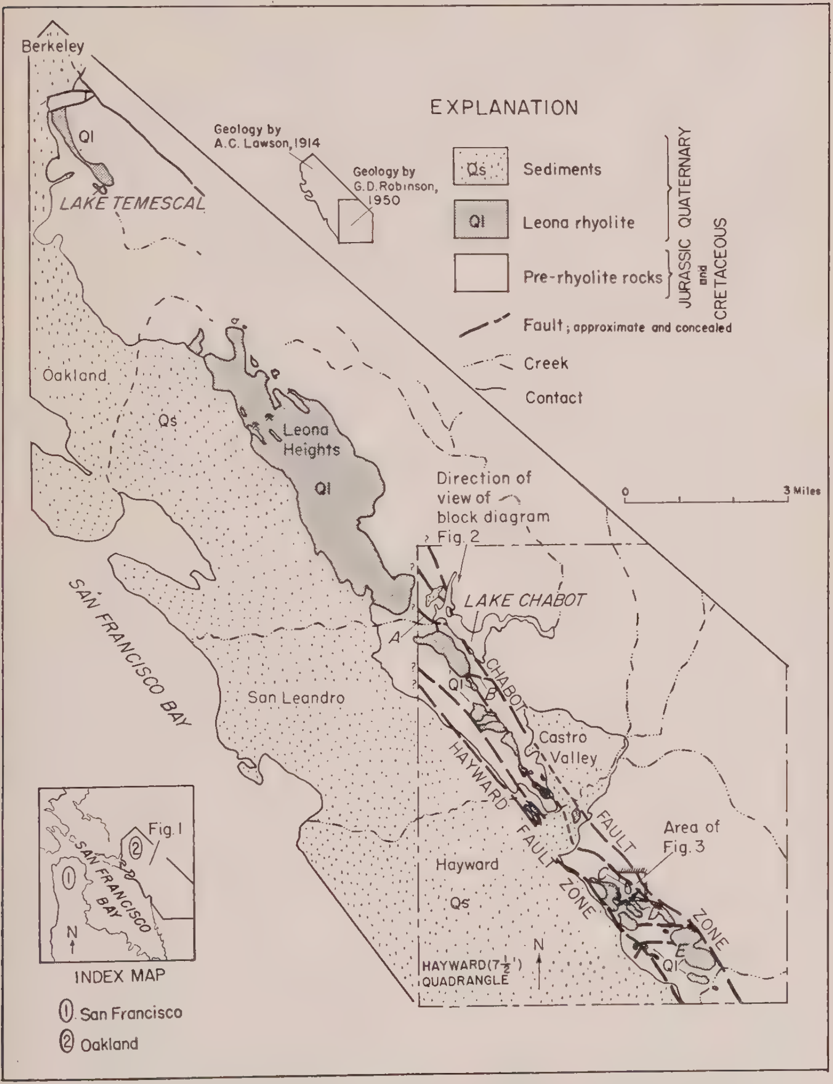

FIG. 1. Distribution of Leona rhyolite, Alameda County, California. The faults which are shown to terminate at the edges of the Hayward Quadrangle are believed to continue beyond it but have not yet been mapped.

crosses the Hayward 7½-minute Quadrangle (see Fig. 1), which I recently mapped and briefly described (Robinson, in preparation). The present paper, which is an expansion of part of the quadrangle report, summarizes existing information on the Leona and presents some new data bearing on its origin and age. Information on the northern half is from Lawson and Clark.

W. T. Schaller's first publication (1903) described the secondary minerals at Leona Heights. Clarence Ross has pioneered in marshalling the evidence favoring the emplacement of large rhyolitic extrusive bodies as welded tuff. Thus it is fitting that a discussion of the Leona rhyolite appear in a publication dedicated to Schaller and Ross. This paper, however, lacks the systematic laboratory approach that characterizes their work. Rather, it is primarily a field study, supported only in small part by laboratory data.

The Leona is deeply altered in most places, and presents a cryptic and unappealing face to casual inspection, which is no doubt why it has been largely neglected since the days of Lawson and Clark. Whether or not the story it has to tell is convincing, this paper will have served its purpose if it stimulates others to undertake exhaustive laboratory studies of the Leona rhyolite.

FIELD RELATIONS

The base of the rugged hills that face San Francisco Bay on the east is a fault- or fault-line scarp, marking the western edge of a zone, 1 to 2 miles wide, riven by a series of northwest-trending faults, linked by subsidiary transverse faults (Fig. 1). This faulted zone has been the site of repeated disturbances at least since the late Tertiary and probably since far back into the Mesozoic. The westernmost faults have had mostly Recent movement; the easternmost ones appear to have been long inactive. In the Hayward quadrangle, these faults have been designated the Hayward fault zone and the Chabot fault zone respectively. Within the faulted zone the principal bedrocks are Upper Jurassic sedimentary, volcanic, and plutonic rocks, overlain by the Leona rhyolite and by Pleistocene gravel.

Outcrops of the rhyolite extend for more than 21 miles between Hamilton Gulch in Berkeley and the southeast corner of the Hayward quadrangle. The rhyolite belt is nowhere more than $1\frac{1}{2}$ miles wide and commonly is less than half a mile wide. It is broken by two major gaps, one $2\frac{1}{2}$ miles long southeast of Lake Temescal in Berkeley, the other $1\frac{1}{2}$ miles long southeast of Hayward. Elsewhere the rhyolite is almost continuous, cut through only by narrow stream canyons. Its highest altitude is about 1100 feet, at Leona Heights; it is exposed in many places less than 100 feet above San Francisco Bay. The original top is nowhere preserved. The present thickness varies abruptly and irregularly, with a maximum of 800 feet near Leona Heights. Most of the rhyolite remnants are less than 100 feet thick, but masses 300 to 400 feet thick are preserved at several places.

The rhyolite usually follows a fault contact between the Upper Jurassic Knoxville formation on the east and a complex assemblage of sedimentary and volcanic rocks of the Upper Jurassic Franciscan formation intruded by serpentine and gabbro on the west. Although largely underlain by Jurassic rocks, the rhyolite is underlain in at least one place by late Tertiary rocks. North of Hayward, in the hills above Hayward Union High School, a small body of siliceous mudstone, correlated with the middle Miocene Monterey group, is present between the serpentine and the rhyolite.

The base of the rhyolite is exposed in a few transverse canyons. These cross sections are V-shaped, as though the rhyolite had flowed down youthful stream valleys cut in the fault zone. In some of them, a few feet of pebble-cobble conglomerate in a rhyolitic tuff matrix underlies the Leona. The pebbles are predominantly Franciscan formation chert and greenstone, with minor amounts of biotitic sandstone from Cretaceous or Tertiary rocks; others are of siliceous shale and chert from the Monterey group.

No younger rocks overlie the Leona in the Hayward quadrangle. Just to the north, however, unconsolidated stream gravels lie on the eroded top of the rhyolite, far above the present valleys and trending athwart them (Clark, 1917, p. 363). Scattered at the highest altitudes in the Hayward area are similar isolated gravel patches, clearly of Pleistocene age, containing pebbles from recognizable Jurassic, Cretaceous, Miocene, and probably Pliocene formations.

The kind and degree of deformation of the Leona rhyolite is important in deducing its age. According to Lawson and Clark, the rhyolite has been much affected by faulting. Their maps show the Leona to be terminated on the north by a west-trending fault, severely displaced by several of the great northwest-striking regional faults, and notably offset by two smaller transverse faults west of Lake Chabot. In the Hayward quadrangle the only significant deformation of the rhyolite is several hundred feet of vertical displacement and perhaps 1200 feet of horizontal displacement on its western edge, in the Hayward fault zone. The two transverse faults west of Lake Chabot are in the Hayward quadrangle (A and B, Fig. 1). Their existence is not questioned, but, in my opinion, the rhyolite is not offset by them. The outcrop pattern of the rhyolite hill-capping that trends across B seems to be entirely erosional. The rhyolite at A, which forms the abutments of the Lake Chabot Dam far below the base of the nearest hill-capping of rhyolite, seems to be a dike, as do several other elongate rhyolite masses on the west side of Lake Chabot. Two of these are shown in a perspective block diagram (Fig. 2). The contacts of three of these masses are well exposed in places, and the rhyolite shows no signs of disturbance, although at the upper contact of the rhyolite exposed on the east side of the San Leandro Rock Co. quarry (see diagram) there is a few feet of black gouge, derived from Franciscan rocks. Apparently these dikes occupy earlier faults. There is no evidence that these bodies are slivers faulted down from a surface flow.

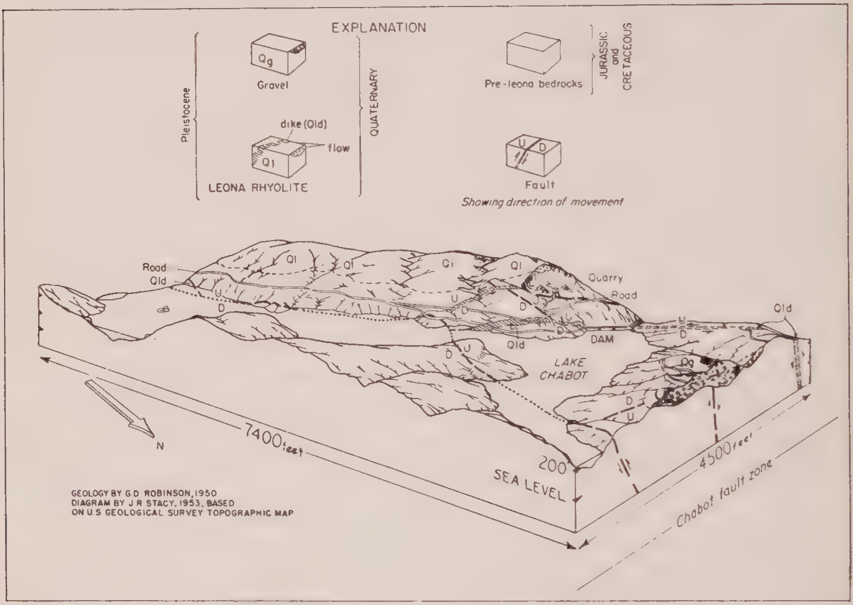

GEOLOGY BY G D ROBINSON, 1950
DIAGRAM BY J R STACY, 1953, BASED
ON U S GEOLOGICAL SURVEY TOPOGRAPHIC MAP

FIG. 2. Perspective block diagram of Leona rhyolite and adjoining formations near Lake Chabot, Hayward Quadrangle, California.

Interpreting the structure is complicated by the presence of old, presumably Franciscan, keratophyric volcanic rocks along much of the western edge of the rhyolite belt. In hand specimens, these rocks are characteristically similar to fresh Leona rhyolite, and they were included with the Leona by Lawson and by Clark. Where well exposed, however, and in thin section, the keratophyric rocks can usually be readily distinguished from the Leona. They have been intensely folded and faulted. If correlated with the Leona they would naturally lead to an exaggerated idea of its deformation.

Southeast of Hayward, on the east side of the belt, three broad rhyolite hill cappings (C, D, E, Fig. 1) narrow abruptly downward into feederlike masses in valleys, which are also the loci of pre-rhyolite faults. Figure 3 is an areal map of one of these (C). These bodies seem best interpreted as eroded domes or as the vent portions of individual short flows.

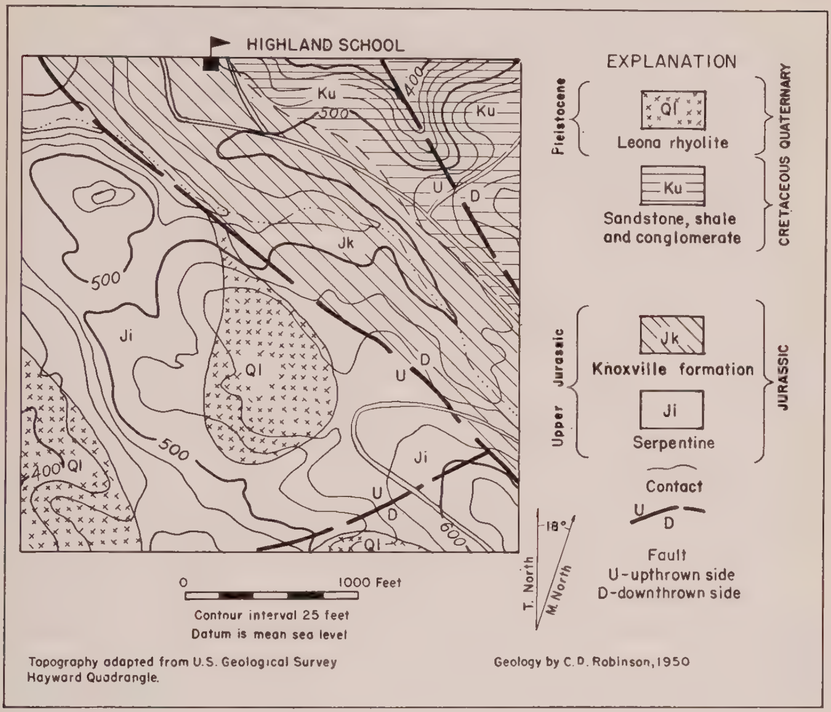

Topography adapted from U.S. Geological Survey Hayward Quadrangle.

Geology by C. D. Robinson, 1950

FIG. 3. Geologic detail near Highland School, Alameda County, California.

INTERNAL FEATURES

The rhyolite, though the most resistant rock in the area, with a tendency to form cliffs, is nearly everywhere deeply altered. Even in quarries, it is commonly a dense mottled, very pale orange to brownish-white mixture of quartz, argillized feldspar, clay, and wisps of chlorite, with iron-stained pits marking former pyrite grains. Innumerable closely spaced fractures are coated with reddish-orange and yellowish-brown iron stains, masking the predominantly light color of the altered rock. Sufficient use of the hammer will usually reveal comparatively fresh rhyolite under a thick carapace of alteration, and the alteration is most intense at higher altitudes and where fractures are most numerous. The alteration, therefore, seems to be largely due to weathering, possibly accelerated by sulfuric acid produced by oxidation of the original disseminated pyrite. The rock is massive, with no sign of layering even in the largest exposures. It is rarely amygdaloidal or vesicular and only locally flow-banded.

The intricate fracturing is apparently due mainly to cooling rather than to deformation. Many fractures are healed with glass or other groundmass material, the brecciation is widespread rather than confined to linear zones, and offsetting across fractures is trivial. Where the rhyolite has been affected by known faults it has cataclastic textures, both macroscopic and microscopic, and the shearing has linear, purely local, distribution. A few fractures are filled with veinlets of quartz or calcite.

Where fresh, the Leona rhyolite is medium bluish or greenish gray. About 30 thin sections from the Hayward quadrangle were studied. They exhibit a few per cent of small poorly oriented phenocrysts of plagioclase (sodic oligoclase to albite), quartz, and sporadically, orthoclase. The phenocrysts are commonly a little resorbed and cracked. Pyroclastic debris, such as broken crystals, glass shards, and relict lapilli, is very rare. The groundmass is typically a felted, locally granophyric, microcrystalline mixture of untwinned albite and quartz. Less commonly, the groundmass is spherulitic glass, in which the spherules are usually chalcedony but in places are feldspar or quartz. Locally the glass is riddled with poorly aligned feldspar microlites. The only ferromagnesian constituents are scattered shreds of chlorite and of biotite, marginally altered to chlorite. Cubes and pyritohedrons of pyrite are disseminated throughout. The mineral proportions vary widely, but the average fresh holocrystalline rock may be visualized as consisting of 60 per cent albite, 30 per cent quartz, 3 per cent oligoclase, 2 per cent each of orthoclase, chlorite, and pyrite, and accessory magnetite, apatite, sphene, zircon, and ilmenite.

The plagioclase, based on many measurements of maximum extinction angles and a few measurements in oils, seems to grade from sodic oligoclase, mostly in the phenocrysts, to somewhat calcic albite (γ 1.538-1.540), mostly in the groundmass. Most of the albite is untwinned, but that approaching oligoclase in composition occasionally exhibits rather broad albite twinning. Zoning was not seen. All of the plagioclase is evidently primary.

Chlorite appears in the freshest rhyolite, which also contains a little biotite, marginally chloritized. The chlorite probably formed during or soon after consolidation of the rhyolite by deuteric alteration of biotite.

In the northern part of the area the phenocrysts are larger and more abundant, making up 5 to 15 per cent of the rock, and the groundmass is more commonly glassy, with much local development of microlitic and spherulitic facies. The bulk mineral composition appears to be about the same as in the southern (Hayward) part.

Three chemical analyses exist from the time of Lawson and Clark; they are reproduced in Table 1 along with one of Daly's averages (1933) for comparison. No recent analyses have been made, but partial analysis of two fresh rhyolite samples for Na_2O and K_2O, made in 1952 in the

TABLE 1. CHEMICAL COMPOSITION OF LEONA RHYOLITE

	(1)	(2)	(3)	(4)
SiO_2	71.00	72.12	71.60	72.80
TiO_2	—	0.17	0.12	0.33
Al_2O_3	12.70	11.49	11.93	13.49
Fe_2O_3	0.66	2.77	3.00	1.45
FeO	2.44	2.30	3.40	0.88
MnO	—	0.10	0.09	0.08
CaO	0.90	0.94	0.52	1.20
MgO	1.39	0.85	1.33	0.38
Na_2O	6.45	5.28	4.62	3.38
K_2O	2.99	0.86	1.90	4.46
P_2O_5	—	0.88	0.62	0.08
SO_3	—	—	0.08	Nr
CO_2	—	1.15	0.38	Nr
FeS_2	—	0.03	—	Nr
H_2O (at 110° C.)	0.28	0.06	0.07	1.47
Ignition	1.56	0.96	0.55	
	100.37	99.96	100.21	100.00

(1) Analyst—C. P. Richmond. From Clark (1917), p. 371, and Lawson (1914),
(2) and (3) Analyst—G. E. Colby p. 12.
(4) Average of 126 analyses of rhyolite, from Daly (1933), p. 9.
Nr, not reported.

laboratories of the U. S. Geological Survey, confirm the proportions of these oxides reported by the earlier analysts.

Elaborate petrologic calculations and deductions based on these analyses would be idle: the data are few and they represent material that was "more or less altered" (Lawson, 1914, p. 12). Even allowing for this the analyses have some features strikingly at variance with the mineralogy as described by Lawson and by Clark. The most significant of these involve the composition of the feldspars. Clark (1917, p. 371) states that "orthoclase, plagioclase, mostly oligoclase, and quartz are the essential constituents of the original rock." But orthoclase and oligoclase cannot be major constituents of a rock containing only 1 to 3 per cent of K_2O and less than 1 per cent of CaO. The present identification of albite as the dominant feldspar, with minor amounts of oligoclase and orthoclase, brings the mineralogy into reasonable agreement with the chemical analyses. The dominance of albite is supported by two partial *x*-ray analyses, made by A. J. Gude, III, of the Geological Survey. Staining tests with sodium cobaltinitrate, made by Lyman C. Huff, also of the Geological Survey, confirm the observation that potash feldspar is sparse and sporadic. Despite this substitution of albite for most of the orthoclase and oligoclase in the mode, the name soda rhyolite applied by Lawson still seems appropriate.

ORIGIN OF THE PYRITE

The ubiquitous pyrite deserves further discussion. Although pyrite is (or was) disseminated throughout the rhyolite, it is absent from the underlying rocks, even at their contacts with pyrite-rich rhyolite, except at one locality where keratophyric volcanics contain a little. It seems reasonable, on this basis alone, to regard the pyrite as a primary mineral in the rhyolite, as Lawson and Clark did. The behavior of pyrite under volcanic conditions, that is, at high temperature and low pressure, is not in conflict with such an origin. It is well-known that pyrite, in a vacuum, decomposes to pyrrhotite and sulfur vapor at about 500° C. But the pyrite-pyrrhotite reaction is reversible, according to Allen, Crenshaw, and Johnston (1912), and their work shows that under only 1 atmosphere of sulfur vapor pressure the dissociation of pyrite is sluggish and incomplete even at 750° C.; at falling temperature, pyrrhotite changes almost completely to pyrite at about 550° C. They found that pyrrhotite in hydrogen sulfide melts at 1183° C. The melting point of pyrite in air is 1171° C. (Handbook of Chemistry and Physics, 1952). The temperature of flowing rhyolite has never been measured, and few really pertinent laboratory experiments are recorded; published speculations range from as low as 600° C. to as high as 1260° C. A number of recent field measurements indicate that the extrusion temperature of basalt in Hawaii is in the range 1030 to 1080° C. (Macdonald and Finch, 1950; Macdonald, 1952); basalt extrusion temperatures near 1170° C. are suggested by recent laboratory experiments (G. C. Kennedy, oral communication). It is generally agreed that rhyolite issues at lower temperature than basalt. In the absence of excess oxygen, then, it would appear that iron sulfide can remain stable at the temperatures expected in rhyolite lava and be preserved as pyrite after cooling.

There is some basis for imagining the pyrite in the Leona to have crystallized early. Many of the pyrite crystals in the unaltered rock are rounded and embayed; some are nearly spherical. The degree of rounding varies widely, even in a single thin section. The surfaces of the rounded crystals have the characteristic luster of pristine pyrite. The possibility is worth considering that early-formed crystals of pyrite were marginally corroded by interaction with the melt, just as the silicate phenocrysts were.

Whether early formed or late, the pyrite does not vein or shoulder aside the other minerals of the rock, and seems syngenetic.

Near Leona Heights, large ovoid masses of pyrite, with very small amounts of chalcopyrite, bornite, sphalerite, and chalcocite, were formerly mined for use in making sulfuric acid. The workings have long been abandoned and inaccessible, but some have been described by Clark (1917) and others by Mace (1911). The pyrite bodies, some more than 100 feet long, appear to have been emplaced in fractures cutting the rhyolite, and the sulfide minerals, according to Clark, have replaced the rhyolite to some extent. The deposits examined by Clark were near the base of the rhyolite, but wholly within it; those studied by Mace were largely within the rhyolite but rested on carbonaceous shale. It was Clark's hypothesis that primary disseminated pyrite had been oxidized by ground water to form acid ferrous sulfate solutions, which were neutralized and reduced below the water table by the rhyolite itself, aided by the carbonaceous shale, to produce the pyrite masses. The process is somewhat difficult to visualize in detail, particularly with respect to the copper and zinc sulfides, and it seems more likely that the massive pyrite and its accompanying sulfides are hydrothermal, and derived originally from the same source as the pyritic rhyolite. Whatever its origin, the massive pyrite at Leona Heights is younger than the rhyolite, and is seemingly not to be correlated with the disseminated pyrite.

EMPLACEMENT OF THE RHYOLITE

The field and laboratory observations, while far from exhaustive, indicate that most of the rhyolite was emplaced by extrusive flow. The rock fabric, with its continuous groundweb, consistently unfragmented phenocrysts, and paucity of pyroclastic debris, clearly suggests that the flowing material was lava and not hot ash. The suggestion of liquid origin is especially forceful where the groundmass is spherulitic glass. The presence of a little pyroclastic material is not unfavorable to this thesis. Incorporation of pyroclastic fragments in any lava flow is to be expected, for ash eruption generally accompanies lava outflow, and some windborne material falls on and mingles with the lava. In addition, the chilled margins of the flow are fragmented as extrusion continues, and these fragments may become widely distributed within the flow.

It does not necessarily follow that the lava issued from a single vent somewhere in the rhyolite belt and traveled for 10 miles or more. Another possibility is suggested by the rhyolite dikes and the three masses that taper downhill, viewed in relation to the regional fault system. Perhaps magma rose, more or less simultaneously, at many places along relatively open west-trending subsidiary fractures of the northwest-trending main fault system, to feed a series of domes and short flows. The main faults, of compressional type, were presumably too tight for magma to pass. Pre-rhyolite stream erosion along the main fault zones, however, provided channels for the lava once it reached the surface. Such a method of emplacement would account for the two long gaps in the belt and for the considerable differences in facies along it.

The proposed emplacement mechanism, in offering multiple vents and short travel for the rhyolite, at the same time provides fairly reasonable avenues for post-lava hydrothermal solutions to disseminate pyrite and, later, even to chloritize and argillize the rock. If so, the solutions were rigorously selective, for they failed to deposit pyrite in the neighboring rocks, although many of them offer environments seemingly as favorable as the rhyolite. Chlorite and clay are widely developed in the underlying rocks (they are abundant primary constituents of the sedimentary rocks, and the ferromagnesian minerals of the volcanic rocks of the Franciscan formation have been largely converted to chlorite), but these same rocks have also been silicified and carbonatized, whereas neither silica nor carbonates have been significantly added to the rhyolite; apparently the chlorite and clay in the rhyolite are not to be correlated with those in the country rocks. While favoring the multiple-extrusion hypothesis for the rhyolite, I prefer not to appeal to it as a mechanism for the hydrothermal introduction of pyrite or chlorite or clay. Pending more thorough study, it is tentatively concluded that the pyrite is primary, that the chlorite is largely deuteric, and that all the clay is the product of weathering.

AGE AND REGIONAL RELATIONS

The Leona rhyolite was dated as late Tertiary, probably Pliocene, by Lawson (1914) and Clark (1917). Subsequent regional studies, and this local one, provide evidence that its age is very likely early or middle-Pleistocene. The presence of bedrock of the Monterey formation and detritus below the rhyolite demonstrate that the rhyolite cannot be older than late Miocene. The very youngest Pliocene rocks throughout the Bay area are reported by all modern workers to be intensely deformed. On the other hand, strata in the Bay area known to contain earlier Pleistocene ("Irvingtonian") continental fauna have gentle dips; beds with unequivocal later Pleistocene ("Rancholabrean") fauna are essentially flat (Savage, 1951, pp. 288-289). Because the rhyolite is little deformed, it is probably post-Pliocene. Because it was deeply eroded before deposition of Pleistocene gravels, themselves now deeply eroded, it appears to be of fairly early Pleistocene age.

Patches of white rhyolite along the west front of the Berkeley Hills north of Berkeley, though similar chemically to the Leona and of about the same age, were considered to be remnants of a separate flow and were named Northbrae rhyolite by Lawson (1914), largely because they contain magnetite rather than pyrite. This difference is, I think, more striking than significant. The Northbrae rhyolite may well prove to be simply another of the many small closely related intrusive masses constituting the Leona rhyolite belt. To the south, near San José, an intrusive mass mapped and named Alum by Crittenden (1951, pp. 46–48) seems to be a correlative of the Leona rhyolite, as he suggests.

Geologic History

The Leona rhyolite is not mentioned in the section on geologic history in Lawson's San Francisco folio (1914), and Clark devotes but a curt paragraph to its geologic history. Doubtless they were prudent rather than negligent. Despite their example, I shall try to reconstruct the history of the rhyolite and its environs. Supporting evidence for details of the regional geology is omitted. These may be found in the Hayward quadrangle report (Robinson, in preparation) and in broader studies, such as those of Taliaferro (1941), Howard (1951) and Louderback (1951).

In late Pliocene time the rhyolite belt was probably dry land, but the nature of the rocks which directly underlay the land surface and the shape of that surface are unknown. At the end of the Pliocene, the region was intensely deformed along northwest-southeast axes. Tight folds were formed, and the Chabot and Hayward fault zones, which may have existed much earlier, were active, with mainly vertical displacement. The early Pleistocene streams tended to be consequent on the folds and faults, flowing northwestward to the ocean. When a ridge-and-valley stage of dissection had been reached, still in early Pleistocene or middle Pleistocene time, another, much milder, episode of deformation reactivated some of the older faults. Rhyolitic magma, from unknown sources, rose along relatively open segments of the faults, largely in complementary fractures rather than on the main breaks. Where magma reached the surface it formed domes or short flows, not more than a few miles long, channeled by the northwest-striking valleys. Probably no large eruption cones were formed, but there was a little explosive activity during the eruptive episode, and some rhyolitic ash was incorporated within and deposited ahead of the slow-moving lava, which subsequently covered it. Although the rhyolite was doubtless much thicker and more widespread than it is today, it probably did not form a continuous blanket of really imposing extent.

When the rhyolite was emplaced, it was about as close to sea level as now, but the shore line was nevertheless farther west, for San Francisco Bay did not yet exist. Extrusion of the rhyolite greatly modified the local drainage pattern, but not for long. Streams, still flowing northwestward, cut into the rhyolite and deposited gravel upon it. Deposition was the dominant process, and by late Pleistocene time the area was a graveled coastal plain. The rhyolite was buried by these gravels.

Then gentle regional tilting produced westerly surface dips, and consequent streams began to run athwart the buried northwest-trending structures and drainage courses. The Hayward fault zone became active, with dominantly vertical displacement. The east side remained stationary or rose slightly, the west side dropped at least 650 feet and possibly several times that much, permitting marine waters to enter here for the first time, perhaps, since the early Pliocene. (Eustatic changes may also have contributed to this invasion.) The west side and northern end of the rhyolite belt were involved in the faulting. The pyrite masses at Leona Heights may have been formed at about this time.

As a result of the very late Pleistocene tilting and faulting, most of the earlier Pleistocene gravels were stripped, and the streams became superposed. Westward tilting and submergence probably continued well into the Recent epoch, and a thick sequence of interbedded marine and stream deposits accumulated under what is now the Bay plain just west of the rhyolite belt. Still more recently westward tilting and submergence gave way to gentle uplift, exposing the Bay plain and entrenching the streams crossing it.

In Recent time, intermittent movements in the Hayward fault zone became mainly horizontal rather than vertical, and rhyolite on the west side of the zone was shifted northwestward.

Downcutting in some of the superposed streams was able to keep pace with uplift, especially where the rhyolite was thin, and canyons were cut across the rhyolite belt. Most streams were diverted by the resistant rhyolite, turning far to the northwest or southeast for outlet. A major outlet developed through the long gap in the rhyolite at Hayward. Gradually, valley cutting on the east and faulting on the west turned the old rhyolite-filled valleys into the rhyolite-capped ridges of today

ACKNOWLEDGMENTS

Professor Howel Williams, of the University of California, and Julius Schlocker and M. G. Bonilla, of the U. S. Geological Survey, visited me in the field and made many helpful suggestions. John R. Stacy constructed the perspective block diagram (Fig. 2).

REFERENCES

ALLEN, E. T., CRENSHAW, J. R., AND JOHNSTON, JOHN (1912), The mineral sulphides of iron: *Am. Jour. Sci.*, 4th ser., **33**, 169–236.

CLARK, C. W. (1917), The geology and ore deposits of the Leona rhyolite: *Univ. Calif., Dept. Geol. Sci. Bull.*, **10**, 361–382.

CRITTENDEN, M. D., JR. (1951), Geology of the San Jose-Mount Hamilton area, California: *Calif. Div. Mines Bull.* **157**.

DALY, R. A. (1933), Igneous Rocks and the Depths of the Earth, 2nd imp., McGraw-Hill Book Co., p. 9.

Handbook of Chemistry and Physics, 34th ed. (1952), Chemical Rubber Publishing Co., p. 512.

HOWARD, A. D. (1951), Development of the landscape of the San Francisco Bay Counties: *Calif. Div. Mines Bull.* **154,** 95–106.

LAWSON, A. C. (1914), *U. S. Geol. Survey Geologic Atlas*, San Francisco folio, no. **193,** 24 p.

LOUDERBACK, G. D. (1951), Geologic history of San Francisco Bay: Geologic Guidebook of the San Francisco Bay Counties, Calif.

MACDONALD, G. A., AND FINCH, R. H. (1950), The June 1950 eruption of Mauna Loa: *Volcano Letter, No.* **509**, 3.

MACDONALD, G. A. (1952), The 1952 eruption of Kilauea: *Volcano Letter, No.* **518,** 10.

MACE, C. H. (1911), Genesis of Leona Heights ore deposit, California: *Mining World*, **35,** 1320.

ROBINSON, G. D. (in preparation), The Hayward quadrangle, California: U. S. Geol. Survey Geologic Quadrangle Map.

SAVAGE, D. E. (1951), Late Cenozoic vertebrates of the San Francisco Bay region: *Univ. Calif., Dept. Geol. Sci. Bull.*, **28,** 215–314.

SCHALLER, W. T. (1903), Minerals from Leona Heights, Alameda County, Calif.: *Univ. Calif., Dept. Geol. Sci. Bull.*, **3,** 191–217.

TALIAFERRO, N. L. (1941), Geologic history and structure of the central Coast Ranges of California: *Calif. Div. Mines Bull.* **118,** 119–163.

HIDALGOITE, A NEW MINERAL*

Robert L. Smith, Frank S. Simons, and Angelina C. Vlisidis,
U. S. Geological Survey, Washington, D. C.

Abstract

Hidalgoite, a new mineral from the San Pascual mine, Zimapan mining district, Hidalgo, Mexico, is a basic sulfate-arsenate of lead and aluminum, with the formula $PbAl_3(AsO_4)(SO_4)(OH)_6$. Hidalgoite is a member of the beudantite group and is the arsenate analogue of the phosphate hinsdalite and the aluminum analogue of beudantite. The unit cell dimensions for both the hexagonal cell and the corresponding rhombohedral cell are: $a_0=7.04$ Å; $c_0=16.99$ Å; $c_0/a_0=2.41$; $a_{rh}=6.97$ Å, $\alpha=60°40'$.

Introduction

The new mineral hidalgoite was collected during a study of the Zimapan mining district, State of Hidalgo, Mexico. This study was made during 1948 as part of a cooperative project between the U. S. Geological Survey, operating under the auspices of the Department of State, and the Comité Directivo para la Investigación de los Recursos Minerales de Mexico of the Government of Mexico. During the course of this study Simons collected specimens of a peculiar white to light-gray material from a vein in the San Pascual mine and submitted them to the U. S. Geological Survey in Washington, D. C., for identification. This material was examined in the laboratory by Smith who found one of the constituents to be a new mineral.

In the preliminary stages of the laboratory investigations, qualitative chemical tests showed the presence of substantial amounts of lead, aluminum, sulfate ion, and water. Spectrographic examination by K. J. Murata confirmed lead and aluminum and established the presence of arsenic—these three elements being the principal metallic constituents. Preliminary *x*-ray examination by J. M. Axelrod placed this mineral in the alunite family, with a pattern close to hinsdalite. The above data together with the optical properties and specific gravity indicated a new mineral, and additional material was therefore requested for detailed study. This material was obtained through the courtesy of Carl Fries, U. S. Geological Survey, Mexico City, Mexico.

The Zimapan mining district is in the western part of the State of Hidalgo. It is about 200 km. north of Mexico City on the road to Laredo, Texas. The San Pascual mine is on the northwest side of the Barranca de San José some 9 km. northwest of Zimapan. Its adit is along a north-trending dike of quartz latite. Both dike and mineralization are probably related to a much larger dike-like body of quartz monzonite, the NW end of which lies some 300 m west of the mine. The monzonite is intrusive principally into calcareous shale of Cretaceous age; the mine is in overlying fanglomerate of probable Miocene or Pliocene age.

---

* Publication authorized by the Director, U. S. Geological Survey.

The hidalgoite was found in a meter-wide vertical vein in the footwall of an east-west fault that dips steeply north where it crosses the adit 115 m from the portal. The fault is barren where the hidalgoite-bearing vein cuts it, to the west of the main N-S structure, but to the east it had the largest ore body of the mine, reportedly containing galena, pyrite, sphalerite, arsenopyrite, cerussite, and minor amounts of anglesite, wulfenite, and alamosite.

Description and Physical Properties

Hidalgoite occurs in white porous or cavernous to dense porcelain-like masses. In some specimens it has much the appearance of "bone" magnesite. Much of the material studied is discolored by streaks or blotches of iron oxide. This is especially true of the more porous specimens.

Owing to the fine-grained nature of hidalgoite, cleavage could not be observed either in hand specimen or under the microscope; fracture, irregular in porous specimens to conchoidal in the porcelain-like masses; hardness, $4\frac{1}{2}$; luster, dull; diaphaneity, translucent; tenacity, brittle.

Optical Data

The fine-grained character of hidalgoite precludes the measurement of any optical properties other than a mean index of refraction. Measurements made on several specimens yielded a mean index of refraction ranging from 1.705 to 1.713 for sodium light. Mean n for the analyzed material is $1.713 \pm .002$ Na. The birefringence is quite low.

In some of the hidalgoite specimens small spherulitic growths have developed. Some of these show extinction crosses which, when tested with the gypsum plate, simulate uniaxial positive interference figures.

Chemical Data

Hidalgoite is insoluble in HCl, HNO_3, and H_2SO_4 at one atmosphere pressure. Solution was effected by heating with 3 ml. of concentrated HCl in a sealed Pyrex tube placed in an oven at 150° C. for 3 hours.

The standard procedures of chemical analysis were employed. Lead was determined as the sulfate and sulfur as barium sulfate. Arsenic and antimony were determined as the pentasulfide. Zinc was precipitated as the sulfide, and ignited to the oxide. Alumina and silica were measured by the usual gravimetric methods, and Fe_2O_3 was determined colorimetrically with KCNS. Total water was determined by the Penfield method using anhydrous sodium tungstate (Na_2WO_4) as a flux.

The chemical analysis and ratios of hidalgoite are shown in Table 1. The calculated analysis of $PbAl_3(AsO_4)(SO_4)(OH)_6$ is included for comparison. Although there is slight departure in ratios from the beudantite structure type, hidalgoite conforms to the formula $PbAl_3(AsO_4)(SO_4)(OH)_6$. There is minor substitution of zinc for lead, iron for aluminum, and antimony for arsenic. The analysis shows a departure from the 1:1 ratio between AsO_4 (or PO_4) and SO_4 ordinarily shown by members of the beudantite group. However, a comparable departure may be observed in some of the published analyses of beudantite and corkite, where SO_4 is predominant over AsO_4 and PO_4, respectively, and in svanbergite, where PO_4 predominates over SO_4. Hidalgoite also has a slight excess of water. Part of the iron may be present as a limonitic impurity.

Table 1. Chemical Analysis and Ratios of Hidalgoite

$PbAl_3(AsO_4)(SO_4)(OH)_6$	Hidalgoite*		
Per cent		*Per cent*	*Ratios*
35.68	PbO	32.84÷223.22=0.14712	
	ZnO	0.88÷ 81.38=0.01081	
		0.15793	1.98
24.51	Al_2O_3	24.25÷101.94=0.23788	
	Fe_2O_3	0.57÷159.70=0.00357	
		0.24145	3.02
18.37	As_2O_5	16.27÷229.82=0.07079	
	Sb_2O_5	0.20÷323.52=0.00062	
		0.07141	0.89
12.80	SO_3	15.03÷ 80.07=0.18771	2.35
8.64	H_2O	9.70÷ 18.00=0.53889	6.75
	SiO_2	0.32	
100.00		100.06	

* Analyst, A. C. Vlisidis.

A qualitative spectrographic analysis of hidalgoite by Janet D. Fletcher showed the presence of Ca, V, Ti, and Cu, in hundredths of one per cent, and Mg, Sr, Ba, B, Cr, and Sc in thousandths of one per cent.

X-RAY DATA AND SPECIFIC GRAVITY

X-ray powder diffraction patterns of hidalgoite were taken using both iron and copper radiation. The iron pattern showed better resolution of reflections than the copper pattern and thus was used as a basis for calculating the unit-cell dimensions.

Hidalgoite is a member of the alunite family (used here to include the alunite, beudantite, and plumbogummite groups) on the basis of its qualitative chemistry and its similarity in structure, as observed in *x*-ray powder patterns, to other members of the family, especially alunite and hinsdalite. Indexing of the reflections was therefore accomplished on a Bunn Chart, after an axial ratio approximately that of other members of the alunite family was assumed. Reflections were present only when $-h+k+l=3n$, the condition satisfying the conventional setting of the rhombohedral cell indexed on hexagonal axes. Lattice parameters for the larger hexagonal cell were then calculated from the *d*-spacings corresponding to the sharpest diffraction lines and when possible where only one form contributed to the reflection. Calculated *d*-spacings from these parameters are in good agreement with the measured values. The unit cell dimensions for both the hexagonal cell and the corresponding rhombohedral cell are: $a_0=7.04$ Å; $c_0=16.99$ Å; $c_0/a_0=2.41$; $a_{rh}=6.97$ Å; $\alpha=60°40'$. The error for a_0 and c_0 is probably within plus or minus 0.02 Å of the stated values.

The powder pattern was indexed for all spacings greater than 1.32. The values for both calculated and observed *d*-spacings are given in Table 2 along with the observed intensities and the hexagonal and rhombohedral indices.

The specific gravity of hidalgoite was determined as 3.96 with an Adams-Johnston fused silica pycnometer of 5-cm. capacity. The specific gravity as calculated from the chemical analysis and the unit-cell dimensions is 4.27. The discrepancy between these values is rather large, but explanation might possibly be found in the very fine-grained nature of hidalgoite.

Features such as the microcrystallinity, the presence of spherulites and spherulitic aggregates, and in some specimens the presence of mosaics of minute cracks (simulating mud cracks) suggest that hidalgoite crystallized from a very viscous or gelatinous material. Assuming such a condition it seems possible that complete crystallization may not have been accomplished and that there is residual interstitial material that has a lower specific gravity. This condition might also explain the slightly higher water content.

Associated Minerals

The material available for study was collected primarily for the purpose of obtaining enough of the new mineral for chemical analysis, and therefore the associated minerals are probably inadequately represented.

TABLE 2. *X*-RAY POWDER DATA FOR HIDALGOITE
Iron Radiation, Manganese Filter, $\lambda = 1.9373$ Å
Effective Camera Diameter 114.59 mm.

$hk\bar{i}l$	$h_rk_rl_r$	Intensity	d (measured)	d (calculated)
$10\bar{1}1$	100	9	5.73	5.74
0003	111			5.66
$01\bar{1}2$	110	1	4.96	4.95
$10\bar{1}4$	211			3.49
$11\bar{2}0$	$10\bar{1}$	9	3.51	3.52
$02\bar{2}1$	$11\bar{1}$	10	2.981	3.00
$11\bar{2}3$	210			2.990
$01\bar{1}5$	221			2.968
$20\bar{2}2$	200	2	2.864	2.869
0006	222	3	2.830	2.832
$02\bar{2}4$	220	4	2.477	2.477
$21\bar{3}1$	$20\bar{1}$	1	2.282	2.283
$20\bar{2}5$	311			2.269
$10\bar{1}7$	322	7	2.257	2.255
$12\bar{3}2$	$21\bar{1}$	4	2.226	2.224
$11\bar{2}6$	321	4	2.204	2.206
$30\bar{3}0$	$2\bar{1}\bar{1}$	5	2.027	2.032
$21\bar{3}4$	310			2.025
$01\bar{1}8$	332	½	2.009	2.006
$03\bar{3}3$	$22\bar{1}$	8	1.911	1.913
$30\bar{3}3$	300			1.913
$12\bar{3}5$	320			1.907
$02\bar{2}7$	331			1.899
0009	333			1.888
$22\bar{4}0$	$20\bar{2}$	6	1.761	1.760
$20\bar{2}8$	422	½	1.746	1.743
$13\bar{4}1$	212	2	1.681	1.683
$22\bar{4}3$	$31\bar{1}$			1.681
$21\bar{3}7$	421	4	1.667	1.671
$11\bar{2}9$	432			1.664
$31\bar{4}2$	301			1.658
$30\bar{3}6$	411	3	1.651	1.651
$03\bar{3}6$	330			1.651
$10\bar{1}\cdot 10$	433	3	1.638	1.637
$13\bar{4}4$	$32\bar{1}$	½	1.570	1.571
$12\bar{3}8$	431			1.562
$40\bar{4}1$	$3\bar{1}\bar{1}$	1	1.514	1.518
$31\bar{4}5$	410			1.514
$04\bar{4}2$	$22\bar{2}$	6	1.496	1.500
$01\bar{1}\cdot 11$	443			1.497
$22\bar{4}6$	420			1.495
$02\bar{2}\cdot 10$	442	6	1.484	1.484
$40\bar{4}4$	400	1	1.434	1.435
$000\cdot 12$	444	½	1.418	1.416
$32\bar{5}1$	$30\bar{2}$	5	1.386	1.394
$04\bar{4}5$	$33\bar{1}$			1.391
$13\bar{4}7$	430			1.387
$30\bar{3}9$	522			1.383
$03\bar{3}9$	441			1.383
$23\bar{5}2$	$31\bar{2}$			1.380
$20\bar{2}\cdot 11$	533	2	1.370	1.378
$21\bar{3}\cdot 10$	532			1.368
$41\bar{5}0$	$3\bar{1}\bar{2}$	3	1.330	1.330
$32\bar{5}4$	$41\bar{1}$			1.329
$31\bar{4}8$	521			1.323

The following minerals were observed in the specimens studied: limonite, hydromica, orthoclase, tourmaline, beudantite, and a mineral tentatively referred to as ferrian hidalgoite.

Limonite

Limonite occurs as a staining in streaks and blotches throughout most of the hidalgoite. In the highly porous and cavernous specimens it may be found concentrated in small earthy or resinous masses.

Hydromica and Orthoclase

A sericitic mineral identified as a hydromica and an alkalic feldspar, here called orthoclase, were identified on the basis of their optical properties. These two minerals occur either together or separately as fine-grained aggregates in pockets in hidalgoite and are most abundant in the limonite-rich cavernous areas. They appear to have formed earlier than hidalgoite.

Tourmaline

Tourmaline was observed in only one specimen, where it occurs in mats of greenish-gray needles associated with orthoclase and hydromica. This mineral was identified by its optical properties and by *x*-ray. The optical properties are as follows: indices of refraction, $\epsilon = 1.62 \pm .002$ and $\omega = 1.643 \pm .002$; pleochroism, ϵ = yellow and ω = pale blue. The indices of refraction were measured using white light.

Beudantite

A dark brownish-green mineral was found in exceedingly small quantity on two specimens of hidalgoite. On the basis of its optical properties and association, it was identified as beudantite. The optical properties that could be determined are: mean n 1.95, low to moderate birefringence, anomalous blue interference colors, lemon-yellow to pale-yellow pleochroism.

An *x*-ray powder pattern was obtained of this mineral which shows a very close similarity to corkite from Beaver County, Utah. The principal difference is the larger cell size of the beudantite.

Ferrian hidalgoite

A mineral tentatively referred to as ferrian hidalgoite occurs in close association with beudantite and hidalgoite. It occurs in small veinlets and spherulitic growths in hidalgoite and in narrow zones surrounding crystals and spherulites of beudantite, separating them from the hidalgoite matrix. This material is light green in color, has a mean index of refraction of 1.79, and a low birefringence. Enough of this mineral was separated to obtain an x-ray powder pattern. This pattern is very close to hidalgoite, but differs in having a slightly larger cell and in the relative positions of a few lines. These few lines show a slight departure from hidalgoite and seem to be related to corresponding lines on the pattern obtained from the associated beudantite.

ACKNOWLEDGMENTS

The writers are indebted to Joseph J. Fahey for aid and advice during the making of the chemical analysis. Especial thanks are due to Donald H. Richter for aid in the x-ray procedure and calculations and to Mrs. Robert L. Smith for aid in the calculations.

REFERENCES

HENDRICKS, STERLING B. (1937), The crystal structure of alunite and the jarosites: *Am. Mineral.*, **22,** 773–784.

PABST, ADOLF (1947), Some computations on svanbergite, woodhouseite, and alunite: *Am. Mineral.*, **32,** 16–30.

PALACHE, C., BERMAN, H., AND FRONDEL, C. (1951), Dana's System of Mineralogy, Seventh Edition, Vol. II, New York, John Wiley and Sons, Inc.

SIMONS, FRANK S., AND MAPES, EDUARDO, Geology and ore deposits of the Zimapan mining district, Mexico (in preparation).

RE-EXAMINATION OF MOSESITE*

George Switzer, W. F. Foshag, *U. S. National Museum, Washington, D. C.*

K. J. Murata, and J. J. Fahey, *U. S. Geological Survey, Washington, D. C.*

Abstract

Mosesite is isostructural with Millon's base ($Hg_2NOH \cdot 2H_2O$) and its salts, the structure being a cubic cristobalite-type configuration of Hg_2N^+ groups. An analysis of mosesite from Huahuaxtla, Mexico, gave Hg^{++} 79.4 per cent, Hg^+ 3.6, Cl 3.3, SO_4 5.4, MoO_4 2.0, CO_3 0.8, N 2.44, and H_2O 3.2, total 100.1 per cent. The unit cell with $a=9.524$ Å contains 8 $[Hg_2N(Cl, SO_4, MoO_4, CO_3) \cdot H_2O]$. The specific gravity is 7.72 (calc. 7.53). Cl, SO_4, MoO_4, and CO_3 are loosely held in large open channels in the structure and may be removed or introduced by anion exchange. Mosesite from El Doctor, Mexico, contains AsO_4 and very little MoO_4, but that from Terlingua, Texas, has only Cl and SO_4 as anions. *X*-ray *d* spacings are given.

Introduction

Mosesite was described as a new mineral by Canfield, Hillebrand, and Schaller (1910) from Terlingua, Brewster County, Tex. Unfortunately, very little material was available for their study, and a definitive description of mosesite was not possible at that time. An incomplete chemical analysis by Hillebrand showed the new mineral to be a mercury-nitrogen compound containing chloride, sulfate, and water. A second discovery at Fitting, Nev., described by Bird (1932), gave some additional data but still not enough to establish the chemical composition of the mineral.

In 1942 Foshag collected several specimens of a mercury mineral at Huahuaxtla, Guerrero, Mexico, which was found by comparison of the *x*-ray powder patterns to be identical with mosesite from Terlingua. The greater abundance of the Huahuaxtla material has made possible the definition of mosesite given in this paper.

Two specimens of mosesite were also obtained from El Doctor, Querétaro, Mexico. There was not enough material from this locality to allow more than a spectrographic analysis.

The writers wish to express their thanks to W. C. Alford, of the National Institute of Health, and Shuford Schuhmann, of the National Bureau of Standards, for their help in the chemical analysis, and to Howard Evans, of the U. S. Geological Survey, for constructing the crystal structure model of mosesite.

---

* Publication authorized by the Secretary, Smithsonian Institution, and by the Director, U. S. Geological Survey.

SUMMARY OF PREVIOUS WORK

Mosesite from Terlingua is in the form of small yellow crystals perched on crystals of calcite, nearly all spinel twins of the simple octahedron. Schaller (Canfield *et al.*, 1910) noted the octahedron as the only form. Later observations by Canfield (1913) gave the additional forms {001}, {011}, {116}, {114}, and {112}.

An incomplete chemical analysis on a 0.04-gram sample by Hillebrand gave 5 per cent of Cl and 3.5 per cent of SO_4. Spectroscopic tests by Nutting (in Canfield *et al.*, 1910) showed prominent lines and bands of mercury, nitrogen, and hydrogen, the last being ascribed to water. No further chemical work has been done on mosesite from Terlingua.

Schaller noted that mosesite is commonly anisotropic but reverts to the isotropic state when heated to about 186° C. The index of refraction was determined by Larsen (1921) to be $n = 2.065 \pm 0.01$. Other data for Terlingua mosesite are: cleavage, octahedral; fracture, uneven, brittle; hardness $= 3\frac{1}{2}$; luster, adamantine; color, lemon yellow to canary yellow, becoming light olive green on long exposure to light; streak, very pale yellow.

Mosesite was also reported by Bird (1932) from the Clock quicksilver mine in the Fitting district, northeast of Lovelock, Pershing County, Nev., where it was found with native mercury and cinnabar. Additional data given by Bird include a determination of the unit cell size to be $a = 9.55$ kX, and a partial chemical analysis, which gave in per cent Hg 83.0, Cl 5.0, SO_3 7.0, NH_3 2.2, sum 97.2.

CONSTITUTION OF MOSESITE

It had not been possible to write a satisfactory formula for mosesite because (1) the analytical data were incomplete and (2) the role of the nitrogen in the structure was not known. A new analysis of mosesite from Huahuaxtla (Table 2) did not immediately improve this situation because of the unknown role of nitrogen and because, in addition to the constituents previously found in mosesite, that from Huahuaxtla was found to contain 2.0 per cent MoO_4 and 0.8 per cent CO_3. To complicate the picture further, a spectrographic analysis of mosesite from El Doctor showed very little molybdenum but several per cent arsenic.

Just at the time the writers were puzzling over the mosesite analysis, Lipscomb (1951) described the structure of Millon's base ($Hg_2NOH \cdot 2H_2O$) and its salts as being a cubic cristobalite-type configuration of Hg_2N^+ groups. The identity of the *x*-ray powder diffraction data of Millon's base with that of mosesite made it apparent that the two materials have the same structure, and the interpretation of the mosesite analysis became a simple matter.

The *d* spacings for Millon's base, as published by Lipscomb, and for mosesite are compared in Table 1. The agreement in *d* spacings is very good. The agreement in intensities is not as good, especially in the low angle region. However, Lipscomb has pointed out (private communication) that the (111) intensity would be decreased by the presence of heavier ions in the interstices of the Hg_2N^+ framework, and that his estimated intensities in the low angle region are somewhat in error, owing to rising background on his films. Also, our intensities have not been corrected for absorption in the sample, which would make the inner ones relatively weaker.

TABLE 1. COMPARATIVE *X*-RAY DIFFRACTION DATA FOR MOSESITE AND MILLON'S BASE

Mosesite Huahuaxtla (U.S.N.M. 105159) $a=9.524\pm0.002$Å Cu/Ni=1.542Å		$Hg_2NOH\cdot 2H_2O$ (Lipscomb, 1951) $a=9.58$Å		*hkl*
I	*d* (A)	I	*d* (A)	
4	5.44	237	5.52	111
8	2.86	65	2.88	311
10	2.74	131	2.76	222
5	2.38	48	2.40	400
6	2.18	43	2.20	331
5	1.83	24	1.84	511, 333
7	1.68	41	1.69	440
6	1.61	36	1.62	531
1	1.45	8	1.46	533
7	1.44	42	1.44	622
2	1.38	11	1.38	444
3	1.33	15	1.34	711, 551
5	1.24	17	1.25	731, 553

Lipscomb determined the structure of $Hg_2NOH\cdot 2H_2O$ to consist of a three-dimensional framework of Hg_2N^+ groups in an idealized cristobalite-type of arrangement. The mercury atoms form linear *sp* bonds, while the nitrogen forms tetrahedral sp^3 bonds, in a face-centered cubic lattice with $a=9.58$ Å ± 0.01. The Hg-N bond distance is 2.07 Å. The space group is $F\,\bar{4}\,3\,m$. The mercury atoms are placed at 1/8, 1/8, 1/8; 1/8, $\bar{1}/8$, $\bar{1}/8$; $\bar{1}/8$, 1/8, $\bar{1}/8$; and $\bar{1}/8$, $\bar{1}/8$, 1/8 plus the face-centered permutation, and the nitrogen atoms are placed in the diamond arrangement at 0, 0, 0 and 1/4, 1/4, 1/4 plus the face-centered permutation. A model of the structure constructed by H. T. Evans, Jr., of the Geological Survey is shown in Figures 1 and 2.

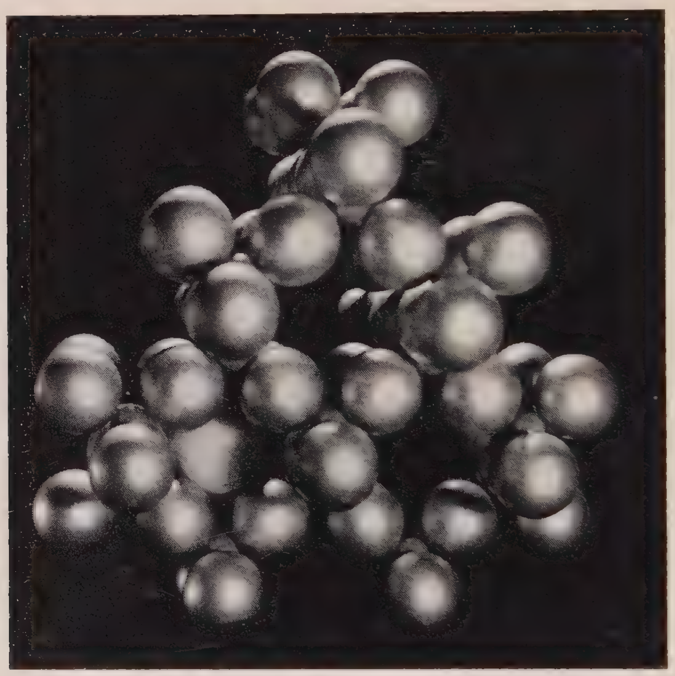

FIG. 1. View along [110] direction showing channels in structure of mosesite. The small nitrogen atoms are located at the centers of tetrahedra formed by large mercury atoms. A chloride ion is present in the lower left channel. Model by H. T. Evans, Jr. Photograph by J. A. Denson.

Lipscomb points out that the Hg_2N^+ three-dimensional network contains large channels in which it is presumed that the negative ions and water molecules are more or less randomly situated in such a way as to satisfy the electrostatic valency. He further found that the base and its salts give substantially the same powder photographs, that is, the powder photographs of the following compounds are essentially identical: $Hg_2NOH \cdot 2H_2O$, $Hg_2NCl \cdot H_2O$, Hg_2NCl, $Hg_2NBr \cdot H_2O$, Hg_2NI, Hg_2NNO_3 and Hg_2NClO_4. The scattering powers of all atoms except mercury are relatively so small that their positions can only be inferred. Probably the amounts of water are not really definite but merely enter into the structure in inexact proportions. The unit cell of Millon's base contains eight $Hg_2NOH \cdot 2H_2O$ units.

INTERPRETATION OF MOSESITE ANALYSIS

The chemical analysis has been calculated on the basis of a formula of the type $Hg_2NCl \cdot H_2O$, with a unit cell containing eight of these formula units, as shown by Lipscomb's structural studies.

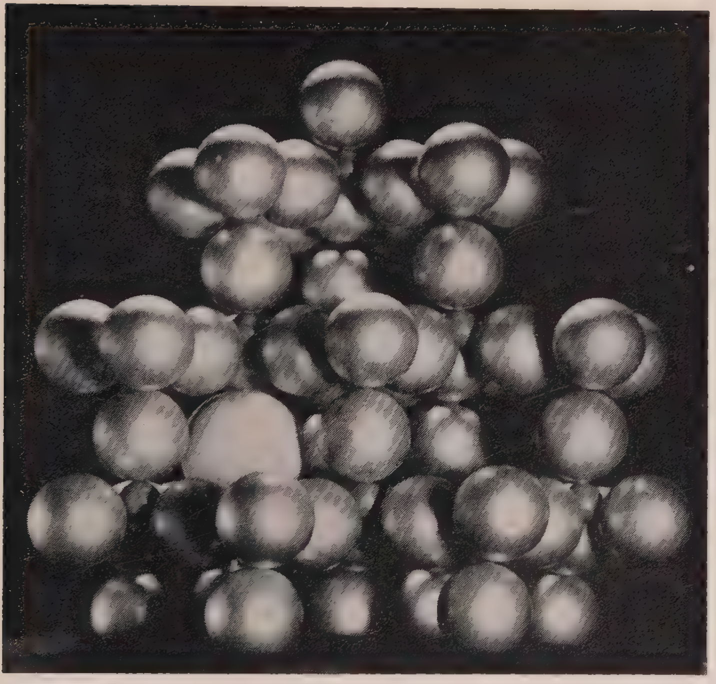

FIG. 2. View along [112] direction in the mosesite structure, showing edge view of sheets parallel to (111). The cleavage of the mineral is parallel to these sheets. The chloride ion is in the same position as in Figure 1.

The sample analyzed contained 3.6 per cent of Hg^+ which has been combined with the 79.4 per cent of Hg^{++}. Theoretically all of the mercury should be in the mercuric state. The reason for the reduction of part of it to the lower valence state is not known. The possibility that Hg^+ is present as calomel is briefly discussed in the footnote to Table 2.

The molecular ratios are given in column 2 of Table 2. The ratios for Cl, SO_4, MoO_4, and CO_3 are combined. These ratios divided by the factor required by a formula of the type $Hg_2NCl \cdot H_2O$ are given in column 3. As stated above, the value for total mercury varies considerably from that required by theory. Values for the other constituents are in better agreement.

In column 4 of Table 2 the individual values for the ratios of Cl, SO_4, MoO_4, and CO_3 are reduced to approximate whole numbers. This gives the relative proportion (average) of these four constituents per unit of structure. In column 5 the unit cell content is listed assuming $8[Hg_2NCl \cdot H_2O]$ as shown by Lipscomb. The unit cell content of Cl, SO_4, MoO_4, and CO_3 respectively is adjusted to match as closely as possible the

TABLE 2. ANALYSIS AND UNIT CELL CONTENT* OF MOSESITE FROM HUAHUAXTLA

	1	2	3	4	5	6	7
Hg^{+2}	79.4 } 83.0	0.414	2.20 2		16	+32	85.6
Hg^{+1}	3.6						
Cl	3.3	0.093		~3	3	− 3	
SO_4	5.4	0.056 } 0.175	0.93 1	~1½	1½	− 3	7.6
MoO_4	2.0	0.013		~ ½	½	− 1	
CO_3	0.8	0.013		~ ½	½	− 1	
N	2.4	0.174	0.93 1		8	−24	3.0
H_2O	3.2	0.178	0.95 1		8		3.8
	100.1					0	100.0

* If the univalent mercury were assumed to be present as HgCl and the ratios in column 3 recomputed, the figures would be 2.04 for Hg, 0.89 for the anions, and 0.97 and 0.99 for N and H_2O, respectively. Because calomel was not definitely recognized as an impurity in the mosesite, this assumption was not adopted in interpreting the analysis.

1. Huahuaxtla. U.S.N.M. 105159. J. J. Fahey, analyst. N determined by W. C. Alford, National Institute of Health.
2. Atomic and molecular proportions.
3. Ratios for $Hg_2N(Cl, SO_4, MoO_4, CO_3) \cdot H_2O$.
4. Approximate ratios of Cl, SO_4, MoO_4, and CO_3 only.
5. Number of atoms per unit cell. Unit cell contains $8[Hg_2N(Cl, SO_4, MoO_4, CO_3) \cdot H_2O]$.
6. Electrical charges associated with each type of atom or radical. The substitution SO_4, MoO_4, or CO_3 for Cl is made on the basis of one SO_4, MoO_4, or CO_3 for two Cl.
7. Theoretical composition of $Hg_2NCl \cdot H_2O$.

amounts indicated by the analysis. The electrical charges are shown in column 6. Substitutions of SO_4, MoO_4, and CO_3 for Cl are figured on the basis of one SO_4, MoO_4, or CO_3 for two Cl. The theoretical composition for $Hg_2NCl \cdot H_2O$ is given in column 7.

The ease with which salts of the Millon's base type can exchange anions has been pointed out by Srinath, Lipscomb, and Sneed (1951), who found that pure solid Hg_2NNO_3 was easily converted to $Hg_2NCl \cdot H_2O$, $Hg_2NBr \cdot H_2O$, Hg_2NI, or $Hg_2NOH \cdot 2H_2O$ by treatment, respectively, with 10 to 20 per cent aqueous solutions of KCl, KBr, KI, or KOH, which treatment displaced substantial quantities of nitrate ion in each case. The large open channels that are present in the structure are analogous to similar channels in zeolites. However, the continuous framework of Millon's base has a net positive charge rather than the net negative charge of zeolites so that anion rather than cation exchange occurs.

For mosesite, assuming a unit cell content of 16 Hg, 3 Cl, 1½ SO_4, ½ CO_3, ½ MoO_4, 16 H, 8 O, and 8 N and a unit cell volume of 847.77 Å^3, the calculated density is 7.53. This compares favorably with the measured density of 7.72 (determined on the analyzed sample from Huahuaxtla). The octahedral cleavage of the mineral follows the (111) planes of NHg_4 tetrahedra.

ANALYTICAL PROCEDURE

The chemical analysis of Huahuaxtla mosesite was made by Fahey on a carefully purified sample, weighing slightly less than one gram, after the specific gravity had been determined by use of a fused silica Adams-Johnston pycnometer. Total Hg and Cl were determined on the same sample. The univalent Hg was precipitated and weighed as HgCl. Sulfate was determined as $BaSO_4$ and the MoO_4 was computed from the MoO_3 obtained by igniting the sulfide. Total H_2O was determined by the Penfield method, using sodium tungstate as a flux. Nitrogen was determined by W. C. Alford, of the National Institute of Health, on a 20-mg. sample using the microkjeldahl procedure. Carbon dioxide was determined by a method previously described (Fahey, 1945), after having been identified as CO_2 by Shuford Schuhmann of the National Bureau of Standards, using the mass spectrograph.

CHEMICAL PROPERTIES

Mosesite is decomposed by HCl, leaving an insoluble residue of HgCl. The solution contains divalent Hg but no NH_3 as stated by Hillebrand (Canfield *et al.*, 1910). Carbon dioxide is liberated as tiny bubbles that appear on the surface of the crystals a few minutes after the addition of concentrated HCl. In 1+1 HCl heated to about 70° C., the CO_2 is evolved much more rapidly. The mosesite had previously been treated with HNO_3, in which it is insoluble, in order to remove any calcite impurity.

The effect of various reagents on mosesite was tested by placing single grains with bright crystal faces in small test tubes with the reagent at room temperature. After eight days each solution was tested for Hg. None was found with H_2SO_4 (concd. or 1+1), HNO_3 (concd. or 1+1), acetic acid (concd. or 1+1), oxalic acid, or water. Some mercury was dissolved by HCl (concd. or 1+1); the concentrated HCl caused the formation of a white coating (HgCl) in one hour; the dilute acid gave a white coating in 24 hours.

SPECTROGRAPHIC ANALYSIS

A qualitative spectrographic analysis was made by Murata of mosesite from Huahuaxtla before quantitative analysis by chemical means was undertaken. The spectrogram revealed the presence of several per cent of molybdenum in this sample. This led to a spectrographic analysis of the type material and of mosesite from El Doctor, Mexico. Molybdenum was not detectable in the type material (from Terlingua, Tex., U.S.N.M. 93292) and was present only in tenths of a per cent in the sample from El Doctor. The latter, however, was found to contain several per cent of arsenic, presumably as arsenate.

The dark outer portion and the light inner core of crystals from Huahuaxtla were separated and found by quantitative spectrographic analysis to contain 0.54 per cent and 2.1 per cent Mo, respectively.

A summary of the results of the spectrographic analysis is given below:

TABLE 3. SPECTROGRAPHIC ANALYSES OF MOSESITE FROM MEXICO

Per cent	Huahuaxtla (U.S.N.M. 105159)	El Doctor (U.S.N.M. 105522)
X0:	Hg	Hg
X:	Mo	As
0.X:	Si Al	Si Al Mg Ca Mo
0.0X–0.00X:	Fe Mg B V Ca Ba Cu	Fe B V Ag Mn
Not found:	As Mn Ag	Cu Ba
Not found in either:	Sb Sn Zn Cd Ge In Tl Pb Bi W Co Ni Cr Ti P Na Sr Y La Be	

DESCRIPTION OF MEXICAN MOSESITE

Mosesite from the two new localities in Mexico, Huahuaxtla and El Doctor, is very similar in appearance and occurrence to the original material from Terlingua, Tex. The crystals range in size from a fraction of a millimeter up to about 2 mm. and are attached to small dogtooth calcite crystals lining vugs in limestone.

The crystals are octahedral, but only rarely in single crystals. The usual habit is complex intergrowths of many crystals, resulting in nearly spherical aggregates. A few single octahedrons were noted, some of them modified by a cube, and a few simple spinel-type twins.

The color of the mosesite is variable, ranging from yellow through amber to nearly black. Some crystals are zoned, with a core of glassy amber-colored mosesite and a softer, lighter-colored surface layer. These two zones differ in molybdenum content, as already discussed, but they give identical *x*-ray powder patterns. The outer, lighter-colored zone seems to be a surface alteration. Powder patterns of the light- and dark-colored crystals are also identical. The cause of this variation in color is not known.

The index of refraction of mosesite from Huahuaxtla is greater than 1.95, and the mineral, like that from Terlingua, is anisotropic at room temperature.

OCCURRENCE AND ASSOCIATION

The mercury mines of Huahuaxtla have produced in the past an abundance of oxidized mercury minerals. Unfortunately, no adequate collection of these minerals has been preserved, but terlinguaite, montroydite, eglestonite, and calomel have been recognized. According to reports, rich masses of these minerals were charged into the retorts for distillation, including quantities of pure montroydite crystals, some of which exceeded an inch in length. Beautiful specimens, some of them containing as many as 10 recognizable varieties of colorful crystals, were consumed in this manner.

The commercial ore bodies at Huahuaxtla occur along ribs of brecciated limestone that formed along the rolls of a low-dipping fault plane. Limestone forms the footwall, and carbonaceous shale the hanging-wall of the fault (Gallagher and Perez-Siliceo, 1948). The chief ore mineral is cinnabar, but metacinnabar is also present and in some places abundant. Marcasite, pyrite, and stibnite are rare. Native mercury is abundant in places and some of it is associated with the oxidized minerals, suggesting their derivation from native mercury rather than from cinnabar.

The mosesite was found in a small cave in the workings of the Huahuaxtla mine known as Pozo Rico. These workings lie immediately below the Aurora tunnel about 100 meters from the entrance. It was reported that Pozo Rico yielded much native mercury, some of which was ladled directly into flasks. The small natural cave appeared to be a solution cavity in a zone of fractured limestone. This irregular cave, about 16 meters long, was lined with a crust of buff-colored steep rhombohedral calcite crystals. Sparsely scattered over these calcite crystals at one end of the cave were small octahedral crystals or aggregated octahedrons of mosesite.

Mosesite was also found with native mercury on calcite from El Doctor, State of Querétaro, Mexico. El Doctor is a famous old silver camp that was active more than a century ago. In the same district are old mercury mines, some of which were operated on a small scale during World War II. Nothing is known of the geology of these mercury deposits other than that they are enclosed in limestone. The specimen available to us contained a number of vugs in limestone lined with steep rhombohedral calcite crystals. A second generation of prismatic calcite crystals sometimes encrusted the first. Sulfur-yellow octahedral crystals or crystal groups of mosesite are scattered sparsely over the first generation calcite. Some irregular solution cavities in the limestone contain montroydite and native mercury.

GENESIS

Mosesite may be easily synthesized by treating HgCl with dilute ammonium hydroxide. The reaction is shown by the equation:

$$4NH_4OH + 4HgCl \rightarrow 2Hg + Hg_2NCl \cdot H_2O + 3H_2O + 3NH_4Cl.$$

In terms of mineral components this would be equivalent to the reaction of ammonia-bearing waters with calomel, yielding native mercury and mosesite. As calomel, mosesite, and native mercury are all found at Terlingua and Huahuaxtla, it is quite probable that the mosesite was formed in just this way, probably at very low temperature because the synthesis may be done at 25° C. The other anions found in mosesite, that is, molybdate, sulfate, arsenate, and carbonate, can be accounted for by anion exchange.

Substantial concentrations of ammonia have been found in thermal waters associated with mercury deposits of Sulphur Banks mine, Lake Co., Calif. (Waring 1915, and Allen and Day, 1927). The presence of tarry organic matter in mercury deposits of many different localities has been discussed by Ross (1942). Such organic matter or its precursors may have been the original source of the ammonia required for the formation of mosesite. At the Huahuaxtla mine, the ammonia may have come from the highly carbonaceous shales lying immediately above the Pozo Rico cave.

REFERENCES

Allen, E. T., and Day, A. L. (1927), Steam wells and other thermal activity at "The Geysers," California: *Carnegie Inst. Washington Pub.* **378,** 33–45.

Bird, Paul H. (1932), A new occurrence and *x*-ray study of mosesite: *Am. Mineral.*, **17,** 541–550.

Canfield, F. A., Hillebrand, W. F., and Schaller, W. T. (1910), Mosesite, a new mercury mineral from Terlingua, Texas: *Am. Jour. Sci.*, 4th ser., **30,** 202–208.

Canfield, F. A. (1913), Mosesite: *Sch. Mines Quart., Columbia Univ.*, **34,** 276–277.

Fahey, J. J., (1945), A volumetric method for the determination of carbon dioxide: *U. S. Geol. Survey Bull.* **950,** 139–141.

Gallagher, David, and Perez-Siliceo, Rafael (1948), Geology of the Huahuaxtla mercury district, State of Guerrero, Mexico: *U. S. Geol. Survey Bull.* **960**-E, 147–175.

Larsen, E. S., Jr. (1921), The microscopic determination of the nonopaque minerals: *U. S. Geol. Survey Bull.* **679,** 294 pp.

Lipscomb, W. N. (1951), The structure of Millon's base and its salts: *Acta Crystall.*, **4,** 156–158.

Ross, C. P. (1942), Some concepts of the geology of quicksilver deposits in the United States: *Econ. Geol.*, **37,** 439–465.

Srinath, D. Arora, Lipscomb, W. N., and Sneed, M. C. (1951), Some aspects of reactions between ammonia and mercury (I) compounds: *Am. Chem. Soc. Jour.*, **73,** 1015–1018.

Waring, G. A. (1915), Springs of California: *U. S. Geol. Survey Water-Supply Paper* **338,** 98–99.

MONTROSEITE, A NEW VANADIUM OXIDE FROM THE COLORADO PLATEAUS*

ALICE D. WEEKS, EVELYN A. CISNEY, AND ALEXANDER M. SHERWOOD
U. S. Geological Survey, Washington, D. C.

ABSTRACT

Montroseite, a new vanadium mineral named from Montrose County, Colo., has been found in four mines in western Colorado and in two mines in eastern Utah. It is black, opaque, submetallic, and occurs in microscopic bladed crystals of the orthorhombic dipyramidal class. The axial ratio is $a:b:c=0.509:1:0.310$, the common forms are *b* {010}, *m* {110}, *p* {121}, and a large vicinal form is approximately {0, 10, 1}. The observed specific gravity is 4.0, and the calculated specific gravity is 4.15. The composition is essentially VO(OH), with some iron commonly substituted for vanadium. Partial oxidation to VO_2 has taken place. Chemical analyses and *x*-ray diffraction data are given. Single crystal study indicated that the space group symmetry is $Pbnm(D_{2h}^{16})$.

INTRODUCTION AND ACKNOWLEDGMENTS

Montroseite was first collected by L. R. Stieff, T. W. Stern, and M. N. Girhard, of the U. S. Geological Survey, during the summer of 1949 at the Bitter Creek mine, Montrose County, Colo., and was studied by the writers in 1950. More montroseite was collected by A. D. Weeks from the Jo Dandy mine, Montrose County, and the Matchless mine, Mesa County, Colo., in 1950; from the Bitter Creek and the Whitney mines, Montrose County, Colo., in 1951, and from the Juniper mine, Grand County, Utah, in 1952. It was collected from the Rex No. 2 mine at Temple Mountain, Emery County, Utah, in 1952 by A. Rosenzweig of the Atomic Energy Commission.

The mineral was named after preliminary morphologic and *x*-ray study and chemical analysis had showed it to be different from any known vanadium mineral (Weeks, Cisney, and Sherwood, 1950). It was not fully described at that time because of the problem of a satisfactory chemical formula. The small unit cell determined by *x*-ray study indicated a simpler formula than was obtained from the chemical analysis.

Thanks are extended to L. R. Stieff, T. W. Stern, and M. N. Girhard, who collected the first sample; H. T. Evans and Stanley Block, of the Geological Survey, who determined the crystal structure and the correct chemical formula; also George Switzer, of the U. S. National Museum, who furnished material for comparison with the new mineral.

This work was done on behalf of the Division of Raw Materials of the U. S. Atomic Energy Commission.

---

* Publication authorized by the Director, U. S. Geological Survey.

OCCURRENCE

Four of the mines in which montroseite has been recognized are located in the Uravan mineral belt (Fischer and Hilpert, 1952) in western Colorado. The fifth locality, the Juniper mine, near Thompsons, Utah, is along a possible northwest extension of the Uravan belt. These five mines are in the Salt Wash sandstone member of the Morrison formation (Late Jurassic). The sixth locality is the Rex No. 2 mine in Shinarump conglomerate (Triassic) at Temple Mountain on the southeast side of the San Rafael swell in Utah. (See Fig. 1.)

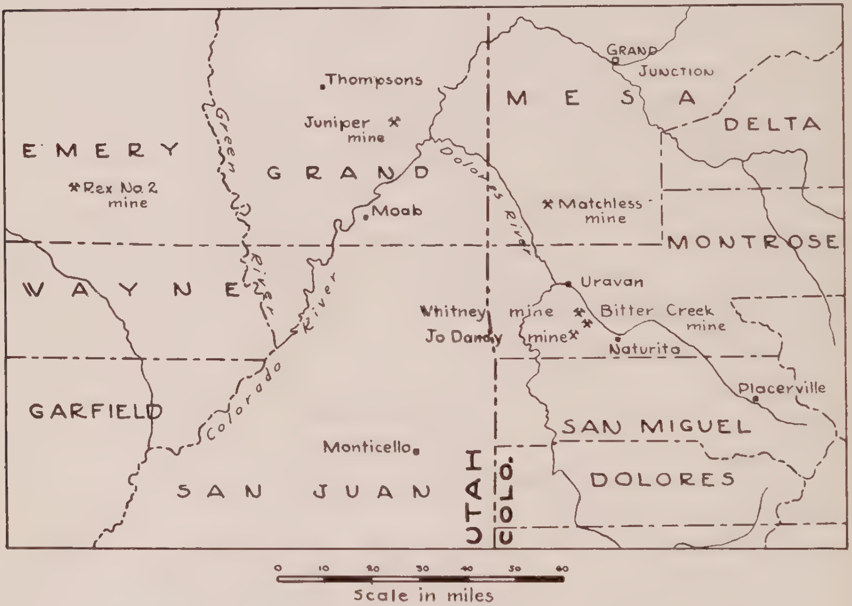

FIG. 1. Index map of localities of montroseite.

Montroseite occurs in black, relatively unoxidized vanadium-uranium ore; it is more abundant in the predominantly blacker ore at the Bitter Creek and the Whitney mines than at the Jo Dandy mine where the ore is generally oxidized and consists of minerals such as carnotite, hewettite, and hummerite. A small amount of pitchblende found at the Juniper and the Rex No. 2 mines is further indication of the relatively unoxidized environment of montroseite.

At the Bitter Creek and Whitney mines montroseite is the chief vanadium ore mineral in the blackest ore but is less abundant than corvusite in the greenish-black or blue-black ore. At the Matchless mine a small amount of montroseite was found in a band of corvusite ore with

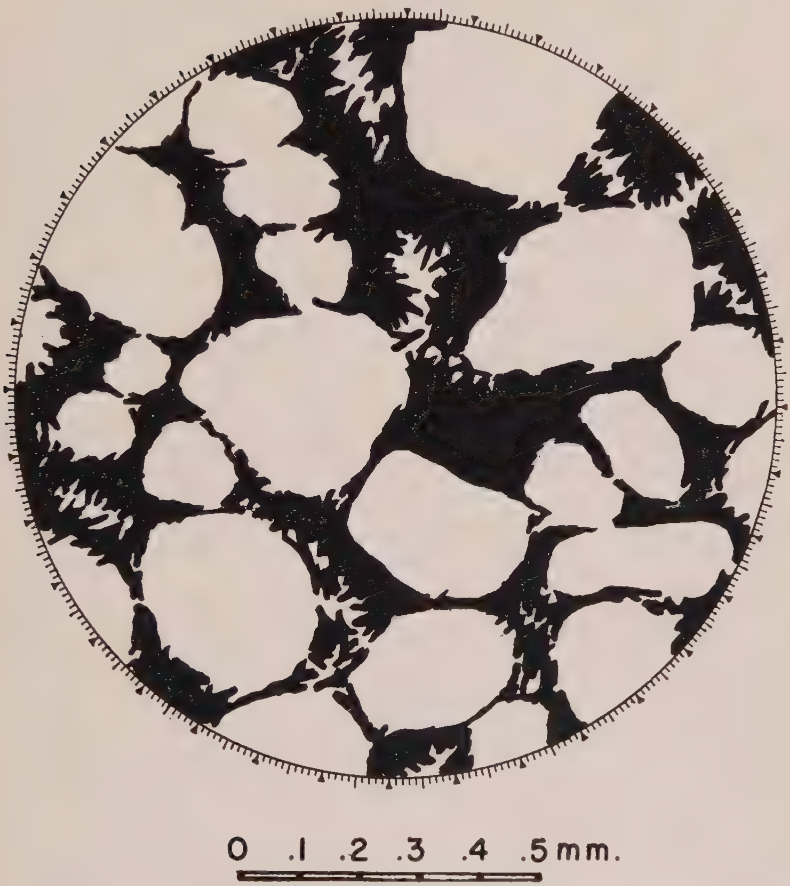

FIG. 2. Drawing of montroseite in thin section of ore sandstone from the Matchless mine, Mesa County, Colo.

thin seam fillings of hewettite. The montroseite is in microscopic crystals interstitial to the quartz grains of the ore-bearing sandstone (Fig. 2). The occurrence at the Jo Dandy mine may represent a further development of the situation at the Matchless mine; at Jo Dandy there is a very small amount of montroseite in dark patches of corvusite ore. At the Juniper mine a specimen of mineralized fossil bone was found to have microscopic tubelike fillings of montroseite in brown apatite.

A. Rosenzweig, of the Atomic Energy Commission, sent a few milligrams of nearly pure montroseite from the Rex No. 2 mine to the writers for identification. The sample consisted of cleavage fragments and aggregates of grains larger than those in other samples, and was the only specimen suitable for measurement of specific gravity on a Berman balance.

PHYSICAL PROPERTIES

Montroseite is black, opaque, with submetallic luster and black streak. It forms microscopic crystals randomly oriented in massive ore, filling interstices between quartz sand grains, or filling small tubelike openings in fossil bone. Only the samples from the Bitter Creek mine contained single crystals large enough for goniometric and x-ray single crystal study. These bladed crystals, of the orthorhombic dipyramidal class, are commonly attached at one end and terminated with dome and pyramid faces on the other end. The crystals have good cleavage parallel to the length of the blade, {010} and {110}, and are brittle. Superficially montroseite resembles melanovanadite in that both form elongated black crystals; but montroseite is orthorhombic and opaque, whereas melanovanadite is triclinic and strongly pleochroic in black and red. From the unit cell dimensions and chemical formula, the specific gravity of montroseite is calculated to be 4.15. The only specimen suitable for measurement of specific gravity, from the Rex No. 2 Mine, Emery County, Utah, gave 4.0. Montroseite can be separated or concentrated from the minerals with which it occurs by the use of methylene iodide and by the Frantz isodynamic separator because it is heavy and more magnetic than the associated minerals.

Goniometric measurements made on several crystals were inaccurate because of poor reflections, small faces, and multiple growth of crystals. They only served to determine the forms present, and the angle table (Table 1) has been computed from the unit cell lengths found by x-ray diffraction. The bladed crystals (Fig. 3) consist chiefly of the brachypinacoid and a steep brachydome, both with rough surfaces. The ρ angle of p{121} could be determined better by finding a small circle including some reflection from the four small faces than by measuring each face

TABLE 1. ANGLES OF MONTROSEITE CRYSTAL

Orthorhombic; dipyramidal, $2/m\ 2/m\ 2/m$
$a:b:c=0.509:1:0.310$ $p_0:q_0:r_0=0.608:0.310:1$
$q_1:r_1:p_1=0.509:1.645:1$ $r_2:p_2:q_2=3.226:1.961:1$

Forms	ϕ	$\rho=$C	ϕ_1	$\rho_1=$A	ϕ_2	$\rho_2=$B
b 010	0°00′	90°00′	90°00′	90°00′	—	0°00′
m 110	62°59′	90°00′	90°00′	27°01′	0°00′	62°59′
p 121	44°26′	40°58′	31°48′	62°41′	58°42′	62°05′
Uncertain form						
d 0, 10, 1	0:00′	72°07′	72°07′	90°00′	90°00′	17°53′

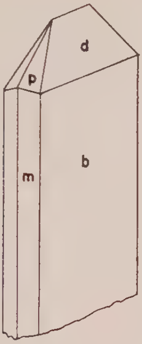

FIG. 3. Drawing of montroseite crystal.

individually, and the angle thus found was between 40° 31′ and 41°, in good agreement with the calculated angle.

X-RAY DIFFRACTION DATA

The x-ray powder pattern distinguishes montroseite from the other black vanadium minerals: melanovanadite, corvusite, and vanoxite (considered a doubtful species by the writers). Morphologic study indicated that montroseite belongs to the orthorhombic system, and this was borne out by x-ray study. Rotation and Weissenberg photographs taken around the c and a axes were poor and did not give sharp reflections, but the extinctions indicated the space group to be *Pbnm* (D_{2h}^{16}). From approximate measurements on the Weissenberg photographs the powder pattern was indexed (Table 2); the unit cell lengths were recalculated from measurements on the powder pattern. The unit cell lengths, $a_0=4.82$, $b_0=9.48$, and $c_0=2.93$, obtained in this way agree more closely with the diffuse lattices than with the sharp lattice of Evans and Block (1953). This is probably because the sample used for the powder pattern was considerably altered to VO_2, whereas the single crystals contained a well-crystallized portion of the original VO(OH).

CHEMICAL ANALYSES

Montroseite presented a problem in chemical analysis because the vanadium is commonly in two valences and some iron substitutes for vanadium. A portion of the sample was digested in H_2SO_4 in the absence of air and was titrated with $K_2Cr_2O_7$. In this titration V_2O_3 is oxidized to V_2O_4, and FeO to Fe_2O_3. A second portion was digested in the same manner and was titrated with $KMnO_4$. In this titration V_2O_3 is oxidized to V_2O_5, V_2O_4 to V_2O_5, and FeO to Fe_2O_3. Total V and Fe were determined on separate portions. The analyses (Table 3) were computed from

TABLE 2. X-RAY DIFFRACTION POWDER PATTERN OF MONTROSEITE. CuKα RADIATION

hkl	*d* (calc) Å	*d* (meas) Å	I
020	4.74	4.75	VF
110	4.30	4.31	S
120	3.38	3.38	M
130	2.643	2.644	S
101	2.507		
021	2.495	2.495	M
111	2.424	2.423	W
121	2.216	2.217	M
220	2.149	2.151	F
131	1.963	1.965	W
230	1.917	1.918	W
041	1.843	1.841	Fb
221	1.734	1.731	W
241	1.690	1.689	W
321	1.605	1.605	W
151	1.512	1.512	M
250	1.491	1.490	W
002	1.467	1.467	W
061	1.391	1.391	W
112	1.388		
170	1.304	1.302	F
132	1.283	1.282	F

these determinations: Total FeO and V_2O_3, total reducing ability of the mineral, total V, and total Fe.

The chemical analyses may be interpreted in the light of information obtained by *x*-ray structure study (Evans and Block, 1953). Ideally the original composition of montroseite was VO(OH), but the substitution of FeO requires an equivalent amount of V_2O_4. In the chemical analyses, the amount of V_2O_4 in excess of that required to balance the FeO represents the oxidation of the original mineral. The amount of water decreases as VO(OH) alters to VO_2. Calculation of the analysis (Table 3, column 3) of the sample from the Matchless mine, indicates about 35 per cent of $[(Fe^{+2}\cdot V^{+4}),V^{+3}]O(OH)$ and about 65 per cent of VO_2.

None of the montroseite samples could be separated completely from the associated minerals, chiefly because montroseite occurs in such fine-grained mixtures. The sample (Table 3, column 2) from the Bitter Creek mine (120 mg.) was a loose aggregate of crystals and probably the purest of the three analyzed samples. The sample from the Matchless mine (Table 3, column 3) contained microscopic grains of montroseite between quartz grains and is only about 90 per cent pure. The sample (about 12 g)

Table 3. Chemical Analyses of Montroseite (in per cent)

Analyst: A. M. Sherwood, U. S. Geological Survey

	1	2	3	4
V_2O_3	89.29	10.5	11.10	
V_2O_4		72.5	66.90	69.35
V_2O_5				0.48
FeO		8.8	8.26	
Fe_2O_3				10.33
H_2O	10.71	5.0	4.82	10.60
SiO_2			6.12	3.56
Al_2O_3			3.00	1.87
UO_3				2.60
MgO				0.56
CaO				0.24
S				0.09
Total	100.0	96.8	100.20	99.68

1. HVO_2 or $V_2O_3 \cdot H_2O$.
2. Partial analysis on a 120-mg sample from Bitter Creek mine.
3. Matchless mine.
4. Whitney mine.

from the Whitney mine (Table 3, column 4) is not more than 85 per cent pure and contains clay, possibly corvusite and a new black uranium mineral, and a little pyrite.

Paragenesis

Montroseite is the least oxidized vanadium mineral thus far found in the Colorado Plateaus uranium-vanadium ores and it is thought to be a primary mineral. It occurs with or in the same environment as pitchblende and a new black uranium mineral not yet described, as well as with pyrite, galena, and other sulfides. In the zone of oxidation it is altered to corvusite, melanovanadite, and the quinquevalent vanadium minerals hewettite, pascoite, and hummerite.

References

Evans, H. T., and Block, S. (1953), The crystal structure of montroseite, a new vanadium member of the diaspore group: *Am. Mineral.*, **38,** 1242–1250.

Fischer, R. P., and Hilpert, L. S. (1952), Geology of the Uravan mineral belt: *U. S. Geol. Survey Bull.* **988-A,** 13 pp.

Weeks, A. D., Cisney, E. A., and Sherwood, A. M. (1950), Hummerite and montroseite, two new vanadium minerals from Montrose County, Colorado: *Geol. Soc. America Bull.*, **61,** 1513 (abstract).

THE CRYSTAL STRUCTURE OF MONTROSEITE, A VANADIUM MEMBER OF THE DIASPORE GROUP*

Howard T. Evans, Jr., and Stanley Block
U. S. Geological Survey, Washington, D. C.

Abstract

An x-ray study of single crystals of montroseite, (V, Fe)O(OH), shows that the mineral has a structure analogous to that of diaspore, AlO(OH). Cell constants are given as: orthorhombic, space group $Pbnm$ (D_{2h}^{16}); $a=4.54$, $b=9.97$, $c=3.03$ Å; cell contents, four formula units. Atomic positions are given with interatomic distances, obtained as a result of a complete structure analysis by Fourier methods. Details of structure are compared with those of other members of the series.

Introduction

Among the many new vanadium minerals discovered during the past five years in the uranium-vanadium ore fields of the Colorado Plateaus is the black crystalline species named montroseite, described by Weeks, Cisney, and Sherwood (1953). It is the first distinct vanadium oxide mineral that has been reported, but current studies show that it is one of a series of structurally related oxides and hydroxides of vanadium in various valence states.

The x-ray patterns of montroseite are multiple, indicating the presence of two or more closely related phases. Rotation photographs show a short spacing of 3.0 Å along the prism axis. Weissenberg and precession photographs exhibit a strong sharp orthorhombic lattice and two weaker diffuse lattices in parallel position, of the same approximate dimensions and symmetry but with minor variations in spacings and intensities. These features suggest that the original montroseite phase corresponding to the sharp lattice has undergone alteration to other phases in which the basic structural framework is not changed. In this paper is described the complete refinement of the structure corresponding to the sharp lattice.

This work is part of a program undertaken by the U. S. Geological Survey on behalf of the Division of Research of the Atomic Energy Commission.

X-ray Crystallography

As described in the previous paper by Weeks, Cisney, and Sherwood, the crystals are jet-black laths up to 0.5 mm. in length flattened normal to the a axis and elongated parallel to the c axis. There is a strong, almost fibrous cleavage parallel to (010) and (110), making it difficult to trim the crystals to suitable dimensions for x-ray study. The sharp spots are somewhat streaked, indicating a twisting of the crystal around [001] of as much as 10°. The diffuse spots are rather strongly developed, and close examination shows that there are two sets of them. The dimensions of the various lattices are given with an accuracy of about ±0.5 per cent in Table 1.

---

* Publication authorized by the Director, U. S. Geological Survey.

TABLE 1. LATTICE DIMENSIONS FOR MONTROSEITE AND RELATED DIASPORE-TYPE STRUCTURES

Species	Composition	a_0 (Å)	b_0 (Å)	c_0 (Å)	V (Å^3)
Montroseite	(V, Fe) O(OH)	4.54	9.97	3.03	136.9
Diffuse A	?	4.80	9.63	2.9_3	135.4
Diffuse B	VO_2	4.89	9.39	2.9_3	134.4
Diaspore[1]	AlO(OH)	4.40	9.39	2.84	129.9
Goethite[1]	FeO(OH)	4.64	10.0	3.03	140.6
Groutite[2]	MnO(OH)	4.58	10.76	2.89	142.5
Ramsdellite[3]	MnO_2	4.53	9.27	2.87	120.5

[1] Hoppe (1941).

[2] Collin and Lipscomb (1949).

[3] Byström (1949).

The extinctions, as shown by Weissenberg and precession photographs, are consistent with the space group *Pbnm* (D_{2h}^{16}), assuming the presence of a center of symmetry (and planes of symmetry normal to the c axis) analogous to other diaspore-type structures. Dimensions of these analogous structures are also given in Table 1.

CRYSTAL STRUCTURE ANALYSIS

Chemical analysis of montroseite did not indicate the chemical nature

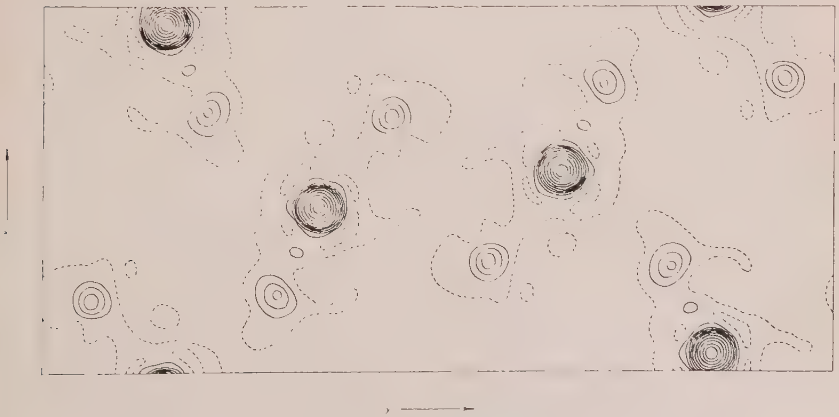

FIG. 1. Electron density projection along [001] of montroseite.

TABLE 2. OBSERVED AND CALCULATED STRUCTURE FACTORS FOR MONTROSEITE

hkl	F_{obs}	F_{calc}	*hkl*	F_{obs}	F_{calc}
020	18.2	−19.5	2.13.0	6.1	− 8.4
040	40.7	−46.0	2.14.0	16.8	18.8
060	31.1	36.6	2.15.0	13.1	13.5
080	4.9	5.6	2.16.0	10.4	−10.3
0.10.0	26.4	−34.8	2.17.0		6.1
0.12.0	9.2	−10.7	2.18.0	11.2	− 9.6
0.14.0	27.6	23.6	2.19.0		−10.5
0.16.0		− 4.3	2.20.0		3.6
0.18.0	12.1	−13.6			
0.20.0	14.1	18.7	310	10.6	3.8
			320	40.6	37.0
110	54.1	57.3	330	36.2	−22.0
120	32.7	22.2	340	4.9	− 5.3
130	51.9	−60.3	350		−10.8
140	50.3	−44.6	360	19.8	−24.4
150	13.5	− 3.5	370	19.4	30.2
160	9.2	−11.9	380	25.5	28.7
170	40.7	38.3	390		− 1.8
180		1.9	3.10.0	7.1	8.0
190	11.4	−14.7	3.11.0	8.4	−10.9
1.10.0		2.6	3.12.0	21.5	−25.2
1.10.0	27.0	−26.7	3.13.0		15.7
1.12.0		− 1.0	3.14.0		3.7
1.13.0	17.0	16.8	3.15.0		1.5
1.14.0		1.3	3.16.0	11.0	9.5
1.15.0	11.0	11.1	3.17.0	14.1	− 9.7
1.16.0	11.4	13.2	3.18.0		− 8.3
1.17.0	16.7	−17.0	3.19.0		− 2.6
1.18.0		− 2.3			
1.19.0		1.7	400	16.4	17.0
1.20.0		− 4.2	410	38.0	25.2
1.21.0	13.3	14.0	420		− 3.7
			430	16.4	25.3
200	18.8	17.7	440	7.8	− 8.0
210	13.9	35.7	450	22.5	−26.0
220	10.8	−11.7	460	7.2	7.1
230	12.1	− 0.4	470	8.8	3.9
240	50.7	−42.8	480		1.4
250	37.0	−37.1	490	21.4	32.8
260	23.3	23.8	4.10.0		− 6.6
270	5.7	1.5	4.11.0	10.4	−19.0
280	24.7	28.2	4.12.0		− 2.6
290	19.8	15.2	4.13.0	21.5	−15.6
2.10.0	20.2	−25.5	4.14.0		5.2
2.11.0	8.4	− 5.9	4.15.0		12.4
2.12.0		5.0	4.16.0		− 0.8

Table 2—(*continued*)

hkl	F_{obs}	F_{calc}	*hkl*	F_{obs}	F_{calc}
4.17.0		−2.5	750		−1.8
4.18.0		−3.7	760	11.6	−12.8
4.19.0	14.3	−10.5	770	12.3	−6.9
			780	10.4	9.8
510		8.5	790		5.8
520	29.6	32.1	7.10.0		3.7
530	10.4	−1.1	7.11.0	10.6	8.9
540	13.3	−15.0	7.12.0		−8.3
550	7.1	6.2			
560	20.2	−20.1	800	20.0	−21.7
570		−8.1	810	9.2	5.6
580	19.6	21.9	820		2.9
590		−3.7	830		7.0
5.10.0	10.0	7.0	840	12.1	10.7
5.11.0		−1.6	850		−6.9
5.12.0	18.2	−20.2	860	10.6	−9.3
5.13.0		−6.6	870		0.3
5.14.0		2.6	880		−1.4
5.15.0		3.9	890		10.6
5.16.0	16.8	13.4	8.10.0	11.4	11.9
600		−6.0	910	9.6	−7.3
610	13.9	23.5	920		3.5
620		3.3	930	14.9	11.5
630	9.6	3.3	940		5.0
640		8.5	950		3.7
650	27.4	−28.2	960		−2.1
660		−5.8	970	5.5	−14.1
670		1.9			
680		−6.6	10.0.0	9.2	5.7
690	21.2	12.7	10.1.0		0.3
6.10.0		5.4	10.2.0		2.9
6.11.0	9.8	−4.8	10.3.0		−0.2
6.12.0		−1.5	10.4.0	11.2	11.9
6.13.0		−8.6	10.5.0		1.2
6.14.0		−5.3	10.6.0	8.2	−7.6
6.15.0	12.3	14.2	10.7.0		0.7
			10.8.0	9.6	−10.4
710	10.2	−8.5			
720	16.5	16.0	11.1.0		−4.4
730	7.8	13.7	11.2.0		−3.6
740	12.1	−13.0	11.3.0	8.8	9.0

of the mineral because some vanadium was replaced by iron. The true nature of the compound was suggested by the size of the unit cell and by the fact that the symmetry of the space group would allow a cell content of only four formula units of the type MO_2. The volume of the unit cell of montroseite is 137 Å^3, which will just accommodate 8 oxygen atoms in close packing (17.1 Å^3 per atom). In the space group *Pbnm* there are only four types of equipoint positions, three fourfold and one eightfold. The oxygen atoms will fit this scheme in several ways, but there can only be one type of vanadium atom in a fourfold position. Thus, the restrictions of unit-cell dimensions and symmetry lead to the empirical formula for montroseite of VO_2 or HVO_2. Reference to the tabulation of MO_2-type structures (Wyckoff, 1948) immediately suggests the comparison of montroseite with the diaspore structure type.

The structure of groutite, MnO(OH), as determined by Collin and Lipscomb (1949), was used as a starting point, and the montroseite structure refined by the usual iterative methods making use of Fourier synthesis and structure factor computations. The final electron density map is shown in Figure 1. The intensities used to determine the amplitudes for this Fourier synthesis were measured by comparing the density of spots on Weissenberg ($hk0$) photographs made with MoKα radiation (films interleaved with nickel foil) against a calibrated strip made from reflections from the same crystal. The values of the structure amplitudes, F, so observed are listed in Table 2, together with those calculated from the final structure. The over-all temperature effect (which modifies the structure factor by the factor e^{-Bs^2}) as determined by a plot of log (F_{obs}/F_{calc}) against $s^2=(\sin\theta)^2/\lambda^2$ was found to have $B=0.4$ Å^2, thus indicating a rather strongly bound structure. The agreement between calculated and observed structure amplitudes is expressed in the usual manner in terms of R, the reliability factor:

$$R=\frac{\sum\left||F_{obs}|-|F_{calc}|\right|}{\sum|F_{obs}|},$$

where $\sum|F_{obs}|$ is set equal to $\sum|F_{calc}|$. For the final structure, $R=0.21$ for 99 observed (non-zero) reflections. Absorption effects have been neglected.

The data for the final structure are shown in Table 3, where the parameters are given in fractions of the cell edge. This table also gives the data for diaspore and goethite as determined by Hoppe (1941, 1942), for groutite after Collin and Lipscomb (1949), and for ramsdellite after Byström (1949).

TABLE 3. PARAMETERS FOR MONTROSEITE AND OTHER DIASPORE-TYPE STRUCTURES

	M		O_I		O_{II}		R
	x	y	x	y	x	y	
Montroseite	−0.051	0.145	0.297	−0.197	−0.197	−0.051	0.213
Diaspore	−0.048	0.146	0.287	−0.199	−0.198	−0.056	0.114
Goethite	−0.045	0.146	0.31	−0.2	−0.20	−0.047	
Groutite	−0.036	0.140	0.27	−0.20	−0.21	−0.05	
Ramsdellite	0.022	0.136	0.167	−0.25	−0.211	−0.033	

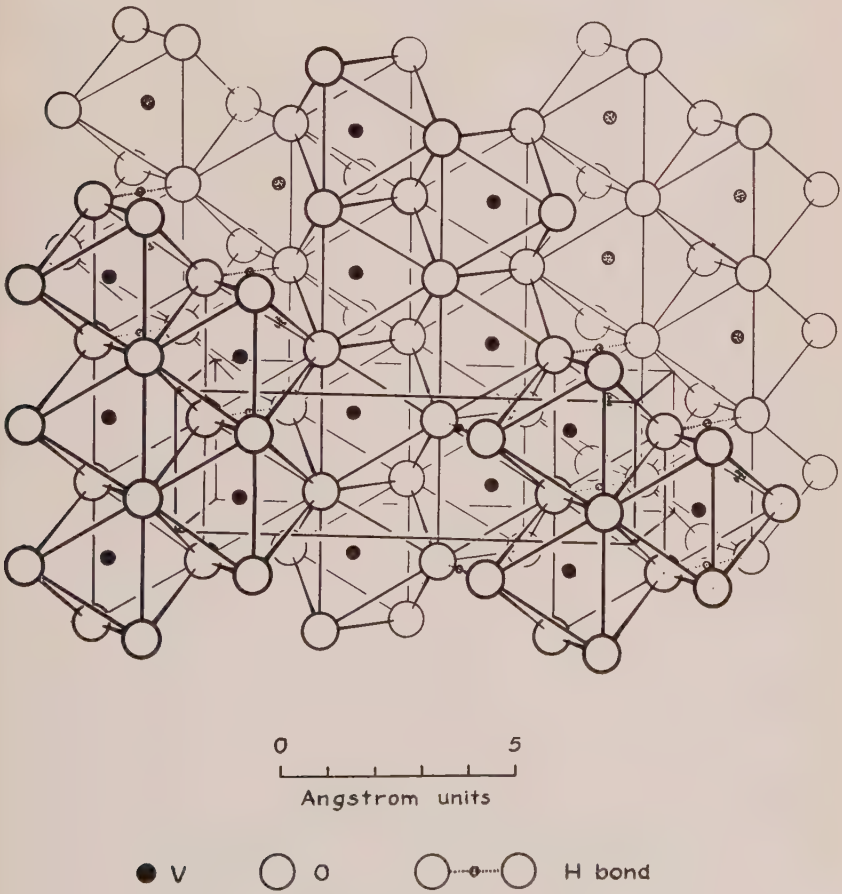

FIG. 2. Pictorial view of crystal structure of montroseite.

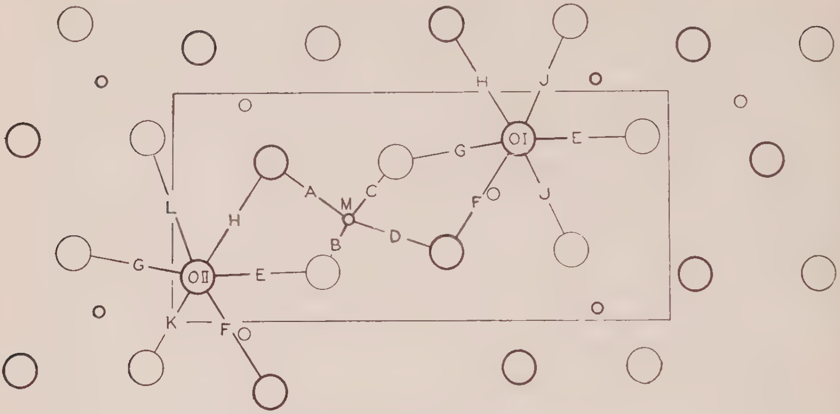

FIG. 3. Interatomic distances in montroseite.

FEATURES OF THE STRUCTURE

The well-known diaspore structure type, shown in a pictorial view in Figure 2, has been much discussed in standard works on crystal chemistry as an important example of a close-packed type of oxide structure (Pauling, 1940; Wells, 1950). A study of bond lengths reveals two outstanding characteristic features: (1) distortions in the octahedral coordination arising from edge-sharing in the chain and (2) the presence of hydrogen bonds between chains. All nearest neighbor interatomic distances, as shown in Figure 3, have been calculated for all structures except those of groutite and ramsdellite, for which accurate data are not yet available. These distances are given in Table 4. Distortion in the chain, expected as a result of the coulombic repulsion of the metal ions, is strongly evident from the short bonds from vanadium to exterior oxygen atoms (1.95 Å, A and B for montroseite) as compared with the longer bonds to interior oxygen atoms (average 2.13 Å, C and D). This effect is accompanied by a contraction to 2.55 Å of the O_{II} O_{II} distance K, which is shared between octahedra. There seems to be a further dimensional compensation within the octahedron in the O_{I}-O_{II} distance F (2.68 Å). Other oxygen-oxygen distances are close to the normal van der Waals diameter, averaging 2.97 Å. These distances for goethite are also very consistent, averaging 2.97 Å, but in diaspore the average is reduced to 2.78 Å, indicating a higher degree of polarization of the oxygen atoms in the aluminum compound. The one remaining exception is the O_{I}-O_{II} distance H (2.72 Å) between chains, and this is the logical place to find the hydrogen atom. The distance is close to that found for most hydrogen bonds (Wells, 1950, p. 238). If the hydrogen atom could be located in this

TABLE 4. INTERATOMIC DISTANCES IN DIASPORE-TYPE STRUCTURES

(Lengths in Å, ±0.03)

Atoms	Vector	Montroseite	Diaspore	Goethite
$M-O_I$	A	1.95	1.84	1.89
	B(2)	1.95	1.86	2.02
$M-O_{II}$	C(2)	2.11	2.03	2.12
	D	2.16	1.99	2.05
O_I-O_{II}	E(2)	2.93	2.76	2.95
	F	2.67	2.62	2.85
	G(2)	2.94	2.78	2.94
	H	2.72	2.60	2.67
O_I-O_I	J(4)	2.93	2.80	2.94
	c-axis (2)	3.03	2.84	3.03
$O_{II}-O_{II}$	K(2)	2.55	2.48	2.56
	L(2)	3.30	3.19	3.31
M–M		3.30	3.12	3.54

structure, it would probably be found on a straight line joining O_I and O_{II}, approaching O_{II} more closely to compensate for the longer $V-O_{II}$ and shorter $V-O_I$ bonds.

CHEMICAL CONSTITUTION OF MONTROSEITE

The montroseite crystals studied in this investigation contained 8.8 per cent FeO (see Weeks, Cisney, and Sherwood, 1953), with iron to vanadium mol-ratio approximately 1:7. The oxidation potentials of Fe^{+2} and V^{+3} are such that the existence of ferric iron in the montroseite structure is unlikely. We may assume instead that Fe^{2+} replaces V^{+3} and that one V^{+4} ion is present for each Fe^{+2} ion.

It was stated earlier that crystals of montroseite give multiple *x*-ray patterns (see Table 1). The relative intensity of the lattices varies widely, but the diffuse B lattice seems to predominate. It is believed that it corresponds to an oxidized phase of composition VO_2. This explanation is consistent with the observations of Weeks, Cisney, and Sherwood that: (1) chemical analysis of montroseite shows a large excess of VO_2 and (2) powder patterns can be indexed on an orthorhombic lattice whose dimensions correspond most nearly with the diffuse B lattice as presented in this paper. Further work on the crystal structure and origin of the diffuse phases is in progress, and the results will be published later.

REFERENCES

BYSTRÖM, A. M. (1949), The crystal structure of ramsdellite, an orthorhombic modification of MnO_2: *Acta Chem. Scand.*, **3**, 163–173.

Collin, R. L., and Lipscomb, W. N. (1949), The crystal structure of groutite: *Acta Cryst.*, **2**, 104–106.

Goldschmidt, V. M. (1926), Crystal structures of the rutile type with remarks on the geochemistry of bivalent and quadrivalent elements: *Norske Vidensk.-akad. Oslo, Skr. I, Mat.-Natur. Kl.* **1926,** no. 1.

Hoppe, W. (1941), Über die Kristallstruktur von α-AlO(OH) (Diaspor) und α-FeO(OH) (Nadeleisenerz): *Zeitschr. Kristallographie* **103,** 73–89.

Hoppe, W. (1942), Über die Kristallstruktur von α-AlO(OH) (Diaspor) II. Fourier Analyse: *Zeitschr. Kristallographie* **104,** 11–17.

International Tables for *X*-ray Crystallography (1952), International Union of Crystallography, Birmingham, England, Kynoch Press.

Pauling, L. (1940), Nature of the chemical bond, Ithaca, N. Y., Cornell University Press.

Weeks, A. D., Cisney, E., and Sherwood, A. M. (1953), Montroseite, a new vanadium oxide from the Colorado Plateaus: *Am. Mineral.*, **38,** 1235–1241.

Wells, A. F. (1950), Structural inorganic chemistry, 2d ed., London, Oxford University Press.

Wyckoff, R. W. G. (1948), Crystal structures, vol. 1, New York, Interscience Publishers, Inc.

SOME THERMODYNAMIC RELATIONS AMONG THE VANADIUM OXIDES, AND THEIR RELATION TO THE OXIDATION STATE OF THE URANIUM ORES OF THE COLORADO PLATEAUS*

Robert M. Garrels, *U. S. Geological Survey, Washington, D. C.*

Abstract

Fields of stability of several vanadium oxides in water solution at 25° C. have been calculated as functions of pH and oxidation potential. The bivalent oxide V_2O_2 is not expected under natural conditions; it should occur only at oxidation potentials below the breakdown potential of water. The oxide corresponding to the mineral montroseite, $V_2O_3 \cdot H_2O$ or VOOH, is predicted to coexist with common metal sulfides and to oxidize to V_2O_4 at about the same potential at which sulfide ion oxidizes to sulfate. Owing to difficulties entailed by the complex chemistry of vanadium, V^{+5}, no attempt was made to calculate a boundary between V_2O_4 and a higher oxide. Diagrams showing the fields of stability of the various oxides have been constructed, and contours showing the activities of the various vanadium ions have been superimposed. The stability fields of the vanadium oxides should be useful in deducing the environment of formation of the carnotite ores and the "blue-black" ores of the Colorado Plateaus.

Introduction

For many years the chief ore minerals from the uranium-vanadium deposits in the Morrison formation of the Colorado Plateaus have been carnotite and a hydrous vanadium silicate. During the past few years another kind of ore has been found in increasing quantities. It is commonly known as "blue-black" ore. The uranium-bearing mineral is probably uraninite or other quadrivalent uranium oxide; vanadium occurs in a variety of compounds, among them the vanadium (III) oxide, montroseite (Weeks *et al.*, 1953).

In general blue-black ore occurs farther from the surface than carnotite ore; it is typically associated with pyrite-bearing light-colored sandstone, whereas carnotite ore is associated with brown-spotted limonitic sandstone. The implication has been drawn by many workers that the ores are essentially equivalent chemically, but that the carnotite ores reflect an oxidizing environment, whereas the blue-black ores formed under reducing conditions.

The present incomplete data on the mineralogy of the ores support this view. Carnotite ore contains V^{+5} compounds, such as carnotite itself, tyuyamunite, hewettite, hummerite, pascoite, rauvite, and many others; Fe^{+++} oxides; U^{+6} compounds; and S^{+6} and Fe^{+++} compounds. The valence state of the vanadium in the hydrous silicate has not been established. Blue-black ore contains V^{+++}, V^{+4}, and V^{+5} compounds, probably largely as oxides; Fe^{++} and S_2^- in pyrite. The valence state of the uranium is probably +4.

---

* Publication authorized by the Director, U. S. Geological Survey.

In anticipation of further mineralogic and geologic work on this problem it seemed worthwhile to summarize present theoretical chemical data on the stability in water solutions of various lower-valence vanadium oxides. Even though the stability fields can be determined only at 25° C. and at atmospheric pressure, they may be useful as general guides to the behavior of the various compounds.

It is shown, for example, in the following, that montroseite ($V_2O_3 \cdot H_2O$) is not stable under ordinary weathering conditions and that V_2O_2 should not be formed at all in ordinary ground water.

PROBABLE MECHANISM OF PRECIPITATION OF VANADIUM OXIDES

Vanadium oxides probably can be precipitated from water solution according to the following reactions:

$$V^{++} + 2OH^- = V(OH)_2 \qquad (1)$$

$$2V(OH)_2 = V_2O_2 + 2H_2O \qquad (2)$$

$$V^{+++} + 3OH^- = V(OH)_3 \qquad (3)$$

$$2V(OH)_3 = V_2O_3 + 3H_2O \qquad (4)$$

$$VO^{++} + 2OH^- = VO(OH)_2 \qquad (5)$$

$$2VO(OH)_2 = V_2O_4 + 2H_2O \qquad (6)$$

If the free energies of the various reactions are known, equilibrium constants for the ionization of the hydroxides (reactions 1, 3, 5) can be calculated. From these equilibria the maximum activity of V^{++}, V^{+++}, and VO^{++} can be calculated at a stipulated pH. If an oxidation potential (Eh) of the system is also stipulated, the equilibrium ratios of these three ions can be calculated. Therefore, it is possible to designate fields of stability of each of the oxides and to calculate the equilibrium activities of vanadium ions ($a_{V^{++}} + a_{V^{+++}} + a_{VO^{++}} + a_{V(OH)_4^+}$) as functions of pH and Eh.

TABLE 1. SOME FREE ENERGIES OF FORMATION

Species	Free Energy of Formation (kilocalories per mol)
V_2O_2	−189
V_2O_3	−271
V_2O_4	−318
H_2O	− 56.7
$V^{++}aq$	− 54.7
$V^{+++}aq$	− 60.6
$VO^{++}aq$	−109
OH^-aq	− 37.6

FREE ENERGY OF FORMATION OF IONS AND COMPOUNDS INVOLVED IN PRECIPITATION OF VANADIUM OXIDES

The free energy changes of reactions 1 through 6 have not been determined, but they can be calculated if the free energy of formation of the chemical species involved are known. Available data are listed in Table 1 (Latimer, 1952).

FREE ENERGY CHANGE FOR FORMATION OF HYDROXIDES FROM CONSTITUENT IONS

The free energy change of reactions 2, 4, and 6 cannot be computed directly because the free energy of formation of the hydroxides is not known (Table 1). However, the free energy change in the reaction from hydrate or hydroxide to oxide plus water is very small in other cases where data are available. For the reactions from $Pb(OH)_2$ to PbO and H_2O, for $Cu(OH)_2$ to $CuO+H_2O$, and $Ni(OH)_2$ to $NiO+H_2O$, the free energy changes are all less than 2 kcal. Similar values are not available for hydroxides of trivalent metals, but for the reactions $Al_2O_3 \cdot H_2O$ to Al_2O_3 and H_2O and for $Al_2O_3 \cdot 3H_2O$ to Al_2O_3 and $3H_2O$, the same rule holds. Therefore the free energy of formation of the various vanadium hydroxides is equal to the sum of the free energies of formation of oxides plus the necessary water, with a probable uncertainty of about 2 kcal.

At 25° C.:

$$V_2O_2 + 2H_2O = 2V(OH)_2 \qquad (2)$$

$$F^\circ_{V_2O_2} + 2F^\circ_{H_2O} = 2F^\circ_{V(OH)_2}$$

$$-189 + (-113) = 2F^\circ_{V(OH)_2}$$

$$F^\circ_{V(OH)_2} = -151 \text{ kcal}$$

$$V_2O_3 + 3H_2O = 2V(OH)_3 \qquad (4)$$

$$F^\circ_{V_2O_3} + 3F^\circ_{H_2O} = 2F^\circ_{V(OH)3}$$

$$-271 + (-170) = 2F^\circ_{V(OH)_3}$$

$$F^\circ_{V(OH)_3} = -221 \text{ kcal}$$

$$V_2O_4 + 2H_2O = 2VO(OH)_2 \qquad (6)$$

$$F^\circ_{V_2O_4} + 2F^\circ_{H_2O} = 2F^\circ_{VO(OH)_2}$$

$$-318 + (-113) = 2F^\circ_{VO(OH)_2}$$

$$F^\circ_{VO(OH)_2} = -216 \text{ kcal}$$

From these values of the free energy of formation of the hydroxides, and the values for formation of the ions in Table 1, the free energy change for the ionization of the hydroxides in water can be determined:

$$V(OH)_2 = V^{++} + 2OH^- \qquad (1)$$

$$\Delta F^\circ = F^\circ_{V^{++}} + 2F^\circ_{OH^-} - F^\circ_{V(OH)_2}$$

$$\Delta F^\circ = -54.7 + (-75.2) - (-151) = +21 \text{ kcal} \pm 2 \text{ kcal}$$

$$V(OH)_3 = V^{+++} + 3OH^- \tag{3}$$

$$\Delta F^\circ = F^\circ_{V+++} + 3F^\circ_{OH^-} - F^\circ_{V(OH)_3}$$

$$\Delta F^\circ = -60.6 + (-113) - (-221) = +47 \text{ kcal} \pm 2 \text{ kcal}$$

$$VO(OH)_2 \rightarrow VO^{++} + 2OH^- \tag{5}$$

$$\Delta F^\circ = F^\circ_{VO++} + 2F^\circ_{OH^-} - F^\circ_{VO(OH)_2}$$

$$\Delta F^\circ = -109 + (-75.2) - (-216) = +32 \text{ kcal} \pm 2 \text{ kcal}$$

IONIZATION CONSTANTS FOR VANADIUM HYDROXIDES

The free energy change for the ionization of the hydroxides is related to the ionization constant K by the equation:

$$\Delta F^\circ = -RT \ln K.$$

At 25° C, RT ln K can be replaced by 1.364 log K when ΔF° is given in kcal.

For equation 1:

$$V(OH)_2 = V^{++} + 2OH^-$$

$$K_{V(OH)_2} = \frac{a_{V++}a^2_{OH^-}}{a_{V(OH)_2}}$$

Because the activity of the precipitated $V(OH)_2$ is unity:

$$\Delta F^\circ = -1.364 \log a_{V++}a^2_{OH^-}$$

$$21 = -1.364 \log a_{V++}a^2_{OH^-}$$

$$K_{V(OH)_2} = a_{V++}a^2_{OH^-} = 10^{-15.4} \tag{7}$$

For equation 3:

$$\Delta F^\circ = -1.364 \log a_{V+++}a^3_{OH^-}$$

$$47 = -1.364 \log a_{V+++}a^3_{OH^-}$$

$$K_{V(OH)_3} = a_{V+++}a^3_{OH^-} = 10^{-34.4} \tag{8}$$

For equation 5:

$$\Delta F^\circ = -1.364 \log a_{VO++}a^2_{OH^-}$$

$$32 = -1.364 \log a_{VO++}a^2_{OH^-}$$

$$K_{VO(OH)_2} = a_{VO++}a^2_{OH^-} = 10^{-23.5} \tag{9}$$

OXIDATION POTENTIAL RELATIONS AMONG THE VANADIUM IONS

The oxidation potential (Eh) of a system can be measured by obtaining the electromotive force generated by the system relative to the standard hydrogen electrode. This can be done by using a circuit containing a hydrogen electrode and an inert electrode, usually platinum. The reaction involved can be described as follows:

$$2H^+ + \text{reduced system} \rightarrow H_2 + \text{oxidized system}.$$

From the standard electrochemical equation for galvanic cells:

$$E = E^\circ - \frac{RT}{nF} \ln \frac{a_{H_2} \text{ (oxidized system)}}{a^2_{H+} \text{ (reduced system)}}.$$

Where E is the measured emf, E° is the emf at unit activity of all constituents, R the gas constant, T the absolute temperature, n*F* the number of Faradays of electricity involved in the reaction. At 25° C,

$$\frac{\mathrm{RT}}{F}\log\cdots = 0.059\log\cdots$$

Because the activity of H_2 and H^+ are unity by definition of the standard hydrogen electrode, the equation reduces to:

$$\mathrm{E} = \mathrm{E}^\circ - \frac{\mathrm{RT}}{\mathrm{n}F}\ln\frac{(\text{oxidized system})}{(\text{reduced system})}$$

By convention, $\mathrm{Eh} = -\mathrm{E}$, so that:

$$\mathrm{Eh} = -\mathrm{E}^\circ + \frac{\mathrm{RT}}{\mathrm{n}F}\ln\frac{(\text{oxidized system})}{(\text{reduced system})}$$

E° is not known for complex natural systems, but if each chemical reaction in the system is in equilibrium with the system as a whole,

$$\mathrm{Eh} = -\mathrm{E}^\circ + \frac{\mathrm{RT}}{\mathrm{n}F}\ln Q$$

Where Q is the product of the activities (or fugacities) of the resulting substances, divided by the product of the activities of the reacting substances, each activity raised to that power whose exponent is the coefficient of the substance in the chemical equation.

For the vanadium ions, the various reactions involved are (Latimer, 1952):

$$\begin{array}{rcll}
\mathrm{V}^\circ & = & \mathrm{V}^{++} + 2\mathrm{e} & \mathrm{E}^\circ = 1.18 \\
\mathrm{V}^{++} & = & \mathrm{V}^{+++} + \mathrm{e} & \mathrm{E}^\circ = 0.255 \\
\mathrm{V}^{+++} + \mathrm{H_2O} & = & \mathrm{VO}^{++} + 2\mathrm{H}^+ + \mathrm{e} & \mathrm{E}^\circ = -0.361 \\
\mathrm{VO}^{++} + 3\mathrm{H_2O} & = & \mathrm{V(OH)_4}^+ + 2\mathrm{H}^+ + \mathrm{e} & \mathrm{E}^\circ = -1.00.
\end{array}$$

The corresponding Eh equations are:

$$\mathrm{Eh} = -1.18 + \frac{0.059}{2}\log\frac{a_{\mathrm{V}^{++}}}{a_{\mathrm{V}^0}} \tag{10}$$

$$\mathrm{Eh} = -0.255 + 0.059\log\frac{a_{\mathrm{V}^{+++}}}{a_{\mathrm{V}^{++}}} \tag{11}$$

$$\mathrm{Eh} = +0.361 + 0.059\log\frac{a_{\mathrm{VO}^{++}}a^2_{\mathrm{H}^+}}{a_{\mathrm{V}^{+++}}} \tag{12}$$

$$\mathrm{Eh} = +1.00 + 0.059\log\frac{a_{\mathrm{V(OH)}^{+}_{4}}a^2_{\mathrm{H}^+}}{a_{\mathrm{VO}^{++}}} \tag{13}$$

Thus the great value of Eh measurements stems from their application to the determination of ionic ratios for all pairs present for which E° values are known; the great danger in using Eh values is in the assumption that the individual reactions are in equilibrium with the system as a whole.

VANADIUM ION ACTIVITIES AS FUNCTIONS OF Eh AND pH

If the Eh and pH ($-\log a_{H^+}$) of an environment are stipulated, the ratios of the various vanadium ions are fixed. Designation of a pH value also fixes the OH^- activity as $a_{H^+}a_{OH^-} = K_{H_2O}$. Knowledge of OH^- activity in turn fixes the activity of V^{++} in equilibrium with $V(OH)_2$, V^{+++} in equilibrium with $V(OH)_3$, and VO^{++} in equilibrium with $VO(OH)_2$ (equations 7, 8, 9).

Consequently if a pair of pH and Eh values are chosen arbitrarily, the concentration of each vanadium ion in equilibrium with its hydroxide can be calculated, and the stable hydroxide also can be determined. For example, on a qualitative basis, V^{++} would be expected to be the predominant species at low Eh values, and $V(OH)_2$ the stable hydroxide. This prediction can be checked quantitatively at a given pair of pH and Eh values by calculating $a_{V^{++}}$ in equilibrium with $V(OH)_2$, then calculating $a_{V^{+++}}$ and $a_{VO^{++}}$ from the Eh equations (11 and 12), and finally testing if these activities are too small to be in equilibrium with either $V(OH)_3$ or $VO(OH)_2$. Calculations of this type show that it is possible to delineate fields of stability of the three vanadium hydroxides of interest here.

A sample calculation may suffice to illustrate the method used.* At the arbitrary values pH 5 and Eh+0.20, the activities of vanadium ion in equilibrium with the hydroxides are:

$$\text{A. } a_{VO^{++}}a^2_{OH^-} = K_{VO(OH)_2} = 10^{-23.5} \qquad (9)$$

$$a_{VO^{++}} = \frac{10^{-23.5}}{(10^{-9})^2} = 10^{-5.5}$$

$$\text{B. } a_{V^{+++}}a^3_{OH^-} = K_{V(OH)_3} = 10^{-34.4} \qquad (8)$$

$$a_{V^{+++}} = \frac{10^{-34.4}}{10^{-27.0}} = 10^{-7.4}$$

$$\text{C. } a_{V^{++}}a^2_{OH^-} = K_{V(OH)_2} = 10^{-15.4} \qquad (7)$$

$$a_{V^{++}} = \frac{10^{-15.4}}{10^{-18.0}} = 10^{2.6}$$

Both $a_{VO^{++}}$ and $a_{V^{+++}}$ are small relative to $a_{V^{++}}$, so it seems likely that either $VO(OH)_2$ or $V(OH)_3$ is the stable hydroxide under the conditions given. Assuming that $VO(OH)_2$ is the stable form, then:

$$Eh = 0.361 + 0.059 \log \frac{a_{VO^{++}}a^2_{H^+}}{a_{V^{+++}}} \qquad (12)$$

$$0.20 = 0.361 + 0.059 \log \frac{10^{-5.5} \times 10^{-10}}{a_{V^{+++}}}$$

$$a_{V^{+++}} = 10^{-12.8}$$

---

* For examples of similar calculations see Krumbein and Garrels (1952), and Delahay, Roe, and Rysselberghe (1950).

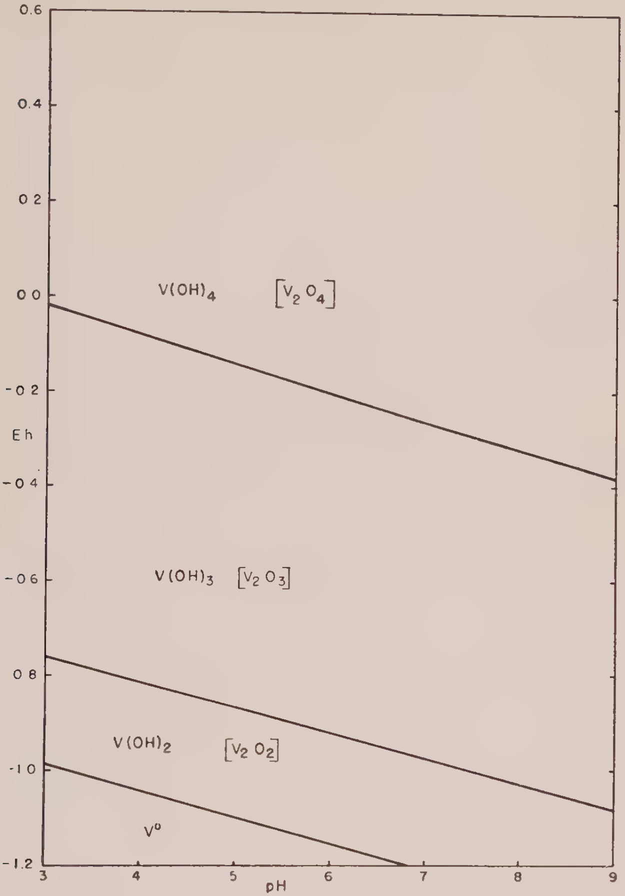

FIG. 1. Stability fields of vanadium hydroxides as functions of Eh and pH.

This result shows that, at Eh 0.2 and pH 5, $VO(OH)_2$ is, as assumed, the stable hydroxide, because the activity of V^{+++} in solution under the assumed condition ($10^{-12.8}$) is far less than that required for equilibrium with $V(OH)_3$($10^{-7.4}$).

The results of a series of such calculations are shown in Figure 1. The position of the boundaries was determined quickly and easily by using the condition that at a boundary both activity products must be satisfied. Therefore at a given pH the ratio of the vanadium ion activities in equilibrium with the two stable solids is fixed. From this known ratio the Eh was determined from the appropriate equation (11 or 12).

Figures 2, 3, 4, and 5 show contours of the activities of V^{++}, V^{+++}, VO^{++}, and $V(OH)^{+}_{4}$, respectively, in relation to the stability fields of the

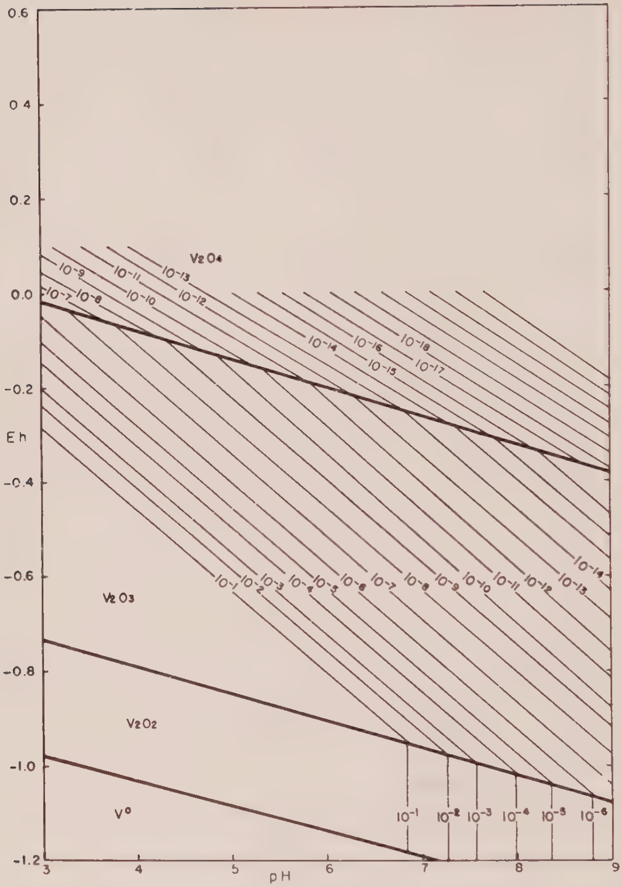

FIG. 2. V^{++} ion activity in equilibrium with various vanadium oxides.

various hydroxides. The calculated values fit the expected general relation that VO^{++} is the most abundant ion in solutions of higher Eh, V^{+++} at intermediate Eh, and V^{++} at lower Eh.

These values represent maximum activities of the various ions in equilibrium with the solid hydroxides at 25° C and at atmospheric pressure, and the values are essentially independent of the composition of the system. The values are, of course, accurate only within the limitations of knowledge of E° and of K values.

Relation of Vanadium Ion Activities and Vanadium Solubility

Although it is possible to calculate vanadium ion activities with reasonable confidence in the order of magnitude of the results, it is very difficult

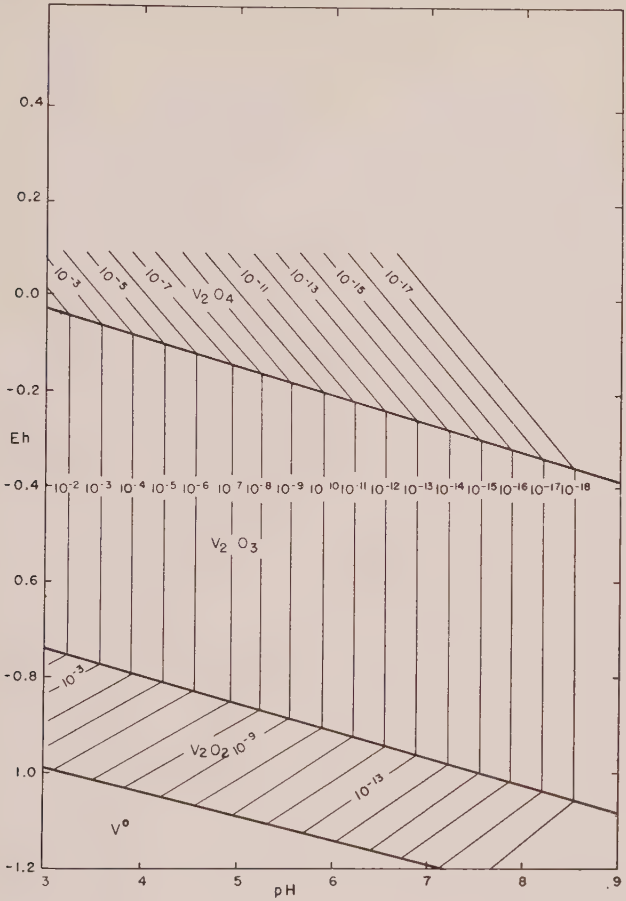

FIG. 3. V^{+++} ion activity in equilibrium with various vanadium oxides.

to relate the values obtained to the stoichiometric solubility. The solubility of vanadium in equilibrium with the hydroxides is equal to the sum of the molalities of all species in solution and can be represented as the sum of the known plus the unknown species:

$$\text{Solubility}_V = \sum m_{V^{++}} + m_{V^{+++}} + m_{VO^{++}} + m_{V(OH)_4^+} + m_{X_1} + m_{X_2} + m_{X_3} \cdots .$$

The activities of V^{++}, V^{+++}, VO^{++}, and $V(OH)_4^+$ are related to the molalities as follows:

$$a_{V^{++}} = \gamma_{V^{++}} m_{V^{++}}$$

$$a_{V^{+++}} = \gamma_{V^{+++}} m_{V^{+++}}$$

$$a_{VO^{++}} = \gamma_{VO^{++}} m_{VO^{++}}$$

$$a_{V(OH)_4^+} = \gamma_{V(OH)_4^+} m_{V(OH)_4^+}$$

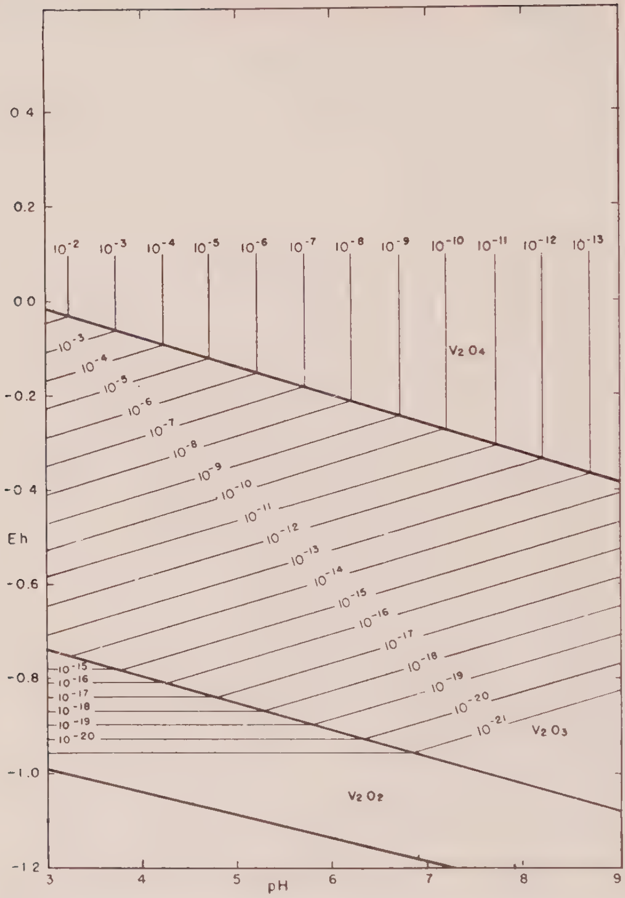

FIG. 4. VO^{++} ion activity in equilibrium with various vanadium oxides.

Therefore $a_i \cong m_i$ only under conditions where $\gamma_i \cong 1$. γ_i is a function of the ionic strength, usually decreasing with increasing ionic strength up to values of ionic strength of 0.1 or 0.2, and then increasing again to unity or more at values of ionic strength of about 1.0. Values of γ_i may drop as low as 0.01 or 0.02 in the range of ionic strength between 0.1 and 1.0. Consequently, because activity usually approximates molality only in very dilute solutions or at specific values of the ionic strength of about 1.0, the error introduced by assuming $a_i = m_i$ is usually an underestimation of the actual value, and the corrective factor may be as large as 100-fold.

The presence of ionic complexes increases solubility; in the vanadium system involved, there is no indication in the literature of the presence

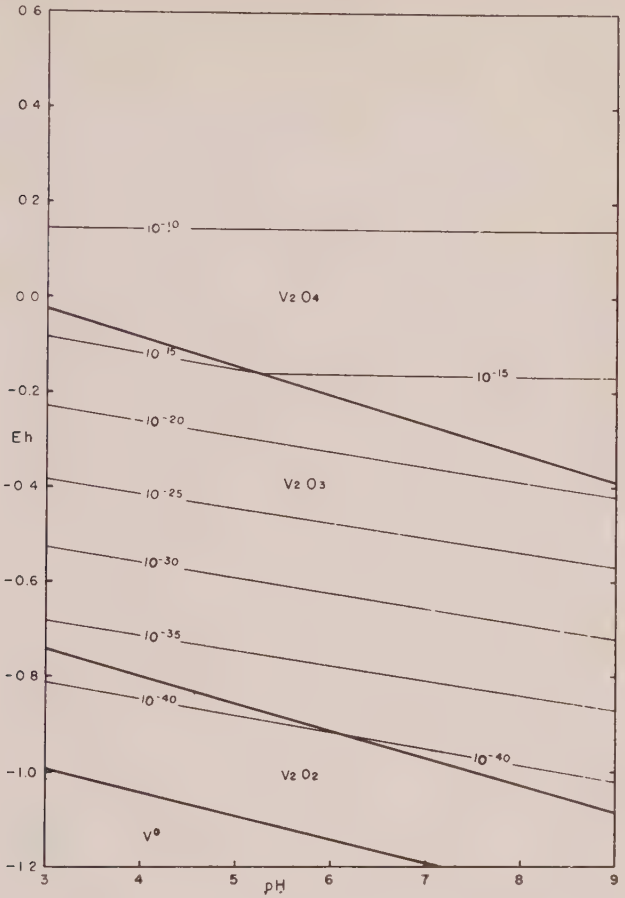

Fig. 5. $V(OH)_4^+$ ion activity in equilibrium with various vanadium oxides.

of soluble complexes with low dissociation constants for the 2-, 3-, and 4-valent ions, at least in solutions containing the typical inorganic ions present in natural waters. Vanadium, V^{+5}, on the other hand, is notorious for the complexity and number of the ions it forms. To a large extent it was this complex behavior of vanadium, V^{+5}, that led to the restriction of this study to the region in which the lower-valent ions are the vastly predominant species. A second consideration is the uncertainty of the reaction mechanism for the precipitation of V_2O_5 in nature.

Figure 6 shows contours of $\sum a_{V^{++}} + a_{V^{+++}} + a_{VO^{++}} + a_{V(OH)_4^+}$ superimposed on the stability fields of the various hydroxides. It can be used as a solubility diagram only for solutions of very low ionic strength with no other ionic species containing vanadium present.

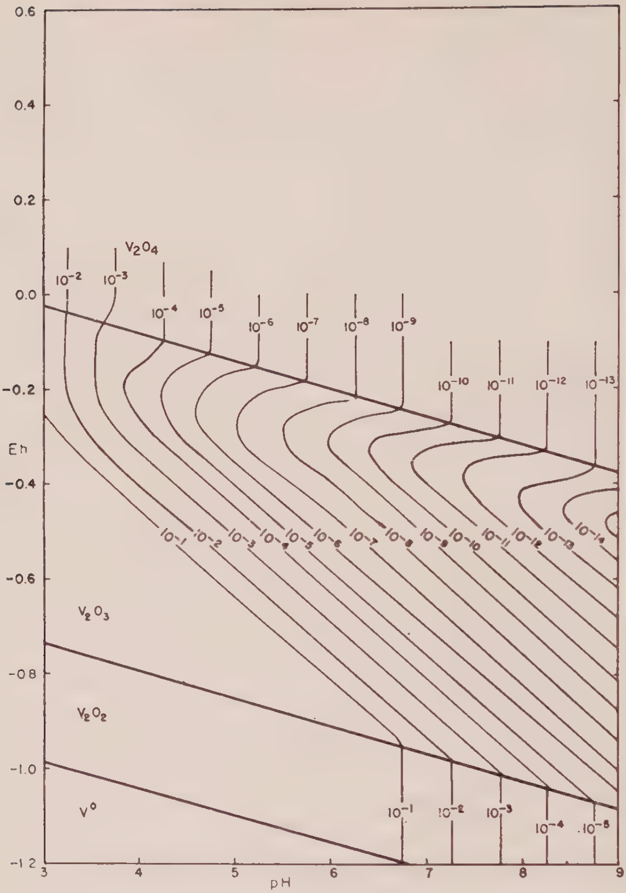

FIG. 6. Equilibrium fields of some vanadium oxides in water. Contours are for activities of vanadium ions in solution $\sum a_{V^{++}} + a_{V^{+++}} + a_{VO^{++}} + a_{V(OH)_4^{+}}$.

In spite of the restrictions imposed on using such diagrams as guides to solubility, it should be reemphasized that phase boundaries are independent of solution composition and are functions only of temperature and pressure. This means, for example, that in spite of the unknown compositional factors in the geologic environment of deposition of these vanadium compounds, there is no escaping the fact that equilibrium conditions for formation of $VO(OH)_2$ and $V(OH)_2$ are mutually exclusive.

Another relation should be emphasized. It is probable that, with various compositional variations, parts of the fields of stability of the compounds shown would be replaced by those of other compounds. This can occur, however, only if the ionic activity in equilibrium with these new compounds is less than that in equilibrium with those shown. Therefore the diagrams show the approximate activity of vanadium ions in equilibrium with the oxides considered and the maximum activity in any other reasonably dilute aqueous system from which other vanadium compounds are formed at equilibrium.

GEOLOGIC IMPLICATIONS

Natural Limits of pH and Eh

Mason (1952, pp. 142–147) points out that the upper and lower limits of Eh for natural waters are determined by the potentials at which oxygen and hydrogen are liberated at atmospheric pressure by decomposition of the waters. The release of oxygen occurs at Eh values well above any shown in this paper; that of hydrogen, however, is well within the range considered, and actually removes the field of stability of $V(OH)_2$ from

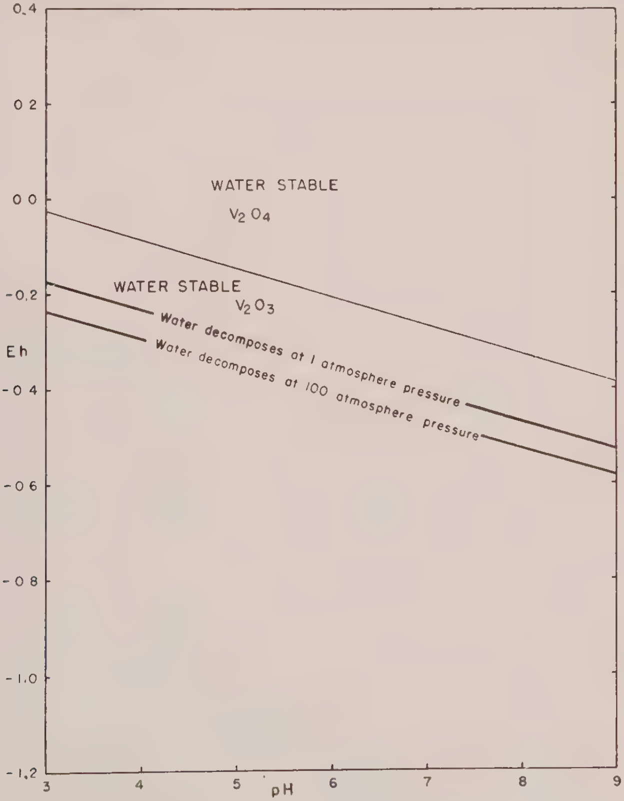

FIG. 7. Conditions for decomposition of water at 1 atmosphere and 100 atmospheres pressure.

the system. Mason points out that equilibrium is not always attained, and somewhat lower than theoretical Eh values may be achieved experimentally without releasing appreciable H_2 from water. Latimer (1952, p. 43) indicates that Eh values a full half volt lower than theoretical may be necessary to release hydrogen. Figure 7 shows the equilibrium values for decomposition of water at 1 atmosphere and at 100 atmospheres pressure at 25° C.

The natural pH range (Mason, 1952) is from 0 to 10 or somewhat higher. The low values usually are achieved under weathering conditions where sulfides are being oxidized to sulfates, with consequent production of hydrogen ion, or in the waters of some volcanic areas, where the source of the H^+ is less well known. Most ground waters range in pH from 4 to 8.

Unfortunately relatively few Eh measurements have been made of natural waters, as opposed to the copious pH data, but surface waters in equilibrium with oxygen under the partial pressure of the atmosphere commonly give empirical Eh values of $+0.1$ to $+0.3$. Eh values of deoxygenated ground waters in the zone of rock-pore saturation ordinarily range from zero to slightly minus values. In the presence of abundant carbonaceous material values as low as -0.5 have been measured. Mason (1952, p. 145) suggests that hydrogen actually may be released from water under such conditions.

Relation of Vanadium Oxide Stability Fields to Natural Conditions

In terms of the range of natural conditions, the theoretical fields of the vanadium oxides show that V_2O_3 (or its hydrate) is the lowest-valent vanadium oxide expected. It should occur under reducing conditions common in nature. It would be expected to oxidize to the next higher-valent vanadium oxide at about the same potential necessary to convert sulfide ion to sulfate. To put this relation in another way, V_2O_3 would be expected to coexist in equilibrium with various metal sulfides, such as pyrite or galena, and to oxidize at about the same potential.

It seems that V_2O_4 would be a transitory phase in most natural situations. The general tendency in nature is to produce either moderate to strong reducing conditions or moderate to strong oxidizing conditions. For example, V_2O_3 below the water table would probably remain indefinitely, but if raised above to a place where moist air or aerated water had free access to it, it would eventually oxidize all the way up to a 5-valent species. Surface conditions would thus ordinarily produce vanadates from V_2O_3. Little is known about the rate of the reaction, but oxidation probably is slow, and many mixed 3–4 valent and 4–5 valent vanadium oxides might have "half-lives" measured in months or years.

Unlike the reaction from sulfide to sulfate, which is essentially irreversible in natural inorganic systems at low temperature, the reaction $V^{+++} \leftrightarrows V^{4+} \leftrightarrows V^{5+}$ apparently goes either way at a finite rate under appropriate conditions.

CONCLUSION

These theoretical equilibrium relations among the vanadium oxides fit well into the concept that the carnotite ore and the blue-black ore are equivalent chemical expressions of differences in oxidation potential of their environment of formation. Whether the blue-black ores represent pre-vanadate stages of oxidation of an original montroseite-pyrite-pitchblende type of ore, or a reduced form of an original carnotite ore, or whether the two types were introduced simultaneously into different environments must be deduced from detailed geologic, mineralogic, and geochemical studies of the field relations. Even at this stage of knowledge, however, there is a surprising correlation between theoretical and observed associations. There seems to be a good possibility that laboratory studies of oxidation and reduction of natural and synthetic materials will be helpful in solving the problem.

ACKNOWLEDGMENTS

The criticisms, discussions, and suggestions of C. L. Christ, H. T. Evans, F. S. Grimaldi, C. R. Naeser, and L. R. Stieff, all of the U. S. Geological Survey, are deeply appreciated.

REFERENCES

DELAHAY, P., ROE, P. J., AND RYSSELBERGHE, P. (1950), Potential-pH diagrams: *Jour. Chem. Education* **27,** 683–688.

KRUMBEIN, W. C., AND GARRELS, R. M. (1952), Origin and classification of chemical sediments in terms of pH and oxidation-reduction potentials: *Jour. Geol.*, **60,** 1–33.

LATIMER, W. M. (1952), Oxidation potentials, 2d ed., New York, Prentice-Hall.

MASON, BRIAN (1952), Principles of geochemistry, New York, John Wiley & Sons.

WEEKS, A. D., CISNEY, E. A., AND SHERWOOD, A. M. (1953), Montroseite, a new vanadium oxide from the Colorado Plateaus: *Am. Mineral.*, **38,** 1235–1241.

OCCURRENCE OF BASSANITE IN TWO DESERT BASINS IN SOUTHEASTERN CALIFORNIA*

Robert D. Allen, and Henry Kramer, *U. S. Geological Survey, Claremont, Calif.*

Introduction

Bassanite, calcium sulfate hemihydrate, has been identified in drill cores from two desert lake basins, about 175 miles apart, in southeastern California. This finding is significant because the only other reported natural occurrences of bassanite known to the writers are at Mt. Vesuvius, Italy, and in the central Asiatic desert. Palache, Berman and Frondel (1951) describe the Mt. Vesuvius occurrence as follows: "Found in cavities of leucite-tephrite blocks thrown out during the April, 1906, eruption of Vesuvius. Also found with gibbsite in fumaroles of the eruption of 1911." Middle Asiatic bassanite deposits (Popov and Vorob'ev, 1947) are found in the desert soils of eastern Turkmenia and northern and western Fergana. The mineral occurs as a white powder, a weathering product sometimes pseudomorphic after gypsum. In southern Fergana the hemihydrate occurs as thin layers in oil-bearing sands.

The California localities are (1) Danby Lake (dry) (lat. 34° 24′ N., long. 115° 17′ W.) at depths of 365 feet and 510 feet; (2) dry lake near Ballarat, Panamint Valley (lat. 36° 02′ N., long. 117° 14′ W.) at a depth of 360 feet.

In both localities the mineral is found in unconsolidated sediments as layers, none more than a few millimeters thick, intercalated with layers of silty clay. Gypsum is associated with the bassanite (1) as crystals included in the clay layers, (2) as light brownish granular layers adjacent to the bassanite, and (3) as a fine crystalline constituent within bassanite laminae. The bassanite is snow white and long fibrous in habit; the fibers, which are distinguishable under a hand lens, are arranged in parallel or slightly divergent bundles. Bassanite fiber axes are nearly parallel to the bedding in Danby samples, but they are oriented at a large angle to the bedding in the Panamint Valley specimen.

The Danby sample from a depth of 510 feet (2½-inch core, Drill Hole No. 1) was pure enough for chemical and spectrographic studies although the quantity available was insufficient for exhaustive analysis. The optical properties tabulated apply to all three samples.

Optical Data

Indices of refraction, determined with sodium light, were as follows; α

---

* Publication authorized by the Director, U. S. Geological Survey.

(perpendicular to fiber direction)—1.550±0.002; γ (parallel to fiber direction)—1.577±0.002. The acicular crystals have parallel extinction, positive elongation, and positive optical character. The mineral is uniaxial or biaxial with small optic axial angle. Winchell (1931) states that $2CaSO_4 \cdot H_2O$ is probably hexagonal; he gives the following optical data: uniaxial positive with $\omega = 1.55$ or slightly less, $\epsilon = 1.57$. Büssem and Gallitelli (1937) conclude that the substance is pseudohexagonal and monoclinic; optical properties are as follows: biaxial positive, $2E = 22°$, $\beta = 1.558 - 1.560$, $\gamma = 1.582 - 1.584$. Popov and Vorob'ev (1947) found indices of refraction 1.556 and 1.583, respectively.

ANALYTICAL DATA

CHEMICAL ANALYSIS OF BASSANITE ($2CaSO_4 \cdot H_2O$), IN PER CENT

	Bassanite from Danby Lake (dry) California	Theoretical
CaO	37.75	38.63
SO_3	54.19	55.16
H_2O	6.37	6.21
Total	98.31	100.00

Spectrographic analysis of the bassanite from Danby Lake (dry) gave the following data, in per cent:

0.X	Sr Mg Na Si
0.0X	Al Fe
0.00X	Mn B Ag
0.000X	Cu

CALCULATED MINERALOGIC ANALYSIS

Petrographic examination shows that the bassanite is contaminated with gypsum, celestite, and clay. The proportions of minerals in the sample have been calculated on the basis of the following assumptions: (1) bassanite is $2CaSO_4 \cdot H_2O$; (2) excess water (in the above analysis) is derived from gypsum; (3) excess SO_3 is derived from celestite. The calculated weight percentages of minerals are: bassanite 97.3 per cent, celestite 1.5 per cent, gypsum 0.8 per cent, clay undetermined, total 99.6 plus per cent.

NATURAL ORIGIN OF THE BASSANITE

Association of bassanite with gypsiferous beds suggests that the hemihydrate was derived from the dihydrate,* either naturally or artifically.

---

* It is not considered likely that bassanite arises from partial hydration of anhydrite, $\beta - CaSO_4$. The hemihydrate is structurally more like $\gamma - CaSO_4$, "soluble anhydrite".

It was at first thought that the material had been produced from gypsum by heat or pressure accompanying core drilling. This is improbable because:

(1) Bassanite is not found in a peripheral zone about the outside of the core, where frictional heat would be greatest. It occurs as horizontal laminae in both internal and external portions of core.

(2) The hemihydrate is not found in core segments from other gypsiferous beds.

(3) The transformation of gypsum to bassanite occurs at 98° C. (Ramsdell and Partridge, 1929; Posnjak, 1938). A liquid-lubricated drill in unconsolidated material probably would not generate a temperature of this magnitude.

(4) The aqueous drill fluid would tend to convert bassanite to gypsum rather than promote the reverse reaction (Milton, 1942).

ACKNOWLEDGMENTS

The material described was collected at the drill sites at Danby Lake (dry) by Fred C. Barstow and at the dry lake near Ballarat in Panamint Valley by George I. Smith, both of the U. S. Geological Survey. Microscopic and x-ray verifications were done by Waldemar T. Schaller and Fred A. Hildebrand, respectively, also of the Survey. The spectrographic analysis was supplied by Hal W. Johnson, Pacific Spectrochemical Laboratory, Los Angeles, California.

REFERENCES

BÜSSEM, W. AND GALLITELLI, P. (1937), Zur Struktur des Calciumsulfat-Halbhydrats $CaSO_4 \cdot \frac{1}{2}H_2O$: *Zeits. Krist.*, **96**, 376–380.

MILTON, C. (1942), Note on the occurrence of calcium sulphate hemihydrate ($CaSO_4 \cdot \frac{1}{2}H_2O$) in thin sections of rocks: *Am. Mineral.*, **27**, 517–518.

PALACHE, C., BERMAN, H. AND FRONDEL C. (1951), Dana's System of Mineralogy, 7th ed., vol. 2, pp. 476, 484, New York.

POPOV, V. I. AND VOROB'EV, A. L. (1947), Zapiski Vserossii. Mineral. Obshchestva (*Mém. soc. russe minéral.*) [2]**76**, 268–270. (*Chem. Abs.* **43**, 2897h, 1949.)

POSNJAK, E. (1938), The system $CaSO_4-H_2O$: *Amer. Jour. Sci.*, **35**A, 247–272.

RAMSDELL, L. S. AND PARTRIDGE, E. P. (1929), The crystal forms of calcium sulphate: *Am. Mineral.*, **14**, 59–73.

WINCHELL, A. N. (1931), Microscopic Characters of Artificial Minerals, 2d. ed., p. 226, New York.

A SIMPLE HIGH-TEMPERATURE MICROSCOPE HEATING STAGE*

Donald H. Richter and Joseph F. Abell, *U. S. Geological Survey, Washington, D. C.*

In the course of geothermometric investigations in the Geochemistry and Petrology Laboratory of the U. S. Geological Survey, a microscope-mounted heating stage capable of producing moderate to high operating temperatures has been constructed. The heating stage, designed primarily for the study of fluid inclusions by the visual or Sorby method, is equally applicable for studies of melting point, phase transition, and other studies that require microscope mounted heating chambers.

The stage (Figs. 1 and 2) is built almost entirely of Marinite, a light heat-insulating material, composed of a mixture of diatomaceous earth and asbestos that can be fabricated with hand or machine tools. The only metal used in the construction, other than legs, bolts, and heating element, is a thin circular plate that gives added strength to the upper assembly of the stage. The upper assembly, which contains the heating chamber, is held above the lower support block by three metal legs. This lower block rests on the microscope stage and is held in place by a circular projection that fits the opening provided for the microscope's removable ring plate. The heating element consists of two flat coils of No. 20 nichrome wire, spaced approximately $\frac{3}{16}$ in. apart in the top and bottom of the heating chamber. Total length of resistance wire used is 12 in. The heating chamber, $\frac{3}{4}$ in. inside diameter by $\frac{1}{4}$ in. deep, has a sloping edge along part of its periphery to facilitate placing the specimen. A cover of the same insulating material, grooved for a thin silica-glass or mica window and lined with aluminum foil, fits snugly over the upper assembly. The window in the cover is kept as small as the microscope objective permits.

The temperature in the cell is controlled by a variable transformer with an input of 6.3 volts supplied by a small stepdown transformer off a 110-volt circuit. At 500° C., the upper limit of the stage for prolonged studies, the power consumption is 20 watts. For short periods temperatures as high as 700° C. may be attained by removing the stepdown transformer. Such high temperatures, however, will decrease the life of the heating element and discolor the enclosing material.

The specimen to be studied, usually a small polished mineral plate, is placed between the coils of the heating element, either on a thin quartz plate, which rests directly on the lower coil, or on a wire support. The

---

* Publication authorized by the Director, U. S. Geological Survey.

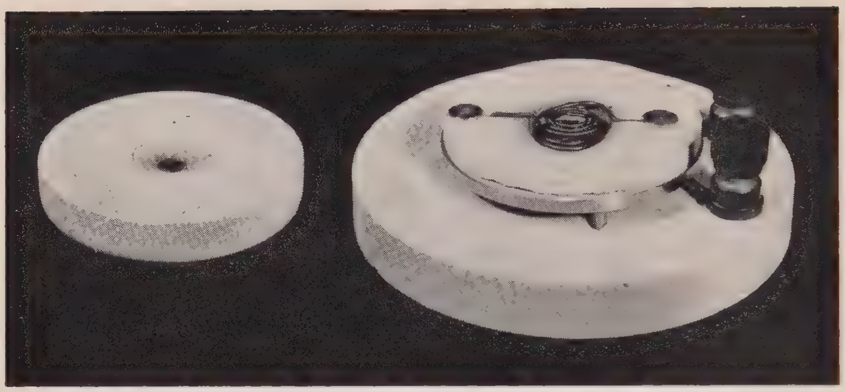

FIG. 1. High-temperature microscope heating stage with cover removed. One half actual size.

specimen is centered with the cover removed before heating has started. Temperatures are measured by a chromel-alumel thermocouple connected to a potentiometer. The thermocouple, which has a thin flat tip, is inserted through a small hole in the side of the chamber and for accurate measurement should make contact with the top or bottom of the mineral plate. For low magnification an ordinary microscope objective is satisfactory; for higher magnification objectives with larger working distances such as those adapted for use with the universal stage, should be used.

For efficient operation and wide application over large temperature ranges the basic requirements of a heating stage are: (1) uniformity of temperature within the heating chamber, (2) minimum conduction and transmission of heat from the chamber, and (3) simple but sturdy construction.

Use of the instrument described here has shown that these requirements have been adequately fulfilled. Convection effects in the chamber are practically negligible at low to moderate temperatures. At 600° C. a temperature variation of only ±10° C. could be detected within the entire heating chamber. The relatively small but all-important region occupied by the mineral plate, however, has at most a variation of 1 or 2° C. The excellent insulating properties of Marinite (conductivity at 800° F. = 0.82 Btu/hr. ft. °F.; and low heat transmission) and the unconventional manner of placing the heating element in the heating chamber minimize radiant-heat problems.

We wish to express our thanks to Clarence S. Ross and David M. Lee, of the U. S. Geological Survey, for their contributions toward the design of this heating stage.

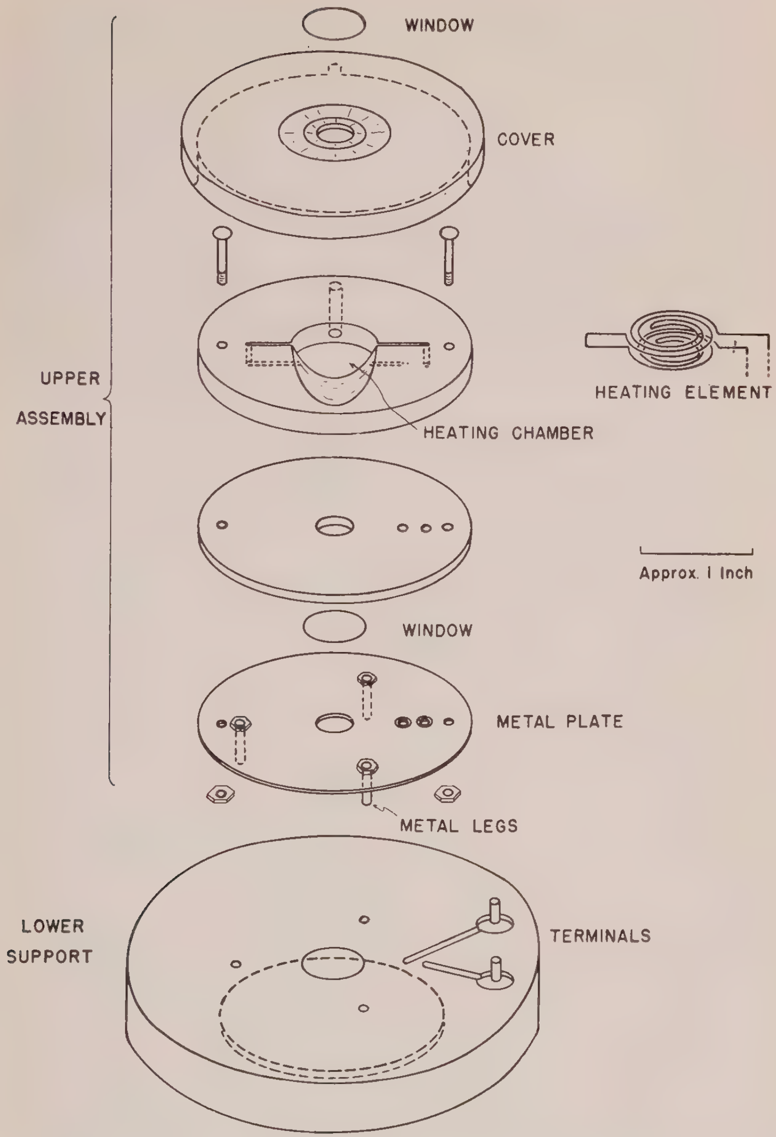

FIG. 2. Exploded isometric diagram of the high-temperature microscope heating stage. Hidden lines are shown only where necessary.

BIBLIOGRAPHY OF CLARENCE SAMUEL ROSS*

(through 1953)

Compiled by Marjorie Hooker, *U. S. Geological Survey, Washington, D. C.*

(with T. E. Savage). The age of the iron ore in eastern Wisconsin: *Am. Jour. Sci.*, (4), **41,** 187–193, illus., (1916).

The "chloritic" material in the ores of southeastern Missouri: *Econ. Geol.*, **11,** 289–290, (1916); abs., *Ill. Acad. Sci. Tr.*, **9,** 209, (1917).

(with E. S. Larsen. Jr.). The R and S molybdenum mine, Taos County, New Mexico: *Econ. Geol.*, **15,** 567–573, (1920).

(with H. D. Miser). Diamond-bearing peridotite in Pike County, Arkansas: *Econ. Geol.*, **17,** 662–674, illus., (1922).

The Lacasa area, Ranger district, north-central Texas: *U. S. Geol. Survey Bull.* **726,** 303–314, illus., (1922).

A method of distinguishing fused cores: *Am. Assoc. Petr. Geol. Bull.*, **6,** 372–374, (1922).

Structure and oil and gas resources of the Osage Reservation, Oklahoma; Tps. 20 and 21 N., R. 12 E.: *U. S. Geol. Survey Bull.* **686,** 171–178, illus., (1922).

Structure and oil and gas resources of the Osage Reservation, Oklahoma; Tps. 21 and 22 N., R. 11 E.: *U. S. Geol. Survey Bull.* **686,** 179–191, illus., (1922).

(with C. F. Bowen and others). Structure and oil and gas resources of the Osage Reservation, Oklahoma; Tps. 21–23 N., Rs. 6–7 E., and Tps. 23–25 N., Rs. 3–5 E.: *U. S. Geol. Survey Bull.* **686,** 279–301, illus., (1922).

(with H. D. Miser). Diamond-bearing peridotite in Pike County, Arkansas: *U. S. Geol. Survey Bull.* **735,** 279–322, illus., (1923).

(with H. D. Miser). Peridotite dikes in Scott County, Arkansas: *U. S. Geol. Survey Bull.* **735,** 271–278, illus., (1923).

Evidences of slumping previous to consolidation in the Pennsylvanian of Oklahoma: *Am. Assoc. Petr. Geol. Bull.*, **8,** 505–510, illus., (1924).

A method of preparing thin sections of friable rocks: *Am. Jour. Sci.*, (5), **7,** 483–485, (1924).

Beds of volcanic material as key horizons: *Am. Assoc. Petr. Geol. Bull.*, **9,** 341–343, (1925).

(and E. V. Shannon). Bentonite and montmorillonite [abs.]: *Am. Mineral.*, **10,** 64, (1925).

(and E. V. Shannon). The chemical composition and optical properties of beidellite: *Washington Acad. Sci. Jour.*, **15,** 467–468, (1925).

Leverrierite and related minerals, *in* Base exchange in ground water by silicates as illustrated in Montana: *U. S. Geol. Survey Water-Supply Paper* **520,** 60–61, (1925).

(and E. V. Shannon). Mordenite and associated minerals from near Challis, Custer County, Idaho: *U. S. Natl. Mus. Proc.*, **64,** art. 19, 19 p., illus., (1925).

(and E. V. Shannon). Nature of bentonite and related clays [abs.]: *Pan-Am. Geol.*, **43,** 364–365, (1925).

(with H. D. Miser). Pre Cambrian rhyolite discovered in well in northwestern Arkansas: *Am. Assoc. Petr. Geol. Bull.*, **9,** 1115, (1925).

(and E. V. Shannon). The so called genthite from Webster, North Carolina: *Am. Mineral.*, **10,** 444–445, (1925).

(and E. P. Henderson). Topaz and associated minerals from the Einstein silver mine, Madison County, Missouri: *Am. Mineral.*, **10,** 441–443, (1925).

(with H. D. Miser). Volcanic rocks in the Upper Cretaceous of southwestern Arkansas and southeastern Oklahoma: *Am. Jour. Sci.*, (5), **9,** 113–126, (1925).

---

* Publication authorized by the Director, U. S. Geological Survey.

A Colorado lamprophyr of the verite type: *Am. Jour. Sci.*, (5), **12,** 217–229, (1926).

Methods of preparation of sedimentary materials for study: *Econ. Geol.*, **21,** 454–468, illus., (1926).

(and E. V. Shannon). The minerals of bentonite and related clays and their physical properties: *Am. Cer. Soc. Jour.*, **9,** 77–96, illus., (1926).

Nephelite-hauynite alnoite from Winnett, Montana: *Am. Jour. Sci.*, (5), **11,** 218–227, (1926).

(and E. V. Shannon). Nickeliferous vermiculite and serpentine from Webster, North Carolina: *Am. Mineral.*, **11,** 90–93, (1926).

(and E. V. Shannon). The origin, occurrence, composition, and physical properties of the mineral iddingsite: *U. S. Natl. Mus. Proc.*, **67,** art. 7, 19 p., illus., (1926).

The optical properties and chemical composition of glauconite: *U. S. Natl. Mus. Proc.*, **69,** art. 2, 15 p., illus., (1927).

Altered Paleozoic volcanic materials and their recognition: *Am. Assoc. Petr. Geol. Bull.*, **12,** 143–164, illus., (1928).

(and W. F. Foshag). Anauxite, a mineral species, based on material from Bilin, Czechoslovakia: *Am. Mineral.*, **13,** 153–155, (1928).

The mineralogy of clays: *First International Congress of Soil Science, June 13–22, 1927, Washington, D. C., Proc. and Papers, Commission 5*, 555–561, (1928).

(and P. F. Kerr). Optical and *x*-ray research on clay minerals [abs.]: *Am. Mineral.*, **13,** 110, (1928).

(and E. V. Shannon and F. A. Gonyer). The origin of nickel silicates at Webster, North Carolina: *Econ. Geol.*, **23,** 528–552, illus., (1928); abs. with title, The formation of nickel silicates by base exchange, *Am. Mineral.*, **13,** 110, (1928).

Physico-chemical factors controlling magmatic differentiation and vein formation: *Econ. Geol.*, **23,** 864–886, (1928).

Preparation of sedimentary materials for study: *Econ. Geol.* **23,** 334, (1928).

Report on the studies of clays [abs.]: *Washington Acad. Sci. Jour.*, **18,** 265, (1928).

Sedimentary analcite: *Am. Mineral.*, **13,** 195–197, (1928); abs. with title, Sedimentary analcite in Arizona, **13,** 111, (1928).

Bentonitic materials, *in* Geology and ground water of Rosebud County, Montana: *U. S. Geol. Survey Water-Supply Paper* **600,** 18, (1929).

Is chromite always a magmatic segregation product? *Econ. Geol.* **24,** 641–645, (1929).

(and E. V. Shannon). The manganese minerals of a hydrothermal vein near Sparta, North Carolina [abs.]: *Am. Mineral.*, **14,** 106, (1929).

Origin of the magnetite and associated rocks of Cranberry, N. C. [abs.]: *Washington Acad. Sci. Jour.*, **19,** 233–234, (1929).

(and H. D. Miser and L. W. Stephenson). Water-laid volcanic rocks of early Upper Cretaceous age in southwestern Arkansas, southeastern Oklahoma, and northeastern Texas: *U. S. Geol. Survey Prof. Paper* **154,** 175–202, illus., (1929).

(and P. F. Kerr). Dickite, a kaolin mineral: *Am. Mineral.*, **15,** 34–39, (1930).

(and P. F. Kerr). The kaolin minerals: *Am. Cer. Soc. Jour.*, **13,** 151–160, (1930)

(and E. P. Henderson and Eugene Posnjak). Clarkeite; a new uranium mineral: *Am. Mineral.*, **16,** 213–220, illus., (1931); abs., **16,** 114, (1931).

(and P. F. Kerr). The clay minerals and their identity: *Jour. Sed. Petr.*, **1,** 55–65, illus., (1931).

(and P. F. Kerr). The kaolin minerals: *U. S. Geol. Survey Prof. Paper* **165,** 151–176, illus., (1931).

The origin of chromite: *Econ. Geol.*, **26,** 540–545, (1931).

The Valles Mountain volcanic center of New Mexico [abs.]: *Am. Geophys. Union Tr.*, **12th. Ann. Mtg.,** 185–186, (1931).

(and P. F. Kerr). The manganese minerals of a vein near Bald Knob, North Carolina: *Am. Mineral.*, **17,** 1–18, illus., (1932).

Titanium deposits of Roseland district, *in* Northern Virginia, *Guidebook 11*, 29–36, illus., *16th Internatl. Geol. Congress*, (1932).

(and E. P. Henderson). Variations in optical properties and composition in the anthophyllite series [abs.]: *Am. Mineral.*, **17,** 114, (1932).

(and P. F. Kerr). The clay minerals, *in* Symposium on the physical chemistry of the alumina-silica refractories: *Am. Cer. Soc. Jour.*, **16,** 57–58, (1933).

Differentiation as a source of vein and ore-forming materials, *in* Ore deposits of the Western States (Lindgren Volume), p. 128–144, Am. Inst. Min. Met. Eng., New York, (1933).

Introduction to chapter, Physical-chemical factors in the development of a deep-seated type of ore-deposit, *in* Ore deposits of the Western States (Lindgren Volume), p. 56–58, Am. Inst. Min. Met. Eng., New York, (1933).

(with R. C. Wells and J. G. Fairchild). Thorianite from Easton, Pa.: *Am. Jour. Sci.*, (5), **26,** 45–54, (1933).

(and P. F. Kerr). Bentonite and related clays [abs.]: *Geol. Soc. Am. Proc.* **1933,** 380, (1934).

Field evidence about the viscosity of lavas: *Am. Geophys. Union Tr.*, **15th Ann. Mtg., Pt. 1,** 255–257, (1934).

The origin of the rutile deposits of the Amherst-Nelson County district [abs.]: *Va. Acad. Sci. Proc.* **1933–1934,** 54–55, (1934).

The role of volatiles in the formation of Virginia titanium deposits [abs.]: *Am. Geophys. Union Tr.*, **15th Ann. Mtg., Pt. 1,** 245, (1934).

Theory trend as to ore genesis: *Eng. Min. Jour.*, **135,** 15–17, illus., (1934).

Copper deposits in the eastern United States, *in* Copper resources of the world, Volume **1,** p. 151–166, illus., *16th Internatl. Geol. Congress*, (1935).

Genetic relations of sphalerite in pegmatite [abs.]: *Am. Mineral.*, **20,** 203, (1935); *Geol. Soc. Am. Proc.* **1934,** 103, (1935).

Origin of the copper deposits of the Ducktown type in the southern Appalachian region: *U. S. Geol. Survey Prof. Paper* **179,** 165 p., illus., (1935).

(and J. V. Lewis). Sulphide deposits of southwest Virginia [abs.]: *Va. Acad. Sci. Proc.*, **1934–1935,** 62–63, (1935).

(with G. R. Mansfield). Welded rhyolitic tuffs in southeastern Idaho: *Am. Geophys. Union Tr.*, **16th Ann. Mtg., Pt. 1,** 308–321, illus., (1935).

Copper deposits of the southern Appalachian region: *Econ. Geol.*, **31,** 428–432, (1936).

(and P. F. Kerr). Halloysite and allophane: *U. S. Geol. Survey Prof. Paper* **185,** 135–148, illus., (1936).

Mineralization of the Virginia titanium deposits: *Am. Mineral.*, **21,** 143–149, (1936); abs., **21,** 192, (1936).

[Review of] Hot springs of the Yellowstone National Park, by E. T. Allen and A. L. Day: *Econ. Geol.*, **31,** 322–325, (1936).

Sphalerite from a pegmatite near Spruce Pine, North Carolina: *Am. Mineral.*, **22,** 643–650, illus., (1937).

Valles volcano, New Mexico [abs.]: *Washington Acad. Sci. Jour.*, **28,** 417, (1938).

Volcanic activity at Magnet Cove, Arkansas: *Am. Geophys. Union Tr.*, **19th Ann. Mtg., Pt. 1,** 263–264, (1938).

(and L. W. Stephenson). Calcareous shells replaced by beidellite: *Am. Mineral.*, **24,** 393–397, illus., (1939).

(with S. B. Hendricks). Chemical composition and genesis of glauconite and celadonite: *Am. Mineral.*, **26,** 683–708, illus., (1941).

(and S. B. Hendricks). Clay minerals of the montmorillonite group, their mineral and chemical relationships, and the factors controlling base exchange: *Soil Sci. Soc. America Proc.*, **6,** 58–62, (1941).

Occurrence and origin of the titanium deposits of Nelson and Amherst Counties, Virginia: *U. S. Geol. Survey Prof. Paper* **198,** 59 p., illus., (1941).

Origin and geometric form of chalcedony-filled spherulites from Oregon: *Am. Mineral.*, **26,** 727–732, illus., (1941); reprinted in *The Mineralogist*, **10,** 171–174, 192–193, illus., (1942).

Sedimentary analcite: *Am. Mineral.*, **26,** 627–629, illus., (1941).

Extreme hydrothermal alteration in the Buck Creek, North Carolina, dunite body [abs.]: *Am. Mineral.*, **27,** 233, (1942).

Presentation of the Roebling Medal of the Mineralogical Society of America to Esper S. Larsen, Jr.: *Am. Mineral.*, **27,** 155–156, (1942).

The titanium district of Roseland, Virginia, *in* Ore deposits as related to structural features, p. 137, Princeton Univ. Press, Princeton, N. J., (1942).

Clays and soils in relation to geologic processes: *Washington Acad. Sci. Jour.*, **33,** 225–235, (1943).

William Shirley Bayley (1861–1943): *Econ. Geol.*, **38,** 263–264, (1943).

Geologic occurrences of rutile [abs.]: *Econ. Geol.*, **39,** 103, (1944).

Memorial of William Shirley Bayley [1861–1943]: *Am. Mineral.*, **29,** 115–120, portrait, (1944).

Minerals and mineral relationships of the clay minerals: *Am. Cer. Soc. Jour.*, **28,** 173–183, (1945).

(and S. B. Hendricks). Minerals of the montmorillonite group, their origin and relation to soils and clays: *U. S. Geol. Survey Prof. Paper* **205,** 23–79, illus., (1946).

Sauconite, a clay mineral of the montmorillonite group: *Am. Mineral.*, **31,** 411–424, (1946); abs. with title, Sauconite, the zinc clay mineral, *Geol. Soc. Am. Bull.*, **56,** 1193, (1945); *Am. Mineral.*, **31,** 206, (1946).

Acceptance of the Roebling Medal of the Mineralogical Society of America: *Am. Mineral.*, **32,** 166–172, portrait, (1947).

Mineralogy of the ballast sands of Japanese balloons [abs.]: *Geol. Soc. Am. Bull.*, **58,** 1222, (1947); *Am. Mineral.*, **33,** 207, (1948).

Virginia titanium deposits: *Econ. Geol.*, **42,** 194–198, (1947).

Volcanic emanations as keys to ore transport, *in* Report of the Committee on research on ore deposits, *Econ. Geol.*, **42,** 537–539, (1947).

Optical properties of glass from Alamogordo, New Mexico: *Am. Mineral.*, **33,** 360–362, illus., (1948).

Photomicrography by inclined illumination: *Am. Mineral.*, **33,** 363–365, illus., (1948).

[Review of] The petrography and petrology of South African clays, by V. L. Bosazza: *Am. Mineral.*, **33,** 650–651, (1948).

Charles Whitman Cross [1854–1949]: *Washington Acad. Sci. Jour.*, **39,** 347–348, (1949).

The dark-field stereoscopic microscope for mineralogic studies: *Am. Mineral.*, **35,** 906–910, illus., (1950).

[Review of] Colloidal chemistry of the silicate minerals, by C. E. Marshall: *Am. Mineral.*, **36,** 921, (1951).

[Review of] Symposium on mineral resources of the southeastern United States: *Am. Mineral.*, **36,** 517–518, (1951).

Provenience of pyroclastic materials [abs.]: *Geol. Soc. Am. Bull.*, **62,** 1473, (1951).

(and M. D. Foster). Studies of minerals in dunites and in olivine-rich inclusions in basaltic rocks [abs.]: *Geol. Soc. Am. Bull.*, **62,** 1472–1473, (1951); *Am. Mineral.*, **37,** 299, (1952).

BIBLIOGRAPHY OF WALDEMAR THEODORE SCHALLER
(through 1953)*

Compiled by Marjorie Hooker, *U. S. Geological Survey, Washington, D. C.*

Chemical analyses, *in* Mineralogical notes, by Arthur S. Eakle: *Calif. Univ. Pubs., Dept. Geology, Bull.*, **2,** 315–325, illus., (1901).

Minerals from Leona Heights, Alameda County, California: *Calif. Univ. Pubs., Dept. Geology, Bull.* **3,** no. 7, 191–217, illus. (1903).

Spodumene from San Diego County, California: *Calif. Univ. Pubs., Dept. Geology, Bull.* **3,** no. 13, 265–275, illus., (1903).

(and W. F. Hillebrand). Crystallographical and chemical notes on lawsonite: *Am. Jour. Sci.*, (4), **17,** 195–197, illus., (1904); with title, Notes on lawsonite, *U. S. Geol. Survey Bull.* **262,** 58–60, illus., (1905).

Notes on some California minerals: *Am. Jour. Sci.*, (4), **17,** 191–194, (1904). Included in Mineralogical notes, *U. S. Geol. Survey Bull.* **262,** 121–126, (1905).

The tourmaline localities of southern California: *Science*, **19,** 266–268 (1904).

Crystallography of lepidolite: *Am. Jour. Sci.*, (4), **19,** 225–226, (1905). Included in Mineralogical notes, *U. S. Geol. Survey Bull.* **262,** 143–144, (1905).

Dumortierite: *U. S. Geol. Survey Bull.* **262,** 91–120, illus., (1905); excerpt, *Am. Jour. Sci.*, (4), **19,** 211–224, illus., (1905); with title, Über Dumortierit, *Z. Kryst.*, **41,** 19–47, illus., (1906).

Mineralogical notes: *U. S. Geol. Survey Bull.* **262,** 121–144, illus., (1905).

(with L. C. Graton). Purpurite, a new mineral: *Am. Jour. Sci.*, (4), **20,** 146–151, (1905); with title, Über Purpurit, ein neues Mineral, *Z. Kryst.* **41,** 433–438, (1906).

Siderite and barite from Maryland: *Am. Jour. Sci.*, (4), **21,** 364–370, illus., (1906); *U. S. Geol. Survey Bull.* **490,** 66–71, illus., (1911); with title, Siderit und Baryt von Maryland, *Z. Kryst.*, **42,** 321–326, illus., (1906).

The chemical composition of molybdic ocher: *Am. Jour. Sci.*, (4), **23,** 297–303, (1907); *U. S. Geol. Survey Bull.* **490,** 84–92, (1911); with title, Die chemische Zusammensetzung des Molybdänockers, *Z. Kryst.*, **43,** 331–337, (1907).

(with W. F. Hillebrand). The mercury minerals from Terlingua, Texas; kleinite, terlinguaite, eglestonite, montroydite, calomel, mercury: *Am. Jour. Sci.*, (4), **24,** 259–274, illus., (1907).

Mineralogical notes: *Am. Jour. Sci.*, (4), **24,** 152–158, illus., (1907); with title, Mineralogische Notizen, *Z. Kryst.*, **44,** 1–8, illus., (1907). Includes material given in 5 papers in *U. S. Geol. Survey Bull.* **490,** (1911), each of which is listed under its title.

Notes on powellite and molybdite: *Am. Jour. Sci.*, (4), **25,** 71–75, (1908); with title, Notiz über Powellit und Molybdit, *Z. Kryst.*, **44,** 9–13, (1907). The section on powellite is given in Notes on powellite, *U. S. Geol. Survey Bull.* **490,** 80–83, (1911).

(with A. Knopf). Two new boron minerals of contact-metamorphic origin: *Am. Jour. Sci.*, (4), **25,** 323–331, illus., (1908); with title, Hulsit und Paigeit, zwei neue Zinn-Eisenborate, *Z. Kryst.*, **48,** 1–15, illus., (1910).

(with W. F. Hillebrand). The mercury minerals from Terlingua, Texas: *U. S. Geol. Survey Bull.* **405,** 174 p., illus., 1909; with title, Die Quecksilbermineralien von Terlingua, Texas, *Z. Kryst.*, **47,** 434–575, illus., (1910).

Some calcite crystals with new forms: *Washington Acad. Sci. Proc.*, **11,** 1–16, illus., (1909); with title, Some new forms of calcite crystals, *U. S. Geol. Survey Bull.* **490,** 99–109, illus., (1911); with title, Calcitkrystalle mit neuen Formen, *Z. Kryst.*, **44,** 321–331, illus., (1908).

---

* Publication authorized by the Director, U. S. Geological Survey.

Barbierite, a monoclinic soda feldspar: *Am. Jour. Sci.*, (4), **30,** 358–359, (1910); *U. S. Geol. Survey Bull.* **509,** 40–41, (1912); with title, La barbierite, un feldspath sodique monoclinique, *Soc. Française de Minéralogie Bull.*, **33,** 320–321, (1910); with title, Barbierit, ein monokliner Natronfeldspat, *Z. Kryst.*, **50,** 347–348, (1912); abs., *Washington Acad. Sci. Jour.*, **1,** 114, (1911).

(and F. L. Ransome). Bismite: *Am. Jour. Sci.*, (4), **29,** 173–176, illus., (1910); with title, Wismutocker, *Z. Kryst.*, **48,** 16–19, illus., (1910).

Chemical composition of hulsite and paigeite: *Am. Jour. Sci.*, (4), **29,** 543–549, (1910).

The identity of stelznerite with antlerite: *Am. Jour. Sci.*, (4), **30,** 311–312, (1910); *U. S. Geol. Survey Bull.* **509,** 114–115, (1912); with title, Die Identität von Stelznerit und Antlerit, *Z. Kryst.*, **49,** 9–10, (1911).

Index of refraction of Canada balsam: *Am. Jour. Sci.*, (4), **29,** 324, (1910); *U. S. Geol. Survey Bull.* **490,** 65, (1911); with title, Der Brechungsexponent von Kanada-Balsam, *Centr. Mineralogie*, 390–391, (1910); abs. with title, Der Brechungsindex von Canadabalsam, *Z. Kryst.*, **53,** 314, (1913).

Ludwigite from Montana: *Am. Jour. Sci.*, (4), **30,** 146–150, (1910); *U. S. Geol. Survey Bull.* **490,** 28–32, (1911); with title, Ludwigit von Montana, U. S. A., *Z. Kryst.*, **48,** 545–549, (1911).

(with F. A. Canfield and W. F. Hillebrand). Mosesite, a new mercury mineral from Terlingua, Texas: *Am. Jour. Sci.*, (4), **30,** 202–208, (1910); with title, Mosesit, ein neues Quecksilbermineral von Terlingua, Texas, *Z. Kryst.*, **49,** 1–8, (1911).

The probable identity of podolite with dahllite: *Am. Jour. Sci.*, (4), **30,** 309–310, (1910); *U. S. Geol. Survey Bull.* **509,** 96–97, (1912); with title, Über die wahrscheinliche Identität von Podolit und Dahllit, *Z. Kryst.*, **48,** 559–561, (1911).

Some pegmatites from southern California [abs.]: *Science*, **31,** 516–517, (1910).

Albite from lawsonite schist, Marin County, California: *U. S. Geol. Survey Bull.* **490,** 48–52, (1911). Included in Krystallographische Notizen über Albit, Phenakit und Neptunit, *Z. Kryst.*, **48,** 550–558, (1911).

The alunite-beudantite group: *Am. Jour. Sci.*, (4), **32,** 359–364, (1911); *U. S. Geol. Survey Bull.* **509,** 70–76, (1912); with title, Die Alunit-Beudantitgruppe, *Z. Kryst.*, **50,** 106–111, (1912); abs., *Washington Acad. Sci. Jour.*, **1,** 112–113, (1911).

Analysis of tourmaline from Elba: *U. S. Geol. Survey Bull.* **490,** 93, (1911).

Axinite from California: *U. S. Geol. Survey Bull.* **490,** 37–47, (1911); with title, Axinit von Californien, *Z. Kryst.*, **48,** 148–157, (1910).

Bismite from Nevada: *U. S. Geol. Survey Bull.* **490,** 33–36, illus., (1911).

Bismuth ochers from San Diego County, California: *Am. Chem. Soc. Jour.*, **33,** 162–166, (1911); with title, Wismuthocker von San Diego Co., Californien, *Z. Kryst.*, **49,** 229–232, (1911); abs., *Washington Acad. Sci. Jour.*, **1,** 37, (1911).

Chemical composition of hulsite and paigeite: *U. S. Geol. Survey Bull.* **490,** 8–24, (1911).

Chemical composition of jamesonite and warrenite: *U. S. Geol. Survey Bull.* **490,** 25–27, (1911); with title, Die Chemische Zusammensetzung von Jamesonit und Warrenit, *Z. Kryst.*, **48,** 562–565, (1911); abs., *Washington Acad. Sci. Jour.*, **1,** 88, (1911).

The chemical composition of nephelite: *Washington Acad. Sci. Jour.*, **1,** 109–112, (1911); *U. S. Geol. Survey Bull.* **610,** 145–147, (1916); with title, Die chemische Zusammensetzung des Nephelins, *Z. Kryst.*, **50,** 343–346, (1912).

Evansite from two American localities: *U. S. Geol. Survey Bull.* **490,** 94–95, (1911).

Ferritungstite, a new mineral: *Am. Jour. Sci.*, (4), **32,** 161–162, (1911); with title, Ferritungstite from Washington, *U. S. Geol. Survey Bull.* **509,** 83–84, (1912); with title,

Ferritungstit, ein neues Mineral, *Z. Kryst.*, **50,** 112–113, (1912); abs., *Washington Acad. Sci. Jour.*, **1,** 24–25, (1911).

(with E. S. Larsen, Jr.). Hinsdalite, a new mineral: *Am. Jour. Sci.*, (4), **32,** 251–255,(1911); with title, Hinsdalit, ein neues Mineral, *Z. Kryst.*, **50,** 101–105, (1912); abs., *Washington Acad. Sci. Jour.*, **1,** 25–26, (1911).

Krystallographische Notizen über Albit, Phenakit, und Neptunit: *Z. Kryst.*, **48,** 550–558, (1911); abs., *Washington Acad. Sci. Jour.*, **1,** 37, (1911). Incorporates material from three articles in *U. S. Geol. Survey Bull.* **490,** (1911).

Manganotantalite from Mount Apatite, Maine: *U. S. Geol. Survey Bull.* **490,** 96–97, (1911).

Mineralogical notes, series 1: *U. S. Geol. Survey Bull.* **490,** 109 p., illus., (1911). Collection of 20 papers, some previously published, others new, each listed individually.

Natramblygonite, a new mineral: *Am. Jour. Sci.*, (4), **31,** 48–50, (1911); with title, Natramblygonite from Colorado, *U. S. Geol. Survey Bull.* **509,** 101–103, (1912); with title, Natronamblygonit, ein neues Mineral, *Z. Kryst.*, **49,** 233–235, (1911); abs., *Washington Acad. Sci. Jour.*, **1,** 37, (1911).

Notes on crystallography of phenacite: *U. S. Geol. Survey Bull.* **490,** 53–54, (1911). Included in Krystallographische Notizen über Albit, Phenakit und Neptunit, *Z. Kryst.*, **48,** 550–558, (1911).

Notes on neptunite: *U. S. Geol Survey Bull.* **490,** 55–57, (1911). Included in Krystallographische Notizen über Albit, Phenakit und Neptunit, *Z. Kryst.*, **48,** 550–558, (1911).

Notes on powellite: *U. S. Geol. Survey Bull.* **490,** 80–83, (1911).

Notes on purpurite and heterosite: *U. S. Geol. Survey Bull.* **490,** 72–79, illus., (1911); abs. with title, The relations of purpurite and heterosite, *Washington Acad. Sci. Jour.*, **1,** 113, (1911); with title, Die Beziehungen zwischen Purpurit und Heterosit, *Z. Kryst.*, **53,** 634, (1914).

Orbicular gabbro from Pala, San Diego County, California: *U. S. Geol. Survey Bull.* **490,** 58–59, (1911).

The refractive index of oil of cinnamon: *U. S. Geol. Survey Bull.* **490,** 60–64, (1911); abs. with title, Der Brechungsindex von Zimmtöl, *Z. Kryst.*, **53,** 624, (1914).

(with B. S. Butler). Some minerals from Beaver County, Utah: *Am. Jour. Sci.*, (4), **32,** 418–424, (1911); with title, Einige Mineralien von Beaver Co., Utah, *Z. Kryst.*, **50,** 114–119, (1912); abs. with title, Beaverite, a new mineral, *Washington Acad. Sci. Jour.*, **1,** 26–27, (1911).

(with B. S. Butler). Thaumasite from Beaver County, Utah: *Am. Jour. Sci.*, (4), **31,** 131–134, (1911); with title, Thaumasit von Beaver County, Utah, *Z. Kryst.*, **49,** 236–238, (1911); abs., *Washington Acad. Sci. Jour.*, **1,** 37, (1911).

Zinnwaldite from Alaska: *U. S. Geol. Survey Bull.* **490,** 98, (1911).

Beitrag zur Kenntnis der Turmalingruppe: *Z. Kryst.*, **51,** 321–343, illus., (1912); abs. with title, A study of the tourmaline group, *Washington Acad. Sci. Jour.*, **3,** 151, (1913).

The composition of the phosphorite minerals: *U. S. Geol. Survey Bull.* **509,** 98–100, (1912).

Crystallized turquoise from Virginia: *Am. Jour. Sci.*, (4), **33,** 35–40, illus., (1912); *U. S Geol. Survey Bull.* **509,** 42–47, illus., (1912); with title, Krystallisierter Türkis von Virginia, *Z. Kryst.*, **50,** 120–125, illus., (1912); abs., *Washington Acad. Sci. Jour.*, **1,** 58–59, (1911).

Crystallized variscite from Utah: *U. S. Natl. Mus. Proc.*, **41,** 413–430, illus., (1912); *U. S. Geol. Survey Bull.* **509,** 48–65, illus., (1912); with title, Krystallisierter Variscit von Utah, *Z. Kryst.*, **50,** 321–342, illus., (1912); abs., *Washington Acad. Sci. Jour.*, **1,** 150–151, (1911).

Cuprodescloizite from California: *U. S. Geol. Survey Bull.* **509,** 88, (1912); abs., *Washington Acad. Sci. Jour.*, **1,** 149–150, (1911); with title, Cuprodescloizit von Californien, *Z. Kryst.*, **53,** 634, (1914).

Hinsdalite from Colorado: *U. S. Geol. Survey Bull.* **509,** 66–69, (1912).

Die Krystallform des Natronamblygonits: *Z. Kryst.*, **51,** 246–247, illus., (1912); abs. with title, The crystallography of natramblygonite, *Washington Acad. Sci. Jour.*, **3,** 152, (1913).

Mineralogical notes, series 2: *U. S. Geol. Survey Bull.* **509,** 115 p., illus., (1912); abs., *Washington Acad. Sci. Jour.*, **2,** 349, (1912). Collection of 17 papers, some previously published, others new, each also listed individually.

Mineralogy of the French phosphorites: *U. S. Geol. Survey Bull.* **509,** 89–95, (1912); abs. with title, Chemical composition of the French phosphorite minerals, *Washington Acad. Sci. Jour.*, **1,** 151, (1911); with title, Chemische Zusammensetzung der französischen Phosphoritmineralien, *Z. Kryst.*, **53,** 635, (1914).

New manganese phosphates from the gem tourmaline field of southern California: *Washington Acad. Sci. Jour.*, **2,** 143–145, (1912).

Notes on minerals from gabbro of Waimea Canyon, Hawaii: *U. S. Geol. Survey Bull.* **509,** 85–87, (1912).

The properties of mosesite: *U. S. Geol. Survey Bull.* **509,** 104–109, (1912).

Some minerals from Beaver County, Utah: *U. S. Geol. Survey Bull.* **509,** 77–82, illus., (1912).

A study of the rutile group: *U. S. Geol. Survey Bull.* **509,** 9–39, (1912); abs., *Washington Acad. Sci. Jour.*, **1,** 177, (1911).

Thaumasite from Beaver County, Utah: *U. S. Geol. Survey Bull.* **509,** 110–113, (1912).

The calculation of mineral formulas: *Washington Acad. Sci. Jour.*, **3,** 97–98, (1913); *U. S. Geol. Survey Bull.* **610,** 163–164, (1916).

(with J. B. Umpleby and E. S. Larsen, Jr.). Custerite, a new contact metamorphic mineral: *Am. Jour. Sci.*, (4), **36,** 385–394, (1913); with title, Custerit, ein neues kontaktmetamorphes Mineral, *Z. Kryst.*, **53,** 321–331, (1914).

(with Charles Palache). Hodgkinsonite, a new mineral from Franklin Furnace, N. J.: *Washington Acad. Sci. Jour.*, **3,** 474–478, illus., (1913); with title, Hodgkinsonit, ein neues Mineral von Franklin Furnace, N. J., *Z. Kryst.*, **53,** 529–532, 675–676, (1914).

Immense bloedite crystals; preliminary note: *Washington Acad. Sci. Jour.*, **3,** 75–76, (1913); with title, Large crystals of bloedite, *U. S. Geol. Survey Bull.* **610,** 148–149, illus., (1916).

The refractive indices of strengite: *Washington Acad. Sci. Jour.*, **3,** 249–250, (1913); *U. S. Geol. Survey Bull.* **610,** 162, (1916).

Über "feste Lösungen" in Turmalin: *Z. Kryst.*, **53,** 181, (1913).

(with E. S. Larsen, Jr.). Cebollite, a new mineral: *Washington Acad. Sci. Jour.*, **4,** 480–482, (1914).

(with F. L. Hess). Colorado ferberite and the wolframite series: *U. S. Geol. Survey Bull.* **583,** 75 p., illus., (1914)

The identity of empressite with muthmannite: *Washington Acad. Sci. Jour.*, **4,** 497–499, (1914).

(with F. L. Hess). Pintadoite and uvanite, two new vanadium minerals from Utah; a preliminary note: *Washington Acad. Sci. Jour.*, **4,** 576–579, (1914).

Four new minerals: *Washington Acad. Sci. Jour.*, **5,** 7, (1915).

The supposed vanadic acid from Lake Superior is copper oxide: *Am. Jour. Sci.*, (4), **39,** 404–406, (1915).

Alunite from Marysvale, Utah: *U. S. Geol. Survey Bull.* **610,** 150–151, (1916).

The amblygonite group of minerals; fremontite (=natramblygonite): *U. S. Geol. Survey Bull.* **610,** 141–142, (1916).

Cassiterite in San Diego County, California: *U. S. Geol. Survey Bull.* **620,** 351–354, (1916)

The chemical composition of tremolite: *U. S. Geol. Survey Bull.* **610,** 133–136, (1916).

The composition and relations of custerite: *U. S. Geol. Survey Bull.* **610,** 152–158, (1916).

The composition of cebollite: *U. S. Geol. Survey Bull.* **610,** 129–130, (1916).

The composition of hodgkinsonite: *U. S. Geol. Survey Bull.* **610,** 159–160, (1916).

The crystallography of fremontite: *U. S. Geol. Survey Bull.* **610,** 143–144, illus., (1916).

The crystallography of thaumasite: *U. S. Geol. Survey Bull.* **610,** 131–132, illus., (1916).

The crystallography of variscite: *U. S. Geol. Survey Bull.* **610,** 69–80, illus., (1916); abs., *Washington Acad. Sci. Jour.*, **2,** 143, (1912).

Crystals of pisanite from Ducktown, Tennessee: *U. S. Geol. Survey Bull.* **610,** 161, illus., (1916).

Gigantic crystals of spodumene: *U. S. Geol. Survey Bull.* **610,** 138, illus., (1916).

(and R. K. Bailey). Intumescent kaolinite: *Washington Acad. Sci. Jour.*, **6,** 67–68, (1916).

Inyoite and meyerhofferite, two new calcium borates: *U. S. Geol. Survey Bull.* **610,** 35–55, illus., (1916).

Koechlinite (bismuth molybdate), a new mineral: *U. S. Geol. Survey Bull.* **610,** 10–34, illus., (1916).

Lucinite, a new mineral; a dimorphous form of variscite: *U. S. Geol. Survey Bull.* **610,** 56–68, illus., (1916).

The melilite group: *U. S. Geol. Survey Bull.* **610,** 109–128, illus., (1916).

Mineralogic notes, series 3: *U. S. Geol. Survey Bull.* **610,** 164 p., illus., (1916); abs., *Washington Acad. Sci. Jour.*, **4,** 354–356, (1914); **6,** 453–454, (1916). Collection of 25 papers, some previously published, others new, each also listed individually.

The natural antimonites and antimonates: *U. S. Geol. Survey Bull.* **610,** 104–105, (1916).

New occurrences of some rare minerals: *U. S. Geol. Survey Bull.* **610,** 137, (1916).

The probable identity of mariposite and alurgite: *U. S. Survey Bull.* **610,** 139–140, (1916)

Romeite: *U. S. Geol. Survey Bull.* **610,** 95–103, illus., (1916).

Schneebergite: *U. S. Geol. Survey Bull.* **610,** 81–94, illus., (1916).

Velardeñite, a new member of the melilite group: *U. S. Geol. Survey Bull.* **610,** 106–108, (1916).

(with G. F. Loughlin). Crandallite, a new mineral: *Am. Jour. Sci.*, (4), **43,** 69–74, illus., (1917).

Gems and precious stones: *U. S. Geol. Survey, Mineral Resources for 1915*, **pt. 2,** 843–858, (1917); **1916, pt. 2,** 887–899, (1919); **1917, pt. 2,** 145–168, (1920); **1918, pt. 2,** 7–14, (1921).

Ilsemannite, hydrous sulphate of molybdenum: *Washington Acad. Sci. Jour.*, **7,** 417–420, (1917). Reprinted in *Chem. News, London*, **116,** 94, (1917).

(with B. S. Butler). Magnesioludwigite, a new mineral: *Washington Acad. Sci. Jour.*, **7,** 29–31, (1917).

Mica: *U. S. Geol. Survey, Mineral Resources for 1915*, **pt. 2,** 277–290, (1917); **1916, pt. 2,** 291–308, (1919); **1917, pt. 2,** 183–195, (1920); **1918, pt. 2,** 629–694, (1921).

Minasragrite, a hydrous sulphate of vanadium: *Washington Acad. Sci. Jour.*, **7,** 501–503, (1917).

On the identity of hamlinite with goyazite: *Am. Jour. Sci.*, (4), **43,** 163–164, (1917).

Lithium minerals: *U. S. Geol. Survey, Mineral Resources for 1916*, **pt. 2,** 7–17, (1919).

Mica, monazite, and lithium minerals: *U. S. Geol. Survey Bull.* **666,** 153–158, (1919).

Planchéite and shattuckite, copper silicates, are not the same mineral: *Washington Acad. Sci. Jour.*, **9,** 131–134, (1919).

Thorium minerals: *U. S. Geol. Survey, Mineral Resources for 1916*, **pt. 2,** 223–237, (1919).

Zirconium and rare-earth minerals: *U. S. Geol. Survey, Mineral Resources for 1916*, **pt. 2,** 377–386, (1919); with illustrations, *Mineral Foote-Notes*, **2,** no. 3, 2–14, (March, 1918).

Gillespite, a new mineral: *Washington Acad. Sci. Jour.*, **12,** 7–8, (1922).

Sincosite, a new mineral (preliminary note): *Washington Acad. Sci. Jour.*, **12,** 195, (1922).

Thorium, zirconium, and rare-earth minerals: *U. S. Geol. Survey, Mineral Resources for 1919*, **pt. 2,** 1–32, (1922).

Argentojarosite, a new silver mineral (preliminary note): *Washington Acad. Sci. Jour.*, **13,** 233, (1923).

The occurrence and properties of sincosite, a new vanadium mineral from Sincos, Peru: *Am. Jour. Sci.*, (5), **8,** 462–480, (1924).

The genesis of lithium pegmatites: *Am. Jour. Sci.*, (5), **10,** 269–279, illus., (1925); abs., *Washington Acad. Sci. Jour.*, **16,** 76, (1926).

(with D. F. Hewett). Hisingerite from Blaine County, Idaho: *Am. Jour. Sci.*, (5), **10,** 29–38, illus., (1925); correction, **11,** 376, (1926).

(with E. S. Larsen, Jr.). The identity of variscite and peganite and the dimorphous form, metavariscite: *Am. Mineral.*, **10,** 23–28, (1925).

Origin of graphic granite [abs.]: *Am. Mineral.*, **11,** 66–67, (1926).

Origin of pegmatite minerals [abs.]: *Am. Mineral.*, **11,** 66, (1926).

(and E. P. Henderson). Purple muscovite from New Mexico: *Am. Mineral.*, **11,** 5–16, (1926).

(with E. S. Larsen, Jr., and F. L. Hess). Uranium minerals from Lusk, Wyoming: *Am. Mineral.*, **11,** 155–164, (1926).

Kernite, a new sodium borate: *Am. Mineral.*, **12,** 24–25, (1927).

The mineralogy of the Tintic Standard mine, Utah [abs.]: *Washington Acad. Sci. Jour.*, **17,** 121, (1927).

Mineral replacements in pegmatites: *Am. Mineral.*, **12,** 59–63, (1927).

Base exchange in artificial autunites [abs.]: *Am. Mineral.*, **13,** 111, (1928).

Hydroboracite from California: Festschrift, Victor Goldschmidt, p. 256–262, illus., Carl Winters Universitätsbuchhandlung, Heidelberg, (1928).

Occurrence of kernite and associated borates [abs.]: *Am. Mineral.*, **13,** 111, (1928).

Potash minerals from the Texas-New Mexico field [abs.]: *Am. Mineral.*, **13,** 111, (1928).

The probable identity of camsellite with szaibelyite: *Am. Mineral.*, **13,** 230–232, (1928); abs., 111, (1928).

Crystallography of the quartz pseudomorphs from Paterson, New Jersey [abs.]: *Am. Mineral.*, **14,** 100, (1929).

Halite-anhydrite intergrowths from Texas [abs.]: *Am. Mineral.*, **14,** 106, (1929).

Introduction, *in* Base exchange in artificial autunites: *Am. Mineral.*, **14,** 265–266, (1929).

The ludwigite group [abs.]: *Am. Mineral.*, **14,** 102, (1929).

(and E. P. Henderson). Mineralogy of potash cores from New Mexico and Texas [abs.]: *Washington Acad. Sci. Jour.*, **19,** 287, (1929).

(and E. P. Henderson). Mineralogy of the potash fields of New Mexico and Texas [abs.]: *Mining and Metallurgy*, **10,** 197–198, (1929).

The properties and associated minerals of gillespite: *Am. Mineral.*, **14,** 319–322, (1929).

Adjectival ending of chemical elements used as modifiers to mineral names: *Am. Mineral.*, **15,** 566–574, (1930); abs. with title, Ending of chemical adjectives in isomorphous minerals, **14,** 102, (1929).

Borate minerals from the Kramer district, Mohave Desert, California: *U. S. Geol. Survey Prof. Paper* **158,** 137–173, illus., (1930).

(with Stephen Taber). Psittacinite from the Higgins mine, Bisbee, Arizona: *Am. Mineral.*, **15,** 575–579, (1930).

The chrysocolla group [abs.]: *Am. Mineral.*, **16,** 112, (1931).

The crystallography of kornelite [abs.]: *Am. Mineral.*, **16,** 116, (1931).

Frank Wigglesworth Clarke [1847–1931]: *Am. Mineral.*, **16,** 405–407, portrait, (1931).

Crystals of sulvanite [abs.]: *Am. Mineral.*, **16,** 114, (1931).

(and T. B. Nolan). An occurrence of spadaite at Gold Hill, Utah: *Am. Mineral.*, **16,** 231–236, illus., (1931).

(with C. A. Schempp). Sulvanite from Utah: *Am. Mineral.*, **16,** 557–562, (1931).

(and J. G. Fairchild). Bavenite, a beryllium mineral, pseudomorphous after beryl, from California: *Am. Mineral.*, **17,** 409–422, illus., (1932); abs. by W. T. Schaller, **17,** 114, (1932).

Chemical composition of cuprotungstite: *Am. Mineral.*, **17,** 234–237, (1932).

The crystal cavities of the New Jersey zeolite region: *U. S. Geol. Survey Bull.* **832,** 90 p., illus., (1932); abs., *Washington Acad. Sci. Jour.*, **22,** 316, 1932.

Memorial of Arthur Starr Eakle [1862–1931]: *Am. Mineral.*, **17,** 94–95, portrait, (1932).

(and E. P. Henderson). Mineralogy of drill cores from the potash field of New Mexico and Texas: *U. S. Geol. Survey Bull.* **833,** 124 p., illus., (1932).

(and E. P. Henderson). Mineralogy of the potash deposits of New Mexico and Texas [abs.]: *Geol. Soc. Am. Bull.*, **43,** 187–188, (1932); brief version, *Pan-Am. Geologist,* **57,** 235, (1932).

The mordenite-ptilolite group; clinoptilolite, a new species: *Am. Mineral.*, **17,** 128–134, (1932).

Ptilolite from Utah: *Am. Mineral.*, **17,** 125–127, (1932).

The refractive indices of bloedite: *Am. Mineral.*, **17,** 530–533, (1932).

[Review of] Snow crystals, by W. A. Bentley and W. J. Humphreys: *Am. Mineral.*, **17,** 123, (1932).

(with E. S. Larson, Jr.). Serendibite from Warren County, New York, and its paragenesis: *Am. Mineral.*, **17,** 457–465, illus., (1932); abs., **14,** 104, (1929).

Ammonioborite, a new mineral: *Am. Mineral.*, **18,** 480–492, illus., (1933); abs., **16,** 114, (1931).

A large monazite crystal from North Carolina: *Am. Mineral.*, **18,** 435–439, illus., (1933).

A tephroite crystal from Franklin Furnace, N. J.: *Am. Mineral.*, **18,** 59–62, (1933).

Pegmatites, *in* Ore deposits of the Western States (Lindgren Volume), p. 144–151, Am. Inst. Min. Met. Eng., New York, (1933).

Mottramite or psittacinite, a question of nomenclature: *Am. Mineral.*, **19,** 180–181, (1934).

Monticellite from San Bernardino County, California, and the monticellite series: *Am. Mineral.*, **20,** 815–827, (1935).

Borates [Kern County, California], *in* Mineral resources of the region around Boulder Dam: *U. S. Geol. Survey Bull.* **871,** 98–105, illus., (1936).

The chemical composition of sepiolite (meerschaum) [abs.]: *Am. Mineral.*, **21,** 202, (1936).

The origin of kernite and borax in the Kramer borate field, California [abs.]: *Am. Mineral.*, **21,** 192, (1936).

Volcanological boron compounds: *Am. Geophys. Union Tr.*, **17th Ann. Mtg., pt. 1,** 234–235, (1936).

(with D. F. Hewett). Braunite from Mason County, Texas: *Am. Mineral.*, **22,** 785–789, (1937).

Crystallography of valentinite (Sb_2O_3) and andorite (?) ($2PbS \cdot Ag_2S \cdot 3Sb_2S_3$) from Oregon: *Am. Mineral.*, **22,** 651–666, illus., (1937).

Borax and borates, *in* Industrial minerals and rocks, p. 149–162, illus., Am. Inst. Min. Met. Eng., New York, (1937).

Lithium minerals, *in* Industrial minerals and rocks, p. 427–432, illus., Am. Inst. Min. Met. Eng., New York, (1937).

(and J. G. Fairchild). Cadmium in smithsonite from New Mexico: *Am. Mineral.*, **23,** 894–897, illus., (1938).

Johannsenite, a new manganese pyroxene: *Am. Mineral.*, **23,** 575–582, illus., (1938).

An unusual form of thaumasite from the Ducktown district, Tennessee: *Am. Mineral.*, **23,** 876–880, illus., (1938); correction, **24,** 346–347, (1939).

(with J. J. Glass). Inesite: *Am. Mineral.*, **24,** 26–39, illus., (1939); correction, 346–347, (1939).

Response to Presentation of the Second Roebling Medal of the Mineralogical Society of America: *Am. Mineral.*, **24,** 56–58, (1939).

A method for making accurate drawings of crystals [abs.]: *Am. Mineral.*, **25,** 214, (1940).

A probably new phosphate-sulphate of aluminum from Utah [abs.]: *Am. Mineral.*, **25,** 213–214, (1940).

Bismoclite from Goldfield, Nevada: *Am. Mineral.*, **26,** 651–654, illus., (1941).

(and R. E. Stevens). The validity of paragonite as a mineral species: *Am. Mineral.*, **26,** 541–545, (1941).

(with Carl Fries, Jr. and J. J. Glass). Bixbyite and pseudobrookite from the tin-bearing rhyolite of the Black Range, New Mexico: *Am. Mineral.*, **27,** 305–322, illus., (1942).

(with D. A. Andrews). Dolomite pseudomorphous after crystals of aragonite: *Am. Mineral.*, **27,** 135–140, illus., (1942).

The identity of ascharite, camsellite, and β-ascharite with szaibelyite; and some relations of the magnesium borate minerals: *Am. Mineral.*, **27,** 467–486, illus., (1942).

(and J. J. Glass). Occurrence of pink zoisite (thulite) in the United States: *Am. Mineral.*, **27,** 519–524, (1942).

Octahedron-like crystals of calcite: *Am. Mineral.*, **27,** 141–143, illus., (1942).

(with R. E. Stevens). The rare alkalies in micas: *Am. Mineral.*, **27,** 525–537, (1942).

An unusual specimen of graphic granite [abs.]: *Am. Mineral.*, **27,** 233, (1942).

Memorial of Frank Charles Schrader [1860–1944]: *Am. Mineral.*, **30,** 148–152, portrait, (1945).

Memorial of Roger Clark Wells [1877–1944]: *Am. Mineral.*, **30,** 163–168, portrait, (1945); *Geol. Soc. Am. Proc.*, **1945,** 279–284, portrait, (1946). Brief version, *Washington Acad. Sci. Jour.*, **34,** 348, (1944).

Presentation of the Sixth Roebling Medal of the Mineralogical Society of America to Clarence Samuel Ross: *Am. Mineral.*, **32,** 163–165, (1947).

An interpretation of the composition of high-silica sericites: *Mineralog. Mag.*, **29,** no. 211, 406–415, illus., (1950).

Miserite from Arkansas; a renaming of natroxonotlite: *Am. Mineral.*, **35,** 911–921, illus., (1950).

(and M. K. Carron). Margarite-ephesite series; theory versus fact [abs.]: *Am. Mineral.*, **37,** 301, (1952).

Presentation of the Mineralogical Society of America Award to Frederick Henry Stewart: *Am. Mineral.*, **38,** 297–298 (1953).

A photographic technique for showing some mineral relations: *U. S. Geol. Survey Bull.* **992,** 83–94, illus., (1953).

You CAN take it with you

...on your TOUGHEST JOBS!

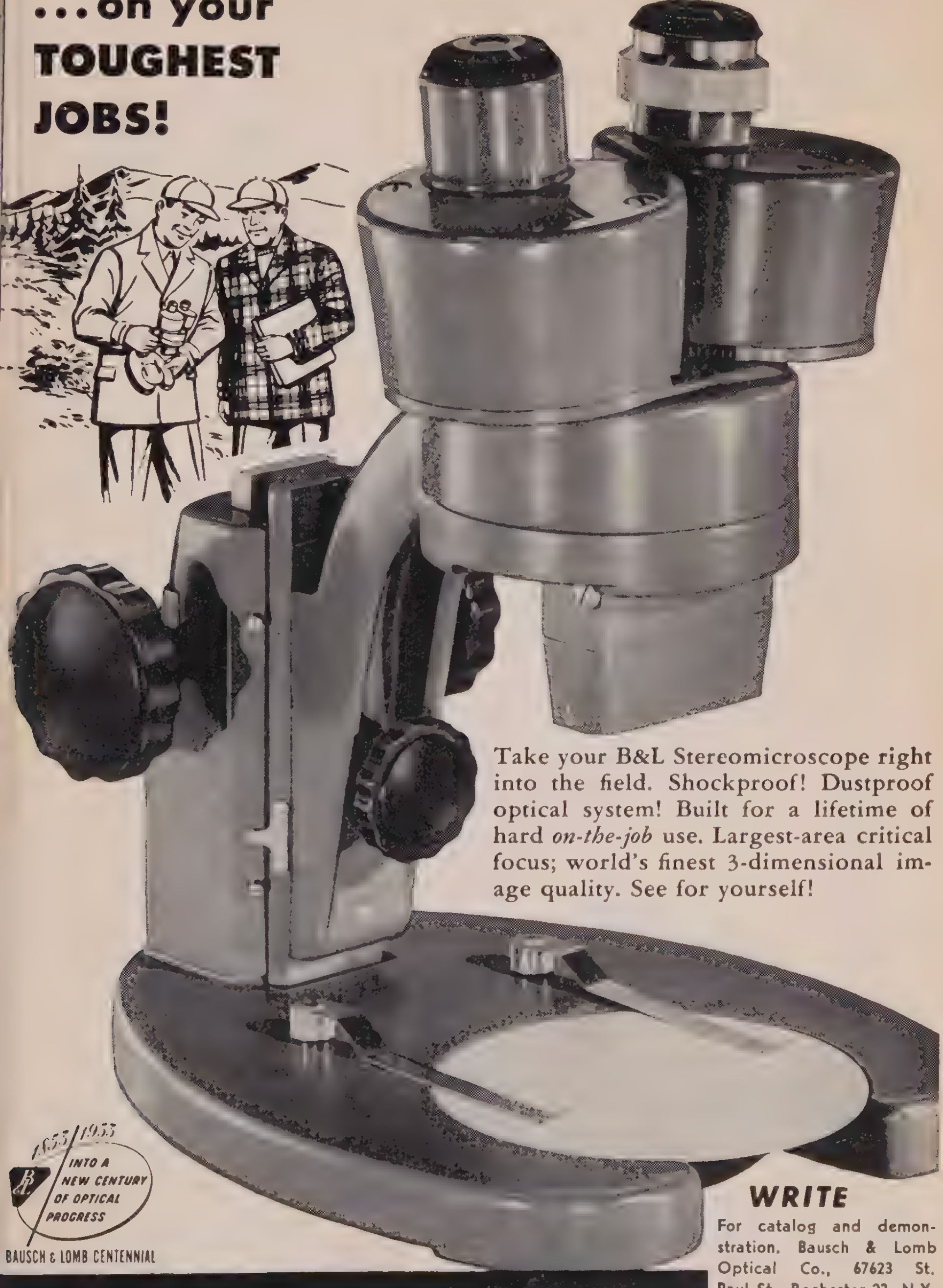

Take your B&L Stereomicroscope right into the field. Shockproof! Dustproof optical system! Built for a lifetime of hard *on-the-job* use. Largest-area critical focus; world's finest 3-dimensional image quality. See for yourself!

1853/1953
INTO A NEW CENTURY OF OPTICAL PROGRESS
BAUSCH & LOMB CENTENNIAL

WRITE

For catalog and demonstration. Bausch & Lomb Optical Co., 67623 St. Paul St., Rochester 23, N.Y.

Bausch & Lomb Stereomicroscopes

OPTICAL "TOOLS"

for Mineralogists

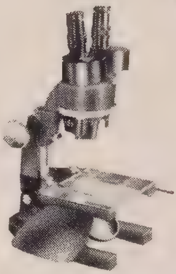

AO STEREOSCOPIC MICROSCOPES

For examining surface characteristics of specimens large and small, nothing surpasses the lifelike, three dimensional image and wide field of view provided by these instruments. Image is right side up unreversed. Many different models available, magnifications from 6.3X to 144X.

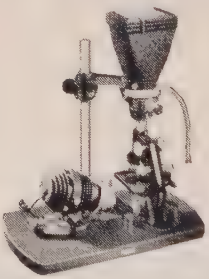

AO PHOTOMICROGRAPHIC CAMERAS

The answer to the demand for a sturdy precise camera that is convenient and rapid to operate. Camera swings easily in and out of position over the microscope without disturbing settings. Provides quick changeover from 4" x 5" to 35mm film.

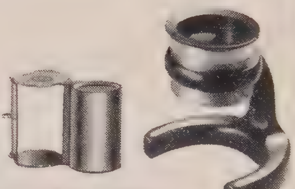

AO MAGNIFIERS

For those who require the finest, AO magnifiers provide good working distance, and clear, undistorted images. Doublet and triplet pocket magnifiers, 6X to 15X, in plain or folding mounts. Large field 4.5X triplet in convenient horseshoe focusing mount.

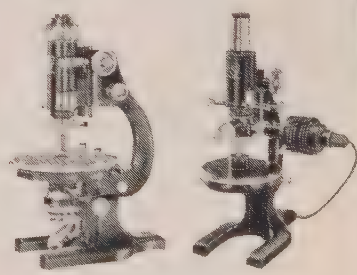

AO POLARIZING MICROSCOPES

These superb instruments offer exceptional variety in equipment and price range . . . from the simple P45A with built-in light source and Polaroid elements, to the large, completely equipped 37A. A new model, 44AV, has an attached high intensity illuminator for studying polished opaque minerals.

Choose AO scientific instruments and *invest* in enduring quality, exceptional performance and readily available service. See your AO distributor or write Dept. **Y7.**

American Optical
INSTRUMENT DIVISION
BUFFALO 15, NEW YORK

idening the use of
your Polarizing microscope

Leitz® UNIVERSAL STAGES

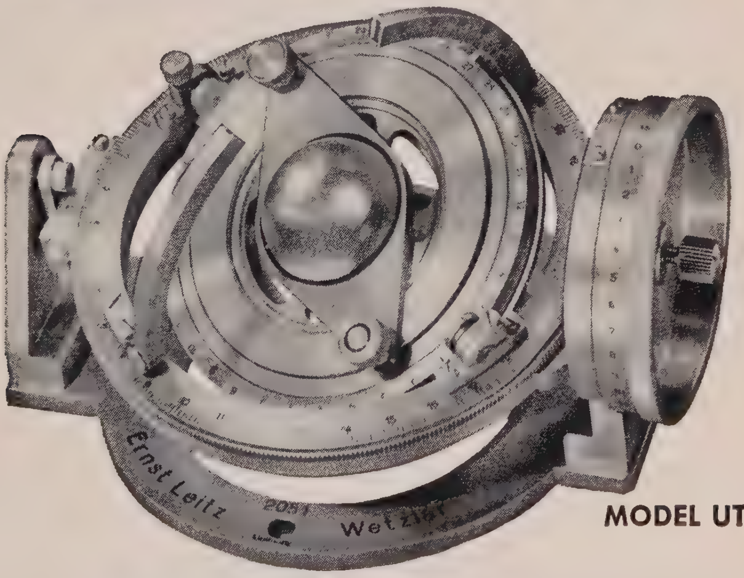

MODEL UT 4

Making your polarizing microscope even more versatile, Leitz Universal Stages permit accurate and rapid determination of the optical properties and orientation of crystal plates and fragments. In addition they embody several vital improvements which enable you to change the slide rapidly and to orient it easily onto the point of junction of the rotating axis.

Several models are available, offering two, four or five axes of rotation. Stages are designed for use with the following Leitz microscopes: Models AM, SY, CMU, IIIM, MOP and PANPHOT.

Four special UM objectives for universal stage methods are now available. Each of the four is equipped with iris diaphragm and corrected for the same free working distance with respect to the segments.

Another fine accessory for the famous Leitz Microscopes—recognized everywhere as the finest microscopes made anywhere.

For details, write Dept. A

E. LEITZ, Inc., 468 Fourth Avenue, New York 16, N.Y.

Z MICROSCOPES • SCIENTIFIC INSTRUMENTS • BINOCULARS
LEICA CAMERAS AND ACCESSORIES

New American

PEAT AND MARL SAMPLER

The instrument embodies the essential features of a design by Professor Davis of the Geographical Survey. It consists of a jacketed plunger with a sharpened end. As the instrument is pressed into the ground, it remains closed. When the proper depth has been reached for taking the sample, the instrument is drawn up about 6 or 8 inches; at this point an internal locking device holds the plunger fast in the upper part of the jacket. This instrument is again forced downward, cutting and retaining the desired sample. Complete with illustrated head, 9 four foot lengths of extension rod and case; catalog number 76-432 sells for $75.00.

SCIENTIFIC INSTRUMENTS & APPARATUS
Eberbach CORPORATION
ANN ARBOR, MICH.
ESTABLISHED 1843

W. HAROLD TOMLINSON
Petrographic Laboratory
260 N. ROLLING RD., SPRINGFIELD, PA.
ROCK SECTIONS ORIENTATED MINERAL SECTIONS

CRYSTALLOGRAPHY

Specializing in choice crystals, singles, groups, from world wide sources. Catalog free.

V. D. HILL
Complete Gem & Mineral Establishment
5450-F Portland Road, Salem, Oregon

NOW

INDEX OF REFRACTION LIQUIDS

High Series; range 1.80 to 2.00; intervals 0.01
Formulas of Meyrowitz and Larsen

Write for leaflet HI-AM

R. P. CARGILLE LABORATORIES, INC.
117 Liberty Street New York 6, N.Y.

The Mineralogical Society of America announces a forthcoming book, the first issue in a new series to be known as Special Publications.

GEORGIUS AGRICOLA'S

DE NATURA FOSSILIUM

(translated by MARK C. AND JEAN A. BANDY)

Georgius Agricola (1494-1555) is well-known as the author of De Re Metallica, a treatise of mining and metallurgy published in 1556. Among Agricola's other works is the first systematic mineralogy, entitled De Natura Fossilium, comprising 210 pages in the original Latin edition published in Basel in 1546. The publication of the translation will make this work available in English to mineralogists, scientists and students of history.

Price $3.00, postpaid

Orders may be sent to the treasurer:

Earl Ingerson
U.S. Geological Survey
Washington 25, D.C.

COOKE

INTERMEDIATE POLARIZING MICROSCOPE
M7021

A MODERATELY PRICED INSTRUMENT FOR INSTRUCTION, CONTROL AND FIELD USE

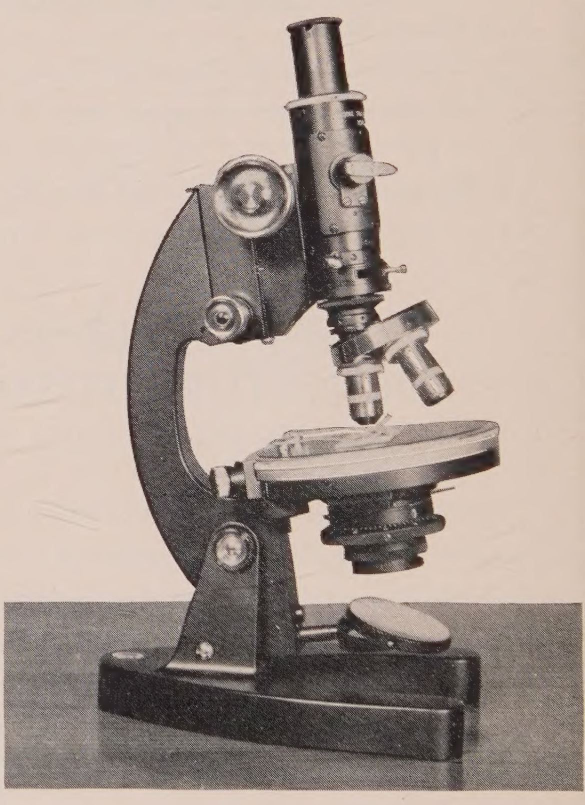

TUBE

Normal size eyepiece tube.

Patented Bertrand Lens and Bertrand Diaphragm of trip-in type

Polaroid analyzer and glass compensator in sliding mount

Slot for compensators

Two-way spring opposed centering adjustment

Revolving nosepiece

STAGE

120 mm. diameter, graduated, with vernier, rotating on plain bearing with clamp.

SUBSTAGE

With Abbe condenser, iris diaphragm, fitting to receive a filter or diffuser and Polaroid polarizer. Polarizer rotatable and graduated with catch at each 90 degree position.

A complete selection of objectives, eyepieces, wedges and compensators, slotted objectives, etc., is available for use with this model.

(Send for complete brochure on the Cooke Polarizing Microscopes)

THE R. Y. FERNER COMPANY, INC., 110 Pleasant Street, Malden 48, Massachusetts

In Canada: Cooke Troughton and Simms, Ltd. 61 College Street, Toronto

(Sold in the United States with service and replacement stock facilities maintained)

Christmas Gift Suggestions:

We recommend any of the following items as ideal Christmas Gifts.

DETECTRON GEIGER COUNTERS

THE NEW MODEL DG-7 is the ultimate in low cost, light weight all-purpose Geiger Counters. This unit is designed for those who desire a Geiger Counter with a detachable probe. The accurate calibration of the DG-7 on all ranges makes it very satisfactory as a laboratory instrument. Complete $135.00

THE NEW MODEL DG-2 is the standard in the low cost field. It compares with instruments costing as much as $250.00! Used by many colleges, universities, the Bureau of Mines and the Atomic Energy Commission. Complete $98.50

THE DG-5 CLAIMSTAKER is America's lowest priced "quality" Geiger Counter. Pocket size but sensitive to radiation from all 54 uranium minerals, reporting their presence in loud, sharp clicks. Complete $37.50

MINERALIGHTS

MINERALIGHT SL-2537 is the ideal short-wave ultra-violet source generally used for laboratory research, mineral prospecting and collecting. Used by the Bureau of Mines and the U.S. Atomic Energy Commission for identifying uranium. Price $39.50

MINERALIGHT SL-3660 is the companion long-wave ultra-violet source for oil analysis, diagnostic and laboratory use, criminology, etc. The mineral collector will like SL-3660 as many minerals respond most brilliantly to this wave length. Price $29.50

LAMP AND BATTERY CASE #505 is designed to carry both the above lamps with batteries for use in the field including daytime viewing feature. Case $22.50. Batteries $5.00

PROSPECTOR'S PICKS

The **ESTWING PROSPECTOR PICK** has been acclaimed as the finest and most desired collecting tool necessary for success of every field trip.

Polished finish $4.00 Black finish $3.75

Shipping weight three pounds each

Transportation additional on all above items

BOOKS FOR THE MINERALOGIST

MINERALS AND HOW TO STUDY THEM—Dana-Hurlbut	$ 4.25
MANUAL OF MINERALOGY—Dana-Hurlbut	6.50
TEXTBOOK OF MINERALOGY—Dana-Ford	7.50
SYSTEM OF MINERALOGY Vol. I—Dana-Palache, Berman, Frondel	12.00
SYSTEM OF MINERALOGY Vol. II—Dana-Palache, Berman, Frondel	15.00
MINERALOGY—Kraus, Hunt and Ramsdell	8.00
FORMATION OF MINERAL DEPOSITS—Bateman	5.50

Books sent Prepaid

SCHORTMANN'S MINERALS

6 McKinley Avenue
Easthampton, Mass.

WARD'S AMERICAN ROCK COLLECTION

This standard reference collection for students of petrography is made up of 100 contrasting examples of commonly occurring igneous, sedimentary and metamorphic rocks from important American localities. Specimens, averaging 3″ × 4″ in size are identified by printed labels attached to their individual trays and are key numbered to additional data in the loose leaf manual* provided. This collection can be conveniently housed in Ward's splendid "Universal" Storage Cabinet, functional designed for economic mineral storage.

Collection, complete with trays and manual (MC 301) $90.00

"Universal" 10 Drawer Cabinet 23⅜″ × 20″ × 43¼″ (complete with lock) $97.50

***Manual of the American Rock Collection.** Contains full data on each of the specimens, including megascopic and microscopic data, pertinent bibliographies, etc. MC 302 $4.50

American Rock Collection Thin Sections. 100 well prepared thin sections on 25 × 45 mm slides in box MC 303 ....$150.50

American Rock Collection Student Sets. Supplementing the American Rock Collection, 100 1″ × 1″ student chips, numbered for ready identification, are provided for study or sectioning. MC 304 ....$5.00

Grain Thin Sections and Multiple Oriented Sections. 40 different mineral slides, each containing several grains of the respective species and illustrating its complete optical characters. Plus a set of 4 slides, illustrating respectively: Interference Figures, 2 v, Bxa-Bxo, and Relief. Complete (MC 210) $110.00 (Full particulars will be sent on request)

Eberbach Slide Filing cabinets. These cabinets provide an expandable filing system. They may be stacked beside or on top of each other as the collection increases. The cabinet holds 25 aluminum trays each of which will hold 30 25 × 46 mm slides. Cabinet sturdily constructed of seasoned hardwood in light oak finish measures 10″ high by 8½″ wide and 12″ deep. Price $51.00

Prices are list at Rochester, N.Y.

Catalogs and price lists.

523 Ward's Geology Catalog. Lists collections, pound materials, and student specimens.

FM 6 Fine Mineral Specimens—a listing of items not included in Catalog 523.

531 Fluorescence and Radiation.

Supplies for the Geologist.

Geology News Letter. Contains items of current interest, recent acquisitions.

Ward's Natural Science Bulletin. 5 issues per year. $1.00

WARD'S *NATURAL SCIENCE ESTABLISHMENT, INC.*
3000 RIDGE ROAD EAST • ROCHESTER 9, N.Y.

GEORGE BANTA PUBLISHING COMPANY, MENASHA, WISCONSIN